รายงานการวิจัยฉบับสมบูรณ์

การพัฒนาและการประยุกต์ใช้ระบบต่อเนื่องสำหรับการศึกษาการดูดซึมได้ของแร่ธาตุและโลหะหนัก

Development and Applications of Continuous Systems for Study of Bioavailability of Minerals and Heavy Metals

ศ.ดร. ยุวดี เชี่ยววัฒนา และคณะ

มกราคม 2551

สัญญาเลขที่ BRG4780002

รายงานการวิจัยฉบับสมบูรณ์

การพัฒนาและการประยุกต์ใช้ระบบต่อเนื่องสำหรับการศึกษา การดูดซึมได้ของแร่ธาตุและโลหะหนัก

Development and Applications of Continuous Systems for Study of Bioavailability of Minerals and Heavy Metals

คณะผู้วิจัย	สังกัด
1. ศ.ดร. ยุวดี เชี่ยววัฒนา	ภาควิชาเคมี คณะวิทยาศาสตร์ มหาวิทยาลัยมหิดล
2. ผศ.ดร. อทิตยา ศิริภิญญานนท์	ภาควิชาเคมี คณะวิทยาศาสตร์ มหาวิทยาลัยมหิดล
3. ดร. น้ำฝน ทองทวี	ภาควิชาเคมี คณะวิทยาศาสตร์ มหาวิทยาลัยมหิดล
4. ดร. รุ่งรัตน์ ปีเตอร์เซ่น	ภาควิชาเคมี คณะวิทยาศาสตร์ มหาวิทยาลัยมหิดล
5. ดร. จรรยา บัวน่วม	ภาควิชาเคมี คณะวิทยาศาสตร์ มหาวิทยาลัยมหิดล
6. ดร. ครรชิต จุดประสงค์	ภาควิชาเคมี คณะวิทยาศาสตร์ มหาวิทยาลัยมหิดล
7. นางสาววีรวรรณ วัยวัฒน์	ภาควิชาเคมี คณะวิทยาศาสตร์ มหาวิทยาลัยมหิดล
8. นางสาววุฒิกา กิจธิคุณ	ภาควิชาเคมี คณะวิทยาศาสตร์ มหาวิทยาลัยมหิดล
9. นางสาวอัปสร โสตถิมัย	ภาควิชาเคมี คณะวิทยาศาสตร์ มหาวิทยาลัยมหิดล
10. นางสาวจีราวรรณ พรหมจันทร์	ภาควิชาเคมี คณะวิทยาศาสตร์ มหาวิทยาลัยมหิดล
11. นางสาวเนตติกานต์ แก้วขอมดี	ภาควิชาเคมี คณะวิทยาศาสตร์ มหาวิทยาลัยมหิดล
12. นางสาวอาทิตยา สามณฑา	ภาควิชาเคมี คณะวิทยาศาสตร์ มหาวิทยาลัยมหิดล
13. นางสาวกนกวรรณ คุณาจิรภรณ์	ภาควิชาเคมี คณะวิทยาศาสตร์ มหาวิทยาลัยมหิดล
14. นายโศภณ ปุระวัฒน์	ภาควิชาเคมี คณะวิทยาศาสตร์ มหาวิทยาลัยมหิดล
15. นายสุทธินันท์ แต่บรรพกุล	ภาควิชาเคมี คณะวิทยาศาสตร์ มหาวิทยาลัยมหิดล
16. นายมธุรส อ่อนไทย	ภาควิชาเคมี คณะวิทยาศาสตร์ มหาวิทยาลัยมหิดล
17. นายวิภาค อนุตรศักดา	ภาควิชาเคมี คณะวิทยาศาสตร์ มหาวิทยาลัยมหิดล

สนับสนุนโดยสำนักงานกองทุนสนับสนุนการวิจัย

กิตติกรรมประกาศ

ขอขอบคุณสำนักงานกองทุนสนับสนุนการวิจัยที่ได้สนับสนุนทุนการวิจัย "ทุนองค์ความรู้ใหม่ที่เป็นพื้นฐานต่อการพัฒนา" เพื่อใช้ในการดำเนินงานวิจัยในโครงการ "การพัฒนาและการประยุกต์ใช้ระบบต่อเนื่องสำหรับการศึกษาการดูดซึมได้ของแร่ธาตุและโลหะหนัก" โดยมีระยะเวลาของโครงการ 3 ปี ตั้งแต่ พฤษภาคม 2547 ถึง เมษายน 2550 ตลอดระยะเวลาดังกล่าวได้รับคำแนะนำและข้อเสนอแนะในการดำเนินโครงการจากบุคลากรที่เกี่ยวข้อง ทำให้สามารถดำเนินงานวิจัยได้อย่างราบรื่น จึงขอขอบคุณไว้ ณ โอกาสนี้ด้วย

ขอขอบคุณหน่วยงานต่างๆ ต่อไปนี้ที่ได้ให้ความอนุเคราะห์ในด้านต่างๆ เป็นอย่างดี

- ศูนย์นวัตกรรมเคมี โครงการพัฒนาบัณฑิตศึกษาและการวิจัยทางเคมี สำหรับทุนการศึกษาของนักศึกษา วัสดุวิจัยและครุภัณฑ์บางส่วนในโครงการวิจัย
- ภาควิชาเคมี คณะวิทยาศาสตร์ มหาวิทยาลัยมหิดล สำหรับสถานที่ เครื่องมือและอุปกรณ์ต่างๆ
- Department of Soil and Environmental Science, Lincoln University, New Zealand สำหรับสถานที่ในการทำวิจัยระยะสั้นของนักศึกษาในโครงการ และคำแนะนำจาก Professor Ronald McLaren
- Department of Chemistry, Technical University of Denmark, Denmark สำหรับสถานที่ในการทำวิจัยระยะสั้นของนักศึกษาในโครงการ และคำแนะนำจาก Professor Elo Harald Hansen
- Department of Chemistry, University of the Balearic Islands, Spain สำหรับสถานที่ในการทำวิจัยระยะสั้นของนักศึกษาในโครงการ และคำแนะนำจาก Dr. Manuel Miró

คณะผู้วิจัย

บทคัดย่อ

รหัสโครงการ: **BRG4780002**

ชื่อโครงการ: **การพัฒนาและการประยุกต์ใช้ระบบต่อเนื่องสำหรับการศึกษาการดูดซึมได้ของแร่ธาตุและโลหะหนัก**

ชื่อนักวิจัย: ศ.ดร.ยุวดี เชี่ยววัฒนา ภาควิชาเคมี คณะวิทยาศาสตร์ มหาวิทยาลัยมหิดล

Email Address: scysw@mahidol.ac.th

ระยะเวลาโครงการ: 1 พฤษภาคม 2547 – 30 เมษายน 2550

การวิเคราะห์ปริมาณทั้งหมดของโลหะหนักหรือแร่ธาตุในตัวอย่างมีประโยชน์จำกัด เพราะธาตุต่างๆ อาจดำรงอยู่ได้ในรูปฟอร์มที่ต่างกันซึ่งมีความสามารถในการเคลื่อนตัว การดูดซึมหรือการนำไปใช้ได้ของโลหะหนักหรือแร่ธาตุนั้นๆ ที่แตกต่างกัน ทำให้มีผลกระทบของธาตุต่างๆ ต่อสิ่งแวดล้อมและชีวิตของมนุษย์ที่ต่างกันด้วย งานวิจัยนี้ได้ประยุกต์ใช้วิธีใหม่ในการประเมินผลกระทบของการปนเปื้อนของโลหะหนักจากกิจกรรมอุตสาหกรรมหลอมโลหะและอุตสาหกรรมการถลุงแร่ โดยใช้ระบบการสกัดเป็นลำดับขั้นแบบไหลต่อเนื่องที่พัฒนาขึ้นใหม่ ทั้งนี้ได้เลือกศึกษากรณีการปนเปื้อนจากโรงงานที่น่าจะมีปัญหาในประเทศไทย คือปัญหาจากการหลอมโลหะตะกั่วจากแบตเตอรี่เก่า และปัญหาจากการถลุงโลหะสังกะสีที่ทำให้เกิดการปนเปื้อนของแคดเมียม โดยได้ศึกษาถึงความสามารถในการเคลื่อนตัวของตะกั่วและแคดเมียมที่ปนเปื้อนอยู่ในดิน ดินตะกอนและอากาศในบริเวณใกล้ๆ กับโรงงานดังกล่าว นอกเหนือจากนั้นได้ศึกษาถึงรูปฟอร์มของตะกรันเหล็กที่เกาะอยู่ในท่อนำส่งแก๊สธรรมชาติ สำหรับงานวิจัยอีกส่วนหนึ่ง ได้ทำการพัฒนาวิธีวิเคราะห์แบบไหลต่อเนื่องเพื่อศึกษาการดูดซึมหรือการนำไปใช้ได้ของแร่ธาตุในอาหาร ระบบที่พัฒนา ขึ้นนี้เป็นการจำลองหลอดแก้วให้เสมือนเป็นระบบการย่อยในกระเพาะอาหารและการดูดซึมสารอาหารในลำไส้เล็ก โดยอาศัยวิธีแบบแบทช์ในการจำลองการย่อยในกระเพาะอาหาร และใช้ระบบการซึมผ่าน เยื่อบางแบบไหลต่อเนื่อง (continuous-flow dialysis, CFD) ในการจำลองการดูดซึมสารอาหารในลำไส้เล็ก ด้วยระบบ CFD ทำให้สามารถเก็บสารละลายตัวอย่างที่ซึมผ่านเยื่อบางออกมาเพื่อการวิเคราะห์ปริมาณแร่ธาตุโดยใช้หน่วยตรวจวัดประเภทต่างๆ ได้ เช่น การวัดการดูดกลืนแสงโดยอาศัยเปลวไฟและความร้อน การวัดการคายแสงของธาตุโดยอาศัยพลาสมาเป็นแหล่งพลังงาน ซึ่งได้ทำการศึกษาถึงวิธีการเชื่อมต่อระบบ CFD ที่พัฒนาขึ้นกับหน่วยตรวจวัดประเภทต่างๆ ทำการประเมินวิธีที่พัฒนาขึ้นใหม่เปรียบเทียบกับวิธีแบบแบทช์ที่ใช้กันอยู่เดิม ในด้านความแม่นยำ ความถูกต้อง และประสิทธิภาพ เพื่อประยุกต์ใช้ในการประเมินค่าการดูดซึมได้ของแร่ธาตุในอาหาร และศึกษาปัจจัยที่มีผลต่อค่าการดูดซึมได้

คำหลัก: ระบบแบบไหลต่อเนื่อง การสกัดลำดับขั้น การซึมผ่านเยื่อบาง

ABSTRACT

Project Code: **BRG4780002**

Project Title: **Development and Applications of Continuous Systems for Study of Bioavailability of Minerals and Heavy Metals**

Investigator: Juwadee Shiowatana

Department of Chemistry, Faculty of Science, Mahidol University

Email Address: scysw@mahidol.ac.th

Project Period: May 1, 2004 – April 30, 2007

The determination of information on total concentration of heavy metals or minerals in samples has limited use because elements can exist in different chemical forms with varying mobility and availability to living organisms and thus can have varying impacts on environment and human life. Chemical speciation is therefore necessary. In this research, a newly developed continuous-flow sequential extraction was applied to assess the impact of heavy metals contamination caused by metal smelting and mining activities. Two major case studies were investigated including lead contamination in soil and air collected from the area nearby lead smelting industry and cadmium contamination in soil and sediment collected from the area in the vicinity of zinc mining industry. In addition, iron speciation in the natural gas pipe line was examined. Further to a different topic, a novel method for the determination of *in vitro* mineral bioavailability, or mineral bioaccessibility, was developed based on a simulated gastric digestion in a batch system followed by a continuous-flow intestinal digestion. The simulated intestinal digestion was performed in a dialysis bag placed inside a channel in a flowing stream of dialyzing solution. The continuous flow dialysis in the intestinal digestion step enables dialysable components to be continuously removed for element detection by various detection methods, including flame atomic absorption spectrometry (FAAS), electrothermal atomic absorption spectrometry (ETAAS), and inductively coupled plasma optical emission spectrometry (ICP-OES). The interfacing between the continuous-flow dialysis system and the detection method was carefully optimized. The precision, accuracy and efficiency of the developed method were compared with the conventional batch analysis. The developed system was applied to examine factors affecting dialyzability, or the mineral bioavailability of food.

Keywords: continuous-flow, sequential extraction, dialysis

Executive Summary

Project Title: Development and Applications of Continuous Systems for Study of Bioavailability of Minerals and Heavy Metals

Investigaor: Juwadee Shiowatana

Department of Chemistry, Faculty of Science, Mahidol University

Email Address: scysw@mahidol.ac.th

Project Period: May 1, 2004 – April 30, 2007

The newly developed continuous-flow sequential extraction has been applied to assess metal mobility, bioavailability, and the impact of heavy metals contaminated in environmental systems. This type of study is considered as a futuristic approach used for planning how to perform environmental management. In addition, a novel method for the determination of *in vitro* mineral bioavailability, or mineral bioaccessibility, has been developed based on a simulated gastric digestion in a batch system followed by a continuous-flow intestinal digestion. The simulated intestinal digestion was performed in a dialysis bag placed inside a channel in a flowing stream of dialyzing solution. The continuous flow dialysis in the intestinal digestion step enables dialysable components to be continuously removed for element detection by various methods, including flame atomic absorption spectrometry (FAAS), electrothermal atomic absorption spectrometry (ETAAS), and inductively coupled plasma optical emission spectrometry (ICP-OES). Moreover, the proposed continuous flow dialysis system offers information on dialysis kinetics, which could be extrapolated to be of some use for absorption studies. The developed system has been applied to examine factors affecting dialyzability, or the mineral bioavailability of food, with the ultimate goal to find ways to overcome mineral deficiency of Thai people.

Seventeen papers have been published in the international journals as follows:

Continuous-Flow Sequential Extraction

1. Samontha, A., Waiyawat, W., Shiowatana, J. & McLaren, R.G. 2007, "Atmospheric deposition of metals associated with air particulate matter: fractionation of particulate-bound metals using continuous-flow sequential extraction", *Science Asia,* vol. 33, pp. 421-428. (impact factor = _)

2. Buanuam, J., Miro, M., Hansen, E.H., Shiowatana, J., Estela, J.M. & Cerda, V. 2007, "A multisyringe flow-through sequential extraction system for on-line monitoring of orthophosphate in soils and sediments", *Talanta,* vol. 71, no. 4, pp. 1710-1719. (impact factor = 2.810)
3. Kaewkhomdee, N., Kalambaheti, C., Predapitakkun, S., Siripinyanond, A. & Shiowatana, J. 2006, "Iron fractionation for corrosion products from natural gas pipelines by continuous-flow sequential extraction", *Analytical and Bioanalytical Chemistry,* vol. 386, no. 2, pp. 363-369. (impact factor = 2.591)
4. Buanuam, J., Tiptanasup, K., Shiowatana, J., Miro, M. & Harald Hansen, E. 2006, "Development of a simple extraction cell with bi-directional continuous flow coupled on-line to ICP-MS for assessment of elemental associations in solid samples", *Journal of Environmental Monitoring,* vol. 8, no. 12, pp. 1248-1254. (impact factor = 1.523)
5. Buanuam, J., Miro, M., Hansen, E.H. & Shiowatana, J. 2006, "On-line dynamic fractionation and automatic determination of inorganic phosphorus in environmental solid substrates exploiting sequential injection microcolumn extraction and flow injection analysis", *Analytica Chimica Acta,* vol. 570, no. 2, pp. 224-231. (impact factor = 2.894)
6. Buanuam, J., Shiowatana, J. & Pongsakul, P. 2005, "Fractionation and elemental association of Zn, Cd and Pb in soils contaminated by Zn minings using a continuous-flow sequential extraction", *Journal of Environmental Monitoring,* vol. 7, no. 8, pp. 778-784. (impact factor = 1.523)
7. Chomchoei, R., Miro, M., Hansen, E.H. & Shiowatana, J. 2005, "Automated sequential injection-microcolumn approach with on-line flame atomic absorption spectrometric detection for implementing metal fractionation schemes of homogeneous and nonhomogeneous solid samples of environmental interest", *Analytical Chemistry,* vol. 77, no. 9, pp. 2720-2726. (impact factor = 5.646)
8. Chomchoei, R., Miro, M., Hansen, E.H. & Shiowatana, J. 2005, "Sequential injection system incorporating a micro-extraction column for automatic fractionation of metal ions in solid samples: Comparison of the extraction profiles when employing uni-, bi-, and multi-bi-directional flow plus stopped-flow sequential extraction modes", *Analytica Chimica Acta,* vol. 536, no. 1-2, pp. 183-190. (impact factor = 2.894)

9. Tongtavee, N., Shiowatana, J., McLaren, R.G. & Gray, C.W. 2005, "Assessment of lead availability in contaminated soil using isotope dilution techniques", *Science of the Total Environment,* vol. 348, pp. 244-256. (impact factor = 2.359)
10. Tongtavee, N., Shiowatana, J. & McLaren, R.G. 2005, "Fractionation of lead in soils affected by smelter activities using a continuous-flow sequential extraction system", *International Journal of Environmental Analytical Chemistry,* vol. 85, no. 8, pp. 567-583. (impact factor = 0.917)
11. Tongtavee, N., Shiowatana, J., McLaren, R.G. & Buanuam, J. 2005, "Evaluation of distribution and chemical associations between cobalt and manganese in soils by continuous-flow sequential extraction", *Communications in Soil Science and Plant Analysis,* vol. 36, no. 19-20, pp. 2839-2855. (impact factor = 0.302)

Continuous-Flow Dialysis

12. Purawatt, S., Siripinyanond, A. & **Shiowatana, J.** 2007, "Flow field-flow fractionation-inductively coupled optical emission spectrometric investigation of the size-based distribution of iron complexed to phytic and tannic acids in a food suspension: Implications for iron availability", *Analytical and Bioanalytical Chemistry,* vol. 389, no. 3, pp. 733-742. (impact factor = 2.591)
13. Judprasong, K., Siripinyanond, A. & **Shiowatana, J.** 2007, "Towards better understanding of in vitro bioavailability of iron through the use of dialysis profiles from a continuous-flow dialysis with inductively coupled plasma spectrometric detection", *Journal of Analytical Atomic Spectrometry,* vol. 22, no. 7, pp. 807-810. (impact factor = 3.630)
14. **Shiowatana, J**., Kitthikhun, W., Sottimai, U., Promchan, J. & Kunajiraporn, K. 2006, "Dynamic continuous-flow dialysis method to simulate intestinal digestion for in vitro estimation of mineral bioavailability of food", *Talanta,* vol. 68, no. 3, pp. 549-557. (impact factor = 2.810)
15. **Shiowatana, J**., Purawatt, S., Sottimai, U., Taebunpakul, S. & Siripinyanond, A. 2006, "Enhancement effect study of some organic acids on the calcium availability of vegetables: Application of the dynamic in vitro simulated gastrointestinal digestion method with continuous-flow dialysis", *Journal of Agricultural and Food Chemistry,* vol. 54, no. 24, pp. 9010-9016. (impact factor = 2.322)
16. Judprasong, K., Ornthai, M., Siripinyanond, A. & **Shiowatana, J.** 2005, "A continuous-flow dialysis system with inductively coupled plasma optical emission spectrometry for in vitro

estimation of bioavailability", *Journal of Analytical Atomic Spectrometry,* vol. 20, no. 11, pp. 1191-1196. (impact factor = 3.630)

17. Promchan, J. & **Shiowatana, J.** 2005, "A dynamic continuous-flow dialysis system with on-line electrothermal atomic-absorption spectrometric and pH measurements for in-vitro determination of iron bioavailability by simulated gastrointestinal digestion", *Analytical and Bioanalytical Chemistry,* vol. 382, no. 6, pp. 1360-1367. (impact factor = 2.591)

Fifteen papers have been presented at the international and national conferences during the past three years as follows:

1. Nattikarn Kaewkhomdee, Chatvalee Kalambaheti, Somruedee Predapitakkun, Atitaya Siripinyanond and Juwadee Shiowatana, Study of iron forms of corrosion products from natural gas pipelines by continuous-flow sequential extraction, **6th International Colloquium on Process Related Analytical Chemistry**, 21-23 March 2007, Dortmund, Germany.
2. Janya Buanuam, Manuel Miró, Ero Harald Hansen, Juwadee Shiowatana, José Manuel Estela and Victor Cerdà, A multisyringe flow injection system for automated fractionation and on-line determination of orthophosphate in solid substrates, **6th International Colloquium on Process Related Analytical Chemistry**, 21-23 March 2007, Dortmund, Germany.
3. Janya Buanuam, Kasipa Tiptanasup and Juwadee Shiowatana**,** Bi-directional continuous-flow sequential extraction system with on-line inductively coupled plasma mass spectrometric detection for study of metal partioning in solid substrates, **2nd Asia-Pacific Winter Conference on Plasma Spectrochemistry,** 27 November – 2 December 2006, Bangkok, Thailand.
4. Kunchit Judprasong, Atitaya Siripinyanond and Juwadee Shiowatana, Use of dialysis profiles from a continuous-flow dialysis system hyphenated with inductively coupled plasma optical emission spectrometry for study of *in vitro* bioavailability of some mineral fortifications, **2nd Asia-Pacific Winter Conference on Plasma Spectrochemistry,** 27 November – 2 December 2006, Bangkok, Thailand.
5. Sopon Purawatt, Atitaya Siripinyanond and Juwadee Shiowatana, Molecular-mass based elemental distribution of food during simulated gastrointestinal digestion, **2nd Asia-Pacific Winter Conference on Plasma Spectrochemistry,** 27 November – 2 December 2006, Bangkok, Thailand.

6. Supharart Sangsawong, Juwadee Shiowatana and Atitaya Siripinyanond, Continuous-flow sequential extraction with on-line field-flow fractionation matrix removal before ICP detections**,** **2nd Asia-Pacific Winter Conference on Plasma Spectrochemistry,** 27 November – 2 December 2006, Bangkok, Thailand.
7. Sopon Purawatt, Atitaya Siripinyanond and Juwadee Shiowatana, Molecular-mass based elemental distribution of food suspension during simulated continuous-flow gastrointestinal digestion, **1st Asia-Pacific Winter Conference on Plasma Spectrochemistry**, 24-30 April 2005, Chiangmai, Thailand.
8. Weerawan Waiyawat, Janya Buanuam and Juwadee Shiowatana, Interference removal in ICPMS measurements of soil extracts, **1st Asia-Pacific Winter Conference on Plasma Spectrochemistry**, 24-30 April 2005, Chiangmai, Thailand.
9. Namfon Tongtavee, Juwadee Shiowatana, Ron McLaren and Colin Gray , Assessment of lead availability in contaminated soils by stable isotope dilution mass spectrometry, **1st Asia-Pacific Winter Conference on Plasma Spectrochemistry,** 24-30 April 2005, Chiangmai, Thailand.
10. Kanokwan Kunajiraporn, Juwadee Shiowatana, Jeerawan Promchan, Continuous-flow dialysis system with online ETAAS/ICPOES and pH measurements for evaluation bioavailability of iron enriched vetgetables, **1st Asia-Pacific Winter Conference on Plasma Spectrochemistry**, 24-30 April 2005, Chiangmai, Thailand.
11. Atitaya Samontha, Nattikarn Kaewkhomdee Ronald McLaren and Juwadee Shiowatana, Elemental fractionation of air particulats using sequential extraction with ICPMS and ICPOES detections, **1st Asia-Pacific Winter Conference on Plasma Spectrochemistry,** 24-30 April 2005, Chiangmai, Thailand.
12. Kanchit Judprasong, Mathuros Ornthai, Atitaya Siripinyanond and Juwadee Shiowatana, A continuous-flow dialysis system with online inductively coupled plasma optical emission spectrometric detections for in vitro estimation of bioavailability, **1st Asia-Pacific Winter Conference on Plasma Spectrochemistry**, 24-30 April 2005, Chiangmai, Thailand.
13. Kanchit Judprasong, Mathuros Ornthai,Sopon Purawatt, Atitaya Siripinyanond and Juwadee Shiowatana, Study of interelemental effects of mineral bioavailability using in vitro continuous-flow dialysis with ICPOES method, **7th International Conference of the Intern.Soc.Trace Element Research in Humans**, 7-12 Nov 2004 Bangkok, Thailand.

14. Sutthinun Taebunpakul, Upsorn Sottimai and Juwadee Shiowatana, Estimation of calcium in vitro bioavailability of vegetables using a novel continuous-flow dialysis system, **7th International Conference of the Intern.Soc.Trace Element Research in Humans**, 7-12 Nov 2004 Bangkok, Thailand.
15. Jeerawan Promchan, Wuttika Kittikhun and Juwadee Shiowatana, A novel continuous-flow dialysis system with online AAS and pH measurements for in vitro iron bioavailability study, **7th International Conference of the Intern.Soc.Trace Element Research in Humans,** 7-12 Nov 2004 Bangkok, Thailand.

Eleven students working on this project have been graduated and three are still working on the project. A 2-day workshop related to this study was organized in May 2007 with 64 participants from 25 organizations at the Faculty of Science, Mahidol University to disseminate the knowledge gained from this study among Thai scientists and researchers.

สารบัญ

		หน้า
กิตติกรรมประกาศ		i
บทคัดย่อ		ii
Abstract		iii
Executive Summary		iv
เนื้อหางานวิจัย		
ตอนที่ 1	การพัฒนาระบบการซึมผ่านเยื่อบางแบบไหลต่อเนื่องเพื่อจำลองระบบการย่อยและดูดซึมสารอาหารสำหรับการประมาณค่าการดูดซึมได้ของแร่ธาตุโดยวิธีในหลอดแก้ว	1
1.1	บทนำ	2
1.2	อุปกรณ์และวิธีการทดลอง	4
1.3	ผลการทดลองและวิจารณ์	8
1.4	บทสรุป	14
1.5	เอกสารอ้างอิง	15
ตอนที่ 2	การพัฒนาระบบไดอะไลซิสแบบไหลต่อเนื่องที่เชื่อมต่อกับ Electrothermal atomic absorption spectrometer (ETAAS) และ pH meter (CFD-ETAAS-pH)	17
2.1	บทนำ	18
2.2	อุปกรณ์และวิธีการทดลอง	18
2.3	ผลการทดลองและวิจารณ์	22
2.4	บทสรุป	25
2.5	เอกสารอ้างอิง	25
ตอนที่ 3	การพัฒนาระบบการซึมผ่านเยื่อบางแบบไหลต่อเนื่องเชื่อมต่อกับหน่วยตรวจวัด ICP-OES เพื่อประมาณค่าการดูดซึมได้ของแร่ธาตุโดยวิธีในหลอดแก้ว	27
3.1	บทนำ	29
3.2	อุปกรณ์และวิธีการทดลอง	29
3.3	ผลการทดลองและวิจารณ์	35
3.4	บทสรุป	59
3.5	เอกสารอ้างอิง	59

ตอนที่ 4 การใช้ระบบเชื่อมต่อระหว่าง Flow field-flow fractionation กับ Inductively coupled plasma optical emission spectrometer ในการศึกษาการกระจายตัวตามขนาดของสารประกอบระหว่างธาตุเหล็กกับ Phytic acid และ Tannic acid ในอาหาร 61
4.1 บทนำ 62
4.2 อุปกรณ์และวิธีการทดลอง 63
4.3 ผลการทดลองและวิจารณ์ 67
4.4 บทสรุป 74
4.5 เอกสารอ้างอิง 74
ตอนที่ 5 บทสรุป 76
Output จากโครงการวิจัย 77
ภาคผนวก ผลงานตีพิมพ์
ผลงานรอการตีพิมพ์

ตอนที่ 1
การพัฒนาระบบการซึมผ่านเยื่อบางแบบไหลต่อเนื่องเพื่อจำลองระบบการย่อยและดูดซึมสารอาหารสำหรับการประมาณค่าการดูดซึมได้ของแร่ธาตุโดยวิธีในหลอดแก้ว

1.1 บทนำ

1.2 อุปกรณ์และวิธีการทดลอง

1.2.1 การออกแบบระบบไดอะไลซิสแบบไหลต่อเนื่อง (Continuous-flow dialysis system)

1.2.2 เครื่องมือ

1.2.3 สารเคมีและตัวอย่าง

1.2.4 วิธีการทดสอบปริมาณแคลเซียมในตัวอย่างหลังการไดอะไลซิส

1.2.5 วิธีการจำลองการย่อยในกระเพาะอาหารและวิธีการหา titratable acidity

1.2.6 วิธีการไดอะไลซิสแบบสมดุล (Equilibrium dialysis system)

1.2.7 วิธีการเลือกอัตราการไหลและความเข้มข้นของสารละลายโซเดียมไบคาร์บอเนตสำหรับระบบไดอะไลซิสแบบไหลต่อเนื่อง

1.2.8 วิธีการไดอะไลซิสแบบไหลต่อเนื่อง (Continuous-flow dialysis system)

1.2.9 วิธีคำนวณค่าความสามารถที่ร่างกายจะนำแร่ธาตุไปใช้ (Dialyzability)

1.3 ผลการทดลองและวิจารณ์

1.3.1 การออกแบบระบบไหลแบบต่อเนื่องเพื่อการประมาณค่าความสามารถที่ร่างกายจะนำแร่ธาตุไปใช้

1.3.2 การเลือกอัตราการไหลที่เหมาะสมของสารละลายโซเดียมไบคาร์บอเนต

1.3.3 การเลือกความเข้มข้นของสารละลายโซเดียมไบคาร์บอเนตที่เหมาะสม

1.3.4 การศึกษาความถูกต้องของระบบที่พัฒนาขึ้น

1.3.5 การศึกษาค่าความสามารถที่ร่างกายจะนำแคลเซียมไปใช้ได้ กรณีตัวอย่าง แคลเซียมคาร์บอเนตแบบเม็ดและเครื่องดื่มนม

1.4 บทสรุป

1.5 เอกสารอ้างอิง

1.1 บทนำ

ปัจจุบันการประเมินค่าปริมาณแร่ธาตุที่ร่างกายจะนำไปใช้ประโยชน์ในกิจกรรมของร่างกายได้มีความจำเป็นที่จะต้องพัฒนาเพื่อให้การประมาณค่าเป็นไปอย่างถูกต้องและง่าย ปริมาณแร่ธาตุทั้งหมดในอาหารไม่ได้บ่งชี้ถึงปริมาณแร่ธาตุที่ร่างกายจะสามารถนำไปใช้ประโยชน์ในกิจกรรมได้ การจำแนกชนิดของสารอาหาร หรือ การศึกษาถึงรูปฟอร์มต่างๆ ในอาหารจึงจำเป็นที่จะทำใช้ทำความเข้าใจและทำนายความสามารถในการดูดซึมของสารอาหาร โดยทั่วไปวิธีการศึกษาค่าปริมาณแร่ธาตุที่ร่างกายจะนำไปใช้ประโยชน์ในกิจกรรมของร่างกายได้ หรือ bioavailability จะทำการศึกษาในมนุษย์ แต่มีข้อจำกัดคือ ใช้เวลานานในการศึกษา ราคาแพง และให้ข้อมูลที่แปรปรวนเนื่องจากปัจจัยของสมรรถภาพและสภาวะของร่างกายที่ไม่สามารถควบคุมให้เหมือนกันได้ ดังนั้นจึงมีการทดลองในสัตว์ทดลองแทนการทดลองในมนุษย์ซึ่งมีราคาถูกกว่า แต่มีข้อจำกัดคือมีความแตกต่างของกระบวนการเมตาบอลิซึมของสัตว์ทดลองกับมนุษย์ อีกทางเลือกหนึ่งคือ การทดลองในหลอดแก้ว ซึ่งวิธีนี้กำลังเป็นที่นิยมเนื่องจากเป็นวิธีที่ง่าย แม่นยำ รวดเร็ว และราคาถูก

การทดลองในหลอดแก้วเริ่มมีการพัฒนาเพื่อใช้ในการประมาณค่าปริมาณแร่ธาตุที่ร่างกายจะดูดซึมได้ตั้งแต่ปี 1930 วิธีการในหลอดแก้วนี้ให้ข้อมูลเกี่ยวกับแร่ธาตุที่ไม่สอดคล้องกับการทดลองในสิ่งมีชีวิต ในปี 1981 Miller และทีมวิจัย ได้พัฒนาวิธีการทดลองในหลอดแก้วเพื่อใช้ในการประมาณค่าปริมาณแร่ธาตุที่ร่างกายมนุษย์จะดูดซึมได้ ซึ่งพบว่าสอดคล้องกับวิธีการทดลองในสิ่งมีชีวิตในกรณีการศึกษาธาตุเหล็ก วิธีการทดลองของ Miller ได้ถูกนำไปพัฒนาต่อเกิดเป็นการทดลองในหลอดแก้วแบบอื่นๆ ซึ่งใช้ประมาณค่าการดูดซึมได้ของธาตุที่หลากหลาย เช่น แคลเซียม และ สังกะสี วิธีการทดลองในหลอดแก้วประกอบด้วยการลอกเลียนแบบกระบวนการย่อยในกระเพาะอาหารและลำไส้เล็กด้วยเอนไซม์ pepsin ที่ pH 2 เป็นเวลา 2 ชั่วโมง ระหว่างขั้นตอนการย่อยในกระเพาะอาหาร และด้วยเอนไซม์ pancreatin และ bile salts ซึ่งมีการเปลี่ยนแปลง pH อย่างต่อเนื่องจาก 2 เป็น 7 ระหว่างขั้นตอนการย่อยในลำไส้เล็ก สัดส่วนของสารที่สามารถแพร่ผ่านรูพรุนของเมมเบรนระหว่างขั้นตอนการย่อยในลำไส้เล็กจะใช้เพื่อทำนายค่า bioavailability ของธาตุต่างๆ

วิธีการของ Miller อาศัยหลักการสมดุลที่ทำให้สารในรูปที่สามารถแพร่ผ่านเมมเบรนได้ระหว่างขั้นตอนการย่อยในลำไส้เล็ก แต่ระบบนี้ยังมีปัญหาเรื่องการพาสารที่แพร่ผ่านออกจากเมมเบรนออกนอกระบบ ซึ่งไม่สามารถทำได้ระหว่างการทำไดอะไลซิสเหมือนกับที่เกิดขึ้นจริงในระบบการย่อยและการดูดซึมของมนุษย์ ทำให้ค่า bioavailability ที่วิเคราะห์ได้จากวิธีนี้มีค่าต่ำ ดังนั้นระบบไดอะไลซิสแบบไหลต่อเนื่องจึงเริ่มพัฒนาอย่างแพร่หลาย โดยทีมวิจัยของ Minihane ได้พัฒนาระบบไดอะไลซิสให้สามารถพาสารที่สามารถแพร่ผ่านเมมเบรนออกมาได้อย่างต่อเนื่อง ระบบดังกล่าวนี้ประกอบด้วย Amicon stirred cell สำหรับการทำไดอะไลซิส pH จะถูกปรับให้เปลี่ยนไปอย่างต่อเนื่องจาก 2 เป็น 7 ภายใน 30 นาที ก่อนเริ่มทำการไดอะไลซิส จากนั้นทีมวิจัยของ Shen ได้พัฒนาให้มีการปรับเปลี่ยน pH ระหว่างทำไดอะไลซิสแทนการปรับ pH ก่อนการไดอะไลซิส Shen ทำไดอะไลซิสโดยการปรับ pH ด้วยการเติมสารละลาย $NaHCO_3$ ใน

ปริมาณที่เท่ากับค่าประมาณของความเป็นกรด (titratable acidity) ของตัวอย่างที่ผ่านการย่อยด้วยเอนไซม์ pepsin แล้ว การไดอะไลซิสจะทำในภาชนะขนาดเล็กภายใต้ความดัน 50 psi

Wolters และทีมวิจัยได้พัฒนาระบบหลอดแก้วสำหรับวิธีไดอะไลซิสแบบไหลต่อเนื่อง โดยใช้ระบบรูพรุนของเมมเบรนแบบท่อกลมกลวง (hollow-fiber) ระบบนี้ประกอบด้วยภาชนะทำปฏิกิริยาที่วางอยู่ใน water bath ที่ปรับอุณหภูมิไว้ 41 องศาเซลเซียส อนุภาคแขวนลอยของอาหารจะถูกปั๊มผ่านท่อดูดไปยังรูพรุนของเมมเบรนแบบท่อกลมกลวงขนาดละเอียดที่ถูกต่อไว้ที่ปลายทางเข้าของ hollow-fiber และมีแท่งแม่เหล็กหมุนเพื่อป้องกันการอุดตันของอนุภาคขนาดใหญ่ อนุภาคที่สามารถแพร่ผ่าน hollow-fiber ได้จะถูกบรรจุลงในขวดพลาสติกเพื่อทำการวิเคราะห์ต่อไป ซึ่งองค์ประกอบต่างๆสามารถถูกย่อยและลำเลียงไปสู่ hollow-fiber จนเสร็จขั้นตอนการไดอะไลซิส

Multicompartmental computer controlled simulated gastrointestinal digestion system ได้ถูกพัฒนาขึ้นและประยุกต์ใช้ในการประเมินค่า bioavailability ระบบนี้ประกอบด้วยส่วนต่างๆ ที่ลอกเลียนแบบระบบการย่อยในกระเพาะอาหารและลำไส้ส่วนต่างๆ (duodenum, jejunum และ ileum) ส่วนต่างๆ นั้นจะถูกต่อเชื่อมกับปั๊มที่ควบคุมการปล่อยเอนไซม์สำหรับการย่อย ระบบนี้จะต่อเข้ากับ rotary pumps และ syringe pumps สำหรับควบคุมความดันน้ำและการหลั่งสาร เนื่องจากงานนี้มีวัตถุประสงค์ในการเลียนแบบระบบการย่อยและการดูดซึมตั้งแต่กระเพาะอาหารจนถึงลำไส้ใหญ่ ileum จึงเป็นระบบที่ค่อนข้างซับซ้อนและไม่ง่ายนักที่จะสร้างขึ้น วิธีการอย่างง่ายที่จะประเมินค่า bioaccessibility ได้ถูกพัฒนาโดยเติมน้ำลายเทียม น้ำย่อยในกระเพาะอาหารและลำไส้เล็ก ซึ่งวิธีการนี้ให้ข้อดีคือ สะดวกและรวดเร็ว แต่อย่างไรก็ตามการดูดซึมใช้เวลาเพียงไม่กี่นาที ตัวอย่างอาหารอาจจะถูกย่อยและดูดซึมเพียงบางส่วนเท่านั้น

ในงานวิจัยนี้ ได้พัฒนาระบบการซึมผ่านเยื่อบางแบบไหลต่อเนื่อง (ระบบไดอะไลซิสแบบไหลต่อเนื่อง)อย่างง่ายโดยวิธีในหลอดแก้วเพื่อจำลองการย่อยในลำไส้เล็ก พิจารณาจากการดูดซึมแร่ธาตุจะเกิดขึ้นที่บริเวณลำไส้เล็ก ระบบที่พัฒนาขึ้นนี้ถูกออกแบบสำหรับการไดอะไลซิสที่ขั้นตอนการย่อยและการดูดซึมที่ลำไส้เล็กโดยการไหลผ่านของสารละลาย (สารละลายเจือจาง $NaHCO_3$) ที่อยู่รอบถุงไดอะไลซิสที่ภายในบรรจุอาหารที่ผ่านการย่อยด้วยเอนไซม์ pepsin ในกระเพาะอาหารแล้ว ขั้นตอนการย่อยในกระเพาะอาหารทำในระบบแบทช์ ทำให้เพิ่ม sample throughput เนื่องจากสามารถทำการย่อยพร้อมๆกันหลายๆตัวอย่างได้ ในขั้นตอนการจำลองการย่อยในลำไส้เล็กนั้นการเปลี่ยนแปลง pH จะเกิดขึ้นใกล้เคียงกับสภาวะที่เกิดขึ้นจริงในลำไส้เล็ก ซึ่งควบคุมได้จากการเลือกใช้อัตราการไหลและความเข้มข้นของสารละลาย $NaHCO_3$ ที่เหมาะสม สารที่สามารถแพร่ผ่านออกมากับสารละลาย $NaHCO_3$ จะเรียกว่า dialysate ซึ่งถูกเก็บในขวดพลาสติกและวิเคราะห์หาปริมาณแร่ธาตุที่สามารถแพร่ผ่านเมมเบรนออกมาได้ กราฟที่พล็อตระหว่างปริมาณแร่ธาตุที่สามารถไดอะไลซ์ได้กับเวลาในการทำไดอะไลซิสยังให้ข้อมูลเชิงจลนศาสตร์ของกระบวนการไดอะไลซิสอีกด้วย และได้ทำการทดสอบประสิทธิภาพของระบบที่พัฒนาขึ้นโดยการประยุกต์ใช้กับตัวอย่าง calcium carbonate tablets และนมผง เพื่อศึกษาค่า dialyzability ของแคลเซียม

1.2 อุปกรณ์และวิธีการทดลอง

1.2.1 การออกแบบระบบไดอะไลซิสแบบไหลต่อเนื่อง

(Continuous-flow dialysis system)

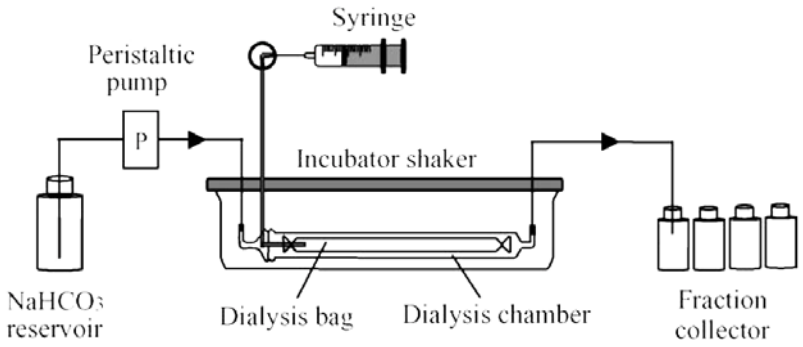

รูปที่ 1.1 ระบบการซึมผ่านเยื่อบางแบบไหลต่อเนื่อง (ระบบไดอะไลซิสแบบไหลต่อเนื่อง) เพื่อใช้เป็นระบบแบบหลอดแก้วในการจำลองการย่อยและดูดซึมอาหารในลำไส้เล็ก

การออกแบบระบบการไดอะไลซิส มีวัตถุประสงค์ 3 ข้อ ดังนี้

- มีการเปลี่ยน pH ในขั้นต้นของการไดอะไลซิส
- มีความสะดวกในการเติมเอนไซม์
- สามารถพา dialysate ออกจากระบบไดอะไลซิสระหว่างการไดอะไลซิสได้

ระบบไดอะไลซิสที่ได้เสนอขึ้นดังแสดงในรูปที่ 1.1 ประกอบด้วยภาชนะมีฝาปิดที่ทำจากแก้ว (dialysis chamber) ความยาว 20 เซนติเมตร และขนาดเส้นผ่านศูนย์กลางภายใน 0.8 เซนติเมตร ภายในภาชนะกับฝาปิดบรรจุด้วยเมมเบรนที่มีรูพรุนขนาด 12,000-4,000 Da ที่มัดเป็นถุงโดยที่ปลายด้านหนึ่งมีท่อซิลิโคน ความยาว 5 เซนติเมตร และขนาดเส้นผ่านศูนย์กลางภายใน 0.2 เซนติเมตร ส่วนปลายอีกด้านของท่อซิลิโคนสอดผ่านฝาปิดของภาชนะเพื่อต่อกับวาล์วสามทาง ซึ่งต่อกับกระบอกฉีดขนาด 3 มิลลิลิตร เพื่อฉีดอาหารที่ผ่านการย่อยด้วยเอนไซม์ pepsinและฉีดเอนไซม์อื่นที่จำเป็นเข้าสู่ถุงไดอะไลซิส ระหว่างภาชนะกับฝาปิดถูกขั้นด้วยแผ่นซิลิโคน โดยทั้งหมดถูกยึดให้ติดเข้าด้วยกัน หลังจากนั้นนำภาชนะแก้วสำหรับไดอะไลซิสวางลงใน water bath ที่ตั้งอุณหภูมิ ณ 37 $\pm$ 1 องศาเซลเซียส และเขย่าขณะไดอะไลซิส สารละลาย $NaHCO_3$ ถูกปั๊มเข้าสู่ระบบไดอะไลซิสด้วยอัตราการไหล 0.5 – 1.0 มิลลิลิตรต่อนาที ซึ่งจากการศึกษาพบว่า อัตราการไหลของสารละลาย $NaHCO_3$ ที่เหมาะสมคือ 1.0 มิลลิลิตรต่อนาที dialysate จะถูกพาออกจากภาชนะแก้วแล้วเก็บในขวดพลาสติกอย่างต่อเนื่อง

ในการไดอะไลซิส ถุงไดอะไลซิสจะต้องสะอาด ก่อนการฉีดตัวอย่างเข้าไป จะต้องไล่อากาศและสารละลายที่อยู่ภายในถุงไดอะไลซิสออกให้หมดโดยใช้กระบอกฉีดที่ต่อเข้ากับท่อซิลิโคนที่สอดอยู่ภายในถุงไดอะไลซิส จากนั้นฉีดตัวอย่างที่ผ่านการย่อยด้วยเอนไซม์ pepsin 2.5 กรัม ผ่านท่อซิลิโคนอันเดิม แล้วพาสารละลาย $NaHCO_3$ เข้าสู่ระบบไดอะไลซิสด้วยอัตราการไหล 1.0 มิลลิลิตรต่อนาที หรือตามที่ต้องการ

1.2.2 เครื่องมือ

Flame atomic absorption spectrometer (FAAS), Perkin-Elmer Model 3100

pH meter, Denver Instrument Model 215 (USA)

Incubater shaker, Grant Instrument Model SS40-D2 (Cambridge, England)

1.2.3 สารเคมีและตัวอย่าง

เอนไซม์ pepsin (P-7000, from porcine stomach mucosa)

เอนไซม์ pancreatin (P-1750, from porcine pancreas)

bile extract (B-6831, porcine) Sigma (St. Louis, MO, USA).

สารละลายแคลเซียมมาตรฐาน (1000 มิลลิกรัมต่อลิตร)

ตัวอย่าง ได้แก่ แคลเซียมคาร์บอเนตแบบเม็ด และ ตัวอย่างนม

การเตรียมสารละลาย pepsin: ละลาย pepsin 0.16 กรัม ในสารละลายกรดไฮโดรคลอริก 0.1 โมลาร์ 1 มิลลิลิตร

การเตรียม pancreatin–bile extract (PBE) mixture: ละลาย pancreatin 0.004 กรัม และ bile extract 0.025 กรัม ในสารละลาย $NaHCO_3$ 0.001 โมลาร์ 5 มิลลิลิตร

1.2.4 วิธีการทดสอบปริมาณแคลเซียมที่มีทั้งหมดในตัวอย่างและปริมาณแคลเซียมที่มีในตัวอย่างหลังการไดอะไลซิส

ในการวิเคราะห์ปริมาณแคลเซียมที่มีทั้งหมดในตัวอย่างทำได้โดยละลายตัวอย่าง (250 มิลลิกรัม สำหรับแคลเซียมแบบเม็ด และ 10.0 กรัม สำหรับเครื่องดื่มนม) แล้วทำการย่อยด้วยสารละลายกรดไนตริกจนกระทั่งได้สารละลายใส จากนั้นเจือจางด้วยน้ำบริสุทธิ์ ปรับปริมาตรเป็น 100.0 มิลลิลิตร สำหรับของผสมที่เหลืออยู่ภายในถุงไดอะไลซิสที่ได้หลังการทำไดอะไลซิส (retentate) นั้น จะถูกถ่ายลงบีกเกอร์ขนาด 100 มิลลิลิตร และล้างถุงไดอะไลซิส 2 ครั้ง ด้วยสารละลาย EDTA 0.01 โมลาร์ และตามด้วยสารละลายกรดไนตริก 2 เปอร์เซนต์ อีก 2 ครั้ง จากนั้นทำการย่อยจนได้สารละลายใส แล้ววิเคราะห์หาปริมาณแคลเซียมด้วยเทคนิค FAAS

1.2.5 วิธีการจำลองการย่อยในกระเพาะอาหารและวิธีการหา Titratable acidity

ขั้นตอนการจำลองการย่อยในกระเพาะอาหารอาศัยหลักการของ Miller สำหรับตัวอย่างแคลเซียมคาร์บอเนตแบบเม็ด ใช้แคลเซียมคาร์บอเนต 1 เม็ด (ตัวอย่างนมผง 10.0 กรัม) ละลายในน้ำ 90 มิลลิลิตร ปรับ pH เป็น 2.0 ด้วยสารละลายกรดไฮโดรคลอริก จากนั้นเติมสารละลาย pepsin 1.5 มิลลิลิตร ปรับ pH เป็น 2.0 อีกครั้งด้วยสารละลายกรดไฮโดรคลอริก แล้วปรับปริมาตรด้วยน้ำเป็น 100 มิลลิลิตร แล้วเขย่าที่อุณหภูมิ 37 องศาเซลเซียส เป็นเวลา 2 ชั่วโมง ปรับ pH เป็น 2.0 ทุกๆ 30 นาที

Titratable acidity ของตัวอย่าง หาได้โดยนำตัวอย่างที่ผ่านการย่อยด้วยเอนไซม์ pepsin 2.5 มิลลิลิตร มาเติม PBE mixture 625 ไมโครลิตร แล้วไทเทรทด้วยสารละลายโซเดียมไฮดรอกไซด์เข้มข้น 0.01 โมลาร์ จนกระทั่งได้ pH 7.5

1.2.6 วิธีการไดอะไลซิสแบบสมดุล (Equilibrium dialysis system)

บรรจุตัวอย่างที่ผ่านการจำลองการย่อยในกระเพาะอาหารด้วยเอนไซม์ pepsin 2.5 กรัมลงในถุงไดอะไลซิสที่บรรจุในภาชนะแก้ว แล้วเติมสารละลาย $NaHCO_3$ 3 มิลลิลิตร ที่มีปริมาณ $NaHCO_3$ สัมพันธ์กับค่า titratable acidity ลงในบริเวณที่ว่างระหว่างถุงไดอะไลซิสกับภาชนะแก้ว จากนั้นเขย่าภาชนะแก้วข้างต้น ณ อุณหภูมิ 37 องศาเซลเซียส เป็นเวลา 30 นาที แล้วเติม PBE mixture 625 ไมโครลิตร ลงในถุงไดอะไลซิส เขย่าภาชนะแก้วข้างต้น ณ อุณหภูมิ 37 องศาเซลเซียส เป็นเวลา 2 ชั่วโมง dialysate จะถูกเก็บในขวดตามลำดับเพื่อวิเคราะห์ปริมาณแคลเซียม

1.2.7 วิธีการเลือกอัตราการไหลและความเข้มข้นของสารละลาย $NaHCO_3$ สำหรับระบบไดอะไลซิสแบบไหลต่อเนื่อง

ขั้นตอนแรก ใช้สารละลายแคลเซียมมาตรฐานที่เตรียมในสารละลายกรดไฮโดรคลอริก 0.01 โมลาร์ เป็นตัวอย่างในการศึกษาถึงอิทธิพลของอัตราการไหลของสารละลาย $NaHCO_3$ ในระบบไดอะไลซิสแบบไหลต่อเนื่อง โดยบรรจุตัวอย่างที่ผ่านการจำลองการย่อยในกระเพาะอาหารด้วยเอนไซม์ pepsin 2.5 กรัม ลงในถุงไดอะไลซิส ทำการไดอะไลซิสด้วยสารละลาย $NaHCO_3$ 0.001 โมลาร์ ที่อัตราการไหลต่างๆ และเก็บสารละลายที่ได้จากการไดอะไลซิส อย่างต่อเนื่อง แล้วนำไปวิเคราะห์ปริมาณแคลเซียม อัตราการไหลที่เหมาะสมคืออัตราการไหลที่การไดอะไลซิสเกิดได้สมบูรณ์โดยใช้เวลาไม่นานและสารละลายที่ได้จากการไดอะไลซิสไม่เกิดการเจือจางมากจนเกินไป

ดังนั้น จะใช้อัตราการไหลของสารละลาย $NaHCO_3$ ที่เหมาะสมในการศึกษาความเข้มข้นของสารละลาย $NaHCO_3$ ต่างๆ ที่มีผลต่อการเปลี่ยนแปลง pH ของตัวอย่างที่ผ่านการจำลองการย่อยในกระเพาะอาหารที่มีค่า titratable acidity ต่างกัน ประกอบด้วย สารละลายกรดไฮโดรคลอริก 0.01 โมลาร์ สารละลายกรดไฮโดรคลอริก 0.01 โมลาร์และสารละลายกรดแอสคอร์บิค 0.04 โมลาร์ สารละลายกรดไฮโดรคลอริก 0.01 โมลาร์และสารละลายกรดแอสคอร์บิค 0.09 โมลาร์ ซึ่งแต่ตัวอย่างนี้มี pH เท่ากับ 2.0

และมีค่า titratable acidity 0.01, 0.05 และ 0.10 โมลาร์ตามลำดับ ตัวอย่างดังกล่าว 2.5 มิลลิลิตร จะถูกฉีดเข้าระบบการจำลองการย่อยในลำไส้ต่อไป

1.2.8 วิธีการไดอะไลซิสในหลอดแก้วแบบไหลต่อเนื่อง

(Continuous-flow dialysis system)

ขั้นแรก เตรียมถุงไดอะไลซิสแล้วบรรจุลงในภาชนะแก้วสำหรับไดอะไลซิสดังที่ได้อธิบายไปแล้ว ใช้แผ่นซิลิโคนคั่นระหว่างฝากับภาชนะแก้วเพื่อให้ปิดสนิท แล้วนำภาชนะแก้วสำหรับไดอะไลซิสนี้ต่อกับท่อที่พาสารละลาย $NaHCO_3$ ทั้งเข้าและออกจากภาชนะแก้ว หลังจากนั้นจุ่มภาชนะแก้วลงใน water bath ที่คุมอุณหภูมิ ณ 37 ± 1 องศาเซลเซียส ฉีดตัวอย่างที่ผ่านการจำลองการย่อยในกระเพาะอาหารเข้าสู่ถุงไดอะไลซิสผ่านท่อซิลิโคนด้วยกระบอกฉีด เริ่มการไดอะไลซิสด้วยการพาสารละลาย $NaHCO_3$ เข้าสู่ระบบด้วยอัตราการไหล 1.0 มิลลิลิตรต่อนาที เก็บ dialysate ลงในขวดพลาสติกทุก 10 นาที หลังจากไดอะไลซิสได้ 30 นาที ฉีด PBE mixture 625 ไมโครลิตร ลงในถุงไดอะไลซิส แล้วทำการไดอะไลซิสต่ออีก 2 ชั่วโมง แล้วนำ dialysate ไปวิเคราะห์ปริมาณธาตุด้วยเทคนิค FAAS ปริมาณธาตุที่ไดอะไลซ์ได้นั้นคำนวณได้จากผลรวมของทุกขวด

1.2.9 วิธีคำนวณค่าความสามารถที่ร่างกายจะนำแร่ธาตุไปใช้ (Dialyzability)

ปริมาณแคลเซียมที่สามารถไดอะไลซ์สามารถ คำนวณเป็นเปอร์เซนต์ Dialyzability ได้ดังสมการ

$$\text{Dialyzability (เปอร์เซนต์)} = \frac{(D - B) \times 100}{W \times A}$$

เมื่อ D คือ ปริมาณของธาตุที่ไดอะไลซ์ได้ในตัวอย่าง

B คือ ปริมาณของธาตุที่ไดอะไลซ์ได้ใน **B**lank

W คือ น้ำหนักตัวอย่าง

A คือ ความเข้มข้นของธาตุในตัวอย่าง

สำหรับวิธีไดอะไลซิสแบบสมดุล แคลเซียมที่ไดอะไลซ์ได้จะคำนวณโดยนำเอาปริมาณที่วิเคราะห์ได้คูณสองในกรณีที่ปริมาตรของตัวอย่างในถุงไดอะไดซิสกับปริมาตรของสารละลาย $NaHCO_3$ ที่ใช้เท่ากัน เนื่องจาก ธาตุที่สามารถไดอะไลซ์ได้เพียงครึ่งเดียวเท่านั้นที่จะแพร่ผ่านเมมเบรนออกมาได้ ถ้าปริมาตรของตัวอย่างในถุงไดอะไลซิสกับปริมาตรของสารละลาย $NaHCO_3$ ที่ใช้ไม่เท่ากัน ต้องคำนวณให้ถูกต้อง

1.3 ผลการทดลองและวิจารณ์

1.3.1 การออกแบบระบบไดอะไลซิสแบบไหลต่อเนื่องเพื่อการประมาณค่าความสามารถที่ร่างกายจะนำแร่ธาตุไปใช้

การดูดซึมแร่ธาตุเกิดขึ้นที่บริเวณลำไส้เล็กส่วนต้น การจำลองสภาวะในลำไส้เล็กจึงเป็นส่วนสำคัญในการพัฒนาระบบเพื่อประมาณค่าการดูดซึมได้ของแร่ธาตุ ถ้าสภาวะกรดด่างในลำไส้ต่างกันจะมีผลต่อการดูดซึมได้ของแร่ธาตุ ดังนั้นการศึกษานี้จึงสนใจกระบวนการเปลี่ยนแปลง pH ซึ่งเป็นตัวแปรที่สำคัญอันหนึ่งในขั้นตอนการทำไดอะไลซิส โดยกราฟการเปลี่ยนแปลง pH ที่ได้จะสอดคล้องกับกราฟไดอะไลซิส วิธีไดอะไลซิสแบบ dynamic ได้ถูกพัฒนาโดยนักวิจัยหลายกลุ่ม เช่น Milller, Minihasnfe, Shen และ Wolters และในงานวิจัยนี้ มีการปรับ pH ที่แตกต่างกัน

การศึกษาอัตราการไหลและความเข้มข้นของสารละลาย $NaHCO_3$ ที่เหมาะสม มีวัตถุประสงค์เพื่อเลียนแบบระบบการย่อยอาหารในลำไส้ของมนุษย์ ดังนี้

1. การเปลี่ยน pH จาก 2.0 เป็น 5.0-6.0 ใน 30 นาที แล้วเปลี่ยน pH เป็น 7.0-7.5 ภายใน 60 นาที และคงที่หลังจากนี้
2. การเติมเอนไซม์สำหรับการย่อย ณ เวลาที่ต้องการผ่านวาล์ว
3. การเก็บ dialysate อย่างต่อเนื่องออกจากระบบไดอะไลซิส

ตามวัตถุประสงค์ข้างต้น จึงศึกษาการอัตราการไหลที่เหมาะสม และ ความเข้มข้นของสารละลาย $NaHCO_3$ ที่เหมาะสม ตามลำดับ

ระบบที่เสนอข้างต้นสามารถนำมาเชื่อมกับเครื่อง FAAS ทำการตรวจวัดแบบ on-line ได้ แต่ในการศึกษานี้จะเก็บสารละลายที่ได้จากการไดอะไลซิสเป็นขวดทุก 5 หรือ 10 นาที แล้ววิเคราะห์ปริมาณแคลเซียมต่อไป ในกรณีนี้ dialysate บางส่วนเท่านั้นที่นำไปวิเคราะห์หาปริมาณธาตุ ซึ่งสามารถเก็บ dialysate นั้นไปวัด pH และสามารถเก็บไว้ตรวจวัดซ้ำได้

1.3.2 การเลือกอัตราการไหลที่เหมาะสมของสารละลายโซเดียมไบคาร์บอเนต

การจำลองการย่อยในกระเพาะอาหารด้วยเอนไซม์ pepsin ที่ pH 2.0 ทำในระบบแบทช์ สำหรับระบบการย่อยในลำไส้เป็นแบบไดอะไลซิสที่สมดุลโดยที่ตัวอย่างจะถูกแช่อยู่ในตัวกลางคือสารละลาย $NaHCO_3$ ที่มีความเข้มข้นเหมาะสม ไหลผ่านถุงไดอะไลซิสที่ภายในบรรจุตัวอย่างที่ผ่านการย่อยด้วยเอนไซม์ pepsin ส่วนของสารละลายที่สามารถแพร่ผ่านเมมเบรนจะถูกเก็บเป็นส่วนๆ ซึ่งได้ทำการศึกษาอัตราการไหลที่เหมาะสมรวมถึงความเข้มข้นของสารละลาย $NaHCO_3$ ที่เหมาะสม ต่อการเปลี่ยนแปลง pH ในการทำไดะไลซิส ในทางทฤษฎี หากใช้อัตราการไหลที่เร็วจะทำให้การเคลื่อนตัวของสารละลายที่ได้จากการไดอะไลซิสออกจากระบบได้เร็ว ดังนั้นสามารถลดเวลาในการทำไดอะไลซิสด้วย

การใช้อัตราการไหลที่เร็วได้ แต่อย่างไรก็ตามจะทำให้เกิดการเจือจางของ dialysate การเลือกอัตราการไหลที่เหมาะสมจึงต้องพิจารณาให้การพาสารละลายที่ได้จากการไดอะไลซิสออกจากระบบได้เร็วและต้องไม่ทำให้เกิดการเจือจางที่มากเกินไป รูปที่ 1.2 แสดงกราฟไดอะไลซิสเมื่อใช้อัตราการไหลต่างๆ ซึ่งแสดงถึงการเปลี่ยนแปลงของแคลเซียมที่สามารถไดอะไลซ์ได้เมื่อใช้อัตราการไหล 0.5, 1.0 และ 2.5 มิลลิลิตรต่อนาที

ในการพา dialysate ออกจากระบบได้อย่างสมบูรณ์นั้น หากใช้อัตราการไหล 2.5 มิลลิลิตรต่อนาที จะใช้เวลาเพียง 50 นาที แต่ถ้าใช้อัตราการไหล 0.5 มิลลิลิตรต่อนาที จะใช้เวลานานประมาณ 100 นาที แต่ความเข้มข้นของแคลเซียมในสารละลายที่ได้จากการไดอะไลซิสจะต่ำกว่าเมื่อใช้อัตราการไหลที่เร็ว ซึ่งเป็นผลจากการเจือจางที่เกิดขึ้น ดังนั้นอัตราการไหลที่เหมาะสมสำหรับการศึกษานี้ ได้แก่ 1.0 มิลลิลิตรต่อนาที เนื่องจากใช้เวลาในการไดอะไลซิสเสร็จสมบูรณ์ภายในเวลา 1 ชั่วโมง และการเจือจางที่เกิดขึ้นอยู่ในเกณฑ์ที่ยอมรับได้

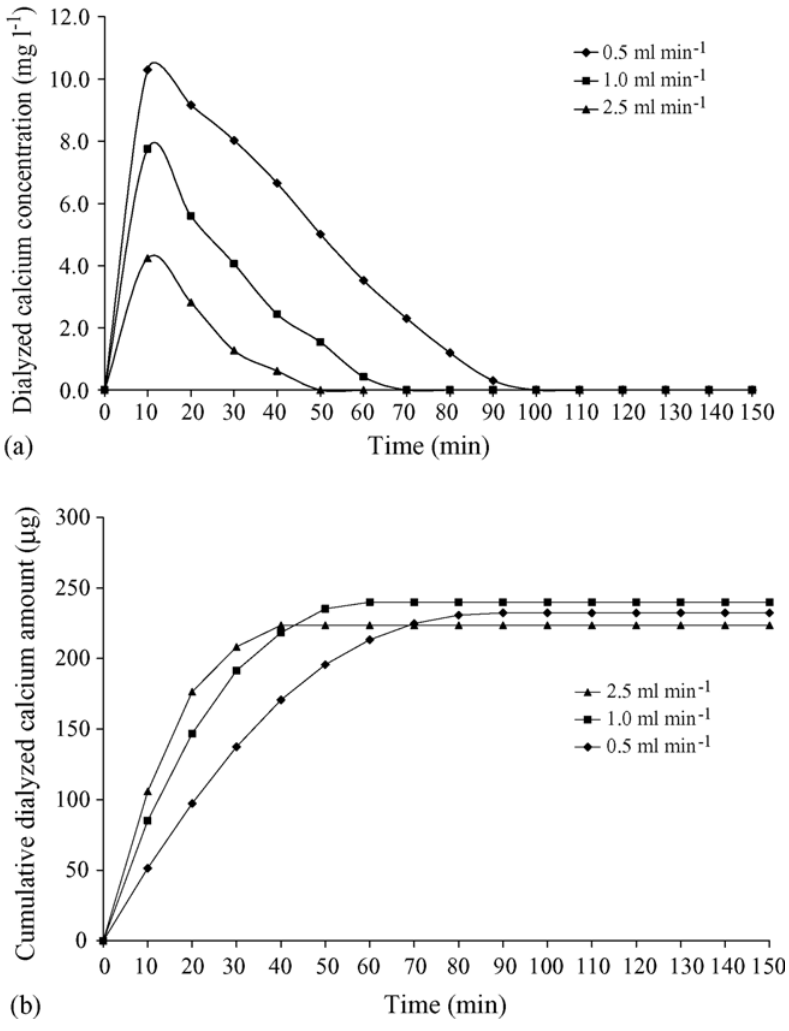

รูปที่ 1.2 กราฟแสดง (a) ปริมาณแคลเซียมที่ถูกไดอะไลซ์ได้ (b) ปริมาณสะสมของแคลเซียมที่ถูกไดอะไลซ์ได้ อัตราการไหลต่างๆ ของ dialyzing solution โดยใช้แคลเซียมเริ่มต้น 100 มิลลิกรัมต่อลิตร ปริมาณ 2.5 มิลลิลิตร

1.3.3 การเลือกความเข้มข้นของสารละลายโซเดียมไบคาร์บอเนตที่เหมาะสม

ทำการศึกษาเพื่อประเมินค่าความเข้มข้นของสารละลายที่ใช้ในการทำไดอะไลซิสเพื่อให้การเปลี่ยนแปลง pH เป็นไปตามสภาวะที่เกิดขึ้นจริง รูปที่ 1.3 แสดงกราฟของการเปลี่ยนแปลง pH เมื่อใช้ความเข้มข้นของสารละลาย $NaHCO_3$ ต่างๆ ไดอะไลซ์ตัวอย่างแคลเซียมแบบเม็ดที่ผ่านการจำลองการย่อยในกระเพาะอาหารซึ่งมีค่า titratable acidity 0.01, 0.05 และ 0.1 โมลาร์ ตามลำดับ ผลการทดลองพบว่า ความเข้มข้นของสารละลาย $NaHCO_3$ ที่เหมาะสมในการไดอะไลซิส กับ ค่า titratable acidity ของตัวอย่าง เป็นดังสมการ

$$\text{ความเข้มข้นของสารละลาย } NaHCO_3 = \frac{\text{Titratable acidity ในหน่วยโมลาร์}}{25}$$

เมื่อทำการไดอะไลซิสตัวอย่างแคลเซียมแบบเม็ดที่มีค่า titratable acidity ต่างๆ โดยใช้ความเข้มข้นของสารละลาย $NaHCO_3$ ที่คำนวนจากสมการข้างต้น พบว่าการเปลี่ยนแปลง pH ขณะไดอะไลซิสใกล้เคียงกับสภาวะจริงเป็นที่น่าพอใจ ดังนั้นสมการข้างต้นจะใช้ในการหาความเข้มข้นของสารละลาย $NaHCO_3$ ที่เหมาะสมในการไดอะไลซิสตัวอย่างแคลเซียมแบบเม็ดต่อไป หากเปลี่ยนชนิดของตัวอย่างจำเป็นจะต้องศึกษาความสัมพันธ์ของความเข้มข้นของสารละลาย $NaHCO_3$ ที่เหมาะสมในการไดอะไลซิส กับ ค่า titratable acidity ในตัวอย่างชนิดนั้นๆ เช่น กรณีตัวอย่างเครื่องดื่มนม พบว่า ความเข้มข้นของสารละลาย $NaHCO_3$ ที่เหมาะสมในการไดอะไลซิส เท่ากับ ค่า titratable acidity ในหน่วยโมลาร์ หารด้วย 50 ความแตกต่างที่เกิดขึ้นน่าจะมีสาเหตุมาจากในตัวอย่างเครื่องดื่มนมที่ผ่านการจำลองการย่อยในกระเพาะอาหารมีปริมาณสารแขวนลอยมากกว่า ซึ่งอาจทำให้อัตราการแพร่ผ่านเมมเบรนช้าลง ดังนั้น สำหรับการศึกษาตัวอย่างต่างชนิดจึงจำเป็นจะต้องศึกษาความสัมพันธ์ของความเข้มข้นของสารละลาย $NaHCO_3$ ที่เหมาะสมในการไดอะไลซิสกับค่า titratable acidity ในตัวอย่างชนิดดังกล่าวด้วย

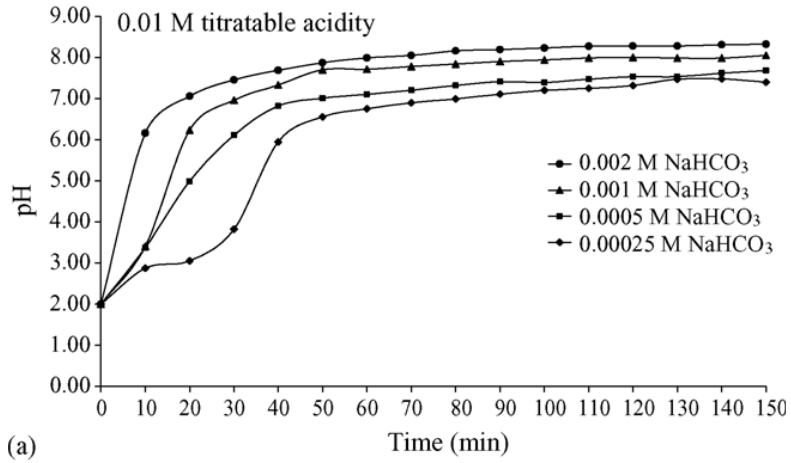

(a)

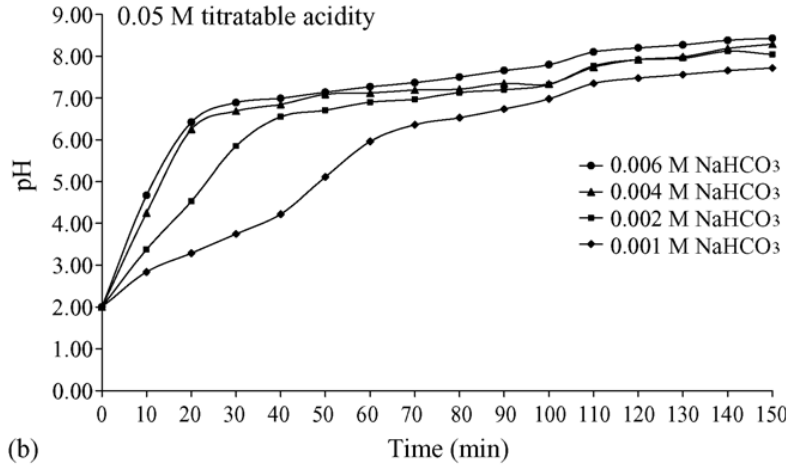

(b)

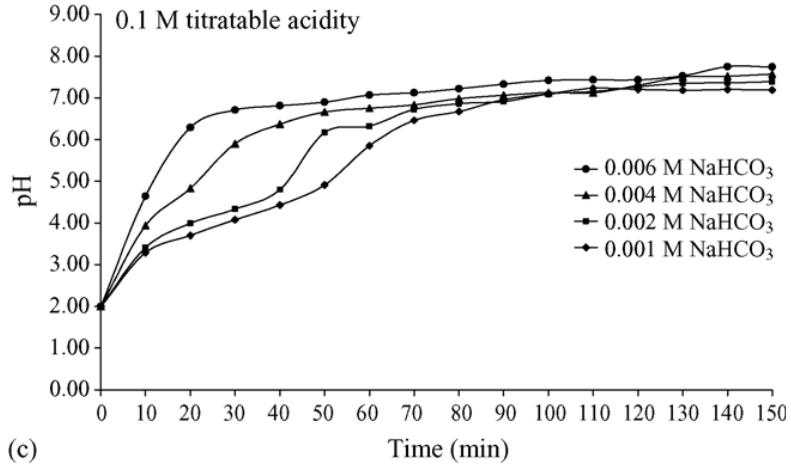

(c)

รูปที่ 1.3 อิทธิพลของความเข้มข้นของ $NaHCO_3$ ต่อการเปลี่ยนแปลงค่า pH ระหว่าง dialysis สำหรับตัวอย่างที่มีค่า titratable acidity ต่างๆ หลังผ่านกระบวนการย่อยด้วย pepsin ที่อัตราการไหล 1.0 มิลลิลิตรต่อนาที

1.3.4 การศึกษาความถูกต้องของระบบที่พัฒนาขึ้น (Method validation)

เนื่องจากไม่มีสารมาตรฐานที่ให้ข้อมูลเกี่ยวกับค่าความสามารถที่ร่างกายจะนำแร่ธาตุไปใช้ได้ จึงมีความจำเป็นในการศึกษาความน่าเชื่อถือของระบบที่พัฒนาขึ้นนี้ โดยทำการศึกษา analytical recoveries ของธาตุที่สนใจ ในการทดลองนี้ใช้ตัวอย่างนมผงเพื่อศึกษาหาค่าความสามารถที่ร่างกายจะนำแร่ธาตุไปใช้และส่วนที่ร่างกายไม่สามารถนำแร่ธาตุไปใช้ได้ ตารางที่ 1.1 แสดงผลการศึกษา พบว่า % dialyzability ใกล้เคียงกัน และพบว่าให้ % recovery ที่ยอมรับได้

ตารางที่ 1.1 ค่า analytical recovery ของธาตุแคลเซียมสำหรับตัวอย่างนมผง (n = 3)

ตัวอย่าง	Dialyzed		Non-dialyzed		%Recovery
	Amount ($mg\ kg^{-1}$)	%Dialyzability	Amount ($mg\ kg^{-1}$)	%Remaining	
นมผง	4680	68.1	1800	26.2	94.3
	4500	65.4	2270	33.1	98.4
	4780	69.5	2080	30.3	99.8
ค่าเฉลี่ย	4650 ± 140	67.6 ± 2.1	2060 ± 240	29.9 ± 3.4	97.5 ± 2.9

Total calcium 6890 ± 120 $mg\ kg^{-1}$

1.3.5 การศึกษาค่าความสามารถที่ร่างกายจะนำแคลเซียมไปใช้ได้ กรณีตัวอย่างแคลเซียมคาร์บอเนตแบบเม็ดและเครื่องดื่มนม

ตัวอย่างการประยุกต์ใช้ระบบที่ได้พัฒนาขึ้นในการประมาณค่าการดูดซึมได้ของแคลเซียมในตัวอย่างเครื่องดื่มนม ได้ผลการทดลองดังแสดงในตารางที่ 1.2 โดยแสดงค่าเปรียบเทียบกับวิธีการไดอะไลซิสของกลุ่มงานวิจัยอื่นๆ ทั้งแบบไดนามิคและแบบสมดุล

เนื่องจากยังไม่มีวิธีไดอะไลซิสใดที่ถูกยอมรับเป็นวิธีมาตรฐานเพื่อใช้ประมาณค่าการดูดซึมได้ของแร่ธาตุในอาหาร ดังนั้นกลุ่มนักวิจัยต่างๆ จึงมีวิธีการและใช้สภาวะต่างกัน นอกจากนั้นแล้วองค์ประกอบต่างๆ ในตัวอย่างก็มีผลต่อการไดอะไลซิส องค์ประกอบบางตัวทำหน้าที่ช่วยให้ไดอะไลซ์ได้มากขึ้น ในขณะที่องค์ประกอบบางตัวจะไปยับยั้งการไดอะไลซิส ซึ่งสาเหตุต่างๆ ดังที่กล่าวมา ทำให้การเปรียบเทียบผลการทดลองจากกลุ่มงานวิจัยต่างๆ เป็นไปได้ยาก

ตารางที่ 1.2 เปรียบเทียบร้อยละของ bioavailability (dialyzability) ของธาตุแคลเซียมในตัวอย่างเครื่องดื่มนมต่างๆ และ calcium carbonate ที่วิเคราะห์ได้จากกลุ่มวิจัยต่างๆ

Sample	In vitro		In vivo	Ref.
	Continuous flow	Equilibrium		
Powder cow milk	42.7 ± 2.5[a]	16.3 ± 1.1[a] (32.6 ±2.2)	-	This work
Powder milk-based formula	67.7 ± 2.1	-	-	This work
Cow milk	-	20.2 ± 1.4	-	[22]
Cow milk	-	17.0 ± 0.8	-	[18]
Milk-based formula	13.9 ± 2.6[b]	10.2 ± 0.7	-	[13]
Milk-based formula	4.3 ± 0.6[c]	-	-	[13]
Cow milk	-	-	46.3 ± 9.5	[23]
Whole milk	-	-	31 ± 3	[24]
Powder cow milk	-	-	37.4 ± 8.7	[25]
Calcium carbonate	72.8 ± 2.2[a]	32.4 ± 1.5[a] (64.8 ± 3.0)	-	This work
Calcium carbonate	-	-	43.0 ± 5.9	[25]
Calcium carbonate	-	-	39 ± 3	[24]

[a] $n = 3$, in brackets are corrected values (ดูตอนที่ 1.2.9)

[b] By Shen's method

[c] By Minihane's method

ผลการทดลองพบว่า ในงานวิจัยนี้ กรณีตัวอย่างเครื่องดื่มนมวัว พบแคลเซียมที่ไดอะไลซ์ได้ 32.6 และ 42.7 เปอร์เซนต์ เมื่อใช้วิธีไดอะไลซิสแบบสมดุลและแบบไดนามิคตามลำดับ มีการศึกษาในตัวอย่างเครื่องดื่มนม ซึ่งพบแคลเซียมที่ไดอะไลซ์ได้มากถึง 67.7 เปอร์เซนต์ โดยค่าประมาณการดูดซึมได้ของแคลเซียมในตัวอย่างเครื่องดื่มนมจากกลุ่มวิจัยต่างๆ พบในช่วง 4.3 ถึง 46.5 เปอร์เซนต์ ซึ่งค่าที่แตกต่างกันนี้ น่าจะมีสาเหตุมาจากความแตกต่างขององค์ประกอบในตัวอย่างเครื่องดื่มนมที่ศึกษา วิธีการทดลอง และ สภาวะที่ใช้

กรณีตัวอย่างแคลเซียมคาร์บอเนตแบบเม็ด งานวิจัยนี้ พบแคลเซียมที่ไดอะไลซ์ได้ 64.8 และ 72.8 เปอร์เซนต์ เมื่อใช้วิธีไดอะไลซิสแบบสมดุลและแบบไดนามิคตามลำดับ นักวิจัยบางกลุ่มรายงานว่า การละลายที่ไม่สมบูรณ์และขีดจำกัดของการละลายแคลเซียมคาร์บอเนตจะส่งผลต่อความสามารถในการไดอะไลซ์ของแคลเซียม ในงานวิจัยนี้ พบว่า หลังการจำลองการย่อยตัวอย่างในกระเพาะอาหารที่ pH 2.0 เป็นเวลา 2 ชั่วโมงนั้น สารละลายที่ได้ค่อนข้างใส แสดงว่าตัวอย่างแคลเซียมคาร์บอเนตละลายได้เกือบหมด ซึ่งอาจจะเป็นสาเหตุที่ได้ค่า dialyzability ที่สูงกว่างานวิจัยอื่น ส่วนค่าที่ได้จากวิธีไดอะไลซิสแบบสมดุลพบว่าต่ำกว่า อาจเนื่องมาจากสารที่ได้จากการไดอะไลซิสบางส่วนหายไปขณะเปลี่ยนภาชนะหลังไดอะไลซิสแล้วนำไปวิเคราะห์ปริมาณ ซึ่งอาจจะติดอยู่ที่ภาชนะซึ่งขั้นตอนนี้ ไม่พบในวิธีไดอะไลซิสแบบไดนามิค

ส่วนผลการทดลองจากวิธีวิเคราะห์ในสิ่งมีชีวิตแบบสมดุล พบว่า ได้ค่า bioavailability ต่ำ (43.0 และ 39 เปอร์เซนต์)

เนื่องด้วยวิธีการไดอะไลซิสแบบในหลอดแก้วสอดคล้องกับการประมาณค่าที่แท้จริง การใช้วิธีการต่างๆ เพื่อศึกษา bioavailability จำเป็นต้องพิจารณาสภาวะที่ใช้อย่างระมัดระวังและการรายงานค่าต่างๆ ควรมาจากการใช้วิธีการเดียวกันภายใต้สภาวะเดียวกัน เพื่อให้มั่นใจว่าในการไดอะไลซิสแต่ละครั้งทำภายใต้สภาวะเดียวกัน งานวิจัยนี้จึงได้เสนอการตรวจวัดค่า pH ที่เปลี่ยนแปลงขณะทำไดอะไลซิส กราฟไดอะไลซิสและกราฟการเปลี่ยนแปลง pH ขณะทำการไดอะไลซิสตัวอย่างแคลเซียมคาร์บอเนตแบบเม็ดหลังจากผ่านการจำลองการย่อยในกระเพาะอาหาร แสดงดังรูปที่ 1.4 กราฟ pH ดังกล่าว ชี้ให้เห็นถึงการเปลี่ยนแปลง pH ที่เป็นไปตามสภาวะจริงที่เกิดขึ้นในมนุษย์ กราฟไดอะไลซิสของแคลเซียมจะมีค่าสูงในส่วนต้น แล้วลดลงอย่างต่อเนื่องเหมือนกับกราฟรูปที่ 1.2 การไดอะไลซิสอย่างสมบูรณ์ใช้เวลาเพียง 60 นาที เหมือนกันกับกรณีตัวอย่างเครื่องดื่มนม

กราฟไดอะไลซิสและการเปลี่ยนแปลง pH น่าจะเป็นประโยชน์ในการศึกษาเปรียบเทียบ dialyzability ของตัวอย่างต่างชนิดและการศึกษาอิทธิพลขององค์ประกอบในตัวอย่างที่มีผลต่อ dialyzability ซึ่งข้อมูลดังกล่าวไม่สามารถวิเคราะห์ด้วยระบบไดอะไลซิสแบบสมดุลได้

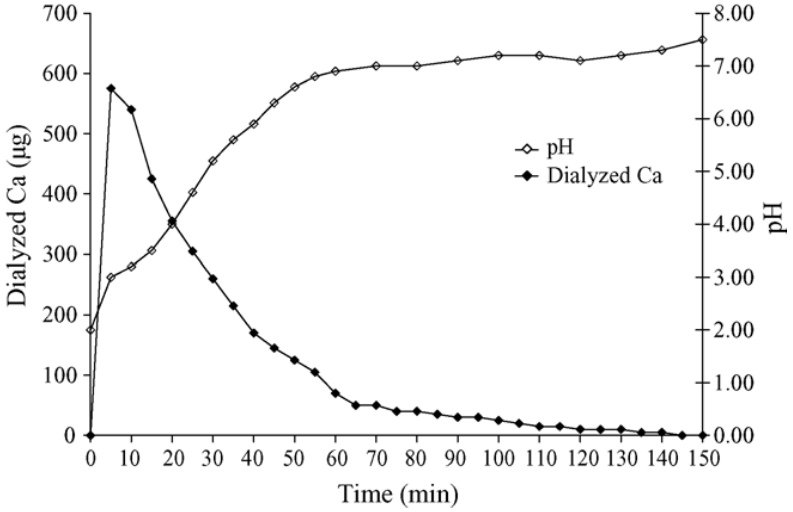

รูปที่ 1.4กราฟแสดงปริมาณธาตุแคลเซียมที่ไดอะไลซ์ได้และการเปลี่ยนแปลง pH ของเม็ด calcium carbonate โดยวิธีการไดอะไลซิสในหลอดแก้วแบบไหลต่อเนื่อง

1.4 บทสรุป

การจำลองระบบการย่อยในลำไส้ได้ถูกพัฒนาขึ้นเพื่อประมาณค่าการดูดซึมได้ของแร่ธาตุ วิธีไดอะไลซิสในหลอดแก้วแบบไหลต่อเนื่องน่าจะเป็นวิธีที่ใกล้เคียงกับระบบจริงที่เกิดขึ้นมากกว่าวิธีไดอะไลซิสในหลอดแก้วแบบสมดุลเนื่องจากสารที่แพร่ผ่านเมมเบรนได้จะถูกพาออกจากระบบขณะทำไดอะไลซิส

ในงานวิจัยนี้ระบบไดอะไลซิส อย่างง่ายแบบไหลต่อเนื่องได้ถูกพัฒนาและใช้ในการประมาณค่าแคลเซียมที่ร่างกายจะสามารถดูดซึมได้ แล้วนำมาเปรียบเทียบกับวิธีไดอะไลซิสแบบสมดุล ส่วนที่สำคัญในการจำลองระบบการดูดซึมให้เหมือนในลำไส้ก็คือ การปรับ pH ขณะเกิดการย่อยในลำไส้ ซึ่งทำได้โดยการใช้อัตราการไหลและความเข้มข้นของสารละลาย $NaHCO_3$ ในการทำไดอะไลซิสให้เหมาะสม เงื่อนไขที่เหมาะสมสำหรับวิธีไดอะไลซิสแบบไหลต่อเนื่อง คือ ใช้อัตราการไหลของสารละลาย $NaHCO_3$ เท่ากับ 1.0 มิลลิลิตรต่อนาที และความเข้มข้นของสารละลาย $NaHCO_3$ ขึ้นกับค่า titratable acidity ของตัวอย่าง นอกจากนั้นแล้วการเตรียม PBE mixture ควรเตรียมในสารละลาย $NaHCO_3$ เข้มข้น 0.001 โมลาร์ เพื่อให้มีผลต่อการเปลี่ยนแปลง pH น้อยที่สุด แทนการเตรียมในสารละลาย $NaHCO_3$ เข้มข้น 0.1 โมลาร์ซึ่งใช้ในระบบไดอะไลซิสแบบสมดุล จากผลการทดลองพบว่าระบบที่ได้เสนอนั้น ให้การเปลี่ยนแปลง pH อย่างต่อเนื่อง วิธีไดอะไลซิสแบบไหลต่อเนื่องไม่ได้ให้ข้อมูลเฉพาะค่า dialyzability ของธาตุต่างๆ เพียงเท่านั้น แต่ยังสามารถให้กราฟไดอะไลซิสเพื่อการศึกษารายละเอียดอื่นๆได้ การเปลี่ยนแปลง pH ขณะไดอะไลซิสจะมีผลต่อค่า dialyzability เนื่องจากบางธาตุเกิดการตกตะกอน จึงได้มีการพัฒนาการตรวจวัดค่า pH อย่างต่อเนื่องไปพร้อมๆ กับการไดอะไลซิส กราฟไดอะไลซิสที่สอดคล้องกับ pH ที่เปลี่ยนแปลงจะช่วยให้เข้าใจถึงการไดอะไลซิส ณ เวลาต่างๆ และอิทธิพลขององค์ประกอบในตัวอย่างที่มีผลต่อค่า dialyzability ของธาตุนั้น

ระบบที่ถูกพัฒนาขึ้นนี้สามารถนำไปเชื่อมต่อกับระบบตรวจวัดธาตุแบบอื่นได้ รวมถึงสามารถตรวจวัดแบบ on-lineได้ ในตอนที่ 1 นี้เสนอการวิเคราะห์เพียงธาตุเดียว คือ แคลเซียม ด้วยเทคนิค FAAS แบบ off-line ในการศึกษาในตอนต่อไป ระบบไดอะไลซิสแบบไหลต่อเนื่องจะถูกเชื่อมต่อกับหน่วยตรวจวัด เช่น ETAAS (ตอนที่ 2), ICP-MS, ICP-OES (ตอนที่ 3)และตรวจวัดแบบ on-line เพื่อให้สามารถตรวจวัดธาตุได้หลายๆ ธาตุไปพร้อมๆ กันและเพื่อแสดงให้เห็นถึงการใช้ประโยชน์ของกราฟไดอะไลซิส

1.5 เอกสารอ้างอิง

1. L.H. Allen, *Am. J. Clin. Nutr.* 1982, **35**, 783.
2. L. Shackleton and R.A. McCance, *Biochem. J.* 1936, **30**, 583.
3. B.S. Narasinga Rao and T. Prabhavathi, *Am. J. Clin. Nutr.* 1978, **31**, 169.
4. S. Lock and A.E. Bender, B*r. J. Nutr.* 1980, **43**, 413.
5. D.D. Miller, B.R. Schricker, R.R. Rasmussen and D. Van Campen, *Am. J. Clin. Nutr.* 1981, **34**, 2248.
6. B.R. Schricker, D.D. Miller, R.R. Rasmussen, D. Van Campen, *Am. J. Clin. Nutr.* 1981, **34**, 2257.
7. T. Hazell and I.T. Johnson, *Br. J. Nutr.* 1987, **57**, 223.
8. R.F. Hurrell, S.R. Lynch, T.P. Trinidad, S.A. Dassenko and J.D. Cook, *Am. J. Clin. Nutr.* 1988, **47**, 102.

9. M.G.E. Wolters, H.A.W. Schreuder, G. Van Den Heuvel, H.J. Van Lonkhuijsen, R.J.J. Hermus and A.G.J. Voragen, *Br. J. Nutr.* 1993, **69**, 849.

10. P. Hocquellet and M.D. L'Hotellier, *J. AOAC Int.* 1997, **80**, 920.

11. J. Veenstra, M. Minekus, P. Marteau and R. Havenaar, *Int. Food Ingredients,* 1993, **3**, 1.

12. A.M. Minihane, T.E. Fox and S.J. Fairweather-Tait, *Proceedings of Bioavailability'93 Nutritional, Chemical and Food Processing Implications of Nutrient Availability, Part II, FRG*, 1993, p. 175.

13. L.H. Shen, I. Luten, H. Robberecht, J. Bindels and H. Deelstra, *Lebensm Unters Forsch,* 1994, **199**, 442.

14. M. Minekus, P. Marteau, R. Havenaar and J.H.J. Huis in't Veld, *Altern. Lab. Anim. (ATLA,)* 1995, **23**, 197.

15. M. Larsson, M. Minekus and R. Havenaar, *J. Sci. Food Agric.* 1997, **74**, 99.

16. C. Krul, A. Luiten-Schuite, R. Baan, H. Verhagan, G. Hohn, V. Feron and R. Havenaar, *Food Chem. Toxicol.* 2000, **38**, 783.

17. M. Chu and D. Beauchemin, *J. Anal. At. Spectrom.* 2004, **19**, 1213.

18. P. Chaiwanon, P. Puwastien, A. Nitithamyong and P.P. Sirichakwal, *J. Food Comp. Anal.* 2000, **13**, 319.

19. D.R. Van Campen and R.P. Glahn, *Field Crop. Res.* 1999, **60**, 93.

20. C. Ekmekcioglu, *Food Chem.* 2002, **76**, 225.

21. D. Bosscher, Z.L. Lu, R. Van Cauwenbergh, M. Van Callie-Bertrand, H. Robberecht and H. Deelstra, *Int. J. Food Sci. Nutr.* 2001, **52**, 173.

22. M.J. Roig, A. Alegria, R. Barbera, R. Farre and M.J. Lagarda, *Food Chem.* 1999, **65**, 353.

23. R.P. Heaney, C.M. Weaver, S.M. Hinders, B. Martin and P.T. Packard, *J. Food Sci.* 1993, **58**, 1378.

24. M.S. Sheikh, C.A. Santa Ana, M.J. Niocar, L.R. Schiller and J.S. Fordtran, *N. Engl. J. Med.* 1987, **317**, 532.

25. M.C. Kruger, B.W. Gallaher and L.M. Schollum, *Nutr. Res.* 2003, **23**, 1229.

26. M.J. Brennan, W.E. Duncan, L. Wartofsky, V.M. Butler and H.L. Wray, *Calcif. Tissue Int.* 1991, **49**, 308.

ตอนที่ 2
การพัฒนาระบบไดอะไลซิสแบบไหลต่อเนื่องที่เชื่อมต่อกับ Electrothermal atomic absorption spectrometer (ETAAS) และ pH meter (CFD-ETAAS-pH)

2.1 บทนำ

2.2 อุปกรณ์และวิธีการทดลอง

2.2.1 สารเคมี

2.2.2 เครื่องมือและอุปกรณ์

2.2.3 อุปกรณ์สำหรับเก็บตัวอย่างเพื่อวิเคราะห์ด้วยเทคนิค ETAAS และอุปกรณ์เพื่อตรวจวัด pH

2.2.4 วิธีการจำลองการย่อยในกระเพาะอาหารและการย่อยในลำไส้

2.2.4.1 วิธีไดอะไลซิสแบบสมดุล

2.2.4.2 วิธีไดอะไลซิสแบบไหลต่อเนื่อง

2.2.4.3 การวิเคราะห์ปริมาณธาตุเหล็กทั้งหมดที่มีในตัวอย่างเครื่องดื่มนมและธาตุเหล็กที่เหลือจากการไดอะไลซิส

2.2.4.4 การคำนวณค่า Dialyzability

2.3 ผลการทดลองและวิจารณ์

2.3.1 กราฟไดอะไลซิส

2.3.2 ค่า Dialyzability ของธาตุเหล็กในตัวอย่างนม

2.3.3 การศึกษาความถูกต้องของระบบที่พัฒนาขึ้น (Method validation)

2.4 บทสรุป

2.5 เอกสารอ้างอิง

2.1 บทนำ

ระบบหลอดแก้วที่จำลองการย่อยอาหารและดูดซึมสารอาหารอย่างง่ายได้ถูกพัฒนาขึ้นดังที่ได้กล่าวไปแล้วในตอนที่ 1 ในการประมาณค่าการดูดซึมได้ของแร่ธาตุที่ร่างกายจะนำไปใช้ประโยชน์ได้ ประกอบด้วยระบบการจำลองการย่อยในกระเพาะแบบแบทช์ จากนั้นเข้าสู่ระบบการจำลองการย่อยในลำไส้ คือระบบไดอะไลซิสแบบไหลต่อเนื่อง ในงานวิจัยนี้ระบบไดอะไลซิสแบบไหลต่อเนื่องจะถูกเชื่อมกับหน่วยตรวจวัดโดยตรงและวิเคราะห์แบบออนไลน์ เพื่อวิเคราะห์ปริมาณธาตุและติดตามการเปลี่ยนแปลง pH ตามลำดับ ขณะทำไดอะไลซิส

งานวิจัยนี้ มีวัตถุประสงค์ในการวิเคราะห์ธาตุที่มีปริมาณต่ำได้ ดังนั้นเทคนิควิเคราะห์ปริมาณธาตุที่เลือกใช้คือ ETAAS นอกจากนั้นแล้วการติดตามการเปลี่ยนแปลง pH ขณะทำไดอะไลซิส ยังมีความจำเป็นเพื่อให้มั่นใจได้ว่า การเปลี่ยนแปลง pH ที่เกิดขึ้นในระบบที่จำลองขึ้นนั้นใกล้เคียงกับสภาวะจริงที่เกิดขึ้นในร่างกายมนุษย์ ในงานวิจัยนี้ได้ประยุกต์วิธีที่พัฒนาขึ้นเพื่อวิเคราะห์ dialyzability ของธาตุเหล็กในตัวอย่างเครื่องดื่มนมชนิดต่างๆ ผลที่ได้จะถูกเปรียบเทียบกับวิธีไดอะไลซิสแบบสมดุล

2.2 อุปกรณ์และวิธีการทดลอง

2.2.1 สารเคมี

สารละลายบัฟเฟอร์ pH 4.00 $\pm$ 0.01, 7.00 $\pm$ 0.01, และ 10.00 $\pm$ 0.01 (Merck, Germany)

สารละลายเหล็กมาตรฐาน (1010 มิลลิกรัมต่อลิตร)

เอนไซม์ pepsin (P-7000, from porcine stomach mucosa)

เอนไซม์ pancreatin (P-1750, from porcine pancreas)

bile extract (B-6831, porcine) Sigma (St. Louis, MO, USA).

ตัวอย่างเครื่องดื่มนม

การเตรียมสารละลาย pepsin: ละลาย pepsin 0.16 กรัม ในสารละลายกรดไฮโดรคลอริก 0.1 โมลาร์ 1 มิลลิลิตร

การเตรียม pancreatin–bile extract (PBE) mixture: ละลาย pancreatin 0.02 กรัม และ bile extract 0.125 กรัม ในสารละลาย $NaHCO_3$ 0.1 โมลาร์ 5 มิลลิลิตร

2.2.2 เครื่องมือและอุปกรณ์

ETAAS (Perkin–Elmer Analyst 100 atomic absorption spectrometer ต่อกับ deuterium arc background corrector และ Perkin–Elmer HGA-800 heated-graphite atomizer)

เครื่องวัด pH (Orion Model PCM500 SensorLink)

Incubator shaker, Grant Instrument Model SS40-D2 (Cambridge, England)

อิเล็กโทรด (Orion, เส้นผ่านศูนย์กลาง 6 มิลลิเมตร)

2.2.3 อุปกรณ์สำหรับเก็บตัวอย่างเพื่อวิเคราะห์ด้วยเทคนิค ETAAS และเพื่อตรวจวัด pH

อุปกรณ์สำหรับเก็บสารละลายตัวอย่างเพื่อวิเคราะห์ด้วยเทคนิค ETAAS ทำจากแก้วซึ่งออกแบบให้กรวยด้านในมีขนาดเล็กและมีปริมาตรน้อยเพื่อให้สามารถตรวจวัด ณ เวลานั้นๆได้ แสดงดังรูปที่ 2.1 โดยที่กรวยด้านในและกรวยด้านนอกมีเส้นผ่านศูนย์กลางภายในขนาด 3 และ 8 มิลลิเมตร ตามลำดับ และกรวยด้านในมีปริมาตรเพียง 60 ไมโครลิตร สารละลายที่ไดอะไลซ์ได้จะถูกปั๊มเข้าสู่กรวยด้านในจากด้านล่างแล้วไหลออกสู่กรวยด้านนอกและไหลออกทางด้านล่างของอุปกรณ์นี้ autosampler ของเครื่อง ETAAS จะเก็บตัวอย่างไปครั้งละ 20 ไมโครลิตร เพื่อวิเคราะห์ปริมาณธาตุเหล็กใน dialysate ทุก 2 นาที (หรือเป็นช่วงเวลาที่ห่างกว่านี้ในกรณีที่ความเข้มข้นของเหล็กที่ไดอะไลซ์มีค่าคงที่) สำหรับการตรวจวัด pH อุปกรณ์สำหรับเก็บสารละลายตัวอย่างถูกออกแบบให้มีขนาดใหญ่กว่าอิเล็กโทรดเพียงเล็กน้อย โดยเชื่อมอิเล็กโทรดกับอุปกรณ์สำหรับเก็บสารละลายตัวอย่างนี้ด้วย o-ring ซึ่ง dialysate ที่ไหลมาอย่างต่อเนื่องจะถูกตรวจวัด pH ในอุปกรณ์สำหรับเก็บสารละลายตัวอย่าง

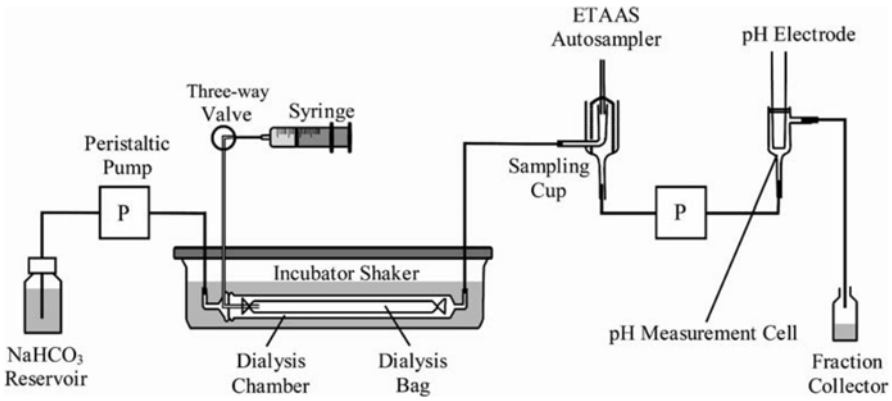

รูปที่ 2.1ระบบไดอะไลซิสแบบไหลต่อเนื่องเชื่อมต่อกับหน่วยตรวจวัดประเภท ETAAS และ pH

2.2.4 วิธีการจำลองการย่อยในกระเพาะอาหารและการย่อยในลำไส้

2.2.4.1 วิธีไดอะไลซิสแบบสมดุล

การจำลองการย่อยในกระเพาะอาหาร (Gastric digestion): เติมตัวอย่าง 5 มิลลิลิตร และน้ำ 5 มิลลิลิตร ลงในภาชนะแก้วขนาด 125 มิลลิลิตร ปรับ pH เป็น 2.0 ด้วยสารละลายกรดไฮโดรคลอ

ริกเข้มข้น 6 โมลาร์ แล้วปรับปริมาตรเป็น 12.5 มิลลิลิตรด้วยน้ำ จากนั้นเติมสารละลาย pepsin 325 ไมโครลิตร นำภาชนะดังกล่าวไปเขย่าที่อุณหภูมิ 37 $\pm$ 1 องศาเซลเซียส เป็นเวลา 2 ชั่วโมง

การจำลองการย่อยในลำไส้ (Intestinal digestion): หลังจากจำลองการย่อยในกระเพาะอาหาร นำสารที่ได้มา 2.5 กรัม (ทำการทดลอง 3 ซ้ำ) ฉีดเข้าถุงไดอะไลซิสซึ่งบรรจุอยู่ในภาชนะแก้วสำหรับไดอะไลซิส จากนั้นเติมสารละลาย $NaHCO_3$ 3.0 มิลลิลิตร ลงในภาชนะไดอะไลซิส นำไปเขย่าที่อุณหภูมิ 37 $\pm$ 1 องศาเซลเซียส เป็นเวลา 30 นาที เติม PBE mixture 625 ไมโครลิตรลงในถุงไดอะไลซิส แล้วทำไดอะไลซิสต่อเป็นเวลา 2 ชั่วโมง dialysate จะถูกเก็บไปวิเคราะห์ปริมาณธาตุเหล็กต่อไป

การศึกษาหาความเข้มข้นของสารละลาย $NaHCO_3$ ที่เหมาะสม: คำนวณจากค่า titratable acidity ซึ่ง titratable acidity คือ ปริมาณที่เท่ากับปริมาณของโซเดียมไฮดรอกไซด์ที่ใช้ในการไทเทรทตัวอย่างที่ผ่านการจำลองการย่อยในกระเพาะอาหาร ให้ได้ pH 7.5 ทำการศึกษาโดยนำตัวอย่างที่ผ่านการย่อยด้วยกระเพาะอาหาร 2.5 กรัมมาเติม PBE mixture 625 ไมโครลิตร แล้วไทเทรทกับสารละลายโซเดียมไฮดรอกไซด์เข้มข้น 0.01 โมลาร์

2.2.4.2 วิธีไดอะไลซิสแบบไหลต่อเนื่อง

การจำลองการย่อยในกระเพาะอาหาร (Gastric digestion): เหมือนวิธีไดอะไลซิสแบบสมดุล

การจำลองการย่อยในลำไส้ (Intestinal digestion): รูปที่ 2.1 แสดงภาพระบบไดอะไลซิสแบบไหลต่อเนื่องเพื่อจำลองการย่อยและดูดซึมสารอาหารในลำไส้เล็กหลังจากจำลองการย่อยในกระเพาะอาหารแล้ว ทำการศึกษาโดยนำสารที่ได้มา 2.5 กรัม ฉีดเข้าถุงไดอะไลซิสซึ่งบรรจุอยู่ในภาชนะแก้วสำหรับไดอะไลซิส ซึ่งปลายทั้งสองข้างของภาชนะไดอะไลซิสต่อกับท่อพาสารละลาย $NaHCO_3$ เพื่อพาสารละลายเข้าและออกจากภาชนะไดอะไลซิส แล้วนำไปเขย่าที่อุณหภูมิ 37 $\pm$ 1 องศาเซลเซียส ปลายด้านที่พาสารละลายออกจากภาชนะไดอะไลซิสจะเชื่อมต่อกับหน่วยตรวจวัด ETAAS และเครื่องวัด pH โดยตรงตามลำดับ เริ่มการไดอะไลซิสด้วยการพาสารละลาย $NaHCO_3$ เข้าสู่ระบบด้วยอัตราการไหล 1.0 มิลลิลิตรต่อนาที หลังจากไดอะไลซิส 30 นาที จึงเติม PBE mixture 625 ไมโครลิตรผ่านวาล์วสามทาง สารละลายที่ไดอะไลซ์ได้จะถูกวิเคราะห์หาปริมาณธาตุเหล็กและวัด pH อย่างต่อเนื่อง อีก 2 ชั่วโมง

การศึกษาหาความเข้มข้นของสารละลาย $NaHCO_3$ ที่เหมาะสม: ความเข้มข้นของสารละลาย $NaHCO_3$ ที่เหมาะสมจะขึ้นกับค่า titratable acidity ของตัวอย่างและอัตราการไหลที่ใช้ หากใช้อัตราการไหลที่ 1.0 มิลลิลิตรต่อนาที ความเข้มข้นของสารละลาย $NaHCO_3$ ที่เหมาะสมจะคำนวณได้โดยนำค่า titratable acidity หารด้วย 50 ซึ่งความเข้มข้นของสารละลาย $NaHCO_3$ ที่คำนวณได้นี้จะเปลี่ยนค่า pH เป็น 5.0 หลังการไดอะไลซิส 30 นาที และเปลี่ยนเป็น 7.0 - 7.5 หลังการเติม PBE mixture

การทำ reagent blank จำเป็นที่จะต้องศึกษาเพื่อหักลบเอาปริมาณธาตุเหล็กที่ปนเปื้อนในสารเคมีต่างๆ รวมถึงเอนไซม์ต่างๆ ที่ใช้ด้วย

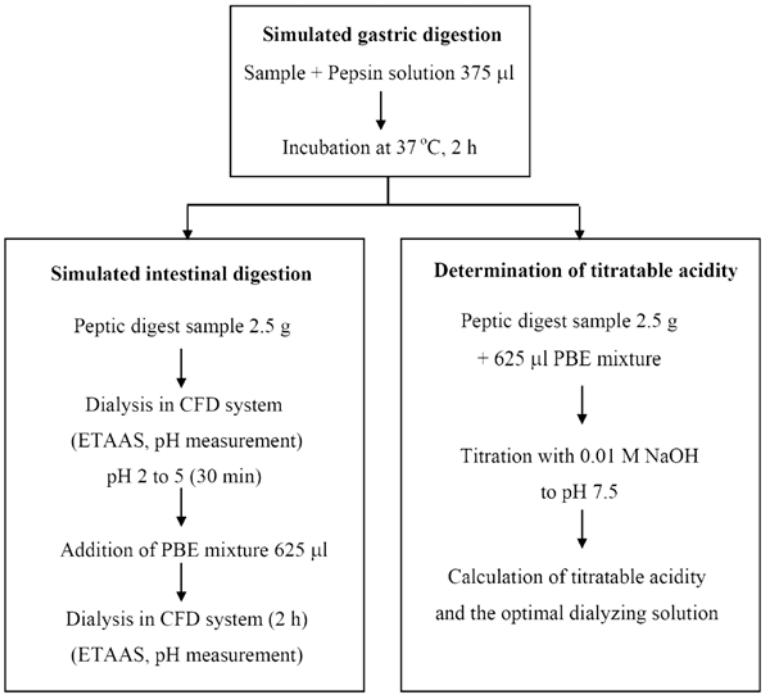

รูปที่ 2.2กระบวนการในการทดลองเพื่อศึกษาการดูดซึมได้ของแร่ธาตุ

2.2.4.3 การวิเคราะห์ปริมาณธาตุเหล็กทั้งหมดที่มีในตัวอย่างเครื่องดื่มนมและธาตุเหล็กที่เหลือจากการไดอะไลซิส

ชั่งตัวอย่าง 1.0 กรัม เติมสารละลายผสมระหว่างกรดไนตริกเข้มข้นกับไฮโดรเจนเปอร์ออกไซด์ 30 เปอร์เซนต์ (อัตราส่วน 3:2) 10.0 มิลลิลิตร ย่อยที่อุณหภูมิ 80 องศาเซลเซียส จนกระทั่งได้สารละลายใส นำไปวิเคราะห์ปริมาณธาตุเหล็กทั้งหมดที่มีในตัวอย่างด้วยเทคนิค ETAAS

กรณีวิเคราะห์ธาตุเหล็กที่เหลือจากการไดอะไลซิส นำของผสมที่เหลืออยู่ภายในถุงไดอะไลซิสที่ได้หลังการทำไดอะไลซิสถ่ายลงบีกเกอร์ขนาด 100 มิลลิลิตร และล้างถุงไดอะไลซิส 2 ครั้งด้วยสารละลาย 0.01 M EDTA 3 มิลลิลิตร ตามด้วยสารละลายกรดไนตริก 2 เปอร์เซนต์ 10.0 มิลลิลิตร อีก 2 ครั้ง เทลงบีกเกอร์เดียวกัน จากนั้นทำการย่อยจนได้สารละลายใส จากนั้นนำไปวิเคราะห์ปริมาณธาตุเหล็กทั้งหมดที่มีในตัวอย่างด้วยเทคนิค ETAAS

2.2.4.4 การคำนวณค่า Dialyzability

ปริมาณธาตุที่สามารถไดอะไลซ์ได้สามารถคำนวณเป็นเปอร์เซนต์ Dialyzability ได้ดังสมการที่แสดงในตอนที่ 1.2.9

ในระบบ CFD ความเข้มข้นของเหล็กในสารละลายที่ได้จากไดอะไลซิสอยู่ในระดับนาโนกรัมต่อมิลลิลิตร ซึ่งวิเคราะห์ได้ด้วยเทคนิค ETAAS ความเข้มข้นที่วิเคราะห์ได้จะเป็นตัวแทน

ของความเข้มข้นของธาตุเหล็กที่สามารถไดอะไลซ์ได้ ณ เวลานั้นๆ เนื่องจากใช้อัตราการไหล 1.0 มิลลิลิตรต่อนาที ดังนั้นหน่วยของปริมาณธาตุเหล็กจะเป็น นาโนกรัมต่อนาที ซึ่งได้มาจากการคูณ ปริมาณกับอัตราการไหล ปริมาณเหล็กที่ไดอะไลซ์ได้โดยรวมจะคำนวณได้จากการอินทิเกรตพื้นที่ใต้กราฟระหว่างปริมาณในหน่วย นาโนกรัมต่อนาที กับเวลาในหน่วยนาที ตลอดการไดอะไลซิส โดยใช้โปรแกรม Origin เวอร์ชั่น 6.0

2.3 ผลการทดลองและวิจารณ์

2.3.1 กราฟไดอะไลซิส

กราฟไดอะไลซิสของธาตุเหล็กและการเปลี่ยนแปลง pH ขณะไดอะไลซิส ของตัวอย่างเครื่องดื่มนมชนิดต่างๆ แสดงดังรูปที่ 2.3 ธาตุเหล็กสามารถแพร่ผ่านเมมเบรนระหว่างการย่อยในลำไส้ได้และแพร่ผ่านได้ลดลงเมื่อ pH เพิ่มขึ้น pH เพิ่มขึ้นเป็น 5.0 อย่างช้าๆ ภายใน 30 นาที เหมือนสภาวะจริงที่เกิดขึ้นในลำไส้ของมนุษย์ แล้ว pH เพิ่มขึ้นเป็น 7.0 อย่างรวดเร็วเนื่องจากเติม PBE mixture หลังจาก pH เป็นกลาง ธาตุเหล็กจะแพร่ผ่านเมมเบรนได้ลดลง ยกเว้น กรณีของตัวอย่างนมธัญพืช UHT และ นมถั่วเหลือง UHT 2 ที่ยังคงไดอะไลซ์ได้ ซึ่งอาจเป็นผลจากองค์ประกอบที่อยู่ในตัวอย่างนี้ ไปช่วยให้ไดอะไลซ์ได้มากขึ้น จากผลการทดลองยังพบว่า ตัวอย่างนมถั่วเหลือง UHT 2 ให้ค่า dialyzability ของธาตุเหล็กสูงกว่ากรณีตัวอย่างนมถั่วเหลือง UHT 1 ทั้งที่มีปริมาณธาตุเหล็กในตัวอย่างน้อยกว่า (แสดงในตารางที่ 2.1)

กราฟไดอะไลซิสของตัวอย่างนมวัวแบบผงที่เสริมแคลเซียม แสดงดังรูปที่ 2.3(a) พบว่าตัวอย่างนมวัวแบบผง 1 ให้ค่า dialyzability ของธาตุเหล็กต่ำ เพียง 1.7 เปอร์เซนต์ ส่วนตัวอย่างนมวัวแบบผง 2 มีค่า dialyzability ของธาตุเหล็กต่ำมากไม่สามารถวิเคราะห์ได้ นักวิจัยหลายกลุ่มรายงานว่าแคลเซียมมีบทบาทไปยับยั้งการดูดซึมธาตุเหล็ก กลไกของการยับยั้งนี้ยังไม่มีคำอธิบายที่ชัดเจน

กราฟไดอะไลซิสของตัวอย่างนมถั่วเหลือง UHT แสดงดังรูปที่ 2.3(b) ตัวอย่างนมถั่วเหลืองทั้งสองชนิดมีองค์ประกอบดังนี้ โปรตีนถั่วเหลือง วิตามินต่างๆ และแคลเซียมที่ปริมาณต่างกัน ซึ่งมีรายงานว่าวิตามินซีและวิตามินเอจะช่วยในการดูดซึมธาตุเหล็ก ส่วนโปรตีนถั่วเหลืองจะไปยับยั้งการดูดซึมธาตุเหล็ก ค่า dialyzability ของธาตุเหล็กในตัวอย่างนมถั่วเหลืองนี้ จึงขึ้นกับอิทธิพลของตัวยับยั้งและตัวช่วยในการดูดซึมได้ของธาตุเหล็ก

สำหรับตัวอย่างนมธัญพืช UHT ธาตุเหล็กสามารถไดอะไลซ์ได้ตลอดการไดอะไลซิส 2.5 ชั่วโมง ในขณะที่ตัวอย่างนมข้าวโพด UHT ธาตุเหล็กที่สามารถไดอะไลซ์มีปริมาณต่ำมากไม่สามารถวิเคราะห์ได้ ดังกราฟไดอะไลซิส รูปที่ 2.3(c) ตัวอย่างนมข้าวโพด UHT มีปริมาณธาตุเหล็กในตัวอย่างน้อยที่สุดในกลุ่มตัวอย่างที่เลือกมาศึกษา

ผลการทดลองพบว่าในตัวอย่างเครื่องดื่มนมชนิดต่างๆ กราฟไดอะไลซิสและความสามารถของธาตุเหล็กในการไดอะไลซ์ได้จะแตกต่างกัน โดยองค์ประกอบของตัวอย่างมีผลต่อลักษณะของกราฟไดอะไลซิส

ดังนั้นกราฟไดอะไลซิสสามารถใช้ประโยชน์ในการศึกษาอิทธิพลขององค์ประกอบต่างๆ ในอาหารต่อค่า dialyzability ของธาตุต่างๆ

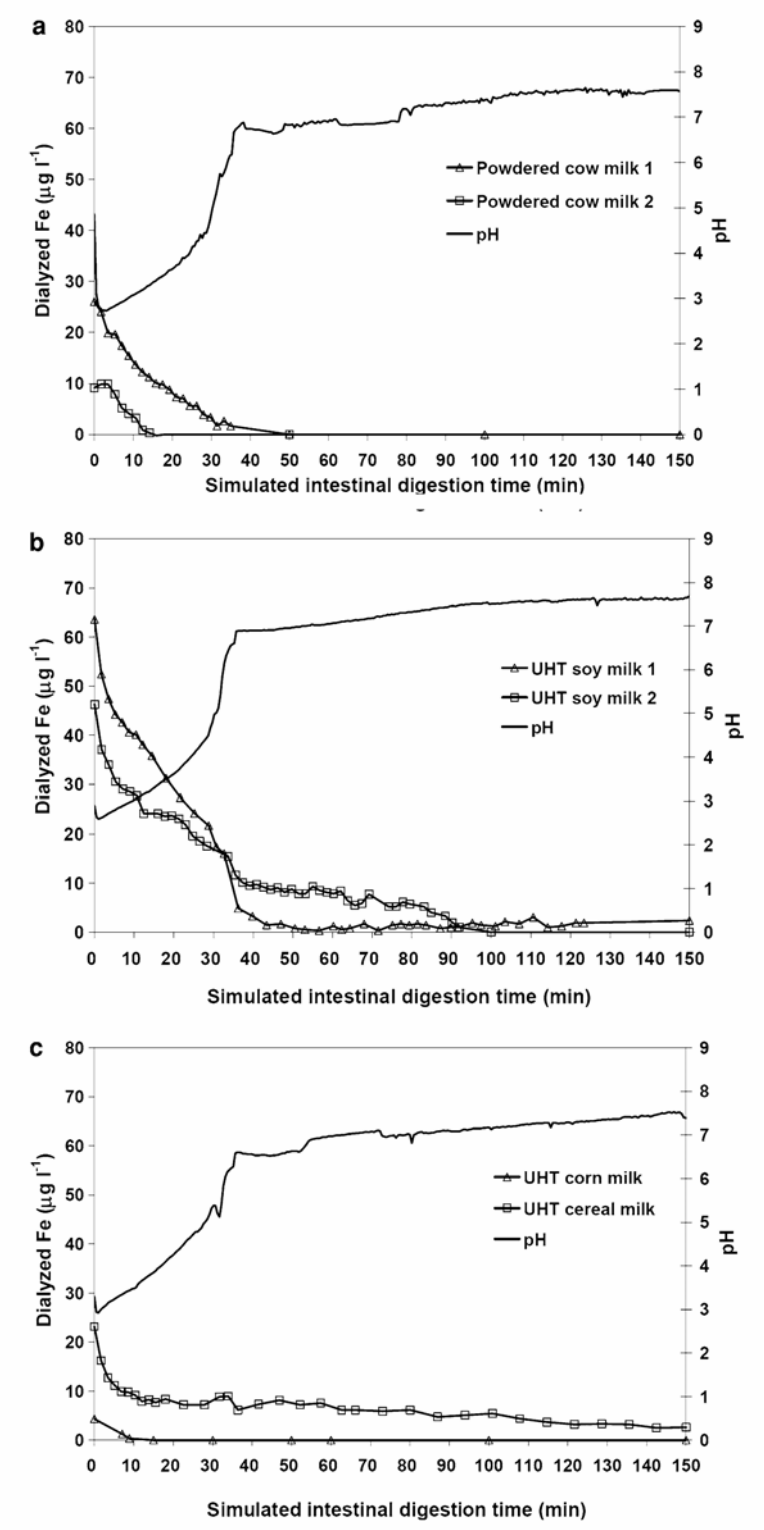

รูปที่ 2.3 กราฟแสดงปริมาณธาตุเหล็กที่ไดละไลซ์ได้และการเปลี่ยนแปลงค่า pH ระหว่างกระบวนการ dialysis สำหรับตัวอย่าง (a) นมผงจากวัว (b) เครื่องดื่มนมถั่วเหลือง UHT (c) เครื่องดื่มนมข้าวโพด UHT วิเคราะห์โดยระบบ CFD–ETAAS–pH โดยใช้อัตราการไหลของ dialyzing solution เท่ากับ 1.0 มิลลิลิตรต่อนาที

2.3.2 ค่า Dialyzability ของธาตุเหล็กในตัวอย่างเครื่องดื่มนม

ค่า Dialyzability ของตัวอย่างเครื่องดื่มนมชนิดต่างๆ ที่วิเคราะห์ด้วยระบบที่ได้พัฒนาขึ้น แสดงดังตารางที่ 2.1 พบว่าในตัวอย่างเครื่องดื่มนมมีปริมาณธาตุเหล็กอยู่ในช่วง 0.8 – 17.1 มิลลิกรัมต่อลิตร ซึ่งพบธาตุเหล็กมากที่สุดในตัวอย่างเครื่องดื่มนมวัว 1 และต่ำที่สุดในตัวอย่างเครื่องดื่มนมข้าวโพด UHT และพบว่าในตัวอย่างเครื่องดื่มนมวัว 1 มีค่า dialyzability 1.7 เปอร์เซนต์ ขณะที่ในกรณีเครื่องดื่มนมวัว 2 และเครื่องดื่มนมข้าวโพด UHT ไม่สามารถประมาณค่าได้ เนื่องจาก dialysate มีปริมาณธาตุเหล็กต่ำกว่าขีดจำกัดของเครื่องมือวัด ในตัวอย่างเครื่องดื่มนมธัญพืช UHT เครื่องดื่มนมถั่วเหลือง UHT 1 และ เครื่องดื่มนมถั่วเหลือง UHT 2 มีค่า dialyzability ของธาตุเหล็ก 20.4, 24.9 และ 37.7 เปอร์เซนต์ ตามลำดับ จากผลการทดลองพบว่า ธาตุเหล็กในตัวอย่างเครื่องดื่มนมถั่วเหลือง UHT สามารถไดอะไลซ์ได้ดีกว่าในตัวอย่างเครื่องดื่มนมวัว (24.9-37.7 เปอร์เซนต์)

ค่า dialyzability ของธาตุเหล็กในตัวอย่างเครื่องดื่มนมชนิดต่างๆ ที่วิเคราะห์ด้วยระบบไดอะไลซิสแบบสมดุล แสดงดังตารางที่ 2.1 พบว่าผลที่ได้จากทั้งสองวิธีไม่แตกต่างกันอย่างมีนัยสำคัญที่ระดับความเชื่อมั่น 95 เปอร์เซนต์ (t-test)

ตารางที่ 2.1 ปริมาณทั้งหมด ปริมาณที่ไดละไลซ์ได้ และร้อยละของการไดอะไลซ์ ของธาตุเหล็กในตัวอย่างเครื่องดื่มนมหลายชนิด ทำการวิเคราะห์โดย CFD-ETAAS และระบบไดอะไลซิสแบบสมดุล (n=3)

Sample	Total iron (mg L^{-1})	Dialyzed iron			
		CFD		Equilibrium dialysis	
		mg L^{-1}	Dialyzability (%)	mg L^{-1}	Dialyzability (%)
Powdered cow milk 1 (calcium and iron fortified)	17.1 ± 0.7	0.28 ± 0.04	1.7 ± 0.3	0.19 ± 0.03	1.1 ± 0.2
Powdered cow milk 2 (calcium fortified)	1.1 ± 0.1	< 0.09 (not detectable)	–	ND	ND
UHT soymilk 1 (high iron, vitamins B, D, E, and soy protein)	5.1 ± 0.0	1.27 ± 0.08	24.9 ± 1.6	1.18 ± 0.15	23.2 ± 3.2
UHT soymilk 2 (high calcium, soy protein, and vitamins A, C and E)	3.0 ± 0.3	1.13 ± 0.07	37.7 ± 2.4	ND	ND
UHT corn milk (high vitamins A and E)	0.80 ± 0.10	< 0.05 (not detectable)	–	ND	ND
UHT cereal milk (high calcium, vitamin B1, B2, E, and soy protein)	4.1 ± 0.3	0.84 ± 0.01	20.4 ± 0.4	0.81 ± 0.03	19.8 ± 0.6

ND for not determined

2.3.3 การศึกษาความถูกต้องของระบบที่พัฒนาขึ้น (Method validation)

เนื่องจากข้อจำกัดของสารมาตรฐานที่ไม่มีข้อมูลเกี่ยวกับ bioavailability ดังนั้นการตรวจสอบความถูกต้องของวิธีที่พัฒนาขึ้นจึงต้องศึกษา analytical recoveries ของสารที่สนใจในตัวอย่างโดยการวิเคราะห์ปริมาณธาตุเหล็กในตัวอย่างนมผงทั้งส่วนที่ไดอะไลซ์ได้และไม่สามารถไดอะไลซ์ได้ ดังแสดงในตารางที่ 2.2 พบว่า % dialyzability ให้ค่าแตกต่างกันเล็กน้อยระหว่างการทำซ้ำ ซึ่งน่าจะมาจาก

ตัวอย่างที่ไม่เป็นเนื้อเดียวกัน และพบว่าให้ % recovery อยู่ในช่วง 77.9 – 90.5 เปอร์เซนต์ เฉลี่ย 83.6 เปอร์เซนต์ ซึ่งธาตุเหล็กบางส่วนอาจจะติดอยู่ในถุงไดอะไลซิส แต่อย่างไรก็ตามข้อผิดพลาดดังกล่าวไม่ได้ส่งผลต่อ % dialyzability

ตารางที่ 2.2 Analytical recovery ของการวิเคราะห์ธาตุเหล็กในตัวอย่างนมผง (n = 3)

Sample	Dialyzed		Non-dialyzed		Recovery (%)
	Amount (mg kg^{-1})	Dialyzability (%)	Amount (mg kg^{-1})	Remaining (%)	
Powdered milk-based formula	3.0	4.8	45.3	73.1	77.9
	2.1	3.4	54.0	87.1	90.5
	3.1	5.1	48.0	77.4	82.4
Average	2.7 ± 0.6	4.4 ± 0.9	49.1 ± 4.5	79.2 ± 7.2	83.6 ± 6.4

Total iron 62.0 ± 1.0 mg kg^{-1}

2.4 บทสรุป

วิธีการประมาณค่าการดูดซึมได้ของธาตุเหล็กโดยวิธีไดอะไลซิสแบบไดนามิคในหลอดแก้วได้ถูกพัฒนาขึ้นโดยเชื่อมต่อระบบไดอะไลซิสแบบไหลต่อเนื่องอย่างง่ายเข้ากับหน่วยตรวจวัด ETAAS และเครื่องวัด pH ระบบนี้สามารถติดตามปริมาณธาตุเหล็กที่ไดอะไลซ์ได้และการเปลี่ยนแปลง pH ได้พร้อมกันในขณะไดอะไลซิส ซึ่งระบบ CFD-ETAAS-pH เป็นเครื่องมือที่ใช้งานได้ดี ราคาไม่แพง เพื่อใช้ในการศึกษา dialyzability และ bioavailability ข้อมูลที่ได้เกี่ยวกับค่า dialyzability ของธาตุต่างๆ นั้น สามารถใช้ประโยชน์ในการประเมินคุณค่าทางโภชนาการได้และยังสามารถใช้ศึกษาอิทธิพลขององค์ประกอบในอาหารต่อค่า dialyzability ของธาตุต่างๆ ความรู้เกี่ยวกับ bioavailability ของสารอาหารนั้นจะเป็นประโยชน์ในการวางแผนการบริโภคที่เหมาะสมและช่วยลดความเสี่ยงในการขาดสารอาหาร

2.5 เอกสารอ้างอิง

1. L.A. Smolin and M.B. Grosvenor, *Nutrition science and applications. Saunders College Publishing, PA, USA*, 1994.
2. A. Scalbert, C. Morand, C. Manach and C. Remesy, *Biomed Pharmacother*, 2002, **56**, 276.
3. R.P Glahn and G.M. Wortley, *J. Agric. Food Chem.* 2002, **50**, 390.
4. S.R. Lynch, *Nutr. Rev.* 1997, **55**, 102.
5. R.F. Hurrell, *Eur. J. Clin. Nutr.* 1997, **51**, S4.
6. M.N. Garcìa-Casal, M. Layrisse, J.P. Peña-Rosas, J. Ramírez, I. Leets and P. Matus, *Nutr. Res.*2003, **23**, 451.

7. M. Tuntawiroon, N. Sritongkul, M. Brune, L. Rossander-Hulten, R. Pleehachinda, R. Suwanik and L. Hallberg, *Am. J. Clin. Nutr.* 1991, **53**, 554.
8. R. Uicich, F. Pizarro, C. Almeida, M. Díaz, J. Boccio, M. Zubillaga, E. Carmuega and A. O'Donnell, *Nutr. Res.* 1999, **19**, 893.
9. S.A. Atkinson, J.K. Shah, C.E. Webber, I.L. Gibsom and R.S. Gibson, *J. Nutr.* 1993, **123**, 1586.
10. W.A. House, *Field Crop Res.* 1999, **60**, 115.
11. K.J.H. Wienk, J.J.M. Marx and A.C. Beynen, *Eur. J. Nutr.* 1999, **38**, 51.
12. D.R. Van Campen and R.P. Glahn, *Field Crop Res.*1999, **60**, 93.
13. M.R. Reddy, R.F. Hurrell and J.D. Cook, *Am. J. Clin. Nutr.* 2000, **71**, 937.
14. B.S. Narasinga Rao and T. Prabhavathi, *Am. J. Clin. Nutr.* 1978, **31**, 169.
15. S. Lock and A.E. Bender, *Brit. J. Nutr.* 1980, **43**, 413.
16. D.D. Miller, B.R. Schricker, R.R. Rasmussen, D. Van Campen, *Am. J. Clin. Nutr.* 1981, **34**, 2248.
17. B.R. Schricker, D.D. Miller, R.R. Rasmussen and D. Van Campen, *Am. J. Clin. Nutr.* 1981, **34**, 2257.
18. M.G.E. Wolters, H.A.W. Schreuder, G. Van Den Heuvel, H.J. Van Lonkhuijsen, R.J.J. Hermus and A.G.J. Voragen, *Br. J. Nutr.* 1993, **69**, 849.
19. L.H. Shen, J. Luten, H. Robberecht, J. Bindels and H. Deelstra, *Lebensm Unters Forsch*, 1994, **199**, 442.
20. M. Minekus, P. Marteau, R. Havenaar and J.H.J. Huis in't Veld, *ATLA*, 1995, **23**, 197.
21. P. Chaiwanon, P. Puwastien, A. Nitithamyong and P.P. Sirichakwal, *J. Food Comp. Anal.* 2000, **13**, 319.
22. B. Chen and R. Beckett, *Analyst*, 2001, **126**, 1588.
23. C. Ekmekcioglu, *Food Chem.* 2002, **76**, 225.
24. L. Hallberg, M. Brune, M. Erlandsson, A.S. Sandberg and L. Rossander-Hulten, *Am. J. Clin. Nutr.* 1991, **53**, 112.

ตอนที่ 3
การพัฒนาระบบการซึมผ่านเยื่อบางแบบไหลต่อเนื่องเชื่อมต่อกับหน่วยตรวจวัด ICP-OES เพื่อประมาณค่าการดูดซึมได้ของแร่ธาตุโดยวิธีในหลอดแก้ว

3.1 บทนำ

3.2 อุปกรณ์และวิธีการทดลอง

3.2.1 เครื่องมือ

3.2.2 วัสดุ และสารเคมี

3.2.3 ตัวอย่างที่ใช้ในการศึกษาและการเตรียมตัวอย่างอาหาร

3.2.4 การวิเคราะห์ปริมาณแร่ธาตุ (total mineral content) ในตัวอย่างอาหาร

3.2.5 ระบบการไดอะไลซ์แบบไหลต่อเนื่อง (Continuous-flow dialysis, CFD) ที่เชื่อมต่อกับการตรวจวัดแบบ on-line ด้วย ICP-OES และเครื่องวัดค่า pH

3.2.6 การวิเคราะห์ปริมาณแร่ธาตุในสารละลายที่ผ่านการย่อยด้วยระบบ CFD (dialysate) และในสารละลายที่เหลือจากการย่อย (residues after dialysis)

3.2.7 การคำนวณหาปริมาณแร่ธาตุที่สามารถดูดซึมได้

3.3 ผลการทดลองและวิจารณ์

3.3.1 การพัฒนา และประเมินประสิทธิภาพของระบบ CFD-ICP-OES เพื่อใช้ในการศึกษาความสามารถในการดูดซึมได้ของแร่ธาตุ

3.3.1.1 การออกแบบ และติดตั้งระบบ CFD-ICP-OES

3.3.1.2 การวัดความเป็นกรดด่าง (pH measurement)

3.3.1.3 ศึกษาผลของ matrix interferences ต่อการวัดด้วย ICP-OES

3.3.1.4 การตรวจสอบความใช้ได้ (Validation) ของระบบ on-line CFD-ICP-OES

3.3.1.5 กราฟการเปลี่ยนแปลงของไดอะไลซิส (Dialysis profile)

3.3.1.6 การประเมินค่าไดอะไลซิสของแร่ธาตุในอาหารชนิดต่างๆ ที่ได้จากใช้ระบบ CFD-ICP-OES

3.3.2 การใช้ประโยชน์ของข้อมูลที่ได้จากระบบ CFD-ICP-OES ในการศึกษาการดูดซึมได้ของแร่ธาตุในสารเสริมแร่ธาตุ

3.3.2.1 การประเมินความสามารถในการไดอะไลซิส และการตรวจสอบความใช้ได้ของวิธี

3.3.2.2 กราฟการเปลี่ยนแปลงของการไดอะไลซิส

3.3.2.3 กราฟการเปลี่ยนแปลงของไดอะไลซิสของธาตุเหล็กในสารเสริมธาตุเหล็กรูปฟอร์มต่างๆ ที่มีการเติมสารส่งเสริม และสารยับยั้งการดูดซึม

3.4 บทสรุป

3.5 เอกสารอ้างอิง

3.1 บทนำ

ระบบไดอะไลซิสแบบไหลต่อเนื่องที่ได้มีการพัฒนาขึ้นนี้ ในช่วงแรกได้มีการเชื่อมต่อกับหน่วยตรวจวัดประเภท AAS ที่ใช้เปลวไฟ และ AAS ที่ไม่ใช้เปลวไฟ (ตอนที่ 1 และ 2 ตามลำดับ) การตรวจวัดด้วยเครื่องเหล่านี้จะทำการตรวจวัดแร่ธาตุได้ครั้งละธาตุ อย่างไรก็ตามในอาหารมีแร่ธาตุที่มีความสำคัญทางโภชนาการหลายชนิด ดังนั้นในการศึกษานี้ได้ทำการต่อเชื่อมระบบ CFD เข้ากับเครื่องตรวจวัดแบบหลายแร่ธาตุด้วยการตรวจวัดครั้งเดียว คือเครื่องอินดัคทีพลีคัพเพิลพลาสมาออพทิคัลอิมิสชันสเปคโทรมิเตอร์ (ICP-OES) วิธีการประมาณค่าด้วยวิธีนี้ได้ทำการจำลองการย่อยในกระเพาะอาหารโดยใช้ระบบแบทช์ (batch) ตามด้วยการจำลองการย่อยในลำไส้แบบไหลต่อเนื่อง (continuous-flow) ซึ่งทำโดยการผ่านสารละลายเข้าไปในท่อที่ภายในมีตัวอย่างอาหารบรรจุอยู่ในถุงไดอะไลซิส ทำการตรวจวัดค่า pH และความเข้มข้นของธาตุในสารละลายที่แพร่ผ่านถุงไดอะไลซิส ด้วยเครื่อง pH meter และ ICP-OES ตามลำดับ ดังนั้นระบบที่พัฒนาขึ้นนี้จึงสามารถใช้ในการตรวจวัดค่า pH และความเข้มข้นของแร่ธาตุต่างๆ ในส่วนที่ผ่านการไดอะไลซ์มาจาก CFD ได้อย่างต่อเนื่องตลอดกระบวนการไดอะไลซิส รายละเอียดของระบบที่พัฒนาขึ้นนี้แสดงไว้ในรูปที่ 3.1

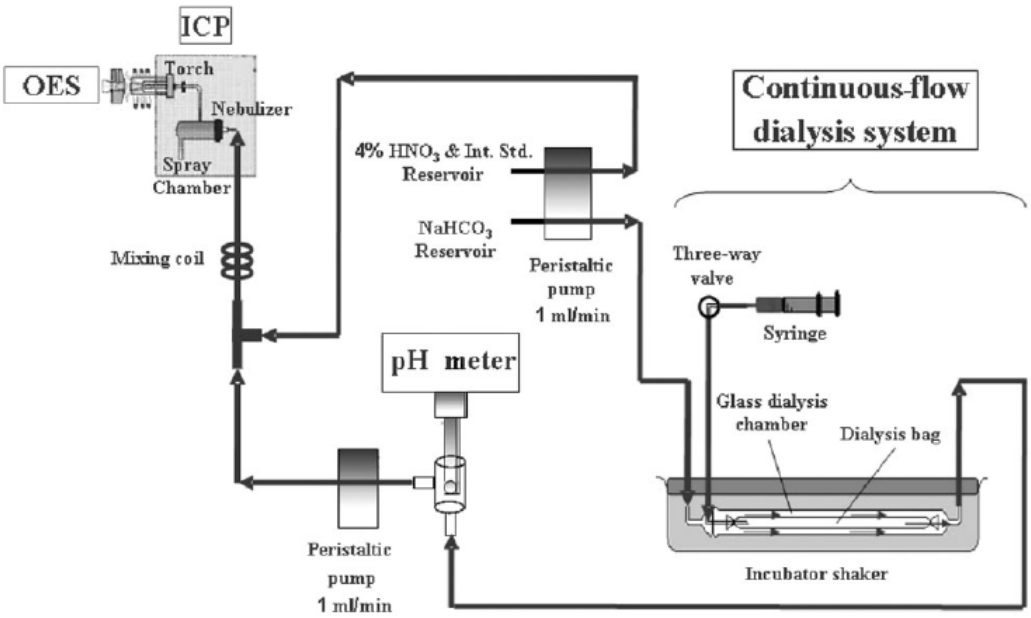

รูปที่ 3.1 ระบบ CFD-ICP-OES ที่ใช้ในการตรวจวัดปริมาณแร่ธาตุที่ไดอะไลซ์ได้ และตรวจวัดค่า pH [Judprasong et al., 2005]

3.2 อุปกรณ์และวิธีการทดลอง

3.2.1 เครื่องมือ

Inductively coupled plasma optical emission spectrometer (ICP-OES)

ตู้อบไมโครเวฟ (Milestone MLS1200 mega, Italy)

เครื่องวัด pH (Orion Model PCM500 SensorLink)

เครื่องชั่งละเอียดทศนิยม 4 ตำแหน่ง (Mettler AJ150, Switzerland)

Incubater shaker, Grant Instrument Model SS40-D2 (Cambridge, England)

Inductively coupled plasma optical emission spectrometer (ICP-OES)

เครื่อง ICP-OES ที่ใช้ในการวัดปริมาณแร่ธาตุต่างๆ คือเครื่องรุ่น SPECTRO CIROS CCD ใช้รูปแบบของตำแหน่งการวัดแบบ axial configuration โดยใช้ spray chamber เป็นแก้ว แบบ double pass, Scott-type และใช้ cross-flow nebulizer (อุปกรณ์ทั้งหมดเป็นของบริษัท SPECTRO, ประเทศเยอรมัน) เพื่อทำให้สารละลายตัวอย่างเกิดเป็นละอองฝอยเล็กๆ เข้าไปสู่พลาสมาที่มีพลังงานสูง (plasma) ที่ทำให้สารตัวอย่างเปลี่ยนเป็นอะตอมอิสระและกระตุ้นอะตอมนี้ให้เปลี่ยนสถานะจากสถานะพื้นไปอยู่ในสถานะเร้า เพื่อทำการตรวจวัดการคายแสง (emission) ของแร่ธาตุต่างๆ โดยหน่วยตรวจวัดความเข้มแสง สภาวะที่ใช้ในการตรวจวัดด้วยเครื่อง ICP-OES ได้แก่กำลัง (power) 1350 วัตต์ ใช้อัตราก๊าซสำหรับ nebulizer 1 ลิตรต่อนาที และใช้อัตราก๊าซสำหรับหล่อเย็นรอบๆคบ (torch coolant gas) 12 ลิตรต่อนาที การวัดปริมาณของแต่ละแร่ธาตุอาศัยหลักของการใช้ Internal standard โดยการเปรียบเทียบธาตุที่ต้องการวัดเทียบกับธาตุที่ไม่มีในธรรมชาติและเติมลงไป (Y) แล้วนำไปสร้าง calibration curve โดยเลือกใช้การคายแสง (emission lines) ของแต่ละธาตุที่มีความจำเพาะเจาะจง ทั้งที่เป็น ionic line (II) และ atomic line (I) โดยไม่มีการรบกวนจากธาตุอื่นๆ ได้แก่ แร่ธาตุแคลเซียม (Ca) ที่ความยาวคลื่น 396.847(II), 317.933(II), และ 422.673(I) นาโนเมตร แมกนีเซียม (Mg) ที่ความยาวคลื่น 279.553(II), 279.079(II) และ 280.270(II) นาโนเมตร ฟอสฟอรัส (P) ที่ความยาวคลื่น 177.495(I) และ 214.914(I) นาโนเมตร เหล็ก (Fe) ที่ความยาวคลื่น 238.204(II), 239.562(II) และ 259.940(II) นาโนเมตร และสังกะสี (Zn) ที่ความยาวคลื่น 202.548(II), 206.191(II) และ 213.856(II) นาโนเมตร สำหรับธาตุที่ใช้เป็น internal standards คือธาตุอิทเทรียม (Y) ที่ความยาวคลื่น 320.332(II), 371.030(II) และ 442.259(II) นาโนเมตร และสแกนเดียม (Sc) ที่ความยาวคลื่น 256.023(II), 361.384(II) และ 440.037(II) นาโนเมตร

3.2.2 วัสดุ และสารเคมี

วัสดุ และสารเคมีที่ใช้พร้อมกับบริษัทผู้ผลิต แสดงอยู่ในตารางที่ 3.1

ตารางที่ 3.1 วัสดุ และสารเคมีที่ใช้

วัสดุ และสารเคมี	ผู้ผลิต
Hydrochloric acid (AR 37% assay)	Merck, Germany
Nitric acid (AR 65% assay)	Merck, Germany
Hydrogen peroxide (AR 30% assay)	BDH Laboratory, England
Sodium bicarbonate (AR 99.7-100.3% assay)	APS Finechem, Australia
Sodium hydroxide (AR 99% assay)	Merck, Germany
Na_2EDTA (AR 99% assay)	Merck, Germany
Ethanol (AR 99% assay)	Merck, Germany
Multielemental solution (QCS 01-5, 100 mg mL^{-1})	AccuStandard, USA
Y (ICP-69N-1 at 1000 mg mL^{-1})	AccuStandard, USA
Sc (ICP-53N-1 at 1000 mg mL^{-1})	AccuStandard, USA
Iron (II) sulphate (AR, >99.5%)	Carlo Erba, Milano, Italy
Ammonium iron(III) sulphate (AR, 99-102%)	UNIVAR, Australia
Standard buffer solutions pH 4.01, 7.00 and 10.01	Thermo-Orion, USA
Enzyme	
Pepsin (P-7000, from porcine stomach mucosa)	Sigma, USA
Pancreatin (P-1750, from porcine pancreas)	Sigma, USA
Bile Extract (B-6831, porcine)	Sigma, USA
Dialysis tubing	
MWCO 12000-14000 Da (Spectra/por® 4)	Spectrum Laboratories, USA
MWCO 6000-8000 Da (Spectra/por® 1)	Spectrum Laboratories, USA

3.2.3 ตัวอย่างที่ใช้ในการศึกษาและการเตรียมตัวอย่างอาหาร

ตัวอย่างที่ใช้ในการศึกษา แสดงอยู่ในตารางที่ 3.2

ตารางที่ 3.2 ตัวอย่างที่ใช้ในการศึกษา

ตัวอย่างที่ใช้ในการศึกษา	ผู้ผลิต หรือ ผู้จำหน่าย
ส่วนที่ 1	
Milk-based infant formula (SRM 1846)	NIST, USA
นมผง (Instant powdered milk) ยี่ห้อ Nestle®	ตลาดในกรุงเทพมหานคร
คะน้า (*Brassica oleracea var. alboglabra, Bail.*)	ตลาดในกรุงเทพมหานคร
ชะอม (*Acacia pennata, L Willd. Subsp.*)	ตลาดในกรุงเทพมหานคร
ถั่วเขียว (*Phaseolus aureus Roxb.*)	ตลาดในกรุงเทพมหานคร
ข้าวหอมมะลิ (*Orya sativa*)	ตลาดในกรุงเทพมหานคร
เนื้อไก่	ตลาดในกรุงเทพมหานคร
ส่วนที่ 2	
Calcium fortificants:	Nutrition Ltd. Partnership,
Calcium carbonate ($CaCO_3$)	กรุงเทพมหานคร
Tri-calcium phosphate ($Ca_3(PO_4)_2$)	
Calcium lactate gluconate ($C_{18}H_{32}O_{20}Ca_2$)	
Calcium citrate ($Ca_3(C_6H_5O_7)_2$)	
Calcium lactate ($Ca(CH_3CH(OH)COO)_2$)	
Iron fortificants:	
Iron(II) sulphate ($FeSO_4.7H_2O$, Fe 36.8%)	Ajax Co., Aubern, Australia
Iron(II) fumarate ($FeC_4H_2O_4$, Fe 32.9%)	Vicky Consolidate Co. Ltd., กรุงเทพมหานคร
Sodium iron (Fe(III)) ethylenediaminetetraacetic acid (NaFe(III)EDTA, Fe 13%)	Akzo Nobel Functional Chemicals Co. Ltd., Arnhem, the Netherlands
Fe(II) lactate ($C_6H_{10}FeO_6$, Fe 20%)	Dr. Paul Lohmann Ltd., Germany
Fe(III) ammonium citrate ($C_6H_8O_7Fe_2.2NH_3$, Fe 20%)	
Zinc fortificants:	Dr. Paul Lohmann Ltd., Germany
Zinc sulphate ($ZnSO_4$)	
Zinc oxide (ZnO)	
Zinc amino complex (containing 10% Zn)	
Ascorbic acid (AR grade, 99.78%)	Fisher Scientific, UK
Citric acid (AR grade, >99%)	Fluka, Switzerland
Phytic acid (AR grade, ~40% in water)	Sigma, USA
Tannic acid (AR grade, >99%)	Fluka, Germany
Oxalic acid (AR grade, >99%)	BDH, England

การเตรียมตัวอย่างอาหาร

ตัวอย่างอาหารที่ใช้ในการศึกษานี้ได้แก่ นมผง คะน้า ชะอม ถั่วเขียว เนื้อไก่ และข้าวหอมมะลิ เตรียมโดยการสุ่มซื้อตัวอย่างจาก 3 ตลาดในกรุงเทพมหานคร แต่ละตัวอย่างซื้อประมาณ 1-3 กิโลกรัม สำหรับตัวอย่างนมผง ถั่วเขียว และข้าวหอมมะลิ เตรียมโดยการนำไปปั่นให้ละเอียดด้วยเครื่องปั่นแบบแห้ง ส่วนคะน้า ชะอม และเนื้อไก่ ทำการล้างด้วยน้ำประปา แล้วตามด้วยน้ำที่ปราศจากแร่ธาตุ 2 ครั้ง นำเฉพาะส่วนที่กินได้ทำให้สุกด้วยการต้ม หลังจากนั้นปั่นให้เป็นเนื้อเดียวกันด้วยเครื่องเตรียมอาหาร (food processor ตรา Tefal® Kaleo Blender, ประเทศฝรั่งเศส) นำไปทำให้แห้งด้วยการอบที่อุณหภูมิ 60 องศาเซลเซียสจนแห้งสนิท (24-48 ชั่วโมง) ปั่นด้วยเครื่องปั่นให้ละเอียด เก็บในถุงพลาสติกแล้วใส่ไว้ในหม้อดูดความชื้น (desiccator) ที่อุณหภูมิห้องจนกว่าจะทำการวิเคราะห์

3.2.4 การวิเคราะห์ปริมาณแร่ธาตุ (total mineral content) ในตัวอย่างอาหาร

ชั่งตัวอย่างอาหารประมาณ 1 กรัมลงใน digestion teflon vessel เติมกรดไนตริก 10 มิลลิลิตรและ ไฮโดรเจนเปอร์ออกไซด์ (H_2O_2) 1 มิลลิลิตร ทำการย่อยด้วยการใช้เครื่องย่อยแบบไมโครเวฟ (microwave digestion) ประกอบด้วย 5 ขั้นตอนคือขั้นแรกที่กำลัง 250 วัตต์เป็นเวลา 1 นาที ขั้นที่ 2 หยุดการให้กำลังเป็นเวลา 1 นาที ขั้นที่ 3 ที่กำลัง 250 วัตต์เป็นเวลา 5 นาที ขั้นที่ 4 ที่กำลัง 400 วัตต์เป็นเวลา 5 นาที และขั้นสุดท้ายที่กำลัง 650 วัตต์เป็นเวลา 5 นาที ทำการย่อยจนได้สารละลายที่ใส ถ้าไม่ใสจะทำซ้ำอีก 1 รอบ หลังจากได้สารละลายที่ใส ทำการเจือจางด้วยน้ำที่ปราศจากแร่ธาตุให้ครบ 50 มิลลิลิตร เพื่อทำการวัดปริมาณแร่ธาตุด้วยเครื่อง ICP-OES ต่อไป

3.2.5 ระบบการไดอะไลซ์แบบไหลต่อเนื่อง (Continuous-flow dialysis, CFD) ที่เชื่อมต่อกับการตรวจวัดแบบ on-line ด้วย ICP-OES และเครื่องวัดค่า pH

ทำการจำลองการย่อยในกระเพาะอาหารด้วยขั้นตอนต่อไปนี้คือ ชั่งตัวอย่างอาหารแห้งประมาณ 0.5-1 กรัมลงใน conical flask ที่มีฝาปิดขนาด 250 มิลลิลิตร ละลายด้วยน้ำ 10 มิลลิลิตร ปรับ pH ให้เป็น 2.0 ด้วยกรดไฮโดรคลอริก (6 M HCl) และปรับปริมาตรสุดท้ายให้เป็น 12.5 กรัมด้วยน้ำที่ปราศจากแร่ธาตุ หลังจากนั้นเติม 375 ไมโครลิตรของสารละลายเอนไซม์เปปซิน นำไปบ่มในอ่างน้ำอุ่นที่อุณหภูมิ 37 องศาเซลเซียส ทำการเขย่าเป็นเวลา 2 ชั่วโมง ได้สารละลายที่ผ่านการย่อยในกระเพาะอาหาร (gastric digest) แบ่งสารละลายที่ได้เป็น 2 ส่วน ส่วนหนึ่งนำไปวิเคราะห์หาความเข้มข้นที่เหมาะสมของสารละลายโซเดียมไบคาร์บอเนตสำหรับระบบ CFD อีกส่วนหนึ่งใช้สำหรับการจำลองการย่อยในลำไส้ต่อไป โดยชั่ง 2.0-2.5 กรัมของสารละลายที่ผ่านการย่อยในกระเพาะอาหารแล้ว ใส่เข้าใน dialysis bag ที่ปิดปลายทั้งสองด้าน เพื่อใส่เข้าไปในท่อแก้วกลวง (dialysis chamber) ด้วยการใช้เข็มฉีดยา (syringe) ฉีดตัวอย่างเข้าไป ท่อแก้วกลวงจะมียางกันซึมวางขั้นอยู่ (silicone rubber gasket) หลังจากใส่ตัวอย่างเข้าไปเรียบร้อยแล้ว ปลายท่อด้านหนึ่งของท่อกลวงจะเชื่อมต่อกับท่อ (tygon tubing) ที่มีการไหล

ของสารละลายโซเดียมไบคาร์บอเนตที่มีความเข้มข้นที่เหมาะสม ส่วนปลายอีกด้านหนึ่งจะต่อท่อเพื่อนำไปเข้าเครื่องวัดค่า pH และ ICP-OES ตามลำดับต่อไป นำท่อแก้วกลวงบ่มไว้ในอ่างน้ำอุ่นที่อุณหภูมิคงที่ 37±0.1 องศาเซลเซียสตลอดช่วงกระบวนการไดอะไลซิส ดังแสดงในรูปที่ 3.1

ให้สารละลายโซเดียมไบคาร์บอเนตที่มีความเข้มข้นที่เหมาะสมไหลเข้าไปในด้านหนึ่งของท่อกลวง ด้วยการเปิดปั๊ม (peristaltic pump) ที่อัตราเร็ว 1 มิลลิลิตรต่อนาที สารละลายที่ได้ออกมาจากระบบ CFD ถูกส่งเข้าไปสู่เครื่องวัดค่า pH และวัดปริมาณแร่ธาตุด้วยเครื่อง ICP-OES ตามลำดับต่อไป หลังจาก 30 นาทีเติมสารละลาย pancreatin bile extract (PBE) จำนวน 625 ไมโครลิตรเข้าไปโดยผ่านวาล์วสามทาง (three-way valve) ทำการ dialyse ต่อไปอีก 2 ชั่วโมง สำหรับการวัดแบบ off-line CFD-ICP-OES จะทำการเก็บส่วนสารละลายที่ได้จากระบบ CFD จำนวนขวดละ 10 มิลลิลิตร เพื่อทำการวัดความเป็นกรดด่าง และวัดปริมาณแร่ธาตุต่อไป

3.2.6 การวิเคราะห์ปริมาณแร่ธาตุในสารละลายที่ผ่านการย่อยด้วยระบบ CFD (dialysate) และในสารละลายที่เหลือจากการย่อย (retentate)

เพื่อให้เกิดประสิทธิภาพที่ดีของการเกิดละอองฝอย (good nebulisation performance) และเพื่อให้แน่ใจว่าแร่ธาตุที่ต้องการวิเคราะห์ยังคงอยู่ในสภาพที่ละลายน้ำได้ ไม่เกิดการตกตะกอนก่อนการตรวจวัด จึงมีความจำเป็นในการเติมกรดไนตริก 4% พร้อมทั้งมี Y และ Sc (internal standards) เข้าผสมกับสารละลายที่ผ่านการย่อย (dialysate) ด้วยอัตราเร็ว 1.0 มิลลิลิตรต่อนาที ก่อนการตรวจวัดด้วย ICP-OES (ดังแสดงในรูปที่ 3.1) การวัดปริมาณความเข้มข้นของแร่ธาตุต่างๆ (Ca, Mg, P, Fe, Zn) ของสารละลายที่เชื่อมต่อมาจากระบบ CFD ในหน่วยไมโครกรัมต่อกรัมตัวอย่างนั้น สามารถคำนวณได้จากการตรวจวัดสารละลายมาตรฐานของธาตุต่างๆ (external calibration) แล้วนำมาหาพื้นที่ใต้กราฟด้วยโปรแกรมคอมพิวเตอร์ (Microcal Origin, Version 6.0) เทียบกับความเข้มข้นของสารละลายมาตรฐาน หลังจากนั้นทำการหาปริมาณของแร่ธาตุที่เหลืออยู่ใน dialysis bag ด้วยการนำไปย่อยด้วยกรดไนตริกจนได้สารละลายที่ใส แล้วนำไปตรวจวัดด้วยเครื่อง ICP-OES

3.2.7 การคำนวณหาปริมาณแร่ธาตุที่สามารถดูดซึมได้ (mineral bioaccessibility, dialysability) [Shiowatana et al., 2006]

ปริมาณแร่ธาตุที่ได้จากระบบไดอะไลซิสหลังจากจำลองการย่อยในลำไส้นั้น สอดคล้องกับปริมาณแร่ธาตุที่ร่างกายดูดซึมได้ (bioaccessibility) ดังรายละเอียดในตอนที่ 1.2.9

3.3 ผลการทดลองและวิจารณ์

ผลการทดลองและวิจารณ์ผลการทดลอง แบ่งออกเป็น 2 ส่วนคือ ส่วนแรกเกี่ยวกับการพัฒนาระบบ CFD ที่ต่อเชื่อมกับการตรวจวัดด้วยเครื่อง ICP-OES เพื่อประมาณค่าการดูดซึมได้ของแร่ธาตุ (mineral bioaccessibility) ส่วนที่สองเป็นการนำผลที่ได้จากระบบที่พัฒนาขึ้นมาใช้ในการศึกษาการดูดซึมได้ของแร่ธาตุโดยวิธีในหลอดแก้วของแร่ธาตุเสริมอาหาร (mineral fortificants) และผลของตัวส่งเสริม (enhancers) และตัวยับยั้ง (inhibitors) การดูดซึมของแร่ธาตุ

ระบบการจำลองการย่อยของมนุษย์ (simulated human gastrointestinal digestion) ความเป็นกรดด่างในสารละลายที่ได้จากระบบ CFD เปลี่ยนแปลงจากค่า pH (pH) 2.0 ไปเป็น 5.0 ภายใน 30 นาที หลังจากนั้นเปลี่ยนจาก 5.0 เป็น 7.0-7.5 โดยคณะวิจัยได้ศึกษาถึงผลของอัตราเร็วในการไหล (flow rate) และความเข้มข้นของสารละลายโซเดียมไบคาร์บอเนตที่ส่งผลต่อการเปลี่ยนแปลงความเป็นกรดด่างดังรายละเอียดในตอนที่ 1 [Shiowatana et al., 2006] พบว่าอัตราเร็วในการไหลที่เหมาะสมคือ 1.0 มิลลิลิตรต่อนาที ซึ่งพิจารณาถึงระยะเวลาของการไดอะไลซิส และการเจือจางของสารละลายจากระบบ CFD และความเข้มข้นที่เหมาะสมของสารละลายโซเดียมไบคาร์บอเนตซึ่งคำนวณได้จากความเป็นกรดที่ไทเทรทได้ในหน่วยโมลาร์ (molarity) หารด้วย 50 สำหรับตัวอย่างยาเม็ดแคลเซียม และผักชนิดต่างๆ [Shiowatana et al., 2006] สำหรับในการศึกษานี้ได้ทำการวิเคราะห์หาปริมาณความเป็นกรดที่ไทเทรทได้ของแต่ละตัวอย่าง และความเป็นกรดของตัวอย่าง ความเข้มข้นที่เหมาะสมของสารละลายโซเดียมไบคาร์บอเนตที่ใช้ในการไหลขึ้นกับชนิดของตัวอย่างและค่าความเป็นกรดที่ไทเทรทได้ดังแสดงในตารางที่ 3.3

3.3.1 การพัฒนาและประเมินประสิทธิภาพของระบบ CFD-ICP-OES เพื่อใช้ในการศึกษาความสามารถในการดูดซึมได้ของแร่ธาตุ

การพัฒนาระบบ CFD ที่เชื่อมต่อแบบ on-line กับการตรวจวัดด้วย ETAAS ได้รายงานไว้ในตอนที่ 2 [Promchan and Shiowatana, 2005] เพื่อใช้ในการติดตามปริมาณแร่ธาตุเหล็ก และความเป็นกรดด่างระหว่างการไดอะไลซิส นอกจากนั้นยังได้มีการออกแบบถ้วยตัวอย่างขนาดเล็ก (sampling cup) (inlet i.d. 2 mm และ outlet i.d. 15 mm) ที่มีปริมาตร 100 ไมโครลิตรเพื่อใช้ในระบบการตรวจวัดด้วย ETAAS แบบต่อเนื่อง และวัดความเป็นกรดด่างต่อไปในภาชนะแก้วขนาดเล็กที่หุ้มอิเล็กโทรด (a small glass combination electrode chamber, i.d. 6 mm) ซึ่งมีวงแหวนซิลิโคน (silicone o-ring) ป้องกันไม่ให้สารละลายไหลออกจากระบบ

สำหรับการศึกษาในตอนที่ 3 นี้ได้มีการใช้ระบบ CFD เชื่อมต่อกับการตรวจวัดแร่ธาตุด้วยเครื่อง ICP-OES และเชื่อมต่อกับเครื่องวัดความเป็นกรดด่าง ระบบที่พัฒนาขึ้นนี้สามารถตรวจวัดปริมาณแร่ธาตุหลายๆ ธาตุในครั้งเดียว ด้วยเครื่อง ICP-OES อย่างต่อเนื่องตลอดการทำไดอะไลซิส ระบบนี้ประกอบด้วย

3 ส่วนหลักๆ คือระบบ CFD ระบบการวัดความเป็นกรดด่าง และระบบการวัดปริมาณแร่ธาตุด้วยเครื่อง ICP-OES

ตารางที่ 3.3 ความเข้มข้นที่เหมาะสมของสารละลายโซเดียมไบคาร์บอเนตที่ใช้ในระบบ CFD

ตัวอย่าง	ความเป็นกรดที่ไทเทรทได้ (Titratable acidity) ($\times 10^{-2}$ โมลต่อลิตร)	ความเข้มข้นที่เหมาะสมของสารละลายโซเดียมไบคาร์บอเนต ($\times 10^{-4}$ โมลต่อลิตร)
ส่วนที่ 1 (ตัวอย่างอาหาร)		
สารละลาย Blank	2.19	4.37
ข้าวหอมมะลิ (Jasmine rice)	3.88	7.77
เนื้อไก่ (Chicken meat)	9.47	18.94
ถั่วเขียว (Mungbean)	6.60	13.21
ชะอม (Acacia pennata)	7.96	15.93
นมผง (Milk powder)	5.71	11.41
คะน้า (Kale)	7.21	14.42
ส่วนที่ 2 สารเสริมแร่ธาตุ (mineral fortificant)		
สารละลาย Blank	2.18	4.36
Calcium carbonate	1.82	3.64
Tri-calcium phosphate	2.66	5.33
Calcium citrate	3.27	6.54
Calcium lactate gluconate	3.51	7.03
Fe(II) sulphate	4.36	8.72
Fe(II) fumarate	4.36	8.72
Fe(II) lactate	2.54	5.09
NaFe(III)EDTA	2.42	4.85
Fe(III) ammonium citrate	2.42	4.85
Zinc sulphate	2.55	5.09
Zinc oxide	2.55	5.09
Zinc amino complex	2.67	5.35

3.3.1.1 การออกแบบระบบ CFD-ICP-OES

เนื่องจากอัตราการไหลของสารละลายโซเดียมไบคาร์บอเนตที่มีความเข้มข้นที่เหมาะสมและอัตราการดูดสารละลาย (uptake rate) ของ ICP-OES มีค่าเท่ากันคือ 1 มิลลิลิตรต่อนาที ดังนั้นการเชื่อมต่อของทั้งสองระบบจึงทำได้สะดวก สำหรับการตรวจวัดความเป็นกรดด่างนั้นใช้ระบบของบริษัท Orion (Model PCM500 SensorLink) ที่มีการใช้อุปกรณ์ต่อพ่วงกับคอมพิวเตอร์ การเชื่อมต่อระบบทั้งสาม

คือ CFD ICP-OES และ pH meter นั้นมีสิ่งสำคัญที่ต้องพิจารณาคือการเชื่อมต่อ สำหรับการวัดความเป็นกรดด่างใช้ภาชนะแก้วขนาดเล็กที่หุ้มอิเล็กโทรดโดยมีการไหลเข้าจากด้านล่าง และไหลออกทางด้านข้างบน เช่นเดียวกับการศึกษาในตอนที่ 2 [Promchan and Shiowatana, 2005] หลังจากนั้นสารละลายจะไหลไปผสมกับกรดไนตริก 4% (ที่มี Y และ Sc อยู่) โดยผ่านวาล์วสามทางที่ทำจากแก้วขนาดเล็ก (glass three-way) แล้วไหลออกไปผสมกันในท่อพลาสติกที่ขดเป็นปม (mixing coil) ก่อนการตรวจวัดด้วยเครื่อง ICP-OES

เครื่อง ICP-OES มีข้อดีหลายด้านคือ ใช้ในการวิเคราะห์ปริมาณแร่ธาตุต่างๆ ที่มีในตัวอย่างทั้งปริมาณสูงและปริมาณต่ำ (macro and trace elements) โดยสามารถทำการวัดหลายๆ ธาตุด้วยการวิเคราะห์ครั้งเดียว (simultaneous detection) มีความเร็วในการวิเคราะห์ และมีความไวในการวิเคราะห์สูง (good sensitivity)

เพื่อเป็นการแสดงให้เห็นว่าสารละลายที่ได้จากระบบ CFD (dialysate) ไม่มีผลรบกวนต่อการตรวจวัดของ ICP-OES (matrix interference) จึงได้ทำการศึกษาตัวอย่างนมผง และผักคะน้าเพื่อใช้เป็นตัวแทน โดยการใช้สารละลายที่ได้จากระบบ CFD ซึ่งอยู่ในโซเดียมไบคาร์บอเนต 0.01 โมลาร์ แล้วนำไปตรวจวัดด้วยเครื่อง ICP-OES เปรียบเทียบผลที่ได้จากการละลายอยู่ในกรดไนตริก 2% พบว่าระดับสัญญาณที่ได้ของแคลเซียมและเหล็กของตัวอย่างนมผงในสารละลายที่มีกรดมีค่าสูงกว่าแบบไม่มีกรดอย่างมีนัยสำคัญทางสถิติ (p<0.05) ดังแสดงในตารางที่ 3.4 นอกจากนั้นการศึกษาในผักคะน้าด้วยระบบ on-line CFD-ICP-OES พบว่าแร่ธาตุแคลเซียม และเหล็กโดยไม่ผสมกรดให้ระดับสัญญาณต่ำกว่าประมาณ 5 และ 3 เท่าตามลำดับ เมื่อเปรียบเทียบกับสารละลายที่มีผสมกับการไหลของกรดไนตริก 4% ดังแสดงในรูปที่ 3.2 และ 3.3

ตารางที่ 3.4 ปริมาณแร่ธาตุต่างๆ ในสารละลายที่ได้จากระบบ off-line ICP-OES (0.01 M $NaHCO_3$) ของตัวอย่างนมผงเปรียบเทียบกับสารละละลายที่มีกรดไนตริกในความเข้มข้นสุดท้าย 2% (n=3)

แร่ธาตุ (ไมโครกรัมต่อกรัม)	สารละละลายที่มีกรดไนตริกในความเข้มข้นสุดท้าย 2% (2% HNO_3)	สารละละลายที่ไม่มีกรดไนตริก (0.01 M $NaHCO_3$)
แคลเซียม (Ca)	5845 ± 175 [a]	4090 ± 55 [a]
แมกนีเซียม (Mg)	865 ± 85	870 ± 60
ฟอสฟอรัส (P)	550 ± 45	510 ± 40
เหล็ก (Fe)	740 ± 55 [b]	375 ± 25 [b]
สังกะสี (Zn)	510 ± 30	495 ± 20

[a, b] ตัวอักษรที่เหมือนกันอยู่ในแถวเดียวกัน แสดงถึงความแตกต่างอย่างมีนัยสำคัญทางสถิติ (p < 0.05)

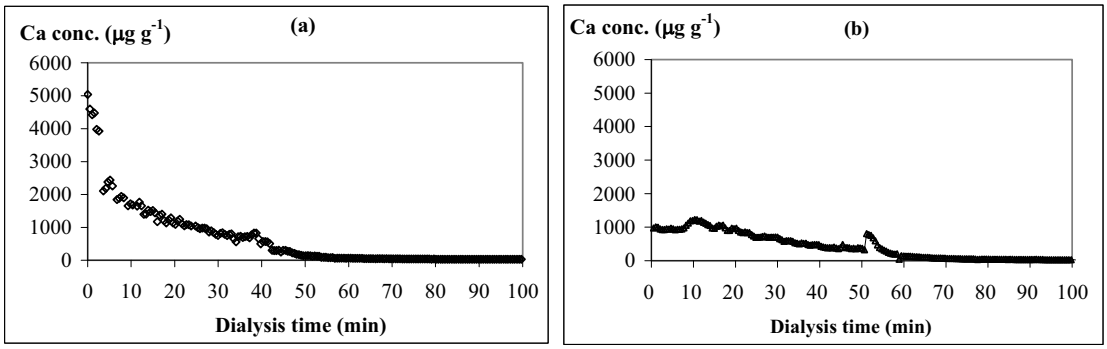

รูปที่ 3.2 กราฟแสดงการไดละไลซิสของแคลเซียมในผักคะน้าที่ได้จากระบบ on-line CFD-ICP-OES ในสารละลายที่มีการผสมของการไหลของกรดไนตริก 4% (a) และไม่มีการผสมกรดไนตริก (b) ตามลำดับ

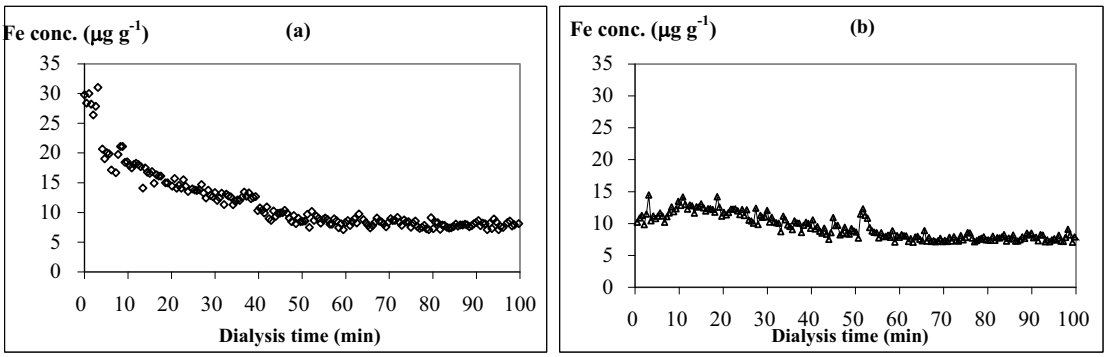

รูปที่ 3.3 กราฟแสดงการไดละไลซิสของธาตุเหล็กในผักคะน้าที่ได้จากระบบ on-line CFD-ICP-OES ในสารละลายที่มีการผสมของการไหลของกรดไนตริก 4% (a) และไม่มีการผสมกรดไนตริก (b) ตามลำดับ

3.3.1.2 การวัดความเป็นกรดด่าง (pH measurement)

เครื่องวัดความเป็นกรดด่างที่ใช้ยี่ห้อ Orion (รุ่น PCM500 SensorLink pH Measurement System) กรณีที่วิเคราะห์แบบต่อเนื่อง (on-line pH measurement) นั้นมีการใช้อิเล็กโทรดขนาดเล็กใส่ไว้ในภาชนะแก้วขนาดเล็ก (sampling cup) และปิดสนิทด้วยยางกันรั่วซึม (rubber o-ring) เมื่อสารละลายไหลจากด้านล่างผ่านเข้าไปท่วมอิเล็กโทรดแล้วไหลออกด้านบนเรียบร้อยแล้ว จึงเริ่มทำการอ่านค่า pH ทำการศึกษาการวัดความเป็นกรดด่างแบบต่างๆ 3 แบบคือ 1)ทำการสอบเทียบในการวัดแบบปกติ (static reading, off-line) กับสารละลายบัฟเฟอร์มาตรฐาน (buffer solution) ที่ความเป็นกรดด่าง 4.0, 7.0 และ 10.0 ตามลำดับ 2) ทำการอ่านค่าสารละลายกรดด่างมาตรฐานที่ผ่านการไหล 1 มิลลิลิตรต่อนาที แล้วทำการอ่านค่าแบบต่อเนื่อง (continuous flow, on-line) และ 3) ทำการอ่านค่า pH ของสารละลายที่มี 0.01 โมลาร์โซเดียมไบคาร์บอเนตไหลผ่านแบบต่อเนื่อง พบว่าความไว (sensitivity โดยอ่านค่าจาก slope ของสมการเส้นตรง) ของการอ่านค่าทั้งแบบปกติ และแบบที่มีการไหลของสารละลายไม่มีความแตกต่างกันอย่างมี

นัยสำคัญทางสถิติ ($p < 0.05$) แต่พบว่าการอ่านค่า pH ของสารละลายโซเดียมไบคาร์บอเนต 0.01 โมลาร์ แบบต่อเนื่องให้ความไวที่ต่ำกว่าเล็กน้อย ดังแสดงในรูปที่ 3.4

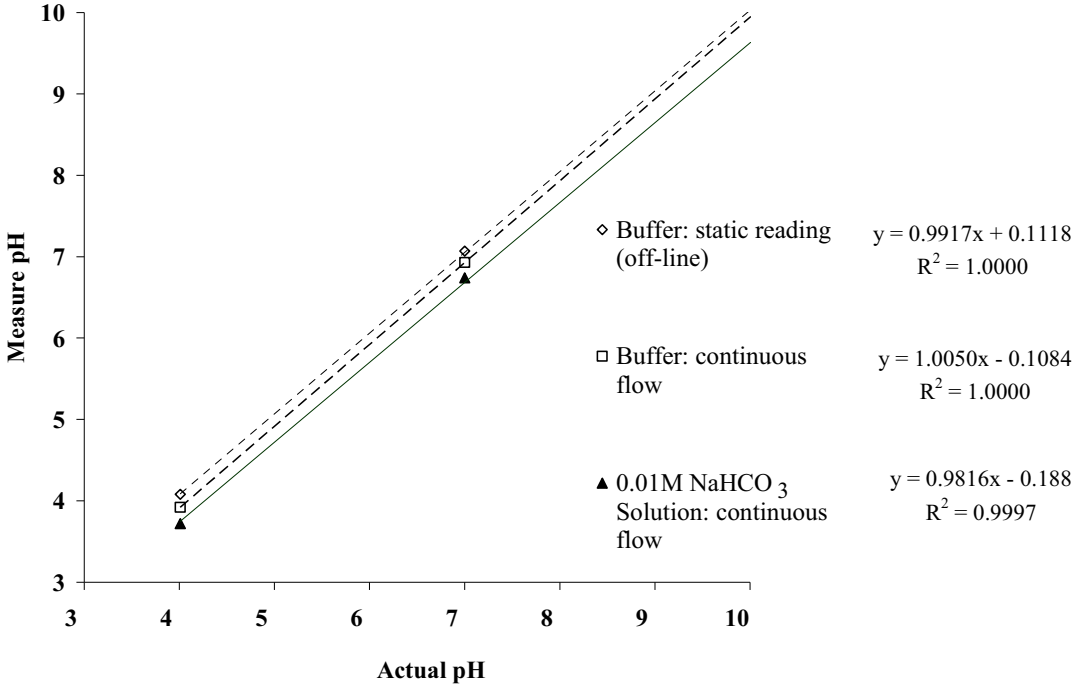

รูปที่ 3.4 เปรียบเทียบความเป็นเส้นตรง (calibration curve) ของการวัดความเป็นกรดด่างแบบต่างๆ

รูปแบบของค่า pH ที่อ่านได้จากการอ่านค่าแบบต่อเนื่อง (on-line) และไม่ต่อเนื่อง (off-line) ของตัวอย่างนมผง ข้าวหอมมะลิ และถั่วเขียว ในสารละลายเดียวกันที่ได้จากระบบ CFD แสดงดังรูปที่ 3.5

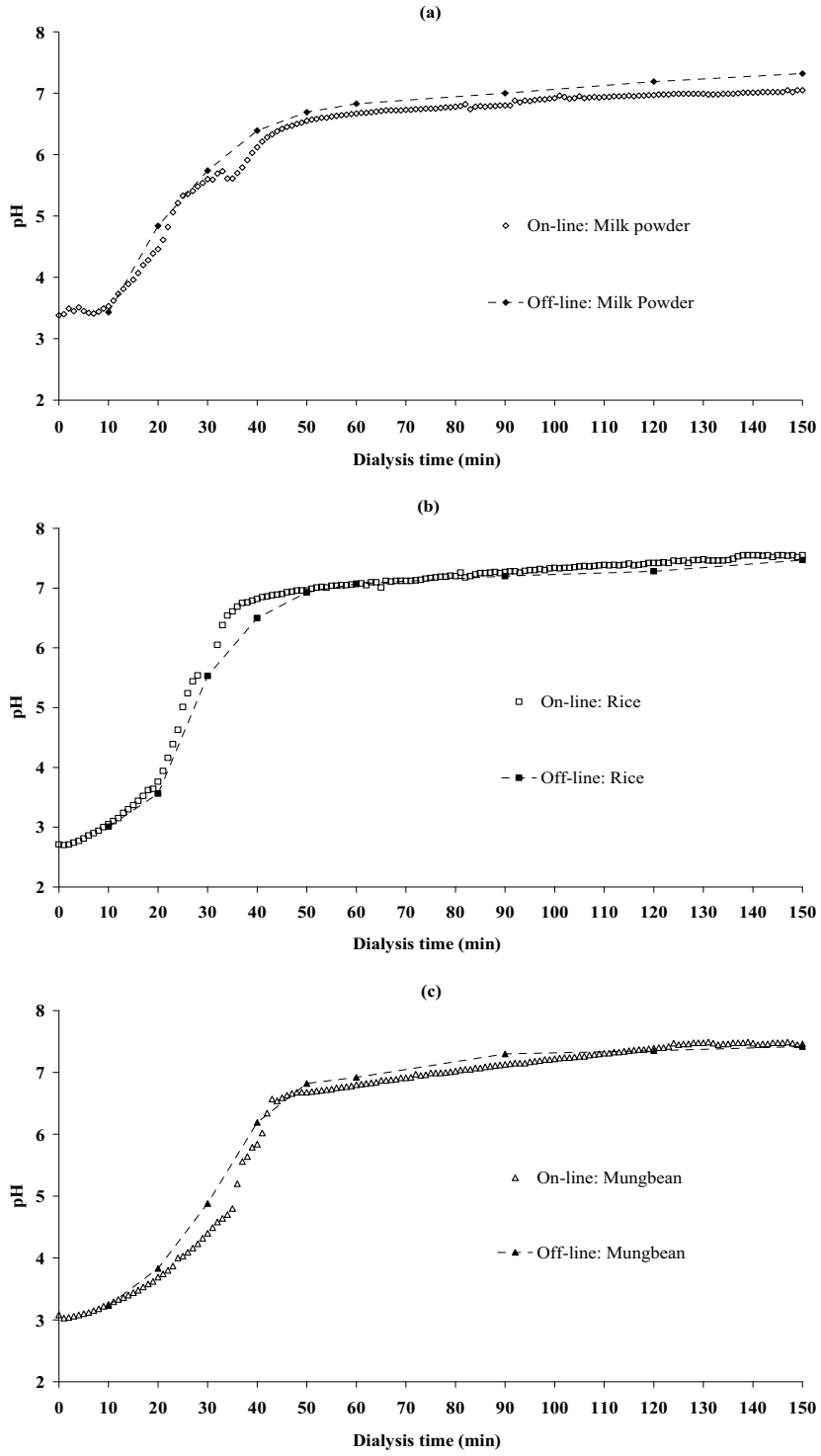

รูปที่ 3.5 ค่า pH ที่เวลาต่างๆ ของการไดอะไลซิสที่อ่านได้จากการอ่านแบบ on-line และ off-line ของตัวอย่างนมผง (a) ข้าวหอมมะลิ (b) และถั่วเขียว (c)

การเปลี่ยนแปลงของการวัดค่า pH ไม่มีความแตกต่างกันระหว่างการวัดแบบ on-line และแบบ off-line โดยแบบ on-line ให้ค่า pH ต่ำกว่าเพียงเล็กน้อย ดังนั้นจึงสามารถใช้การวัดความเป็นกรดด่างในการวัดแบบ on-line เพื่อใช้ในการติดตามการเปลี่ยนแปลงความเป็นกรดด่างของการไดอะไลซิส

3.3.1.3 ศึกษาผลของ matrix interferences ต่อการวิเคราะห์ด้วย ICP-OES

ผลของการรบกวนการตรวจวัดจาก matrix ต่างๆ กัน เกิดขึ้นได้โดยอาจทำให้เกิดการเพิ่มหรือลดสัญญาณของการตรวจวัด ซึ่งเกิดขึ้นจากคุณลักษณะทางกายภาพและทางเคมีที่ต่างกันระหว่างสารละลายมาตรฐานกับสารละลายตัวอย่าง ทางกายภาพ เช่นความหนืด แรงตึงผิวเป็นต้น ส่วนทางเคมี อาจทำให้เกิดการขยับของสมดุลไอออนในพลาสมาโดยเฉพาะเมื่อสารละลายตัวอย่างมีความเข้มข้นของเกลือกรด หรือ matrix ที่ต่างจากสารละลายมาตรฐาน เพื่อป้องกันปัญหาอันเกิดจากสาเหตุนี้ จึงจำเป็นต้องทำให้สารละลายของสารมาตรฐาน และสารละลายตัวอย่าง มีคุณลักษณะใกล้เคียงกัน (มี matrix ที่เหมือนกัน)

การวิเคราะห์ปริมาณสารโดยใช้วิธีการที่เรียกว่า “standard additions” เป็นวิธีการที่นิยมใช้ในการป้องกันและแก้ไขปัญหาอันเกิดจากการรบกวนของ matrix และเป็นวิธีที่มีความถูกต้องมาก ทำได้โดยเติมสารละลายมาตรฐานหลายๆ ความเข้มข้นลงในสารละลายตัวอย่าง ดังนั้นการรบกวนของ matrix ในสารละลายต่างๆ จึงเหมือนกัน นั่นคือไม่มีผลกระทบจากสิ่งรบกวน นอกจากนั้นวิธีนี้ยังเป็นวิธีที่ใช้ในการตรวจสอบว่าเกิดการรบกวนของ matrix หรือไม่ ด้วยการเปรียบเทียบความชัน (slope) ของสมการเส้นตรงระหว่างสารละลายมาตรฐานกับสารละลายที่เติมสารมาตรฐานหลายๆ ความเข้มข้น ถ้าหากความชันมีค่าแตกต่างกันแสดงว่าสารรบกวนการวิเคราะห์มีผลต่อการวัด

สารละลายที่ใช้ในการทำไดอะไลซิสคือโซเดียมไบคาร์บอเนตที่ความเข้มข้นประมาณ 10^{-4}-10^{-5} โมลาร์ และมีการเติมกรดไนตริกให้ได้ประมาณ 2% ดังนั้นจึงได้ทำการเตรียมสารละลายมาตรฐานและ สารละลาย blank ในสารละลายโซเดียมไบคาร์บอเนต การศึกษาผลของสิ่งรบกวนการวัดของสารละลายที่ได้จากการทำไดอะไลซิสด้วยการเปรียบเทียบความชันของสมการเส้นตรงระหว่างสารละลายมาตรฐานกับสารละลายที่เติมสารมาตรฐานหลายๆ ความเข้มข้น แสดงในตารางที่ 3.5 พบว่าความชันของสมการเส้นตรงของแต่ละ emission line และของแต่ละธาตุ (แคลเซียม แมกนีเซียม ฟอสฟอรัส เหล็ก และสังกะสี) ไม่มีความแตกต่างกัน นั่นคือไม่เกิดการรบกวนการวัดของสิ่งรบกวนการวัด ดังนั้นจึงสามารถทำการตรวจวัดปริมาณแร่ธาตุต่างๆ ด้วย ICP-OES ในสารละลายที่ได้จากการทำไดอะไลซิสได้

ตารางที่ 3.5 เปรียบเทียบความชันของสมการเส้นตรงระหว่างสารละลายมาตรฐาน (External calibration curve) กับสารละลายที่เติมสารมาตรฐานหลายๆ ความเข้มข้น (Standard Addition) ในโซเดียมไบคาร์บอเนต 0.01 โมลาร์

	External calibration curve	**Standard addition**
แคลเซียม (Ca)		
Ca 396.847 nm	y = 6651.6x - 46722.3	y = 6551.6x + 96443.5
Ca 422.673 nm	y = 365.5x - 131.1	y = 356.1x + 9301.1
Ca 317.933 nm	y = 186.3x - 1941.5	y = 186.0x + 3372.3
แมกนีเซียม (Mg)		
Mg 279.079 nm	y = 3.493x + 116.5	y = 3.492x + 104.2
Mg 279.553 nm	y = 982.2x + 44786.7	y = 964.8x + 340916.9
Mg 280.270 nm	y = 485.9x + 30927.5	y = 490.4x + 161596.7
ฟอสฟอรัส (P)		
P 177.495 nm	y = 29.05x + 33.87	y = 31.61x + 506.80
P 214.914 nm	y = 12.38x + 62.26	y = 13.38x + 735.06
เหล็ก (Fe)		
Fe 238.204 nm	y = 107.16x - 688.68	y = 107.17x + 1159.72
Fe 239.562 nm	y = 77.58x - 759.20	y = 63.77x + 629.73
Fe 259.940 nm	y = 128.40x - 833.16	y = 123.05x - 1378.91
สังกะสี (Zn)		
Zn 202.548 nm	y = 96.08x + 617.33	y = 95.29x + 45602.30
Zn 213.856 nm	y = 62.55x + 1271.39	y = 56.88x + 28929.30

3.3.1.4 การตรวจสอบความใช้ได้ของระบบ on-line CFD-ICP-OES

เนื่องจากไม่มีตัวอย่างสารมาตรฐาน (reference material) เกี่ยวกับการดูดซึมได้ของแร่ธาตุ ดังนั้นการตรวจสอบความใช้ได้ (validation) ของระบบ CFD-ICP-OES จึงเป็นสิ่งสำคัญ ทำโดยการศึกษา %recovery ของแร่ธาตุของการวิเคราะห์ทั้งหมด ซึ่งเลือกอาหารมาตรฐานของหน่วยงาน NIST (SRM 1846) คืออาหารเลี้ยงทารก (milk-based infant formula) เป็นตัวแทน โดยใช้เป็นตัวอย่างอาหารในระบบ CFD แล้วทำการวิเคราะห์หาปริมาณแร่ธาตุทั้งส่วนที่ไดอะไลซ์ได้ (dialysate) จากระบบ CFD และส่วนที่เหลือจากการไดอะไลซ์ (non-dialysable, retentate) ด้วยการใช้กรดย่อยสลายส่วนที่เหลือจนได้สารละลายใส แล้วนำทั้งสองส่วนไปวิเคราะห์หาปริมาณแร่ธาตุต่างๆ ด้วยเครื่อง ICP-OES ได้ผลการทดลองดังแสดงในตารางที่ 3.6 พบว่าการวิเคราะห์หาปริมาณแร่ธาตุทั้งหมด (total amount) มีค่าไม่แตกต่างจากค่าที่ระบุไว้ (certified values) นอกจากนั้นค่าผลรวมของแร่ธาตุจากส่วนที่ไดอะไลซ์ได้และส่วนที่เหลือจากการไดอะไลซ์มีค่าไม่

แตกต่างจากที่ระบุไว้เช่นเดียวกัน มีค่า % recoveries ตั้งแต่ 90 $\pm$ 5% ของธาตุเหล็ก จนถึง 104 $\pm$ 6% ของธาตุฟอสฟอรัส

ตารางที่ 3.6 ผลของการตรวจสอบความใช้ได้ของปริมาณแร่ธาตุที่ได้วิเคราะห์ได้จากระบบ CFD-ICP-OES ในตัวอย่างอาหารมาตรฐาน (milk-based infant formula, SRM 1846) (n=3)

	ปริมาณแร่ธาตุ				
	แคลเซียม (Ca)	**แมกนีเซียม (Mg)**	**ฟอสฟอรัส (P)**	**เหล็ก (Fe)**	**สังกะสี (Zn)**
ค่าที่ระบุ (Certified value, $\mu g\ g^{-1}$)	**3670 $\pm$ 200**	**538 $\pm$ 29**	**2610 $\pm$ 150**	**63.1 $\pm$ 4.0**	**60.0 $\pm$ 3.2**
แร่ธาตุทั้งหมด (Total minerals, $\mu g\ g^{-1}$)*	3760 $\pm$ 160	541 $\pm$ 17	2490 $\pm$ 96	66.6 $\pm$ 1.5	62.8 $\pm$ 1.8
ส่วนที่ไดอะไลซ์ได้ (Dialysed minerals, $\mu g\ g^{-1}$)*	2810 $\pm$ 140	428 $\pm$ 10	1730 $\pm$ 200	17.7 $\pm$ 2.2	51.5 $\pm$ 3.7
ส่วนที่เหลือจากการไดอะไลซ์ (Non-dialysed minerals, $\mu g\ g^{-1}$)*	790 $\pm$ 46	86 $\pm$ 12	1040 $\pm$ 94	42.4 $\pm$ 5.5	7.8 $\pm$ 1.0
Dialysed + non-dialysed mineral ($\mu g\ g^{-1}$)	3600 $\pm$ 140	514 $\pm$ 6	2690 $\pm$ 145	60.1 $\pm$ 5.0	59.0 $\pm$ 4.9
ร้อยละของไดอะไลซิส (Dialysis, %)	76.3 $\pm$ 3.7	79.6 $\pm$ 1.9	69.6 $\pm$ 5.0	26.5 $\pm$ 3.2	85.7 $\pm$ 5.7
ร้อยละของส่วนที่เหลือ (Element retained, %)	21.6 $\pm$ 1.2	16.0 $\pm$ 2.2	41.8 $\pm$ 3.8	63.6 $\pm$ 5.2	12.5 $\pm$ 1.6
ร้อยละของผลรวม (Sum, %)	**97.9 $\pm$ 3.7**	**95.6 $\pm$ 1.2**	**103.8 $\pm$ 5.8**	**90.1 $\pm$ 5.4**	**94.2 $\pm$ 8.6**

* ได้ทำการหักลบ blank ออกแล้ว (blank subtracted)

3.3.1.5 กราฟการเปลี่ยนแปลงของไดอะไลซิส (Dialysis profile)

ระบบ CFD นอกเหนือจากจะให้ข้อมูลของร้อยละการไดอะไลซิสแล้ว ยังให้ข้อมูลของการเปลี่ยนแปลงค่า pH และการเปลี่ยนแปลงระดับแร่ธาตุต่างๆ ด้วย ซึ่งช่วยทำให้เข้าใจการเปลี่ยนแปลงที่เกิดขึ้นระหว่างการไดอะไลซิส และปัจจัยที่ส่งผลถึงการไดอะไลซิส โดยพิจารณาจากแกนด้านขวาของกราฟการเปลี่ยนแปลงของความเป็นกรดด่างในรูปที่ 3.6 พบว่าค่า pH เปลี่ยนแปลงจากประมาณ 2.0 ในการย่อยของกระเพาะอาหารไปเป็นประมาณ 5.0 ภายใน 30 นาทีของการย่อยในลำไส้ และเปลี่ยนเป็น 7.0-7.5 หลังจาก 1 ชั่วโมงซึ่งใกล้เคียงกับการเปลี่ยนแปลงที่เกิดขึ้นในระบบการย่อยของมนุษย์ ค่าการเปลี่ยนแปลงของแร่ธาตุในตัวอย่าง blank แสดงในรูปที่ 3.6 พบว่าปริมาณแร่ธาตุต่างๆ มีค่าต่ำคือน้อยกว่า 4 mg L^{-1} สำหรับทุกธาตุ สูงสุดคือฟอสฟอรัสที่ความเข้มข้น 3 ถึง 7 mg L^{-1} เนื่องจากธาตุนี้เป็นองค์ประกอบของเอนไซม์ต่างๆ อย่างไรก็ตามในการศึกษาครั้งนี้ได้ทำการหักลบค่าของ blank ออก

กราฟการเปลี่ยนแปลงของไดอะไลซิสของแร่ธาตุต่างๆ ในตัวอย่างนมผง และคะน้า ที่ได้ทำการศึกษาด้วยระบบ CFD-ICP-OES แสดงอยู่ในรูปที่ 3.7 พบว่ารูปแบบการเปลี่ยนแปลงของไดอะไลซิสมีลักษณะใกล้เคียงกัน มีค่าสูงสุดที่ประมาณ 10 นาทีของการไดอะไลซิส หลังจากนั้นค่อยลดลงจนถึงระดับคงที่ (baseline) การเปลี่ยนแปลงในช่วงประมาณ 30-40 นาทีเกิดขึ้นเนื่องจากผลของการฉีดสารละลาย PBE เข้าไปในระบบ ณ เวลา 30 นาที

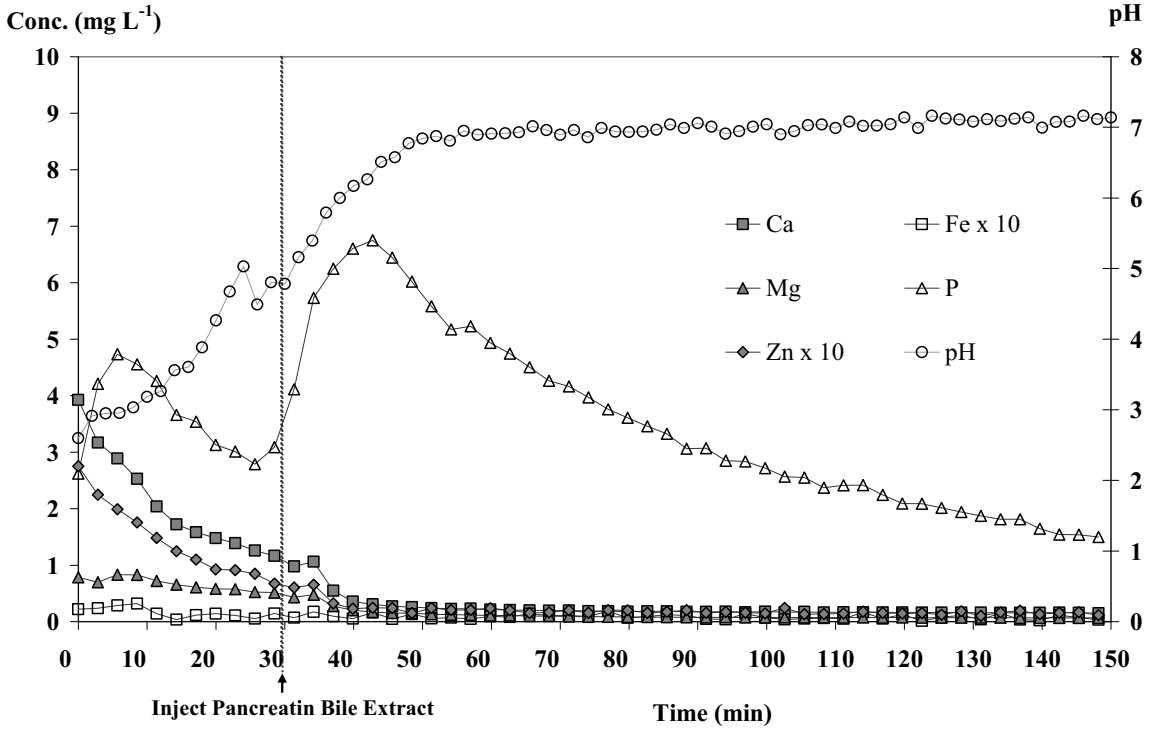

รูปที่ 3.6 กราฟการเปลี่ยนแปลงของไดอะไลซิสของ blank

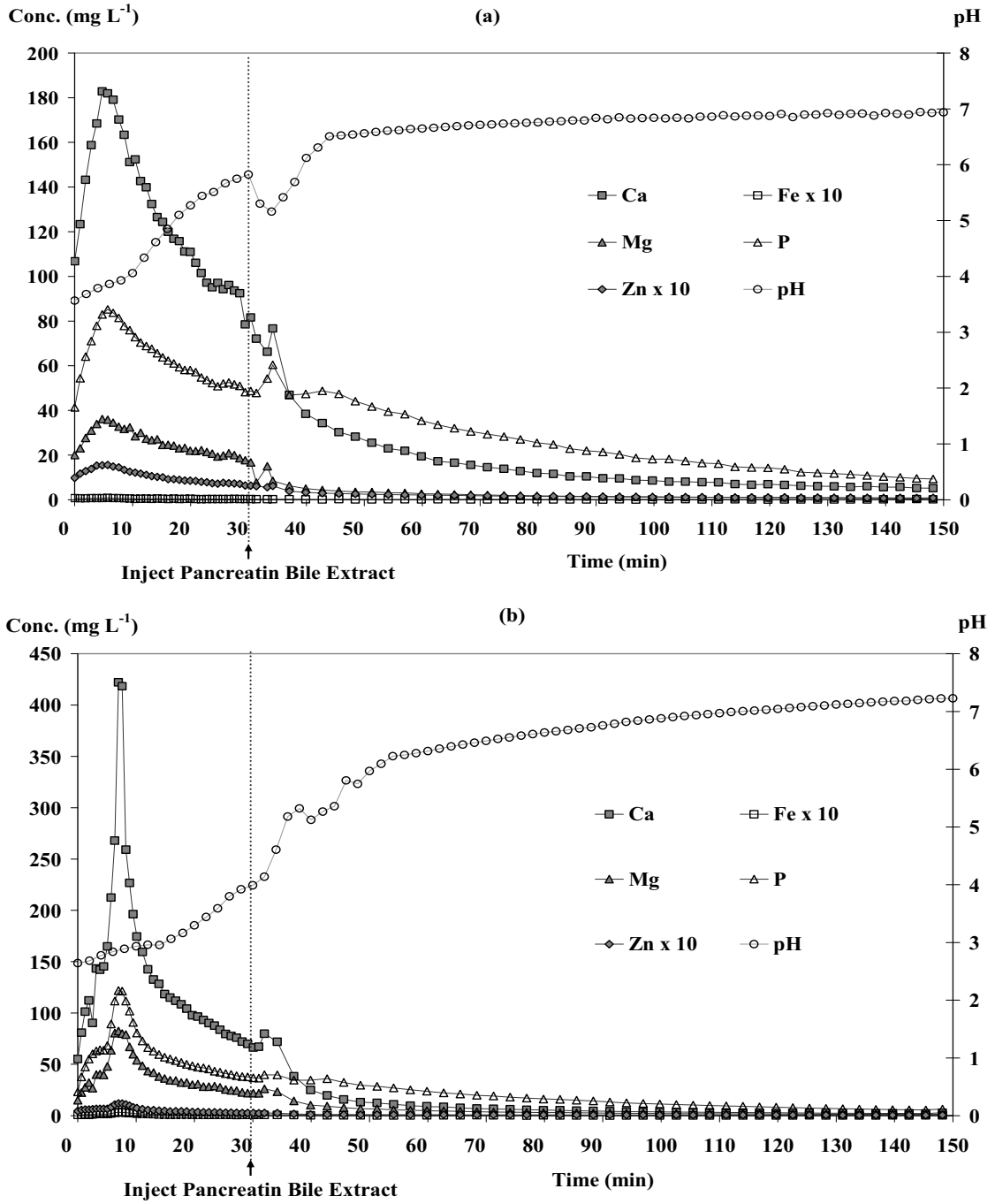

รูปที่ 3.7 กราฟการเปลี่ยนแปลงของไดอะไลซิสของตัวอย่างนมผง (a) และคะน้า (b)

รูปที่ 3.8 แสดงกราฟการเปลี่ยนแปลงของไดอะไลซิสของแคลเซียม (แสดงเป็นตัวแทนของธาตุต่างๆ)ในตัวอย่างอาหารที่ใช้ในการศึกษา พบว่าในตัวอย่างคะน้าและนมผงมีการไดอะไลซ์ได้อย่างรวดเร็วตั้งแต่ช่วงเริ่มต้นจนถึงประมาณ 30 นาที โดยภาพรวมปริมาณการไดอะไลซ์ได้ของแคลเซียมเรียงจากมากไปน้อยแสดงได้คือ คะน้า>นมผง>อาหารเสริมทารก>ชะอม>เนื้อไก่>ข้าวหอมมะลิ>ถั่วเขียว (จากปริมาณ 13867 ถึง 56 $\mu g\ g^{-1}$) ขึ้นกับปริมาณแคลเซียมที่ไดอะไลซ์ได้

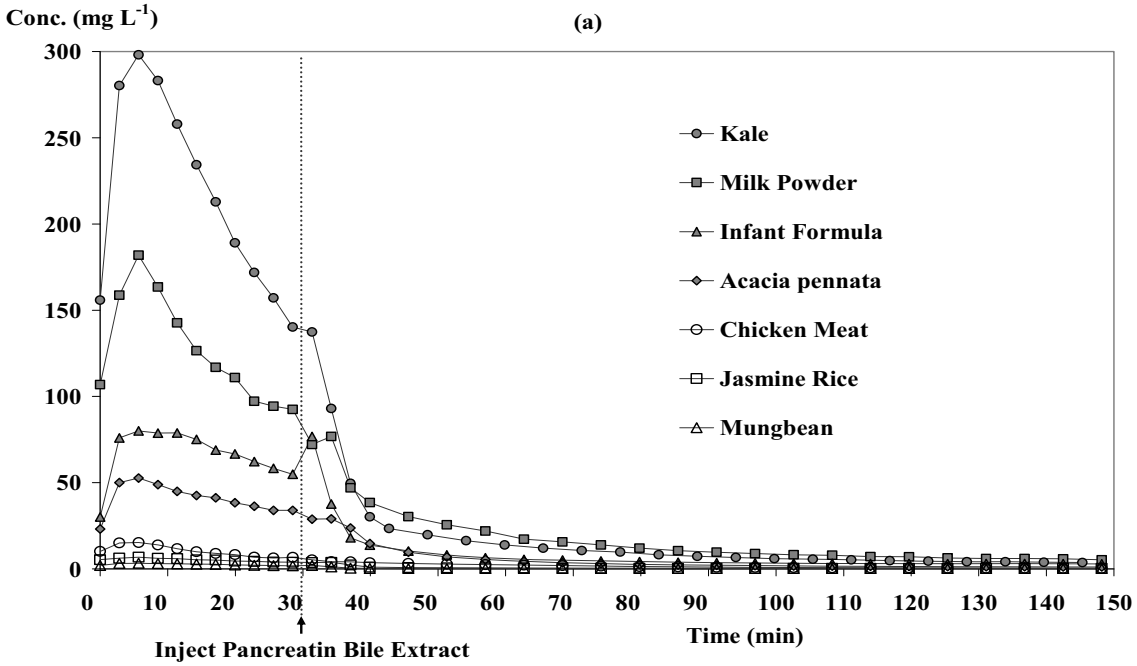

รูปที่ 3.8 กราฟการเปลี่ยนแปลงของไดอะไลซิสของแคลเซียมในตัวอย่างอาหารต่างๆ

3.3.1.6 การประเมินค่าไดอะไลซิสของแร่ธาตุในอาหารชนิดต่างๆ ที่ได้จากการใช้ระบบ CFD-ICP-OES

ค่าความสามารถในการไดอะไลซิส (dialysability) คำนวณได้จากการหาค่าพื้นที่ใต้กราฟของการไดอะไลซ์จากระบบที่พัฒนาขึ้นเทียบกับสารละลายมาตรฐานของแร่ธาตุต่างๆ ตารางที่ 3.7 แสดงปริมาณแร่ธาตุที่วิเคราะห์ได้ทั้งปริมาณแร่ธาตุในอาหารของน้ำหนักแห้ง ปริมาณแร่ธาตุที่ไดอะไลซ์ได้ และส่วนที่เหลือจากการไดอะไลซ์ ปริมาณแร่ธาตุแคลเซียมมีค่าต่ำสุดในตัวอย่างข้าวหอมมะลิ (56 ± 3 $\mu g\ g^{-1}$) และสูงสุดในผักคะน้า (13870 ± 540 $\mu g\ g^{-1}$) ร้อยละของการไดอะไลซิสในตัวอย่างต่างๆ มีค่าระหว่างร้อยละ 61 ถึง 93 ร้อยละส่วนที่เหลือจากการไดอะไลซ์มีค่าร้อยละ 4 ถึง 40 และผลรวมของทั้งสองส่วนมีค่าร้อยละ 94 ถึง 105 ส่วนธาตุอื่นมีค่าดังแสดงในตารางที่ 3.8 โดยสรุปคือการไดอะไลซ์ได้ของแร่ธาตุขึ้นอยู่กับชนิดของตัวอย่างและปริมาณแร่ธาตุที่มีในตัวอย่าง เช่นนมผงและคะน้ามีปริมาณแคลเซียม แมกนีเซียม ฟอสฟอรัส และสังกะสีสูง ส่วนเนื้อไก่มีเหล็กสูง เป็นต้น ร้อยละของการไดอะไลซิสของแคลเซียม แมกนีเซียม และสังกะสีมีค่าตั้งแต่ร้อยละ 36 ถึง 93 ส่วนธาตุฟอสฟอรัสมีค่าแตกต่างกันมากตั้งแต่ $9 \pm 1\%$ ในข้าวสารถึง $56 \pm 3\%$ ในนมผง ในขณะที่ธาตุเหล็กมีค่าไดอะไลซิสต่ำร้อยละ 5-10 เท่านั้น ผลรวมของทั้งส่วนที่ไดอะไลซ์ได้และส่วนที่เหลือจากการไดอะไลซ์ของแร่ธาตุแมกนีเซียม ฟอสฟอรัส เหล็ก และสังกะสีมีค่าในช่วงที่ยอมรับได้คือร้อยละ 82-107, 79-107, 86-103 และ 87-108 ตามลำดับ

ตารางที่ 3.8 ปริมาณแร่ธาตุจากระบบ CFD-ICP-OES ในอาหารชนิดต่างๆ (ต่อน้ำหนักแห้ง) (n=3)

	Jasmine rice	**Chicken meat**	**Mungbean**	**Acacia pennata**	**Milk powder**	**Kale**
Calcium						
Total minerals ($\mu g\ g^{-1}$)	56 ± 3	299 ± 13	819 ± 43	1650 ± 30	6890 ± 120	13870 ± 540
Dialysed minerals ($\mu g\ g^{-1}$)	44 ± 2	279 ± 9	714 ± 35	1220 ± 55	5560 ± 280	8520 ± 430
Non-dialysed minerals ($\mu g\ g^{-1}$)	8 ± 2	12 ± 5	119 ± 27	482 ± 25	1030 ± 30	5520 ± 240
Dialysed + non-dialysed minerals ($\mu g\ g^{-1}$)	52 ± 4	290 ± 13	842 ± 26	1760 ± 91	6580 ± 280	14030 ± 520
Dialysis (%)	78 ± 3	93 ± 3	87 ± 4	74 ± 3	81 ± 4	61 ± 3
Element Retained (%)	14 ± 3	4 ± 2	15 ± 3	31 ± 2	15 ± 0.5	40 ± 2
Sum (%)	94 ± 6	100 ± 4	103 ± 3	105 ± 6	96 ± 4	101 ± 4
Magnesium						
Total minerals ($\mu g\ g^{-1}$)	157 ± 3	878 ± 30	1410 ± 3	1980 ± 12	763 ± 29	4690 ± 310
Dialysed minerals ($\mu g\ g^{-1}$)	95 ± 4	814 ± 13	1050 ± 40	1640 ± 44	628 ± 46	3130 ± 100
Non-dialysed minerals ($\mu g\ g^{-1}$)	34 ± 6	47 ± 2	459 ± 3	417 ± 7	69 ± 3	1470 ± 40
Dialysed + non-dialysed minerals ($\mu g\ g^{-1}$)	129 ± 3	861 ± 14	1507 ± 43	2080 ± 50	697 ± 45	4600 ± 90
Dialysis (%)	60 ± 2	93 ± 2	74 ± 3	84 ± 2	82 ± 6	67 ± 2
Element Retained (%)	22 ± 4	5 ± 0.2	33 ± 0.2	21 ± 1	9 ± 0.4	31 ± 1
Sum (%)	82 ± 2	98 ± 2	107 ± 3	105 ± 2	91 ± 6	98 ± 2
Phosphorus						
Total minerals ($\mu g\ g^{-1}$)	839 ± 41	6060 ± 209	4000 ± 60	8540 ± 220	6610 ± 310	5990 ± 60
Dialysed minerals ($\mu g\ g^{-1}$)	77 ± 8	2720 ± 90	525 ± 13	3250 ± 120	3680 ± 180	3240 ± 210
Non-dialysed minerals ($\mu g\ g^{-1}$)	699 ± 26	2490 ± 340	3750 ± 40	5390 ± 260	1610 ± 30	1840 ± 40
Dialysed + non-dialysed minerals ($\mu g\ g^{-1}$)	776 ± 25	5210 ± 370	4280 ± 60	8630 ± 340	5160 ± 140	5280 ± 60
Dialysis (%)	9 ± 1	45 ± 1	13 ± 0.3	38 ± 1	56 ± 3	54 ± 3
Element Retained (%)	83 ± 3	45 ± 1	94 ± 1	63 ± 3	23 ± 2	31 ± 1
Sum (%)	92 ± 3	90 ± 2	107 ± 1	101 ± 4	79 ± 2	88 ± 1

ตารางที่ 3.8 ปริมาณแร่ธาตุจากระบบ CFD-ICP-OES ในอาหารชนิดต่างๆ (ต่อน้ำหนักแห้ง) (n=3) (ต่อ)

	Jasmine rice	**Chicken meat**	**Mungbean**	**Acacia pennata**	**Milk powder**	**Kale**
Iron						
Total minerals ($\mu g\ g^{-1}$)	3.8 ± 0.1	15.2 ± 0.8	46.8 ± 2.1	113.4 ± 10.2	69.0 ± 1.4	90.9 ± 8.6
Dialysed minerals ($\mu g\ g^{-1}$)	0.2 ± 0.1	0.7 ± 0.2	2.2 ± 0.3	11.8 ± 0.9	3.7 ± 0.7	4.8 ± 0.4
Non-dialysed minerals ($\mu g\ g^{-1}$)	3.2 ± 0.1	14.0 ± 0.3	41.4 ± 1.4	104.9 ± 1.9	55.5 ± 3.1	85.5 ± 2.8
Dialysed + non-dialysed minerals ($\mu g\ g^{-1}$)	3.5 ± 0.1	14.7 ± 0.4	43.6 ± 1.4	116.7 ± 2.7	59.2 ± 3.4	90.4 ± 2.6
Dialysis (%)	6 ± 1	5 ± 1	5 ± 1	10 ± 1	5 ± 1	5 ± 1
Element Retained (%)	84 ± 3	92 ± 2	89 ± 3	92 ± 2	80 ± 4	94 ± 3
Sum (%)	91 ± 3	96 ± 2	93 ± 3	103 ± 2	86 ± 5	100 ± 3
Zinc						
Total minerals ($\mu g\ g^{-1}$)	19.4 ± 0.6	27.5 ± 1.8	29.6 ± 0.4	44.0 ± 3.2	50.7 ± 2.3	32.0 ± 4.0
Dialysed minerals ($\mu g\ g^{-1}$)	10.8 ± 1.3	22.9 ± 0.7	21.3 ± 0.2	15.9 ± 0.6	38.3 ± 1.7	18.2 ± 0.9
Non-dialysed minerals ($\mu g\ g^{-1}$)	6.5 ± 0.7	6.9 ± 0.2	10.4 ± 0.8	22.9 ± 0.8	7.2 ± 0.1	15.1 ± 0.8
Dialysed + non-dialysed minerals ($\mu g\ g^{-1}$)	17.3 ± 1.4	29.8 ± 0.7	31.5 ± 0.6	38.8 ± 0.6	44.3 ± 1.1	32.6 ± 0.8
Dialysis (%)	55 ± 7	83 ± 2	72 ± 1	36 ± 1	76 ± 3	57 ± 3
Element Retained (%)	33 ± 4	25 ± 1	35 ± 3	52 ± 2	14 ± 0.2	47 ± 2
Sum (%)	89 ± 7	108 ± 3	106 ± 2	88 ± 2	87 ± 2	102 ± 3

3.3.2 การใช้ประโยชน์ของข้อมูลที่ได้จากระบบ CFD-ICP-OES ในการศึกษาการดูดซึมได้ของแร่ธาตุในสารเสริมแร่ธาตุ [Judprasong et al., 2007]

3.3.2.1 การประเมินความสามารถในการไดอะไลซิสและการตรวจสอบความใช้ได้ของวิธี

เช่นเดียวกับในตอนที่แล้วเนื่องจากไม่มีตัวอย่างสารมาตรฐาน (reference material) เกี่ยวกับการดูดซึมได้ของแร่ธาตุ ดังนั้นการตรวจสอบความใช้ได้ (validation) ของระบบ CFD-ICP-OES ของตัวอย่างแร่ธาตุที่เติมลงในอาหารในรูปฟอร์มต่างๆ (mineral fortificants) จึงจำเป็นที่ต้องศึกษา ทำโดยการศึกษา %recovery ของแร่ธาตุทั้งหมด (แคลเซียม เหล็ก และสังกะสี) ทำการวิเคราะห์หาปริมาณแร่ธาตุทั้งส่วนที่ไดอะไลซ์ได้ (dialysate) จากระบบ CFD และส่วนที่เหลือจากการไดอะไลซ์ (non-dialysable, retentate) แล้วนำทั้งสองส่วนไปวิเคราะห์หาปริมาณแร่ธาตุต่างๆ ด้วยเครื่อง ICP-OES ได้ผลการวิเคราะห์

ดังแสดงในตารางที่ 3.9 พบว่าผลรวมของส่วนที่ไดอะไลซ์ได้ และส่วนที่เหลือจากการไดอะไลซ์มีค่าใกล้เคียงกับปริมาณแร่ธาตุทั้งหมด ซึ่งมี %recovery ในช่วงร้อยละ 94.5-102.8 โดยมีค่าความแม่น (repeatability, RSD) ของธาตุทั้งสาม (Ca, Fe, Zn) น้อยกว่าร้อยละ 3

ร้อยละของความสามารถในการไดอะไลซ์ของแคลเซียมในสารเสริมแคลเซียม (calcium fortificants) ในรูปฟอร์มต่างๆ มีค่าไม่แตกต่างกันอยู่ในช่วงประมาณร้อยละ 75-80 พบสูงสุดในรูปของแคลเซียมซิเตรต (calcium citrate, 81.8$\pm$2.5%) ส่วนของสารเสริมสังกะสี (zinc fortificants) มีค่าตั้งแต่ร้อยละ 45.0$\pm$2.2 ในรูปของสารประกอบสังกะสี-กรดอะมิโน (zinc amino complex) จนถึงร้อยละ 53.1$\pm$2.7 ในรูปของสังกะสีซัลเฟต (zinc sulphate) สำหรับรูปฟอร์มต่างๆ ของสารเสริมธาตุเหล็ก (iron fortificants) มีค่าความสามารถในการไดอะไลซ์แตกต่างกัน เหล็ก(II)ซัลเฟต (iron(II)sulphate), เหล็ก(II)แล็คเตส (iron(II)lactate) และเหล็ก(II)ฟูเมอเรท (iron(II)fumarate) มีค่าร้อยละ 41-45 ซึ่งไม่แตกต่างกัน ส่วนสารเสริมเหล็กในรูปของ NaFe(III)EDTA มีค่าความสามารถในการไดอะไลซ์สูงสุด (81.3$\pm$2.2%) ทั้งนี้สามารถอธิบายจากค่า stability ระหว่างสารประกอบ iron-EDTA (log K of 25.7 for Fe(III) and 14.3 for Fe(II) [Hurrell RF, 1997; Furia TE, 1980]) ค่าความสามารถในการเกิดสารเชิงซ้อนระหว่าง EDTA กับโลหะขึ้นอยู่กับค่า effective stability constant (K_{eff}) ณ ค่า pH หนึ่งๆ โดยค่า K_{eff} นี้สามารถคำนวณได้ ณ ที่ความเป็นกรดด่างต่างๆ เช่น K_{eff} ของ EDTA และ Fe(III) มีค่า 12.3 ที่ความเป็นกรดด่าง 2, 19.2 ที่ความเป็นกรดด่าง 5, 22.4 ที่ความเป็นกรดด่าง 7 และ 25.7 ที่ความเป็นกรดด่าง 12 นอกจากนั้นยังมีค่าสูงสุดเมื่อเปรียบเทียบกับธาตุอื่นๆ คือทองแดง Cu(II) (log K 18.8), สังกะสี Zn(II) (log K 16.5) และแคลเซียม Ca(II) (log K 10.7) ดังนั้นเมื่อ EDTA อยู่ในสภาวะความเป็นกรดด่างของกระเพาะอาหาร จึงคาดได้ว่าเกิดเป็นสารประกอบระหว่าง EDTA กับ Fe(III) และป้องกันการตกตะกอนของ Fe(III) ในอาหารเมื่อค่า pH สูงขึ้น [Hurrell RF, 1997]

ตารางที่ 3.9 ผลการตรวจสอบความใช้ได้ของตัวอย่างสารเสริมแร่ธาตุ Ca, Fe และ Zn mineral fortificants (n=3)

สารเสริมแร่ธาตุ (Fortificants)	ความเข้มข้นของแร่ธาตุ (μg g^{-1} fortificant)[a]			
	ปริมาณทั้งหมด	ส่วนที่ไดอะไลซ์ได้ (Dialysed)	ส่วนที่เหลือจากการไดอะไลซ์ (Non-dialysed)	Dialysed + Non-dialysed
Calcium fortificants:				
Calcium carbonate	4890 ± 270	3630 ± 100 (74.2 ± 2.1)	1130 ± 210 (23.2 ± 4.2)	4750 ± 170 (98.8 ± 4.9)
Tri-calcium phosphate	4460 ± 260	3360 ± 110 (75.3 ± 2.5)	970 ± 110 (21.7 ± 2.5)	4340 ± 50 (95.7 ± 3.5)
Calcium lactate gluconate	3740 ± 270	2940 ± 90 (78.6 ± 2.4)	710 ± 80 (19.0 ± 2.2)	3660 ± 50 (96.5 ± 3.1)
Calcium citrate	4050 ± 230	3310 ± 100 (81.8 ± 2.5)	740 ± 90 (18.3 ± 2.1)	4060 ± 60 (99.0 ± 3.1)
Iron fortificants:				
Fe(II) sulphate	1200 ± 84	507 ± 16 (42.4 ± 1.3)	660 ± 15 (54.8 ± 1.3)	1170 ± 25 (97.3 ± 2.0)
Fe(II) fumarate	1280 ± 33	524 ± 16 (40.9 ± 1.2)	680 ± 6 (53.2 ± 1.0)	1210 ± 15 (94.5 ± 1.1)
Fe(II) lactate	1350 ± 53	609 ± 19 (45.0 ± 1.4)	751 ± 35 (55.5 ± 2.6)	1360 ± 44 (100.5 ± 3.3)
Sodium iron EDTA	1340 ± 50	1090 ± 30 (81.3 ± 2.2)	287 ± 20 (21.5 ± 1.0)	1380 ± 30 (102.8 ± 2.2)
Fe(III) ammonium citrate	1440 ± 54	364 ± 10 (25.2 ± 0.7)	994 ± 76 (73.5 ± 5.6)	1360 ± 78 (100.4 ± 5.8)
Zinc fortificants:				
Zinc sulphate	683 ± 9	363 ± 19 (53.1 ± 2.7)	323 ± 21 (48.1 ± 3.1)	692 ± 26 (101.2 ± 3.8)
Zinc oxide	1124 ± 20	516 ± 27 (46.1 ± 2.4)	586 ± 18 (52.4 ± 1.6)	1002 ± 39 (98.4 ± 3.4)
Zinc amino complex	1140 ± 30	514 ± 25 (45.0 ± 2.2)	577 ± 24 (50.5 ± 2.0)	1090 ± 20 (95.5 ± 1.6)

[a]ค่าที่อยู่ในวงเล็บแสดงความเข้มข้นของแร่ธาตุ

3.3.2.2 กราฟการเปลี่ยนแปลงของการไดอะไลซิส

ระบบไดอะไลซิสทั่วไป โดยเฉพาะในระบบ batch dialysis ให้คำตอบเฉพาะในเรื่องของค่าไดอะไลซิสเท่านั้น ส่วนในระบบการไหลแบบต่อเนื่อง (continuous-flow dialysis) นั้นให้ข้อมูลเพิ่มขึ้นมากกว่าคือได้ข้อมูลของการเปลี่ยนแปลงแร่ธาตุระหว่างไดอะไลซิส และข้อมูลการเปลี่ยนแปลงในช่วงเวลาต่างๆ (time-based dialysis profile) ระบบ CFD-ICP-OES ที่พัฒนาขึ้นนี้มีข้อมูลของกราฟสองรูปแบบ คือ การเปลี่ยนแปลงของแร่ธาตุและความเป็นกรดด่างระหว่างไดอะไลซิส (dialysis profiles and pH change) ดังแสดงในรูปที่ 3.9 (ด้านบน) และการเปลี่ยนแปลงแบบสะสมในช่วงเวลาต่างๆ (time-dependent cumulative plot) ดังแสดงในรูปที่ 3.9 (ด้านล่าง) ซึ่งข้อมูลของกราฟระหว่างความเข้มข้นของแร่ธาตุต่างๆ ที่ไดอะไลซ์ได้เทียบกับเวลา ให้ข้อมูลในเชิงจลนศาสตร์ (kinetic information) ค่าอัตราการไดอะไลซิสสามารถคำนวณได้จากค่าความชัน (slope) ของกราฟระหว่างไดอะไลซิส

ค่า pH เปลี่ยนแปลงจากประมาณ 2.0 เป็นประมาณ 5.0 ภายใน 30 นาที และเปลี่ยนเป็น 7.0-7.5 หลังจาก 1 ชั่วโมงดังแสดงในรูปที่ 3.9 (ด้านบน) ส่วนกราฟสะสมของปริมาณเหล็กที่ไดอะไลซ์ได้แสดงอยู่ด้านล่าง พบว่าธาตุเหล็กที่ไดอะไลซ์ได้เพิ่มขึ้นอย่างรวดเร็วในช่วงก่อนฉีดเอนไซม์ PBE แล้วเพิ่มขึ้นอีกเล็กน้อย และสุดท้ายก็คงที่ ร้อยละของไดอะไลซิสสามารถคำนวณได้จากความชันของกราฟนี้ (กราฟด้านล่าง ขวามือ) ผลของสารต่างๆ ที่มีผลต่อการไดอะไลซิสสามารถแสดงได้อย่างชัดเจนด้วยกราฟนี้ เช่นในรูปที่ 3.9 ด้านล่าง พบว่าวิตามินซี (ascorbic acid) แสดงผลของการส่งเสริมการดูดซึมธาตุเหล็กโดยเฉพาะในช่วงหลังจาก 20 นาที (ความเป็นกรดด่างมากกว่า 4) หลังจากไดอะไลซิส นอกจากนั้นจะเห็นได้ว่าการไดอะไลซ์ของธาตุเหล็กไม่เปลี่ยนแปลงเมื่อความเป็นกรดด่างมีค่ามากกว่า 6 ในทั้งกรณีที่มีและไม่มี ascorbic acid เป็นผลให้ธาตุเหล็กในรูปของซัลเฟตที่มีการเติมวิตามินซีมีค่าไดอะไลซิสร้อยละ 63 เมื่อเปรียบเทียบกับที่ไม่มีการเติมวิตามินซี (ร้อยละ 49) กราฟที่แสดงทั้งสองแบบนี้จะใช้ในการศึกษาการดูดซึมได้ของแร่ธาตุ รวมทั้งผลของสารส่งเสริมและสารยับยั้งการดูดซึม

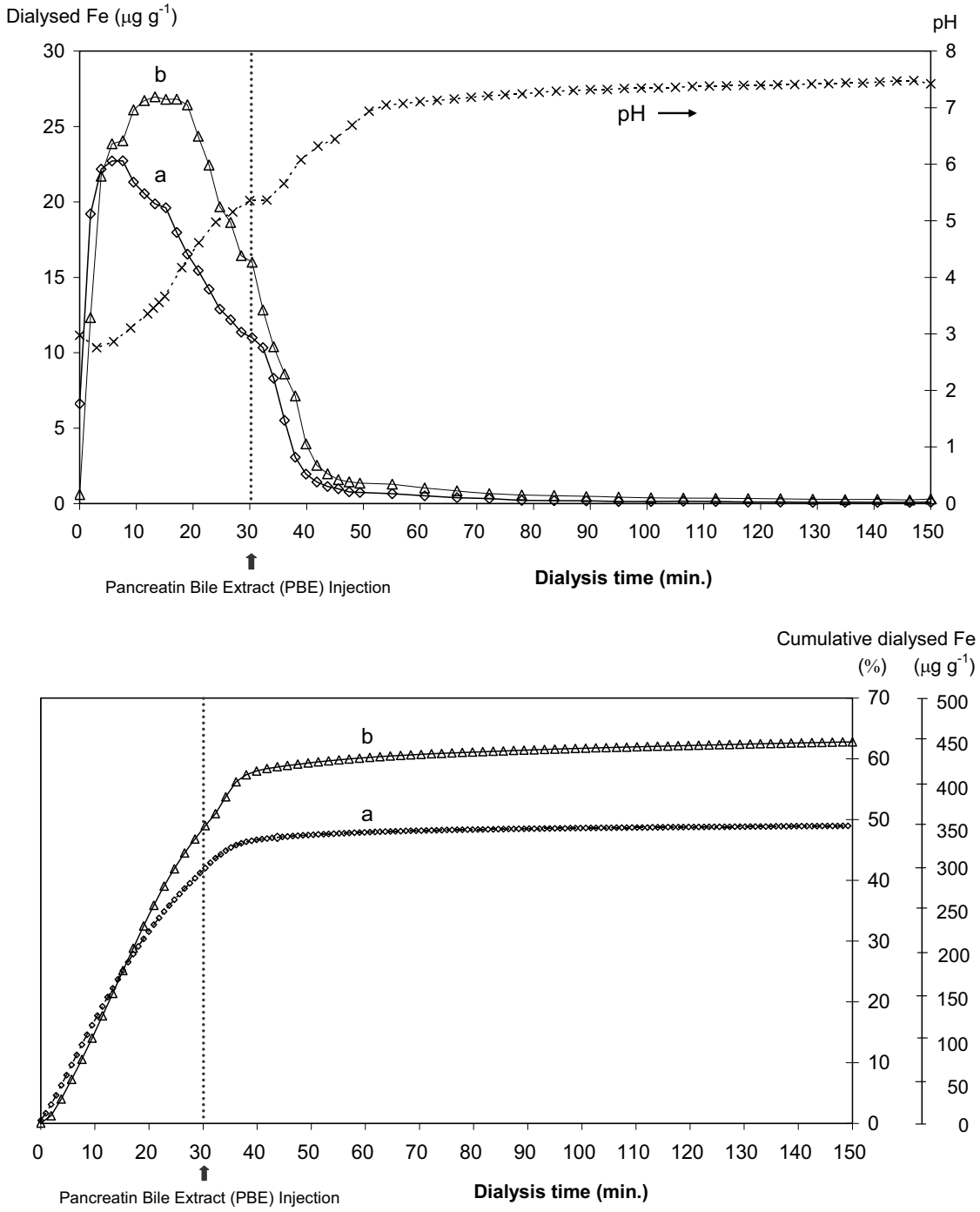

รูปที่ 3.9 กราฟการเปลี่ยนแปลงของไดอะไลซิสของธาตุเหล็กและค่า pH (รูปด้านบน) และกราฟการเปลี่ยนแปลงแบบสะสมในช่วงเวลาต่างๆ (cumulative plot) ของธาตุเหล็กและร้อยละของไดอะไลซิส (รูปด้านล่าง) สำหรับ $FeSO_4$ ที่ไม่มี ascorbic acid (a) และมี ascorbic acid (b)

3.3.2.3 กราฟการเปลี่ยนแปลงของไดอะไลซิสของธาตุเหล็กในสารเสริมธาตุเหล็กรูปฟอร์มต่างๆ ที่มีการเติมสารส่งเสริมและสารยับยั้งการดูดซึม

สารเสริมแร่ธาตุเหล็ก แคลเซียมและสังกะสี มีการใช้กันอย่างกว้างขวางในผลิตภัณฑ์อาหารที่เสริมแร่ธาตุต่างๆ ได้ทำการศึกษาทั้งสารเสริมธาตุเหล็ก (iron fortificants) สารเสริมธาตุแคลเซียม (calcium fortificants) และสารเสริมสังกะสี (zinc fortificants) แต่เพื่อให้เห็นภาพได้ชัดเจนของการใช้ข้อมูลที่ได้จากระบบ online CFD-ICP-OES จึงขอนำเสนอเฉพาะในส่วนที่เป็นสารเสริมธาตุเหล็กเท่านั้น

สารเสริมธาตุเหล็กที่นิยมใช้มีหลายรูปฟอร์ม แต่ที่ใช้ในการศึกษาครั้งนี้คือเหล็กในรูปของ Fe(II) sulphate, Fe(II) fumarate, NaFe(III)EDTA, Fe(II) lactate และ Fe(III) ammonium citrate เนื่องจากความสามารถในการดูดซึม ราคาไม่สูงมาก และมีการใช้กันมาก กราฟการเปลี่ยนแปลงของธาตุเหล็กที่ไดอะไลซ์ได้ และการเปลี่ยนแปลงค่า pHในรูปฟอร์มของสารเสริมเหล็กต่างๆ แสดงในรูปที่ 3.10 พบว่าสามารถแบ่งได้เป็น 3 กลุ่มตามร้อยละของการไดอะไลซ์คือกลุ่มที่มีค่าระดับต่ำ (ร้อยละ 25 สำหรับ Fe(III) ammonium citrate) ระดับกลาง (ร้อยละ 41-45% สำหรับ Fe(II) sulphate, Fe(II) fumarate และ Fe(II) lactate) และระดับสูง (ร้อยละ 81 สำหรับ NaFe(III)EDTA) กราฟการเปลี่ยนแปลงของไดอะไลซิสของธาตุเหล็กในรูปของ Fe(III) ammonium citrate พบว่ามีอัตราการไดอะไลซิสต่ำในช่วง 30 นาทีแรกและคงที่ในที่สุด ทำให้มีค่าไดอะไลซิสเพียงร้อยละ 25.2 เท่านั้น ส่วนกราฟการเปลี่ยนแปลงของไดอะไลซิสของธาตุเหล็กในรูปของ Fe(II) sulphate, Fe(II) lactate และ Fe(II) fumarate มีค่าไดอะไลซิสร้อยละ 42, 45 และ 41 ตามลำดับ แต่จะเห็นได้ว่ากราฟเหล่านี้มีความซับซ้อนมากขึ้นเมื่อมีหลายรูปแบบของการเปลี่ยนแปลง ดังนั้นจึงได้มีการประมวลข้อมูลให้สามารถเข้าใจได้ง่ายด้วยการทำเป็นกราฟการเปลี่ยนแปลงของไดอะไลซิสของธาตุเหล็กในรูปของการสะสมปริมาณ (cumulative plot) ดังแสดงอยู่ในรูปที่ 3.10 (ด้านล่าง) ซึ่งแสดงทั้งปริมาณธาตุเหล็ก ($\mu g\ g^{-1}$) และร้อยละของการไดอะไลซิสของสารเสริมธาตุเหล็กในรูปฟอร์มต่างๆ ความชันของกราฟที่ได้นี้สามารถบ่งบอกถึงอัตราการไดอะไลซ์ของธาตุเหล็กในตัวอย่าง อัตราการไดอะไลซ์ก่อนฉีดเอนไซม์ PBE มีค่าสูง และแตกต่างกันไปตามชนิดของสารเสริมธาตุเหล็ก สารเสริมธาตุเหล็กในรูปของ NaFe(III)EDTA มีค่าการไดอะไลซ์สูงสุด (ร้อยละ 81) ในขณะที่สารเสริมธาตุเหล็กในรูปของ Fe(III) ammonium citrate มีค่าต่ำสุด (ร้อยละ 25) ทั้งนี้เนื่องจากค่าคงที่ (stability constant) ของสารประกอบ EDTA และ citrate กับเหล็ก(III) มีค่าแตกต่างกันมาก (log K = 25.7 and 11.8, respectively [Furia TE, 1980]) นอกจากนั้นยังเห็นชัดเจนได้จากอัตราการไดอะไลซ์ในช่วงระหว่าง 0-30 นาทีในรูปฟอร์มของ NaFe(III)EDTA มีค่าสูงสุดในขณะที่ Fe(III) ammonium citrate มีค่าต่ำสุด ในขณะที่รูปฟอร์มอื่นมีอัตราไดอะไลซ์อยู่ระหว่างนี้ การเปลี่ยนจากเหล็ก(II) ไปเป็นเหล็ก(III) แล้วตกตะกอนเป็น $Fe(OH)_3$ นั้นเกิดขึ้นที่ค่า pH มากกว่า 4 [Salovaara et al., 2003] ดังนั้นความสามารถในการไดอะไลซ์ของสารเสริมธาตุเหล็กรูปฟอร์มต่างๆ มีค่าคงที่หรือหยุดการไดอะไลซ์หลังจากเวลาผ่านไป 30 นาที (ค่า pHประมาณ 5) ยกเว้นรูปฟอร์มของ NaFe(III)EDTA ซึ่งพบอัตราการไดอะไลซ์สูงสุดตั้งแต่เริ่มกระบวนการไดอะไลซิส นอกจากนั้นหลังจากฉีด PBE แล้ว (ค่า pHประมาณ 5-7) รูปฟอร์มนี้ยังคงไดอะไลซ์ได้อย่างต่อเนื่อง ร้อยละ

ของไดอะไลซิสของฟอร์มนี้ในช่วงก่อนฉีด PBE นั้นมีค่าสูงถึงร้อยละ 58 เมื่อเทียบกับทั้งหมดที่ไดอะไลซ์ได้ (ร้อยละ 81)

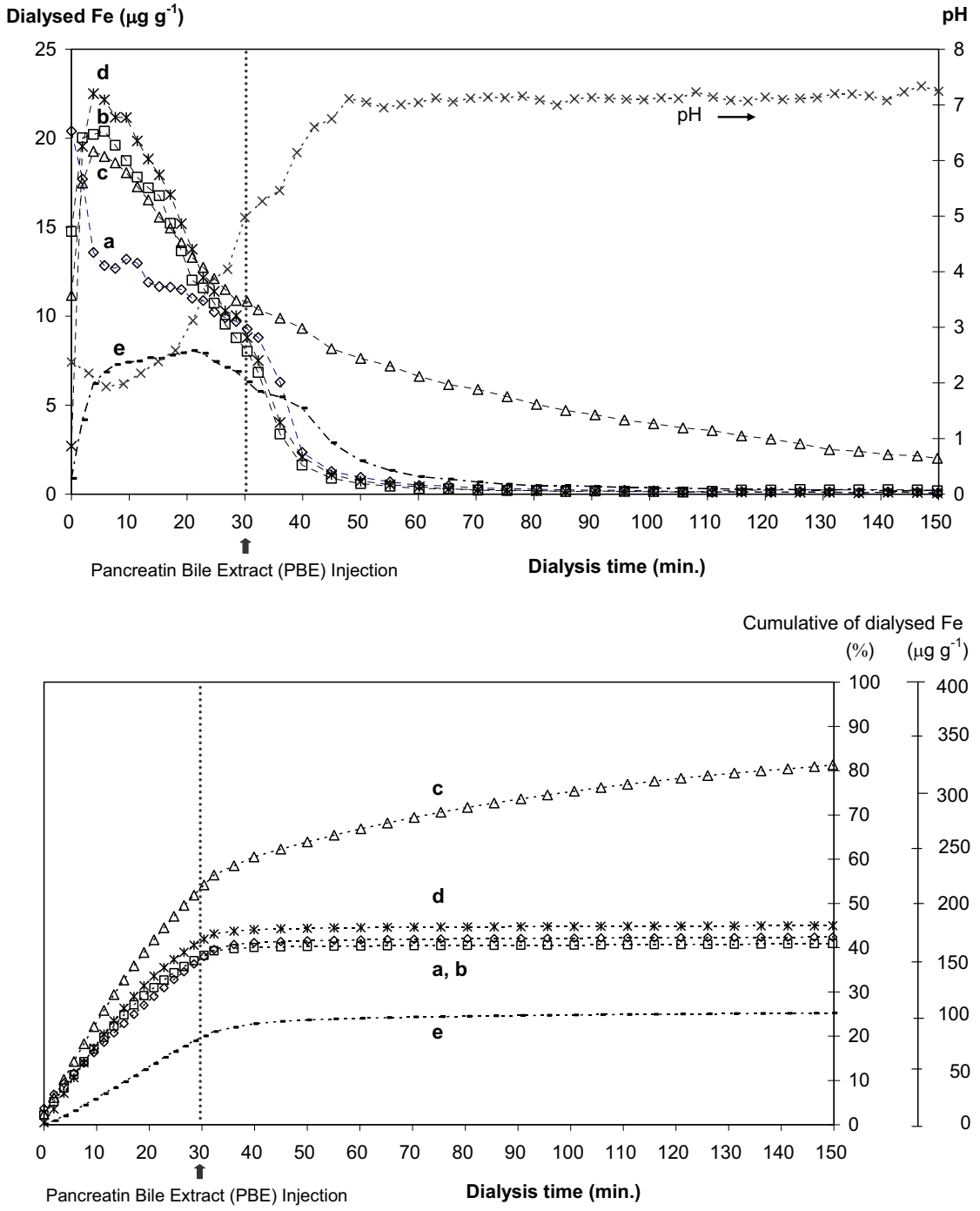

รูปที่ 3.10 กราฟการเปลี่ยนแปลงของไดอะไลซิสของธาตุเหล็ก และค่า pH (รูปด้านบน) และกราฟการเปลี่ยนแปลงแบบสะสมในช่วงเวลาต่างๆ (cumulative plot) ของธาตุเหล็กและร้อยละของไดอะไลซิส (รูปด้านล่าง) ในสารเสริมธาตุเหล็กในรูปฟอร์มต่างๆ a) Fe(II) sulphate b) Fe(II) fumarate c) NaFe(III)EDTA d) Fe(II) lactate และ e) Fe(III) ammonium citrate

หลายรายงานที่ได้ศึกษาถึงผลของกรดอินทรีย์ต่างๆ (Organic acids) ที่มีผลต่อการดูดซึมได้ของธาตุเหล็ก พบว่าวิตามินซีมีผลส่งเสริมการดูดซึมของธาตุเหล็กในรูปที่เป็น non-heme iron ทั้งที่เป็นสารในธรรมชาติและสารสังเคราะห์ [Hallberg and Brune, 1986] ทั้งการศึกษาในแบบหลอดทดลอง (*in vitro*) [Nayak and Nair, 2003, Salovaara et al., 2003] และในแบบการทดลองกับสิ่งมีชีวิต (*in vivo*) [Siengenberg et al.,1991; 50] ดังนั้นจึงมีการเติมวิตามินซีในผลิตภัณฑ์อาหารหลายชนิดเพื่อป้องกันผลที่เกิดจากสารยับยั้งการดูดซึมประเภทไฟเตทที่พบมาในพืชผักชนิดต่างๆ มีการศึกษาพบว่ากรดซิตริก (Citric acid) ที่เติมลงในอาหารทดสอบที่มีข้าวและถั่วเหลืองเป็นองค์ประกอบหลัก มีผลเพิ่มการดูดซึมของธาตุเหล็ก 2-3 เท่า [Gillooly et al, 1983, Derman et al., 1987] สารประกอบเหล่านี้ได้ใช้ในการศึกษาของสารส่งเสริมและสารยับยั้งการดูดซึมของธาตุเหล็ก รูปที่ 3.11 (ด้านบน) แสดงการเปลี่ยนแปลงของไดอะไลซิสของธาตุเหล็ก และค่า pHของเหล็กในรูปของ Fe(II) sulphate ที่มีการเติมสารเสริมการดูดซึม (วิตามินซี กรดซิตริก) และสารยับยั้งการดูดซึม (กรดไฟติก แทนนิค และออกซาลิค) ที่สัดส่วนต่อธาตุเหล็กคือ 3:1 ถึง 4:1 ดังการศึกษาของ Lynch และ Stoltzfus [Lynch and Stoltzfus, 2003] จากการศึกษาพบว่าสารที่เติมลงในอาหาร (additives) มีผลอย่างมากต่อการเปลี่ยนแปลงของไดอะไลซิสของธาตุเหล็กในรูปของ Fe(II) sulphate โดยเฉพาะวิตามินซี เห็นได้ชัดในช่วงแรก (0-30 นาที) ของการไดอะไลซิส ทั้งนี้เนื่องจากวิตามินซีลดอัตราการเปลี่ยนฟอร์มจาก Fe(II) ไปเป็น Fe(III) เมื่อค่า pH มีค่าสูงขึ้น วิตามินซีจะแสดงบทบาทนี้ได้ดีเมื่อค่า pH มีค่าน้อยกว่า 6.0 ถึง 6.8 เมื่อค่า pH สูงกว่านี้วิตามินซีจะไม่สามารถแสดงบทบาทนี้ [Derman et al., 1987] นอกจากนี้วิตามินซียังเกิดเป็นสารประกอบที่ละลายน้ำได้ (soluble complexes) กับเหล็กเมื่อค่า pH มีค่าต่ำทำให้สารประกอบนี้ยังคงละลายน้ำได้และดูดซึมได้ แต่เมื่อค่าเป็นกรดด่างสูงขึ้นดังที่พบในบริเวณลำไส้เล็ก [Hurrell RF, 1997] ทำให้เกิดการเปลี่ยนจาก Fe(II) ไปเป็น $Fe(OH)_3$ ดังจะเห็นได้จากการหยุดการไดอะไลซ์ของเหล็ก(II)ซัลเฟตที่เติมวิตามินซี เมื่อค่า pH มากกว่า 6 (รูปที่ 3.11 รูปด้านบน) อัตราการไดอะไลซ์ของเหล็ก(II)ซัลเฟตที่เติมวิตามินซีและกรดซิตริกในช่วง 0-40 นาที (ค่า pH น้อยกว่า 6) มีค่าสูงมากกว่าที่ไม่ได้มีการเติมวิตามินซีและกรดซิตริก (รูปที่ 3.11 รูปด้านล่าง) ซึ่งเห็นได้อย่างชัดเจนว่าสามารถแบ่งแยกความแตกต่างระหว่างสารเพิ่มการดูดซึมและสารยับยั้งการดูดซึมของธาตุเหล็ก ส่วนผลการเพิ่มอัตราการไดอะไลซิสในช่วงก่อนฉีด PBE เมื่อเติมสารเพิ่มการดูดซึมพบได้ชัดในกรณีของวิตามินซี ในขณะที่กรดซิตริกแสดงบทบาทชัดเจนในช่วงหลังฉีด PBE ทั้งนี้เนื่องจากคุณสมบัติในการ chelate ของกรดซิตริกด้วยหมู่ carboxylic และ hydroxyl ที่ช่วยป้องกันไม่ให้ธาตุเหล็กเปลี่ยนไปเป็น iron hydroxides ซึ่งไม่สามารถละลายน้ำได้ และยังทำให้เกิดเป็นสารประกอบ Fe(III)-citrate ที่ยังคงละลายน้ำได้ [Salovaara et al., 2003] นอกจากนั้นจะเห็นได้จากการที่ค่าคงที่ (log K, stability constant) ของเหล็ก(III)กับกรดซิตริกสูงกว่ากรณีของเหล็ก(II) คือ 11.8 และ 3.2 ตามลำดับ ดังนั้นกรดซิตริกจึงสามารถเกิดสารประกอบได้กับทั้งเหล็ก(II) และเหล็ก(III) ที่ความเป็นกรดด่างประมาณ 3-4 เหล็ก(II) สามารถเกิดเป็น tridentate complex กับกรดซิตริก $[Fe(II)\ cit]^-$ ด้วยหมู่ carboxylic 2 ตัวและหมู่ hydroxyl 1 หมู่ กระบวนการ oxidation และ hydrolysis ของเหล็ก(II) ทำให้เกิดเป็นสารประกอบ tridentate ferric-citrate $[Fe(III)OH\ cit]^-$ ซึ่งจะถูกไฮโดรไลซ์ไปเป็นสารประกอบ bidentate, $[Fe(III)OH2\ cit]^{2-}$ ที่ละลายน้ำได้ [Salovaara et al., 2003]

ในทางตรงกันข้าม ในกรณีที่มีสารยับยั้งการดูดซึมธาตุเหล็ก สารที่มีการศึกษากันมานานแล้วพบว่ามีผลชัดเจนคือกรดไฟติก (phytic acid) พบว่าถ้าเติมกรดไฟติกลงในเหล็ก(II)ซัลเฟต ปริมาณเหล็กที่ไดอะไลซ์ได้ต่ำมากกว่าที่ไม่ได้เติมโดยเฉพาะในช่วง 0-30 นาทีแรกของไดอะไลซิส (รูปที่ 3.11d ด้านล่าง) ทั้งนี้เนื่องจากกรดไฟติกมีประจุลบ (negatively charged) สามารถทำปฏิกิริยากับประจุบวกของเหล็กทำให้เหล็กดูดซึมได้ลดลง หลังจากฉีด PBE เข้าไปพบว่ากราฟการเปลี่ยนแปลงของปริมาณธาตุเหล็กระหว่างไดอะไลซิสของเหล็ก(II)ซัลเฟตที่เติมกรดออกซาลิก (oxalic acid) แสดงว่าไดอะไลซ์ได้น้อยลงเช่นกัน (รูปที่ 3.11f) ค่าคงที่ (log K, stability constant) ของกรดออกซาลิกกับเหล็ก(III) มีค่า 9.4 โดยเมื่อพิจารณาที่ค่า effective stability constants (log K_{eff}) ที่ค่า pH 5, 6 และ 7 มีค่า 2.9, 4.7 และ 6.1 ตามลำดับ [Furia TE, 1980] ด้วยเหตุนี้เหล็กที่เกิดสารประกอบกับออกซาลิกจึงยังคงไดอะไลซ์ได้แม้ว่าค่า pH มีค่ามากกว่า 5

ผลของความสามารถในการไดอะไลซ์ได้ของธาตุเหล็กที่มีสารส่งเสริมและสารยับยั้งการดูดซึมแสดงอยู่ในตารางที่ 3.10 โดยแสดงค่าเหล็กที่ไดอะไลซ์ได้เป็น สองช่วงคือช่วงก่อน และช่วงหลังการฉีด PBE เข้าไปในระบบ CFD เพื่อติดตามพฤติกรรมของสารที่ใช้ในศึกษาปริมาณธาตุเหล็กในรูปเหล็กซัลเฟตที่มีการเติมวิตามินซี และกรดซิตริก พบว่ามีค่าไดอะไลซิสร้อยละ 62.8$\pm$1.6 และ 61.9$\pm$2.3 ตามลำดับ ในช่วงก่อนฉีด PBE ผลของวิตามินซีส่งผลเพิ่มการไดอะไลซ์ได้ชัดเจนมากกว่ากรดซิตริก (ร้อยละ 48.8 กรณีที่เติมวิตามินซี ร้อยละ 42.9 กรณีที่เติมกรดซิตริก เปรียบเทียบกับร้อยละ 41.6 ในกรณีที่เป็นเหล็กซัลเฟตที่ไม่ได้เติมสารใด) ในช่วงหลังฉีด PBE วิตามินซีกลับแสดงผลการส่งเสริมการไดอะไลซ์ของเหล็กได้น้อยกว่ากรดซิตริก (ร้อยละ 14.0 และ 18.9 เปรียบเทียบกับร้อยละ 7.4 กรณีที่ไม่เติมสารใด) สำหรับกรณีที่เติมกรดไฟติกพบว่ามีค่าไดอะไลซิสต่ำกว่าที่ไม่ได้เติมประมาณครึ่งหนึ่ง ในขณะที่การเติมกรดแทนนิก และกรดออกซาลิก ส่งผลลดการไดอะไลซ์เล็กน้อย (ประมาณร้อยละ 40 เปรียบเทียบกับร้อยละ 49 ที่ไม่ได้เติมสารใด) โดยสรุปความสามารถในการไดอะไลซ์ของธาตุเหล็กในฟอร์มเหล็ก(II)ซัลเฟต เรียงลำดับจากมากไปน้อยดังนี้คือกรณีที่เติมวิตามินซี (ร้อยละ 63) > กรณีเติมกรดซิตริก (ร้อยละ 62) > ไม่ได้เติมสารใด (ร้อยละ 49) > กรณีเติมกรดออกซาลิก (ร้อยละ 41) > กรณีเติมกรดแทนนิก (ร้อยละ 38) > กรณีเติมกรดไฟติก(ร้อยละ 21)

ตารางที่ 3.10 ปริมาณธาตุเหล็กทั้งหมดและเหล็กที่ไดอะไลซ์ได้ในเหล็ก(II)ซัลเฟต ที่มีการเติมสารส่งเสริมและสารยับยั้งการดูดซึม (n=3)

Iron fortificants	**Fe(II) sulphate ($FeSO_4$)**	**$FeSO_4$ with ascorbic acid**	**$FeSO_4$ with citric acid**	**$FeSO_4$ with phytic acid**	**$FeSO_4$ with tannic acid**	**$FeSO_4$ with oxalic acid**
Total Fe in each study is 1210 ± 24 ($\mu g\ g^{-1}$)						
Dialysed Fe ($\mu g\ g^{-1}$) and percent dialysis (%)						
- Before 30 min	502 ± 20 (41.6)[a]	589 ± 15 (48.8)	518 ± 19 (42.9)	225 ± 31 (18.7)	407 ± 15 (33.7)	350 ± 9 (29.0)
- After 30 min	89 ± 4 (7.4)	169 ± 4 (14.0)	229 ± 9 (18.9)	26 ± 4 (2.2)	51 ± 2 (4.2)	146 ± 4 (12.1)
- Sum	592 ± 24 (49.0 ± 2.0)	758 ± 20 (62.8 ± 1.6)	747 ± 28 (61.9 ± 2.3)	251 ± 34 (20.8 ± 2.8)	458 ± 17 (37.9 ± 1.4)	496 ± 13 (41.1 ± 1.1)
Non-dialysed Fe ($\mu g\ g^{-1}$)	564 ± 12 (46.7 ± 1.0)	396 ± 36 (32.8 ± 3.0)	520 ± 16 (43.1 ± 1.3)	952 ± 34 (78.9 ± 2.9)	704 ± 25 (58.3 ± 2.1)	700 ± 10 (58.0 ± 0.9)
Dialysed + non-dialysed Fe ($\mu g\ g^{-1}$)	1156 ± 25 (95.7 ± 2.0)	1155 ± 47 (95.7 ± 3.9)	1267 ± 25 (101.4 ± 2.1)	648 ± 58 (99.7 ± 3.9)	1162 ± 23 (96.2 ± 1.9)	1196 ± 10 (99.1 ± 0.9)

[a] ค่าที่อยู่ในวงเล็บแสดงค่าร้อยละของไดอะไลซิส

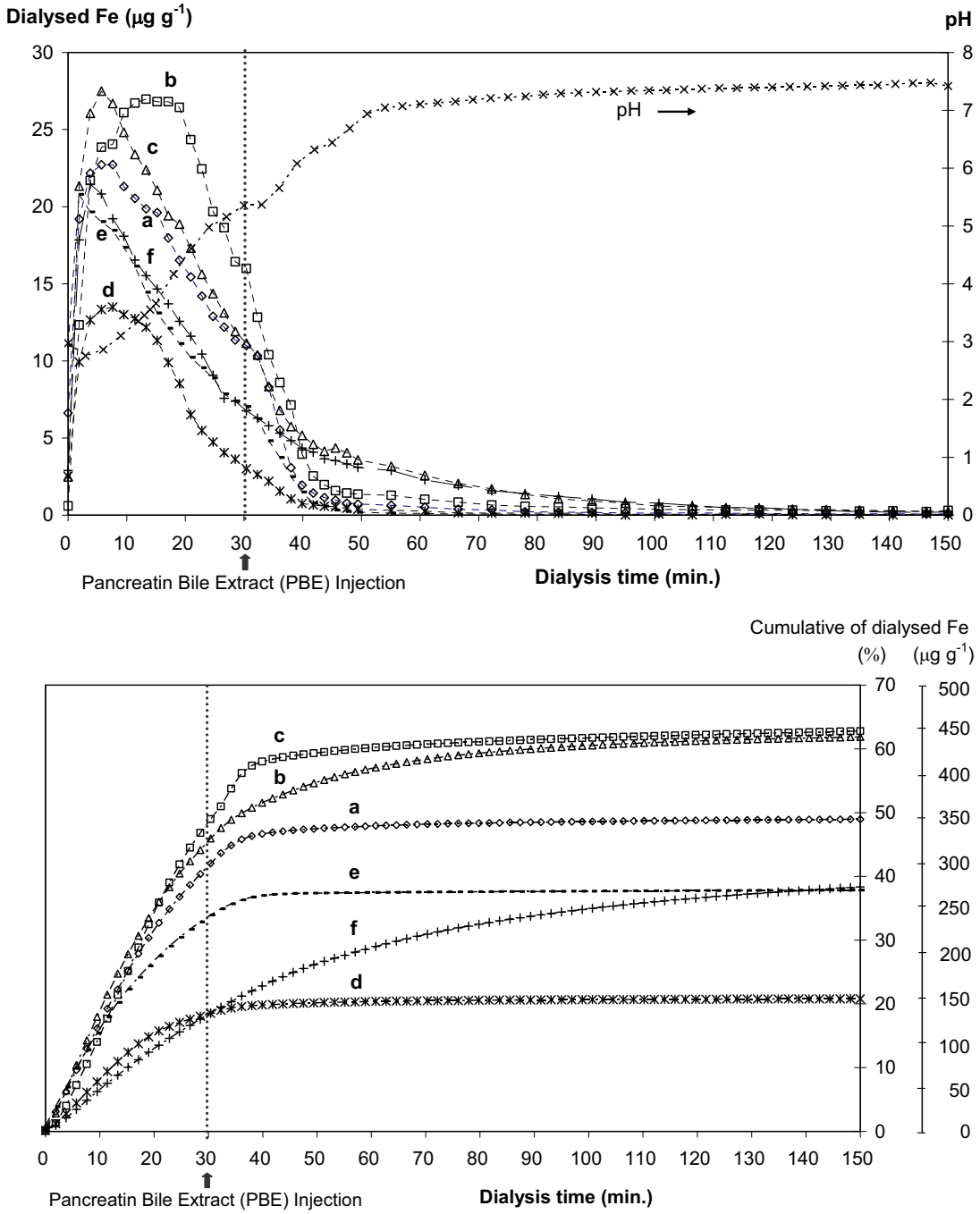

รูปที่ 3.11 กราฟการเปลี่ยนแปลงของไดอะไลซิสของธาตุเหล็กในฟอร์มเหล็ก(II)ซัลเฟต ที่เติมสารส่งเสริมและยับยั้งการดูดซึม (รูปด้านบน) และกราฟการเปลี่ยนแปลงแบบสะสมในช่วงเวลาต่างๆ (cumulative plot) ของธาตุเหล็กและร้อยละของไดอะไลซิส (รูปด้านล่าง) ในสารเสริมธาตุเหล็กในรูปฟอร์มเหล็ก(II)ซัลเฟตที่มีการเติมสารต่างๆ a) ไม่เติมสารใด b) เติมวิตามินซี c) เติมกรดซิตริก d) เติมกรดไฟตริก e) เติมกรดแทนนิก และ f) เติมกรดออกซาลิก

3.4 บทสรุป

ระบบ CFD-ICP-OES ที่พัฒนาขึ้นนี้เป็นระบบที่ง่าย รวดเร็ว และสามารถตรวจวัดแร่ธาตุครั้งละหลายๆ ธาตุพร้อมกันได้อย่างต่อเนื่อง นอกจากนั้นยังสามารถติดตามความเป็นกรดด่าง และการเปลี่ยนแปลงของแร่ธาตุระหว่างไดอะไลซิสไปพร้อมๆ กัน ได้ทดสอบระบบที่พัฒนาขึ้นนี้กับตัวอย่างต่างๆ หลายชนิด ข้อมูลของความสามารถในการไดอะไลซ์ของแร่ธาตุ กราฟการเปลี่ยนแปลงของความเป็นกรดด่าง และการเปลี่ยนแปลงของแร่ธาตุระหว่างไดอะไลซิสนั้น เป็นประโยชน์สำหรับการประเมินความสามารถในการดูดซึมได้ของแร่ธาตุ และใช้ในการศึกษาผลของปัจจัยต่างๆที่มีผลต่อการดูดซึมนั้น ทำให้เข้าใจการเปลี่ยนแปลงที่เกิดขึ้นระหว่างไดอะไลซิส

ระบบ CFD-ICP-OES-pH ที่พัฒนาขึ้นนี้สามารถใช้ในการติดตามกระบวนการไดอะไลซิสของแร่ธาตุต่างๆ และค่า pHได้ในทุกช่วงเวลา (time-dependent dialysis) ระบบนี้ได้นำมาประยุกต์ใช้ในการศึกษาสารเสริมแร่ธาตุบางชนิดที่ใช้เติมในอาหาร และการศึกษาผลของสารส่งเสริมและสารยับยั้งการดูดซึมของแร่ธาตุ ซึ่งเป็นการใช้ระบบไดอะไลซิสในการศึกษาเป็นครั้งแรก กราฟการเปลี่ยนแปลงของไดอะไลซิสของแร่ธาตุ และกราฟการเปลี่ยนแปลงแบบสะสมในช่วงเวลาต่างๆ (cumulative plot) ของปริมาณแร่ธาตุและร้อยละของไดอะไลซิส ได้แสดงให้เห็นอย่างชัดเจนในการติดตามการเปลี่ยนแปลงระหว่างไดอะไลซิสที่มีผลมาจากสารที่เติมลงในอาหาร ซึ่งไม่สามารถเห็นได้ด้วยกระบวนการไดอะไลซิสแบบทั่วไป ระบบนี้จึงมีประโยชน์ในการใช้เป็นเครื่องมือสำหรับการประเมินค่าความสามารถในการดูดซึมได้ของแร่ธาตุในอาหาร และสารที่เติมลงในอาหาร

3.5 เอกสารอ้างอิง

1. D. Derman, D. Ballot, T. Bothwell, B. Macfarlane, R. Baynes, A. MacPhail and et al., *British Journal of Nutrition* 1987, **57(3)**, 345.
2. T.E. Furia, *CRC handbook of Food Additives* 2nd ed, CRC press, 1980.
3. M. Gillooly, T. Bothwell, J. Torrance, A. MacPhail, D. Derman, W. Bezwoda and et al., *British Journal of Nutrition* 1983, **49(3)**, 331.
4. R.F. Hurrell, *Nutrition Reviews* 1997, **55(6)**, 210.
5. L. Hallberg and M. Brune *Human nutrition Applied nutrition* 1986, **40(2)**, 97.
6. K. Judprasong, M. Ornthai, A. Siripinyanond and J. Shiowatana, *Journal of Analytical Atomic Spectrometry*, 2005, **11**, 1191.
7. K. Judprasong, A. Siripinyanond and J. Shiowatana, *Journal of Analytical Atomic Spectrometry*, 2007, **22**, 807.

8. S.R. Lynch and R.J. Stoltzfus, *The Journal of Nutrition* 2003, **133(9)**, 2978S.
9. D.D. Miller, B.R. Schricker, R.R. Rasmussen and D.V. Campen, *The American Journal of Clinical Nutrition* 1981, **34**, 2248.
10. B. Nayak and K. Nair, *Food Chemistry* 2003, **80**, 545.
11. J. Promchan and J. Shiowatana, *Analytical and Bioanalytical Chemistry* 2005, **382(6)**, 1360.
12. S. Salovaara, A-S. Sandberg and T. Andlid, *Journal of Agricultural and Food Chemistry* 2003, **51(26)**, 7820.
13. D. Siengenberg, R. Baynes, T. Bothwell, B. Macfarlane, R. Lamparelli, N. Car and et al., *The American Journal of Clinical Nutrition* 1991, **53**, 537.
14. J. Shiowatana, W. Kitthikhun, U. Sottimai, J. Promchan and K. Kunajiraporn, *Talanta* 2006, **68(3)**, 549.

ตอนที่ 4

การใช้ระบบเชื่อมต่อระหว่าง Flow field-flow fractionation กับ Inductively coupled plasma optical emission spectrometer ในการศึกษาการกระจายตัวตามขนาดของสารประกอบระหว่างธาตุเหล็กกับ Phytic acid และ Tannic acid ในอาหาร

4.1 บทนำ

4.2 อุปกรณ์และวิธีการทดลอง

4.2.1 สารเคมีและตัวอย่าง

4.2.2 วิธีการศึกษาการจับตัวระหว่างธาตุเหล็กกับ Phytic acid และ Tannic acid

4.2.3 วิธีการบ่มตัวอย่างในสภาวะกรดเบสเสมือนระบบการย่อยอาหารโดยปราศจากเอนไซม์

4.2.4 วิธีการจำลองการย่อยในระบบการย่อยในหลอดแก้ว

4.2.5 เครื่องมือ

4.2.6 วิธีการคำนวณการกระจายตัวของธาตุเหล็กตามขนาด

4.3 ผลการทดลองและวิจารณ์

4.3.1 การเทียบมาตรฐานของการแยกด้วยระบบ Flow field-flow fractionation (FlFFF)

4.3.2 การกระจายตัวของธาตุเหล็กเมื่อมี Phytic acid และ Tannic acid

4.3.3 การกระจายตัวของธาตุเหล็กในสารสกัดผักคะน้าและน้ำชาในสภาวะกรดเบสเสมือนระบบการย่อยอาหารโดยปราศจากเอนไซม์

4.3.4 การกระจายตัวของธาตุเหล็กในสารสกัดผักคะน้าและน้ำชาหลังการย่อยในระบบการย่อยในหลอดแก้ว

4.4 บทสรุป

4.5 เอกสารอ้างอิง

4.1 บทนำ

ปัญหาการขาดแคลนธาตุเหล็กจัดเป็นปัญหาทางโภชนาการที่พบมากทั่วโลก โดยคิดเป็นอัตราส่วนร้อยละ 20 ของประชากรโลก มีการนำเสนออาหารเสริมธาตุเหล็กและวิธีทางโภชนาการเพื่อเพิ่มปริมาณการรับและนำไปใช้ประโยชน์ของธาตุเหล็กในร่างกาย ธาตุเหล็กที่อยู่ในรูป non-heme iron จัดเป็นธาตุเหล็กที่ร่างกายได้รับจากอาหารมากที่สุด โดยร่างกายจะดูดซึมธาตุเหล็กชนิดนี้ที่เซลล์ลำไส้เล็กในรูปแบบของไอออนอิสระ ซึ่งปริมาณการดูดซึมและนำไปใช้ประโยชน์ขึ้นอยู่กับปัจจัยหลายอย่าง โดยอาหารบางชนิดมักพบสารยับยั้งการดูดซึมธาตุเหล็กที่อยู่ในรูป non-heme iron เป็นองค์ประกอบ ได้แก่ phytic acid และ tannic acid

Phytic acid เป็นสารประกอบ Myo-inositol ที่พบมากในอาหารจำพวกธัญพืชและผักบางชนิด จากการที่ phytic acid มีโครงสร้างที่มีหมู่ Phosphate เป็นองค์ประกอบถึง 6 หมู่ จึงส่งผลให้เป็นสารคีเลตที่มีความสามารถสูงในการยึดจับกับธาตุหลายชนิดซึ่งรวมไปถึงธาตุเหล็กด้วย โดยในหลายงานวิจัยพบว่าสารประกอบของธาตุเหล็กกับ phytic acid เป็นสารประกอบที่ไม่สามารถดูดซึมได้ที่ลำไส้เล็ก

Tannic acid จัดเป็นสารประกอบ polyphenolic compound ที่พบได้ในเครื่องดื่มหลายชนิด เช่น ไวน์แดง เบียร์ กาแฟ ชาดำ และชาเขียว นอกจากนี้ยังพบได้ในอาหารหลายชนิดเช่น ข้าวฟ่าง องุ่น แพร กล้วย ถั่วดำ ถั่วแขก และช็อกโกแลต โดย tannic acid เมื่ออยู่ในสภาวะที่เป็นกรดจะทำให้เกิดหมู่ galloyl ที่มีผลยับยั้งการดูดซึมธาตุเหล็ก จากการที่องค์ประกอบของอาหารมีความสลับซับซ้อน ธาตุเหล็ก อาจมีการรวมตัวกับโมเลกุลยับยั้งการดูดซึมข้างต้นหรืออนุภาคขนาดต่างๆ ซึ่งส่งผลต่อความสามารถในการดูดซึมของแร่ธาตุเหล็ก การศึกษาการกระจายตัวของธาตุเหล็กตามขนาดจะให้ข้อมูลที่เป็นประโยชน์และมีความเข้าใจมากขึ้นในเรื่องของการดูดซึมของธาตุเหล็กในระบบการย่อยอาหาร

ในการศึกษาการกระจายตัวของธาตุเหล็กตามขนาดจะต้องใช้เทคนิคเชื่อมต่อระหว่างเทคนิคการแยกตัวอย่างตามขนาดอนุภาคและหน่วยตรวจวัดปริมาณธาตุตวามไวสูง เทคนิคทางโครมาโตกราฟีได้รับการนำเสนออย่างกว้างขว้างในการศึกษาดังกล่าวเช่น การใช้เทคนิค gel chromatography ร่วมกับเทคนิค flame atomic absorption ในการศึกษาการกระจายตัวอย่างอิสระและยึดจับกับโมเลกุลอื่นของ แคดเมียม สังกะสี ทองแดง และเงินในต่อมน้ำย่อยของกุ้ง lobster การใช้เทคนิค size exclusion chromatography (SEC) ที่ต่อเข้ากับเทคนิค Inductively coupled plasma mass spectrometry (ICP-MS) ในการศึกษาการจับตัวและปลดปล่อยของโลหะในโปรตีนภายใต้สภาวะการทดลองต่างๆ และในการศึกษาการกระจายตัวของโลหะในสารประกอบที่มีขนาดโมเลกุลต่างๆ ในตัวอย่างเห็ด แต่ด้วยเทคนิคโครมาโต กราฟีมีข้อจำกัดบางประการเช่น ต้องมีการเตรียมให้สารที่ต้องการวิเคราะห์มีความบริสุทธิ์ เช่นการสะกัดด้วยตัวทำละลายอินทรีย์ซึ่งมีความยุ่งยาก ประกอบกับการใช้ตัวทำละลายอินทรีย์เป็นตัวทำละลายและเฟสที่เคลื่อนที่ในคอลัมน์อาจส่งให้เกิดปัญหา Carbon overloading ในการตรวจวัดด้วยเทคนิค ICP-MS

สำหรับเทคนิคการแยกแบบ non-chromatographic techniques อย่าง FlFFF ที่เชื่อมต่อเข้ากับเทคนิคตรวจวัดธาตุความไวสูงอย่าง ICP-OES หรือ ICP-MS ได้ถูกนำเสนอในหลายงานวิจัยที่เกี่ยวข้องกับ

การศึกษาการกระจายตัวตามขนาดของธาตุชนิดต่างๆ ในตัวอย่างหลายชนิดเช่น โปรตีน มหโมเลกุล และแบคทีเรียเป็นต้น จากตัวอย่างงานวิจัยของ Barnes และ Siripinyanond ได้นำเสนอเทคนิค FlFFF-ICP-MS เพื่อใช้ในการศึกษาการกระจายตัวตามขนาดของโลหะต่างๆในโปรตีนหลายชนิดเช่น metallothionein, carbonic anhydrase, ceruloplasmin, alcohol dehydrogenase และ thyroglobulin อีกตัวอย่างงานวิจัยหนึ่งคือ งานของ Jackson et al ที่ได้นำเสนอการใช้เทคนิค FlFFF-ICP-MS เพื่อศึกษาพฤติกรรมการดูดซับธาตุยูเรเนียมของแบคทีเรีย นอกจากนี้ยังมีอีกหลายงานวิจัยที่ประสบความสำเร็จในการใช้ FlFFF-ICP-MS และ FlFFF-ICP-OES ในการศึกษาการกระจายตัวตามขนาดของธาตุต่างๆ ในตัวอย่างหลายชนิด

ในงานวิจัยนี้ได้ทำการศึกษาการจับตัวระหว่างธาตุเหล็กกับ phytic acid และ tannic acid โดยติดตามจากการกระจายตัวตามขนาดของธาตุเหล็ก นอกจากนี้ยังทำการศึกษาการกระจายตัวตามขนาดของธาตุเหล็กในตัวอย่างสารสกัดผักคะน้าและน้ำชาซึ่งมีรายงานว่ามี phytic acid และ tannic acid เป็นองค์ประกอบตามลำดับ โดยการทดลองจะศึกษาการกระจายตัวของธาตุเหล็กในตัวอย่างหลังบ่มในสภาวะกรดเบสเสมือนระบบการย่อยอาหารโดยปราศจากเอนไซม์ ซึ่งจะมีการปรับสภาพกรดเบสตัวอย่างให้เหมือนกับในระบบการย่อยอาหารของมนุษย์ นอกจากนี้ได้ทำการศึกษาการกระจายตัวของธาตุเหล็กในตัวอย่างหลังผ่านการย่อยในระบบการย่อยในหลอดแก้วโดยเติมเอ็นไซม์ pepsin และ pancreatic bile extract ลงในตัวอย่าง ระบบ FlFFF-ICP-OES ได้ถูกพัฒนาและนำมาใช้ในการศึกษาการกระจายตัวตามขนาดของธาตุเหล็กในตัวอย่างดังกล่าว

4.2 อุปกรณ์และวิธีการทดลอง

4.2.1 สารเคมีและตัวอย่าง

เอ็นไซม์ pepsin (P-7000, from porcine stomach mucosa)

เอ็นไซม์ pancreatin (P-1750, from porcine pancreas)

bile extract (B-6831, porcine) Sigma (St. Louis, MO, USA)

phytic acid (FW = 660.04 Da; Fluka, Italy)

tannic acid (FW = 1700.79 Da; Fluka, Italy)

monodisperse polystyrene sulfonate 4.3, 17 and 49 kDa (PSS) (Fluka, Italy)

สารละลายเหล็กมาตรฐาน (1000 มิลลิกรัมต่อลิตร)

การเตรียมสารละลาย pepsin: ละลาย pepsin 0.16 กรัม ในสารละลายกรดไฮโดรคลอริก 0.1 โมลาร์ 1 มิลลิลิตร

การเตรียม pancreatin–bile extract (PBE) mixture: ละลาย pancreatin 0.004 กรัม และ bile extract 0.025 กรัม ในสารละลายโซเดียมไบคาร์บอเนต 0.001 โมลาร์ 5 มิลลิลิตร

การเตรียมตัวอย่างผักคะน้า: ล้างผักคะน้าด้วยน้ำปราศจากไอออน อบที่อุณหภูมิ 65ºC จนแห้งและมีน้ำหนักคงที่ บดให้ละเอียด

การเตรียมตัวอย่างน้ำชา: น้ำชาถุงกึ่งสำเร็จรูปแช่ในน้ำ 120 มิลลิลิตรที่อุณหภูมิ 80ºC เป็นเวลา 10 นาที นำน้ำชามา centrifuge ที่ความเร็ว 3000 รอบต่อนาที เป็นเวลา 20 นาที เพื่อทำการแยกส่วนละลาย

การเตรียม carrier liquid ของระบบ FlFFF ที่ pH 2.0: เจือจางสารละลาย 0.8 มิลลิลิตรของกรดไฮโดรคลอริก 37% ในน้ำปราศจากไอออน 1 ลิตร

การเตรียม carrier liquid ของระบบ FlFFF ที่ pH 5.0: เจือจางสารละลาย 0.8 มิลลิลิตรของกรดไฮโดรคลอริก 37% ในน้ำปราศจากไอออน 800 มิลลิลิตร ปรับ pH ของสารละลายเท่ากับ 5 ด้วยสารละลายโซเดียมไบคาร์บอเนต หลังจากนั้นทำการปรับปริมาตรของสารละลายเท่ากับ 1 ลิตรด้วยน้ำปราศจากไอออน

การเตรียม carrier liquid ของระบบ FlFFF ที่ pH 7.0: เจือจางสารละลาย 0.8 มิลลิลิตรของกรดไฮโดรคลอริก 37% ในน้ำปราศจากไอออน 800 มิลลิลิตร ปรับ pH ของสารละลายเท่ากับ 5 ด้วยสารละลายโซเดียมไบคาร์บอเนต และปรับ pH ของสารละลายเท่ากับ 7 ด้วยสารละลายโซเดียมไฮดรอกไซด์ หลังจากนั้นทำการปรับปริมาตรของสารละลายเท่ากับ 1 ลิตรด้วยน้ำปราศจากไอออน

4.2.2 วิธีการศึกษาการจับตัวระหว่างธาตุเหล็กกับ Phytic acid และ Tannic acid

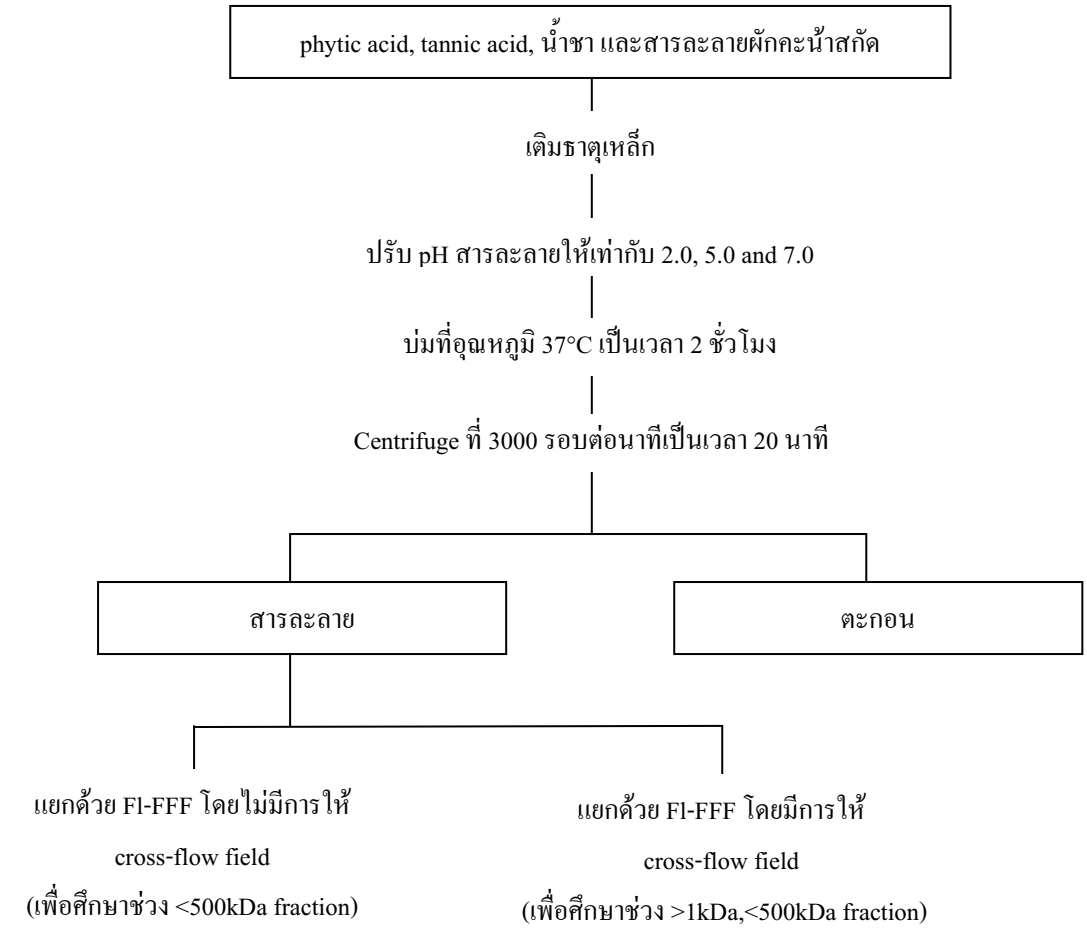

รูปที่ 4.1 วิธีการบ่มตัวอย่างในสภาวะกรดเบสเสมือนระบบการย่อยอาหารโดยปราศจากเอนไซม์เพื่อใช้ในการศึกษาการกระจายตัวตามขนาดของธาตุเหล็ก

ทำการเตรียมตัวอย่างตามขั้นตอนดังแสดงในรูปที่ 4.1 โดยจะทำการเตรียมให้ตัวอย่างมีอัตราส่วนน้ำหนักระหว่างธาตุเหล็กและ phytic acid (หรือ tannic acid) เท่ากับ 1:10, 1:50 และ 1:100 โดยมีความเข้มข้นของธาตุเหล็กเท่ากับ 300 มิลลิกรัม ต่อ ลิตร สำหรับการปรับ pH ของสารละลายทำได้โดยการเติมสารละลายเจือจางของกรดไฮโดรคลอริก โซเดียมคาร์บอเนต หรือโซเดียมไฮดรอกไซด์

4.2.3 วิธีการบ่มตัวอย่างในสภาวะกรดเบสเสมือนระบบการย่อยอาหารโดยปราศจากเอนไซม์

ทำการเตรียมตัวอย่างตามขั้นตอนดังแสดงในรูปที่ 4.1 สำหรับตัวอย่างสารสกัดคะน้าจะทำการปรับ pH ตัวอย่าง 2.5 มิลลิลิตรให้เท่ากับ 2.0, 5.0 และ 7.0 และปรับปริมาตรเป็น 5 มิลลิลิตร สำหรับตัวอย่างสารสกัดคะน้าและน้ำชาที่ทำการเติมสารละลายเหล็กเพิ่ม ทำการเติม 1.5 มิลลิลิตรของสารละลาย

เหล็กมาตรฐานที่มีความเข้มข้น 1000 มิลลิกรัมต่อลิตร ลงในตัวอย่างที่มีปริมาตร 2.5 มิลลิลิตรทำการปรับ pH ให้เท่ากับ 2.0, 5.0 และ 7.0 และปรับปริมาตรเป็น 5 มิลลิลิตร

4.2.4 วิธีการจำลองการย่อยในระบบการย่อยอาหารของร่างกาย

ในการจำลองการย่อยในระบบการย่อยในหลอดแก้ว ตัวอย่างจะถูกย่อยในระบบ gastric digestion ด้วยเอ็นไซม์ pepsin และย่อย pancreatic digestion ด้วยเอ็นไซม์ PBE ตามลำดับ โดยทำตามวิธีการใน รูปที่ 4.2

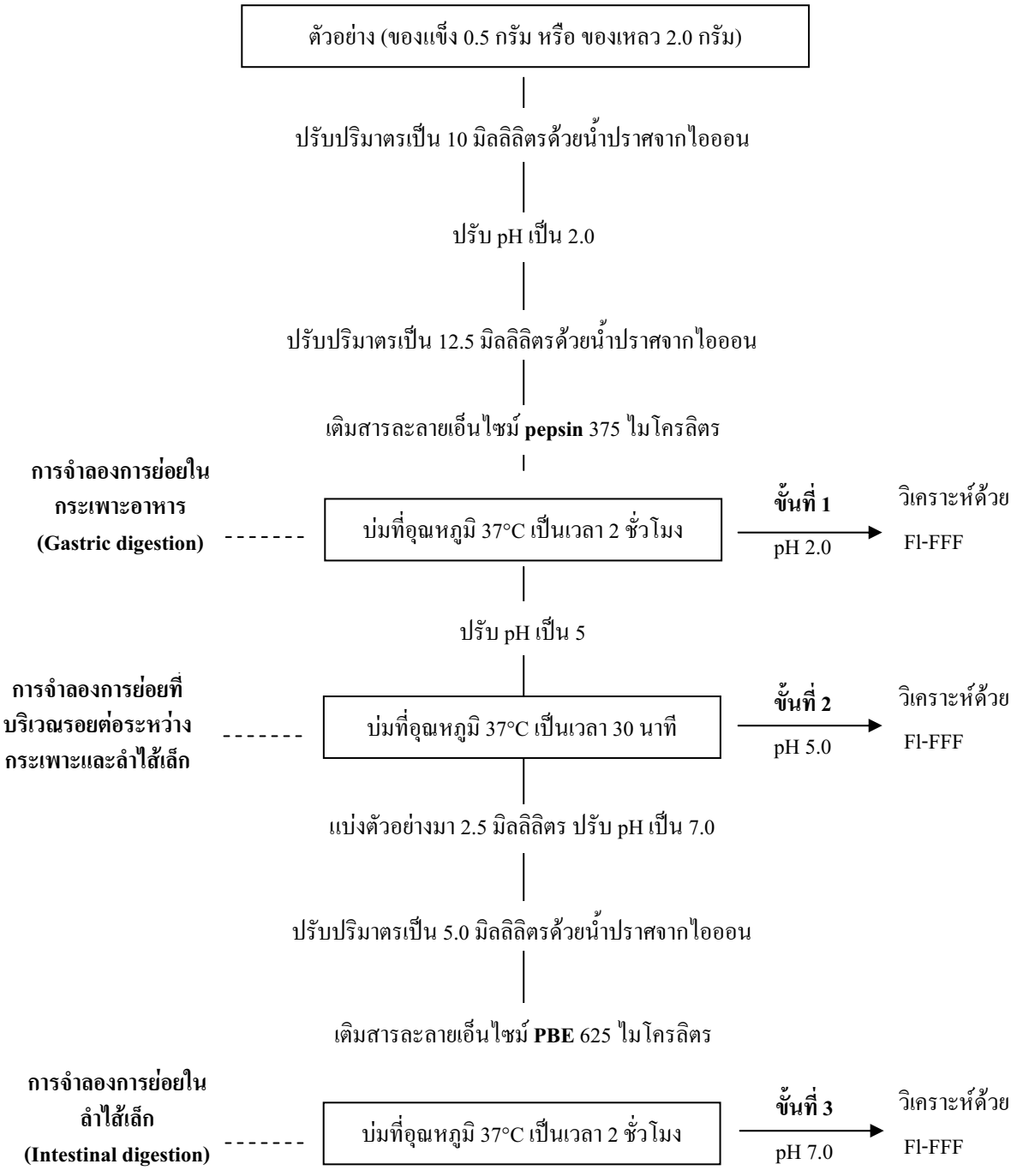

รูปที่ 4.2 วิธีการจำลองการย่อยในระบบการย่อยอาหารของร่างกาย

4.2.5 เครื่องมือ

pH meter, Denver Instrument Model 215 (USA)

Incubater shaker, Grant Instrument Model SS40-D2 (Cambridge, England)

FlFFF system (Model PN-1021-FO, Postnova Analytics, Landsberg, Germany)

ICP-OES system Spectro CirosCCD (SPECTRO Analytical Instruments, Kleve, Germany)

ในการทดลอง ระบบ FlFFF ที่มีหน่วยตรวจวัดเป็น UV spectrophotometer จะต่อเข้ากับ ICP-OES โดยทำการวิเคราะห์ภายใต้เงื่อนไขที่กำหนด ใน ตารางที่ 4.1

ตารางที่ 4.1 เงื่อนไขของเครื่องมือในการวิเคราะห์

FlFFF	
Carrier liquid	
- pH 2.0	0.01 M HCl
- pH 5.0	0.01 M HCl adjusted to pH 5.0 by $NaHCO_3$
- pH 7.0	0.01 M HCl adjusted to pH 7.0 by NaOH
Membrane	1000 Da MWCO, poly(cellulose acetate)
Channel flow rate / mL min^{-1}	0.75
Cross flow rate / mL min^{-1}	2

ICP-OES	
RF generator frequency / MHz	27.2
RF power / W	1350
Nebulizer gas flow rate / L min^{-1}	1
Coolant gas flow rate / L min^{-1}	12
Auxiliary gas flow rate / L min^{-1}	1

4.3 ผลการทดลองและวิจารณ์

4.3.1 การเทียบมาตรฐานของการแยกด้วยระบบ Flow field-flow fractionation (FlFFF)

ในการเทียบมาตรฐานของการแยกด้วยระบบ FlFFF นั้น เลือกใช้ monodisperse polystyrene sulfonate (PSS) ที่ขนาดโมเลกุลต่างๆ เป็นสารมาตรฐานโดยจะทำการวิเคราะห์แยก PSS ขนาด 4.3, 17 และ 49 kDa ในระบบ FlFFF ที่ใช้ carrier liquid ที่มี pH 2.0, 5.0 และ 7.0 จากนั้นทำการสร้างกราฟ

มาตรฐานและคำนวนสมการความสัมพันธ์เชิงเส้นระหว่างค่า logarithm ของ retention time (t_r) และขนาดโมเลกุล (M)

$$\log t_r = 0.572 \log M - 0.556, \; R^2 = 0.984 \quad \text{.....(1)}$$

$$\log t_r = 0.437 \log M - 0.065, \; R^2 = 0.999 \quad \text{.....(2)}$$

$$\log t_r = 0.526 \log M - 0.100, \; R^2 = 0.994 \quad \text{.....(3)}$$

สมการที่ (1)-(3) เป็นสมการความสัมพันธ์เชิงเส้นที่ได้จากการแยก PSS ในระบบ FlFFF ที่ใช้ carrier liquid ที่มี pH 2.0, 5.0 และ 7.0 ตามลำดับ โดยสมการดังกล่าวนี้จะถูกนำไปใช้ในการคำนวณขนาดโมเลกุลของตัวอย่างแยกในระบบ FlFFF ที่ใช้ carrier liquid ที่มี pH 2.0, 5.0 และ 7.0 ตามลำดับ

4.3.2 การกระจายตัวของธาตุเหล็กเมื่อมี Phytic acid และ Tannic acid

เนื่องจากในระบบการย่อยอาหารของมนุษย์ pH จะมีการเปลี่ยนอย่างช้าๆ จาก 2.0 ที่กระเพาะอาหารไปเป็น 7.0 ที่บริเวณลำไส้เล็ก ซึ่งเป็นบริเวณที่ร่างกายมีการดูดซึมแร่ธาตุสูงที่สุด ในการวิจัยนี้จึงสนใจศึกษาการกระจายตัวของธาตุเหล็กตามขนาดที่ pH 2.0, 5.0 และ 7.0 โดยใช้เทคนิค FlFFF-ICP-OES

จากรูปที่ 4.3(a-d) พบว่าเมื่อวิเคราะห์ธาตุเหล็กโดยไม่มีการเติม phytic acid ไม่พบว่ามีการกระจายตัวของธาตุเหล็กในช่วงที่วิเคราะห์ได้ในช่วง >1 kDa, >500 kDa (รูปที่ 4.3(d),ขวา) ทั้งนี้เกิดจาก ธาตุเหล็กอิสระมีขนาดเล็กกว่า membrane ในระบบ FlFFF ทำให้ธาตุเหล็กถูกกำจัดออกจากระบบ FlFFF ในกรณีที่มีการเติม phytic acid ธาตุเหล็กและ phytic acid จะเกิดเป็นสารประกอบที่มีขนาดใหญ่ขึ้น และจะให้สัญญาณธาตุเหล็กกระจายตัวในช่วงที่ FlFFF-ICP-OES สามารถวิเคราะห์ได้ในช่วง 1 – 1.5 นาทีแรกของการแยกหรือช่วงขนาดโมเลกุล ~1 kDa และการกระจายตัวของธาตุเหล็กดังกล่าวให้ผลสอดคล้องกับสัญญาณ molecular absorption ที่ได้จาก UV-spectrophotometer (รูปที่ 4.3 (a)-(c),ซ้าย) โดยให้ peak maxima ที่ตำแหน่งเดียวกันในทุกๆ กรณี นอกจากนี้สัญญาณของธาตุเหล็กในช่วงนี้จะสูงขึ้นเมื่อเพิ่มปริมาณ phytic acid ให้สูงขึ้น และจากการทดลองเมื่อพิจารณาให้ปริมาณ phytic acid คงที่ พบว่าเมื่อ pH สูงขึ้นการจับตัวระหว่างธาตุเหล็กและ phytic acid จะสูงขึ้นด้วยโดยสังเกตได้จากสัญญาณการกระจายตัวของธาตุเหล็กในช่วง ~1 kDa ที่สูงขึ้น

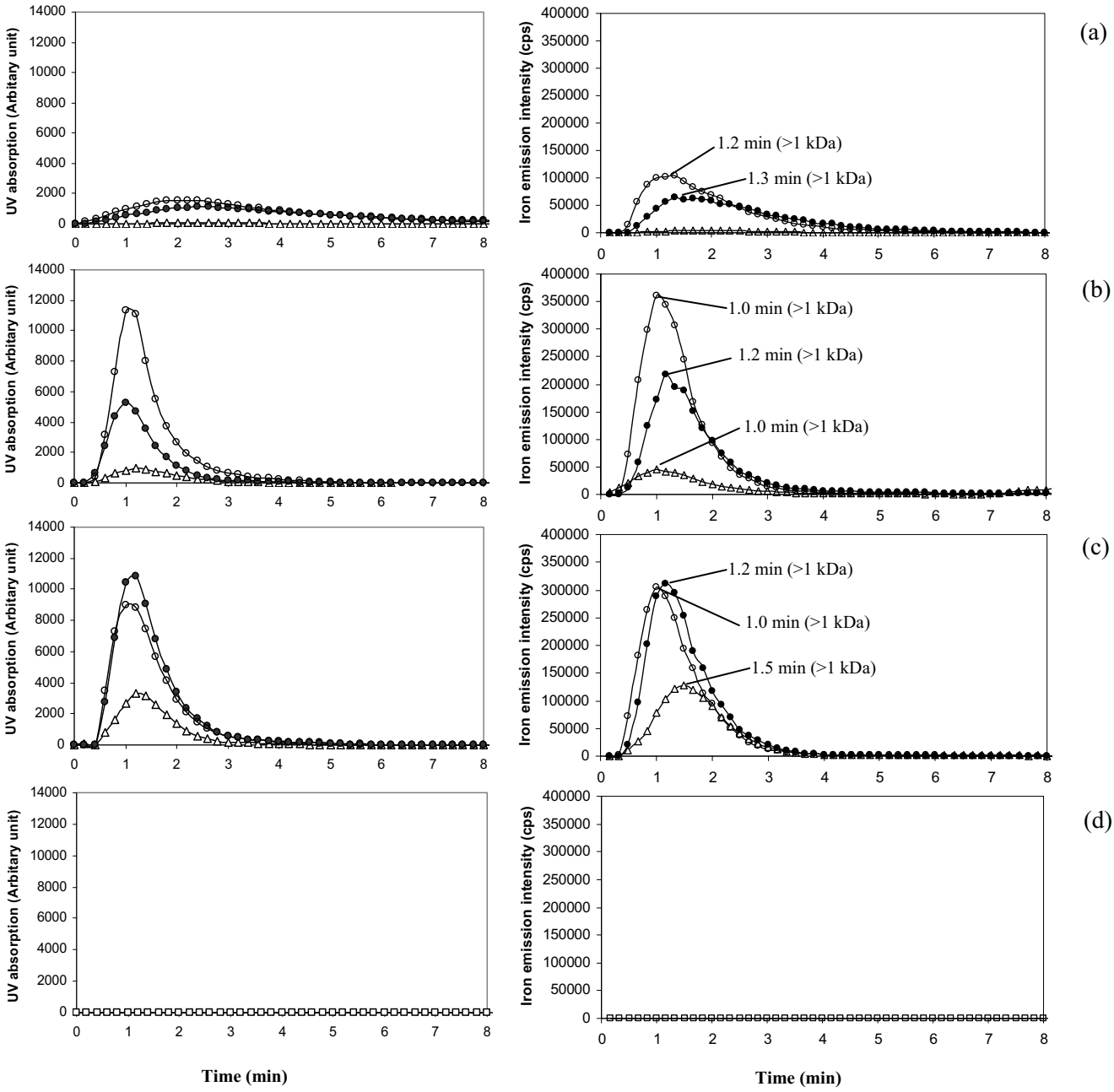

รูปที่ 4.3(a-d) การกระจายตัวตามขนาดของธาตุเหล็ก(สัญญาณจาก UV spectrophotometer ซ้ายและICP–OES ขวา) เมื่อมี phytic acid ปริมาณต่างๆ โดยทำการศึกษาที่ pH 2.0 (a), 5.0 (b), และ 7.0 (c) รูป d แสดงการกระจายตัวตามขนาดของธาตุเหล็กเมื่อไม่มีการเติม phytic acid; ธาตุเหล็ก : phytic acid เท่ากับ 1:10 (สามเหลี่ยม), 1:50 (วงกลมทึบ), และ 1:100 (วงกลมโปร่ง)

การกระจายตัวของธาตุเหล็กตามขนาดถูกจำแนกออกเป็นสามช่วงคือ

(a) <1 kDa

(b) >1 kDa แต่ <500 kDa

(c) >500 kDa

ตารางที่ 4.2 ร้อยละการกระจายตัวตามขนาดของธาตุเหล็กเมื่อมี phytic acid และ tannic acid ปริมาณต่างๆ โดยทำการบ่มตัวอย่างในสภาวะกรดเบสเสมือนระบบการย่อยอาหารโดยปราศจากเอนไซม์ที่ pH 2.0, 5.0 และ 7.0

ตัวอย่าง	pH	ร้อยละการกระจายตัวตามขนาดของธาตุเหล็ก (%)		
		<1 kDa	**>1 kDa, <500 kDa**	**>500 kDa**
ธาตุเหล็ก : phytic acid	2.0	16.0	2.0	81.9
(1:10)	5.0	3.9	25.5	70.7
	7.0	6.0	45.5	48.4
ธาตุเหล็ก : phytic acid	2.0	49.6	50.4	0.0
(1:50)	5.0	19.8	66.0	14.2
	7.0	0.0	93.8	6.2
ธาตุเหล็ก : phytic acid	2.0	45.2	54.8	0.0
(1:100)	5.0	17.2	82.8	0.0
	7.0	4.5	95.5	0.0
ธาตุเหล็ก : tannic acid	2.0	98.9	1.1	n.d.
(1:10)	5.0	0.5	0.4	99.1
	7.0	0.1	0.6	99.3
ธาตุเหล็ก : tannic acid	2.0	98.9	1.2	0.0
(1:50)	5.0	0.9	0.7	98.4
	7.0	1.1	0.6	98.2
ธาตุเหล็ก : tannic acid	2.0	98.9	1.1	n.d.
(1:100)	5.0	2.5	16.1	81.5
	7.0	1.7	1.7	96.6

ตารางที่ 4.2 แสดงการกระจายตัวของธาตุเหล็กตามขนาดโดยแสดงเป็นสัดส่วนร้อยละของการกระจายตัวตามขนาดในช่วงต่างๆ ที่กำหนดข้างต้น จากผลการทดลองพบว่า phytic acid มีประสิทธิภาพในการยึดจับธาตุเหล็กสูง โดยการทดลองที่อัตราส่วนน้ำหนัก 1:10 ธาตุเหล็กตกตะกอนร่วมกับ phytic acid (>500 kDa) ในการทดลองที่ทุกๆ pH สำหรับการทดลองที่อัตราส่วน 1:50 และ 1:100 ธาตุเหล็กส่วนใหญ่จะอยู่ในช่วง <1 kDa และเมื่อ pH สูงขึ้นเป็น 5.0 และ 7.0 จะเปลี่ยนไปกระจายตัวสูงขึ้นในช่วง >1 kDa, <500 kDa

สำหรับผลการทดลองของ tannic acid พบว่า ธาตุเหล็กส่วนใหญ่จะกระจายตัวในช่วง <1 kDa เมื่อ pH เท่ากับ 2.0 และตกตะกอนทันทีเมื่อ pH สูงขึ้นเป็น 5.0 และ 7.0 กระจายตัวในช่วง >500 kDa ยกเว้นการทดลองที่อัตราส่วน 1:100 จะพบธาตุเหล็กประมาณร้อยละ 16 กระจายตัวในช่วง >1 kDa, <500 kDa ที่ pH เท่ากับ 5.0 ดังแสดงใน รูปที่ 4.4

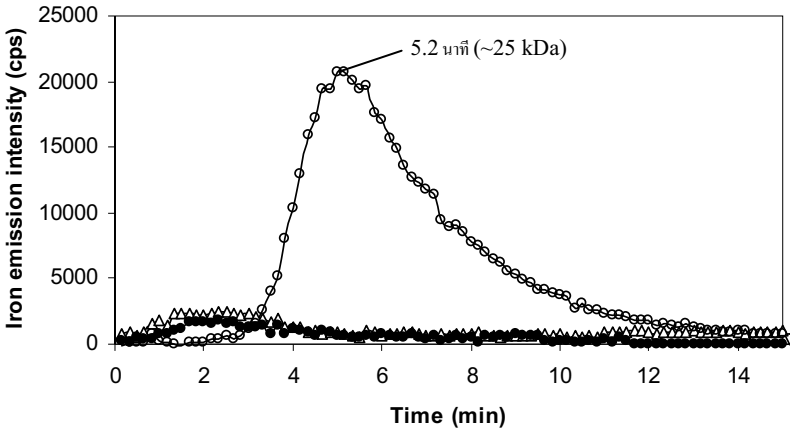

รูปที่ 4.4 การกระจายตัวตามขนาดของธาตุเหล็กเมื่อมีสัดส่วนโดยน้ำหนักธาตุเหล็กต่อ phytic acid เท่ากับ 1 : 100 โดยทำการบ่มตัวอย่างในสภาวะกรดเบสเสมือนระบบการย่อยอาหารโดยปราศจากเอนไซม์ที่ pH 2.0 (สามเหลี่ยม), 5.0 (วงกลมโปร่ง) และ 7.0 (วงกลมทึบ)

จะเห็นได้ว่าธาตุเหล็กมีความสามารถในการยึดจับได้ดีกับทั้ง phytic acid และ tannic acid โดยเฉพาะที่ pH 5.0 และ 7.0 ซึ่งเป็นช่วง pH ที่สอดคล้องกับสภาวะที่ลำไส้เล็ก ดังนั้นจะเห็นได้ว่า phytic acid และ tannic acid มีผลยับยั้งการดูดซึมของธาตุเหล็ก

4.3.3 การกระจายตัวของธาตุเหล็กในสารสกัดผักคะน้าและน้ำชาในสภาวะกรดเบสเสมือนระบบการย่อยอาหารโดยปราศจากเอนไซม์

จากการที่ผักคะน้าและน้ำชามีสารยับยั้งการดูดซึมธาตุเหล็กเป็นองค์ประกอบ ได้แก่ phytic acid และ tannic acid ตามลำดับ ซึ่งสามารถส่งผลยับยั้งการดูดซึมธาตุเหล็กได้ ในการทดลองนี้จึงได้ทำการศึกษาการกระจายตัวตามขนาดของธาตุเหล็กในสารสกัดผักคะน้า และน้ำชา โดยตัวอย่างจะถูกเตรียมด้วยวิธีการบ่มตัวอย่างในสภาวะกรดเบสเสมือนระบบการย่อยอาหารโดยปราศจากเอนไซม์ และวิธีการจำลองการย่อยในระบบการย่อยในหลอดแก้วแบบเติมเอ็นไซม์ โดยจะทำการศึกษาที่ pH 2.0, 5.0 และ 7.0 แต่เนื่องจากปริมาณธาตุเหล็กที่มีอยู่เดิมในน้ำชาอยู่ในระดับต่ำ ดังนั้นจึงได้ทำการเติมธาตุเหล็กลงในตัวอย่างน้ำชาให้มีความเข้มข้นเท่ากับ 300 มิลลิกรัมต่อลิตร

จากผลการกระจายตัวตามขนาดของธาตุเหล็กหลังผ่านการบ่มในสภาวะกรดเบสเสมือนระบบการย่อยอาหารโดยปราศจากเอนไซม์ที่ในตารางที่ 4.3 พบว่าที่ pH 2.0 ธาตุเหล็กจะอยู่ในรูปธาตุเหล็กอิสระคือกระจายตัวในช่วงขนาด <1 kDa แต่การกระจายตัวของธาตุเหล็กดังกล่าวจะเกิดการเปลี่ยนแปลงทันทีเมื่อ pH สูงขึ้นเป็น 5.0 และ 7.0 โดยในตัวอย่างสารสกัดผักคะน้าจะพบการกระจายตัวของธาตุเหล็กใน

ช่วง >1 kDa, <500 kDa ดังแสดงในรูปที่ 4.5(a) ซึ่งสอดคล้องกับผลการทดลองของ phytic acid ก่อนหน้านี้ แต่ในกรณีตัวอย่างสารสกัดคะน้าที่มีการเติมธาตุเหล็กจะตกตะกอนอย่างเฉียบพลันเมื่อ pH สูงขึ้นเป็น 5.0 และ 7.0 และพบว่าธาตุเหล็กกระจายตัวอยู่ในช่วงดังกล่าวคือ >500 kDa แต่ยังคงพบธาตุบางส่วนกระจายตัวในช่วง >1 kDa, <500 kDa เช่นกัน ดังแสดงในรูปที่ 4.5(b)

ตารางที่ 4.3 ร้อยละการกระจายตัวตามขนาดของธาตุเหล็กในสารสกัดผักคะน้า สารสกัดผักคะน้าที่มีการเติมธาตุเหล็ก น้ำชาที่มีการเติมธาตุเหล็ก โดยทำการบ่มตัวอย่างในสภาวะกรดเบสเสมือนระบบการย่อยอาหารโดยปราศจากเอนไซม์ที่ pH 2.0, 5.0 และ 7.0

ตัวอย่าง	pH	ร้อยละการกระจายตัวตามขนาดของธาตุเหล็ก (%)		
		<1 kDa[(a)]	>1 kDa, <500 kDa[(b)]	>500 kDa[(c)]
สารสกัดผักคะน้า	2.0	100.0	0.0	0.0
	5.0	36.5	63.5	0.0
	7.0	4.2	95.8	0.0
สารสกัดผักคะน้าที่มีการเติมธาตุเหล็ก	2.0	100.0	n.d.	n.d.
	5.0	3.3	3.9	92.8
	7.0	3.0	3.5	93.5
น้ำชาที่มีการเติมธาตุเหล็ก	2.0	91.9	n.d.	8.1
	5.0	21.0	18.5	60.5
	7.0	18.5	7.2	74.3

(a) พื้นที่ใต้กราฟการกระจายตัวของธาตุเหล็กเมื่อไม่ให้ cross flow field หักลบด้วย (b)

(b) พื้นที่ใต้กราฟการกระจายตัวของธาตุเหล็กเมื่อให้ cross flow field

(c) ปริมาณธาตุเหล็กทั้งหมดหักลบด้วย (a) และ (b)

n.d. มีความเข้มข้นต่ำกว่า detection limit (0.2 มิลลิกรัม ต่อ ลิตร)

ในกรณีของตัวอย่างน้ำชาที่มีการเติมธาตุเหล็ก พบว่าเมื่อ pH สูงขึ้นเป็น 5.0 และ 7.0 เกิดการตกตะกอนอย่างเฉียบพลัน และพบว่าธาตุเหล็กกระจายตัวอยู่ในช่วงดังกล่าวคือ >500 kDa และพบธาตุบางส่วนกระจายตัวในช่วง >1 kDa, <500 kDa ที่ pH 5.0 และมีลักษณะการกระจายตัวดังแสดงในรูปที่ 4.5(b) ซึ่งสอดคล้องกับผลการทดลองของ tannic acid ก่อนหน้านี้

4.3.4 การกระจายตัวของธาตุเหล็กในสารสกัดผักคะน้าและน้ำชาหลังการย่อยในระบบการย่อยในหลอดแก้ว

ตารางที่ 4.4 แสดงการกระจายตัวตามขนาดของธาตุเหล็กหลังการย่อยด้วยระบบการย่อยอาหารในหลอดแก้ว โดยจากผลการทดลองพบว่าหลังผ่านการย่อยในทุกๆ ขั้นตอน ทุกตัวอย่างแสดงการกระจายตัวในสองช่วงคือ <1 kDa และ >500 kDa ผลดังกล่าวแสดงให้เห็นว่าการเติมเอ็นไซม์จะช่วยย่อย

สารประกอบที่อยู่ในช่วง >1 kDa, <500 kDa ไปเป็นสารประกอบที่มีขนาด <1 kDa ซึ่งเป็นส่วนที่คาดว่าร่างกายสามารถดูดซึมได้ ทำให้ไม่พบการกระจายตัวในช่วง >1 kDa, <500 kDa สำหรับธาตุเหล็กที่กระจายตัวในช่วง >500 kDa คาดว่าเป็นธาตุเหล็กที่จับตัวอยู่กับสารยับยั้งการดูดซึมและเกิดการตกตะกอนโดยเป็นส่วนที่ไม่สามารถย่อยได้

ตารางที่ 4.4 ร้อยละการกระจายตัวตามขนาดของธาตุเหล็กในสารสกัดผักคะน้าที่มีการเติมธาตุเหล็ก และน้ำชาที่มีการเติมธาตุเหล็ก หลังการย่อยในระบบการย่อยในหลอดแก้วที่ pH 2.0, 5.0 และ 7.0

ตัวอย่าง	ขั้นที่	ร้อยละการกระจายตัวตามขนาดของธาตุเหล็ก (%)		
		<1 kDa	>1 kDa, <500 kDa	>500 kDa
สารสกัดผักคะน้า	1 (pH 2.0)	94.8	nd	5.2
	2 (pH 5.0)	29.7	nd	70.3
	3 (pH 7.0)	15.5	nd	84.5
น้ำชาที่มีการเติมธาตุเหล็ก	1 (pH 2.0)	82.8	nd	17.2
	2 (pH 5.0)	27.5	nd	72.5
	3 (pH 7.0)	21.2	nd	78.8

รูปที่ 4.6 แสดงกราฟเปรียบเทียบการกระจายตัวตามขนาดของธาตุเหล็กในตัวอย่างน้ำชาที่มีการเติมธาตุเหล็กหลังผ่านการบ่มในสภาวะกรดเบสเสมือนระบบการย่อยอาหารโดยปราศจากเอนไซม์และหลังการย่อยในระบบการย่อยในหลอดแก้ว จากผลแสดงให้เห็นว่าธาตุเหล็กที่จับอยู่กับสารยับยั้งการดูดซึมบางส่วนสามารถถูกย่อยได้ด้วยเอนไซม์และทำให้เพิ่มธาตุเหล็กที่กระจายตัวในช่วงที่ร่างกายสามารถดูดซึมได้คือ <1 kDa

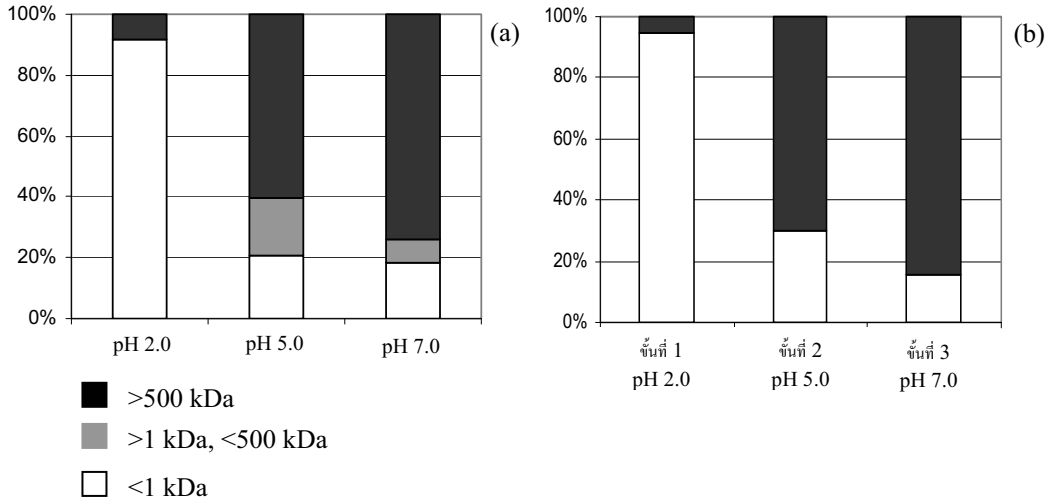

รูปที่ 4.6 ร้อยละการกระจายตัวตามขนาดของธาตุเหล็กในน้ำชาที่มีการเติมธาตุเหล็กโดยเปรียบเทียบระหว่างผลการบ่มในสภาวะกรดเบสเสมือนระบบการย่อยอาหารโดยปราศจากเอนไซม์ (a) และหลังการย่อยในระบบการย่อยในหลอดแก้ว (b)

4.4 บทสรุป

เทคนิค FlFFF-ICP-OES มีศักยภาพในการศึกษาการกระจายตัวตามขนาดของธาตุเหล็กในอาหารระหว่างการย่อยในขั้นตอนต่างๆ ในระบบการย่อยจำลอง ระบบที่พัฒนาขึ้นสามารถใช้ในการศึกษาพฤติกรรมการยึดจับตัวของธาตุเหล็กกับองค์ประกอบอื่นของอาหารที่ส่งผลยับยั้งการดูดซึมในลำไส้เล็กเช่น phytic acid และ tannic acid และระบบที่พัฒนาขึ้นนี้มีข้อได้เปรียบที่เหนือระบบการแยกแบบโครมาโตกราฟีคือ สามารถแยกตัวอย่างในช่วงขนาดและ pH ที่กว้างกว่า อย่างไรก็ดีการแยกด้วยระบบ FlFFF ยังคงมีข้อจำกัดในด้านประสิทธิภาพของการแยกที่ด้อยกว่า

จากผลการทดลองการยึดจับตัวของธาตุเหล็กกับ phytic acid พบว่ามีการยึดจับที่ดีในทุกๆ pH ในขณะที่ tannic acid ให้ผลการยึดจับธาตุเหล็กที่ดีที่ pH 5.0 และ 7.0 และผลการทดลองของสารสกัดคะน้าและน้ำชาให้ผลที่สอดคล้องกับ phytic acid และ tannic acid ตามลำดับ และผลการทดลองยังแสดงให้เห็นความสามารถในการยับยั้งการดูดซึมธาตุเหล็กที่ดีของสารยับยั้งการดูดซึมในสารสกัดคะน้าและน้ำชา

4.5 เอกสารอ้างอิง

1. N. Martinez-Navarrete, M.M. Camacho, J. Martinez-Lahuerta, J. Martinez-Monzo and P. Fito, *Food Res Int*, 2002, **35**, 225.
2. H.W. Lopez, F. Leenhardt, C. Coudray and C. Remesy, *Int J Food Sci Technol*, 2002, **37**, 727.
3. R.P. Glahn, G.M. Wortley, P.K. South and D.D. Miller, *J Agric Food Chem*, 2002, **50**, 390.
4. P. Brigide and S.G. Canniatti-Brazaca, *Food Chem*, 2006, **98**, 85.
5. E. Graf, J.R. Mahoney, R.G. Bryant and J.W. Eaton, *J Biol Chem*, 1984, **259**, 3620.
6. E. Graf, K. Empson and J. Eaton, *J Biol Chem*, 1987, **262**, 11647.
7. E. Graf E and J.W. Eaton, *Free Radical Biol Med*, 1990, **8**, 61.
8. E. Vasca, S. Materazzi, T. Caruso, O. Milano, C. Fontanella and C. Manfredi, *Anal Bioanal Chem*, 2002, **374**, 173.
9. A.S. Sandberg and U. Svanberg, *J Food Sci*, 1991, **56,** 1330.
10. R. Engle-Stone, A. Yeung, R. Welch and R. Glahn, *J. Agric Food Chem*, 2005, **53**, 10276.
11. P.K. South and D.D. Miller, *Food Chem*, 1998, **63**, 167.
12. A. King and G. Young, *J Am Diet Assoc*, 1999, **99**, 213.
13. K-T. Chung, T.Y. Wong, C-I. Wei, Y-W. Huang, and Y. Lin, *Crit Rev Food Sci and Nutr*, 1998, **38**, 421.
14. M. Brune, L. Hallberg and A.B. Skaanberg, *J Food Sci*, 1991, **56**, 128.

15. C.L. Chou, J.F. Uthe and R.D. Guy, *J AOAC Inter*, 1993, **76**, 794.
16. B.B.M. Sadi, A.P. Vonderheide, J.S. Becker and J.A. Caruso, *ACS Symp Ser*, 2005, **893**, 168.
17. R.G. Wuilloud, S.S. Kannamkumarath and J.A. Caruso, *J Agri Food Chem*, 2004, **52**, 1315.
18. A. Siripinyanond and R.M. Barnes, *J Anal At Spectrom*, 1999, **14**, 1527.
19. B. Stolpe, M. Hassellov, K. Andersson and D.R. Turner, *Anal Chim Acta*, 2005, **535**, 109.
20. L.J. Gimbert, K.N. Andrew, P.M. Haygarth and P.J. Worsfold, *Trends Anal Chem*, 2003, **22**, 615.
21. C. Contado, G. Blo, F. Fagioli, F. Dondi and R. Beckett, *Colloids Surf A*, 1997, **120**, 47.
22. E. Bolea, M.P. Gorriz, M. Bouby, F. Laborda, J.R. Castillo and H. Geckeis, *J Chromatogr A*, 2006, **1129**, 236.
23. B.P. Jackson, J.F. Ranville and A.L. Neal, *Anal Chem*, 2005, **77**, 1393.
24. F. Hurrell Richard, *J Nutr*, 2003, **133**, 2973S.
25. W.J. Evans and C.J. Martin, *J Inorg Biochem*, 1991, **41**, 245.

ตอนที่ 5
บทสรุป

งานวิจัยนี้ มีองค์ประกอบหลัก 2 ส่วนๆแรกเป็นการศึกษาพัฒนาระบบและวิธีการใหม่ และเพื่อเป็นการยืนยันถึงศักยภาพและประโยชน์ของระบบที่พัฒนาขึ้น งานวิจัยนี้จึงได้นำระบบที่พัฒนาไปศึกษาวิจัยเชิงประยุกต์ ดังแบ่งได้เป็นสองกลุ่มดังนี้ ทั้งนี้ งานวิจัยเชิงประยุกต์ ยังคงดำเนินต่อไป เพื่อนำเสนอแนวทางการใช้ประโยชน์จากเทคนิคที่พัฒนาขึ้น

5.1 การประยุกต์ใช้ระบบการสกัดเป็นลำดับขั้นแบบไหลต่อเนื่อง

จากที่ได้มีการพัฒนาระบบการสกัดเป็นลำดับขั้นแบบไหลต่อเนื่องขึ้นดังรายละเอียดในรายงานวิจัยฉบับสมบูรณ์ตามสัญญาเลขที่ BRG05/2543 นั้น ทำให้สามารถวิเคราะห์ประเมินความสามารถในการเคลื่อนตัว การดูดซึมหรือการนำไปใช้ได้ของโลหะหนักหรือแร่ธาตุนั้นๆ ที่แตกต่างกัน ซึ่งทำให้มีผลกระทบต่อสิ่งแวดล้อมและชีวิตของมนุษย์ที่ต่างกันด้วย งานวิจัยนี้ได้ประยุกต์ใช้วิธีที่พัฒนาขึ้นดังนี้ (รายละเอียดในภาคผนวก)

- ประเมินผลกระทบของการปนเปื้อนของโลหะหนักจากกิจกรรมอุตสาหกรรมหลอมโลหะและอุตสาหกรรมการถลุงแร่
- ศึกษาถึงความสามารถในการเคลื่อนตัวของตะกั่วและแคดเมียมที่ปนเปื้อนอยู่ในดิน ดินตะกอนและอากาศในบริเวณใกล้ๆ กับโรงงานหลอมตะกั่ว และแหล่งถลุงโลหะสังกะสี
- ศึกษาถึงรูปฟอร์มของตะกรันเหล็กที่เกาะอยู่ในท่อนำส่งแก๊สธรรมชาติ

5.2 การประยุกต์ใช้วิธีวิเคราะห์แบบไหลต่อเนื่องเพื่อศึกษาการดูดซึมหรือการนำไปใช้ได้ของแร่ธาตุในอาหาร

ในงานวิจัยนี้ได้ทำการพัฒนาวิธีวิเคราะห์แบบไหลต่อเนื่องเพื่อศึกษาการดูดซึมหรือการนำไปใช้ได้ของแร่ธาตุในอาหาร ระบบที่พัฒนาขึ้นนี้เป็นการจำลองหลอดแก้วให้เสมือนเป็นระบบการย่อยในกระเพาะอาหารและการดูดซึมสารอาหารในลำไส้เล็ก โดยอาศัยวิธีแบบแบทช์ในการจำลองการย่อยในกระเพาะอาหาร และใช้ระบบการซึมผ่านเยื่อบางแบบไหลต่อเนื่อง (continuous-flow dialysis, CFD)ในการจำลองการดูดซึมสารอาหารในลำไส้เล็ก ด้วยระบบ CFD ทำให้สามารถเก็บสารละลายตัวอย่างที่ซึมผ่านเยื่อบางออกมาเพื่อการวิเคราะห์ปริมาณแร่ธาตุโดยใช้หน่วยตรวจวัดประเภทต่างๆ ได้ นอกเหนือจากที่ได้สรุปไว้ในรายงานในตอนที่ 1-4 แล้ว ได้มีการประยุกต์ใช้วิธีที่พัฒนาขึ้นดังนี้ (รายละเอียดในภาคผนวก)

- ศึกษาอิทธิพลของกรดอินทรีย์ต่อการนำไปใช้ได้ของธาตุแคลเซียมในผักต่างๆ
- ศึกษาอิทธิพลของกรดอินทรีย์ในอาหารไทยต่อการนำไปใช้ได้ของธาตุแคลเซียม

RESEARCH ARTICLE
doi: 10.2306/scienceasia1513-1874.2007.33.421

ScienceAsia 33 (2007): 421-428

Atmospheric Deposition of Metals Associated with Air Particulate Matter: Fractionation of Particulate-Bound Metals Using Continuous-Flow Sequential Extraction

Atitaya Samontha,[a] Weerawan Waiyawat,[a] Juwadee Shiowatana[a*] and Ronald G. McLaren[b]

[a] Department of Chemistry, Faculty of Science, Mahidol University, Rama VI Rd., Bangkok 10400, Thailand.
[b] Soil and Physical Sciences Group, Agriculture and Life Sciences Division, PO Box 84, Lincoln University, Canterbury, New Zealand.

* Corresponding author, E-mail: scysw@mahidol.ac.th

Received 26 Jan 2007
Accepted 4 Jun 2007

ABSTRACT: The fractionation and elemental association of some heavy metals in air particulate matter from two different sources, a smelter and heavy vehicle traffic, were investigated using a continuous-flow sequential extraction procedure. Air particulate matter (a combination of wet and dry deposition) was collected monthly for one year and was analyzed by a four-step continuous-flow sequential extraction procedure employing a modified Tessier scheme. Examination of crustal enrichment factors (EF_{crust}) suggested that the Cd, Zn and Pb in the air particulate matter were predominantly of anthropogenic origin. Total Pb deposition in the dry season was found to be higher than that in the wet season, and may be attributed to soil dust. However, the fractional distribution of metals between forms did not differ between seasons. The results showed that the reducible phase (Fe/Mn oxides) was the largest fraction of Pb in air particulate matter from both the smelter and heavy traffic sites. The overlain metal extraction profiles demonstrated a close elemental association between Al and Pb in the acid-soluble phase of air particulate matter. In the reducible fraction, Pb was found to dissolve earlier than Fe indicating that Pb could occur adsorbed onto Fe oxide surfaces in the air particulate matter.

KEYWORDS: air particulate matter, continuous-flow sequential extraction, enrichment factor.

INTRODUCTION

Air particulate matter, together with associated metal contaminants, can be formed as the result of both natural and anthropogenic processes. Typical natural sources are the sea, giving rise to saline particles, or wind-blown dust derived from the land. Human activity produces air particulate matter as a result of industrial activities, traffic emissions and combustion processes. In particular, mining and smelting activities are important sources of heavy metals in the environment. For example, lead smelters are one of the most important sources of Pb pollution in the environment. Another source of Pb, still important in some countries, is the combustion of leaded gasoline. Lead is a toxic element and is dangerous to human health even at relatively low levels. Knowledge of the bulk concentrations of metal contaminants is essential for an assessment of ecosystem risk. Lead contamination in the vicinity of smelters is mainly airborne and represents a long-term pollution effect on the environment.

Environmental risk assessment of metals associated with air particulates has usually been based on the total concentrations of the metals. This can provide information on the degree of contamination, however, the mobility of metals in the environment depends not only on their total concentration but also on the associations and forms present in the solid phase by which they are bound. These forms include the following broad categories: soluble; exchangeable; carbonate-bound; Fe and Mn oxide-bound; organic matter-bound and residual[1]. Understanding the mode of occurrence of metals in air particulates is essential for the environmental assessment of this form of contamination.

One approach to the study of the distribution of metals among these physicochemical phases is the use of phase-selective chemical extractions involving multiple extracting reagents[2]. The reagents employed in sequential extractions have been chosen on the basis of their selectivity and specificity towards particular physicochemical forms. Sequential extraction techniques are widely used to fractionate metals in solid samples on the basis of the leachability/extractability of different metal forms[3,4].

In our previous work, a continuous-flow extraction system has been developed to perform chemical

speciation by sequential extraction of both metals[5] and nonmetals[6] in solid materials. Compared with batch extraction systems, the procedure is rapid, has less risk of contamination, has the possibility of further automation, and is easy to perform. The system has also been found to have less problems of readsorption due to the shorter extraction times required[7]. In addition, the extractogram (a graphical plot of concentration versus extraction volume) offers additional information about chemical association of metals in the solid phases.

This study aims to investigate the use of a continuous-flow sequential extraction system to determine the fractionation of metals in air particulate matter. Another objective was to use the extractograms obtained from the dynamic extraction system for interpretation of elemental associations in the various air particulate fractions. Results obtained from this work should improve our understanding of the forms and elemental associations of metals in air particulate matter.

Materials and Methods

Sampling Sites

The study sites are an area surrounding a small lead smelter located in Saraburi province, approximately 110 km north of Bangkok, Thailand and a heavy traffic area in central Bangkok, Thailand. The smelter has been operating for the last 10 years and its main activity is to recycle lead from old batteries. The criterion for the location of monitoring stations of air particulate matter was that each site should be clear of shelter from the wind and not overhung by electricity cables or tall trees. For sampling at the lead smelter site, three sampling locations were chosen at distances of 2 km, 1 km and 300 m from the smelter. The site in central Bangkok was located in one of the busiest traffic junctions (near Victory Monument). At each site, atmospheric deposition of particulates and metals was monitored for a period of one year. At all sites, duplicate samplers were installed within 20 m of each other.

Design of Air Particulate Collectors

Passive air particulate collectors provide a relatively simple method for monitoring dust particles deposited by both dry and wet deposition. The plastic cones used as collectors were constructed from polyethylene funnels and were 25 cm in diameter with an internal depth of 12.5 cm. The edges of the plastic funnels were cut in a zigzag shape to discourage birds from perching and thus minimize contamination from bird excreta (Fig. 1). At each monitoring site, the plastic funnels were mounted on posts 1.6-1.8 m above ground level to avoid contamination by saltating soil particles. The tubing connecting the plastic funnels to the receiving bottles, and the bottles themselves, were shielded with black plastic sheeting to prevent algal growth. Rainfall and particles passively deposited into the plastic funnel were collected in a 4-L bottle which was replaced monthly. A known volume of high purity water was used to flush particles out of the plastic funnel down the tube into the bottle at the time of sample collection. After collection and transport to the laboratory, samples were filtered through a glass microfibre filter (Whatman GF/B (Maidstone, UK), 47 mm diameter, 1 micron particle retention) and the sample volume determined. The pH of the samples was also measured. The particulate matter retained on the filter was then subjected to continuous flow extraction, and the filtered solutions containing soluble constituents were analysed separately.

The volume of samples for wet season months (June-October) was quite consistent at approximately 3 L, and in dry season months at approximately 0.1 L. Air particulates in August were chosen to represent the wet season, and air particulates in March, the dry season. These two months were selected because they are in the middle of the wet and dry seasons, respectively, and less likely to be affected by instability of changing weather.

Chemicals and Apparatus

All chemicals used were of analytical grade. Multi-

Fig 1. The photograph of an air particulate collector.

element stock solution for ICP-MS (AccuStandard, Inc. CT, USA) was used for the preparation of standard solutions. An inductively coupled plasma quadrupole mass spectrometer (ICP-QMS, Perkin Elmer ELAN 6000) was used for the elemental determination of air particulate extracts.

Fractionation Scheme

A modified Tessier sequential extraction scheme[2] was carried out using the following solutions:

Step 1 (F1): 0.01 M $Mg(NO_3)_2$ (exchangeable fraction)

Step 2 (F2): 0.11 M CH_3COOH (acid soluble fraction; carbonate or specifically sorbed)

Step 3 (F3): 0.01 M $NH_2OH.HCl$ adjusted to pH 2 with HNO_3, 85°C (reducible fraction; Fe/Al/Mn oxide-bound)

Step 4 (F4): 8:3 v/v (30% H_2O_2:0.02 M HNO_3), 75°C (oxidizable fraction; organic-bound)

Step 5 (F5): Aqua Regia (residue fraction)

Continuous-Flow Extraction System

Extraction Chamber

An extraction chamber was designed to allow containment and stirring of air particulate samples. Extractants could flow sequentially through the chamber and leach metals from the targeted phases. The chambers and their covers were constructed from borosilicate glass to have a capacity of approximately 10 mL. The outlet of the chamber was furnished with a glass microfibre filter GF/B (47 mm diameter, 1 µm particle retention, Whatman, Maidstone, UK) to allow dissolved matter to flow through. Extractant was pumped through the chamber using a peristaltic pump (Micro tube pump, MP-3N, EYELA, Tokyo Rikakikai Co. Ltd.) at varying flow rates using tygon tubing. Heating of the extractant in steps 3 and 4 was carried out by passing the extractant through a glass heating coil approximately 120 cm in length, which was placed in a water bath. The flow extraction setup is shown in Fig. 2.

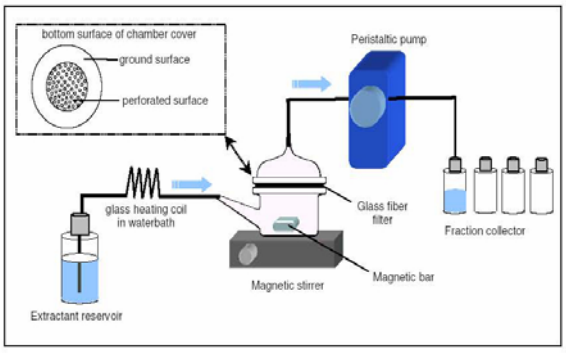

Fig 2. The set-up of the continuous-flow extraction system.

Extraction Procedure

Since it was impossible to remove air particulate matter from the filters collected from the samplers without loss of material, the whole central portion of the filter through which the solution had passed was cut from the filter and transferred to a clean extraction chamber. Following addition of a magnetic bar, a glass microfibre filter was then placed on the outlet followed by a silicone rubber gasket, and the chamber cover was securely clamped in position. The chamber was connected to the extractant reservoir and the collector vial using tygon tubing and placed on a magnetic stirrer. The magnetic stirrer and peristaltic pump were switched on to start the extraction. The extracting reagents continuously flowed through the chamber to effect sequential extraction. The extract passing the membrane filter was collected at 30 mL volume intervals to obtain six subfractions for each extractant. Extraction was carried out until all four extraction steps were completed. Elemental concentrations in extracts were determined by ICP-QMS.

Dissolution of Residues

A closed-vessel microwave digestion system (Milestone model MLS-1200 Mega, Bergamo, Italy) was used for pseudo-total digestion of air particulate matter residues. Residues from the extraction chamber were transferred to the digestion vessels together with concentrated HNO_3 (4 mL) and 37% HCl (2 mL). The vessel was then tightly sealed and subjected to microwave digestion. After cooling, the digested solutions were made up to volume in volumetric flasks before ICP-QMS measurements. The total amounts of metals associated with the particles were determined by summation of metals in exchangeable, acid soluble, reducible, oxidizable and residual fractions.

Quality Control

Analytical quality assurance was addressed by undertaking duplicate analysis of all extracted solutions. Blank analysis was performed frequently and every time a change of reagents or materials was used.

Results and Discussion

Total Metal Deposition and Enrichment Factors

The samples were obtained in this study using sample collectors modified from Gray et al.[8] as described in section 2.2. The material collected would have resulted from a combination of both wet and dry deposition processes. Total metal deposition was calculated from a combination of the amounts of soluble metals, as determined in the original sample filtrates, and the amounts of metals determined in the various particulate matter fractions. At each sampling, at all

four sites, solution and air particulate samples from both duplicate samplers were analyzed. The volume and pH of the rainwater harvested by the samplers, together with total metal depositions (solution plus particulate) are shown in Table 1.

In the dry season, harvested rainwater ranged from 1.6 to 13.2 mm month^{-1}, and from 52 to 70 mm month^{-1} in the wet season. The rainwater pH was around 8 in the wet season and varied from 4 to 7 in the dry season. The higher pH of rainwater harvested in the wet season was attributed to activities including biomass burning which produces oxides of Ca, Mg and K to neutralize the acidity of rainwater. In the wet and dry seasons, photochemical processes, driven by sunlight presumably cause oxidation of SO_2 and NO_x to give acidic rainwater[9].

Pb, Cd and Zn are the most common toxic metal contaminants in air particulates because they appear in gasoline, car components, oil lubricants and are widely used in industry. Sources of metal contamination in air particulates have been reviewed[10]. Table 1 shows that the concentration of Pb in air particulate matter adjacent to the lead smelter area (L1) is distinctly elevated and decreases with distance from the smelter in both dry and wet seasons, implicating the lead smelter as the point source of contamination. The highest Zn content was obtained at sampling site L4, most likely originating from traffic-related sources (vehicle tyres).

Total Pb depositions at locations L1 and L2 were substantially higher in the dry compared with the wet season, in spite of the much higher rainfall in the latter. This may be related to a greater deposition of wind-blown dust material in the dry season. Nriagu[11] has indicated that wind-blown dusts are a major source of Pb emissions worldwide.

Trace metals in aerosols are derived from a variety of sources including the earth's crust, the oceans, the biosphere, and a number of anthropogenic processes. The degree to which a trace metal in an aerosol is enriched, or depleted, relative to a specific source can be assessed to a first approximation using an enrichment factor (EF_{crust})[12]. The enrichment factor (EF_{crust}) of an element in an aerosol sample is defined as

$$EF_{crust} = \left(\frac{\left(Cxatm / CAlatm \right)}{\left(Cxcrust / CAlcrust \right)} \right)$$

where (C_{xatm}) and (C_{Alatm}) are the concentrations of the atmospheric trace metal and Al, respectively, and (C_{xcrust}) and ($C_{Alcrust}$) are their concentrations in average crustal material. The enrichment factor (EF_{crust}) was determined in this study based on the total depositions of trace elements and Al relative to their average crustal concentrations as reported by Mason and Moore[13].

As an approximate guide, values of EF_{crust} lower than 10 (in effect 10 times the level of samples with no enrichment) are believed to have originated from normal weathering of crustal material. Values of EF_{crust} larger than about 10^1 are referred to as enriched elements and may have some sources other than crustal weathering, possibly anthropogenic. The higher the value of EF_{crust}, the more likely that an anthropogenic source is involved.

The high enrichment factors ($10^1 - 10^3$) for Pb, Cd and Zn suggest a substantial anthropogenic input for these three metals. Not only the lead smelter, but also vehicular exhaust emission was a major source of Pb contamination. Pb is still persistent in road dust from earlier vehicular exhaust emission before leaded gasoline was banned, because of its long residence time in the environment[14]. Similar to earlier reports[10,15], particulate Zn in ambient air probably has its origin from automobile sources, i.e., wear and tear of vulcanized rubber tyres, lubricating oil and corrosion of galvanized vehicular parts. Cadmium is being emitted mainly from industrial activities and industrial and domestic wastes related with paints and batteries. In contrast, iron (Fe) shows no enrichment (EF_{crust} H•1) and EF_{crust} for Al by definition is 1.0. The metals Pb, Cd and Zn are all relatively volatile metals, and because they are readily transported in air, have been referred to as atmosphile elements[16]. Previous studies have reported the accumulation of Pb and Cd in the soil

Table 1. Rainwater volumes, pH and total metal depositions (g ha^{-1} month^{-1}) for representative dry and wet season months (n =2).

Location	Rainfall (mm month^{-1})		pH of rainfall		Pb		Cd		Zn	
	Dry	Wet	Dry	Wet	Dry	Wet	Dry	Wet	Dry	Wet
L1	1.6	52.0	8.04	7.25	78.51 ± 64.50	10.26 ± 7.25	0.41 ± 0.33	0.91 ± 0.00	106.2 ± 34.92	116.7 ± 33.73
L2	2.0	65.2	8.51	7.57	8.25 ± 1.83	0.92 ± 0.083	1.25 ± 0.17	0.34 ± 0.17	71.3 ± 36.25	70.9 ± 5.83
L3	2.2	67.8	8.06	6.14	0.22 ± 0.008	0.26 ± 0.092	1.16 ± 0.00	0.33 ± 0.25	54.0 ± 22.33	52.4 ± 9.20
L4	13.2	70.3	8.34	4.59	2.84 ± 0.33	2.42 ± 1.04	1.42 ± 0.33	0.17 ± 0.00	110.2 ± 25.00	233.3 ± 51.53

L1, L2, L3: 0.3, 1 and 2 km from lead smelter, respectively.
L4: Heavy traffic area.

surrounding the smelter[17,18].

Fractionation of Metals in Air Particulate Samples

For Pb and Zn, concentrations of these metals in the filtered solutions obtained from the air samplers were all below detection limits, i.e. all of the Pb and Zn were associated with the air particulate matter. In the case of Cd, for three samples (L2 and L3 wet season, L4 dry season) some Cd was detected in the water-soluble fraction, equivalent to depositions of between 0.42 and 1.24 g Cd ha^{-1} $month^{-1}$, and accounting for between 23 and 84% of the total Cd deposition for those samples. For the other samples, all of the Cd was associated with the air particulate matter.

Information on the fractionation of metals in air particulate matter is essential for considering their mobility, mechanisms of transformation and also their environmental risk. The fractionation of Pb, Cd and Zn in air particulate matter has been studied previously using sequential extraction procedures[1,19,20]. These studies found that Pb was strongly associated with carbonate and Fe-Mn oxide phases.

Metal fractionation data for the four sites is shown in Table 2. However, it should be noted that for sites L2 and L3in particular, the concentrations of metals in several fractions were close to the detection limits. The samples from the most contaminated sites (L1 and L4) provide the most complete sets of data. For these sites,

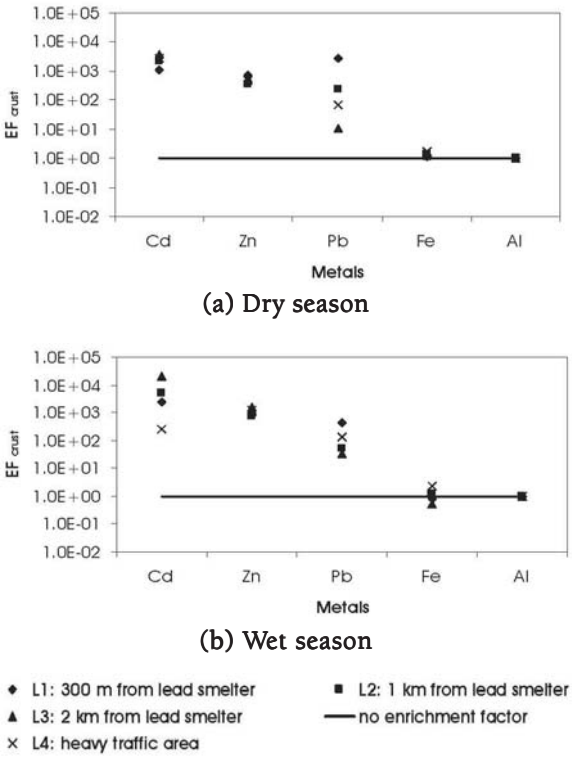

Fig 3. Mean EF_{crust} values for metals (Pb, Cd, Zn, Fe and Al) deposited at different sites (L1-L4).

Table 2. Fractional distribution of metals in representative air particulate matter from dry and wet seasons as determined using a continuous-flow sequential extraction procedure.

.

Fraction	Metal deposition in air particulate fractions (g ha^{-1} $month^{-1}$)							
	L1		L2		L3		L4	
	Dry season	Wet season	Dry season	Wet season	Dry season	Wet season	Dry season	Wet season
				Lead				
F1	ND (<0.04)	ND (<0.04)	ND (<0.04)	ND (<0.04)	ND (<0.04)	ND (<0.04)	ND (<0.04)	ND (<0.04)
F2	5.25 ± 4.50	0.42 ± 0.25	ND (<0.04)	ND (<0.04)	ND (<0.04)	ND (<0.04)	0.50 ± 0.00	ND (<0.04)
F3	61.92 ±61.50	6.25 ± 8.08	ND (<0.16)	ND (<0.16)	ND (<0.16)	ND (<0.16)	1.67 ± 0.17	1.25 ± 0.33
F4	9.67 ± 2.75	1.42 ± 2.00	6.75 ± 2.17	ND (<0.04)	ND (<0.04)	ND (<0.04)	ND (<0.04)	0.17 ± 0.17
F5	1.67 ± 1.17	2.17 ± 0.92	1.50 ± 0.33	0.92 ± 0.083	0.22 ± 0.008	0.26 ± 0.092	0.67 ± 0.17	1.00 ± 0.08
Sum	78.51 ± 64.50	10.26 ± 7.25	8.25 ± 1.83	0.92 ± 0.083	0.22 ± 0.008	0.26 ± 0.092	2.84 ± 0.33	2.42 ± 1.04
				Cadmium				
F1	ND (<0.01)	ND (<0.01)	ND (<0.01)	ND (<0.01)	ND (<0.01)	ND (<0.01)	ND (<0.01)	ND (<0.01)
F2	0.33 ± 0.33	0.83 ± 0.08	ND (<0.0003)	ND (<0.0003)	ND (<0.0003)	ND (<0.0003)	1.25 ± 0.08	ND (<0.0003)
F3	ND (<0.002)	ND (<0.002)	1.08 ± 0.17	0.17 ± 0.17	1.08 ± 0.08	0.33 ± 0.25	ND (<0.002)	ND (<0.002)
F4	ND (<0.001)	ND (<0.001)	ND (<0.001)	ND (<0.001)	ND (<0.001)	ND (<0.001)	ND (<0.001)	ND (<0.001)
F5	0.08 ± 0.00	0.08 ± 0.00	0.17 ± 0.00	0.17 ± 0.00	0.08 ± 0.08	ND (<0.003)	0.17 ± 0.00	0.17 ± 0.00
Sum	0.41 ± 0.33	0.91 ± 0.00	1.25 ± 0.17	0.34 ± 0.17	1.16 ± 0.00	0.33 ± 0.25	1.42 ± 0.33	0.17 ± 0.00
				Zinc				
F1	2.1 ± 2.92	4.1 ± 5.83	ND (<0.12)	1.2 ± 1.67	ND (<0.12)	0.7 ± 0.92	ND (<0.12)	2.8 ± 4.00
F2	25.5 ± 21.17	22.0 ± 2.90	ND (<0.22)	ND (<0.22)	ND (<0.22)	ND (<0.22)	38.5 ± 11.00	6.8 ± 5.33
F3	8.2 ± 11.58	1.1 ± 1.50	ND (<0.08)	ND (<0.08)	ND (<0.08)	ND (<0.08)	34.3 ± 8.83	9.3 ± 3.75
F4	2.1 ± 3.00	2.2 ± 3.08	10.0 ± 1.17	ND (<0.25)	3.8 ± 5.33	4.0 ± 5.58	6.6 ± 1.25	7.4 ± 2.25
F5	68.3 ± 44.50	87.3 ± 54.17	61.3 ± 35.08	69.7 ± 4.25	50.2 ± 17.00	47.7 ± 0.17	30.8 ± 43.67	207.0 ± 39.92
Sum	106. ± 34.92	116.7 ± 33.73	71.3 ± 36.25	70.9 ± 5.83	54.0 ± 22.33	52.4 ± 9.20	110. ± 25.00	233.3 ± 51.53

ND: Not detectable.
L1, L2, L3: 0.3, 1 and 2 km from lead smelter, L4: Heavy traffic area.
F1: Exchangeable, F2: Acid soluble, F3: Reducible, F4: Oxidizable, F5: Residue fractions.

it was observed that Pb occurred predominantly in the reducible fraction, with much smaller amounts occurring in the acid-soluble, oxidizable and residual fractions. There was no Pb in the exchangeable fraction. The predominance of Pb in the Fe-Mn oxide (reducible) fraction is in broad agreement with previous reports for air particles[1,19,20] and soil dusts[15,21]. The adsorption of Pb cations onto the Fe-Mn oxide phase is considered as a reasonably universal fixation process.

Cadmium occurred predominantly in the in acid soluble or reducible phases, while the highest proportions of Zn occurred mainly in the residual phase. Zinc in this fraction is unlikely to be easily released under natural conditions, however at sites L1 and L4 there were also reasonable amounts of Zn present in the acid-soluble fraction.

Elemental Associations of Lead in Air Particulate Samples Based on Extractograms

For investigation of elemental associations, comparison of extractograms obtained from continuous-flow sequential extraction can be used (graphic plots of metal concentrations in subfractions versus subfraction number) It is possible to evaluate the elemental associations in the various extracted solid phases by comparing the details of peak profiles and peak shapes of overlain extractograms.

The distribution and chemical associations of Pb and major elements (Al and Fe) in air particulate matter for contaminated air particulate samples (300 m from lead smelter and heavy traffic area) can be evaluated using the extractograms shown in Fig. 4. Chemical associations of Pb in air particulate matter were not studied at sampling sites L2 and L3 because of the low concentrations of Pb in each fraction (Table 2).

For the contaminated air particulate matter at the lead smelter site (L1), although the Pb occurred predominantly in the reducible phase, Pb and Al had similar dissolution patterns within the acid soluble phase in both wet and dry seasons (Fig. 4: 1a and b). This indicates a close association between Pb and Al in the acid soluble phase of contaminated air particulate matter. In contrast, in the reducible phase, the Pb peak was found to increase rapidly early in the fraction, preceding the bulk of the Fe (and Al) dissolution in this phase. This has been taken as an indication that the Pb is mostly adsorbed on oxide (Fe/Al) surfaces; the results being very similar to the extractograms of soil samples collected at the same site[17]. The air particulates are probably therefore derived mainly from wind-blown dust at the site.

Extractograms for contaminated air particulate matter from the heavy traffic area site (L4) also show associations of Pb with the Fe/Al oxide phases (Fig. 4: 2a and b). Therefore, irrespective of the source of the contamination, the extractograms appear quite similar.

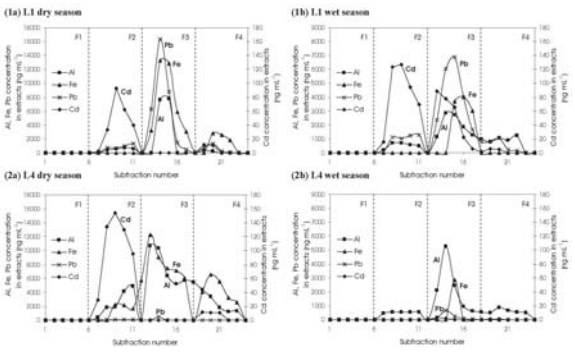

Fig 4. Extractograms for air particulate matter obtained using the continuous-flow sequential extraction procedure for contaminated air particulate: L1 in the dry season (1a) and L1 in the wet season (1b), L4 in the dry season (2a) and L4 in the wet season (2b).

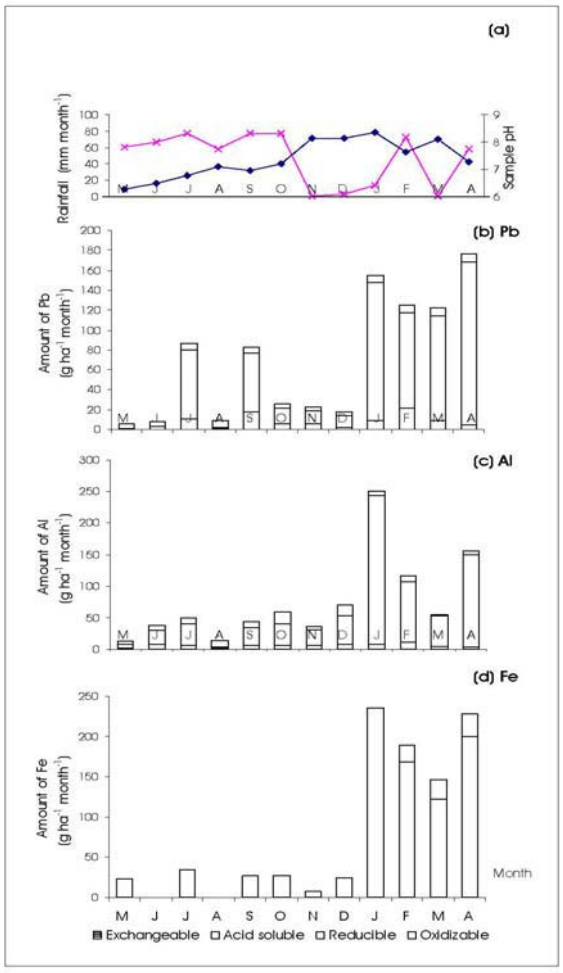

Fig 5. Monthly rainfall data (a) and fractional distribution of Pb (b), Al (c), and Fe (d) for air particulate matter collected near a lead smelter (site L1).

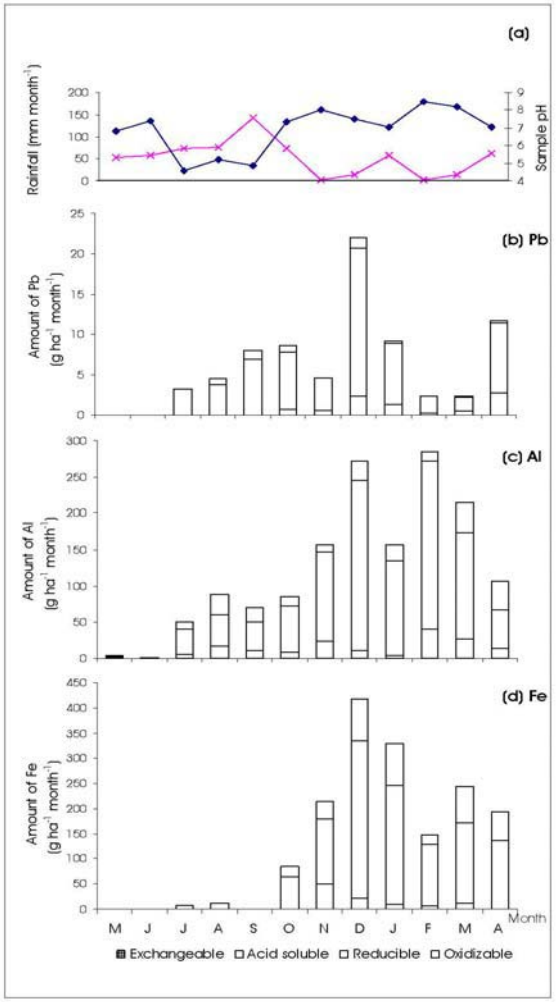

Fig 6. Monthly rainfall data (a) and fractional distribution of Pb (b), Al (c), and Fe (d) for air particulate matter collected near a heavy traffic area (site L4).

Monthly Fractional Distribution of Pb in Air Particulate Matters

Monthly data for the fractional distribution of Pb in air particulate matter are shown in Fig. 5-6. The data are shown together with rainfall (mm) and pH from May, 2004 to April, 2005.

At both sites, the fractional distribution of Pb, Al and Fe between chemical forms in contaminated air particulate matter was quite similar for all months, with no obvious differences between the dry and wet seasons. It can therefore be concluded that seasonal change does not affect the distribution of chemical forms of Pb, Al and Fe in air particulate matter. Considering the metal content of the particulate matter, it was clearly observed that total metal concentrations were higher in the dry compared with the wet months (Fig. 5 and 6). This was most clearly observed at sampling site L1. Soil aerosols normally make the largest contribution to atmospheric pollution with Al and Fe as the most abundant metals acting as markers[22,23]. In the dry season, wind-blown dusts are likely to be more abundant at both the smelter and heavy traffic sites with resulting deposition of particulate matter occurring by sedimentation or diffusion.

Conclusion

A continuous-flow sequential extraction system was used to study the fractionation and elemental association of metals in air particulate matter. For air particulate matter from the lead smelter and traffic-related dust examined in this study, Pb was predominantly present in the reducible fraction, with moderate amounts occurring in the oxidizable and residual fractions, and a small amount being associated with the acid soluble phase. Examination of extractograms showed close associations between Al and Pb in the acid soluble phase for the contaminated air particulate matter from the lead smelter. In contrast, in the reducible fraction, Pb appeared to dissolve earlier than Fe and Al suggesting that Pb is adsorbed on Fe/Al oxide surfaces in air particulate matter. Similar extractograms for soil collected from the same location suggests wind-blown dust to be the source of the particulate matter. Extractograms of Pb in particulate matter from a heavy traffic area also showed close associations of Pb with the major elements Al and Fe. Total Pb deposition in the dry season was found higher than in the wet season supporting the suggestion that soil dust is the predominant source of the atmospheric particulate matter. The fractional distribution of Pb, Al and Fe in particulate matter was very similar for both dry and wet seasons.

Acknowledgements

The authors would like to gratefully thank the Thailand Research Fund and the Postgraduate Education and Research Program in Chemistry (PERCH), Higher Education Development Project of the Commission on Higher Education for financial support.

References

1. Harrison RM, Laxen DPH and Wilson SJ (1981) Chemical associations of lead, cadmium, copper, and zinc in street dusts and roadside soils. *Environ Sci Technol* **15**, 1378-83.
2. Tessier A, Campbell PGC and Bisson M (1979) Sequential extraction procedure for the speciation of particulate trace metals. *Anal Chem* **51**, 844-51.
3. Gleyzes C, Tellier S and Astruc M (2002) Fractionation studies of trace elements in contaminated soils and sediments: a review of sequential extraction procedures. *Trac-Trend Anal*

Chem **21**, 451-67.
4. Sahuquillo A, Rigol A and Rauret G. (2003) Overview of the use of leaching/extraction tests for risk assessment of trace metals in contaminated soils and sediments. *Trac-Trend Anal Chem* **22**, 152-59.
5. Shiowatana J, Tantidanai N, Nookabkaew S and Nacapricha D (2001) A flow system for the determination of metal speciation in soil by sequential extraction. *Environ Inter* **26**, 381-87.
6. Shiowatana J, McLaren RG, Chanmekha N and Samphao A (2001) Heavy metals in the environment. *J Environ Qual* **30**, 1940-49.
7. Chomchoei R, Shiowatana J and Pongsakul P (2002) Continuous-flow system for reduction of metal readsorption during sequential extraction of soil. *Anal Chim Acta* **472**, 147-59.
8. Gray CW, McLaren RG and Roberts AHC (2003) Atmospheric accessions of heavy metals to some New Zealand pastoral soils. *Sci Total Environ* **305**, 105-15.
9. Railsback LB (1997) Lower pH of acid rain associated with lightning: evidence from sampling within 14 showers and storms in the Georgia Piedmont in summer 1996. *Sci Total Environ* **198**, 233-41.
10. Fang GC, Wu YS, Huang SH and Rau JY (2005) Review of atmospheric metallic elements in Asia during 2000-2004. *Atmos Environ* **39**, 3003-13.
11. Nriagu JO (1979) Global inventory of natural and anthropogenic emissions of trace metals to the atmosphere. *Nature* **279**, 409-11.
12. Duce RA, Hoffman GL and Zoller WH (1974) Atmospheric trace metals at remote northern and southern hemispheric sites: pollution and natural. *Science* **187**, 59-61.
13. Mason B and Moore CB (1982) Principles of Geochemistry, 4th ed. John Wiley and Sons, Inc.
14. Karar K, Gupta AK, Kumar A and Biswas AK (2006) Characterization and identification of the sources of chromium, zinc, lead, cadmium, nickel, manganese and iron in PM10 particulates at the two sites of Kolkata, India. *Environ Monit Assess* **120**, 347-60.
15. Banerjee ADK (2003) Heavy metal levels and solid phase speciation in street dusts of Delhi, India. *Environ Pollut* **123**, 95-105.
16. Wang X, Sato T, Xing B, Tamamura S and Tao S (2005) Source identification, size distribution and indicator screening of airborne trace metals in Kanazawa, Japan. *J Aerosol Sci* **36**, 197-210.
17. Tongtavee N, Shiowatana J and McLaren RG (2005) Fractionation of lead in soils affected by smelter activities using a continuous-flow sequential extraction system. *Intern J Environ Anal Chem* **85**, 567-83.
18. Tongtavee N, Shiowatana J, McLaren RG and Gray CW (2005) Assessment of lead availability in contaminated soil using isotope dilution techniques. *Sci Total Environ* **348**, 244-56.
19. Fernández AJ, Ternero M, Barragán FJ and Jiménez JC (2000) An approach to characterization of sources of urban airborne particles through heavy metal speciation. *Chemosphere Global Change Science* **2**, 123-36.
20. Espinosa AJF, Rodríguez MT, Rosa FJB and Sánchez JCJ (2002) A chemical speciation of trace metals for fine urban particles. *Atmos Environ* **36**, 773-80.
21. Li X, Poon CS and Liu PS (2001) Heavy metal contamination of urban soils and street dusts in Hong Kong. *Appl Geochem* **16**, 1361-68.
22. Peirson DH, Cawse PA, Salmon L and Cambray RS (1973) Trace elements in the atmospheric environment. *Nature* **241**, 252-56.
23. Querol X, Alastuey A, Rosa JDL, Campa ASDL, Plana F and Ruiz CR (2002) Source apportionment analysis of atmospheric particulates in an industrialised urban site in southwestern Spain. *Atmos Environ* **36**, 3113-25.

Intern. J. Environ. Anal. Chem.
Vol. 85, No. 8, 15 July 2005, 567–583

Taylor & Francis
Taylor & Francis Group

Fractionation of lead in soils affected by smelter activities using a continuous-flow sequential extraction system

NAMFON TONGTAVEE*†, JUWADEE SHIOWATANA† and RONALD G. McLAREN‡

†Department of Chemistry, Faculty of Science, Mahidol University, Rama VI Road, Bangkok 10400, Thailand
‡Soil and Physical Sciences Group, Agriculture and Life Sciences Division, PO Box 84, Lincoln University, Canterbury, New Zealand

(*Received 15 December 2004; in final form 29 March 2005*)

A continuous-flow sequential extraction system was used to study the distribution of Pb, and its association with other elements (Fe, Al and Ca), in soils around a Pb smelter. Soil samples were analysed by a four-step continuous-flow sequential extraction procedure employing a modified Tessier/BCR scheme. Recoveries of Pb using the flow system (88–111%) were higher than those obtained using a conventional batch extraction system. There were also some differences in Pb distribution between fractions as determined using the two extraction systems. The most abundant fraction of Pb was extracted during the dissolution of soil oxides (Fe/Al). Extractograms (plots of concentration of elements *vs.* extractant volume/time) indicated that anthropogenic Pb was predominantly adsorbed onto Fe oxide surfaces in contaminated soils. In soil profiles, the highest amounts of Pb were found in the topsoil surface layers (0–5 cm) of the contaminated soils with only limited movement into subsurface layers.

Keywords: Continuous-flow extraction system; Elemental association; Sequential extraction; Pb; Smelter

1. Introduction

Many heavy metals are very common in industrial and domestic usage. Consequently, wastes containing heavy metals have been dispersed into the environment through their improper management and disposal. Metal smelters are important industrial point sources of heavy metals. Toxic metals emitted into the atmosphere can be re-deposited onto the land and accumulate in the soil. Moreover, the accumulated metals in soil may be taken up by plants, which could cause human health problems through the food chain. Therefore it is important to assess soil contamination in order to understand the potential adverse effects and to impose appropriate control measures.

*Corresponding author. Fax: +662-259 2097. Email: namfon@swu.ac.th

International Journal of Environmental Analytical Chemistry
ISSN 0306-7319 print: ISSN 1029-0397 online
DOI: 10.1080/03067310500140345

In most circumstances, risk assessment to human health from contamination of soils by heavy metals has usually been based on total concentrations of metals in soil. This can provide information on the degree of contamination [1]. Unfortunately, the potential risk from contaminated soil is not dependent on the total concentration of the element alone, but on the chemical reactivity of the element or the chemical species of the element of interest. The identification of chemical species or forms and their quantitative data should be used to assess the bioavailability, toxicity and environmental impact of contaminant metals. In recent years, there has been development of chemical testing procedures to measure bioavailability to plants of metals and metalloids in soil [2]. In general, sequential extraction using a series of chemicals of increasing strength is a widely used method for metal fractionation and evaluation of the potential of metal leaching [3]. The sequential extraction approach can provide detailed information about the origin, mode of occurrence, biological and physicochemical availability, mobilization, and transport of metals [4]. Elements extracted in the same extraction steps have been used as evidence of their chemical association (e.g. [5]). However, this may not always be absolutely correct, because elements extracted from the same phase may not have dissolved simultaneously but at different times during the same extraction step. In our previous work, we have developed a continuous-flow system for sequential extraction [6, 7], which has shown many advantages over the batch system such as speed, ease of operation, less vulnerability to variation in extraction conditions, high extraction efficiency and freedom from operational contamination. The flow system has also been proved to reduce the problem of metal readsorption and redistribution during extraction in comparison with the batch system [8]. Extractograms, i.e. plots of concentration of element extracted *vs.* subfraction number (in effect time) obtained using the system also provides kinetic information and information on solid phase elemental associations [9].

The purpose of the present study is to investigate the use of a continuous flow extraction system to determine the distribution of Pb in soils contaminated by atmospheric fallout from a metal smelter. The study compares the results obtained using the flow system with those obtained for the same soils using a traditional batch extraction system. A secondary objective was to use the extractograms obtained from the flow extraction system for interpretation of elemental associations in the various soil fractions. Results obtained from this work should help improve our understanding of the transformations of contaminant Pb at an industrially contaminated field site.

2. Materials and methods

2.1 *Soil samples*

Surface soil samples (0–5 cm) were sampled from the area surrounding a small Pb smelter located in Saraburi Province, approximately 110 km north of Bangkok, Thailand (figure 1). The smelter has been operating for the last 10 years and it is used essentially to recycle Pb from old batteries. Sampling was carried out at distances of between 0 and 2.5 km from the smelter by taking several subsamples with a trowel, and bulking from an area of approximately 0.5 m^2 at each location. Since the land surrounding the smelter has many different private owners, only parts of the area were accessible. The areas sampled were all uncultivated grassland. A preliminary

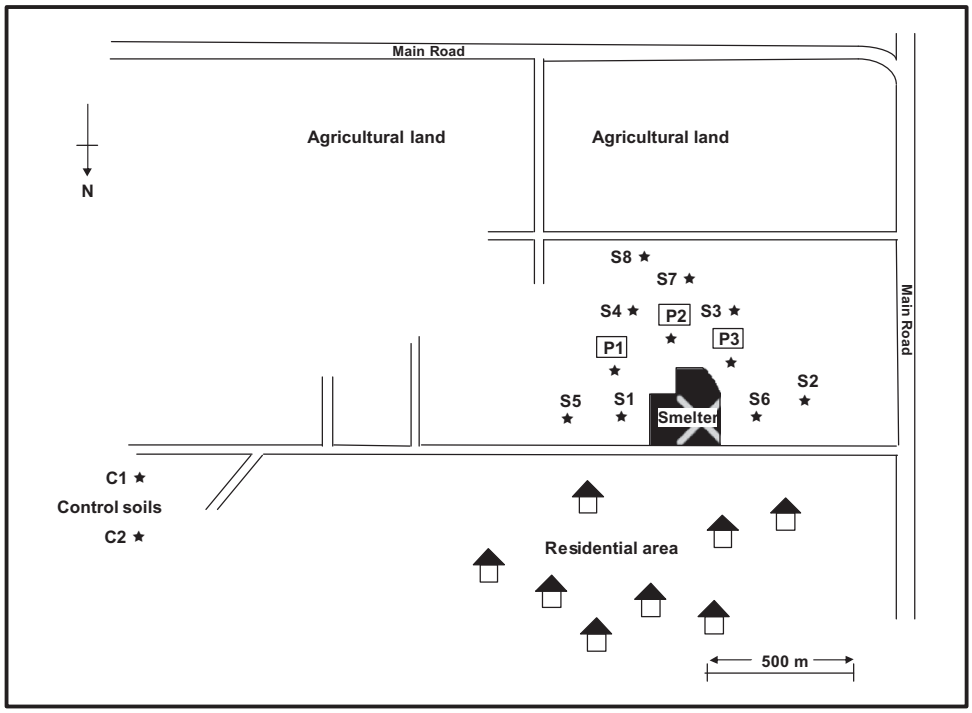

Figure 1. Map showing the sampling sites in the area adjacent to the smelter.

Table 1. General soil characteristics.

Soil	Total Pb ($mg\,kg^{-1}$)	pH	Sand (%)	Silt (%)	Clay (%)	Org. C (%)	Total Fe (%)	Total Al (%)	Total Ca ($mg\,kg^{-1}$)
Control C1	21.2	5.54	21.3	56.9	21.8	2.23	5.1	1.8	2844
Soil S1	69.9	6.51	20.5	63.6	15.9	2.89	7.6	1.2	3282
Soil S2	99.2	6.17	24.6	61.9	13.5	1.47	4.7	0.8	2259
Soil S3	143.0	5.91	17.1	65.1	17.8	1.81	3.3	1.1	1875
Soil S4	246.6	5.73	20.5	61.4	18.1	2.65	3.4	1.1	2251

sampling of topsoils from the site was carried out and the total concentrations of Pb in these samples were determined. The results showed that total Pb concentrations varied in the range of 20–250 $mg\,kg^{-1}$ Pb. Five of the topsoil samples were then chosen for further study to represent a range from background to high concentrations of Pb (Samples C1, S1, S2, S3 and S4). Background topsoil samples were sampled at a distance of 2 km from the smelter. The chemical and physical properties of these five soils are shown in table 1. For studying the distribution of Pb with soil depth, three soil profiles were sampled at depths of 0–5 and 5–10 cm from the surface at distances of less than 200 m from the Pb smelter (locations P1, P2 and P3, figure 1). A further sample was taken from the base of each profile (20–30 cm) in the expectation that the soil at this depth would most likely be completely unaffected by the smelter emissions. Soil samples were dried at 30°C in an oven for 5 d. All the samples were then ground and sieved through a 2-mm stainless steel sieve. All soils were stored in

a desiccator prior to laboratory analysis. Soil pH was measured in a water suspension using a soil/solution ratio of 1 : 2.5 after the suspensions were shaken for 24 h on a reciprocating shaker at 20°C [10]. Total carbon content was determined by a LECO CNS 2000 Analyser. Soil texture was obtained using the Malvern Laser Sizer method [11]. Total Pb, Fe, Al and Ca were determined by acid digestion as described by Kovacs *et al*. [12] followed by atomic absorption spectrophotometric detection.

2.2 *Standard reference material (SRM)*

SRM 2711 was purchased from the National Institute of Standards and Technology (NIST) (Gaithersburg, MD). This is a moderate contaminated soil (particle size < 74 μm) from Montana. It has been prepared to achieve a high degree of homogeneity with certified total elemental concentrations provided. Hence, it is suitable for use to validate the proposed continuous-sequential extraction method. The SRM is guaranteed for homogeneity provided that analyses are performed using a minimum sample size of 250 mg.

2.3 *Preparation of standard solutions and glassware*

The chemical reagents in this work were of analytical grade. Ultra-pure water from a MilliQ water purification unit (Millipore, Bedford, MA) was used throughout this work. All glassware used was cleaned and soaked in 10% HNO_3 and rinsed with ultrapure water before use. Standard stock solutions (1000 mg L^{-1}) were purchased from Merck, (Darmstadt, Germany) or prepared in-house from pure metals. Working standard solutions for calibration of graphite furnace atomic absorption spectrophotometry (GFAAS) measurements were prepared by diluting the stock solution with ultrapure water or with extracting reagents before use.

2.4 *Fractionation scheme*

The fractionation scheme used was based essentially on the Tessier *et al*. [13] and BCR [14] schemes but with substantial modifications to enable its use with the flow extraction system. The geochemical phase at each extraction step is operationally defined according to the reagents used as shown in table 2. The phases extracted should be considered as nominal rather than absolute chemical fractions. For step I

Table 2. Sequential fractionation procedure.

Step	Nominal fraction	Extractant	Extraction conditions (Batch method)
I	Exchangeable	0.01 M $Mg(NO_3)_2$[a]	Shaken 24 h, 25°C
II	Acid-soluble (carbonate or specifically sorbed)	0.11 M CH_3COOH[b]	Shaken 16 h, 25°C
III	Reducible (Fe/Al/Mn oxide-bound)	0.1 M $NH_2OH \cdot HCl$, pH 2[b]	Shaken 6 h, 96°C
IV	Oxidizable (organic-bound)	30% H_2O_2 : 0.02 M HNO_3 (8 : 3 v/v)[a]	Shaken 5 h, 85°C
V	Residual	$HNO_3 + H_2O_2$[c]	Acid digestion

[a] Modification from Tessier *et al*. scheme [13, 15].
[b] Modification from BCR scheme [14].
[c] Acid digestion, Kovacs *et al*. procedure [12].

(exchangeable phase), which is not required in the BCR scheme, 0.01 M $Mg(NO_3)_2$ was used as the extractant. Many authors use 1 M $MgCl_2$ for this phase following the Tessier *et al*. [13] scheme. However, using a nitrate salt reduces the background absorption when determining Pb with GFAAS. The lower strength salt was used to simulate desorption of the most weakly bound ions (exchangeable) into the soil solution (e.g. [15, 16]). For Steps II and III the reagents used in the BCR sequential extraction scheme were used [14]. Step IV was modified from the Tessier *et al*. [13] scheme by using only 30% H_2O_2 : 0.02 M HNO_3 (8 : 3 v/v) because intermittent addition of NH_4OAc during extraction is not practical in the flow system. The last step (Step V) was performed using the HNO_3/H_2O_2 digestion procedure of Kovacs *et al*. [10]. Such digestions are often referred to as pseudo-total analyses [17] since they do not include metals trapped within the lattices of silicate minerals. However, true total analyses are not considered necessary for the assessment of metal-contaminated soils since only those metals potentially available for leaching and biological processes are usually of interest [18].

In the batch extraction system, the soil sample was weighed accurately into a centrifuge tube and the extractions at each step were carried out using the equilibration times as shown in table 2. A water bath was used for the extraction steps where higher temperatures were required. Centrifugation (10,000 rpm for 10 min), decantation and filtration steps (Whatman filter paper, No. 52) were used for separation of the liquid and solid phases at each step. This differs from the Tessier *et al*. [13] procedure in which supernatants were removed by pipette. In this work, the original five soil samples (C1, S1–S4) were fractionated using both batch and continuous-flow extraction systems to examine the accuracy and efficiency of these two extraction systems. The sets of samples taken from different depths (P1–P3) were fractionated using the flow extraction system only.

2.5 *Continuous-flow extraction system*

2.5.1. The extraction chamber. An extraction chamber was designed to allow containment and stirring of a weighed sample of soil. Extractants are pumped sequentially through the chamber and leach metals from the targeted phases. The chambers and covers were constructed from borosilicate glass to have a capacity of approximately 10 mL [6, 7]. The outlet of the chamber was furnished with a filter (Whatman [Maidstone, UK]) glass microfibre filter GF/B, 47-mm diameter, 1-μm particle retention). Extractant was pumped through the chamber using a peristaltic pump (Micro tube pump, MP-3N, EYELA [Tokyo Rikakikai Co., Ltd.]) at varying flow rates using tygon tubing of 2.25 mm inner diameter. Heating of the extractants in Steps III and IV was carried out by passing the extractants through a glass heating coil approximately 120 cm in length, placed in a water bath. However, because of heat loss problems, even when the glass heating coil was immersed in a thermostat water bath controlled at 95°C, the maximum temperatures achieved in the extraction chamber were between 80 and 85°C. Thus, for Step IV in particular, the temperatures used were somewhat lower than those used for the batch system (table 2).

2.5.2. Extraction procedure. A weighed sample (1.00 g) was transferred to a clean extraction chamber together with a magnetic bar. A glass microfibre filter was then

placed on the outlet followed by a silicone rubber gasket, and the chamber cover was securely clamped in position. The chamber was connected to the extractant reservoir and the collector vial using tygon tubing and placed on a magnetic stirrer. The magnetic stirrer and peristaltic pump were switched on to start the extraction. The extracting reagents were continuously and sequentially pumped through the chamber. The extracts passing through the membrane filter were collected in subfractions of 10–30 mL volume intervals until all four leaching steps were completed. For most soils examined, it was found that 120–180 mL were sufficient to leach the metals completely for each step.

2.5.3. Residue digestion. Residue digestion was performed using an acid digestion method [12] on a heating block. This system was equipped with a heating program. Amounts of 0.5–1.0 g of dried soil sample or residue from the extraction chamber were transferred to digestion tubes together with 5 mL of HNO_3 (70%) and 5 mL of H_2O_2 (30%). The digestion tubes were placed on a heating block and the digestion was operated following the recommended heating program for 6 h [12]. The digest solutions were cooled to room temperature, and filtered through Whatman filter paper No. 52, were then made up to volume in a volumetric flask. Total metal concentrations were determined by both a single digestion of non-fractionated soil and by summation of extractable metals in each subfraction of the exchangeable, acid-soluble, reducible, oxidizable and residual fractions.

2.6 *Analysis of extracts and acid digests*

Lead concentrations in extracts were determined using graphite furnace atomic absorption spectrophotometry (GFAAS). The GFAAS measurements were performed with a Perkin Elmer (Norwalk, CT) Analyst 100 equipped with a deuterium background corrector and an HGA-800 heated graphite atomizer. The sample was introduced to the atomizer using an AS-72 autosampler. Flame atomic absorption (FAAS) measurements for Fe, Al and Ca were performed using a Perkin Elmer Model 3100 spectrometer equipped with deuterium background correction. Concentrations of metals were obtained by the matrix-matched standard calibration method. Working standard solutions were prepared in the same extracting reagent as the sample solutions.

3. Results and discussion

3.1 *Validation of the continuous-flow sequential extraction system using a standard reference material*

We initially evaluated the proposed continuous-flow sequential extraction system by carrying out a sequential extraction of 0.25 g of NIST standard reference material (SRM 2711). The resulting analytical data are shown in table 3. The sums of each element determined (Pb, Fe, Al and Ca) found in all fractions (I + II + III + IV + Residue) were compared with the reference values of acid leaching data provided by NIST. It was found that they agreed reasonably well within the range of reference values provided indicating that the extraction data obtained from the continuous-flow extraction system are reliable.

Table 3. Comparison of analytical results for summation of elemental concentrations determined using the continuous-flow sequential extraction system for SRM 2711 ($mg\,kg^{-1} \pm$ s.d., $n = 3$).

Element	Step I	Step II	Step III	Step IV	Residue	Sum of fractions	Leached value[a]	Certified value[b]
Pb	3.7 ± 0.5	309 ± 9	710 ± 90	23 ± 8	91 ± 17	1138 ± 56	930–1500	1162 ± 31
Fe	ND	228 ± 12	964 ± 119	123 ± 10	14860 ± 460	16170 ± 460	17000–26000	28900 ± 600
Al	ND	ND	1290 ± 107	160 ± 18	20660 ± 550	22100 ± 430	12000–23000	28800 ± 800
Ca	3970 ± 90	11920 ± 700	3820 ± 140	25 ± 4	89 ± 13	19820 ± 660	20000–25000	65300 ± 900

ND = non-detectable.
[a] Acid leaching values for SRM 2711 provided by NIST.
[b] Certified values for total concentrations of SRM 2711 provided by NIST.

3.2 *Comparison of Pb fractionation obtained using continuous-flow and batch sequential extraction techniques*

Table 4 compares the distribution of Pb in soils obtained using the flow system and a conventional batch method. In the flow system, the amounts of Pb in each individual phase were obtained by summation of the amounts in all subfractions of each step. In general, the flow system gave better recoveries of Pb compared to the batch system for all samples analysed. The summation of Pb fractions obtained using the flow method also showed good agreement with the total concentrations from a single total analysis. The recoveries in the batch system were poorer, probably as a result of losing particulate matter at each stage during centrifugation and filtration. However, the flow extraction is a closed system, which effectively solves this problem. The precision (repeatability) of the flow system appears to be slightly lower than for the batch system (see standard deviations in table 4). This is probably due to the summation of data from several subfractions for each fraction in the flow system.

Although the overall recoveries of Pb was higher using the flow system, in the first two exchangeable and acid soluble phases, the amounts of Pb extracted using the flow system were lower than those obtained using the batch system. Lead is very strongly sorbed onto soil and the flow rate of extractant at 3–5 mL min^{-1} (calculated as approximately 0.5 h total contact time) may have been too fast to allow adequate equilibration between solution and solid phases. In contrast, in the batch system, equilibration was carried out for 16 or 24 h for these fractions (table 2). In addition, although not significant in terms of overall recoveries, the Pb concentrations in subfractions of Steps I and II were often near or below detection limits. For the soil oxides (Fe/Al); extraction step, the amounts of Pb extracted using the flow system were higher than those obtained using the batch system. Conversely in the following step (oxidizable), the amounts of Pb extracted using the flow system were lower than those obtained using the batch system. These observations can be explained by the readsorption of Pb in the batch system. Chomchoei *et al*. [8] have investigated and compared the readsorption process in both batch and flow systems. For Pb, their results clearly showed that for the conventional batch system, there was significant readsorption in both the reducible and oxidizable steps. Some Pb extracted in the reducible phase was readsorbed and could be dissolved in the next step; the oxidizable phase. Hence the batch system tends to underestimate the Pb associated with the Fe/Al oxides and overestimates the Pb associated with the oxidizable fraction. In contrast, readsorption is not observed for the continuous-flow extraction system [8]. Little readsorption occurs in the flow system because the extracted Pb is gradually removed from the system in the flowing extractant before it can be readsorbed on the solid phase. According to the results of the present work, the amount of Pb in the reducible step appears to be more completely dissolved and removed in the flow system. It can be observed from the extractograms (figure 2) that the concentration of Pb approaches the baseline towards the end of the reducible step. However, this is not the case for the oxidizable step, which normally takes a longer time to complete because of clogging of the filter paper by dispersed soil. This is often found in the flow extraction for this step because the oxidizable phase is often complex and the extraction temperature achievable is not high enough for rapid dissolution of organic matter in this phase. The concentration of some elements remained well above the baseline when the extraction (Step IV) was discontinued. This also suggests an additional reason

Table 4. Comparison of analytical results for batch and flow sequential extraction methods of Pb for soil samples (mg kg^{-1} ± s.d., $n = 2$).

Sample	Method	Step I	Step II	Step III	Step IV	Residue	Sum of fractions	Total
Control C1	Flow	0.11 ± 0.00	0.06 ± 0.01	11.7 ± 3.9	0.87 ± 0.25	8.77 ± 1.06	21.54 ± 3.05	20.8 ± 2.9
	Batch	0.19 ± 0.06	0.99 ± 0.17	7.44 ± 0.5	1.23 ± 0.09	4.6 ± 0.15	14.45 ± 0.30	
Soil S1	Flow	0.16 ± 0.01	0.06 ± 0.01	41.6 ± 3.1	0.78 ± 0.11	19.53 ± 3.04	62.16 ± 0.15	69.9 ± 9.0
	Batch	0.27 ± 0.07	2.21 ± 0.38	21.4 ± 1.1	5.42 ± 0.17	14.15 ± 1.43	43.36 ± 0.90	
Soil S2	Flow	0.14 ± 0.05	0.71 ± 0.10	96.8 ± 1.2	1.68 ± 0.53	11.23 ± 2.72	110.54 ± 2.19	99.2 ± 8.5
	Batch	0.25 ± 0.08	3.01 ± 0.22	54.0 ± 3.1	11.67 ± 0.29	7.30 ± 0.10	76.22 ± 1.60	
Soil S3	Flow	0.19 ± 0.10	1.73 ± 0.07	124.0 ± 0.1	1.99 ± 0.42	17.42 ± 2.86	145.29 ± 3.90	143.0 ± 2.1
	Batch	0.45 ± 0.04	3.52 ± 0.15	78.0 ± 0.2	15.89 ± 0.98	10.60 ± 0.20	108.46 ± 0.52	
Soil S4	Flow	0.03 ± 0.01	3.52 ± 0.27	229.5 ± 0.3	4.12 ± 0.09	21.81 ± 2.50	259.00 ± 2.95	246.6 ± 6.7
	Batch	0.19 ± 0.04	4.78 ± 0.83	131.2 ± 8.8	25.9 ± 0.87	18.70 ± 2.90	180.86 ± 4.70	

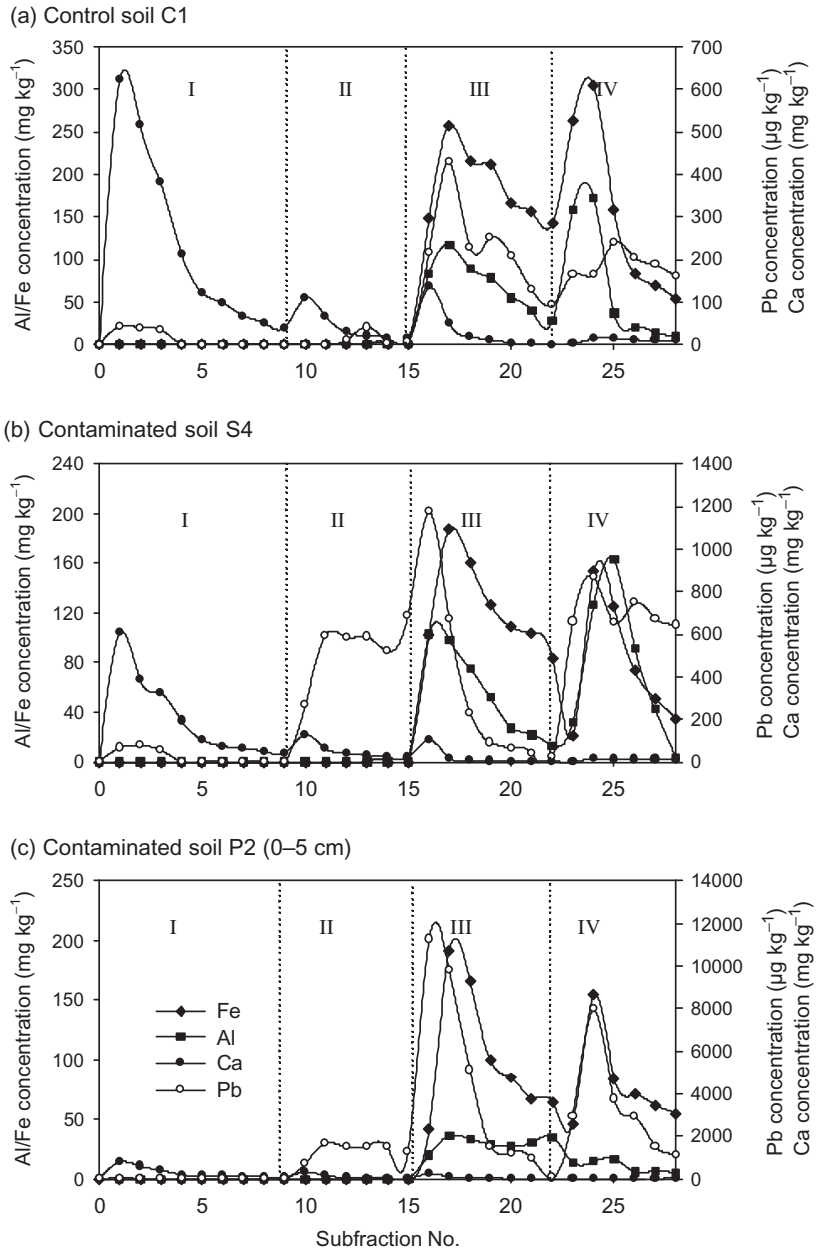

Figure 2. Extractograms obtained using the continuous-flow method for (a) control C1, (b) contaminated soil S4, and (c) contaminated soil P2 (0–5 cm). For purposes of clarity, Pb concentrations in fraction III have been scaled down by factors of 10 (C1 and P2) or 100 (S4).

why the amounts of Pb extracted in this step in the flow system are lower than those obtained in the batch system (table 4), with some of Pb in effect being carried over to the residual phase. The mean proportions of Pb present in individual fractions obtained from the both batch and flow extraction systems are shown in figure 3.

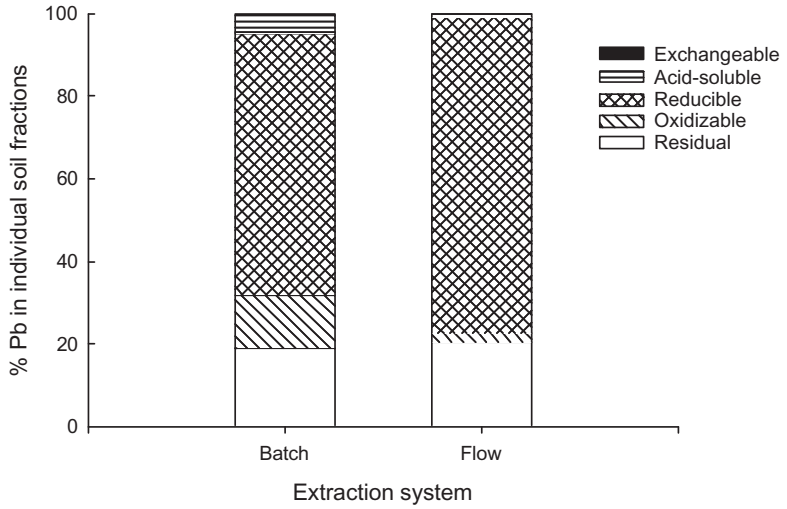

Figure 3. A comparison of mean fractional distributions of Pb in soils as determined by batch and continuous-flow methods.

Table 5. The distribution of contaminant Pb determined using the flow sequential extraction system.

	Contaminant Pb[a] ($mg\,kg^{-1}$)					
Sample	Step I	Step II	Step III	Step IV	Residue	Sum
Soil S1	0.05	0.00	29.86	−0.09	10.76	40.85
Soil S2	0.03	0.65	85.05	0.81	2.46	89.00
Soil S3	0.08	1.67	112.26	1.12	8.65	123.78
Soil S4	−0.08	3.46	217.77	3.25	13.04	237.44
Mean %	0.005	0.88	87.89	0.74	10.44	
Control C1 %	0.51	0.28	54.41	4.04	40.75	

[a] Pb concentrations in fractions of control C1 have been subtracted.

Although clearly there are differences between the two systems, in both systems the highest proportion of Pb was found in the reducible fraction (60–80%), followed by the residual (10–40%), organic/sulphide bound (1–15%), acid-soluble (0.8%) and exchangeable (0.005%) fractions. However, for the following parts of this study, only the flow system has been used. This system was selected because of advantages in reducing soil loss, potential contamination and readsorption phenomena, and providing better overall Pb recoveries.

3.3 *Examination of anthropogenic Pb in the soil using the flow system*

When anthropogenic Pb is deposited and incorporated into the soil, it can be distributed and fixed by different soil phases [19]. Table 5 shows the differences in amounts of Pb ($mg\,kg^{-1}$) in individual fractions between the control and the contaminated samples (i.e. anthropogenic Pb) as determined using the flow extraction system. It can be seen that in the contaminated soils, the anthropogenic Pb is distributed between all the individual phases. However, the distribution is substantially

different to that of the native soil Pb found in the control soil. Considering each fraction, there are very small proportions of contaminant Pb in the exchangeable, acid soluble phases, and oxidizable phases; 0.005, 0.883 and 0.74% respectively. Most of the contaminant Pb appears in the reducible phases (88%), with an approximate 10% in the residual fraction. This result is in agreement with earlier reports that soil oxides are important scavengers of heavy metals in soils (e.g., [20]). However, previous studies, including soils with relatively high organic matter contents, have shown that in such soils, anthropogenic Pb may occur predominantly in the oxidisable fraction [21, 22].

The above results demonstrate considerable soil pollution with Pb in the vicinity of the smelter. Our sequential extraction data also agrees with some previous studies, which have measured metal concentrations of soils affected by smelters [23–25]. Such studies have suggested that sequential extraction investigations are good tools to distinguish between contaminated and native soils. The mineral phases that hold heavy metals appear to be significantly different in the native soils compared to contaminated soils. The typically lithogenic metals Fe, Al, Ca and Pb usually occur in uncontaminated soils predominantly in the most stable fractions. Lead of anthropogenic origin has considerably higher proportions in mobile fractions and correspondingly lower proportions in residual phases.

3.4 *Lead fractionation in samples from different depths*

Data on metal fractionation of soil at different soil depths is essential for considering the processes of metal transformation, mobility and bioavailability as well as the long-term risk assessment. Total Pb concentrations in different layers of polluted soils have been measured and monitored previously [23, 24]. These studies found that Pb fractionation differed between topsoils and subsoils. Mobile Pb (exchangeable and acid soluble fractions) was high in topsoils and much lower in subsoils.

In this present study, in order to assess the vertical extent of soil contamination, topsoil and subsoil concentrations of Pb were compared using the flow sequential extraction technique (table 6). In all three profiles sampled, at a distance of 0.2 km from the emission point source, the highest concentrations of Pb were found in the topsoils, ranging from 350–450 mg kg^{-1} (table 6). However, Pb concentrations in the subsurface layers (5–10 cm and 20–30 cm) were much lower and differed from one point to another. The concentrations of Pb at a depth of 30 cm are the lowest and similar to background concentrations (ca 10–15 mg kg^{-1}). This indicates that the Pb of anthropogenic origin showed high accumulations at the soil surface and only moves slowly downward through the soil profile. The Pb fractionation data for the different depth samples are summarized in table 6. The results demonstrate that there are significant increases of anthropogenic Pb (mg kg^{-1}) in topsoil samples found in the first two most mobile fractions; the exchangeable and acid-soluble fractions. However, most anthropogenic Pb was present in the reducible fraction due to the ability of soil oxides (Fe/Al) to fix Pb. The enhancement of the available/mobile pool in the topsoil is probably responsible for the limited movement of Pb down into the deeper layers. However, most of the Pb leached from the topsoil appears to be fixed by soil oxides in the 5–10 cm layer, limiting any further movement to deeper layers. These results are similar to those reported in many previous studies [23, 24, 26]. For example, Ettler *et al.* [26] have estimated downward penetration rates of between

Table 6. Fractionation of Pb in soil profiles (mg kg^{-1} ± s.d., $n = 2$).

Sample	Depth (cm)	Step I	Step II	Step III	Step IV	Residue	Sum of fractions	Total
P1	0–5	0.040 ± 0.002 (0.012)	8.36 ± 0.20 (2.63)	313.19 ± 13.26 (86.50)	2.29 ± 0.26 (0.63)	38.02 ± 10.75 (10.50)	361.8 ± 5.3	337 ± 25
	5–10	0.009 ± 0.002 (0.002)	0.73 ± 0.03 (2.29)	18.47 ± 0.12 (57.95)	1.76 ± 0.08 (5.62)	10.89 ± 1.87 (34.17)	31.87 ± 1.8	35 ± 2
	20–30	0.009 ± 0.001 (0.073)	0.11 ± 0.03 (0.903)	9.78 ± 0.56 (80.29)	0.41 ± 0.15 (3.36)	1.95 ± 0.01 (16.00)	12.18 ± 0.79	15 ± 0.5
P2	0–5	0.041 ± 0.002 (0.009)	8.02 ± 0.03 (1.809)	391.57 ± 17.81 (88.38)	20.85 ± 6.47 (4.70)	22.85 ± 5.78 (5.15)	443.3 ± 5.5	376 ± 55
	5–10	0.031 ± 0.006 (0.110)	0.63 ± 0.04 (2.26)	13.25 ± 1.45 (47.57)	1.70 ± 0.06 (6.10)	12.24 ± 1.29 (43.94)	27.85 ± 2.55	31 ± 4
	20–30	0.003 ± 0.001 (0.13)	0.07 ± 0.004 (3.07)	1.76 ± 0.01 (77.19)	0.08 ± 0.01 (3.50)	0.35 ± 0.00 (15.35)	2.28 ± 0.07	3.7 ± 0.2
P3	0–5	0.028 ± 0.006 (0.006)	6.04 ± 0.02 (1.47)	366.64 ± 11.69 (89.50)	16.29 ± 0.01 (3.97)	20.64 ± 1.23 (5.03)	409.3 ± 10.9	420 ± 45
	5–10	0.030 ± 0.001 (0.055)	0.71 ± 0.05 (1.32)	37.77 ± 0.10 (70.18)	4.18 ± 1.04 (7.76)	11.13 ± 0.18 (20.68)	53.82 ± 0.52	69 ± 1
	20–30	0.005 ± 0.001 (0.030)	0.071 ± 0.002 (0.42)	14.16 ± 0.89 (87.46)	0.18 ± 0.05 (1.11)	1.78 ± 0.30 (10.99)	16.19 ± 0.80	11 ± 0.07

Figures in parenthesis show % of total concentration in each fraction.

0.3 and 0.36 cm y^{-1} for Pb in soils surrounding a Pb smelter. On this basis, since the smelter in the current study has been operating for only 10 years, it is probably not surprising that Pb movement downwards appears to be somewhat limited.

3.5 *Chemical associations of Pb and major elements (Fe, Al and Ca) in soil fractions using extractograms*

One of the problems when using batch sequential extraction to study chemical associations is the non-absolute evidence of elemental associations. Elements extracted in the same extraction step have been used as evidence of their chemical associations. However, this may not always be absolutely correct, because elements extracted in the same extraction step may not have dissolved simultaneously but at different times during the extraction step. For the continuous-flow sequential extraction, the extractants were continuously and sequentially pumped through the chamber containing the soil samples. The extracts were collected at set volume intervals (subfractions) with time until each extraction step was completed, as indicated by the extraction profiles reaching baseline. The graphical plot of metal concentrations in subfractions *vs*. subfraction number is called an extractogram. Using overlayed extractograms for different elements, and by comparing detailed peak profiles and peak shapes, it is possible to evaluate the elemental associations in the various extracted solid phases [9, 27]. If two elements are closely associated in a particular geochemical phase, they should show similar peak shapes, and a high correlation between amounts extracted in each subfraction of the particular phase. Metals, which are not closely associated, but are leached in the same extraction step, will show peak profiles, which do not coincide with time during the extraction. As a result, the extractogram enables a detailed examination of possible associations between elements, and therefore provides an insight into the sources of elements present in each fraction.

The distribution and chemical associations of Pb and major elements in soil (Fe, Al and Ca) for a control and contaminated soils (topsoils) can be evaluated using the extractograms shown in figure 2. Variations in the Pb extraction profiles between the control and contaminated soils are most likely due to the difference between the lithogenic and anthropogenic origin of Pb particularly in the reducible phase. The extractograms for the exchangeable phase show little difference in extraction profiles of Pb between the contaminated and control soils. In the exchangeable fraction, very small amounts of Pb were found and extracted along with Ca extracted in the early stages.

Some previous studies of the Pb smelting process have reported that the Pb emission from smelters is predominantly in the form of Pb sulphates ($PbSO_4$, angelsite) [28, 29], or as a combination of Pb sulphates and chlorides ($PbCl_2$, cotunnite) [25]. Although $PbSO_4$ is less soluble than $PbCl_2$, both compounds will dissolve in the soil, and therefore the very small amounts of Pb in the exchangeable fraction found in this work may be derived from these sources. The more soluble $PbCl_2$ in particular could also be responsible for the slight downward movement of Pb observed in this study. Li and Thornton [29] also suggested that the large amounts of Ca (55%) present in the exchangeable fraction were due to the possible presence of $CaSO_4$ in the area surrounding the smelter. However, they could also be due to Ca adsorbed by the exchange complex.

In the acid soluble phase, it is difficult to see the profile of Pb present in the control soil since Pb in this particular fraction was found at very low concentrations. However, the Pb profile seems to be lagging behind the Ca profile in both the control and contaminated samples. The small amounts of Ca extracted most probably results from the low contents of $CaCO_3$ in our soil samples. The concentrations of Pb found in the contaminated soils in the acid soluble step remained relatively high with no sign of approaching the baseline. These continuous leaching signals are possibly a contribution from Pb sorbed on the surface of soil oxides. Dissolution of Fe oxide was negligible as no Fe peak was observed in this particular step.

In the reducible and oxidizable steps, Fe and Al were found in significant amounts. The predominant fraction for Pb appeared in the reducible fraction. However, there are some significant visual differences observed in the extractograms between the control and contaminated soils. It can be seen in the extractogram of the control soil (figure 2a) that Pb does appear to dissolve at the same time as Fe and Al in the reducible fraction (Step III). This indicates a close association between Pb and soil oxides. In contrast, for the contaminated soils, the initial Pb peak was found to rise rapidly in the early part of this stage, and preceded the bulk of the Fe and Al dissolution. Data obtained using batch methods are unable to provide this type of information.

On the basis of the above patterns observed in the extractograms, it could be concluded that Pb was predominantly absorbed on the Fe/Al oxide surfaces, indicating an anthropogenic origin. The results also suggest that Fe/Al oxides are the major components of importance in fixing heavy metals in the soils at this contaminated site.

In the oxidizable fractions, the extraction step could not be carried out to completion as discussed previously. However enough data was produced to consider the chemical associations in this step. The extractograms of Pb do not show up as well-defined peaks decreasing to the baseline by the end of the fraction, and there is no clear correlation of the Pb extractograms with those Fe, Al and Ca.

The visual interpretation of elemental associations using the extractogram is strongly supported by examination of the extraction data using plots of mole ratios of Pb/Fe in the reducible phase. The mole ratio of Pb/Fe in each subfraction was plotted against subfraction number for this particular phase as shown in figure 4. It can be seen that high ratios of Pb/Fe were found in the early subfractions in contaminated soils and correspond to Pb adsorbed on the Fe oxide surfaces. According to the plots of the Pb/Fe mole ratios of the contaminated soils, the Pb/Fe mole ratios decreased with subfraction number and approached a constant value. The more highly contaminated soils show higher Pb/Fe mole ratios in the early subfractions. This mole ratio plot can be used as a tool for identification of anthropogenic origin and degree of contamination.

4. Conclusions

A continuous-flow extraction procedure was applied to contaminated soils from an area adjacent to a Pb smelter. The results obtained from this study demonstrate that the flow system was an effective and accurate method for fractionating soil Pb. The sum of Pb in all subfractions obtained using this method gave good recoveries when compared with results of total concentration obtained from total digestion.

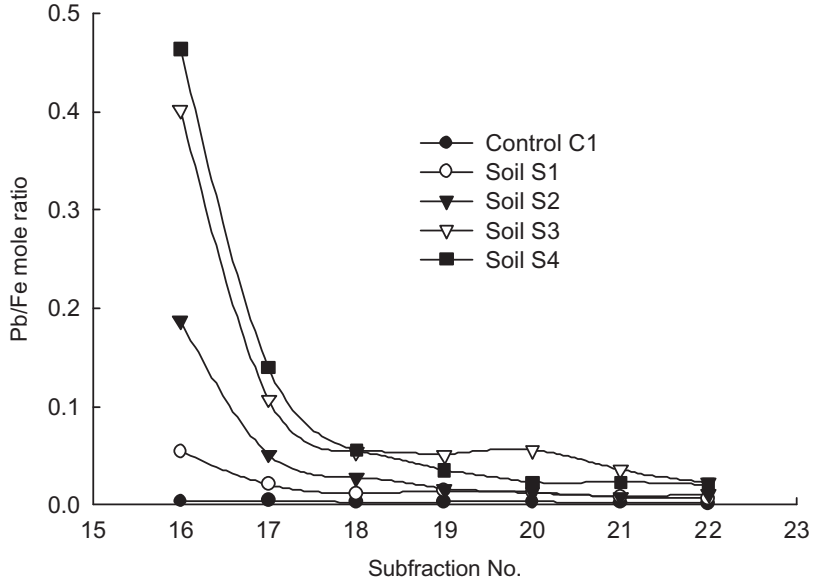

Figure 4. Pb/Fe mole ratio plots for subfractions in the reducible phases of the control and contaminated soils.

In addition, the continuous-flow system eliminates some tedious procedures, such as centrifugation and manual filtration that are required for the batch method. However, it must be recognized that the results obtained using the continuous-flow system, in terms of Pb distribution between fractions, are likely to differ to some extent from those obtained using conventional batch techniques. The reasons for this have been fully discussed above. For the soil samples examined in this study, Pb was predominantly present in the reducible and residual phases. The most predominant fractions for Fe and Al are the residual phases, followed by the reducible phases. In contrast, most Ca is in the exchangeable and residual phases.

An additional advantage of the flow system is the detailed information obtained from the extractogram. Detailed investigations using extractograms, particularly for inter-element comparisons, can clearly provide useful information not possible with the batch technique. The flow system has a high potential for evaluating elemental associations and the modes of occurrence of Pb in soil samples. The fractionation profiles/extractograms of Pb were found to depend strongly on the metal origin. For contaminated soils in this study, the extractograms have shown that Pb was predominantly adsorbed on soil oxide surfaces, especially in topsoil samples, indicating anthropogenic origin. The visual interpretation of Pb adsorption on the surface using extractograms is strongly supported by an examination of the Pb/Fe mole ratio plots. Total concentrations of anthropogenic Pb were much higher in topsoils than in subsoils. However, enhancement of Pb in the most available/mobile fractions (exchangeable and acid soluble) in the topsoil (0–5 cm) had resulted in a limited movement of Pb into the underlying soil (5–10 cm). There was no further detectable movement of Pb below this layer.

Acknowledgements

The authors would like to gratefully thank the Royal Golden Jubilee Grant and the Thailand Research Fund for funding this project, and the Postgraduate Education and Research Program in Chemistry (PERCH) for partial support.

References

[1] R.L. Chaney, J.A. Ryan. *Risk Based Standards for As, Pb, and Cd in Urban Soils*, p. 25, DECHEMA, Frankfurt, Germany (1994).
[2] M.J. McLaughlin, B.A. Zarcinas, D.P. Stevens, N. Cook. *Commun. Soil. Sci. Plant Anal.*, **31**, 1661 (2000).
[3] A.V. Filgueiras, I. Lavilla, C. Bendicho. *J. Environ. Monit.*, **4**, 823 (2002).
[4] A.K. Das, R. Chakraborty, M.L. Cervara, M. de la Guardia. *Talanta*, **42**, 1007 (1995).
[5] Z. Li, R.G. McLaren, A.K. Metherell. *Aust. J. Soil Res.*, **39**, 951 (2001).
[6] J. Shiowatana, N. Tantidanai, S. Nookabkaew, D. Nacapricha. *J. Environ. Qual.*, **30**, 1195 (2001).
[7] J. Shiowatana, N. Tantidanai, S. Nookabkaew, D. Nacapricha. *Environ. Inter.*, **26**, 381 (2001).
[8] R. Chomchoei, J. Shiowatana, P. Pongsakul. *Anal. Chim. Acta*, **472**, 147 (2002).
[9] D. Hinsin, L. Pdungsap, J. Shiowatana. *Talanta*, **58**, 1365 (2002).
[10] L.C. Blakemore, P.L. Searle, B.K. Daly. *Methods for Chemical Analysis of Soils*, New Zealand Soil Bureau, Wellington (1987).
[11] J.K. Singer, J.B. Anderson, M.T. Ledbetter, I.N. McCave, K.P.N. Jones, R.J. Wright. *Sediment. Petrol.*, **58**, 534 (1988).
[12] B. Kovács, J. Prokisch, Z. Györi, A.B. Kovács, A.J. Palencsár. *Commun. Soil Sci. Plant Anal.*, **31**, 1949 (2000).
[13] A. Tessier, P.G.C. Campbell, M. Bisson. *Anal. Chem.*, **51**, 844 (1979).
[14] C.M. Davidson, P.C.S. Ferreira, A.M. Ure. *Fresenius J. Anal. Chem.*, **363**, 446 (1999).
[15] C.W. Gray, R.G. McLaren, A.H.C. Roberts, L.M. Condron. *Aust. J. Soil Res.*, **36**, 199 (1998).
[16] D. Singh, R.G. McLaren, K.C. Cameron. *Aust. J. Soil Res.*, **35**, 1253 (1997).
[17] H. Hödrejärv, A. Vaarmann. *Anal. Chim. Acta*, **396**, 293 (1999).
[18] Y.K. Soon, S. Abboud. In *Soil Sampling and Methods of Analysis*, M.R. Carter (Ed.), pp. 101–108, Lewis Publishers, Boca Raton (1993).
[19] R.G. McLaren, K.C. Cameron. *Soil Science. An Introduction to the Properties and Management of New Zealand Soils*, pp. 237–247, Oxford University Press, Auckland, New Zealand (1996).
[20] R.M. Mckenzie. *Aust. J. Soil Res.*, **18**, 61 (1980).
[21] J.R. Bacon, I.J. Hewitt, P. Cooper. *J. Environ. Monit.*, **6**, 766 (2004).
[22] J.R. Bacon, I.J. Hewitt, P. Cooper. *Sci. Total Environ.*, **337**, 191 (2005).
[23] J.F. Verner, M.H. Ramsey. *Appl. Geochem.*, **11**, 11 (1996).
[24] A. Karczewska. *Appl. Geochem.*, **11**, 35 (1996).
[25] V. Ettler, A. Vaněk, M. Mihaljevič, P. Bezdička. *Chemosphere*, **58**, 1449 (2005).
[26] V. Ettler, M. Mihaljevič, M. Komárek. *Anal. Bioanal. Chem.*, **378**, 311 (2004).
[27] J. Shiowatana, R.G. McLaren, N. Chanmekha, A. Samphao. *J. Environ. Qual.*, **30**, 1940 (2001).
[28] D.J. Oyedele, I.B. Obioh, J.A. Adejumo, A.F. Oluwole, P.O. Aina, O.I. Asubiojo. *Sci. Total Environ.*, **172**, 189 (1995).
[29] X. Li, I. Thornton. *Appl. Geochem.*, **16**, 1693 (2001).

Communications in Soil Science and Plant Analysis, 36: 2839–2854, 2005

ISSN 0010-3624 print/1532-2416 online
DOI: 10.1080/00103620500306023

Evaluation of Distribution and Chemical Associations between Cobalt and Manganese in Soils by Continuous-Flow Sequential Extraction

N. Tongtavee and J. Shiowatana
Department of Chemistry, Faculty of Science, Mahidol University, Bangkok, Thailand

R. G. McLaren
Soil and Physical Sciences Group, Agriculture and Life Sciences Division, Lincoln University, Canterbury, New Zealand

J. Buanuam
Department of Chemistry, Faculty of Science, Mahidol University, Bangkok, Thailand

Abstract: In this study, a strong association between cobalt (Co) and manganese (Mn) in different geochemical soil phases (fractions) was evaluated using a continuous-flow sequential extraction technique employing a modified Tessier extraction scheme. With the flow system, detailed extraction profiles of Co and Mn in soils could be obtained by plotting concentrations of the elements extracted against extraction time (plots referred to as extractograms). Extractograms may be used as an indicator of whether the elements dissolving in the same extraction step are closely associated, or are merely extractable with the same reagent. From the soil samples studied, the coincidence of Co and Mn peaks seems to indicate a close association of these elements in the exchangeable, reducible, and oxidizable fractions. Analysis of flow extraction data suggested that the association between Co and Fe is not as strong as reported in previous studies based on the statistical analysis of batch fractionation data.

Keywords: Manganese oxides, flow, sequential extraction, fractionation

Received 22 February 2004, Accepted 6 April 2005
Address correspondence to J. Shiowatana, Department of Chemistry, Faculty of Science, Mahidol University, Rama VI Road, Bangkok 10400, Thailand. E-mail: scysw@mahidol.ac.th

INTRODUCTION

Most micronutrients in the soil have been inherited from soil parent materials, in which the micronutrients occur in the crystal structure of various primary and secondary minerals. During soil development, micronutrients are released as soluble ions, which can either be lost from the soil by leaching, be reincorporated into new secondary minerals, or react in a variety of ways with other soils constituents (McLaren and Cameron, 1996). Cobalt (Co), although not essential for all plants, is required for the fixation of nitrogen by rhizobium bacteria. It is also essential in the diets of ruminant animals for the formation of vitamin B_{12}. Deficiency results in anemia, loss of appetite, and poor growth rates. Deficiencies are likely to occur in cows and sheep if pasture Co levels are less than 0.08 mg Co/kg dry matter (McLaren and Cameron, 1996). Soil Co availability to plants is very dependent on both soil pH and soil moisture status (McLaren, 2002). It has also been demonstrated that soil Co reactivity and solubility are also significantly influenced by soil manganese (Mn) status through the strong fixing ability and redox reactions of Mn oxides (Taylor et al., 1964; McKenzie, 1969; Taylor and McKenzie, 1966). In a soil fractionation study, Li et al. (2001b) have also shown a significant correlation between soil Co and Mn. This study indicated the presence of substantial amounts of Co and Mn in soil iron (Fe) oxide fractions, and multiple regression analysis suggested that Fe and Mn oxides have a considerable influence on the distribution of Co in soils. The chemistry of Co, and its availability to plants, therefore appears to be dominated by its association with Mn oxide minerals. Understanding the relationship between these two elements could be important for the management of pastures that are deficient in Co for grazing animals. Indeed, some previous studies have attempted to investigate the importance of the sorption of Co by Mn minerals in soils in relation to plant Co uptake (Adams et al., 1969; Tiller et al., 1969).

Sequential extraction using batch methods to fractionate metals in solid materials has become widely used and well recognized and is a useful technique for determining chemical phases of metals in soil materials. Elements extracted in the same extraction steps have been used as evidence of their chemical association. However, this may not always be absolutely correct, because elements extracted from the same phase may not have dissolved simultaneously but at different times during the same extraction step.

In previous work, a continuous-flow system was developed for the sequential extraction of soils (Shiowatana et al., 2001a, 2001b), which has shown many advantages over the batch system including speed, ease of operation, less vulnerability to variation in extraction conditions, high extraction efficiency and freedom from operational contamination. The flow system has been proven to reduce the problem of metal readsorption and redistribution during extraction in comparison with the batch system (Chomchoei et al., 2002). Extractograms, i.e., plots of concentration of element extracted

vs. subfraction number (in effect time) obtained using the system also provides kinetic information and information on solid-phase elemental associations.

The aim of the present study is to use the continuous-flow sequential extraction system to investigate the elemental associations between Co, Mn, and Fe in a range of soil samples.

MATERIALS AND METHODS

Soil Samples and Standard Reference Material

Four soil samples, from the study by Li et al. (2001b), differing substantially in Co and Mn status, and in chemical and physical properties, were selected for this study. The chemical properties of the experimental soils are given in Table 1. Soil samples were air-dried and ground to pass through a 2 mm stainless steel sieve, and were stored in a desiccator prior to laboratory analysis.

For the validation of the detection method and the extraction system, a standard reference material (SRM 2711) was also used. This material (particle size $<74\,\mu m$) was a moderately contaminated soil from Montana in the United States.

Preparation of Standard Solutions and Glassware

The chemical reagents in this work were of analytical grade. Ultra-pure water from a MilliQ water purification unit (Millipore, Bedford, MA) was used

Table 1. Properties of the soils used for cobalt and manganese fractionation[a]

	Soil			
	Waimakariri	Mangaotaki	Magaopiko	Makarewa
New Zealand classification[b]	Recent soil	Allophanic soil	Recent soil	Gley soil
Soil pH	5.61	4.92	4.97	4.95
Sand (%)	52.4	26.1	49.8	47.6
Silt (%)	33.1	48.9	40.2	42.6
Clay (%)	14.5	25.0	10.0	9.8
Org.C (%)	2.37	5.53	9.81	6.18
Total Fe (%)	2.08	2.44	3.04	4.08
Total Al (%)	1.16	2.28	6.92	3.22
Total Co (mg/kg)	6.09	6.37	7.57	14.0
Total Mn (mg/kg)	301	697	965	1030

[a]Data from Li et al. (2001a).
[b]Hewitt (1993).

throughout this work. All glassware used was cleaned and soaked in 10% HNO_3 and rinsed with ultra-pure water before use. Standard metal solutions (1000 mg/L) were purchased from Merck, (Darmstadt, Germany) or prepared in-house from pure metals. Working standard solutions were prepared by diluting the stock solution with ultrapure water or with extracting reagents before use.

Fractionation Scheme

The fractionation scheme used was slightly modified from the Tessier scheme (Tessier et al., 1979). The geochemical phases at each step are largely operationally defined by the reagents used as shown in Table 2. The phases extracted should be considered as nominal rather than absolute chemical fractions. All soil samples and SRM 2711 were fractionated using both the batch and the continuous-flow extraction systems.

Continuous-Flow Extraction System

The Extraction Chamber

An extraction chamber was designed to allow containment and stirring of a weighed sample of soil. Extractants are pumped sequentially through the chamber and leach metals from the targeted phases. The chambers and covers, as shown in Fig. 1, were constructed from borosilicate glass to have a capacity of approximately 10 mL. The outlet of the chamber was furnished with a filter [Whatman (Maidstone, U.K.) glass microfiber filter GF/B, 47-mm diameter, 1-μm particle retention] to allow dissolved matter to flow through. Extractant was pumped through the chamber using a peristaltic pump [Micro tube pump, MP-3 N, EYELA (Tokyo likakikai Co., Ltd.)] at varying flow rates using tygon tubing of 2.25 mm inner diameter. Heating of

Table 2. Sequential fractionation procedure for soil cobalt and manganese

Step	Nominal fraction	Extractant	Extraction conditions (Batch method)
I	Exchangeable	0.01 M $Ca(NO_3)_2$	Shake 24 h, 25°C
II	Acid-soluble (specifically sorbed)	0.11 M CH_3COOH	Shake 16 h, 25°C
III	Reducible (Fe/Mn oxides)	0.1 M NH_2OH. HCl, pH 2	Shake 6 h, 96°C
IV	Oxidizable (Organic-bound)	30% H_2O_2: 0.02 M HNO_3 (8:3 v/v)	Shake 5 h, 85°C
V	Residual	$HNO_3 + HF$	Microwave digestion

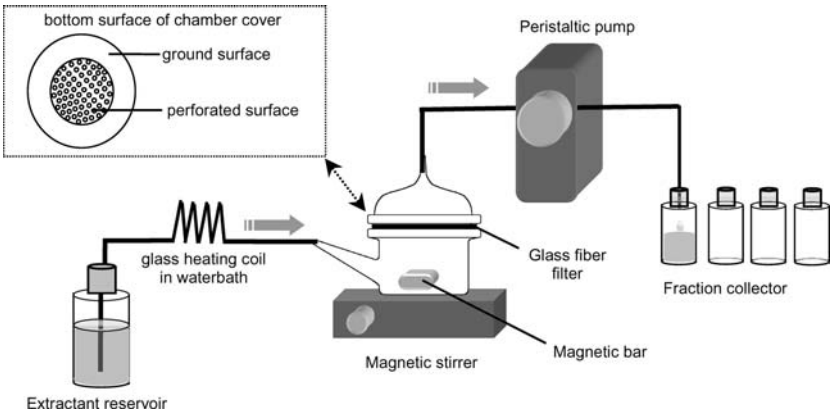

Figure 1. Continuous-flow extraction system (modified from Shiowatana et al., 2001b).

the extractants in Steps III and IV was carried out by passing the extractants through a glass heating coil approximately 120 cm in length, placed in a water bath. However, because of heat-loss problems, even when the heating coil was immersed in a thermostat water bath controlled at 95°C, the maximum temperatures achieved in the extraction chamber were between 80 and 85°C. Thus, for Step IV in particular, the temperatures used were somewhat lower than used for the batch system (Table 2).

Extraction Procedure

A weighed sample (0.25–1.00 g) was transferred to a clean extraction chamber together with a magnetic bar. A glass microfiber filter was then placed on the outlet followed by a silicone rubber gasket, and the chamber cover was securely clamped in position. The chamber was connected to the extractant reservoir and the collector vial using tygon tubing and placed on a magnetic stirrer. The magnetic stirrer and peristaltic pump were switched on to start the extraction. The extracting reagents were continuously and sequentially pumped through the chamber. The extracts passing through the membrane filter were collected in subfractions of 10–30 mL volume intervals until all four leaching steps were completed. For most soils examined, it was found that 120–180 mL were sufficient to leach the metals completely for each step.

Residue Digestion

Residue digestion was performed using a Milestone microwave digestion system model MLS-1200 Mega. This system was equipped with a MLS-1200 plus EM-45 Exhaust Module for operations with MDR Microwave

digestion Rotors and 240 control Terminal. Amounts of 0.1 g of dried soil sample or residue from the extraction chamber was transferred to each vessel together with 4 mL of HNO_3 (70%), 4 mL of H_2O_2 (30%), and 2 mL of HF (48%). The vessels were placed in a microwave digester and the digestion was carried out following the recommended heating program for 30 min. The clear digest solutions were cooled to room temperature, and were then brought up to a final volume of 50.00 mL in a volumetric flask. Total metal concentrations were determined by both a single digestion of non-fractionated soil and by summation of extractable metals in each subfraction of the exchangeable, acid-soluble, reducible, oxidizable, and residual fractions.

Analysis of Extracts and Digests

Cobalt concentrations in the extracts were determined using graphite furnace atomic absorption spectrophotometry (GFAAS). The GFAAS measurements were performed with a Perkin Elmer (Norwalk, CT) Analyst 100 equipped with a deuterium-arc background corrector and an HGA-800 heated graphite atomizer. The sample was introduced to the atomizer using an AS-72 autosampler. Flame atomic absorption (FAAS) for Mn and Fe was performed using a Perkin Elmer Model 3100 spectrometer equipped with deuterium background correction. Concentrations of metals were obtained by the standard matrix-matching calibration method. Working standard solutions were prepared in the same extracting reagent as the sample solutions to be measured.

RESULTS AND DISCUSSION

Distributions of Cobalt and Manganese in Soil Determined by Flow and Batch Systems

In order to evaluate the flow extraction system, both the batch and flow extraction systems were used for the same sets of samples. For examination of the accuracy and precision of the proposed flow system, SRM 2711 was analyzed and the results were compared with the certified values. The analytical results are shown in Table 3. It was found that both flow extraction and batch extraction methods gave good recoveries for the elements studied. This indicates that the extraction data obtained from the continuous-flow extraction system is reliable. Based on these findings, the four soil samples were then extracted to study the distributions and chemical association between Co, Mn, and Fe in soils.

Table 4 compares the distributions of Co, Mn, and Fe in soil samples using the flow system and a conventional batch method. In the proposed

Table 3. Comparison of analytical results for batch and flow sequential extraction methods for SRM 2711 (mg/kg ± s.d., $n = 2$)

Element	Method	Step I	Step II	Step III	Step IV	Residue	Sum of fractions	Total	Certified value
Co	Batch	<0.1 ± 0.00	1.6 ± 0.00	1.7 ± 0.21	0.3 ± 0.00	4.1 ± 0.24	7.8 ± 0.14	7.6 ± 0.47	10.00[a]
	Flow	<0.1 ± 0.00	2.1 ± 0.10	0.8 ± 0.02	<0.1 ± 0.00	3.0 ± 0.29	5.9 ± 0.15		
Mn	Batch	1.4 ± 0.10	239 ± 5	121 ± 13	21 ± 0.5	231 ± 22	613 ± 12	616 ± 19	638 ± 38
	Flow	2.4 ± 0.02	278 ± 2	101 ± 3	1.2 ± 0.32	201 ± 30	584 ± 18		
Fe	Batch	0.6 ± 0.21	7.8 ± 0.44	2532 ± 410	503 ± 35	18142 ± 498	21185 ± 546	26413 ± 453	28900 ± 600
	Flow	<0.1 ± 0.00	285 ± 58	1854 ± 78	499 ± 69	19742 ± 193	22380 ± 765		

[a]Non-certified value.

Table 4. Comparison of analytical results for batch and flow sequential extraction methods for soil samples (mg/kg ± s.d., $n = 2$)

Soil/element	Method	Step I	Step II	Step III	Step IV	Residue	Sum of fractions	Total
Soil 1								
Co	Batch	0.1 ± 0	0.6 ± 0	1.3 ± 0.03	0.2 ± 0.01	3.3 ± 0.24	5.4 ± 0.11	4.9 ± 0.31
	Flow	<0.1 ± 0	0.2 ± 0.12	1.3 ± 0.06	0.2 ± 0.02	2.3 ± 0.35	4.2 ± 0.15	
Mn	Batch	14.7 ± 0.13	37.3 ± 0.15	71 ± 3	11.7 ± 0.11	198 ± 7	333 ± 3	354 ± 5
	Flow	18.6 ± 0.48	20.5 ± 2.89	93 ± 3	14.7 ± 2.56	175 ± 22	322 ± 10	
Fe	Batch	0.8 ± 0	15.9 ± 3.47	3016 ± 30	991 ± 10	15390 ± 780	19414 ± 390	25918 ± 907
	Flow	<0.1 ± 0	<0.1 ± 0	1995 ± 333	756 ± 56	17984 ± 1357	20735 ± 807	
Soil 2								
Co	Batch	0.1 ± 0	0.3 ± 0.04	2.4 ± 0.02	0.3 ± 0	3.3 ± 0.09	6.4 ± 0.04	6.0 ± 0.30
	Flow	0.1 ± 0.03	0.1 ± 0.06	1.9 ± 0.03	0.3 ± 0.12	3.0 ± 0.07	5.3 ± 0.07	
Mn	Batch	94 ± <1	104 ± 14	298 ± 63	39.8 ± 0.42	269 ± 12	805 ± 30	974 ± 32
	Flow	105 ± 10	54 ± 13	411 ± 12	54 ± 15	292 ± 15	915 ± 13	
Fe	Batch	15.5 ± 0.63	13.1 ± 0.83	8080 ± 2173	5481 ± 257	17573 ± 2020	31163 ± 1332	33296 ± 3911
	Flow	<0.1 ± 0	<0.1 ± 0	2878 ± 537	1179 ± 112	25781 ± 3553	29840 ± 2076	
Soil 3								
Co	Batch	0.2 ± 0	0.5 ± 0.07	2.0 ± 0.11	0.4 ± 0.02	3.4 ± 2.81	6.4 ± 1.26	8.8 ± 1.51
	Flow	0.1 ± 0.04	<0.1 ± 0.03	1.4 ± 0.05	0.2 ± 0.03	5.5 ± 2.44	7.3 ± 1.09	
Mn	Batch	62 ± 1	83 ± 5	309 ± 23	23.7 ± 1.81	300 ± 4	778 ± 11	854 ± 31
	Flow	77 ± 2	41 ± 13	291 ± 3	31.6 ± 4.96	533 ± 16	974 ± 8	
Fe	Batch	9.9 ± 0.59	10.3 ± 0.44	4560 ± 1	1795 ± 111	23344 ± 988	29720 ± 445	38759 ± 1847
	Flow	<0.1 ± 0	<0.1 ± 0	2700 ± 90	815 ± 96	25410 ± 2159	28926 ± 2962	
Soil 4								
Co	Batch	0.1 ± 0	0.5 ± 0.07	2.3 ± 0.06	0.2 ± 0	3.3 ± 0.44	6.4 ± 0.20	6.4 ± 0.03
	Flow	0.2 ± 0.09	<0.1 ± 0.03	1.8 ± 0.22	0.4 ± 0.16	3.4 ± 0.35	5.8 ± 0.21	
Mn	Batch	68 ± 7	114 ± 14	406 ± 3	11.3 ± 0.49	258 ± 39	858 ± 18	719 ± 33
	Flow	73 ± 17	35 ± 3	498 ± 27	60 ± 22	201 ± 30	778 ± 18	
Fe	Batch	1.0 ± 2.99	3.4 ± 1.29	5212 ± 55	1602 ± 61	27123 ± 901	33940 ± 856	37150 ± 1850
	Flow	<0.1 ± 0	<0.1 ± 0	2212 ± 276	654 ± 45	27953 ± 1830	30819 ± 724	

flow system, the amount of each element in an individual phase was obtained by summation of the amounts in all subfractions of each step. For all samples analyzed, the concentrations of Co extracted were found to be slightly lower for the flow system compared to the batch method, probably because of limitations of analytical detection in each subfraction, especially in the exchangeable and acid-soluble phases. Cobalt in some subfractions was not detectable because of a dilution effect. However, it can be seen from the results in Table 4 that the summation of Co fractions was, on average, within $\pm 10\%$ of the single total Co determinations.

For Mn fractionation, the summation of Mn fractions obtained using the flow method showed reasonable agreement with those obtained using both the conventional batch method, and with the single total Mn determination. For Fe fractionations, the summation of Fe fractions was found to be consistently 20% lower than the total Fe determinations. These errors were probably caused by high concentrations of Fe in the subfractions. Each subfraction needed a considerable dilution prior to measurement by FAAS. In general, for all elements, the repeatability of the flow system appears to be as acceptable as that obtained using the batch system.

The elemental distributions between fractions on a proportional basis using both the batch and flow methods are shown in Fig. 2. Considerable variations in elemental distributions between the different soils, depending on the geochemical composition of each soil were observed. For most soils, very small proportions of Co were found in the first two fractions (exchangeable and acid-soluble) while the largest proportion in most soils was found in the residual fraction. For Mn, small amounts of Mn were found in the oxidizable (organic-bound) fraction, and the largest proportions were found in the residual and reducible (Fe-Mn oxides) fractions. For Soils 1, 2, and 4, the distributions of Co and Mn between fractions were similar for the batch and flow systems. However, there appeared to be some differences between the two methods for Soil 3. In this case, both the proportions of Co and Mn in the Fe-Mn oxides fraction were smaller, and those in the residual fraction were higher in the flow compared to the batch system. Overall the mean proportions of total soil Co present in different fractions decreased in the order: Residual $>$ Fe-Mn oxides $>$ organic-bound $\approx$ acid-soluble $>$ exchangeable fractions. The proportional distribution of Mn in each fraction differed slightly from that for Co decreasing in the order: Residual $>$ Fe-Mn oxides $>$ acid-soluble $\approx$ exchangeable $>$ organic-bound fractions.

For Fe fractionations, the highest proportions of Fe were found in the residual and in the Fe-Mn oxides fractions. For all samples, the distributions of Fe determined with the flow system appeared slightly different from those distributions determined using the batch system. The proportions of Fe determined in the Fe-Mn oxides and organic-bound fractions as determined using the flow system were smaller than those obtained using the batch system. The greatest proportion ($>86\%$) of Fe extracted using the flow system was found in the residual fraction. This can be explained by the fact

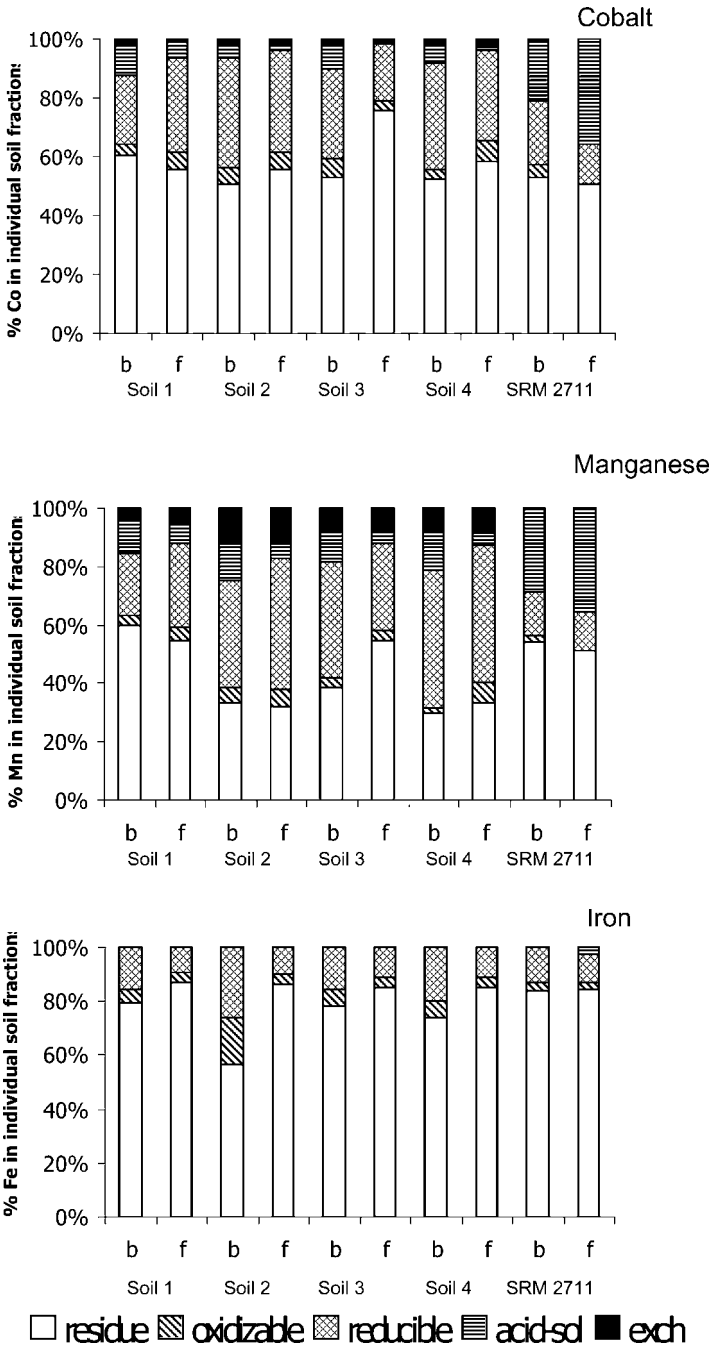

Figure 2. Comparison of elemental distribution (Co, Mn, Fe) in soils, on a proportional basis, as determined by batch (b) and continuous-flow (f) methods.

that the temperature in the heated Steps (III and IV) in the flow system was about 15–20°C lower than the temperatures achieved in the batch system. As discussed, this is due to heat loss during the transfer of the extractant from the heating bath to the extraction chamber. The temperature was probably not high enough to dissolve all of the crystalline iron oxide forms in the reducible fraction. Particularly in Soil 2, there was a large difference between the flow and batch systems in the proportion of Fe determined in the residual phase (Fig. 2). This was probably caused by a high content of silt and clay in this soil, resulting in low extraction efficiency for the flow system. On average, the distribution of Fe in each fraction decreased in the order: Residual $\ggg$ Fe-Mn oxides $>$ organic-bound $\ggg$ acid-soluble $\approx$ exchangeable.

Evaluation of Elemental Distributions and Associations Using Extractograms

The distributions and chemical association between Co, Mn, and Fe in soils were evaluated employing the continuous-flow extraction system, in which the extractants were continuously and sequentially pumped through the chamber containing the soil sample. The extracts were collected at set volume intervals (subfractions) with time until each extraction step was completed, as indicated by the extraction profiles reaching baseline.

By using overlayed extractograms for different elements, and by comparing detailed peak profiles and peak shapes, it is possible to evaluate the elemental associations in the various extracted solid phases (Shiowatana et al., 2001c; Hinsin et al., 2002). If two elements are closely associated in a particular geochemical phase, it is expected that they should show similar peak shapes, and a high correlation between amounts extracted in each subfraction of the particular phase. These metals, which are not closely associated, but are leached in the same extraction step, will show peak profiles, which do not coincide with time during the extraction. As a result, correlations between concentrations of the different elements in the subfractions will be poor.

Elemental distributions and chemical associations of Co, Mn, and Fe for the four soils in the present study can be evaluated using the extractograms shown in Figs. 3a and 3b. Variations between the four sets of extractograms are due to the geochemical/mineralogical differences between the soils. The extractograms show some evidence for the association of Co and Mn. Although not explicit in the first two phases (exchangeable and surface adsorbed) since Co in particular was found in very small concentrations. However, for Soil 1, the extractograms clearly show a close association between Co and Mn in the acid-soluble phase (II). For all four samples, the extractograms show that the predominant phase (excluding the residual fraction) for both Co and Mn is the reducible phase (Fe-Mn oxides). In this phase, the strong coincidence of the peak shapes for Co and Mn indicate

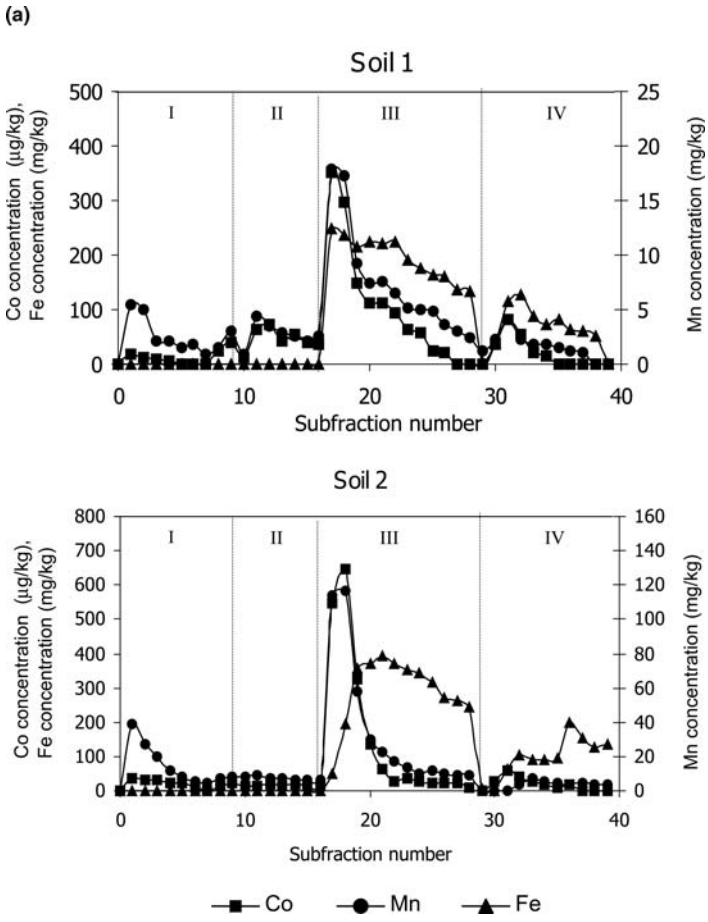

Figure 3a. Extractograms obtained using the continuous-flow method for Soil 1 and Soil 2. (Sample/chamber volume ratio 0.75 g/10 mL; subfraction volumes of 10, 15, 30, and 30 mL in fractions I, II, III, and IV, respectively.)

simultaneous dissolution of the two elements, providing clear evidence of their elemental association in all four samples. However, Fe (which was also extracted in the same phase) gave a much broader peak throughout the extraction step and therefore did not appear to be closely associated with either Mn or Co. In Soil 4, the Co peak appeared simultaneously with the first Mn peak, but not associate with the second Mn peak.

The extractograms obtained from the continuous-flow extraction system show that, apart from the large amounts in the residue (Table 4), Fe was found predominantly in the reducible and oxidizable (organic-bound) phases. In all cases, there was significant dissolution of both Co and Fe in those two phases. However, the extraction peak shapes of Co and Fe in the

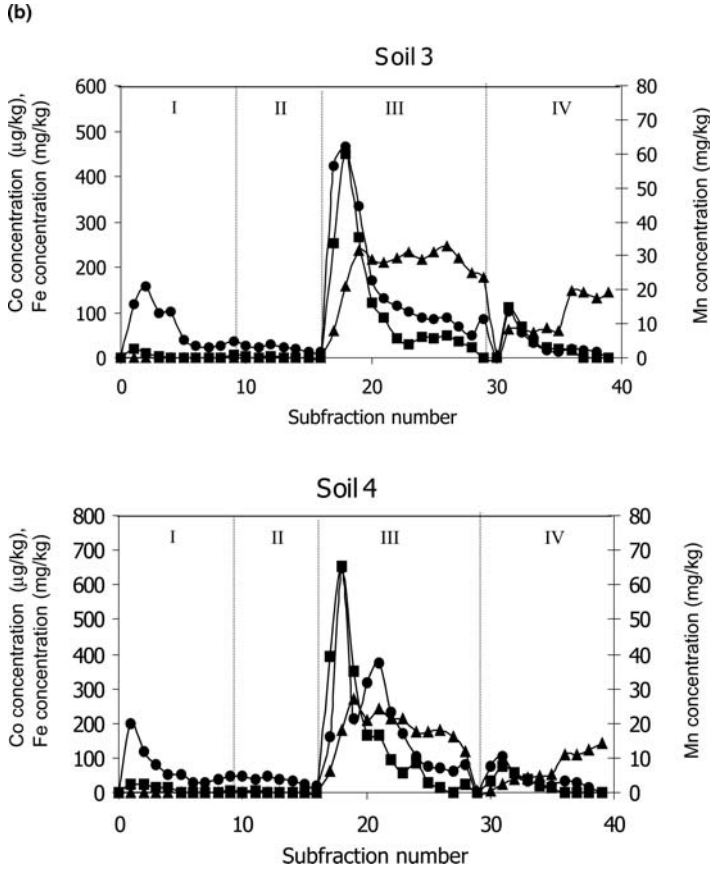

Figure 3b. Extractograms obtained using the continuous-flow method for Soil 3 and Soil 4. (Conditions as in Fig. 3a)

reducible fraction (III) were distinctly different from each other. As can be seen in the extractogram of Soil 1 (Fig. 3a), Co does appear to dissolve at the same time as Fe in the early stages of the reducible fraction. This might indicates some association between Co and Fe; however the divergence between the Co and Fe extractograms later in the fraction would mean that the distribution of Co within Fe oxides is not uniform. The coincidence of an early Fe peak with the main Co and Mn peaks could possibly be due to the dissolution of amorphous Fe oxides; however for Soils 2, 3, and 4, the initial Fe peak clearly lagged behind those of Co and Mn. It would therefore appear that there was no simultaneous dissolution of Co and Fe in the subfractions of the reducible phase.

The close relationship between Co and Mn, but not with Fe, was also observed in the oxidizable (organic-bound) phase (Figs. 3a and 3b).

The extraction profiles of Co and Mn showed up as a peaks decreasing to the baseline by the end of the fraction, whereas for Fe, for three of the soils, concentrations remained well above baseline when the extraction (Step IV) was discontinued.

Evaluation of Association between Elements Using Statistical Correlations

In previous studies (Li et al., 2001a) batch sequential extraction data has been used to evaluate the chemical association between Co and Mn in the soil. Chemical associations are examined by the calculation of correlation coefficients (r) between the amounts (or proportions) of Co and Mn determined in the same extraction step. Highly significant correlations have been interpreted as the two elements having close associations. Nevertheless, results from such studies have demonstrated that the amounts of Co and Mn extracted in the reducible phase are strongly correlated (Jarvis, 1984), and it has been suggested that the association is due to the strong sorption of Co by Mn oxides. More recently, Li et al. (1999, 2001a, 2001b) have reported chemical relationships and associations between Co, Mn, and Fe for batch extraction data, based on linear correlation analysis. However, since the batch system provides only a single metal concentration value for each extraction step, correlations as found using the batch technique may not always indicate a true elemental association. Elements may be dissolved at different times during the same extraction step.

To further investigate possible relationships between Co, Mn, and Fe in soil, Li et al. (2001b) also used multiple regression modeling based on batch fractionation data. Their multiple regression models suggested that the Fe content of the soils strongly influences the proportions of both Co and Mn present in exchangeable, reducible, and organic-bound fractions.

In this current work, linear correlation (r) was used to evaluate the relationships between Co and Mn and between Co and Fe, using the flow extraction data. For each phase of each sample, the r value was calculated for the linear correlations between extractable Co and extractable Mn concentrations in the subfractions of that phase. The r values between Co and Mn, and between Co and Fe, calculated in this way from the flow extraction data, are summarized in the first four columns of Tables 5 and 6. For comparison purposes, correlations calculated using the batch extraction data for all four samples are shown in the last columns of Tables 5 and 6.

It was found that, in the flow system, concentrations of Co and Mn in the reducible phase were highly and significantly correlated for three of the soils ($r > 0.95$). For Soil 4, the correlation was not as high ($r = 0.80$) and as noted previously, the extractogram for this soil showed a second Mn peak that was not accompanied by a corresponding peak for Co. In comparison to the correlations between Co and Mn in the reducible phase, those between Co and Fe

Table 5. Correlations (r) between Co and Mn concentrations in fractions obtained from flow and batch extractions

Fraction	Flow extraction[a]				Batch extraction (all soils)[b]
	Soil 1	Soil 2	Soil 3	Soil 4	
Exchangeable	0.91*** (9)	0.86** (9)	0.68* (9)	0.90*** (9)	0.66
Acid-soluble	0.88** (8)	0.34 (8)	0.81* (8)	0.44 (8)	0.71
Reducible	0.99*** (12)	0.99*** (12)	0.96*** (12)	0.80** (12)	0.90
Oxidizable	0.88*** (11)	0.20 (11)	0.69* (11)	0.85*** (11)	0.67

*$P < 0.05$; ** $P < 0.01$; ***$P < 0.001$.

[a]r values calculated from concentrations in individual subfractions; number of subfractions for each soil/fraction shown in parenthesis.

[b]r values calculated from metal concentrations in particular fractions of the four soils.

were not significant for three of the soils and only significant at $P > 0.05$ for the fourth soil (Table 6). It is interesting to note that for the batch extraction data, equally high r values were calculated for the reducible fraction, between Co and Mn, and between Co and Fe. However, because of the small number of samples neither r value was statistically significant.

Apart from the reducible fraction, correlations between Co and Mn for the flow extraction data were also generally high for the exchangeable fraction (Table 5). However, correlations for the acid-soluble and oxidizable fractions were much more variable, ranging from highly significant for some soils to nonsignificant for others. Correlations between Co and Fe in the oxidizable fraction were much poorer than between Co and Mn in the same fraction. Correlations were not calculated between Co and Fe in the

Table 6. Correlations (r) between Co and Fe concentrations in fractions obtained from flow and batch extractions

Fraction	Flow extraction[a]				Batch extraction[b] (all soils)
	Soil 1	Soil 2	Soil 3	Soil 4	
Exchangeable	ND	ND	ND	ND	0.89
Acid-soluble	ND	ND	ND	ND	0.11
Reducible	0.69* (12)	0.32 (12)	0.46 (12)	0.14 (12)	0.86
Oxidizable	0.66* (11)	0.24 (11)	0.42 (11)	0.58 (11)	0.37

*$P < 0.05$.

[a]r values calculated from concentrations in individual subfractions; number of subfractions for each soil/fraction shown in parenthesis.

[b]r values calculated from metal concentrations in particular fractions of the four soils.

ND = not determined since Fe concentrations at or below detection limit.

exchangeable and acid-soluble fractions because of the negligible concentrations of Fe extracted.

In the case of the batch extraction data, in addition to the high (but nonsignificant) r values between Co and Mn or Fe in the reducible fraction, relatively high r values were obtained for some of the other fractions (Tables 5 and 6). However, unlike the flow extraction data, these did not generally agree with the trends between elements observed in the extractograms.

CONCLUSIONS

This study has demonstrated that a continuous-flow extraction system can be used to fractionate Co, Mn, and Fe in soils with similar precision and accuracy to those obtained using a traditional batch fractionation procedure. In addition, the continuous-flow system reduces some tedious procedures, such as centrifugation and manual filtration that are required for the batch method. A four-step continuous-flow extraction can be completed within 5–7 h, compared with 5 days for a batch method. Although clearly requiring a greater number of chemical analyses than the batch system, an additional advantage of the flow system is the detailed information obtained from the extractogram. This appears to be a very useful tool for evaluating a true chemical association between elements. The visual interpretation of elemental associations using the extractograms is strongly supported by examination of the flow extraction data using a statistical correlation technique. In contrast, there are clearly limitations in using the data obtained from batch extractions to examine the association between elements.

For the soils in this study, results from the flow extraction system suggest a clear association between Co and Mn but little direct evidence of a strong Co interaction with Fe. This contrasts with some previous studies using batch fractionations, in which statistical correlations between Co and Fe have been taken as evidence for an association between these elements.

ACKNOWLEDGMENTS

The authors would like to gratefully thank the Royal Golden Jubilee Grant and the Thailand Research Fund for funding this project, and the Postgraduate Education and Research Program in Chemistry (PERCH) for partial support.

REFERENCES

Adams, S.N., Honeysett, J.L., Tiller, K.G., and Norrish, K. (1969) Factors controlling the increase of cobalt in plants following the addition of a cobalt fertilizer. *Australian Journal of Soil Research*, 7: 29–42.

Chomchoei, R., Shiowatana, J., and Pongsakul, P. (2002) Continuous-flow system for reduction of metal readsorption during sequential extraction of soil. *Analytical Chimica Acta*, 472: 147–159.

Hewitt, A.E. (1993) *New Zealand Soil Classification: Landcare Research Science Series No. 1*; Manaaki Whenua Press: Lincoln, New Zealand.

Hinsin, D., Pdungsap, L., and Shiowatana, J. (2002) Continuous-flow extraction system for elemental association study: a case of synthetic metal doped iron hydroxide. *Talanta*, 58: 1365–1373.

Jarvis, S.C. (1984) The association of cobalt with easily reducible manganese in some acidic permanent grassland soils. *Journal of Soil Science*, 35: 431–438.

Li, Z., McLaren, R.G., and Metherell, A.K. (1999) The effect of soil manganese status on the bioavailability of soil cobalt for pasture uptake in New Zealand soils. *Proceeding of the New Zealand Grassland Association*, 61: 133–137.

Li, Z., McLaren, R.G., and Metherell, A.K. (2001a) Cobalt and manganese relationship in New Zealand soils. *New Zealand Journal of Agriculture Research*, 44: 191–200.

Li, Z., McLaren, R.G., and Metherell, A.K. (2001b) Fractionation of cobalt and manganese in New Zealand soils. *Australian Journal of Soil Research*, 39: 951–967.

McKenzie, R.M. (1969) The reaction of cobalt with manganese dioxide minerals. *Australian Journal of Soil Research*, 8: 97–106.

McLaren, R.G. (2002) Cobalt and iodine. In *Encyclopedia of Soil Science*; Lal, R., ed.; Marcel Dekker Inc. New York.

McLaren, R.G. and Cameron, K.C. (1996) *Soil Science: Sustainable Production and Environmental Protection*; Oxford University Press: Auckland, New Zealand.

Shiowatana, J., Tantidanai, N., Nookabkaew, S., and Nacapricha, D. (2001a) A flow system for the determination of metal speciation in soil by sequential extraction. *Environment International*, 26: 381–387.

Shiowatana, J., Tantidanai, N., Nookabkaew, S., and Nacapricha, D. (2001b) A novel continuous-flow sequential extraction procedure for metal speciation in solids. *Journal of Environmental Quality*, 30: 1195–1205.

Shiowatana, J., McLaren, R.G., Chanmekha, N., and Samphao, A. (2001c) Fractionation of arsenic in soil by a continuous-flow sequential extraction method. *Journal of Environmental Quality*, 30: 1940–1949.

Taylor, R.M., McKenzie, R.M., and Norrish, K. (1964) The mineralogy and chemistry of manganese in some Australian soils. *Australian Journal of Soil Research*, 2: 235–48.

Taylor, R.M. and McKenzie, R.M. (1966) The association of trace elements with manganese minerals in Australian soils. *Australian Journal of Soil Research*, 4: 29–39.

Tessier, A., Campbell, P.G.C., and Bisson, M. (1979) Sequential extraction procedure for the speciation of particulate trace metal. *Analytical Chemistry*, 66: 3562–3565.

Tiller, K.G., Honeysette, J.L., and Hallsworth, E.G. (1969) The isotopically exchangeable form of native and applied cobalt in soils. *Australian Journal of Soil Research*, 7: 43–56.

Anal Bioanal Chem (2007) 389:733–742
DOI 10.1007/s00216-007-1308-x

ORIGINAL PAPER

Flow field–flow fractionation–inductively coupled optical emission spectrometric investigation of the size-based distribution of iron complexed to phytic and tannic acids in a food suspension: implications for iron availability

Sopon Purawatt · Atitaya Siripinyanond · Juwadee Shiowatana

Received: 31 January 2007 / Revised: 11 April 2007 / Accepted: 12 April 2007 / Published online: 30 May 2007

Abstract Flow field–flow fractionation–inductively coupled plasma optical emission spectrometry (FlFFF–ICP–OES) was applied to achieve the size-based fractionation of iron in a food suspension in order to gain insights into iron availability. The binding of iron with phytic and tannic acids, employed as model inhibitors of iron availability in foods, was investigated at pH 2.0 (representing stomach fluid), pH 5.0 (the transition stage in the upper part of the duodenum), and pH 7.0 (the small intestine). In the presence of phytic acid, iron was found as a free ion or it was associated with molecules smaller than 1 kDa at pH 2.0. Iron associated with molecules larger than 1 kDa when the pH of the mixture was raised to 5.0 and 7.0. In the presence of tannic acid, iron was again mostly associated with molecules smaller than 1 kDa at pH 2.0. However, at pH 5.0, iron and tannic acid associated in large molecules (~25 kDa), while at pH 7.0, most of the iron was associated with macromolecules larger than 500 kDa. Iron size-based distributions of kale extract and tea infusion containing phytic and tannic acids, respectively, were also examined at the three pH values, with and without enzymatic digestion. Without enzymatic digestion of the kale extract and the tea infusion at pH 2.0, most of the iron was released as free ions or associated with molecules smaller than 1 kDa. At other pH values, most of the iron in the kale extract and the tea infusion was found to bind with ~2 kDa and >500 kDa macromolecules, respectively. Upon enzymatic gastrointestinal digestion, the iron was not observed to bind to macromolecules >1 kDa but <500 kDa, due to the enzymatic breakdown of large molecules to smaller ones (<1 kDa).

Keywords Iron · FlFFF · ICP–OES · Size-based elemental fractionation

S. Purawatt · A. Siripinyanond · J. Shiowatana (✉)
Department of Chemistry, Faculty of Science, Mahidol University, Rama VI Rd.,
Bangkok 10400, Thailand
e-mail: scysw@mahidol.ac.th

Introduction

Iron deficiency is one of the commonest nutritional problems worldwide, affecting ~20% of the world's population. Various iron fortification and dietary strategies have been proposed to maximize the intake and the bioavailability of iron [1]. Non-heme Fe, which comprises most of the Fe taken in, is absorbed in ionic form by receptors on the mucosa cells, and its bioavailability varies depending on the Fe status of the subjects and different dietary factors. Some food components show a marked inhibitory effect on the absorption of non-heme Fe in humans [2]. The strong inhibitory effects of phytic acid (PA) and tannic acid (TA) on iron absorption have been documented previously [3, 4]. Phytic acid (myo-inositol-1,2,3,4,5,6-hexakisphosphate) is the most abundant myo-inositol compound. It is reported to occur as highly phosphorylated molecules that are present in cereal grains and seeds, and it is an excellent chelator of metal ions [5–7]. Owing to the presence of six phosphate groups in very close proximity in the molecule, it strongly binds practically any metal ion. According to its pK_a of ~1.1 [8], phytic acid is present in ionic form under slightly acidic conditions and is thus able to bind with free metal ions. Most research suggests that the formation of

phytate–metal complexes in the intestinal tract prevents metal absorption [2–4, 9, 10].

TA is a hydrolyzable tannin that was reported to have a high capacity to bind iron to form a stable complex [11]. TA is a polyphenolic compound found, along with other condensed tannins, in beverages such as red wine, beer, coffee, black tea, green tea, as well as many foodstuffs such as grapes, pears, bananas, sorghum, black-eyed peas, lentils, and chocolate [12, 13]. TA is hydrolyzed by acid to form glucose and gallic acid. The latter contains a galloyl group, which has been implicated in the inhibition of iron absorption through the binding of iron [14].

As food compositions are very complex, iron and other minerals may be associated with molecules or particles of different sizes. Therefore, knowledge of the size-based distribution of iron in food suspensions during gastrointestinal digestion should lead to a better understanding of iron absorption. To study size-based elemental distribution, it is necessary to couple a separation unit with elemental detection. Gel chromatography with flame atomic absorption and polarographic detection was used to study the distributions of free and bound cadmium, zinc, copper, and silver in lobster digestive gland extract [15]. Size-based metal distributions (of free ion, low molecular weight bound, and medium molecular weight bound forms) provide information about metal–protein binding and release behavior under different conditions. Size exclusion chromatography (SEC) hyphenated with inductively coupled plasma mass spectrometry (ICP–MS) was found to be useful for exploring metal binding and association behavior, as reviewed by Sadi [16]. Wuilloud et al. employed SEC–UV–ICP–MS to determine the molecular weight distributions of associations of metal with various compounds in edible mushroom [17]. A Superdex-75 column was used to examine the association of metals with molecules of different molecular weights in fungi porcini mushroom. In chromatographic techniques, organic solvents are often used as the carrier liquid, and a sample pretreatment step is necessary to clean up the sample prior to sample introduction. The organic solvent can cause carbon overloading in the plasma of the ICP-MS.

The non-chromatographic technique flow field–flow fractionation (FlFFF), when coupled with a highly sensitive elemental detection unit such as an inductively coupled plasma optical emission spectrophotometer (ICP–OES) or ICP–MS, has been exploited to investigate the binding and association of elements with various kinds of molecules, such as proteins [18], macromolecules [19–22], and bacteria [23]. Barnes and Siripinyanond performed a feasibility study of the applicability of FlFFF–ICP–MS to metal fractionation in a protein standard including metallothionein, carbonic anhydrase, ceruloplasmin, alcohol dehydrogenase, and thyroglobulin [18]. The simple interface between the FlFFF and ICP–MS, resulting from their compatible flow rates, makes this a potentially promising and versatile technique for elemental fractionation in proteins. Jackson et al. successfully used FlFFF–ICP–MS to investigate uranium sorption behavior on bacterial cells [23]. Recent reports have suggested that FlFFF–ICP–MS and FlFFF–ICP–OES are highly capable techniques for investigating metal binding and association behavior via size-based metal distributions.

In this work, the binding of iron with phytic acid and tannic acid in food suspensions was investigated using FlFFF–ICP–OES. The size-based distribution of iron in kale extract and tea infusion with and without enzymatic digestion was also examined. Non-enzymatic incubation of the sample at pH 2.0, 5.0 and 7.0 was performed in order to mimic the pH conditions of the gastrointestinal digestion processes in the stomach, the upper part of the duodenum, and the small intestine, respectively. To obtain enzymatic incubations, pepsin and pancreatic bile extract, which are predominantly found and known to be active in the respective stages of gastrointestinal digestion, were added. To our knowledge, this is the first attempt to use hyphenated FlFFF–ICP–OES to investigate the size-based distribution of an element in a food suspension at various pHs during simulated gastrointestinal digestion.

Experimental

Chemicals and samples

Deionized water (MilliQ plus, 18.2 MΩ cm^{-1}) was used throughout the experiments. All glassware was washed with liquid detergent, rinsed with water, soaked overnight in 10% HNO_3, and rinsed again before use. All chemicals were of analytical grade. All standard working solutions of iron were prepared by diluting a 1000 mg L^{-1} standard solution of iron (prepared from Fe(III) nitrate by Merck, Darmstadt, Germany) with deionized water. Phytic acid (FW=660.04 Da; Fluka, Milan, Italy) and tannic acid (FW= 1700.79 Da; Fluka, were weighed and dissolved in deionized water to create stock solutions for the iron-inhibitor binding study. The enzymes pepsin (P-7000, from porcine stomach mucosa), pancreatin (P-1750, from porcine pancreas), and bile extract (B-6831, porcine) were from Sigma (St. Louis, MO, USA). A pepsin solution was prepared by dissolving 0.16 g of pepsin in 1 mL of 0.1 M hydrochloric acid, and a pancreatin bile extract (PBE) mixture was made by dissolving 0.004 g of pancreatin and 0.025 g of bile extract in 5 mL of 0.001 M $NaHCO_3$.

Fresh Chinese kale was washed with deionized water. It was then dried at 65 °C to constant weight and ground up before being stored in a desiccator until required. To prepare

the tea infusion, instant tea was bought from a local market and prepared by following the recommended instructions. A tea bag was dipped in 120 mL of deionized water and heated at 80 °C for 10 min. To obtain kale extract, 1 g of dried, ground Chinese kale was added to 10 mL of deionized water and heated at 80 °C for 10 min. The suspension was then centrifuged at 3000 rpm for 20 min in order to separate out the precipitated residue. The tea infusion and the Chinese kale extract was stored at 4 °C until use.

The carrier liquid for FlFFF operating at pH 2.0, 0.01 M HCl, was prepared by diluting 0.8 mL of 37% HCl (Merck) in 1000 mL of deionized water. Carrier liquids at pH 5.0 and 7.0 were prepared by adding 0.8 mL of HCl to 800 mL of deionized water and then adjusting to the required pH using $NaHCO_3$ and NaOH solutions. The solution volume was finally made up to 1000 mL. Monodisperse polystyrene sulfonates (PSS) (Fluka), which were used as FlFFF molecular weight calibrating standards (4.3, 17, and 49 kDa), were individually prepared by diluting in deionized water to obtain 10 mg mL^{-1}. All samples were centrifuged at 3000 rpm for 20 min to eliminate large particles before the FlFFF investigation.

Iron-inhibitor binding study

A flow chart for this sample preparation process is shown in Fig. 1. According to the literature, an iron:phytic acid weight ratio in excess of 1:10 (~1:1 mole ratio) clearly inhibits iron availability [24]. To demonstrate the degree of iron binding that causes the inhibition of iron absorption, 1:10, 1:50, and 1:100 weight ratios were therefore selected. Phytic and tannic acids were individually mixed with 300 mg L^{-1} iron at weight ratios (iron:phytic acid/tannic acid) of 1:10, 1:50 and 1:100. The pH was adjusted with dilute HCl or $NaHCO_3$ or NaOH solutions in order to investigate iron binding at pH values of 2.0, 5.0, and 7.0.

Non-enzymatic incubation

For the unspiked kale extract, the pH of 2.5 mL of the kale extract was adjusted to either 2.0, 5.0, or 7.0. The final volume was adjusted to 5.0 mL. For the iron-spiked kale extract or tea infusion, 1.5 mL of the 1000 mg L^{-1} standard solution of iron was added to 2.5 mL of the kale extract or tea infusion before pH adjustment. The solution volume was finally made up to 5.0 mL. The flow chart for this sample preparation process is shown in Fig. 1.

Gastrointestinal digestion

Simulated gastrointestinal digestion of food samples was carried out starting with peptic digestion with pepsin, and then pancreatic digestion with PBE (see Fig. 2). In the simulated peptic digestion step, a portion of the sample (0.5 g for a solid sample or 2.0 mL for a liquid sample) was added to 10.0 mL of purified water and adjusted to pH 2.0 with 6 M hydrochloric acid. The volume of the sample suspension was finally adjusted to 12.5 mL with purified water, and 375 μL of pepsin solution was added. This digestion step was performed in an incubator shaker at 37± 1 °C for 2 h. After that, the suspension pH was adjusted to 5.0 and incubated for 30 min to simulate the digestion in the upper part of the duodenum, at the juncture between the stomach and the intestine. An aliquot of 2.5 mL of the digestate at pH 5.0 was taken, adjusted to pH 7.0, and diluted to 5.0 mL. The freshly prepared PBE mixture (625 μL) was then added, and the incubation was continued for 2 h.

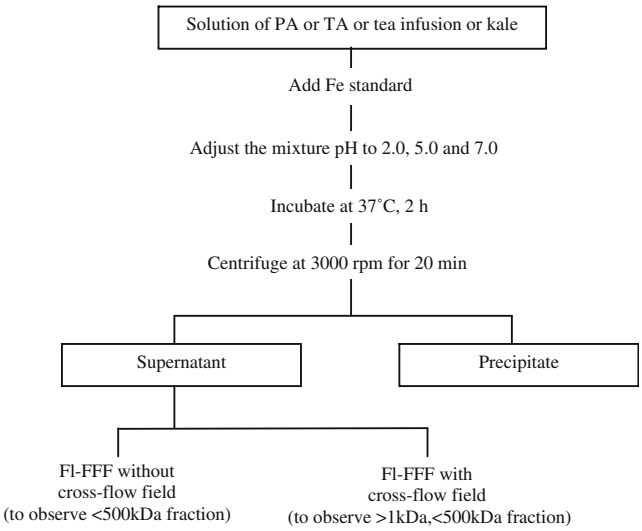

Fig. 1 Non-enzymatic mixing of test samples (kale extract and tea infusion) containing phytic acid (PA) or tannic acid (TA) with iron solution, at various pH values, to investigate the size-based iron distribution

Instrumentation

A pH meter (model 215, Denver Instrument, Denver, CO, USA) with a glass combination electrode was used for all pH measurements. Commercial standard buffers (Merck) of pH 4.00 and 7.00 were employed for the pH calibration. An incubator shaker, model SS40-D2 from Grant Instruments (Cambridge, UK), was used to incubate the samples at 37± 1 °C. A FlFFF system (model PN-1021-FO, Postnova Analytics, Landsberg, Germany) equipped with a 1000-Da molecular weight cut-off poly(cellulose acetate) membrane (Postnova Analytics) was used. The FlFFF channel was 27 cm long, 2.0 cm wide and 0.0254 cm thick. A high-pressure liquid chromatography (HPLC) pump (model PN 2101, Postnova Analytics) was employed to deliver the channel flow. Another HPLC pump of the same model was employed to regulate the cross-flow. The FlFFF can be

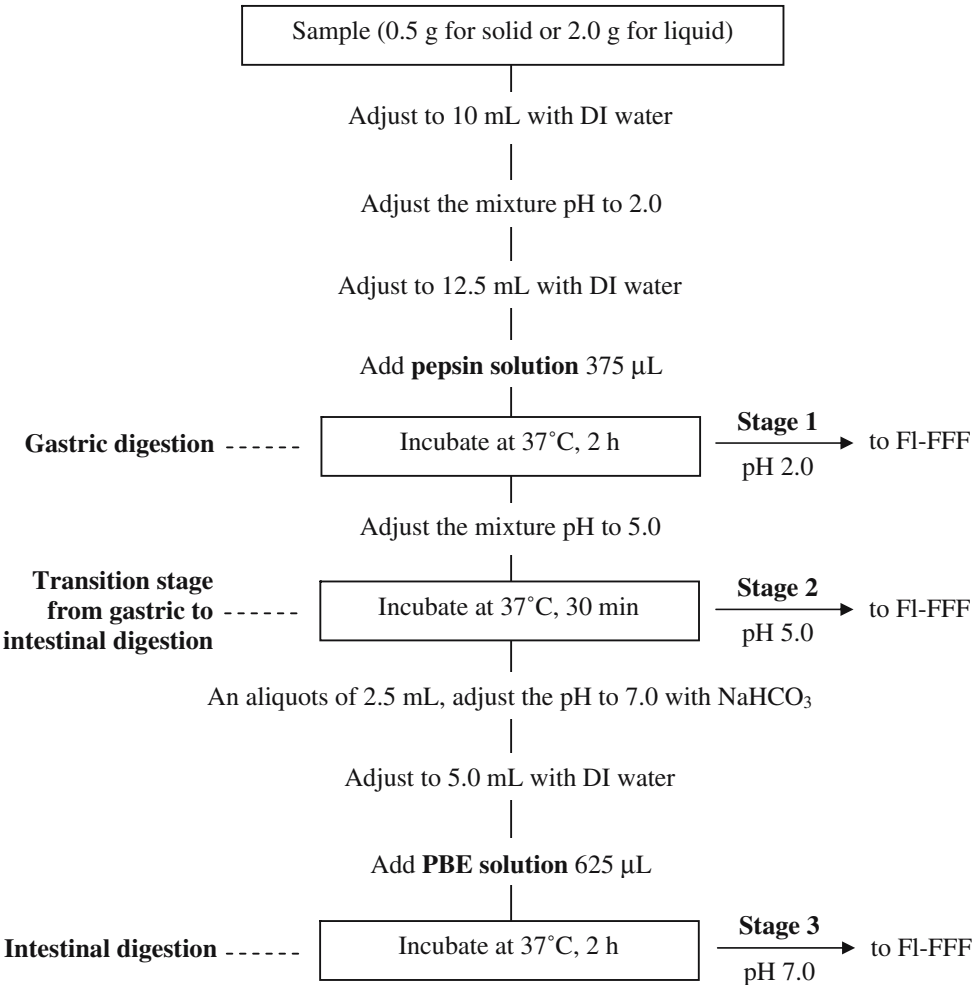

Fig. 2 Enzymatic digestion procedure used to simulate gastrointestinal digestion

operated in two modes; with and without cross-flow. In the presence of cross-flow, sample components that are smaller than the membrane cutoff (1 kDa) are forced through a membrane and leave the channel, whereas the remaining components are separated under cross-flow field. Without using cross-flow, all sample components are retained in the channel and leave the channel through the outlet connected to the detectors. UV absorption of the eluted molecules was monitored at 254 nm by a UV-visible spectrophotometer (model S 3210, Postnova Analytics). An end-on view Spectro CirosCCD ICP–OES system (Spectro Analytical Instruments, Kleve, Germany) was used as an elemental detector. The outlet of the spectrophotometer flow cell was connected directly to the modified Lichte nebulizer of the ICP–OES system with poly(tetrafluoroethylene) tubing. The operating conditions employed when taking FlFFF and ICP-OES measurements are summarized in Table 1. The iron emission was monitored at 238.20(II), 259.94(II) and 239.56(II) nm.

Calculating the iron distribution

To gauge the total iron concentrations in the phytic and tannic acid experiments, including those involving the iron-spiked and unspiked kale extracts and the tea infusion, their wet acid digestates were measured by ICP–OES using external calibration. After enzymatic and non-enzymatic incubation, the sample suspension was separated into supernatant (assumed to be the <500 kDa fraction) and precipitation phases (assumed to be the >500 kDa fraction). The total iron in the supernatant was calculated from the area of the iron fractogram obtained without cross-flow field of the supernatant. The iron in the precipitation phase (>1 kDa but <500 kDa) was calculated from the area of the iron fractogram obtained with cross-flow field of the supernatant.

The iron associated with the supernatant was calculated by subtracting the iron in the precipitation phase from the total iron in the supernatant. The >500 kDa fraction was

Table 1 Instrumental operating conditions

FlFFF condition	
Carrier liquid	
pH 2.0	0.01 M HCl
pH 5.0	0.01 M HCl adjusted to pH 5.0 by $NaHCO_3$
pH 7.0	0.01 M HCl adjusted to pH 7.0 by NaOH
Membrane	1000 Da MWCO, poly(cellulose acetate)
Channel flow rate (mL min^{-1})	0.75
Cross flow rate (mL min^{-1})	2
ICP–OES condition	
RF generator frequency (MHz)	27.2
RF power / W	1350
Nebulizer gas flow rate (L min^{-1})	1
Coolant gas flow rate (L min^{-1})	12
Auxiliary gas flow rate (L min^{-1})	1

obtained by subtracting the total iron concentration in the supernatant from the total iron concentration in the samples. The percentage distributions were calculated by dividing the iron concentration in each fraction by the total iron concentration and multiplying by 100.

Results and discussion

I. FlFFF channel calibration

To calibrate the FlFFF channel effectively, the type of molecular weight standard used should be selected carefully. In this study, poly(styrene sulfonate) standards were selected for two reasons. The first reason is the similar secondary structure (a random coil) of the phytic and tannic acids and the poly(styrene sulfonate). Second, in contrast to protein standards, poly(styrene sulfonate) maintains its structural integrity at the pH values examined in this work. As FlFFF has rarely been performed at pH 2, we carefully evaluated the feasibility of performing size characterization at this acidic pH, and found that satisfactory results were obtained.

By calibrating the FlFFF channel with known molecular weight poly(styrene sulfonate) standards (4.3, 17.0, and 49 kDa), calibration functions were obtained for each pH value, as follows:

$$\log t_r = 0.572 \log M - 0.556, R^2 = 0.984 \text{ for pH } 2.0$$
$$\log t_r = 0.437 \log M - 0.065, R^2 = 0.999 \text{ for pH } 5.0$$
$$\log t_r = 0.526 \log M - 0.100, R^2 = 0.994 \text{ for pH } 7.0$$

The parameters t_r and M represent retention time (min) and molecular weight (kDa), respectively. The retention time (t_r) was measured at the peak maximum of the fractogram. These equations were used to translate the retention time into molecular weight information. The slightly different calibration equation at each pH may be due to changes in the properties of the FlFFF membrane at different pH values, which could lead to a slight shift in retention. Therefore, channel calibration must be performed at all pH values studied.

II. The size-based distribution of iron in the presence of inhibitors

FlFFF–ICP–OES fractograms were obtained in order to study the binding behavior of iron to phytic and tannic acids at pH 2.0, 5.0, and 7.0 (Fig. 3a–d, right, and Fig. 4), considering the pH change from ~2.0 to ~7.0 in the gastrointestinal pathway where iron and other minerals are absorbed. The amount of phytic acid was varied by employing weight ratios (Fe:PA) of 1:10, 1:50 and 1:100, and size-based distribution profiles of iron at pH 2.0, 5.0, and 7.0 were obtained. The molecular weight at the peak was calculated from the molecular weight calibration equation obtained at each pH value. Initially, fractograms of iron solution with phytic and tannic acids were examined. Without any phytic or tannic acids, iron in its free form is not retained in the FlFFF channel, and it is thus forced to pass through the channel membrane and leave the channel. Therefore, no iron distribution is seen in the fractogram, as shown in Fig. 3d, right. However, upon binding with an inhibitor with a large molecular weight, the iron phytate chelation results in larger molecules which are retained above the channel membrane, gaving an iron signal at 1–1.5 min, equivalent to a molecular weight of ~1 kDa. The UV fractograms of the retained molecules showed similar profiles to those of the iron distribution profiles, suggesting that iron was highly associated with the phytic acid molecules (Fig. 3a–d, left). The UV fractograms and iron distributions gave peak maxima at the same retention time for every phytic acid iron ratio. The peak areas of UV absorption and iron distribution increased when the phytic acid to iron ratio was increased.

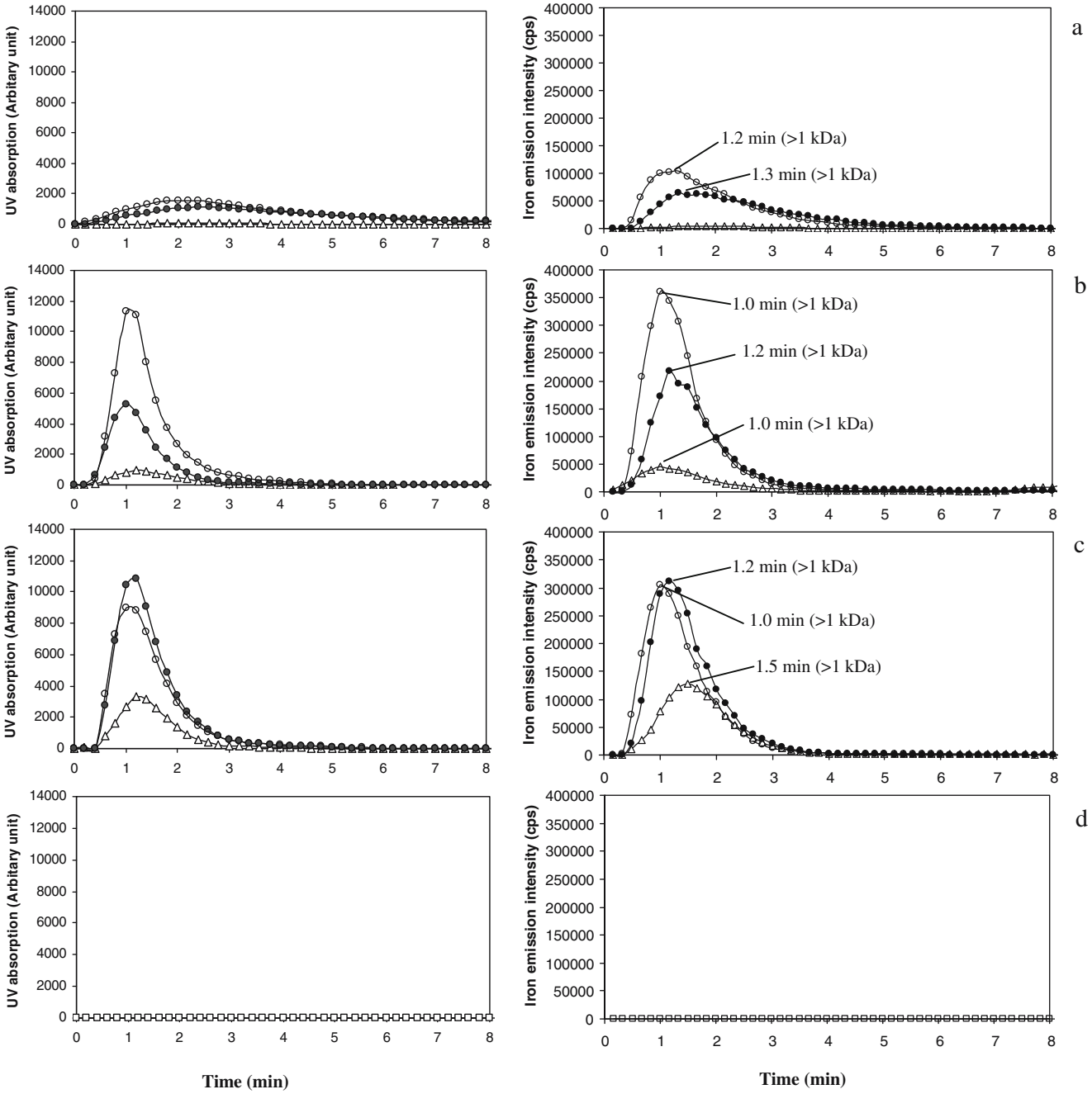

Fig. 3a–d Fractograms (UV detection on the *left* and ICP–OES detection on the *right*) for iron in the presence of varying amounts of phytic acid at pH 2.0 (**a**), 5.0 (**b**), and 7.0 (**c**). **d** shows fractograms of iron without phytic acid. Fe:PA was 1:10 (*triangles*), 1:50 (*filled circles*), and 1:100 (*unfilled circles*)

At all pH values studied, the iron association in the FlFFF-observable range of >1 kDa but <500 kDa was found to increase when more phytic acid was added. The highest association, as observed from the peak areas in Fig. 3, right), was found for weight ratios of 1:50 and 1:100 at pH 7.0. For a fixed amount of phytic acid, the binding of iron and phytic acid increased when the pH was increased.

Three molecular weight ranges were then classified: (a) <1 kDa; (b) >1 kDa but <500 kDa; and (c) >500 kDa. The size-distributions of the iron associations for all three weight ranges are summarized in Table 2. Fraction (b) was calculated from area under the fractogram, as observed using FlFFF–ICP–OES. The iron associated with molecules smaller than 1 kDa (a) was obtained from the area of the

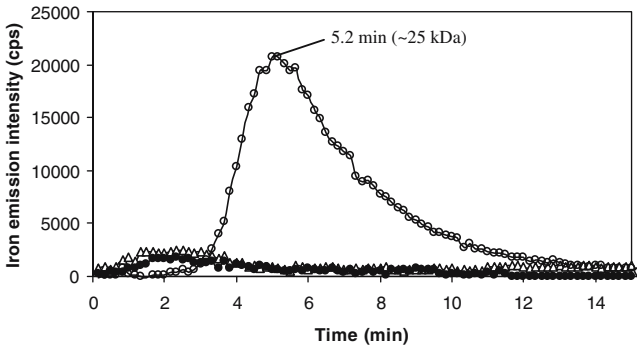

Fig. 4 Iron fractograms of iron in tannic acid (weight ratio 1:100) at pH 2.0 (*triangles*), 5.0 (*unfilled circles*) and 7.0 (*filled circles*)

fractogram yielded by FlFFF–ICP–OES without the application of cross-flow field minus the same value for (b). The equivalent value for the fraction larger than 500 kDa (c) was calculated by subtracting the values for (a) and (b) from the total iron value.

High associations between iron and phytic acid were observed for every pH and every iron:phytic acid ratio. For an iron:phytic acid ratio of 1:10, the iron was largely distributed in the >500 kDa fraction at all pH values tested. For the other iron:phytic acid ratio, the amount of iron in this fraction was less significant. This phenomenon was in agreement with the results reported by Evan and Martin [25], who found that iron phytate precipitated at ratios of approx. 1:10 and 1:40. Free iron or iron associated with molecules smaller than 1 kDa was clearly predominant at pH 2.0. The amount of iron in this fraction decreased when solution pH was increased to 5.0 and 7.0. At pH 5.0 and 7.0, the iron was concentrated in the fraction associated with phytic acid (>1 kDa), as observed in the FlFFF fractogram. Most of the iron was associated with phytic acid.

In the presence of tannic acid, iron was associated with small molecules (<1 kDa) at pH 2.0 (Table 2). At pH 5.0 and 7.0, however, iron only appeared in the >500 kDa fraction, except for an iron:tannic acid ratio of 1:100 at pH 5.0, as illustrated in Fig. 4. The association of iron with macromolecules (~25 kDa) was observed at t_r = 5.2 min. At high levels of tannic acid and for slightly acidic conditions, the iron that formed macromolecules with tannic acid did not precipitate completely. For other ratios and at pH 5.0 and 7.0, precipitation readily occurred when the iron and tannic acid solutions were mixed. The amount of free iron or iron associated with molecules smaller than 1 kDa was extremely low. It can therefore be concluded that iron was completely bound to tannic acid when the pH was higher than 5.0.

At pH 5.0 and 7.0, most of the iron was associated with the phytic acid or tannic acid. The phytic and tannic acids

Table 2 Size-based distributions of iron in the presence of various concentrations of phytic acid (PA) and tannic acid (TA) at pH 2.0, 5.0, and 7.0

Sample	pH	Proportions of iron (%)		
		<1 kDa[(a)]	>1 kDa, <500 kDa[(b)]	>500 kDa[(c)]
Fe + PA (1:10)	2.0	16.0	2.0	81.9
	5.0	3.9	25.5	70.7
	7.0	6.0	45.5	48.4
Fe + PA (1:50)	2.0	49.6	50.4	0.0
	5.0	19.8	66.0	14.2
	7.0	0.0	93.8	6.2
Fe + PA (1:100)	2.0	45.2	54.8	0.0
	5.0	17.2	82.8	0.0
	7.0	4.5	95.5	0.0
Fe + TA (1:10)	2.0	98.9	1.1	n.d.
	5.0	0.5	0.4	99.1
	7.0	0.1	0.6	99.3
Fe + TA (1:50)	2.0	98.9	1.2	0.0
	5.0	0.9	0.7	98.4
	7.0	1.1	0.6	98.2
Fe + TA (1:100)	2.0	98.9	1.1	n.d.
	5.0	2.5	16.1	81.5
	7.0	1.7	1.7	96.6

[(a)] Obtained from the area of the iron profile yielded by FlFFF–ICP–OES without the cross-flow field minus the value for (b)
[(b)] Obtained from the area of the iron profile yielded by FlFFF–ICP–OES with the cross-flow field
[(c)] Obtained from the total iron minus the values for (a) and (b)
n.d., not determined, as the concentration in this fraction was lower than the detection limit of 0.2 mg L^{-1}
Total iron concentration was 300 mg L^{-1}.

showed high potential to produce iron complexes which are reportedly not absorbable by the intestine [2–4, 9, 10].

III. Size-based distributions of iron in kale extract and tea infusion

Kale and tea contain inhibitor molecules—phytic acid and tannic acid, respectively. The inhibitors in kale and tea can bind with the iron to form iron complexes, and so they exhibit an inhibition effect. Therefore, the size-based distribution of iron in kale extract and tea infusion was investigated at pH 2.0, 5.0, and 7.0 under both non-enzymatic and enzymatic conditions. Due to the low iron content in tea itself, free iron was spiked into the tea infusion to a level of 300 mg L^{-1} prior to investigation.

Table 3 shows the proportions of iron in each of three size groups for kale extract and tea infusion. The proportions were calculated as in the iron-inhibitor binding study (Table 2).

From Table 3, the proportions of iron in the small size fraction (<1 kDa) were similar for all sample types. The highest proportion of iron was observed at pH 2.0. At an acidic pH of 2.0, iron was in the free form (or was associated in molecules of <1 kDa), except in the case of iron-spiked tea infusion, when precipitation was observed.

For the unspiked kale extract, the iron was concentrated in the FlFFF-observable range (>1 kDa, <500 kDa) at pH 5.0 and 7.0. The distribution profiles shown in Fig. 5a show that iron was associated with macromolecules of approximately the same molecular weight as in Fig. 2 (>1 kDa). Phytic acid, which binds to the iron, may be present in kale extract. Iron-spiked kale also gave iron distribution profiles

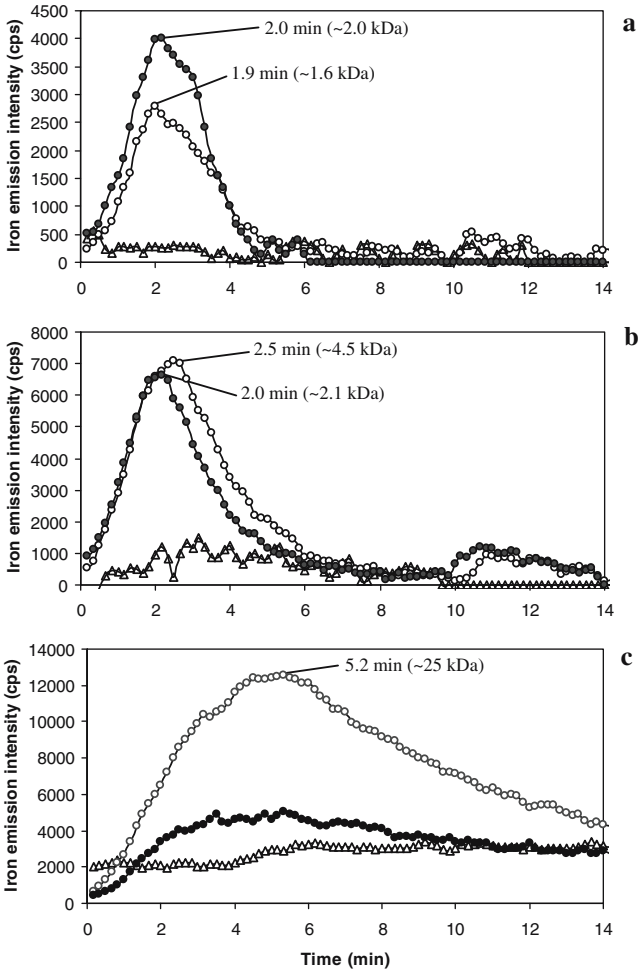

Fig. 5a–c Iron fractograms for iron in kale extract (**a**), iron-spiked kale extract (**b**) and iron-spiked tea infusion (**c**) at pH 2.0 (*triangles*), 5.0 (*unfilled circles*) and 7.0 (*filled circles*)

Table 3 Size-based distributions of iron for kale extract, iron-spiked kale extract and iron-spiked tea infusion at pH 2.0, 5.0, and 7.0

Sample	pH	Proportions of iron (%)		
		<1 kDa[a]	>1 kDa, <500 kDa[b]	>500 kDa[c]
Kale extract	2.0	100.0	0.0	0.0
	5.0	36.5	63.5	0.0
	7.0	4.2	95.8	0.0
Iron-spiked kale extract	2.0	100.0	n.d.	n.d.
	5.0	3.3	3.9	92.8
	7.0	3.0	3.5	93.5
Iron-spiked tea infusion	2.0	91.9	n.d.	8.1
	5.0	21.0	18.5	60.5
	7.0	18.5	7.2	74.3

[a] Obtained from the area of the iron profile yielded by FlFFF–ICP–OES without cross-flow field minus the value for (b)
[b] Obtained from the area of the iron profile yielded by FlFFF–ICP–OES with cross-flow field
[c] Obtained from the total iron minus (a) and (b)
n.d., not determined, as the concentration in this fraction was lower than the detection limit of 0.2 mg L^{-1}

Table 4 Size-based distributions of iron in iron-spiked tea infusion and kale extract at each stage of gastrointestinal digestion

Sample	Stage	Proportions of iron (%)		
		<1 kDa[a]	>1 kDa, <500 kDa[b]	>500 kDa[c]
Tea infusion (iron-spiked)	1 (pH 2.0)	94.8	nd	5.2
	2 (pH 5.0)	29.7	nd	70.3
	3 (pH 7.0)	15.5	nd	84.5
Kale extract	1 (pH 2.0)	82.8	nd	17.2
	2 (pH 5.0)	27.5	nd	72.5
	3 (pH 7.0)	21.2	nd	78.8

[a] Obtained from the area of the iron profile yielded by FlFFF–ICP–OES without cross-flow field minus the value for (b)
[b] Obtained from the area of the iron profile yielded by FlFFF–ICP–OES with cross-flow field
[c] Obtained from the total iron minus the values of (a) and (b)
n.d., not determined, as the concentration in this fraction was lower than the detection limit of 0.2 mg L^{-1}

that peaked in the FlFFF-observable range (>1 kDa, <500 kDa) at pH 5.0 and 7.0, as shown in Fig. 5b.

From Table 3, it is clear that most of the iron was distributed in the small molecular size fraction at pH 2.0. The iron was found in the large molecular size fraction when the pH was raised to 5.0 and 7.0. At pH 5.0, iron associated with macromolecules was observed, as the peak maximum occurred at 5 min or ~25 kDa (Fig. 5c), in agreement with the iron–tannic acid binding experiment (Fig. 4).

The fractograms for the kale extract (Fig. 5a) and the iron-spiked kale extract (Fig. 5b) show a similar degree of association in the range of >1 kDa but <500 kDa. Insufficient numbers of phytic acid binding sites in kale and the high iron concentration may have caused precipitation at slightly acidic (pH 5.0) and neutral (pH 7.0) conditions. Most of the unbound iron in iron-spiked kale precipitated and was distributed in the large molecular fraction (>500 kDa) at pH 5.0 and 7.0, as shown in Table 3.

IV. Size-based distributions of iron in kale and tea infusion after gastrointestinal digestion

To observe the change in the size-based distribution of iron as a result of gastrointestinal digestion, simulated enzymatic digestion was carried out by peptic and then pancreatic digestion. The iron distribution after each stage of gastrointestinal digestion of the kale extract and iron-spiked tea infusion is shown in Table 4. Both samples showed different iron distributions compared to those obtained after non-enzymatic incubation. No iron was observed in the FlFFF-observable size range (>1 kDa, <500 kDa). This shows that, upon gastrointestinal digestion, the iron-bound molecules were digested and converted to free irons and iron associated with molecules smaller than 1 kDa. The inhibitor in the sample was believed to bind with iron, forming an insoluble iron compound, especially at stages 2 and 3 of the simulated gastrointestinal digestion, as can be seen in Table 4.

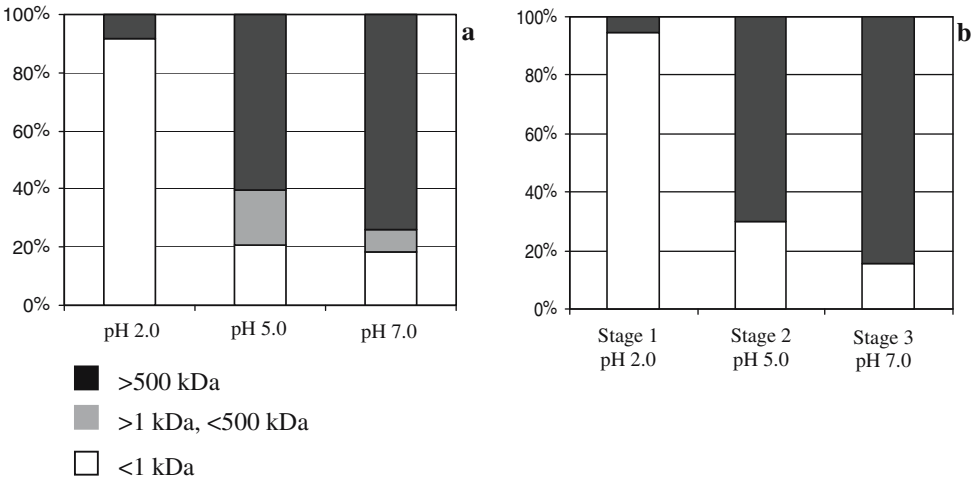

Fig. 6a–b Size-based distribution of iron in iron-spiked tea infusion after (**a**) non-enzymatic mixing at different pH values and (**b**) enzymatic gastrointestinal digestion

In the gastrointestinal digestion of iron-spiked tea infusion, iron did not completely precipitate after full gastrointestinal digestion at pH 7.0. This suggests that the tea infusion may contain less tannic acid than was added in the iron–tannic acid binding experiment.

In Fig. 6, size-based distributions of iron in the spiked tea infusion at different pH values both with and without enzymatic gastrointestinal digestion are compared. The distributions were found to be similar at pH 2.0. The results from the non-enzymatic study at pH 5.0 and 7.0 show that the soluble iron is partially associated with the inhibitor, as shown by the proportions in the range >1 kDa, <500 kDa. In contrast, the enzymatic digestion results in a negligible iron macromolecule binding fraction, as seen from the FlFFF fractogram. It seems probable that the iron in the molecular range of >1 kDa, <500 kDa is digested during enzymatic digestion; it is partially released as free forms and as some iron chelate precipitates.

All soluble iron was present as free iron or iron associated with molecules smaller than 1 kDa, which is absorbable. The iron bound to macromolecules may be digested to small molecules and released as free iron or precipitated after enzymatic digestion, depending on the nature and composition of the food sample.

Conclusion

A hybrid technique where flow field–flow fractionation (FlFFF) is coupled to inductively coupled plasma optical emission spectrometry (ICP–OES) has shown the potential to be an alternative investigation tool for monitoring the size-based distributions of elements in food suspensions during simulated gastrointestinal digestions. Using the technique, iron binding with food components—exemplified by phytic acid and tannic acid in this study—can be investigated. The FlFFF exhibited several advantages over chromatographic techniques due to its ability to investigate wider pH and molecular size ranges. However, the FlFFF has limitated applicability in other studies that require higher resolution.

With or without enzymatic digestion, iron strongly associates with phytic acid at every pH, whereas strong association with tannic acid was observed only when the pH was raised to 5.0 and 7.0. The investigation provides a better understanding of the elemental fractionation of iron–phytic acid and iron–tannic acid complexes during gastrointestinal digestion processes. Tea and kale, which contain tannic and phytic acids, respectively, exhibited the potential to bind with iron and yield similar distributions to those obtained for iron–phytic acid and iron–tannic acid. The ingestion of non-heme iron-containing foods with tea and kale may cause iron absorption to be inhibited during gastrointestinal digestion. The fractionation power of Fl-FFF coupled with the highly sensitivity of ICP–OES is potentially a useful technique for estimating the in vitro iron bioavailability, circumventing the need for a tedious and lengthy procedure. The study of bioavailability will lead to further management strategies for counteracting inhibition and promoting better mineral bioavailability.

Acknowledgement The authors are grateful for financial support from the Thailand Research Fund and the Center for Innovation in Chemistry: Postgraduate Education and Research Program in Chemistry, Higher Education Development Project, Ministry of Education.

References

1. Martinez-Navarrete N, Camacho MM, Martinez-Lahuerta J, Martinez-Monzo J, Fito P (2002) Food Res Int 35:225–231
2. Lopez HW, Leenhardt F, Coudray C, Remesy C (2002) Int J Food Sci Technol 37:727–739
3. Glahn RP, Wortley GM, South PK, Miller DD (2002) J Agric Food Chem 50:390–395
4. Brigide P, Canniatti-Brazaca SG (2006) Food Chem 98:85–89
5. Graf E, Mahoney JR, Bryant RG, Eaton JW (1984) J Biol Chem 259:3620–3624
6. Graf E, Empson K, Eaton J (1987) J Biol Chem 262:11647–11650
7. Graf E, Eaton JW (1990) Free Rad Biol Med 8:61–69
8. Vasca E, Materazzi S, Caruso T, Milano O, Fontanella C, Manfredi C (2002) Anal Bioanal Chem 374:173–178
9. Sandberg AS, Svanberg U (1991) J Food Sci 56:1330–1333
10. Engle-Stone R, Yeung A, Welch R, Glahn R (2005) J Agric Food Chem 53:10276–10284
11. South PK, Miller DD (1998) Food Chem 63:167–172
12. King A, Young G (1999) J Am Diet Assoc 99:213–218
13. Chung K-T, Wong TY, Wei C-I, Huang Y-W, Lin Y (1998) Crit Rev Food Sci Nutr 38:421–464
14. Brune M, Hallberg L, Skaanberg AB (1991) J Food Sci 56:128–167
15. Chou CL, Uthe JF, Guy RD (1993) J AOAC Int 76:794–798
16. Sadi BBM, Vonderheide AP, Becker JS, Caruso JA (2005) ACS Symp Ser 893:168–183
17. Wuilloud RG, Kannamkumarath SS, Caruso JA (2004) J Agri Food Chem 52:1315–1322
18. Siripinyanond A, Barnes RM (1999) J Anal Atom Spectrom 14:1527–1531
19. Stolpe B, Hassellov M, Andersson K, Turner DR (2005) Anal Chim Acta 535:109–121
20. Gimbert LJ, Andrew KN, Haygarth PM, Worsfold PJ (2003) Trends Anal Chem 22:615–633
21. Contado C, Blo G, Fagioli F, Dondi F, Beckett R (1997) Colloids Surf A 120:47–59
22. Bolea E, Gorriz MP, Bouby M, Laborda F, Castillo JR, Geckeis H (2006) J Chromatogr A 1129:236–246
23. Jackson BP, Ranville JF, Neal AL (2005) Anal Chem 77:1393–1397
24. Hurrell Richard F (2003) J Nutr 133:2973S–2977S
25. Evans WJ, Martin CJ (1991) J Inorg Biochem 41:245–252

Towards better understanding of *in vitro* bioavailability of iron through the use of dialysis profiles from a continuous-flow dialysis with inductively coupled plasma spectrometric detection†

Kunchit Judprasong,[ab] Atitaya Siripinyanond[a] and Juwadee Shiowatana*[a]

Received 11th January 2007, Accepted 19th March 2007
First published as an Advance Article on the web 11th April 2007
DOI: 10.1039/b700470b

A continuous-flow dialysis (CFD) method with an on-line inductively coupled plasma optical emission spectrometric (ICP-OES) simultaneous multielement measurement for the study of *in vitro* mineral bioavailability was previously reported. The method was based on a simulated gastric digestion in a batch system followed by a continuous-flow intestinal digestion—dialysis with on-line measurement of dialysed mineral concentration by ICP-OES. This study demonstrates how the dialysis profiles obtained could be exploited to understand differences of mineral dialysability and the effect of enhancers and inhibitors. The graphical plot of time-dependent cumulative dialysed mineral concentrations and percent dialysis was efficiently used for these purposes. Iron fortificants in various chemical forms were used to demonstrate the effect of their anionic parts on dialysability together with enhancement and inhibition effects from food acids.

Introduction

Mineral bioavailability has usually been determined by *in vivo* measurements. As an alternative to human and animal *in vivo* studies, the availability of minerals or trace elements has also been estimated by simple, rapid and inexpensive *in vitro* methods.[1] *In vitro* methods based on simulated gastrointestinal digestion with continuous-flow dialysis (CFD) were developed.[2–5] These methods measure the fraction of mineral accessible pool in diets which is of potential absorption. Although a true absorption is not determined, *in vitro* methods have frequently been used to predict and compare the bioavailability of minerals from different foods.[6,7]

In our previous reports, the CFD system was operated with flame AAS,[4] electrothermal AAS[5] and inductively coupled plasma optical emission spectrometric (ICP-OES)[8] detections for studies of minerals of nutritional importance (Ca, Mg, P, Fe and Zn). The objective of this study was to demonstrate the use of dialysis profiles to understand the differences of dialysability of minerals, taking the advantage of the time-dependent dialysis data obtained from the developed CFD method. Effects of the different chemical forms of mineral fortificant and the inhibition and enhancement effects from common components in food were elaborated.

Being carried out by an *in vitro* equilibrium batch dialysis method, previous studies provided no insight information to explain the dialysability results obtained. This work shows how to exploit the time-dependent dialysis information from the continuous-flow dialysis approach to clearly demonstrate the factors affecting *in vitro* bioavailability. Such investigation has been exemplified for Ca, Fe and Zn. In order to illustrate the concept, however, only Fe is described in this manuscript.

Experimental

Instrument and equipment

The detail of continuous-flow dialysis (CFD) system connected to a pH measurement module and ICP-OES detection unit has been described elsewhere.[8] A shaking water bath (Memmert®, Memmert GmbH, Germany), controlled at 37 ± 1 °C was used both for simulated gastric and intestinal digestions. The Orion SensorLink pH measurement system (ThermoOrion, USA), model PCM500, equipped with a PCMCIA slot and a personal computer, was used to monitor pH during digestion and dialysis.

Determination of iron by ICP-OES was performed using a SPECTRO CIROS CCD, axial configuration, equipped with a glass spray chamber (double pass, Scott-type) and a cross-flow nebuliser (all from SPECTRO, Kleve, Germany). The ICP-OES operating conditions were as follows: power 1350 W; nebuliser gas flow 1 L min^{-1}; and auxiliary gas flow 12 L min^{-1}. Selected emission lines were: Fe, 238.204 (II), 239.562 (II) and 259.940 (II). Emission lines for internal standards were: Y, 320.332 (II), 371.030 (II) and 442.259 (II) and Sc: 256.023 (II), 361.384 (II) and 440.037 (II) nm.

Reagents and solutions

The enzymes: pepsin (P-7000, from porcine stomach mucosa); pancreatin (P-1750, from porcine pancreas) and bile extract (B-6831, porcine) were from Sigma (St. Louis, Missouri, USA). The preparation procedures of the digestive enzyme

[a] *Department of Chemistry, Faculty of Science, Mahidol, 66 2 2015122, Thailand. E-mail: scysw@mahidol.ac.th*
[b] *Institute of Nutrition, Mahidol University, Salaya, Putthamonthon, Nakorn Pathom, 73170, Thailand. E-mail: nukjp@mahidol.ac.th*
† Presented at the Second Asia–Pacific Winter Conference on Plasma Spectrochemistry, Bangkok, Thailand, November 27–December 2, 2006.

pepsin, pancreatin bile extract (PBE) have been described elsewhere.[4]

Three sets of stock solution containing multi-element standards (QCS 01-5 at 100 μg mL^{-1}), Y (ICP-69N-1 at 1000 (μg mL^{-1}) and Sc (ICP-53N-1 at 1000 (μg mL^{-1}); as internal standards, were from Accutrace™ (AccuStandard®, Connecticut, USA). Standard solutions were prepared immediately before use by dilution of stock standard with 2% HNO_3.

Sample preparation

Five iron fortificants including iron(II) sulfate (Ajax Co. Ltd., Aubern, Australia), iron(II) fumarate (Vicky Consolidate Co. Ltd., Bangkok, Thailand), sodium iron(III) ethylenediaminetetraacetic acid (Akzo Nobel Functional Chemicals Co. Ltd., Arnhem, The Netherlands), iron(II) lactate, iron(III) ammonium citrate (Dr Paul Lohmann® Co. Ltd., Emmerthal, Germany) were investigated. The iron concentration for simulated gastrointestinal digestion experiment was approx. 1 mg metal mL^{-1}.

Ascorbic acid and citric acid (Fisher Scientific, Leicestershire, England) were selected to study enhancement of mineral absorption at molar ratio of enhancer to mineral of 3 : 1. For inhibition experiments, phytic acid (Sigma, USA), tannic acid (Fluka, Steinheim, Germany) and oxalic acid (BDH, Poole, England) were used at the same molar ratio of 3 : 1.

Simulated gastrointestinal digestion procedure and determination of dialysability

To study *in vitro* bioavailability of minerals, an *in vitro* gastric digestion was performed in a batch system (mimicking digestion in the stomach where no mineral absorption takes place), followed by an intestinal digestion in a CFD system. The CFD in the intestinal digestion step enables dialyzable components to be continuously removed for element detection. Gastric digestion was performed according to the procedure of Miller.[1] Dried samples were accurately weighed (0.5–1.0 g), mixed with 10 g of Milli-Q water, adjusted to pH 2.0 with 6 M HCl and adjusted to 12.5 g using pure water. To carry out pepsin–HCl digestion, 375 μL of pepsin solution (16% w/v) was added. The mixture was then incubated for 2 h at 37 ± 1 °C in a shaking water-bath. This mixture was further used in the following intestine digestion.

For intestinal digestion and dialysis, a CFD-ICP-OES system was used.[8] A portion of the mixture after gastric digestion (2.0 g) was injected into the flattened dialysis bag (MWCO 12–14 kDa) 10 mm flat wide, 17.6 cm in length (cellu-Sep®H1, Membrane Filtration Products, Texas, USA) in the dialysis chamber *via* a syringe. The dialysing solution of optimum concentration (3–9 × 10^{-4} M $NaHCO_3$) flowed through the chamber around the bag at 1 mL min^{-1} and the temperature was controlled at 37 ± 1 °C. A 625-μL freshly prepared pancreatin-bile extract (PBE) mixture containing 0.4% w/v pancreatin and 2.5% w/v bile extract was slowly injected after 30 min and dialysis was continued for an additional 2 h. The dialysable components were transported in the dialysing solution into the pH measurement cell and finally to the ICP-OES. To obtain good nebulisation performance and to ensure that iron remained soluble, the stream of dialysing solution was acidified by mixing with a stream of 4% nitric acid, which also contained 1 mg L^{-1} of Y and Sc, used as internal standards at 1.0 mL min^{-1}. A blank of gastrointestinal digestion-dialysis was also performed in each experiment.

The iron concentration of the dialysate (μg mL^{-1}) was obtained by on-line ICP-OES measurement with external calibration using standard solutions in $NaHCO_3$ of similar concentration to the dialysing solution. Total dialysed amount was determined by integration of the signal through the whole dialysis time using a computer program (Microcal Origin, Version 6.0). Dialysability in percent was calculated as follows: Dialysability (%) = 100 × D/C, where D = dialysed iron content (μg g^{-1} sample) and C = total iron content (μg g^{-1} sample).

Results and discussion

CFD-ICP-OES: Analytical recoveries and dialysability assessment

To validate the analytical procedure, the recoveries of iron were determined. The iron concentrations in the dialysate and the non-dialysed counterparts in the retentate were measured. Non-dialysed iron concentration in the retentate was determined after acid decomposition of the remains of sample suspension in the dialysis tube with subsequent ICP-OES detection. The total iron content of the sample was also determined after microwave decomposition of the sample. The summations of dialysed and non-dialysed amounts were compared with the total iron content. For all iron fortificants studied herein, the sum values of the dialysed and non-dialysed iron contents were close to the total values with recoveries ranging from 94.5 to 102.8%. Repeatability of percent dialysability of iron in all fortificants determined was better than 3% RSD.

Various chemical forms of iron fortificants provided significantly different iron dialysability. Iron(II) sulfate, iron(II) lactate, and iron(II) fumurate provided similar percent dialysability of 41–45%. Iron(III) ammonium citrate shows lowest percent dialysability (24–26%). The protected iron compound, NaFe(III)EDTA, gave the highest percent dialysability (79–83%). This phenomena can be explained by high stability constants of iron–EDTA complexes having the value log K of 25.7 for Fe(III) and 14.3 for Fe(II).[8,9] Formation of complexes prevents iron(III) in food from precipitating when pH rises resulting in high dialysability.

Dialysis profiles

While a batch dialysis system provides only a single value of dialysed amount at equilibrium, the continuous-flow dialysis system (CFD) offers both dialysed amount and time-based dialysis profile information. Dialysis profiles and pH change (Fig. 1 and 2, upper frame) and time-dependent cumulative plot of dialysed iron amount (Figs. 1 and 2, lower frame) can be obtained from the continuous measurement of dialysed iron concentrations and pH. The pH change (right axis of upper frame) from approx. 2.0 of the gastric digest to *ca.* 5.0 within 30 min of intestinal digestion and to *ca.* 7.0–7.5 after 1 h was close to what occurs in the human gastrointestinal tract. The

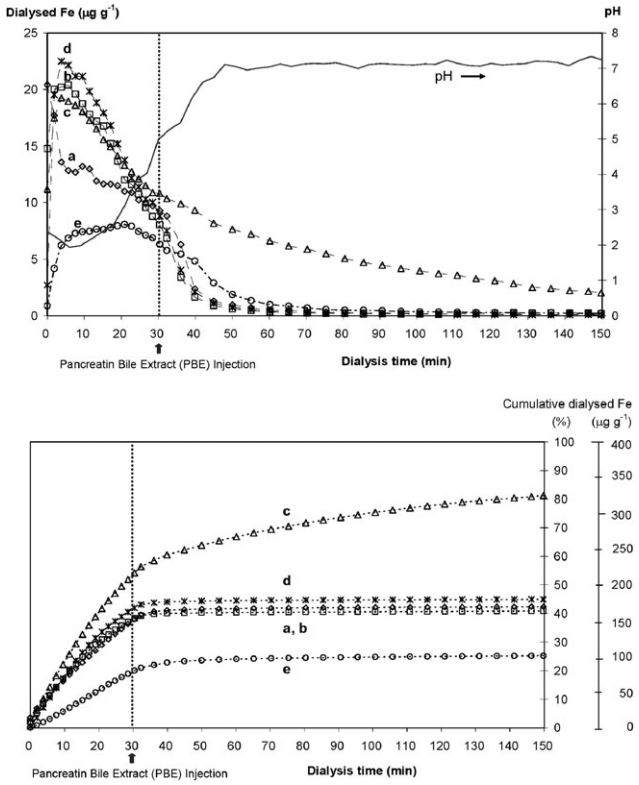

Fig. 1 Dialysis profiles of iron with pH change (upper frame) and corresponding cumulative plots (lower frame) for different chemical forms of iron fortificants: (a) iron(II) sulfate, (b) iron(II) fumarate, (c) NaFe(III)EDTA, (d) iron(II) lactate and (e) iron(III) ammonium citrate.

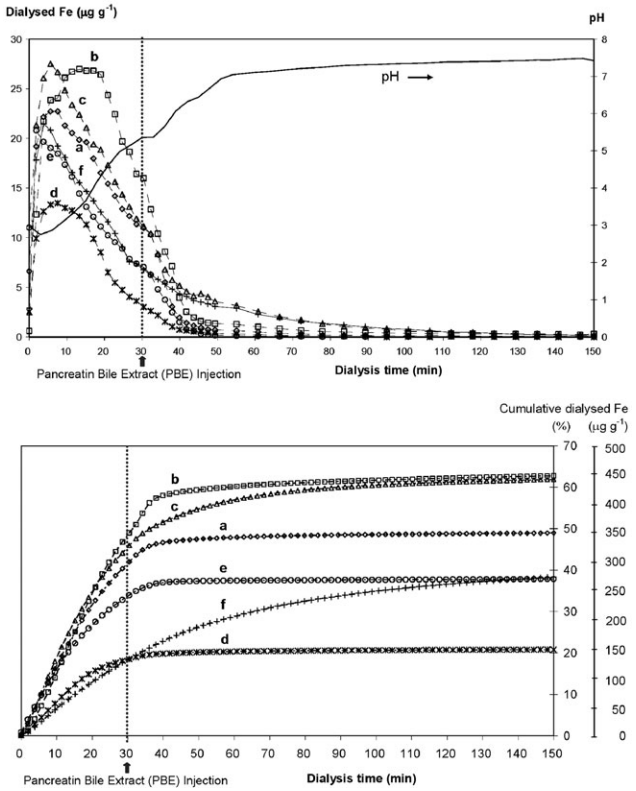

Fig. 2 Dialysis profiles of iron(II) sulfate with enhancers and inhibitors (upper frame) and their cumulative plots and percentage dialysis (lower frame): (a) $FeSO_4$ only; (b), (c), (d), (e), (f) for $FeSO_4$ with ascorbic, citric, phytic, tannic and oxalic acids, respectively.

graphical plot of dialysed iron concentration with respect to the dialysis time offers kinetic information of dialysis. The cumulative dialysed iron (Fig. 1 and 2, lower frame) increased before PBE injection, gradually increased after PBE injection and finally became constant. The slope of this graphical plot could demonstrate the rate of dialysis process. From this plot (Fig. 1, lower frame), iron fortificants can be divided into three groups according to their dialysability (low at 25% for iron(III) ammonium citrate; medium at 41–45% for iron(II) sulfate, iron(II) fumarate, iron(II) lactate; and high at 81% for NaFe(III)EDTA). The slopes are distinguished in two parts, before and after PBE injection at 30 min (Fig. 1, lower frame). The low dialysability (trace (e)) resulted from small slope before 30 min and almost zero thereafter. The medium dialysability (traces (a), (b) and (d)) can be seen to originate from higher slope before 30 min and almost zero thereafter. The high dialysability (trace (c)) was obtained from high slope before 30 min and small slope thereafter. The conversion of Fe(II) to $Fe(OH)_3$ is preferred at pH above 4.[10] Therefore, the dialysability of all studied iron fortificants ceased after 30 min (pH $\sim$ 5) except that of the protected compound NaFe(III)EDTA.

Effect of enhancers and inhibitors on iron dialysability

Many organic acids have been reported to show enhancement (ascorbic,[11–15] citric acids[16,17]) and inhibition (phytic, tannic and oxalic acids) effects. These compounds were used for the study of effect of enhancer and inhibitor on iron dialysability.

Fig. 2 (upper frame) shows profiles of iron dialysability of iron(II) sulfate with some enhancers (ascorbic and citric acids) and inhibitors (phytic, tannic and oxalic acids) at molar ratio of enhancer/inhibitor and iron between 3 : 1 to 4 : 1 (as used by Lynch and Stoltzfus[18]). Dialysis profiles of iron(II) sulfate were obviously affected by the presence of additives. The dialysis profile of iron(II) sulfate with ascorbic acid added at molar ratio of ascorbic acid to iron of 3 : 1 remarkably shows higher degree of dialysis in the first 30 min of dialysis. This is probably because ascorbic acid can decrease the transformation rate of iron(II) to iron(III) when pH increases. Iron(III) can be reduced by ascorbic acid only when the pH is below a limit, somewhere between pH 6.0 and 6.8. Above that pH limit, ascorbic acid is no longer an effective reducing agent for Fe(III).[19] In addition, ascorbic acid can form soluble complexes with iron at low pH that makes it remain soluble and absorbable at a more alkaline duodenal pH. Higher pH favors the conversion of Fe(II) to $Fe(OH)_3$. The reduction rate of iron(III) by ascorbic acid decreases markedly as the pH increases. Dialysability of iron(II) sulfate with ascorbic acid ceased at pH >6 (Fig. 2, upper frame). The dialysis rates (at 0–40 min, pH <6) of iron(II) sulfate with ascorbic and citric acids added were higher than that of iron(II) sulfate alone (Fig. 2, lower frame). The cumulative plots of iron(II) sulfate with and without enhancers and inhibitors are clearly distinguished.

The dominant increasing effect was observed before PBE injection in the case of ascorbic acid while citric acid showed significant effect after PBE injection. This is due to the chelating property of citric acid that presumably occurs through its carboxylic and hydroxyl groups, preventing iron from formation of insoluble iron hydroxides.[10] The stability constant (log *K*) of citric acid with Fe(II) and Fe(III) are 3.2 and 11.8, respectively.[9] So, the dialysability of the citrate complex of Fe(III) at pH >5 gradually increased.

On the other hand, dialyses of iron(II) sulfate with phytic or tannic acids, well-known strong iron inhibitors, were dramatically lower than that of iron(II) sulfate, especially in the first 30 min of dialysis (Fig. 2(d) and (e)). Since phytate and tannate are negatively charged, they can react with positively charged Fe ions, leading to the inhibition effect. After PBE injection (pH >5), the dialysis profile of iron(II) sulfate with oxalic acid showed a gradual increase of dialysed iron (Fig. 2(f), lower frame). The stability constant (log *K*) of oxalate with Fe(III) is 9.4, with the effective stability constants at pH 5, 6 and 7 being 2.9, 4.7 and 6.1, respectively.[9] As a result, dialysis of the oxalate complex of Fe(III) continues even at pH >5. In conclusion, the descending order of the iron dialysability is $FeSO_4$ with ascorbic acid (63%) $\sim$ with citric acid (62%) $>$ $FeSO_4$ only (49%) $>$ with oxalic acid (41%) $>$ with tannic acid (38%) $>$ with phytic acid (21%).

Conclusions

The CFD-ICP-OES-pH system was used for monitoring time-dependent dialysed minerals concentration and pH during dialysis. The system was applied to study the dialysability and effect of food components for iron fortificants. The mechanisms of enhancement and inhibition were investigated for the first time by a dynamic dialysis system. Dialysis profiles and their cumulative plots showed the changes of dialysis in the simulated intestinal digestion as affected by other food components. Such study is not possible using a batch dialysis system. The proposed approach is anticipated to be a useful tool to evaluate bioavailability of food or even non-food components consumed by humans.

Acknowledgements

The authors are grateful for financial support from the Thailand Research Fund and Center for Innovation in Chemistry: Postgraduate Education and Research Program in Chemistry, Higher Education Development Project, Ministry of Education.

References

1 D. D. Miller, B. R. Schricker, B. S. Rasmussen and D. Van Campen, *Am. J. Clin. Nutr.*, 1981, **34**, 2248–2556.
2 M. G. E. Wolters, H. A. W. Schreuder, G. Van Den Heuvel, H. J. Van Lonkhuijsen, R. J. J. Hermus and A. G. J. Voragen, *Br. J. Nutr.*, 1993, **69**, 849–861.
3 L. H. Shen, J. Luten, H. Robberecht, J. Bindels and H. Deelstra, *Z Lebensm.-Unters. -Forsch.*, 1994, **199**, 442–445.
4 J. Shiowatana, W. Kitthikhun, U. Sottimai, J. Promchan and K. Kunajiraporn, *Talanta*, 2006, **68**, 549–557.
5 J. Promchan and J. Shiowatana, *Anal. Bioanal. Chem.*, 2005, **382**, 1360–1367.
6 M. J. Roig, A. Alegria, R. Barbera and M. J. Lagarda, *Food Chem.*, 1999, **65**, 353–357.
7 K. J. H. Wienk, J. J. M. Marx and A. C. Beynen, *Eur. J. Nutr.*, 1999, **38**, 51–75.
8 K. Judprasong, M. Ornthai, A. Siripinyanond and J. Shiowatana, *J. Anal. At. Spectrom.*, 2005, **20**, 1191–1196.
9 T. E. Furia, in *CRC Handbook of Food Additives*, CRC Press, Boca Raton, FL, USA, 2nd edn, 1980.
10 S. Salovaara, A.-S. Sandberg and T. Andlid, *J. Agric. Food Chem.*, 2003, **51**, 7820–7824.
11 L. Hallberg, M. Brune and L. Rossander, *Hum. Nutr. Appl. Nutr.*, 1986, **40**, 97–113.
12 B. Nayak and K. M. Nair, *Food Chem.*, 2003, **80**, 545–550.
13 S. Salovaara, A.-S. Sandberg and T. Andlid, *J. Agric. Food Chem.*, 2003, **51**, 7820–7824.
14 L. Davidsson, P. Galan, P. Kastenmayer, F. Cherouvrier, M. A. Juillerat, S. Hercberg and R. F. Hurrell, *Pediatr. Res.*, 1994, **36**, 816–822.
15 D. Siegenberg, R. D. Baynes, T. H. Bothwell, B. J. Macfarlane, R. D. Lamparelli, N. G. Car, P. Macphail, U. Schmidt, A. Tal and F. Mayet, *Am. J. Clin. Nutr.*, 1991, **53**, 537–541.
16 M. Gillooly, T. H. Bothwell, J. D. Torrance, A. P. MacPhail, D. P. Derman, W. R. Bezwoda, W. Mills, R. W. Charlton and F. Mayet F, *Br. J. Nutr.*, 1983, **49**, 331–342.
17 D. P. Derman, D. Ballot, T. H. Bothwell, B. J. MacFarlane, R. D. Baynes, A. P. MacPhail, M. Gillooly, J. E. Bothwell, W. R. Bezwoda and F. Mayet F, *Br. J. Nutr.*, 1987, **57**, 345–353.
18 S. R. Lynch and R. J. Stoltzfus, *J. Nutr.*, 2003, **133**, 2978S–2984S.
19 Y.-H. P. Hsieh and Y. P. Hsieh, *J. Agric. Food Chem.*, 1997, **45**, 1126–1129.

Available online at www.sciencedirect.com
SCIENCE DIRECT
Talanta 68 (2006) 549–557
Talanta
www.elsevier.com/locate/talanta

Dynamic continuous-flow dialysis method to simulate intestinal digestion for in vitro estimation of mineral bioavailability of food

Juwadee Shiowatana*, Wutthika Kitthikhun, Upsorn Sottimai, Jeerawan Promchan, Kanokwan Kunajiraporn

Department of Chemistry, Faculty of Science, Mahidol University, Rama VI Rd., Bangkok 10400, Thailand

Available online 13 June 2005

Abstract

A system for dynamic continuous-flow dialysis during intestinal digestion for an in vitro simulation of gastrointestinal digestion is presented as an alternative to human and animal in vivo methods for estimation of the bioavailability of minerals. The method is based on the in vitro batch dialysis method described by Miller, which was developed into a continuous-flow system of a simple design to perform dynamic dialysis in the intestinal digestion stage. A flow dialysis system has the advantages of simulation being close to in vivo physiological conditions because pH change during dialysis is gradual and dialyzed components are continuously removed. The proposed new design performed dialysis during a continuous flow of dialyzing solution ($NaHCO_3$) around a dialysis bag containing peptic digest, which is placed inside a glass dialysis chamber. Gradual change of dialysis pH, similar to that occurring in the gastrointestinal tract, was obtained by optimization of flow rate and concentration of $NaHCO_3$. The dialysate collected in fractions was analyzed to determine dialyzed minerals and pH change in the course of dialysis. The method was tested by determination of calcium bioavailability of powder milk and calcium carbonate tablets.

Keywords: In vitro method; Bioavailability; Continuous-flow

1. Introduction

The total concentration of a mineral micronutrient in food does not provide information about its bioavailability. Speciation of a micronutrient or the determination of its chemical forms in food and in the gastrointestinal tract is essential to the understanding and the prediction of its availability for absorption [1]. This is often difficult to perform. Nutrient bioavailability has usually been estimated by in vivo human study. In vivo experiments, however, are time consuming and very expensive and often give variable results caused by uncontrollable physiological factors. Laboratory in vivo experiments in animals are sometime used as a model for human. Experiments with animals are less expensive but are limited by uncertainties with regard to differences in metabolism between animals and human. As an alternative to in vivo human and animal studies, nutrient bioavailability has also been estimated through in vitro methods [2–9]. These methods have gained popularity because of their simplicity, precision, speed of analysis and relatively low cost.

Interest in development of in vitro methods for estimating bioavailability of essential mineral elements dates back to at least the early 1930s [2]. These methods provide insights on minerals and trace element nutrition that are not achievable by human or animal experiments. The earliest trial [2] assumed ionizable minerals as potentially available and determined ionizable iron in food by extracting with complexing agents such as α,α′-dipyridyl and bathophenanthroline. Another approach attempted to simulate gastrointestinal digestion conditions and determined soluble or dialyzable minerals [3–9]. Particularly, the in vitro method developed in 1981 by Miller et al. [5] has been reported to provide availability measurements that correlate well with in vivo studies for iron. This method has been the basis for several in vitro methods for estimation of the bioavailability of iron and other minerals such as calcium and zinc [10,11]. The in vitro method

* Corresponding author. Tel.: +66 2 201 5124; fax: +66 2 354 7151.
E-mail address: scysw@mahidol.ac.th (J. Shiowatana).

0039-9140/$ – see front matter © 2005 Elsevier B.V. All rights reserved.
doi:10.1016/j.talanta.2005.04.068

involves a simulated gastrointestinal digestion with pepsin at pH 2 for 2 h during the gastric stage and with a mixture of pancreatin and bile salts along with a gradual pH change from 2 to 7 during the intestinal stage. The proportion of the compounds diffusing across a semipermeable membrane during the intestinal stage is used as a prediction of the elemental bioavailability.

In Miller's method, equilibrium dialysis is performed to obtain dialyzable compounds during intestinal digestion. The drawback is that dialyzed components are not removed during dialysis, as occurred in the real situation of the digestive tract. This may cause lower dialyzability. Therefore, a modified continuous dialysis in vitro method was developed by Minihane et al. [12] in which dialyzed components were removed continuously. The model developed by Minihane et al. used an Amicon stirred cell for continuous dialysis. The pH was adjusted gradually over a 30 min period from 2.0 to 7.0 before dialysis was started. Minihane's method was further modified by Shen et al. [13] to obtain a gradual pH change during the dialysis instead of adjusting the pH before dialysis. Shen et al. performed continuous dialysis by introducing a gradual pH adjustment using a small dialysis bag filled with an amount of $NaHCO_3$ equivalent to the predetermined titratable acidity of the peptic digest. The dialysis was carried out in a vessel under a pressure of 50 psi.

Wolters et al. [9] developed an in vitro method for continuous dialysis of minerals and trace elements based on a hollow-fiber system. The hollow-fiber system for continuous dialysis consists of a reaction vessel placing in a water bath at 41 °C. The food suspension in this vessel is pumped via a peristaltic pump through a suction tube into the hollow-fiber membrane. A fine filter cloth stretched across the inlet of the hollow-fiber and a magnetic stirrer was used to prevent clogging of the hollow-fiber by large particles. Components in the suspension that could pass through the hollow-fiber membrane were dialyzed and collected in a plastic bottle for subsequent analysis. That part of the suspension that could not pass through the hollow-fiber membrane was pumped back into the reaction vessel where these components could be digested further and recirculated into the hollow-fiber for complete dialysis.

A multicompartmental computer controlled simulated gastrointestinal digestion system has been developed [14] and applied [15,16] for evaluation of bioavailability. The system consists of several successive compartments to simulate the digestion in the stomach, duodenum, jejunum and ileum. Compartments are connected by peristaltic valve pumps to regulate the transfer of digestive enzymes. The system was also equipped with rotary pumps, syringe pumps for water pressure and secretion controls. Because the model aimed to mimic the whole GI-tract from stomach to ileum, it was rather complicated and not easy to perform. A simple method to access maximum bioaccessibility based on flow injection leaching of food sample by artificial saliva, gastric juice and intestinal juice was recently developed [17]. The method has the advantages of rapidity and simplicity. However, because leaching was accomplished in only a few minutes, the food sample may only be partially digested and leached.

In the present study, a simple setup for continuous-flow dialysis to perform an in vitro simulated intestinal digestion was developed. Considering that mineral absorption takes place mainly at the intestinal digestion stage [5], this setup was designed for dialysis in the intestinal digestion stage to occur by a continuous flow of dialyzing solution (dilute $NaHCO_3$ solution) around the dialysis tubing containing the gastric digestate. The gastric digestion was performed in a batch manner to effect high sample throughput because a large number of samples could be digested at the same time. In the simulated intestinal digestion stage, gradual change of pH, similar to that occurring in the intestinal tract, was obtained by optimization of flow rate and concentration of $NaHCO_3$. The dialysate collected in fractions was analyzed to determine the amount of dialyzed minerals. The graphical plot of dialyzed minerals with time of dialysis provides kinetic information of the dialysis process. The feasibility of the developed system was tested by applying it to evaluate dialyzability of calcium in calcium carbonate tablets and powder milk.

2. Experimental

2.1. Design and setup of continuous-flow dialysis system

A continuous-flow dialysis system was designed to serve three objectives: a gradual pH change at the early stage of dialysis, a convenient means of addition of enzymes at will and continuous removal of dialyzable components during dialysis.

The proposed dialysis system is presented schematically in Fig. 1. A dialysis chamber was designed to allow containment of a dialysis tubing, around which dialyzing solution could flow during dialysis. The chamber (ca. 20 cm in length and 0.8 cm inner diameter) and its cover were constructed in-house from borosilicate glass. Dialysis tubing MMCO 12,000–14,000 Da (Spectra/Por, Thomas Scientific, USA) was used. To prepare the dialysis chamber, a dialysis tubing

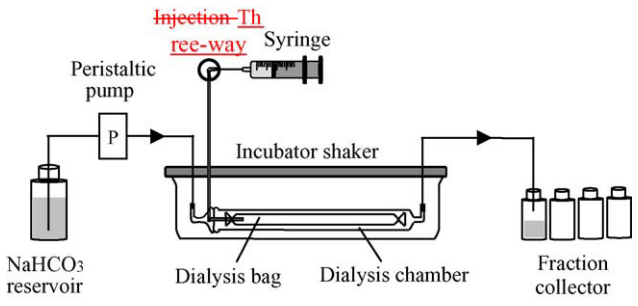

Fig. 1. Schematic diagram of the proposed continuous flow in vitro dialysis setup.

of 10 mm flat width and ca. 17.5 cm in length was tied at both ends, one end with a silicone tube (2 mm inner diameter and 5 cm long) inserted for the injection of a peptic digest sample and required enzymes. The other end of this silicone tube is pierced through an aperture in the chamber cover to allow convenient addition of a peptic digest aliquot and PBE mixture via a three-way valve by a 3 ml disposable syringe (both were purchased from a local medical equipment supplier). The cover was tightly sealed onto the chamber with a silicone gasket and a rubber band. The dialysis chamber was placed in a shaking water bath at $37 \pm 1\,^{\circ}C$. The dialyzing solution ($NaHCO_3$) from the reservoir was pumped through the chamber using a peristaltic pump (Eyela, Model MP-3N, Japan). The dialysis flow can be adjusted between 0.5 and 10 ml min^{-1} but 1.0 ml min^{-1} was found to be optimal. Dialyzable components in the peptic digest suspension could pass through the dialysis membrane and collected in plastic collectors.

To perform dialysis, the prewashed [18] dialysis tubing is prepared as above. Before adding the peptic digest, the dialysis tubing is flattened to remove any air bubbles or liquid inside using a syringe connecting to the silicone tube insert. Peptic digest aliquot of 2.5 ml is then injected through the same silicone tube. The dialyzing solution of optimum concentration is flowed through at 1.0 ml min^{-1} or at the required flow rate.

2.2. Instrument and equipment

Determination of calcium by flame atomic absorption spectrometer (FAAS) was performed using a Perkin-Elmer Model 3100 equipped with deuterium background correction (CT, USA), providing a background corrected signal. The operating parameters for measurement of calcium were 422.7, 0.7 nm band width and air–acetylene flame. The calcium contents of the dialysate and digested samples were determined using standard addition method.

A pH meter of Denver Instrument Model 215 (USA) with a glass combination electrode was used for all pH measurements. Commercial standard buffers (Damstadt, Germany) of pH 4.00 ± 0.01 and 7.00 ± 0.01 were employed for the pH meter calibration.

An incubator shaker from Grant Instrument, Model SS40-D2 (Cambridge, England), was used to shake and incubate samples at $37 \pm 1\,^{\circ}C$.

2.3. Chemicals and test materials

Enzymes pepsin (P-7000, from porcine stomach mucosa), pancreatin (P-1750, from porcine pancreas) and bile extract (B-6831, porcine) were from Sigma (St. Louis, MO, USA). Ca standard solution (1000 mg l^{-1}) was a certified NIST standard.

A pepsin solution was prepared by dissolving 0.16 g pepsin (P-7000, from porcine stomach mucosa) in 1 ml of 0.1 M of hydrochloric acid.

A pancreatin–bile extract (PBE) mixture was prepared by weighing 0.004 g pancreatin and 0.025 g bile extract into a beaker and dissolving in 5 ml of 0.001 M sodium bicarbonate. The concentration of sodium bicarbonate in PBE solution was prepared at 0.001 M so that addition of PBE (after 30 min of intestinal digestion) will not disturb the pH change already optimized.

Calcium carbonate tablets (dietary supplement) were from Vitamin World (New York, USA). Milk samples were obtained from a local supermarket.

2.4. Determination the total calcium content in test materials and in residues after dialysis

To determine the total calcium content of each calcium source, the sample (250 mg for tablet and 10.0 g for milk powder) was dissolved by wet digestion with nitric acid to clear solution and diluted to 100.0 ml with pure water. For residues after dialysis, the food suspension after dialysis was transferred from the dialysis tube into a beaker (100 ml) and rinsed with two aliquots (3 ml each) of 0.01 M EDTA washing and two aliquots (10 ml each) of 2% HNO_3 washing before subsequent digestion to clear solution. The calcium contents were determined by flame atomic absorption spectrometry using standard addition method.

2.5. Peptic digestion and determination of titratable acidity

Peptic digestion was performed according to the procedure of Miller [5]. For calcium carbonate tablet, 90 ml of pure water was added to one tablet (250 mg) and the pH was adjusted to 2.0 with diluted HCl. For milk samples, powder milk of 10.0 g and pure water were added into a 100 ml flask and the mixture was shaken to obtain a suspension of 90 ml. The pH was adjusted to 2.0 by addition of a dilute HCl solution. To each sample suspension, 1.5 ml of pepsin solution was added and pH was adjusted again to 2.00 before the total volume was adjusted to 100.0 ml with pure water and the sample was incubated in a shaking water bath at 37 °C for 2 h. The pH was adjusted to 2.00 every 30 min.

Titratable acidity of peptic digest was determined by titrating a 2.5 ml aliquot to which 625 μl of PBE mixture was added, using standard 0.01 M NaOH as a titrant to a pH of 7.5.

2.6. In vitro equilibrium dialysis method

A 2.5 ml portion of the peptic digest was added into the dialysis bag in the dialysis chamber. Then, 3.0 ml of dialyzing solution containing an amount of $NaHCO_3$ equivalent to the titratable acidity of the peptic digest was injected into the dialysis chamber to fill the space in the chamber outside of the dialysis bag. The sample was incubated in a shaking water bath at 37 °C for 30 min before 625 μl of PBE mixture was added and incubation continued for an additional 2 h.

The dialysate was collected for subsequent determination of calcium content.

2.7. Optimization of flow rate and concentration of sodium bicarbonate for continuous-flow dialysis

Firstly, standard calcium solution in 0.01 M HCl was subjected to continuous-flow dialysis with varying flow rate of sodium bicarbonate. The sample (2.5 ml) was introduced into the flattened dialysis tubing. The dialysis was performed using 0.001 M sodium bicarbonate and the dialysate fractions were collected continuously for calcium determination. The flow rate that gave a complete dialysis in a short time without too much dilution effect of dialysate was considered as optimal.

Then, the optimal sodium bicarbonate flow rate was used to study the effect of its concentration on pH change. Peptic digest samples of varying titratable acidities, including peptic digest containing 0.01 M HCl, peptic digest containing 0.01 M HCl with 0.04 M ascorbic acid, and peptic digest containing 0.01 M HCl with 0.09 M ascorbic acid, were used. These peptic digests had pH values and titratable acidities of 2.0, 0.01 M; 2.0, 0.05 M and 2.0, 0.10 M, respectively. Each sample (2.5 ml) was subjected to the simulated intestinal digestion.

2.8. In vitro dialysis method with continuous flow

To start the simulated pancreatic intestinal digestion, a segment of dialysis tubing was prepared and placed in the dialysis chamber as described earlier. A silicone gasket was placed on the outlet, and the chamber cover was securely clamped. The chamber was connected to the sodium bicarbonate reservoir and the collector containers using tygon tubings and placed in a water bath. A 2.5 ml pepsin digest sample was injected into the dialysis tubing via the silicone tube insert using a syringe. The bath temperature was maintained at $37 \pm 1\,^{\circ}C$. The peristaltic pump was switched on to start the dialysis. The dialysis flow rate was 1 ml min^{-1}. The dialysate was collected at 10 ml intervals in plastic containers for 30 min before a 625 μl freshly prepared PBE mixture was added and dialysis was continued for an additional 2 h. The dialysate fractions were subjected to FAAS measurement after all fractions were collected. Then, the dialyzed amount of an element was calculated by summation of the amounts in all dialysate fractions.

2.9. Calculation of dialyzability

The amount of dialyzed calcium is expressed as a percentage of the total amount present in the sample as follows:

$$\text{Dialyzability}\,(\%) = \frac{(D - B) \times 100}{W \times A}$$

where D and B are the total and blank amounts (μg), respectively, of mineral dialyzed, W the dry weight (g) of sample used for dialysis and A is the concentration of calcium in the dry sample (μg g^{-1}). For equilibrium dialysis, the dialyzed calcium is calculated as twice of the amount dialyzed when the volumes of the peptic digest and the dialyzing solution were equal because the dialyzed amount accounted for only one half of the dialyzable amount in equilibrium dialysis. When the volumes were not equal, correction was made accordingly.

3. Results and discussion

3.1. Design of continuous-flow system for in vitro determination of mineral bioavailability

As the absorption of minerals and trace elements is taking place in the earlier part of the small intestine, simulation of the conditions prevailing in the small intestine is the most critical step for in vitro methods aiming at prediction of the bioavailability of minerals and trace elements. Variation in the pH conditions in the course of intestinal digestion is a major cause of variability of results of dialyzability [13,19–21]. Therefore, this study has given particular attention to the process resulting in pH change and considered it important to provide a pH profile during dialysis corresponding to the dialysis profile. The dynamic in vitro methods developed by Miller [5], Minihane [12] and Shen et al. [13], Wolters et al. [9] and this study have slight differences in the pH change during dialysis and duration of dialysis as summarized in Table 1.

Optimization of the flow rate and concentration of dialyzing solution has been performed to achieve the following requirements for a close simulation of intestinal digestion in human:

1. Change of pH from 2.0 to about 5.0–6.0 in 30 min and to approximately 7.0–7.5 in 60 min and being constant thereafter.
2. Addition of digestive enzymes at required time via a three-way valve.
3. Continuous removal of dialyzed minerals from the dialysis system for determination.

Aiming at the above requirements, firstly a flow rate was selected. Then, the concentration of sodium bicarbonate was optimized.

Although the proposed dialysis system can be connected to the FAAS instrument for online detection, this study chose to collect the dialysate fractionwise (every 5 or 10 min) for subsequent calcium determination. By this way, dialysate samples are not totally consumed and can be kept for pH measurements and for repeated confirmation.

3.2. Selection of dialyzing solution flow rate

The peptic digestion was performed in pepsin solution at pH 2 in a batch system. For intestinal digestion, in contrast to

Table 1
A diagram comparing in vitro gastrointestinal digestion procedures

Item		Time (min) 0 30 60 90 120 150
1. pH adjustment and dialysis process		
(Miller) [5]	Place dialysis bag containing equivalent amount of $NaHCO_3$ in the digestion vessel; dialysis occurs through this dialysis bag	
(Minihane & Shen) [13]	Place a small dialysis bag containing equivalent amount of $NaHCO_3$ in an Amicon stirred cell; dialysis occurs through dialysis membrane at the bottom of the Amicon cell	
(This work)	Flow suitable concentration of $NaHCO_3$ to adjust pH and to continuously remove dialyzable minerals from peptic digest inside a dialysis tube	
2. Addition of PBE (same for all methods)		↓ PBE addition
3. pH change		
(Miller)		2.0 5.0 7.0
(Minihane & Shen)		2.0 7.0 7.0
(This work)		2.0 7.0 7.0
4. Dialysis process and duration of dialysis		
(Miller)	passive diffusion + equilibrium	
(Minihane)	diffusion under pressure of 50 psi + continuous removal of dialyzed minerals	
(Shen)	diffusion under pressure of 50 psi + continuous removal of dialyzed minerals	
(This work)	dialyzing solution flow accelerated diffusion + continuous removal of dialyzed minerals	
5. Dialysis membrane		
(Miller)	MMCO 6,000-8,000 Da	
(Minihane)	MMCO 1,000 Da	
(Shen)	MMCO 1,000 Da	
(This work)	MMCO 12,000-14,000 Da	

the equilibrium dialysis method where samples are incubated in sodium bicarbonate solution of sufficient concentration, optimal concentration of sodium carbonate solution was continuously flowed around the dialysis tubing containing peptic digest and the dialysate was collected fractionwise. Thus, the optimal flow rate was selected and the effect of concentration of sodium bicarbonate on pH change during the course of dialysis was studied. In theory, a faster flow rate can facilitate removal of the dialyzed minerals from the system and can speed up the dialysis. However, a fast flow can result in dilution of the dialyzed minerals in the dialyzing solution. The optimal flow rate should assist fast transfer of dialyzable mineral through the membrane and should not cause too much dilution of the dialyzed minerals. The dialysis profiles were obtained at different flow rates as shown in Fig. 2. Dialysis profiles show the kinetics of dialyzable calcium penetrating through the semipermeable membrane for 0.5, 1.0 and 2.5 ml min^{-1} flow rates.

It can be seen that faster flow rate at 2.5 ml min^{-1} could remove dialyzable calcium faster and quantitative dialysis was obtained in about 50 min while slow flow rate at 0.5 ml min^{-1} took a longer time (ca. 100 min) to complete the removal. However, the concentration of calcium in dialysate was lower for the faster flow as a result of dilution effect. Therefore, 1.0 ml min^{-1} flow rate was considered as a compromised flow rate for this application because the dialysis could be completed within 1 h and the dilution effect was acceptable.

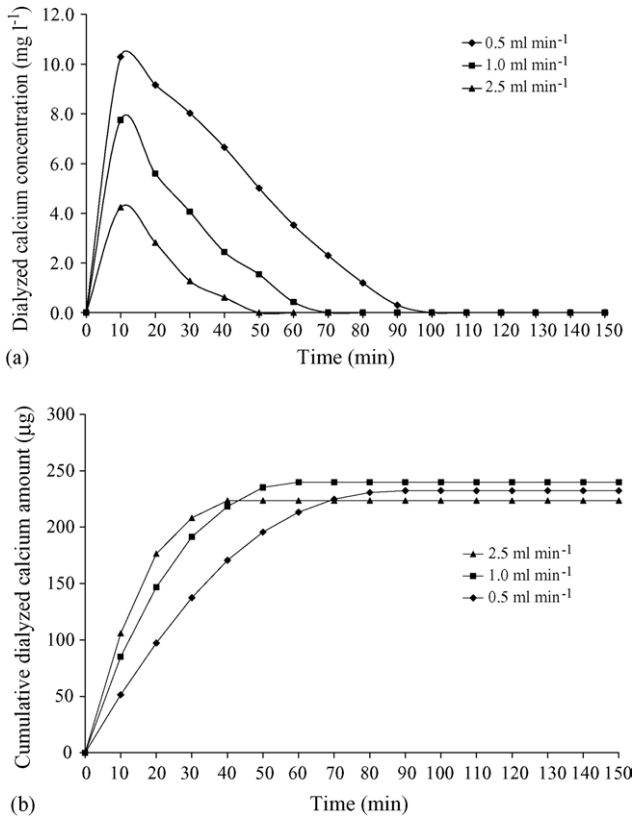

Fig. 2. Profiles of dialyzed amount (a) and cumulative dialyzed amount (b) of calcium at varying flow rate of dialyzing solution. Standard calcium (100 mg l^{-1}) 2.5 ml was used.

3.3. Optimization of concentration of sodium bicarbonate dialyzing solution

The concentration of dialyzing solution has to be optimized to obtain the required pH increase during the course of dialysis. It was found that $NaHCO_3$ concentration of 0.002 M was optimal for peptic digest of calcium carbonate tablets having titratable acidity of 0.05 M (Fig. 3b). The dialysis pH profiles for peptic digest of 0.01 and 0.1 M titratable acidities at various concentrations of dialyzing solution are also

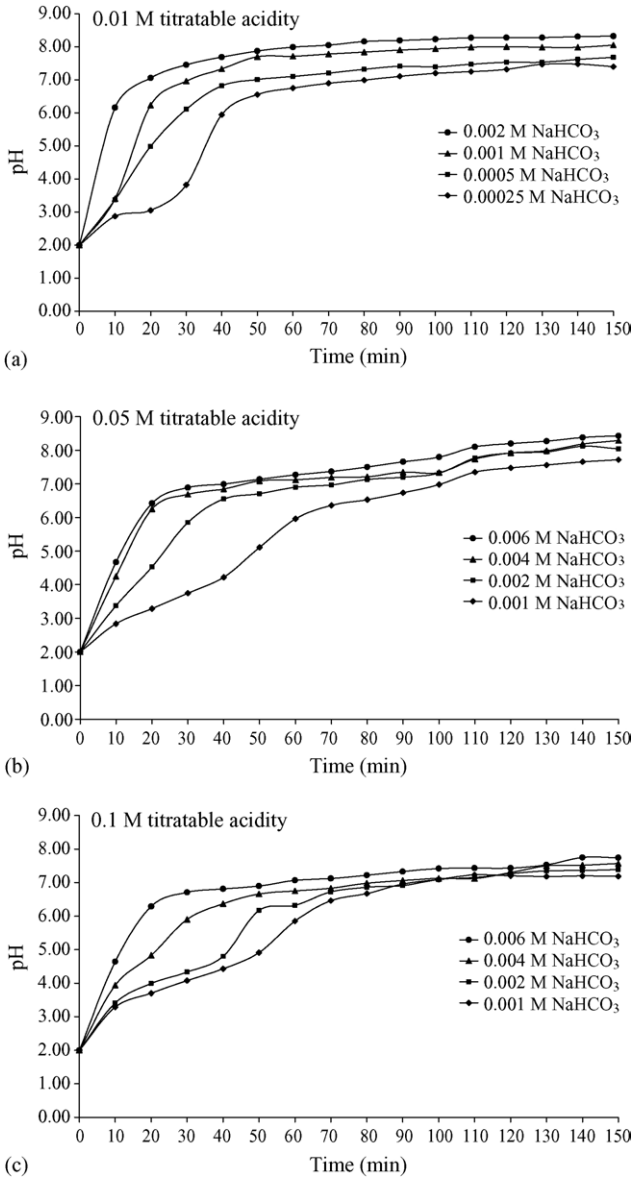

Fig. 3. Effect of concentration of dialyzing solution ($NaHCO_3$) on pH change during dialysis for peptic digests of different titratable acidities. Flow rate 1.0 ml min^{-1}.

Table 2
Analytical recovery of calcium for powder milk sample (three individual replicates are shown)

Sample	Dialyzed		Non-dialyzed		%Recovery
	Amount (mg kg^{-1})	%Dialyzability	Amount (mg kg^{-1})	%Remaining	
Powder milk-based formula	4680	68.1	1800	26.2	94.3
	4500	65.4	2270	33.1	98.4
	4780	69.5	2080	30.3	99.8
Average	4650 ± 140	67.6 ± 2.1	2060 ± 240	29.9 ± 3.4	97.5 ± 2.9

Total calcium 6890 ± 120 mg kg^{-1}.

shown in Fig. 3a and c. From the results of Fig. 3, optimum concentration of dialyzing solution was found to show an approximate linear relationship with the titratable acidity and the following equation can be drawn:

$$\text{Optimum } NaHCO_3 \text{ concentration} = \frac{\text{titratable acidity in M}}{25}$$

The optimal $NaHCO_3$ concentration for more than 10 peptic digests of calcium carbonate tablet samples with different titratable acidities were calculated using the above equation and the pH profiles were found to demonstrate satisfactory pH change during dialysis. So this equation will be used to obtain appropriate concentration of dialyzing solution for calcium carbonate peptic digests. It should be noted that the above equation can be applied for calcium carbonate and other tablets, and may not be applied to other types of food digest. For peptic digests of powder cow milk, the optimum dialyzing solution was found to be one fiftieth of the titratable acidity in M. This difference is probably due to the higher concentration of suspended matter in peptic digest of powder cow milk which resulted in slow rate of mass transfer in the dialysis tube and across the dialysis membrane. Therefore, this should be determined when different new types of sample are to be studied.

3.4. Method validation by analytical recovery study

Since there is no reference materials providing bioavailability data available, validation of the proposed method can only be done by studying of analytical recoveries of the mineral of interest. A milk sample was subjected to the proposed analytical procedure to determine the dialyzable calcium in the dialysate and the non-dialyzable calcium in the retentate. The results are given in Table 2. It can be seen that percent dialyzability of calcium is reproducible and the percent recoveries are acceptable.

3.5. Application of the proposed method to estimate calcium dialyzability of calcium carbonate tablets and milk samples

As examples to show the applicability of the dialysis system developed, calcium dialyzability for calcium carbonate tablets and milk samples was studied. Table 3 shows the results of dialyzable calcium determined by the developed continuous-flow method and the equilibrium method together with some previously reported values.

Since there has not been an accepted standard procedure for in vitro method for estimation of bioavailability, different authors used different procedures or conditions in their work. Furthermore, components in the samples (especially for formulated milk, which may contain different additives)

Table 3
Comparison of percent bioavailability (or dialyzability) of calcium for milk samples and calcium carbonate by different authors and procedures

Sample	In vitro		In vivo	Ref.
	Continuous flow	Equilibrium		
Powder cow milk	42.7 ± 2.5[a]	16.3 ± 1.1[a] (32.6 ± 2.2)	–	This work
Powder milk-based formula	67.7 ± 2.1	–	–	This work
Cow milk	–	20.2 ± 1.4	–	[22]
Cow milk	–	17.0 ± 0.8	–	[18]
Milk-based formula	13.9 ± 2.6[b]	10.2 ± 0.7	–	[13]
Milk-based formula	4.3 ± 0.6[c]	–	–	[13]
Cow milk	–	–	46.3 ± 9.5	[23]
Whole milk	–	–	31 ± 3	[24]
Powder cow milk	–	–	37.4 ± 8.7	[25]
Calcium carbonate	72.8 ± 2.2[a]	32.4 ± 1.5[a] (64.8 ± 3.0)	–	This work
Calcium carbonate	–	–	43.0 ± 5.9	[25]
Calcium carbonate	–	–	39 ± 3	[24]

[a] $n = 3$, in brackets are corrected values as indicated in Section 2.9.
[b] By Shen's method.
[c] By Minihane's method.

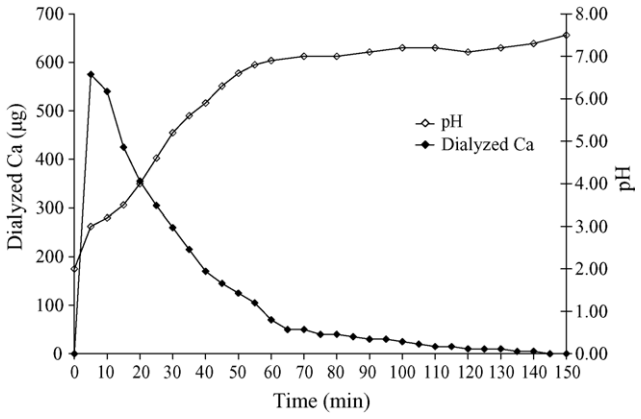

Fig. 4. Profile of dialyzed calcium and the pH change for peptic digest of calcium carbonate tablet by a continuous flow in vitro method.

may inhibit or promote dialyzability. This makes it rather impossible to compare results of different authors.

For milk samples, it was found in this work that dialyzability of calcium in powder cow milk was 32.6 and 42.7% for equilibrium and continuous-flow methods, respectively. The powder milk-based formula has a high dialyzability at 67.7%. Many authors have reported different values of bioavailability of calcium in milk ranging from 4.3 [13] to 46.3% [23]. This probably was attributed to the different sample compositions, procedures and conditions being used. For calcium carbonate tablet, our results of %dialyzability were very high at 64.8 and 72.8 for equilibrium and continuous-flow methods, respectively. Some authors indicated that incomplete disintegration and/or dissolution of the tablet could limit the degree of dialysis [26]. In this study, the peptic digest was seen to be clear after 2 h of peptic digestion at pH 2.0 indicating of solubilization very close to completion. This could possibly be the reason for high dialyzability. The dialyzability for equilibrium method gave slightly lower value probably due to loss during transfer of the dialysate from the dialysis chamber for AAS measurement, the step not required in the continuous-flow method. The in vivo result from a balance study [24,25] reported lower bioavailability values (43.0 and 39%).

Because in vitro dialysis method is a relative rather than an absolute estimation, the use of this method to estimate bioavailability has to be done with careful consideration of dialysis conditions [20,21] and report should serve as a relative evaluation under the same dialysis procedure and conditions. To confirm the similar conditions of dialysis being performed, this work considers monitoring of pH during dialysis a crucial necessity. Fig. 4 shows the dialysis profiles and the pH change during dialysis for calcium carbonate after peptic digestion. The pH profiles demonstrate pH change following the physiological conditions. The dialyzed calcium profiles show maximum value at the first dialysate fraction and gradually lower values similar to the profile of Fig. 2. The dialysis took about 60 min to complete. Similar observation was also evident for milk samples (not shown).

The continuous-flow dialysis profile and pH change are expected to be useful for comparative study of dialyzability of different foods and the study of the effects of food components on dialyzability. Such detailed investigation is not possible using the equilibrium dialysis system.

4. Conclusions

Simulated intestinal digestion has been developed for estimation of nutrient bioavailability. The continuous flow in vitro method is believed to be more representative of in vivo physiological conditions than that based on equilibrium dialysis because dialyzable components are continuously removed from the simulated intestinal digestion system during dialysis. In this study, a simple in vitro continuous-flow dialysis method was developed and used for estimation of calcium availability in comparison with the conventional in vitro equilibrium dialysis method. The most important part for successful simulation of the intestinal absorption was the pH adjustment during intestinal digestion. This was obtained by flowing dialyzing solution of appropriate concentration through a glass dialysis chamber containing the dialysis tubing with peptic digest inside. The optimum conditions for continuous flow in vitro method were a flow rate of 1.0 ml min^{-1} and varying concentration of dialyzing solution ($NaHCO_3$) depending on titratable acidity of the sample. In order that the PBE mixture would not drastically affect the pH change on its addition, PBE was prepared in 0.001 M sodium bicarbonate instead of 0.1 M as in the equilibrium dialysis. As a result, this proposed method achieved a gradual change of pH. The results from continuous-flow dialysis system not only can be used for estimating dialyzability of minerals but also provide dialysis profiles for detailed investigation. Since pH change during dialysis can greatly affect dialyzability due to precipitation for some elements, simultaneous monitoring of the pH change was also performed. The dialysis profiles of dialyzed mineral together with corresponding pH change can help understand the dialysis changes with time and the effect of food components on mineral dialyzability.

Although other elements, elemental detection systems and online measurement can be performed to demonstrate additional advantages of this proposed system, only calcium with a FAAS and off-line detection was attempted to prove the feasibility of the concept in this report. Future studies with online and other elemental detection systems such as inductively-coupled plasma spectrometry will be performed to cover more elements and to show the usefulness of the dialysis profiles obtained.

Acknowledgements

The authors are grateful for the financial support from the Thailand Research Fund and the Postgraduate Education and Research Program in Chemistry, Higher Education Development Project, Ministry of Education.

References

[1] L.H. Allen, Am. J. Clin. Nutr. 35 (1982) 783.
[2] L. Shackleton, R.A. McCance, Biochem. J. 30 (1936) 583.
[3] B.S. Narasinga Rao, T. Prabhavathi, Am. J. Clin. Nutr. 31 (1978) 169.
[4] S. Lock, A.E. Bender, Br. J. Nutr. 43 (1980) 413.
[5] D.D. Miller, B.R. Schricker, R.R. Rasmussen, D. Van Campen, Am. J. Clin. Nutr. 34 (1981) 2248.
[6] B.R. Schricker, D.D. Miller, R.R. Rasmussen, D. Van Campen, Am. J. Clin. Nutr. 34 (1981) 2257.
[7] T. Hazell, I.T. Johnson, Br. J. Nutr. 57 (1987) 223.
[8] R.F. Hurrell, S.R. Lynch, T.P. Trinidad, S.A. Dassenko, J.D. Cook, Am. J. Clin. Nutr. 47 (1988) 102.
[9] M.G.E. Wolters, H.A.W. Schreuder, G. Van Den Heuvel, H.J. Van Lonkhuijsen, R.J.J. Hermus, A.G.J. Voragen, Br. J. Nutr. 69 (1993) 849.
[10] P. Hocquellet, M.D. L'Hotellier, J. AOAC Int. 80 (1997) 920.
[11] J. Veenstra, M. Minekus, P. Marteau, R. Havenaar, Int. Food Ingredients 3 (1993) 1.
[12] A.M. Minihane, T.E. Fox, S.J. Fairweather-Tait, Proceedings of Bioavailability'93 Nutritional, Chemical and Food Processing Implications of Nutrient Availability, Part II, FRG, 1993, p. 175.
[13] L.H. Shen, I. Luten, H. Robberecht, J. Bindels, H. Deelstra, Lebensm Unters Forsch 199 (1994) 442.
[14] M. Minekus, P. Marteau, R. Havenaar, J.H.J. Huis in't Veld, Altern. Lab. Anim. (ATLA) 23 (1995) 197.
[15] M. Larsson, M. Minekus, R. Havenaar, J. Sci. Food Agric. 74 (1997) 99.
[16] C. Krul, A. Luiten-Schuite, R. Baan, H. Verhagan, G. Hohn, V. Feron, R. Havenaar, Food Chem. Toxicol. 38 (2000) 783.
[17] M. Chu, D. Beauchemin, J. Anal. At. Spectrom. 19 (2004) 1213.
[18] P. Chaiwanon, P. Puwastien, A. Nitithamyong, P.P. Sirichakwal, J. Food Comp. Anal. 13 (2000) 319–327.
[19] D.R. Van Campen, R.P. Glahn, Field Crop. Res. 60 (1999) 93.
[20] C. Ekmekcioglu, Food Chem. 76 (2002) 225.
[21] D. Bosscher, Z.L. Lu, R. Van Cauwenbergh, M. Van Callie-Bertrand, H. Robberecht, H. Deelstra, Int. J. Food Sci. Nutr. 52 (2001) 173.
[22] M.J. Roig, A. Alegria, R. Barbera, R. Farre, M.J. Lagarda, Food Chem. 65 (1999) 353.
[23] R.P. Heaney, C.M. Weaver, S.M. Hinders, B. Martin, P.T. Packard, J. Food Sci. 58 (1993) 1378.
[24] M.S. Sheikh, C.A. Santa Ana, M.J. Niocar, L.R. Schiller, J.S. Fordtran, N. Engl. J. Med. 317 (1987) 532.
[25] M.C. Kruger, B.W. Gallaher, L.M. Schollum, Nutr. Res. 23 (2003) 1229.
[26] M.J. Brennan, W.E. Duncan, L. Wartofsky, V.M. Butler, H.L. Wray, Calcif. Tissue Int. 49 (1991) 308.

JOURNAL OF AGRICULTURAL AND FOOD CHEMISTRY

Enhancement Effect Study of Some Organic Acids on the Calcium Availability of Vegetables: Application of the Dynamic in Vitro Simulated Gastrointestinal Digestion Method with Continuous-Flow Dialysis

JUWADEE SHIOWATANA,* SOPON PURAWATT, UPSORN SOTTIMAI, SUTTHINUN TAEBUNPAKUL, AND ATITAYA SIRIPINYANOND

Department of Chemistry, Faculty of Science, Mahidol University, Rama VI Road, Bangkok 10400, Thailand

The effect of added organic acids on the calcium availability of vegetables was investigated using the dialysis profiles obtained from an in vitro simulated gastrointestinal digestion with continuous-flow dialysis method. Citric acid was the most effective enhancer followed by tartaric, malic, and ascorbic acids. For amaranth, which has a low calcium availability (5.4%), a significant increase of availability was observed with increasing concentrations of all acids studied. With the continuous-flow dialysis approach, organic acids could be observed to promote the dialyzability even at an elevated intestinal pH. An enhancement effect from added organic acids was not clearly observed for Chinese kale, which itself contains a high amount of available calcium (52.9%).

KEYWORDS: Calcium availability; vegetables; organic acid; in vitro method; continuous flow

INTRODUCTION

Vegetables, especially green leafy vegetables, are known as a rich source of dietary calcium. Unfortunately, some vegetables with high contents of calcium show very low availability. The low calcium availability in vegetables was derived from the presence of some substances (phytate, oxalate, and dietary fiber components) which bind calcium to form unabsorbable compounds (*1*, *2*).

The effect of some organic acids on calcium availability has been documented. An enhancement effect by ascorbic acid (*3*) and citric acid (*4*, *5*) was reported. Many literature data on the effect of an enhancer or an inhibitor on the mineral availability are available. These studies were often carried out by adding the enhancer or inhibitor directly to foods followed by an in vitro or an in vivo availability evaluation. The in vitro method was widely performed by the method or modified methods of Miller (*6*) using a simulated gastrointestinal digestion with an equilibrium dialysis procedure. The methods involve enzymatic digestion with pepsin at pH 2 followed by digestion−dialysis in the presence of pancreatin−bile extract (PBE) at a gradual pH change from 2 to 7.5. The earlier conventional dialysis procedure provides a single value of the dialyzable amount of the element of interest at the equilibrium condition. It is simple and has been well accepted. However, in the equilibrium method, the dialyzed components are not continuously removed, as occurred in the intraluminal digestive tract, and therefore, this approach does not mimic the dynamic absorption process in the body and does not give information of time-dependent changes of dialysis during the course of gastrointestinal digestion.

Therefore, in vitro gastrointestinal digestion with continuous-flow dialysis procedures have been proposed as a closer simulation of the in vivo physiological conditions as opposed to that based on equilibrium dialysis, because dialyzable components are continuously removed from the digestion mixture during dialysis (*7*−*10*). The continuous-flow procedures also are readily adaptable to automatic computer control (*9*) and on-line detection (*11*, *12*). The computer-controlled in vitro dynamic system was applied for many case studies of the bioavailability of both minerals (*13*, *14*) and food mutagens (*15*).

Continuous monitoring of dialyzed minerals and pH change during dialysis provides profiles which are believed to be useful for the interpretation of enhancing or inhibiting effects. The aim of this work was to apply the dynamic in vitro simulated gastrointestinal digestion with continuous-flow dialysis method for the first time to demonstrate the use of dialysis profiles to investigate the effect of some organic acids on the calcium dialyzability of vegetables by looking into the time-dependent profiles obtained. Amaranth and Chinese kale were selected in this study to represent vegetables of low and high calcium availability, respectively (*16*). Four common organic acids, i.e., ascorbic, citric, tartaric, and malic acids, were studied.

EXPERIMENTAL DETAILS

Equipment and Materials. For measurement of calcium in dialysates, a Perkin-Elmer model 3100 flame atomic absorption/emission spectrometer (FAAS/FAES) was used. Calibration standards were

* To whom correspondence should be addressed. Phone: +66-2-201-5122. Fax: +66-2-354-7151. E-mail: scysw@mahidol.ac.th.

10.1021/jf062073t CCC: $33.50
Published on Web 11/08/2006

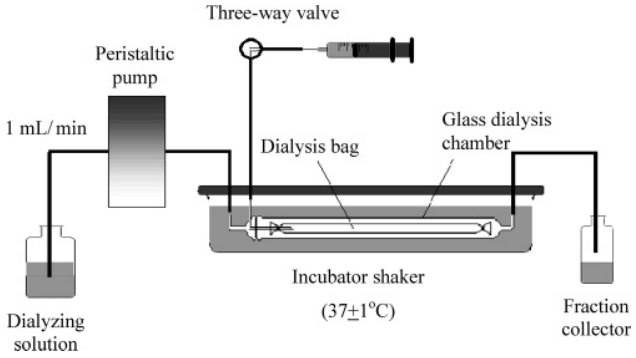

Figure 1. Diagram of the proposed continuous-flow in vitro dialysis system.

prepared in sodium bicarbonate of the same concentration as the dialyzing solution. The measurement was carried out with an air−acetylene flame. The calcium emission intensity was monitored at 422.7 nm with a 0.7 nm slit width.

A pH meter (Denver Instrument model 215, Colorado) with a glass combination electrode was used for all pH measurements. Commercial standard buffers (Merck, Darmstadt, Germany) of pH 4.00 ± 0.01 and 7.00 ± 0.01 were employed for the pH calibration. An incubator shaker from Grant Instrument, model SS40-D2 (Cambridge, England), was used to incubate the samples at 37 ± 1 °C.

Chemicals and Samples. The enzymes pepsin (P-7000, from porcine stomach mucosa), pancreatin (P-1750, from porcine pancreas), and bile extract (B-6831, porcine) were from Sigma (St. Louis, MO). A pepsin solution was prepared by dissolving 0.16 g of pepsin in 1 mL of 0.1 M hydrochloric acid and a PBE mixture by dissolving 0.004 g of pancreatin and 0.025 g of bile extract in 5 mL of 0.001 M sodium bicarbonate (*6*). Calcium standard solution (1000 mg/L) was prepared by dissolving an appropriate amount of calcium carbonate (Carlo Erba, Italy) in 1% (v/v) hydrochloric acid. The dialyzing solution was prepared by dissolving an appropriate amount of sodium bicarbonate in 1 L of purified water. The optimum concentration of sodium bicarbonate was determined from the titratable acidity, which was determined by titrating a 2.5 mL aliquot of peptic-digested sample to which 625 μL of PBE mixture was added, using standard 0.01 M NaOH as a titrant, to a pH of 7.5 (*10*). Ascorbic, malic, citric, and tartaric acids were obtained from Fluka Chemicals (Switzerland) and were confirmed to contain an undetectable amount of calcium at the concentrations being used.

Fresh amaranth, Chinese kale, and other vegetables were purchased from local markets and were cleaned and rinsed with purified water. Only the edible parts were then dried at 65 °C to constant mass and ground to store in a desiccator for use throughout the study to ascertain that similar vegetable lots were used.

Determination of the Total Calcium Content of Food Samples. A 0.5 g amount of sample was accurately weighed in a TFM vessel, and 10 mL of a HNO_3/H_2O_2 (3:2 v/v) mixture was added. Then acid dissolution was performed in a microwave digestion system (Milestone, model MLS-1200 Mega, Connecticut) according to the manufacturer's instructions. The clear solution was diluted with purified water to obtain a volume of 50.0 mL. The solution was then transferred to a polyethylene bottle. The calcium content was determined by flame atomic emission spectrometry using standard addition calibration.

Design and Setup of the Continuous-Flow Dialysis System (*10*). A continuous-flow dialysis (CFD) system was designed to serve three objectives as follows: to facilitate a gradual pH change at the early stage of dialysis (30 min), with the pH being maintained at 7.5 at the later stage (after 60 min), to provide a convenient means of addition of enzymes at the time and amount required, and to enable continuous removal of dialyzable components during dialysis.

The proposed dialysis system is presented schematically in **Figure 1**. A dialysis chamber was designed to allow containment of the dialysis tubing, around which the dialyzing solution could flow during dialysis. The chamber (ca. 20 cm in length and 0.8 cm inner diameter) and its covers were constructed in-house from borosilicate glass. Dialysis tubing of MWCO 12000−14000 (Spectro/Por, Thomas Scientific) was used. To prepare the dialysis chamber, dialysis tubing of 10 mm flat width and ca. 17.5 cm length was tied at both ends, one end with a silicone tube (2 mm inner diameter and 5 cm long) inserted for the injection of a peptic digest sample and required enzymes. The other end of this silicone tube was pierced through an aperture in the chamber cover to allow convenient addition of a peptic digest aliquot and PBE mixture via a three-way valve by a syringe. The cover was tightly sealed onto the chamber with a silicone gasket and a rubber band. The dialysis chamber was placed in a shaking water bath at 37 ± 1 °C. The dialyzing solution ($NaHCO_3$) from the reservoir was pumped through the chamber using a peristaltic pump (Eyela, model MP-3N, Japan) with a flow rate of 1.0 mL/min. Dialyzable components in the peptic digest suspension could pass through the dialysis membrane and be collected in plastic collectors.

Although the proposed dialysis system can be connected to the pH meter and elemental detection instrument for on-line detection, in this study we chose to collect the dialysate fractionwise for subsequent calcium determination. In this way, dialysate samples are not totally consumed and can be kept for further analyses or later confirmation.

Simulated Gastrointestinal Digestion Procedure with Continuous-Flow Dialysis. Simulated gastrointestinal digestion of food samples was carried out starting with peptic digestion with pepsin in a batch system, followed by pancreatic digestion with PBE in the CFD system (see the flow chart in **Figure 2**).

In the simulated peptic digestion step, a dried homogeneous vegetable sample (0.5 g) or cooked vegetable (equivalent to a 0.5 g dry mass) was suspended in 10 mL of purified water and adjusted to pH 2 with 6 M hydrochloric acid. The sample suspension volume was finally adjusted to 12.5 mL with purified water and spiked with 375 μL of pepsin solution. This digestion process was performed in an incubator shaker at 37 ± 1 °C for 2 h. The titratable acidity of the peptic digest was determined by titrating a 2.5 mL aliquot to which 625 μL of PBE mixture was added, using standard 0.01 M NaOH as a titrant, to a pH of 7.5. This titratable acidity was used for calculation of the optimal concentration of the dialyzing solution (*10*).

After the simulated peptic digestion, intestinal digestion with continuous-flow dialysis was carried out. The dialysis chamber was prepared as described earlier. Before use, the dialysis tubing was flattened to remove any air bubbles or liquid inside. Then, the 2.5 g peptic-digested sample was added via the three-way valve using a syringe connected to the silicone tube insert. The dialysis temperature was maintained at 37 ± 1 °C. The peristaltic pump was switched on to start the pancreatic digestion with a flow rate of 1 mL/min. The dialysate from the chamber was collected at 10 mL intervals in plastic vials for 60 min and then at 10 or 30 mL intervals for an additional 90 min. The freshly prepared PBE mixture (625 μL) was added into the dialysis bag by means of syringe injection via the three-way valve at 30 min. All dialysate fractions were subjected to pH measurement and calcium determination after completion of the pancreatic digestion.

Simulated Gastrointestinal Digestion Procedure with Equilibrium Dialysis. The peptic digestion was carried out similarly as mentioned above. Then a 2.5 mL portion of the peptic digest was added into the dialysis bag in the chamber of the dialysis system setup. However, instead of flowing the dialyzing solution, 3.0 mL of dialyzing solution containing an amount of $NaHCO_3$ equivalent to the titratable acidity of the peptic digest was injected into the dialysis chamber to fill the space in the chamber outside the dialysis bag. The sample was incubated in a shaking water bath at 37 ± 1 °C for 30 min before 625 μL of pancreatin−bile extract mixture was added and incubation continued for an additional 2 h. The dialysate was collected for subsequent determination of the calcium content.

Estimation of Calcium Availability. The amount of dialyzed calcium in a sample after the simulated gastrointestinal digestion was calculated from the summation of dialyzed calcium in all dialysate fractions and was expressed as a percentage of the total amount of calcium present in the sample:

$$\text{availability (\%)} = (D \times 100)/(WA)$$

where D = total amount of dialyzed calcium (μg), W = amount of sample used (g) as the dry mass of the original sample, and A = concentration of calcium in the original dry sample (μg/g).

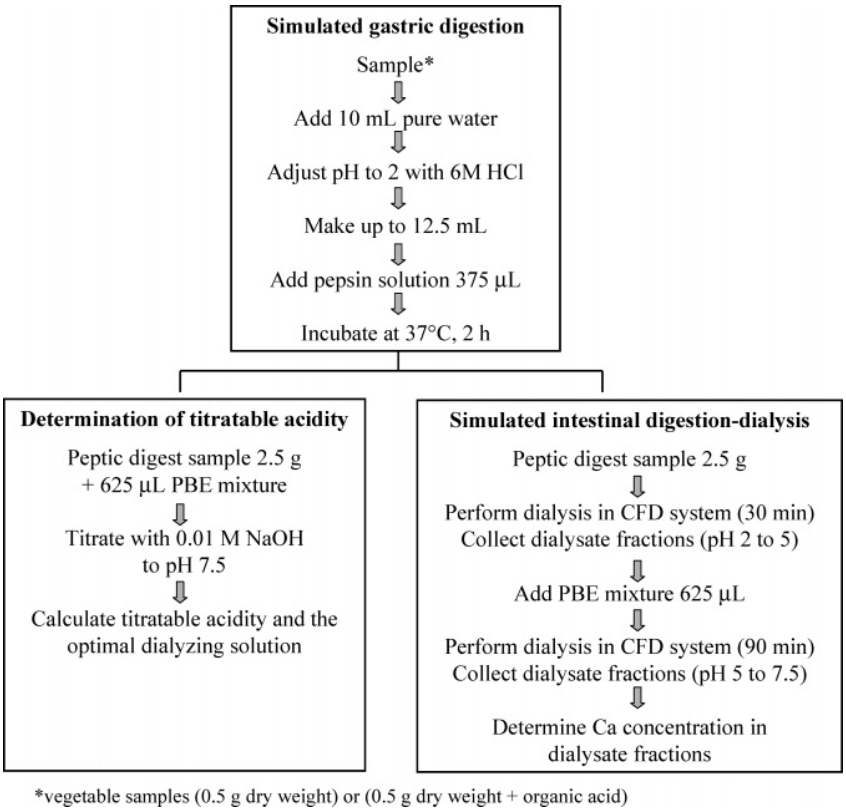

Figure 2. Flow chart of the simulated gastrointestinal digestion with continuous-flow intestinal digestion–dialysis.

RESULTS AND DISCUSSION

In Vitro Simulated Gastrointestinal Digestion: Equilibrium vs Dynamic Dialysis Approaches. The differences between the in vitro gastrointestinal dialysis with traditional equilibrium and the continuous-flow dialysis approaches are important to consider. Only a single value of the dialyzable amount of minerals at the equilibrium condition is obtained from the equilibrium dialysis procedure, whereas a time-dependent change of the dialyzed amount of mineral during the course of gastrointestinal digestion is obtained from the continuous-flow approach. A dynamic in vitro method with continuous removal of dialyzed components should be a better estimation of availability than the equilibrium in vitro method. Naturally, the results obtained from the two approaches are different, owing to the fact that the equilibrium method is based on the dialysis equilibrium of minerals between both sides of the dialysis membrane. Dialysis ceases when the concentrations of dialyzable components on both sides are equal. On the other hand, in the dynamic continuous-flow in vitro method, all the dialyzable components could possibly permeate through the membrane because fresh dialyzing solution was fed to the system continuously. To demonstrate this fact, standard 100 μg/mL calcium carbonate in 1% (v/v) HCl was subjected to the two dialysis procedures using the procedure described. The calcium availability as determined by the continuous-flow in vitro method was higher than that obtained from the equilibrium dialysis method (**Table 1**). The dialyzed amounts obtained from the equilibrium approach were found to be dependent on the volume ratio of the peptic digest and the dialyzing solution as summarized in **Table 1**. For a given case in which the volumes of the peptic digest and the dialyzing solution are equal (10 mL each), the dialyzed amount from the continuous-flow in vitro method was approximately 2 times that of the equilibrium in vitro method. In other words, the dialyzed amount accounted for only half of the dialyzable amount in the equilibrium dialysis. Since the continuous-flow approach provides the total dialyzable amount through continuous removal of dialyzable minerals, the results from the equilibrium dialysis should be corrected to match the value obtained from the continuous-flow dialysis procedure using the following equation:

$$D_{\text{corrected}} = D_{\text{uncorrected}}(V_s + V_d)/V_d$$

where $D_{\text{corrected}}$ (%) = the corrected D (%), $D_{\text{uncorrected}}$ (%) = the D (%) obtained from the amount dialyzed in the equilibrium dialysis, V_s = sample volume (mL), and V_d = dialyzing solution volume (mL).

This rationale was confirmed by examining the effects of the sample volume and dialyzing solution volume on the dialyz-

Table 1. Effect of the Sample Volume to Dialyzing Solution Volume Ratio (S:D) on Dialyzability in the Equilibrium Dialysis Method[a]

dialysis method	sample vol (mL)	dialyzing solution vol (mL)	S:D	D[b] (%) $D_{\text{uncorrected}}$ (%)	D[b] (%) $D_{\text{corrected}}$ (%)
equilibrium	10.0	20.0	0.5	28.1 ± 1.0	42.2 ± 1.5
	10.0	10.0	1.0	22.0 ± 1.1	44.0 ± 2.2
	10.0	5.0	2.0	12.6 ± 0.8	37.8 ± 2.4
continuous flow	2.5	flowing		41.2 ± 1.4	

[a] The sample was a 100 μg/mL (2.5 mL) standard calcium carbonate solution ($n = 3$). [b] D for the equilibrium method is provided as uncorrected values ($D_{\text{uncorrected}}$) and corrected values ($D_{\text{corrected}}$), while that of the continuous-flow method needs no correction. Each $D_{\text{corrected}}$ value shows no significant difference with the D obtained from the continuous-flow method as evaluated by the t test at $P = 0.05$.

Table 2. Total Calcium Content and Availability of Calcium from Various Vegetables As Determined by in Vitro Simulated Gastrointestinal Digestion with Continuous-Flow and Equilibrium Dialysis

		availability (%) ($n = 3$)			
			equilibrium in vitro method		
vegetable	total calcium concn (mg/g dried sample) ($n = 3$)	continuous-flow in vitro method[a]	uncorrected	corrected[b]	availability (%) (other researchers)
amaranth, leaves	26.7 ± 0.4	5.4 ± 0.4	3.0 ± 0.5	6.0 ± 1.0	4.1[c] (Kamchan et al. (*16*))
awltree, leaves	38.7 ± 0.6	10.1 ± 1.2	5.1 ± 1.0	10.2 ± 2.0	
cabbage, edible parts	4.5 ± 0.4	48.2 ± 1.3	21.6 ± 0.5	43.2 ± 1.0	64.9[d] (Weaver et al. (*20*))
Chinese kale, edible parts	16.1 ± 0.3	52.9 ± 1.1	22.2 ± 1.7	44.4 ± 3.4	58.8[d] (Weaver et al. (*20*))
cumin, leaves	23.6 ± 0.6	13.2 ± 0.6	5.5 ± 0.2	11.0 ± 0.4	
hairy basil, leaves	20.4 ± 0.5	31.2 ± 0.3	13.3 ± 0.9	26.6 ± 1.8	
Indian penny wort, leaves	15.3 ± 0.5	39.6 ± 0.7	17.1 ± 0.3	34.2 ± 0.6	
ivy gourd, leaves and tips	9.3 ± 0.6	38.4 ± 0.8	16.1 ± 0.6	32.2 ± 1.2	
kitchen mint, leaves	18.5 ± 0.4	33.9 ± 1.7	16.5 ± 1.6	33.0 ± 3.8	
betel, leaves	22.8 ± 0.5	2.25 ± 0.1	1.3 ± 0.2	2.6 ± 0.4	2.5[c] (Kamchan et al. (*16*))
sesbania, tender tips	10.1 ± 0.4	24.8 ± 0.2	10.1 ± 0.7	20.2 ± 1.4	
spinach, edible parts	10.3 ± 0.5	4.6 ± 0.5	1.9 ± 0.2	3.8 ± 0.4	4.6[d] (Peterson et al. (*19*))

[a,b] The correlation plot of data from the continuous-flow (*a*) and equilibrium (*b*) methods shows that $b = 0.853a + 0.638$, $r^2 = 0.991$. [c] Values from the in vitro method. [d] Values from the in vivo method.

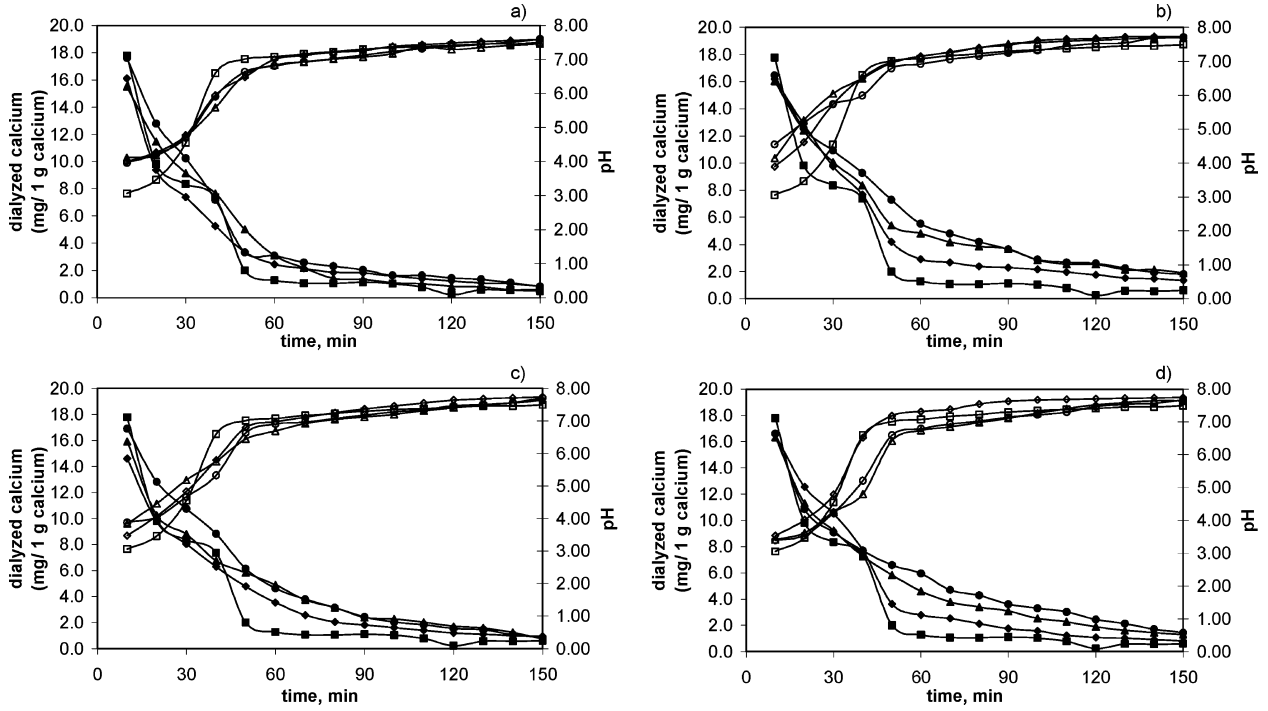

Figure 3. Dialyzed calcium and pH change during simulated intestinal digestion for amaranth with addition of varying concentrations of ascorbic acid (**a**), citric acid (**b**), malic acid (**c**), and tartaric acid (**d**), where ■, ◆, ▲, and ● represent amaranth with 0%, 1.0%, 2.5%, and 5% (w/w) acid, respectively. The corresponding pH profiles are presented with open symbols of the same type.

ability of a calcium standard as presented in **Table 1**, which shows a lower $D_{\text{uncorrected}}$ when the dialyzing solution volume is increased. $D_{\text{corrected}}$ gave results comparable with those of continuous-flow dialysis. This correction method should always be applied to get $D_{\text{corrected}}$, which is an accurate value expressing the dialyzable fraction for the equilibrium method.

In Vitro Availability of Calcium for Various Local Vegetables. The calcium availability of some vegetables as determined by the in vivo method has been reported (*16*−*20*). Total calcium and its availability of various local vegetables by an in vitro method based on continuous-flow dialysis and equilibrium approaches were determined, and the results are shown in **Table 2**. Some reported availability data are given in the last column for comparison. The results show that the corrected availability values of the equilibrium method were approximately 85% of the values obtained from the continuous-flow dialysis as calculated from the correlation plot ($b = 0.853a + 0.638$, $r^2 = 0.991$). The slightly lower availability values (%) from the equilibrium method could be due to systematic error from the correction factors obtained from the sample and dialyzing solution volumes used for correction. The accurate volumes were difficult to measure since the dialysis membrane may swell during use. This observation can also suggest that the results from the continuous-flow method should be more reliable than those obtained from the equilibrium method.

The in vitro availability of calcium for cabbage, Chinese kale, and spinach by the continuous-flow method was found to be 48.2%, 52.9%, and 4.6%, respectively. These results are close

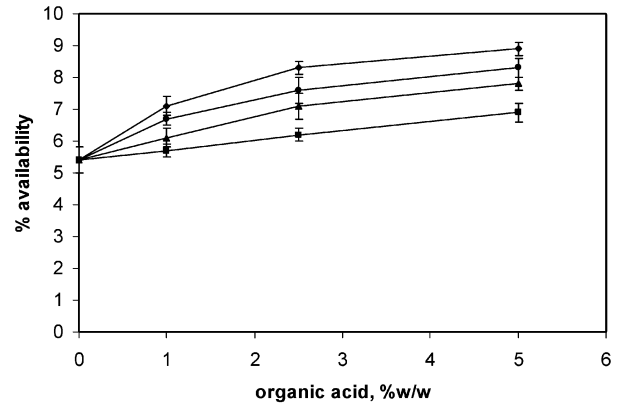

Figure 4. Relationship between the concentration (%) of organic acids added and the calcium availability (%) for amaranth: ascorbic acid (■), citric acid (◆), malic acid (▲), and tartaric acid (●).

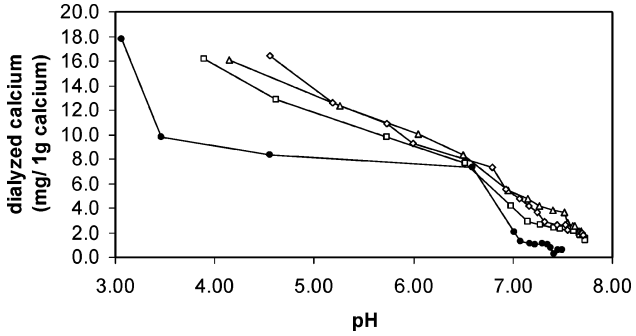

Figure 5. Dialysis profile as a graphical plot of dialyzed calcium against the pH value of the dialysate for amaranth with addition of varying concentrations of citric acid: 0% (●), 1% (□), 2.5% (△), and 5% (◇). Data were obtained from **Figure 3b**.

to the values of in vivo study reports of 64.9%, 58.8% (*20*), and 4.6% (*19*), respectively.

Some vegetables such as amaranth, awltree, cumin, betel leaves, and spinach were found to contain high amounts of calcium but a very low in vitro availability (%). The reasons for the low availability were reported to be related to the inhibitors (phytate, oxalate, and dietary fiber components) which bind calcium to form unabsorbable compounds (*1*, *2*).

Amaranth and Chinese kale were selected as representative vegetables for low and high calcium availability, respectively, for the study of the effect of organic acids on availability.

Effect of Organic Acids on the Calcium Availability of Amaranth. Chemical bindings of calcium with food components are major factors affecting availability. Some food components favorably promote mineral absorption. The influence of various organic acids on calcium availability has been investigated. Some authors reported an enhancing effect by organic acids (*4*, *5*). Therefore, the effect of organic acids, commonly found in foods, on the calcium availability of vegetables was systematically studied. Ascorbic, citric, tartaric, and malic acids were directly added into the chosen vegetables at concentrations of 1% (w/w), 2.5% (w/w), and 5% (w/w) of the vegetable (dry mass), and the calcium availability was determined in the same manner. The results are depicted in **Figure 3**.

The dialysis profiles obtained from the dynamic continuous-flow system, showing the effect of the concentration of added organic acids, are illustrated in **Figure 3**. The changes in the dialyzed amount could be observed from the dialysis profiles. The profiles show an enhancing effect on calcium dialyzability at increased concentrations of organic acids. For example, the dialysis profiles of amaranth without citric acid dropped to the baseline when the pH of dialysis approached 7. On the contrary, dialysis went on even at pH higher than 7 when 1−5% citric acid was added. Other organic acids gave similar results. From

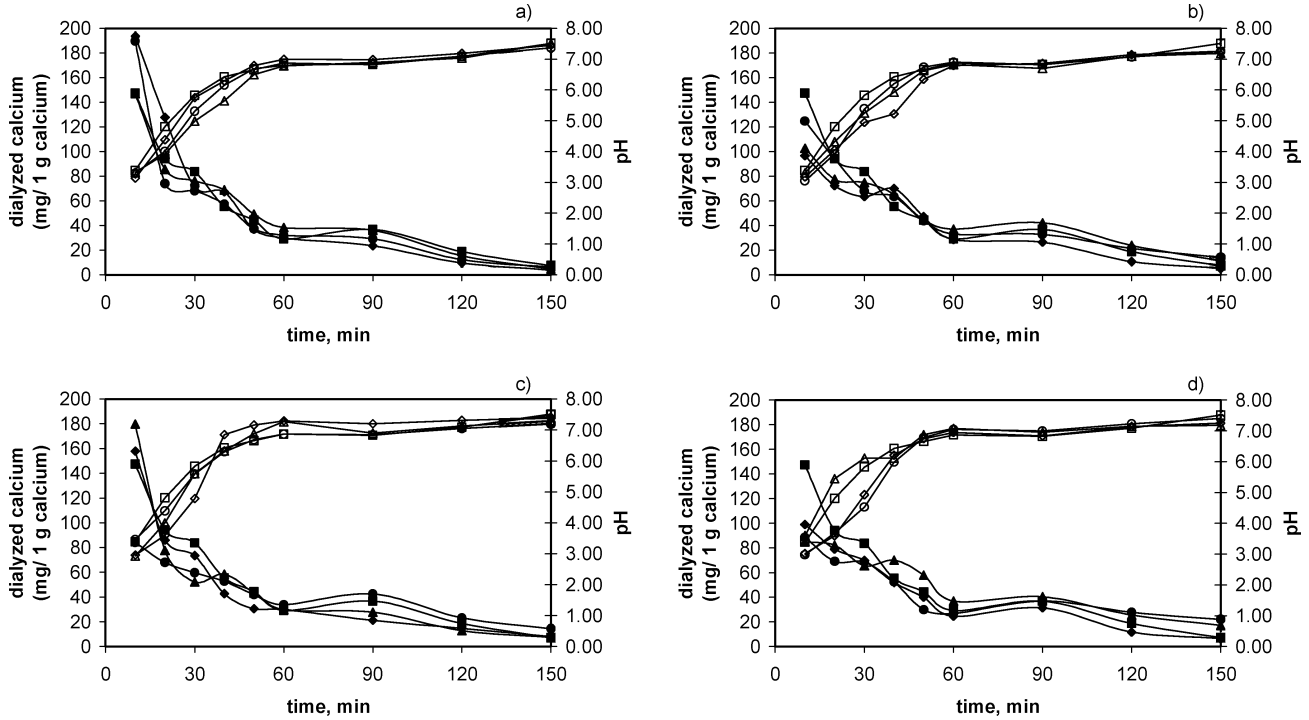

Figure 6. Dialyzed calcium and pH change during simulated intestinal digestion for Chinese kale at varying concentrations of ascorbic acid (**a**), citric acid (**b**), malic acid (**c**), and tartaric acid (**d**), where ■, ◆, ▲, and ● represent Chinese kale with 0%, 1.0%, 2.5%, and 5% (w/w) acid, respectively. The corresponding pH profiles are presented with open symbols of the same type.

the dialysis profiles (**Figure 3**), the enhancement effect was most pronounced when citric and tartaric acids of 5% were added.

Figure 4 illustrates the effect of the percentage of organic acid added on calcium availability, as calculated from the summation of dialyzed calcium in all dialysate fractions, for the amaranth sample. The effect on calcium dialyzability in a decreasing order is as follows: citric acid > tartaric acid > malic acid > ascorbic acid. This appears to be the same order as that of the first stability constants (log K_1) of calcium complexation with these organic ligands: citric acid (3.50), tartaric acid (1.80), malic acid (1.80), and ascorbic acid (0.19) (*21*).

From the observation of dialysis profiles, the following can be speculated. Most of the calcium in vegetables is bound with other dietary constituents. During the simulated gastrointestinal digestion, these constituents are broken down, and calcium is released as dialyzable forms. At low pH, the dialyzability is naturally higher than at high pH, owing to the favorable binding of anions with protons, leaving calcium as an ionic soluble form. When the pH increases, binding with various ligands occurs. Oxalate and phytate can bind with calcium to form precipitates which are not dialyzed. However, with the presence of organic acids, the organic acids favorably bind with calcium even at an elevated pH, resulting in the enhancement of calcium dialyzability. To demonstrate the dialysis of calcium at high pH in the presence of the organic acids studied, **Figure 3b** was replotted to obtain **Figure 5** showing the effect of citric acid on the dialyzed calcium at various pH values. This graph illustrates that the change in dialyzability was not solely contributed by the pH change, but also due to the organic acid added. This information cannot be obtained from the equilibrium dialysis approach.

Effect of Organic Acids on the Calcium In Vitro Availability of Chinese Kale. The dialysis profiles showing the effect of added organic acids in Chinese kale are presented in **Figure 6**. No enhancement of calcium dialyzability was observed when various organic acids were added at various concentrations. Because of the naturally existing promoters (citric and malic acids) in Chinese kale, most calcium was already present in readily dialyzable forms. The dialysis profiles (**Figure 6**) show continuing dialysis even after pH has reached 7.0. In relation to the high calcium availability of Chinese kale, some authors reported a low concentration of inhibitors (precipitators) such as phytate and oxalate in Chinese kale (*16*). Moreover, high concentrations of enhancers such as citric and malic acids were found as the major organic acids in Chinese kale at 22.13 and 1.51 mg/g, respectively (*22*). Lucarini et al. (*23*) presented *brassica* vegetables (e.g., broccoli, green cabbage, and kale) as a good source of dietary calcium and showed that dialyzable calcium in these vegetables was in both ionic and bound forms with a large fraction in the bound forms. Hence, the added organic acid did not show an observable effect on the calcium dialyzability in Chinese kale.

Conclusion. The calcium availability of various vegetables was determined by the in vitro simulated gastrointestinal digestion with continuous-flow dialysis method. The calcium in vitro availability in the vegetables studied was found to vary between 4.6% and 52.9%. The in vitro availability obtained as compared to the reported availability data from the in vivo measurement was very similar. This indicates the possibility of using the in vitro method as a rapid evaluation method for the availability study.

The study of the effect of organic acids on calcium dialysis showed a significant increase of availability at increasing concentrations of acid for amaranth. Citric acid was the most effective enhancer followed by tartaric, malic, and ascorbic acids as could be predicted from their stability constants of complexation with calcium. An enhancement effect was not clearly observed for Chinese kale, which was a representative vegetable of high calcium availability.

The dialysis profiles from continuous-flow dialysis, showing a time-dependent dialyzed amount and pH change, provide information which is not obtained from the equilibrium method. Thus, the enhancement effect of some organic acids on calcium availability was proved to be caused by calcium remaining dialyzable even at elevated pH conditions in the intestinal digestion stage. The dialysis profiles were proved to be useful for understanding the effect of food components on mineral dialyzability in the simulated gastrointestinal digestion model.

LITERATURE CITED

(1) Kennefick, S.; Cashman, K. D. Investigation of an *in vitro* model for predicting the effect of food components on calcium availability from meals. *Int. J. Food Sci. Nutr.* **2000**, *51*, 45−54.

(2) Aletor, V. A.; Adeogun, O. A. Nutrient and anti-nutrient components of some tropical leafy vegetables. *Food Chem.* **1995**, *53*, 375−379.

(3) Mehansho, H.; Kanerva, R. L.; Hudepohl, G. R.; Smith, K. T. Calcium bioavailability and iron-calcium interaction in orange juice. *J. Am. Coll. Nutr.* **1989**, *8*, 61−68.

(4) Wolters, M. G.; Diepenmaat, H. B.; Hermus, R. J. J.; Voragen, A. G. J. Relation between *in vitro* availability of minerals and food composition: a mathematical model. *J. Food Sci.* **1993**, *58*, 1349−1355.

(5) Pak, C. Y. C.; Harvey, J. A.; Hsu, M. C. Enhanced calcium bioavailability from a solubilized form of calcium citrate. *J. Clin. Endocr. Metab.* **1987**, *65*, 801−805.

(6) Miller, D. D.; Schricker, B. R.; Rasmussen, R. R.; Campen, D. V. An *in vitro* method for estimation of iron availability from meals. *Am. J. Clin. Nutr.* **1981**, *34*, 2248−2256

(7) Shen, L. H.; Luten, I.; Robberecht, H.; Daeel, P. V.; Deelstra, H. Modification of an in-vitro method for estimating the bioavailability of zinc and calcium from foods. *Lebensm. Unters. Forsch.* **1994**, *199*, 442−445.

(8) Wolters, M. G. E.; Schreuder, H. A. W.; Heuvel, G. V. D.; Lonkhuijsen, H. J. V.; Hermus, R. J. J.; Voragen, A. G. J. A continuous *in vitro* method for estimation of the bioavailability of minerals and trace elements in foods: Application to breads varying in phytic acid content. *Br. J. Nutr.* **1993**, *69*, 849−861.

(9) Larsson, M.; Minekus, M.; Havenaar, R. Estimation of the bioavailability of iron and phosphorus in cereals using a dynamic *in vitro* gastrointestinal model. *J. Sci. Food Agric.* **1997**, *74*, 99−106.

(10) Shiowatana, J.; Kitthikhun, W.; Sottimai, U.; Promchan, J.; Kunajiraporn, K. Dynamic continuous-flow dialysis method to simulate intestinal digestion for *in vitro* estimation of mineral bioavailability of food. *Talanta* **2006**, *68*, 549−557.

(11) Promchan, J.; Shiowatana, A dynamic continuous-flow dialysis system with on-line electrothermal atomic-absorption spectrometric and pH measurements for *in-vitro* determination of iron bioavailability by simulated gastrointestinal digestion. *Anal. Bioanal. Chem.* **2005**, *382*, 1360−1367.

(12) Judprasong, K.; Ornthai, M.; Siripinyanond, A.; Shiowatana, J. A continuous-flow dialysis system with inductively coupled plasma optical emission spectrometry for *in vitro* estimation of bioavailability. *J. Anal. At. Spectrom.* **2005**, *20*, 1191−1196.

(13) Larsson, M.; Minekus, M.; Havenaar, R. Estimation of the bioavailability of iron and phosphorus in cereals using a dynamic *in vitro gastrointestinal model. J. Sci. Food Agric.* **1997**, *74*, 99−106.

(14) Dominy, N. J.; Davoust, E.; Minekus, M. Adaptive function of soil consumption: an *in vitro* study modeling the human stomach and small intestine. *J. Exp. Biol.* **2004**, *207*, 319−324.
(15) Krul, C.; Luiten-Schuite, A.; Baan, R.; Verhagen, H.; Mohn, G.; Feron, V.; Havenaar, R. Application of a dynamic *in vitro* gastrointestinal tract model to study the availability of food mutagens, using heterocyclic aromatic amines as model compounds. *Food Chem. Toxicol.* **2000**, *38*, 783−792.
(16) Kamchan, A.; Puwastien, P.; Sirichakwal, P. P.; Kongkachauichai, R. *In vitro* calcium bioavailability of vegetables, legumes and seed. *J. Food Compos. Anal.* **2004**, *17*, 311−320.
(17) Toba, Y.; Takada, Y.; Tanaka, M.; Aoe, S. Comparison of the effects of milk components and calcium source on calcium bioavailability in growing male rats. *Nutr. Res.* **1999**, *19*, 449−459.
(18) Heaney, R. P.; Recker, R. R.; Weaver, C. M. Absorbability of calcium sources: the limited role of solubility. *Calcif. Tissue Int.* **1990**, *46*, 300−304.
(19) Peterson, C. A.; Eurell, J. A. C.; Erdman, J. W. Bone composition and histology of young growing rats fed diets of varied calcium bioavailability: spinach, nonfat dry milk, or calcium carbonate added to casein. *J. Nutr.* **1992,** *122*, 137−144.
(20) Weaver, C. M.; Plawecki, K. L. Dietary calcium: Adequacy of a vegetarian diet. *Am. J. Clin. Nutr.* **1994**, *59* (Suppl.), 1238s−1241s.
(21) Thomas, E. F. *CRC Handbook of Food Additives*; Taylor and Francis, CRC Press: Boca Raton, FL, 1972.
(22) Ayaz, F. A.; Glew, R. H.; Millson, M.; Huang, H. S.; Chuang, L. T.; Sanz, C.; Ayaz, S. H. Nutrient contents of kale (*Brassica oleraceae* L. *var. acephala* DC.). *Food Chem.* **2006**, *96*, 572−579.
(23) Lucarini, M.; Canali, R.; Cappelloni, M.; Di, Lullo, G.; Lombardi-Boccia, G. *In vitro* calcium availability from *brassica* vegetables (*Brassica oleracea* L.) and as consumed in composite dishes. *Food Chem.* **1999**, *64*, 519−523.

Received for review July 22, 2006. Revised manuscript received September 22, 2006. Accepted September 29, 2006. We are grateful for financial support from the Thailand Research Fund and the Postgraduate Education and Research Program in Chemistry, Higher Education Development Project, Ministry of Education.

JF062073T

ARTICLE

JAAS
www.rsc.org/jaas

A continuous-flow dialysis system with inductively coupled plasma optical emission spectrometry for *in vitro* estimation of bioavailability†

Kunchit Judprasong,[ab] Mathuros Ornthai,[a] Atitaya Siripinyanond[a] and Juwadee Shiowatana*[a]

[a] *Department of Chemistry, Faculty of Science, Mahidol University, Rama VI Rd., Bangkok 10400, Thailand. E-mail: scysw@mahidol.ac.th; Fax: 66 2 3547151; Tel: 66 2 2015122*

[b] *On study leave from Institute of Nutrition, Mahidol University, Salaya, Putthamonthon, Nakorn Pathom 73170 Thailand. E-mail: nukjp@mahidol.ac.th; Fax: 66 2 4419344; Tel: 66 2 8002380*

Received 17th June 2005, Accepted 8th September 2005
First published as an Advance Article on the web 22nd September 2005

A continuous-flow dialysis (CFD) method with on-line inductively coupled plasma optical emission spectrometric (ICP-OES) simultaneous multielement measurement for the study of *in vitro* mineral bioavailability was developed. The method was based on a simulated gastric digestion in a batch system followed by a continuous-flow intestinal digestion. The simulated intestinal digestion was performed in a dialysis bag placed inside a channel in a flowing stream of dialyzing solution ($NaHCO_3$). The mineral concentrations in the dialysate were determined by ICP-OES using Y and Sc as internal standards. The pH of the dialysate was also monitored on-line to ensure pH changes similar to the situation in the gastrointestinal tract.The developed system was applied to determining the dialysability of five essential elements (Ca, Mg, P, Fe, Zn) for various kinds of foods, *i.e.*, milk-based infant formula reference material (NIST SRM 1846), milk powder, kale, mungbean, chicken meat, jasmine rice, and *Acacia pennata*. The dialysis profiles of elements and pH change profiles can be useful in understanding the dialysis change and factors affecting dialysability. All studied elements were rapidly dialysed in the first 30 min of simulated intestinal digestion. It is expected that this system will be useful for estimation of dialysability and for studying the mutual effects of components in food.

Introduction

Mineral deficiency is usually caused by a low mineral content in the diet when rapid body growth is occurring and/or when minerals from the diet are poorly absorbed. Mineral bioavailability has usually been determined by *in vivo* measurement.[1] Ideally, mineral bioavailability studies should be performed *in vivo* and in humans; however, they are difficult, expensive, and provide limited data with each experiment.[2] While animal assays are less expensive, they are somewhat limited by uncertainties with regard to differences in metabolism between animals and humans. As an alternative to human and animal *in vivo* studies, the availability of minerals or trace elements has also been estimated by simple, rapid and inexpensive *in vitro* methods.[3] The earlier *in vitro* methods estimated bioavailability by measuring the dialysability of minerals through a semipermeable membrane in equilibrium after simulated enzymatic digestion of foods, which was known as ''Miller's method''. However, in this equilibrium method, the dialysed components are not continuously removed, as occurrs in the intraluminal digestive tract. Many modifications have been made to Miller's method in an attempt to improve the analytical methodology. Continuous-flow dialysis (CFD) *in vitro* methods were developed[4–6] in which dialysed components were continuously removed. These methods measure the fraction of the available mineral pool in diets which is potentially capable of absorption. Although a true absorption is not determined, *in vitro* methods have frequently been used to predict and compare the availability of different foods because they are simple, rapid, inexpensive and easy-to-control. In addition, certain parameters can be monitored during *in vitro* dialysis. Some studies reported poor correlation between *in vitro* and *in vivo* bioavailability,[7,8] whereas some studies reported good correlation between results obtained from the two methods.[9,10] An example of disagreement between the two methods was reported for bioavailability estimation of Ca.[8] The *in vivo* studies of Ca showed higher values than *in vitro* studies because some of the Ca bound species was released into the large intestine and might be absorbable.[8] Therefore, to obtain a reliable and meaningful *in vitro* bioavailability study, a clear need exists for the development of a dialysis method that can mimic *in vivo* functions.

A CFD system, by which dialysed components were continuously removed during simulated intestinal digestion, has been developed to obtain a closer simulation of the mineral absorption in the body.[6] It involves an *in vitro* gastric digestion in a batch system (mimicking digestion in the stomach where no mineral absorption takes place), then intestinal digestion in a CFD system. The CFD in the intestinal digestion step enables dialysable components to be continuously removed for element detection. Moreover, the proposed CFD system offers information on dialysis kinetics, which could be extrapolated to be of some use for absorption studies. In our previous reports, the CFD system was operated with off-line flame AAS,[6] and on-line electrothermal AAS detection[11] for the study of Ca and Fe dialysability, respectively. However, many essential minerals are of nutritional interest, for example Ca and P are two essential elements for optimal bone mineralization.[12] The roles

† Presented at the First Winter Conference on Plasma Spectrochemistry, Chiang Mai, Thailand, April 25–30, 2005.

DOI: 10.1039/b508639f

of other major and trace elements (Mg, Fe, Zn, Cu, Se, *etc.*) are also of particular interest. Magnesium, Zn, and Fe serve metabolic and enzymatic functions. Zinc is essential for normal growth and development of the immune response.[13] So, the CFD system with multielement detection capability for the determination of major and trace elements was aimed in this direction. An inductively coupled plasma optical emission spectrometric (ICP-OES) detection was chosen for this study. An ICP-OES spectrometer was connected on-line sequentially after an on-line pH measurement module to the CFD system to continuously monitor the dialysed multielement content and pH change during dialysis. The developed method was validated and applied for determination of mineral (Ca, Mg, P, Zn and Fe) dialysability for various kinds of food.

Experimental

Reagents and solutions

All reagents were of analytical grade, and ultrapure water of 18 MΩ cm specific resistivity obtained from a Milli-Q purification system (Millipore Corp., MA, USA) was used throughout. Glass and polyethylene containers were soaked in 10% nitric acid for at least 24 h and then rinsed three times with ultrapure water before use.

A pepsin solution was prepared by dissolving 0.16 g of pepsin (P-7000, porcine stomach mucosa, Sigma, St.Louis, MO, USA) in 1 mL of 0.1 mol L^{-1} HCl. A pancreatin–bile extract (PBE) mixture was prepared by dissolving 0.004 g of pancreatin (P-1750, porcine pancreas, Sigma) and 0.025 g of bile extract (B-6831, porcine, Sigma) in 5 mL of 0.001 mol L^{-1} $NaHCO_3$. Flat dialysis membranes (MWCO 12–14 kDa) 10 mm wide and 17.6 cm in length (cellu-Sep®H1, Membrane Filtration Products, Texas, USA) were used in the intestinal digestion procedure. The membranes were boiled for 30 min in 40% ethanol, soaked in 1 mM ethylenediamine tetraacetic acid (EDTA; BDH Ltd., Poole, UK) for 30 min, rinsed several times with Milli-Q water, stored in 0.01 M $NaHCO_3$ and rinsed with Milli-Q water before use. A multielemental stock solution (QCS 01–5 at 100 μg mL^{-1}), Y (ICP-69N-1 at 1000 g mL^{-1}) and Sc (ICP-53N-1 at 1000 g mL^{-1}), as internal standards, were from AccutraceTM (AccuStandard®, USA). Standard solutions were prepared immediately before use by dilution of stock standard with 2% HNO_3.

Instrument and equipment

The CFD system used in this study was described elsewhere.[6] The outlet of the CFD system was connected to a pH measurement module and ICP-OES detection unit (Fig. 1). A shaking water bath (Memmert®, Memmert GmbH, Germany), controlled at 37 ± 1 °C, was used for both gastric and intestinal digestions. The Orion SensorLink pH measurement system (ThermoOrion, USA), Model PCM500, equipped with PCMCIA slot and personal computer, was used to determine pH during digestion and dialysis.

Determination of minerals by ICP-OES was performed using a SPECTRO CIROS CCD, axial configuration, equipped with a glass spray chamber (double pass, Scott-type) and a cross-flow nebulizer (all from SPECTRO Analytical Instruments, Germany). The ICP-OES operating conditions were as follows: power 1350 W; nebulizer gas flow 1 L min^{-1}; and auxiliary gas flow 12 L min^{-1}. Selected emission lines were: Ca, 396.847 (II), 317.933 (II), and 422.673 (I); Mg, 279.553 (II), 279.079 (II) and 280.270 (II); P, 177.495 (I) and 214.914 (I); Fe, 238.204 (II), 239.562 (II), 259.940 (II); and Zn, 202.548 (II), 206.191 (II), 213.856 (II) nm. Emission lines for internal standards were: Y, 320.332 (II), 371.030 (II) and 442.259 (II); and Sc: 256.023 (II), 361.384 (II), and 440.037 (II) nm. A closed microwave digestion unit (Milestone MLS 1200 mega, Italy) equipped with 6 Teflon vessels was used to mineralize 0.5–1 g of food samples with 10.0 mL of concentrated nitric acid prior to determination of the total mineral contents by ICP-OES.

Sample collection and preparation

Milk-based infant formula (NIST SRM 1846) was used for method validation. Representative samples of cow milk, kale (*Brassica oleracea* var. alboglabra, Bail.), *Acacia pennata* (L., Willd. Subsp.), mungbean (*Phaseolus aureus* Roxb.), chicken meat, and jasmine rice (*Orya sativa*) were examined. Three samples for each food item, 1–3 kg, were purchased randomly in three local markets in metropolitan areas of Bangkok, Thailand. After purchase, the samples were transported as soon as possible to the laboratory. Milk powder, jasmine rice, and mungbean were used as purchased. Kale, *Acacia pennata* and chicken meat were cleaned once with tap water, and twice with Milli-Q water. The inedible portions of each sample were recorded and discarded. The edible parts in all samples except milk powder and infant formula were cooked by boiling,

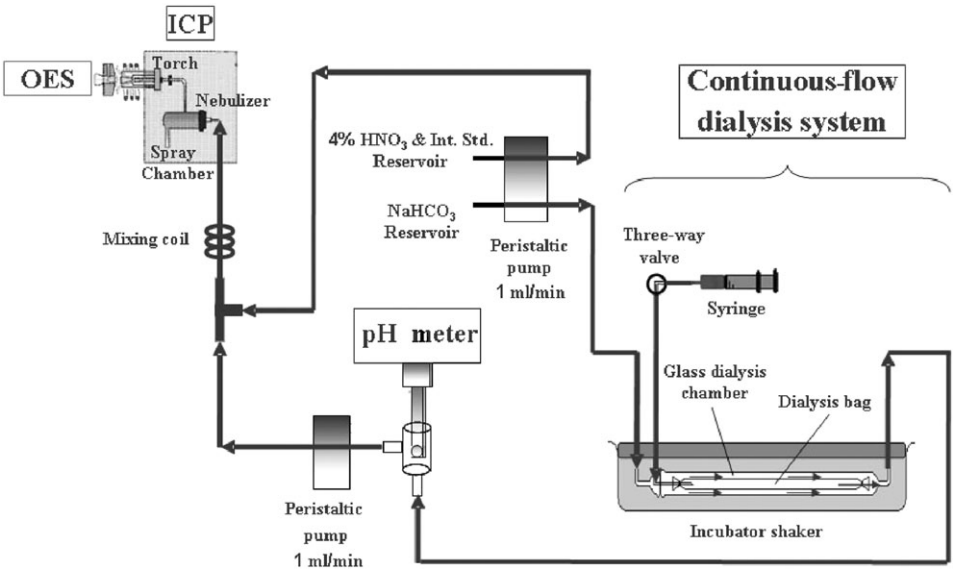

Fig. 1 Schematic diagram of continuous-flow dialysis system with on-line ICP-OES and pH measurements. A 2.5 mL pepsin digest sample was injected into the dialysis bag using a syringe. A 625 μL aliquot of pancreatin–bile extract was introduced into the dialysis bag after the first 30 min of the dialysis process. Dialysis was continued for 150 min. The dialysate flow was sequentially subjected to pH and ICP-OES measurements.

Table 1 Optimum concentrations of $NaHCO_3$ for each food sample

Sample	Optimum $NaHCO_3$/mol L^{-1}
Jasmine rice	7.77×10^{-4}
Chicken meat	1.89×10^{-3}
Mungbean	1.32×10^{-4}
Acacia pennata	1.59×10^{-3}
Milk powder	1.14×10^{-3}
Kale	1.44×10^{-3}

homogenized by a food processor (Tefal® Kaleo Blender, France), kept in an acid-washed screw-capped plastic bottle, and stored at −20 °C. A representative portion of the homogenized samples was dried at 60 °C and ground to fine particles, and then stored in a sealed plastic bag in a desiccator at room temperature until analysis.

Analytical procedure

***In vitro* gastrointestinal digestion method.** Gastric digestion was performed according to the procedure of Miller.[3] Dried samples were weighed (0.5–1 g), mixed with 10 g of Milli-Q water, adjusted to pH 2.0 with 6 M HCl and adjusted to 12.5 g using pure water. To carry out pepsin–HCl digestion, 375 µl of pepsin solution was added. The mixture was then incubated for 2 h at 37 °C in a shaking water bath.

For intestinal digestion and dialysis, a dynamic CFD system was used (Fig. 1). A portion of the mixture after gastric digestion (2.0–2.5 g) was injected into the flattened dialysis bag in the dialysis chamber *via* a syringe. The dialysing solution, $NaHCO_3$ of optimum concentration, determined by titratable acidity[6] for each food sample as summarized in Table 1, flowed through the outer surface of the bag at 1 mL min^{-1} and the temperature was controlled at 37 °C. The dialysable components in the dialysing solution were transported into the pH measurement cell and finally to the ICP-OES. To obtain good nebulization performance and to ensure that the analyte elements remained soluble, the stream of dialysing solution was acidified by mixing with a stream of 4% nitric acid, which also contained 1 mg L^{-1} of Y and Sc, used as internal standards at 1.0 mL min^{-1} (see Fig. 1). Blanks for gastric and intestinal digestions were also performed in each experiment to control possible contamination problems.

Mineral content determination. A known amount of sample (approximately 1.0 g) was digested by microwave digestion using 10.0 mL of concentrated HNO_3. The microwave digestion program comprised five steps: 1, 250 W for 1 min; 2, no power for 1 min; 3, 250 W for 5 min; 4, 400 W for 5 min; and 5, 650 W for 5 min. Digestion was performed to obtain a clear solution. In each digestion round, five vessels were used for food samples and one vessel was left for blank HNO_3 to check for the presence of contamination during each run. Acid digestion of an SRM 1846 milk-based infant formula standard reference material was also performed using a microwave digestion system to check for analytical recovery. The mineral total contents were measured by ICP-OES.

In the CFD method, the concentration of each mineral in the dialysate (µg mL^{-1}) was obtained by on-line ICP-OES measurement by external calibration using freshly prepared standard solution in $NaHCO_3$ of similar concentration to the dialysing solution, which was acidified to contain 2% HNO_3 before use. The total amount of dialysed minerals was determined by integration of the signal through the whole dialysis time using a computer program (Microcal Origin, Version 6.0).

Dialysability in percent was calculated as follows: dialysability (%) = $100 \times D/C$, where D represents dialysed mineral content (µg g^{-1} sample) and C represents the total mineral content (µg g^{-1} sample). After dialysis, mineral contents in the residue inside the dialysis bag were determined by ICP-OES after acid digestion, and the percentages of mineral remaining were calculated.

Results and discussion

I. Setup of continuous-flow dialysis system with on-line detections

The design of the continuous-flow dialysis (CFD) system for *in vitro* determination of mineral bioavailability, the selection of dialysing solution flow rate and optimization of dialysing solution ($NaHCO_3$) have been reported elsewhere.[6] The optimum flow rate of dialysing solution in the CFD and the uptake rate of ICP-OES were similar at 1 mL min^{-1}, therefore they can be readily coupled. Nonetheless, to obtain good nebulization performance, sample solution was acidified before reaching the nebulizer by merging the stream of sample solution with a stream of 4% nitric acid. The signal intensities of Ca and Fe in acidified samples were increased remarkably, in comparison with those which were not acidified.

II. Validation of analytical method

Because a reference material, which would provide bioavailability data, is not available, validation of the proposed method was performed by studying the analytical recoveries of all elements of interest. Milk-based infant formula reference material (SRM 1846) was subjected to the proposed analytical procedure to determine the dialysable minerals in the dialysate and the non-dialysable ones in the retentate. The non-dialysable mineral in the retentate was determined by ICP-OES after acid digestion of the remaining of food suspension in the dialysis tube. The total mineral content of the sample was determined after total digestion of the sample. The results are given in Table 2. The results of total concentration obtained by ICP-OES after acid digestion agreed well with the certified values for all elements studied, suggesting good performance of ICP-OES detection. In addition, a summation of the dialysed

Table 2 Validation of method using milk-based infant formula (SRM 1846) ($n = 3$)

	Mineral contents				
	Ca	Mg	P	Fe	Zn
Certified value/µg g^{-1}	3670 ± 200	538 ± 29	2610 ± 150	63.1 ± 4.0	60.0 ± 3.2
Total minerals/µg g^{-1}[a]	3760 ± 160	541 ± 17	2490 ± 96	66.6 ± 1.5	62.8 ± 1.8
dialysed minerals/µg g^{-1}[a]	2800 ± 140	428 ± 10	1730 ± 200	17.7 ± 2.2	51.5 ± 3.7
Non-dialysed minerals/µg g^{-1}[a]	792 ± 46	86 ± 12	1040 ± 94	42.4 ± 5.5	7.8 ± 1.0
dialysed + non-dialysed mineral/µg g^{-1}	3600 ± 140	514 ± 6	2690 ± 145	60.1 ± 5.0	59.0 ± 4.9
Dialysis (%)	76 ± 4	80 ± 2	70 ± 5	27 ± 3	82 ± 6
Element retained (%)	22 ± 1	16 ± 2	42 ± 4	64 ± 5	18 ± 2
Sum (%)	98 ± 4	96 ± 1	104 ± 6	90 ± 5	94 ± 9

[a] Blank subtracted.

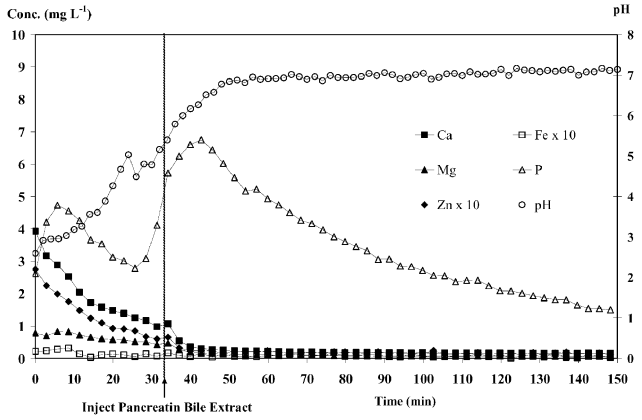

Fig. 2 Dialysis profiles and pH changes obtained from the CFD-pH-ICP-OES system for blank analysis.

minerals (by CFD-ICP-OES) and non-dialysed minerals contents was similar to the certified values with recoveries ranging from 90 ± 5% for Fe to 104 ± 6% for P, suggesting good performance of the CFD system and the absence of matrix interferences from the dialysable components and therefore the reliability of an on-line ICP-OES determination of dialysable minerals without prior acid digestion. With the proposed CFD-ICP-OES system, a quantitative recovery was obtained.

III. Dialysis profile

Not only was the percent dialysability obtained but also the dialysis profiles of elements and pH change profiles, which can be useful in understanding the dialysis change and factors affecting dialysability. The pH changes (right axis of Fig. 2) from approximately 2.0 for gastric digests to *ca*. 5.0 within 30 min of intestinal digestion and to *ca*. 7.0–7.5 after 1 h were

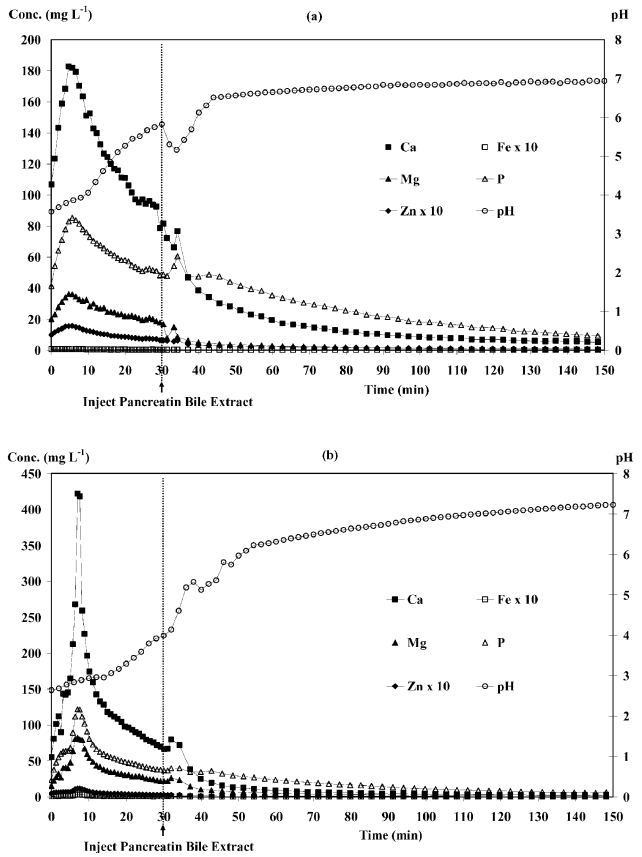

Fig. 3 Dialysis profiles and pH changes in milk powder (a) and kale (b).

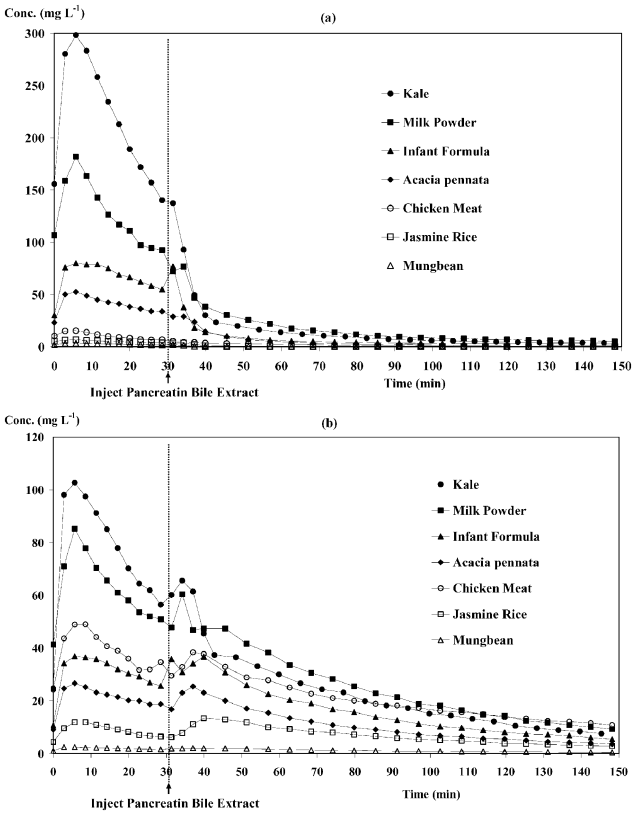

Fig. 4 Dialysis profiles of calcium (a) and phosphorus (b) in various foods.

close to what occurs in the human gastrointestinal tract.[4] The blank dialysis (Fig. 2) was found to give low values (<4 mg L^{-1} for all elements, highest for P at 3–7 mg L^{-1}, which was considerably low and could be estimated to be less than 10% of the dialysable components). Nevertheless, blank correction was performed and subtracted in all analyses. Figs. 3(a) and 3(b) show dialysis profiles of Ca, Mg, P, Fe and Zn for milk powder and kale digests, respectively. All elements show similar profiles, giving peak maxima at about 10 min of dialysis and a gradual decrease to baseline; in this system, such profiles equate to "absorption", seen here as loss of mineral from the model intestine. The irregular pH change and dialysis profiles at 30–40 min were probably affected by PBE injection at 30 min.

Fig. 4 shows dialysis profiles of Ca (a) and P (b) in different food digests. Calcium and phosphorus in kale and milk powder were rapidly dialysed in the first 30 min. It was found that P dialysis profiles showed a second peak after PBE injection, as illustrated in Fig. 4(b), as a result of digestion of food components by PBE enzymes. The descending order of the total calcium content (Table 3) is as kale > milk powder > infant formula > *Acacia pennata* > chicken meat > jasmine rice > mungbean (ranged from 13 867 to 56 μg g^{-1}) considering their dialysed calcium.

IV. Profile of molar ratio plot

From a nutritional point of view, the ratio of Ca and P intake is believed to be important: the optimum molar ratio of Ca/P is 1, although a Ca/P ratio of 1/1.5 is acceptable. Injurious effects can appear when this relationship is not met.[14] It is important to maintain a good ratio of Ca and P intake for optimal bone mineralization.[15] Anderson,[16] in a review of the relationship of Ca and P and human bone development, stated that a potential mechanism for the development of low bone mass in the United States was related to a low ratio of Ca/P intake. Consumed diets with low Ca in dairy foods can also potentially

Table 3 Total and dialysed minerals (as per dry weight) in various kinds of foods ($n = 3$)

	Jasmine rice	Chicken meat	Mungbean	*Acacia pennata*	Milk powder	Kale
Calcium						
Total minerals/μg g^{-1}	56 ± 3	299 ± 13	819 ± 43	1650 ± 30	6890 ± 120	13 870 ± 540
Dialysed minerals/μg g^{-1}	44 ± 2	279 ± 9	714 ± 35	1220 ± 55	5560 ± 280	8520 ± 430
Non-dialysed minerals/μg g^{-1}	8 ± 2	12 ± 5	119 ± 27	482 ± 25	1030 ± 30	5520 ± 240
Dialysed + non-dialysed minerals/μg g^{-1}	52 ± 4	290 ± 13	842 ± 26	1760 ± 91	6580 ± 280	14 030 ± 520
Dialysis (%)	78 ± 3	93 ± 3	87 ± 4	74 ± 3	81 ± 4	61 ± 3
Element retained (%)	14 ± 3	4 ± 2	15 ± 3	31 ± 2	15 ± 0.5	40 ± 2
Sum (%)	94 ± 6	100 ± 4	103 ± 3	105 ± 6	96 ± 4	101 ± 4
Magnesium						
Total minerals/μg g^{-1}	157 ± 3	878 ± 30	1410 ± 3	1980 ± 12	763 ± 29	4690 ± 310
Dialysed minerals/μg g^{-1}	95 ± 4	814 ± 13	1050 ± 40	1640 ± 44	628 ± 46	3130 ± 100
Non-dialysed minerals/μg g^{-1}	34 ± 6	47 ± 2	459 ± 3	417 ± 7	69 ± 3	1470 ± 40
Dialysed + non-dialysed minerals/μg g^{-1}	129 ± 3	861 ± 14	1507 ± 43	2080 ± 50	697 ± 45	4600 ± 90
Dialysis (%)	60 ± 2	93 ± 2	74 ± 3	84 ± 2	82 ± 6	67 ± 2
Element retained (%)	22 ± 4	5 ± 0.2	33 ± 0.2	21 ± 1	9 ± 0.4	31 ± 1
Sum (%)	82 ± 2	98 ± 2	107 ± 3	105 ± 2	91 ± 6	98 ± 2
Phosphorus						
Total minerals/μg g^{-1}	839 ± 41	6060 ± 209	4000 ± 60	8540 ± 220	6610 ± 310	5990 ± 60
Dialysed minerals/μg g^{-1}	77 ± 8	2720 ± 90	525 ± 13	3250 ± 120	3680 ± 180	3240 ± 210
Non-dialysed minerals/μg g^{-1}	699 ± 26	2490 ± 340	3750 ± 40	5390 ± 260	1610 ± 30	1840 ± 40
dialysed + non-dialysed minerals/μg g^{-1}	776 ± 25	5210 ± 370	4280 ± 60	8630 ± 340	5160 ± 140	5280 ± 60
Dialysis (%)	9 ± 1	45 ± 1	13 ± 0.3	38 ± 1	56 ± 3	54 ± 3
Element retained (%)	83 ± 3	45 ± 1	94 ± 1	63 ± 3	23 ± 2	31 ± 1
Sum (%)	92 ± 3	90 ± 2	107 ± 1	101 ± 4	79 ± 2	88 ± 1
Iron						
Total minerals/μg g^{-1}	3.8 ± 0.1	15.2 ± 0.8	46.8 ± 2.1	113.4 ± 10.2	69.0 ± 1.4	90.9 ± 8.6
dialysed minerals/μg g^{-1}	0.2 ± 0.1	0.7 ± 0.2	2.2 ± 0.3	11.8 ± 0.9	3.7 ± 0.7	4.8 ± 0.4
Non-dialysed minerals/μg g^{-1}	3.2 ± 0.1	14.0 ± 0.3	41.4 ± 1.4	104.9 ± 1.9	55.5 ± 3.1	85.5 ± 2.8
dialysed + non-dialysed minerals/μg g^{-1}	3.5 ± 0.1	14.7 ± 0.4	43.6 ± 1.4	116.7 ± 2.7	59.2 ± 3.4	90.4 ± 2.6
Dialysis (%)	6 ± 1	5 ± 1	5 ± 1	10 ± 1	5 ± 1	5 ± 1
Element retained (%)	84 ± 3	92 ± 2	89 ± 3	92 ± 2	80 ± 4	94 ± 3
Sum (%)	91 ± 3	96 ± 2	93 ± 3	103 ± 2	86 ± 5	100 ± 3
Zinc						
Total minerals/μg g^{-1}	19.4 ± 0.6	27.5 ± 1.8	29.6 ± 0.4	44.0 ± 3.2	50.7 ± 2.3	32.0 ± 4.0
Dialysed minerals/μg g^{-1}	10.8 ± 1.3	22.9 ± 0.7	21.3 ± 0.2	15.9 ± 0.6	38.3 ± 1.7	18.2 ± 0.9
Non-dialysed minerals/μg g^{-1}	6.5 ± 0.7	6.9 ± 0.2	10.4 ± 0.8	22.9 ± 0.8	7.2 ± 0.1	15.1 ± 0.8
Dialysed + non-dialysed minerals/μg g^{-1}	17.3 ± 1.4	29.8 ± 0.7	31.5 ± 0.6	38.8 ± 0.6	44.3 ± 1.1	32.6 ± 0.8
Dialysis (%)	55 ± 7	83 ± 2	72 ± 1	36 ± 1	76 ± 3	57 ± 3
Element retained (%)	33 ± 4	25 ± 1	35 ± 3	52 ± 2	14 ± 0.2	47 ± 2
Sum (%)	89 ± 7	108 ± 3	106 ± 2	88 ± 2	87 ± 2	102 ± 3

contribute to a low Ca/P ratio.[17] Wyatt and co-workers[18] found that beans and corn tortillas were the main contributors of Ca and P in the diet, contributing higher levels of P than Ca, which resulted in Ca/P of 1 : 1.8.

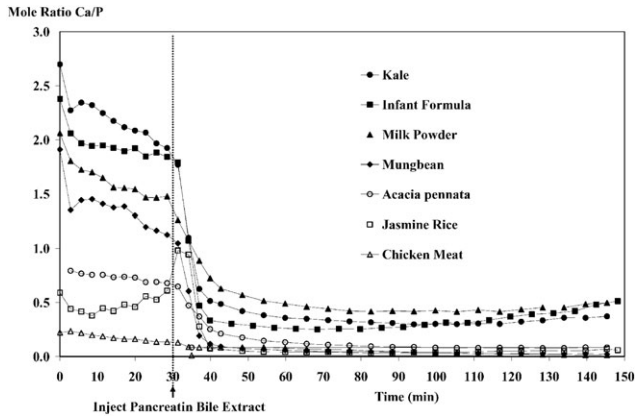

Fig. 5 Dialysis profiles of molar ratio Ca/P for various foods.

From the Ca and P levels found in the dialysed samples, the Ca/P ratio was calculated. The molar ratio plot of Ca/P in various kinds of food is markedly different (see Fig. 5). The ratio of Ca/P of dialysed amount is higher than that of the total mineral content in the same food (Table 4). The molar ratio of Ca/P from total mineral content in milk powder is 0.81 in this study, which is similar to an earlier report.[19] In contrast, the Ca/P ratio from total mineral content in kale is 1.80, which differs from the values in an earlier study[20] of 2.44–3.01, possibly owing to the fact that kales were from different geographical areas and might be of different species. However, this ratio for dialysed amount is, in all cases, higher because Ca gives higher % dialysis than P in all food samples (see Table 3). Although the Ca/P is important in determining their biological activity, this does not extend to absorption. Nonetheless, the study of the molar ratio profile might be of potential use in the future.

V. Application of the proposed system to estimate mineral dialysability of various foods

Dialysability was calculated by the summation of dialysed amounts of mineral during intestinal digestion. The results

Table 4 Molar ratio of Ca/P in dialysed and total minerals (calculated from Table 3)

	Jasmine rice	Chicken meat	Mungbean	*Acacia pennata*	Milk powder	Kale
Molar ratio of Ca/P (dialysed)	0.44	0.08	1.05	0.29	1.17	2.03
Molar ratio of Ca/P (total)	0.05	0.04	0.16	0.15	0.81[a]	1.80[b]

[a] A value of 0.81 reported.[19] [b] 2.44–3.01 reported.[20]

from the determination of the dialysability of essential elements from different kinds of food by the proposed method are shown in Table 3. Total Ca content was low in jasmine rice (56 ± 3 μg g^{-1}) and high in kale ($13\,870 \pm 540$ μg g^{-1}). The percentage of dialysis in all samples ranged from 61 to 93%, the percentage of Ca remained ranged from 4 to 40% and the sum of these values ranged from 94 to 105%. Magnesium content in studied foods ranged from 157 ± 3 μg g^{-1} in jasmine rice to 4690 ± 310 μg g^{-1}in kale. The percentage of dialysis varied from 60% in jasmine rice and 93% in chicken meat. Percent Mg remaining ranged from 5 to 33% and the sum of these values ranged from 82 to 105%. Most studied foods contained high amounts of total P (more than 2490 μg g^{-1}) except that of jasmine rice (839 μg g^{-1}). The percent dialysis of P was lower than 56% and the sum of percent dialysis and percent remained minerals was 79–107%. The percent dialysis of Fe was lowest at 5–10%, and the recovery was 86–103%. For Zn, the summation of dialysed and remaining Zn was also acceptable (87–108%).

In summary, total element and percent dialysability of each element is markedly influenced by the nature of the food. Kale and milk powder contained high total amounts of Ca, Mg, P, and Zn. Chicken meat contained a high total Fe content, whereas mungbean was high in total Mg content. The dialysabilities of Ca, Mg, and Zn are relatively high (36–93%). All studied foods had varying P dialysability, 9 ± 1% in jasmine rice and 56 ± 3% in milk powder. In contrast, the Fe dialysability is lowest at 5–10%.

Conclusions

The developed CFD-pH-ICP-OES system is simple, rapid and capable of continuous multielement detection. The system can be used for simultaneous monitoring of dialysed minerals concentration and pH during dialysis. The developed system was successfully applied to estimate the essential minerals dialysability of various kinds of foods. Information about minerals dialysability can be useful for the nutritional evaluation of foods and for the study of the effect of food components on mineral bioavailability. The dialysis profiles of elements and pH change profiles can be useful to understand the dialysis change and factors affecting dialysability. All studied elements were rapidly dialysed in the first 30 min of simulated intestinal dialysis. Not only was the profile of dialysed minerals obtained but also the molar ratio profiles of elements, which can be useful for nutritional evaluation of foods. Knowledge of mineral bioavailability is useful for managing mineral intake and for reduction of the health risk from mineral deficiency.

Acknowledgements

The authors are grateful for financial support from the Thailand Research Fund and the Postgraduate Education and Research Program in Chemistry, Higher Education Development Project, Ministry of Education.

References

1 K. Van Dyck, S. Tas, H. Robberecht and H. Deelstra, *Int. J. Food Sci. Nutr.*, 1996, **47**, 499–506.
2 M. Hansen, B. Sandstrom and B. Lonnerdal, *Pediatr. Res.*, 1996, **40**(4), 547–552.
3 D. D. Miller, B. R. Schricker, B. S. Rasmussen and D. Van Campen, *Am. J. Clin. Nutr.*, 1981, **34**, 2248–2556.
4 M. G. E. Wolters, H. A. W. Schreuder, G. Van Den Heuvel, H. J. Van Lonkhuijsen, R. J. J. Hermus and A. G. J. Voragen, *Br. J. Nutr.*, 1993, **69**, 849–861.
5 L. H. Shen, J. Luten, H. Robberecht, J. Bindels and H. Deelstra, *Z. Lebensm. Unters. Forsch.*, 1994, **199**, 442–445.
6 J. Shiowatana, W. Kitthikhun, U. Sottimai, J. Promchan and K. Kunajiraporn, *Talanta*, 2005, in the press; DOI: 10.1016/j.talanta.2005.04.068.
7 M. J. Roig, A. Alegria, R. Barbera and M. J. Lagarda, *Food Chem.*, 1999, **65**, 353–357.
8 M. Santaella, I. Martinez, G. Ros and J. Periago, *Meat Sci.*, 1997, **45**, 473–483.
9 M. Lucarini, R. Canali, M. Cappelloni, G. Di Lullo and G. Lombardi-Boccia, *Food Chem.*, 1999, **64**, 519–523.
10 K. J. H. Wienk, J. J. M. Marx and A. C. Beynen, *Eur. J. Nutr.*, 1999, **38**, 51–75.
11 J. Promchan and J. Shiowatana, *Anal. Bioanal. Chem.*, 2005, **382**, 1360–1367.
12 J. M. Pettifor, 'Rickets', in *Dietary Calcium Deficiency*, ed. F. H. Glorieux, Raven Press, New York, 1991, pp. 123–143.
13 F. Cámara, M. A. Amaro, R. Barberá and G. Clemente, *Food Chem.*, 2004, **92**, 481–489.
14 P. Aranda and J. Llopis in *Nutrition Dietetic: Aspects Sanitarios*, Consejo General de Colegios Oficiales de Farmaceuticos, Madrid, 1993, pp. 183–233.
15 I. Martinez, M. Santaella, G. Ros and J. Periago, *Food Chem.*, 1998, **63**(3), 299–305.
16 J. J. B. Anderson, *J. Nutr.*, 1996, **126**, 1153s–1158s.
17 J. J. Barger-Lux, R. P. Heaney, P. T. Packard, J. M. Lappe and R. R. Reeker, *Clin. Appl. Nutr.*, 1992, **2**, 39–45.
18 C. J. Wyatt, M. E. Hemandez-Lozano, R. O. Mendez and M. E. Valencia, *Nutr. Res.*, 2000, **20**(3), 427–437.
19 A. Lante, G. Lomolino, M. Cagnin and P. Spettoli, *Food Control*, 2004, in the press (DOI:10.1016/j.foodcont.2004.10.010).
20 M. Umetaa, C. E. West and H. Fufaa, *J. Food Compos. Anal.*, 2005, **18**, 803–817.

Anal Bioanal Chem (2005) 382: 1360–1367
DOI 10.1007/s00216-005-3288-z

ORIGINAL PAPER

Jeerawan Promchan · Juwadee Shiowatana

A dynamic continuous-flow dialysis system with on-line electrothermal atomic-absorption spectrometric and pH measurements for in-vitro determination of iron bioavailability by simulated gastrointestinal digestion

Received: 10 February 2005 / Revised: 20 April 2005 / Accepted: 23 April 2005 / Published online: 10 June 2005

Abstract A dynamic continuous-flow dialysis (CFD) method with on-line electrothermal atomic absorption spectrometric (ETAAS) and pH measurements for study of simulated gastrointestinal digestion has been developed for prediction of iron bioavailability. The method used to estimate mineral bioavailability was based on gastric digestion in a batch system then dynamic continuous-flow intestinal digestion. The intestinal digestion was performed in a dialysis bag placed inside a chamber containing a flowing stream of dialyzing solution. Mineral concentration and dialysate pH were monitored by ETAAS and use of a pH meter, respectively. The amount of dialyzed minerals in the intestinal digestion stage was used to evaluate the dialyzability. The dialysis profile and pH change can be used to understand or examine differences between the dialyzability of different food samples. To test the proposed system it was used to estimate the iron dialyzability of different kinds of milk. Iron dialyzability for powdered cow milk, cereal milk, and two brands of soymilk was found to be 1.7, 20.4, 24.9, and 37.7%, respectively. The developed CFD–ETAAS–pH system is a simple, rapid, and inexpensive tool for bioavailability studies, especially for minerals at ultratrace levels.

Keywords Continuous-flow · Dialysis · Gastrointestinal digestion

Abbreviation ETAAS: Electrothermal atomic-absorption spectrometry · CFD: Continuous-flow dialysis

J. Promchan · J. Shiowatana (✉)
Department of Chemistry, Faculty of Science,
Mahidol University, Rama VI Road, Bangkok 10400,
Thailand
E-mail: scysw@mahidol.ac.th
Tel.: +66-2-2015122
Fax: +66-2-3547151

Introduction

Minerals are needed by the body in different amounts, depending on the element, to maintain good health. The terms trace minerals or trace elements can refer to essential, non-essential, or toxic elements which are found in very small amounts in human body [1]. Trace minerals are found in foods from both plant and animal sources. An adequate dietary intake of an essential trace element does not guarantee that the body can meet its needs; absorption efficiency must also be considered. Some food constituents for example phytates, oxalates, tannins, and polyphenols can inhibit absorption of trace elements whereas other food components can promote bioavailability [2–7].

Bioavailability of trace minerals has attracted increasing interest in studies of nutrition. Bioavailability is a term used to describe the proportion of a nutrient in food that can be utilized for normal body functions. Many techniques have been proposed for quantification of bioavailability. The most reliable methods for bioavailability studies are in-vivo measurement of absorption in humans with or without using a labeling technique [7–13]. Human in-vivo studies are, however, time-consuming, very expensive, and complicated, and produce variable results. Laboratory animal in-vivo studies are less expensive but are limited by uncertainties with regard to differences between the metabolism of animals and human. In-vitro methods have several advantages, for example simplicity, rapidity, precision, and low cost, but their results may not always agree with those from real human body mineral absorption studies. Many in-vitro methods were presented in the last half of the twentieth century [14–20]. The in-vitro method developed in 1981 by Miller et al. [16], in particular, has been shown to provide availability measurements that correlate well with human in vivo studies. The method involves simulated gastrointestinal digestion then measurement of dialyzable minerals in the intestinal stage.

This method has been the basis for several in-vitro methods for estimation of the bioavailability of iron and other minerals [18, 19]. In Miller's equilibrium dialysis method the dialyzed components are not continuously removed, as occurs in the intraluminal digestive tract. Continuous-flow dialysis (CFD) in-vitro methods were therefore developed by Wolters et al. [18] and Shen et al. [19] in which dialyzed components were continuously removed. A dynamic multicompartmental computer-controlled in-vitro gastrointestinal-tract model was designed by Minekus et al. [20] to simulate various parts of the digestive tract—stomach, duodenum, jejunum, and ileum. Because the objective of the method was to imitate the whole gastrointestinal tract, it was very complicated and not easy to follow.

In this work, a simple and inexpensive CFD method has been developed. It involves simulated gastric digestion in a batch system then simulated intestinal digestion in a CFD system. The batch system in the gastric digestion stage enables high sample-throughput, because many samples can be digested in parallel. The CFD in the intestinal digestion step enables dialyzable components to be continuously removed for element detection. For on-line detection the system is connected to an electrothermal atomic-absorption spectrometer (ETAAS) and a pH meter to continuously monitor dialyzed mineral content and pH change during dialysis. The objective of using ETAAS as a detector is to enable the determination of minerals at very low levels. Monitoring of pH is necessary to ensure the dialysis pH is close to physiological pH. To evaluate the usefulness of the proposed method the iron dialyzability of different kinds of milk was determined and results were compared those from the widely used equilibrium dialysis method.

Experimental

Chemicals and materials

Deionized water (Milli Q plus, 18.2 MΩ cm^{-1}) was used throughout the experiments. All glassware was washed with liquid detergent, rinsed with water, soaked overnight in 10% HNO_3, rinsed again, and dried. All chemicals were analytical grade.

Pepsin solution was prepared by dissolving 0.16 g pepsin (P-7000, from porcine stomach mucosa) in 1.0 mL 0.1 mol L^{-1} hydrochloric acid.

Pancreatin bile extract (PBE) mixture contained 0.02 g pancreatin (P-1750, from porcine pancreas) and 0.125 g bile extract (B-6831, porcine) dissolved in 5.0 mL 0.1 mol L^{-1} sodium bicarbonate.

Dialysis tubing was prewashed before use. The tubing was boiled for 10 min in 40% ethanol, and washed with distilled water, and rewashed with 0.01 mol L^{-1} EDTA in 2% $NaHCO_3$ solution to remove trace element impurities. The tubing was then rinsed several times with deionized water. The ready-to-use dialysis tubing was kept in 0.001 mol L^{-1} $NaHCO_3$ in the refrigerator (4°C). It was rinsed again a few times with deionized water before use [21].

All Fe(II) working standard solutions were prepared by diluting 1010 mg L^{-1} Fe(II) standard solution (AccuStandard, USA) with 0.001 mol L^{-1} $NaHCO_3$ solution.

Test samples, ultra-high-temperature (UHT) corn milk, UHT cereal milk, UHT soymilk, and powdered cow milk, were obtained from a local supermarket. All milk samples were used as obtained except powdered cow milk, which was prepared by dissolving 25 g in 200 mL deionized water.

Instrument and equipment

The iron content of the solution was determined by means of a Perkin–Elmer Analyst 100 atomic absorption spectrometer equipped with a deuterium arc background corrector and a Perkin–Elmer HGA-800 heated-graphite atomizer. The Perkin–Elmer Model AS-72 autosampler was used to introduce standard and necessary solutions into the graphite tube. Pyrolytically coated graphite tubes with integrated platforms from the same manufacturer were used throughout and measurements were based on peak area. An iron hollow-cathode lamp was operated at 25 mA and the wavelength 248.3 nm was used. The spectral bandwidth was 0.7 nm. The furnace operating conditions for iron measurement are given in Table 1. The atomic signals were monitored by means of a Compaq computer with a Hewlett–Packard 870 printer to print out the analytical data. Standard stock solution (1010 mg Fe L^{-1}) was used to prepare working standard solutions of iron. Peak area was used to construct calibration plots. A six-point calibration plot in the range 0–40 μg Fe L^{-1} was constructed. When peak area under these operating conditions (Table 1) was used, standard solutions in different matrices in this work were found to give the same calibration slope. Therefore, a single calibration plot can be used for samples with different matrices.

An Orion Model PCM500 SensorLink pH Measurement System equipped with a PCMCIA slot laptop was used. The PCMCIA card was connected to a small glass combination electrode (6-mm diameter) from Orion. Commercial standard buffer solutions of pH 4.00 ± 0.01, 7.00 ± 0.01, and 10.00 ± 0.01 from Merck, Germany, were used to calibrate the pH meter.

Table 1 Furnace operating conditions for iron

Step	Temperature (°C)	Ramp/hold time (s)	Argon flow (mL min^{-1})
Drying	150	10/30	250
Pyrolysis	1300	1/10	250
Pre-atomization	500	1/5	250
Atomization	2400	0/5	0
Clean up	2600	1/3	250

An incubator shaker from Grant Instrument, model SS40-D2 (Cambridge, UK), was used to shake and incubate samples at 37 ± 1°C.

Design of the CFD system

A dialysis system was designed to serve three objectives. First, a gradual pH change from 2.0 of gastric digestion to 7.0–7.5 of intestinal digestion within 60 min of the CFD must be achieved. Second, pancreatin-bile extract can be added to the digestion mixture at the time required. Finally, dialyzed components must be continuously removed throughout the duration of the simulated intestinal digestion.

The proposed dialysis system is presented schematically in Fig. 1. A dialysis chamber was designed to enable containment of a dialysis tubing, and through which dialyzing solution could flow during dialysis. The chamber and its cover were constructed from borosilicate glass (ca. 20 cm in length and 0.8 cm inner diameter). Dialysis tubing was Spectro/Por MMCO 12,000–14,000 Da (Thomas Scientific, USA) and dialysis was performed with a piece 17.6 cm long (10 mm flat width). Although larger tubing can be used, this size is preferred to give a large contact surface with the surrounding dialysis solution. The tubing was tied at both ends, one end having silicone rubber tubing of 2 mm inner diameter and 7 cm long inserted for introduction of the sample and the required enzymes. The other end of this silicone tubing was inserted through an aperture in the glass chamber cover to enable convenient addition of a peptic digest sample and pancreatin-bile extract mixture through a three-way valve by means of a syringe. The cover was tightly sealed on to the chamber with a silicone rubber gasket. The dialysis chamber was placed in a water bath at 37 ± 1°C for pancreatic digestion. The dialyzing solution ($NaHCO_3$) was pumped through the chamber using a peristaltic pump (Eyela model MP-3N, Japan). The dialysis flow was adjusted to 1 mL min^{-1}. Dialyzable components in the peptic digest suspension could pass through the dialysis membrane and were carried by the dialyzing solution to the ETAAS sampling cup, to the pH measurement cell, and finally to the fraction collector.

To perform dialysis, the prewashed dialysis tubing was prepared as above. Before adding the peptic digest, the dialysis tubing was flattened to remove any air bubbles or liquid inside using a syringe connected to the silicone tube insert. A peptic digest sample (2.5 g) was then injected through the same silicone rubber tube. The dialyzing solution of optimum concentration flowed through at 1 mL min^{-1}. Although it took approximately 4 min for dialyzing solution to reach the ETAAS sampling cup for first ETAAS detection, this first ETAAS measurement was taken as the amount dialyzed at $t = 0$ in the dialysis profile to indicate the first point of data collection.

ETAAS sampling cup and pH measurement cell

An ETAAS sampling cup (Fig. 1) was constructed from borosilicate glass to have a small inner cone volume to enable real-time measurement of the element in the flowing stream [22]. The i.d. of the inner and outer cones of the sampling cup were 3 and 8 mm, respectively, and the inner cone volume was 60 μL. The dialysate from the CFD system flowed through the inlet at the bottom of the sampling cup, overflowed to the top of the inner cone, and drained to the outlet of the sampling cup. Determination of the concentration of iron (ng mL^{-1}) in the dialysate was performed by an ETAAS with an autosampler which sampled 20 μL dialysate every 2 min (or less frequently when the dialyzed iron concentration was steady at the later stage of dialysis). A pH measurement cell was designed to have a slightly larger size than the microelectrode (6-mm diameter) to enable the microelectrode to fit into the cell using a rubber O-ring. The dialysate flowed into the cell for continuous pH measurement.

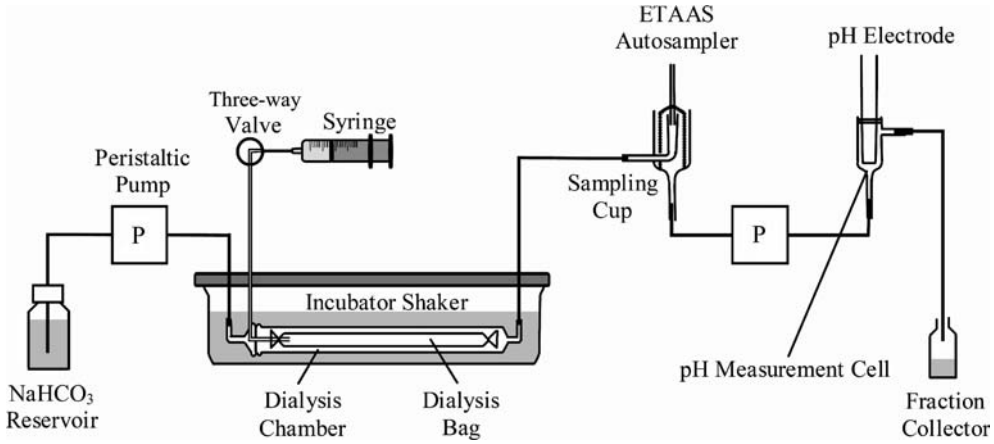

Fig. 1 Diagram of the CFD system with on-line ETAAS and pH measurement

Simulated gastrointestinal digestion procedures

Equilibrium dialysis method

Gastric digestion The in-vitro simulated gastric digestion with equilibrium dialysis was performed according to Miller et al. [16]. Deionized water (5 mL) was added to a test sample (5 mL) in a 125-mL conical flask and the pH was adjusted to 2.0 with 6 mol L^{-1} HCl. The sample was made up to 12.5 g with deionized water and 375 μL freshly prepared pepsin solution was added. The mixture was subsequently incubated in an incubator shaker at 37 ± 1°C for 2 h.

Intestinal digestion After the simulated gastric digestion, a triplicate 2.5 g peptic digest sample was weighed and introduced into the proposed dialysis bags that were placed in glass dialysis chambers. After transferring the peptic digest samples into the dialysis bag, 3.0 mL dialyzing solution was injected to the dialysis chamber. The temperature of the incubator was maintained at 37 ± 1°C. The freshly prepared PBE mixture (625 μL) was added into the dialysis bag via a three-way valve after 30 min intestinal digestion and incubation was continued for an additional 2 h. The dialysate was collected for subsequent determination of iron content.

Determination of the optimum concentration of $NaHCO_3$ The optimum $NaHCO_3$ concentration for equilibrium dialysis can be calculated from titratable acidity [16]. Titratable acidity was defined as the number of equivalents of NaOH required to titrate the amount of digest to a pH of 7.5. It was determined, using standard 0.01 mol L^{-1} NaOH as titrant, on a 2.5 g aliquot of the peptic digest to which 625 μL of PBE mixture had been added.

Continuous-flow dialysis method

Gastric digestion The simulated gastric digestion procedure was the same as the equilibrium method.

Intestinal digestion The system setup as shown in Fig. 1 was used. After simulated gastric digestion 2.5 g peptic digest was weighed and introduced into a dialysis bag. The chamber was connected to the sodium bicarbonate solution reservoir and the collector vials using Tygon tubing and placed in an incubator shaker. The other end of the chamber was connected to a sampling cup for ETAAS and to the pH measurement system. The temperature of the incubator was maintained at 37 ± 1°C. The peristaltic pump was switched on to start the intestinal digestion. The dialyzing solution flow rate was 1 mL min^{-1}. The dialysate from the CFD chamber was analyzed for iron content and pH change by means of ETAAS and a pH meter, respectively. The freshly prepared PBE mixture (625 μL) was added into the dialysis bag via a three-way valve after 30 min intestinal digestion. The dialyzed iron content and pH change were measured for an additional 2 h.

Determination of the optimum concentration of $NaHCO_3$ The optimum $NaHCO_3$ concentration for the CFD method depends on the titratable acidity of the sample and the dialysis flow rate. Titratable acidity was determined as already described. For the dialysis flow rate of 1 mL min^{-1} the optimum concentration of $NaHCO_3$ was calculated by dividing the titratable acidity by 50. This concentration of $NaHCO_3$ was found to change the pH of the dialysate to 5.0 after 30 min of dialysis and gradually increase it to 7.0–7.5 on addition of the PBE mixture.

A reagent blank was analyzed for iron content to correct for impurities in the reagents or enzymes being used (Fig. 2).

Determination of the total iron content of milk samples and in residues after dialysis

A known amount of sample (approx. 1.0 g) was digested using 10.0 mL HNO_3 and 30% H_2O_2 mixture (3:2) at 80°C. Digestion was performed until the mixture was clear. For residues after dialysis, the food suspension after dialysis was transferred from the dialysis tube into a beaker (100 mL) and the dialysis tubing was rinsed with 0.01 mol L^{-1} EDTA (2×3 mL) and 2% HNO_3 (2×10 mL), into the same beaker, before subsequent digestion to furnish a clear solution. The accurate weight of digested samples was reconstituted with deionized water and the iron content was determined by ETAAS.

Calculation of dialyzability

The amount of dialyzed mineral in dialysate from the simulated gastrointestinal digestion was used to calculate the percentage of the total amount of mineral present in the sample (or dialyzability). The dialyzability was calculated according to the equation:

$$\text{Dialyzability}(\%) = [(D - B) \times 100]/(W \times A)$$

where D is the total amount of dialyzed mineral in the dialysate (μg), B the total amount of dialyzed mineral in the blank (μg), W the weight of sample used for intestinal digestion (g), and A the total concentration of mineral in the sample (μg g^{-1}).

For the equilibrium method amounts of dialyzable minerals were calculated as twice the amount dialyzed when the volumes of peptic digest and dialyzing solution were equal, because the dialyzed amount accounted for only one half of the dialyzable iron in equilibrium dialysis [18]. When the volumes were not equal, correction was made accordingly.

In the CFD method the concentration of iron in the dialysate (ng mL^{-1}) was obtained by ETAAS

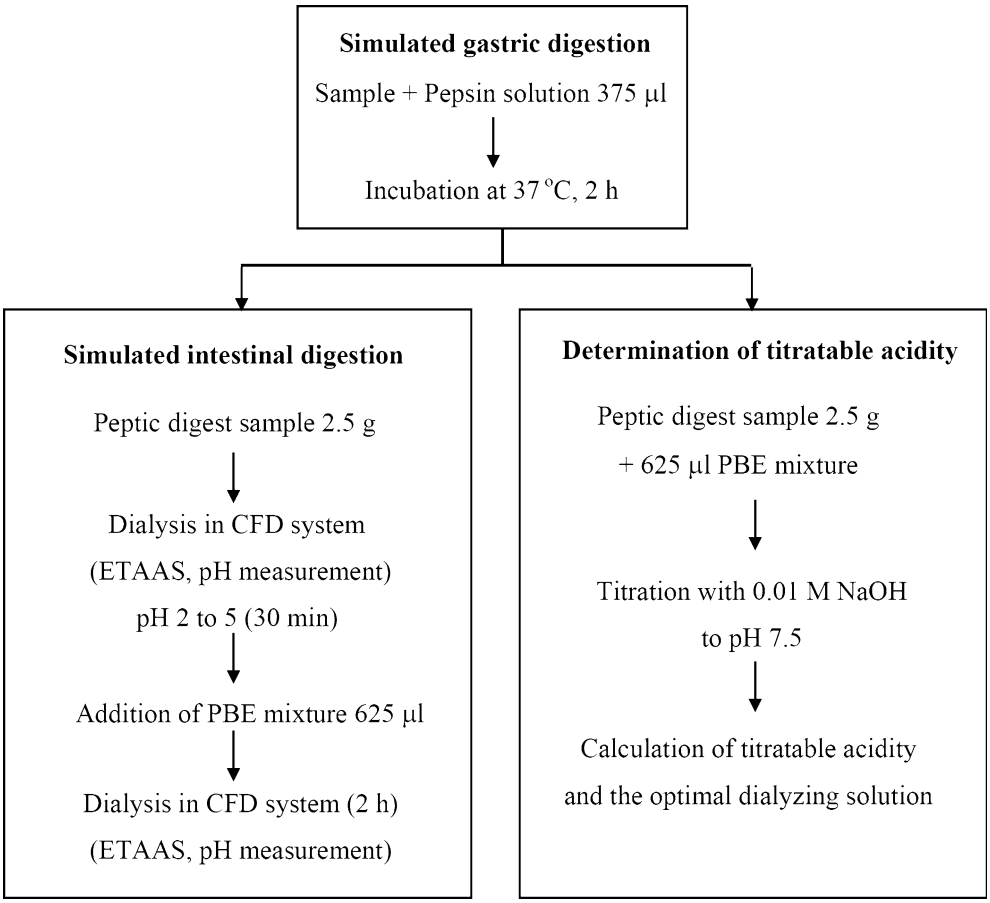

Fig. 2 Flow chart of simulated gastrointestinal digestion with the CFD–ETAAS–pH system

measurement. This concentration represented the concentration of iron in the dialysate at the time of sampling. Because a flow rate of 1 mL min^{-1} was used, the amount of iron in ng min^{-1} was obtained by multiplying the iron concentration in ng mL^{-1} by 1 mL min^{-1}. Total amount of dialyzed iron was determined by integration of the signal in ng min^{-1} through the whole dialysis time using a computer program, Microcal Origin Version 6.0.

Results and discussion

Dialysis profile

On-line ETAAS detection and pH measurement were coupled with the CFD system to enable simultaneous monitoring of low levels of dialyzed minerals and pH change during dialysis.

The dialysis profiles of iron and pH change during dialysis for different kinds of milk are shown in Fig. 3. Iron can gradually dialyze through the semipermeable membrane during intestinal digestion and dialysis decreases as pH increases. The pH of dialysate changed slowly to reach pH 5 in approximately 30 min, similar to physiological conditions in the human intestine [23]. The pH then increased rapidly to 7.0 as a result of PBE addition. After reaching a neutral pH, iron dialysis ceased except for UHT cereal milk and UHT soymilk 2, for which dialysis continued. This is probably because of the different components in these types of milk, which may help promote dialyzability. As a result, UHT soymilk 2 has higher iron dialyzability than UHT soymilk 1 although the total iron content is lower (Table 2).

In Fig. 3a, dialysis profiles for two types of calcium-fortified milk are compared. The results showed that iron dialyzability was very low (1.7%) for powdered cow milk 1 and too low to be determined for powdered cow milk 2. Many researchers have reported that calcium can inhibit iron absorption [11–13, 24]. However, the effect of calcium is complex and the mechanisms by which it reduces iron absorption are unknown. Further study of the effect of added calcium on the dialysis profiles of both elements is in progress to understand the mechanism more clearly.

Dialysis of UHT soymilk (Fig. 3b) also resulted in different profiles for iron. These UHT soymilk samples contained soy protein, different vitamins, and different amounts of calcium. Vitamin C or ascorbic acid has been reported as a most potent enhancer of iron absorption [4, 5]. At high enough concentrations ascorbic acid was found to overcome the inhibitory effect of phytic acid in cereal and in soy formula. Addition of vitamins A and C to a meal was also found to improve iron absorption [6]. Some proteins found in

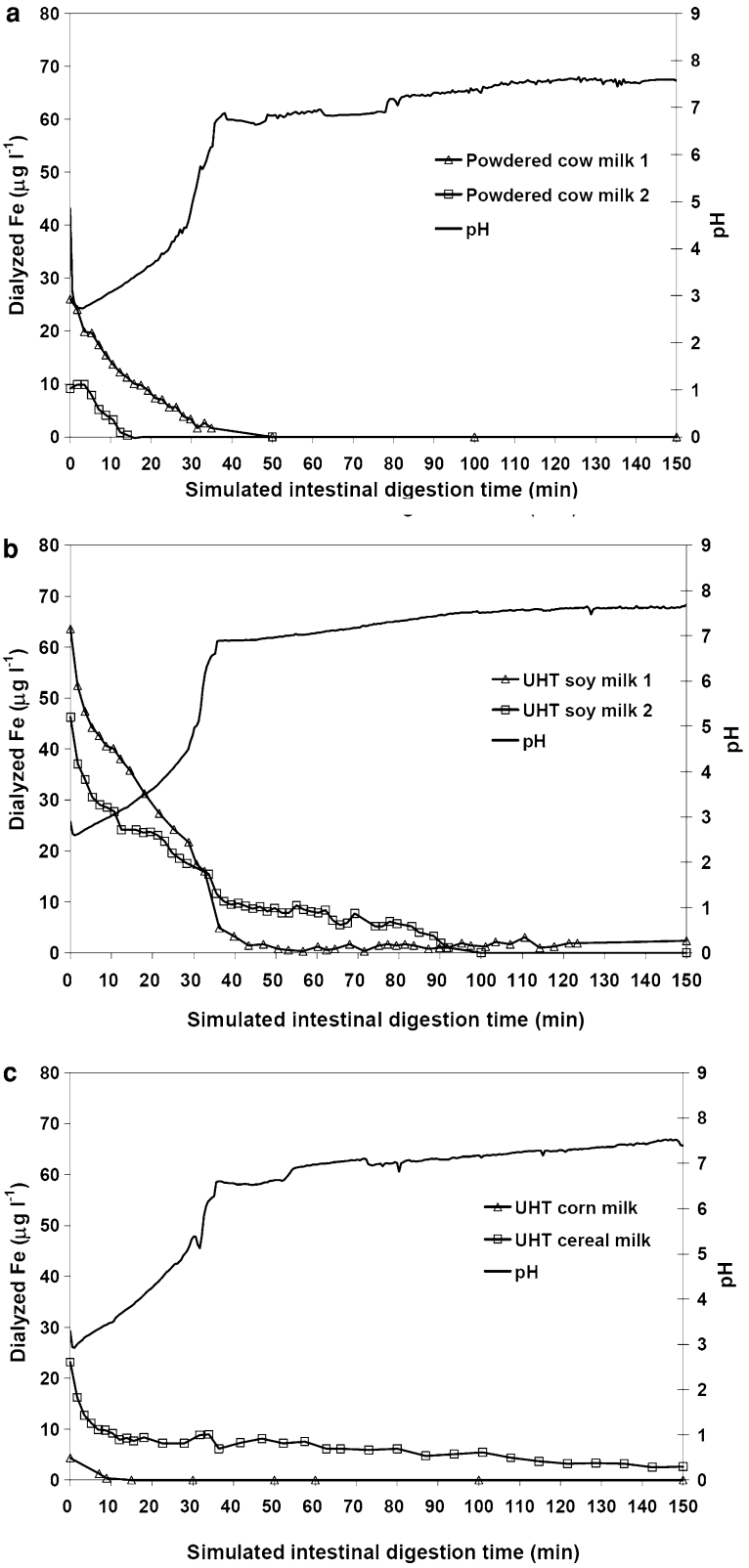

Fig. 3 Dialysis profiles of iron and pH change during continuous dialysis of **a** powdered cow's milk, **b** UHT soymilk and **c** UHT corn milk and UHT cereal milk by means of the CFD–ETAAS–pH system. The dialysis flow rate was 1 mL min^{-1}

soybeans may inhibit iron absorption. The iron dialyzability of soymilk was therefore possibly affected by both inhibitor (calcium and phytate) and enhancer (vitamins A and C).

For UHT cereal milk, iron can be gradually dialyzed until the end of 2.5 h intestinal digestion at which time dialyzed iron from UHT corn milk was too low to be detectable (Fig. 3c). The total iron content of UHT corn

milk was the lowest among the different kinds of milk studied.

The results for iron dialyzability obtained in this study show that dialysis profiles and degrees of dialyzability are different for different kinds of milk. Obviously, dialysis profile is affected by components in the digested meals and this, in turn, results in different degrees of dialyzability. The dialysis profile can be a useful tool for investigation of the effects of food components on dialyzability to provide a better understanding of dialyzability of minerals.

Iron dialyzability for different milk samples

Dialyzability was calculated by summation of dialyzed amounts of iron during intestinal digestion. The results from determination of the iron dialyzability of different kinds of milk by an in-vitro method based on CFD are shown in Table 2. The total iron content was found to vary from 0.8 to 17.1 mg L^{-1}, being highest for iron-fortified powdered cow milk 1 and lowest for UHT corn milk. The iron dialyzability was found to be 1.7% for fortified powdered cow milk 1 and not determinable for powdered cow milk 2 and UHT corn milk, because levels of dialyzable iron were undetectable. The iron dialyzability was 20.4, 24.9, and 37.7% for UHT cereal milk, UHT soymilk 1, and UHT soymilk 2, respectively. The iron dialyzability was higher for UHT soymilk (24.9–37.7%) than for powdered cow milk.

The iron dialyzability of some milk samples (cow milk 1, soymilk 1, and cereal milk) was also determined by the equilibrium dialysis method; the results are presented in the last two columns of Table 2. The iron dialyzability determined by two methods was not significantly different at a confidence level of 95% when tested by the *t*-test method.

Method validation by analytical recovery study

Because no reference material with bioavailability data is available, validation of the proposed method can be achieved only by studying analytical recoveries of the mineral of interest. A milk sample was subjected to the proposed analytical procedure to determine the dialyzable iron in the dialysate and the non-dialyzable iron in the retentate. The non-dialyzable iron in the retentate was determined by transferring the food suspension in the dialysis tubing into a beaker (100 mL) and rinsing the dialysis tubing with 0.01 M EDTA (2×3 mL) and with 2% HNO_3 (2×10 mL), into the same beaker, before subsequent digestion and iron determination. The total iron content of the samples were also determined after total digestion of the milk samples. The results are given in Table 3. It can be seen that dialyzed and non-dialyzed amounts differ slightly between replicates, probably because of inhomogeneity of the sample being used. Recoveries were between 77.9 and 90.5% with an average of 83.6%. This is thought to be partly because of incomplete removal of iron from the dialysis bag to determine the retained fraction despite repeated washing. This error will not, however, affect the percentage dialyzability results.

Conclusions

A dynamic in-vitro simulated gastrointestinal digestion method for determination of iron dialyzability was developed by connecting a simple CFD system to ETAAS and pH measurement. The system can be used for simultaneous monitoring of dialyzed metal concentration and dialysate pH during dialysis. The CFD–ETAAS–pH system was shown to be a practical and inexpensive tool for studies of dialyzability and

Table 2 Total content, amount dialyzed, and dialyzability of iron for different kinds of milk as determined by on-line CFD-ETAAS and equilibrium dialysis methods ($n = 3$)

Sample	Total iron (mg L^{-1})	Dialyzed iron			
		CFD		Equilibrium dialysis	
		mg L^{-1}	Dialyzability (%)	mg L^{-1}	Dialyzability (%)
Powdered cow milk 1 (calcium and iron fortified)	17.1 ± 0.7	0.28 ± 0.04	1.7 ± 0.3	0.19 ± 0.03	1.1 ± 0.2
Powdered cow milk 2 (calcium fortified)	1.1 ± 0.1	< 0.09 (not detectable)	–	ND	ND
UHT soymilk 1 (high iron, vitamins B, D, E, and soy protein)	5.1 ± 0.0	1.27 ± 0.08	24.9 ± 1.6	1.18 ± 0.15	23.2 ± 3.2
UHT soymilk 2 (high calcium, soy protein, and vitamins A, C and E)	3.0 ± 0.3	1.13 ± 0.07	37.7 ± 2.4	ND	ND
UHT corn milk (high vitamins A and E)	0.80 ± 0.10	< 0.05 (not detectable)	–	ND	ND
UHT cereal milk (high calcium, vitamin B1, B2, E, and soy protein)	4.1 ± 0.3	0.84 ± 0.01	20.4 ± 0.4	0.81 ± 0.03	19.8 ± 0.6

ND for not determined

Table 3 Analytical recovery of iron from powdered milk sample (three individual replicates are shown)

Sample	Dialyzed		Non-dialyzed		Recovery (%)
	Amount (mg kg^{-1})	Dialyzability (%)	Amount (mg kg^{-1})	Remaining (%)	
Powdered milk-based formula	3.0	4.8	45.3	73.1	77.9
	2.1	3.4	54.0	87.1	90.5
	3.1	5.1	48.0	77.4	82.4
Average	2.7 ± 0.6	4.4 ± 0.9	49.1 ± 4.5	79.2 ± 7.2	83.6 ± 6.4

Total iron 62.0 ± 1.0 mg kg^{-1}

bioavailability. Information about mineral dialyzability can be useful for nutritional evaluation of foods and for study of the effect of food components on mineral bioavailability. Knowledge of nutrient bioavailability is useful for managing mineral intake and for reduction of the health risk from mineral deficiencies.

Acknowledgements The authors are grateful for financial support from the Thailand Research Fund and the Postgraduate Education and Research Program in Chemistry, Higher Education Development Project, Ministry of Education.

References

1. Smolin LA, Grosvenor MB (1994) Nutrition science and applications. Saunders College Publishing, PA, USA
2. Scalbert A, Morand C, Manach C, Remesy C (2002) Biomed Pharmacother 56:276–282
3. Glahn RP, Wortley GM (2002) J Agric Food Chem 50:390–395
4. Lynch SR (1997) Nutr Rev 55:102–110
5. Hurrell RF (1997) Eur J Clin Nutr 51:S4–S8
6. Garcìa-Casal MN, Layrisse M, Peña-Rosas JP, Ramírez J, Leets I, Matus P (2003) Nutr Res 23:451–463
7. Tuntawiroon M, Sritongkul N, Brune M, Rossander-Hulten L, Pleehachinda R, Suwanik R, Hallberg L (1991) Am J Clin Nutr 53:554–557
8. Uicich R, Pizarro F, Almeida C, Díaz M, Boccio J, Zubillaga M, Carmuega E, O'Donnell A (1999) Nutr Res 19:893–897
9. Atkinson SA, Shah JK, Webber CE, Gibsom IL, Gibson RS (1993) J Nutr 123:1586–1593
10. House WA (1999) Field Crop Res 60:115–141
11. Wienk KJH, Marx JJM, Beynen AC (1999) Eur J Nutr 38:51–75
12. Van Campen DR, Glahn RP (1999) Field Crop Res 60:93–113
13. Reddy MR, Hurrell RF, Cook JD (2000) Am J Clin Nutr 71:937–943
14. Narasinga Rao BS, Prabhavathi T (1978) Am J Clin Nutr 31:169–175
15. Lock S, Bender AE (1980) Brit J Nutr 43:413–420
16. Miller DD, Schricker BR, Rasmussen RR, Van Campen D (1981) Am J Clin Nutr 34:2248–2256
17. Schricker BR, Miller DD, Rasmussen RR, Van Campen D (1981) Am J Clin Nutr 34:2257–2263
18. Wolters MGE, Schreuder HAW, Van Den Heuvel G, Van Lonkhuijsen HJ, Hermus RJJ, Voragen AGJ (1993) Br J Nutr 69:849–861
19. Shen LH, Luten J, Robberecht H, Bindels J, Deelstra H (1994) Lebensm Unters Forsch 199:442–445
20. Minekus M, Marteau P, Havenaar R, Huis in't Veld JHJ (1995) ATLA 23:197–209
21. Chaiwanon P, Puwastien P, Nitithamyong A, Sirichakwal PP (2000) J Food Comp Anal 13:319–327
22. Chen B, Beckett R (2001) Analyst 126:1588–1593
23. Ekmekcioglu C (2002) Food Chem 76:225–230
24. Hallberg L, Brune M, Erlandsson M, Sandberg AS, Rossander-Hulten L (1991) Am J Clin Nutr 53:112–119

Available online at www.sciencedirect.com
ScienceDirect
Talanta 71 (2007) 1710–1719
Talanta
www.elsevier.com/locate/talanta

A multisyringe flow-through sequential extraction system for on-line monitoring of orthophosphate in soils and sediments

Janya Buanuam [a], Manuel Miró [b,*], Elo Harald Hansen [c], Juwadee Shiowatana [a], José Manuel Estela [b], Víctor Cerdà [b]

[a] *Department of Chemistry, Faculty of Science, Mahidol University, Rama VI Road, Bangkok 10400, Thailand*
[b] *Department of Chemistry, Faculty of Sciences, University of the Balearic Islands, Carretera de Valldemossa km. 7.5, E-07122 Palma de Mallorca, Illes Balears, Spain*
[c] *Department of Chemistry, Technical University of Denmark, Kemitorvet, Building 207, DK-2800 Kgs. Lyngby, Denmark*

Received 16 May 2006; received in revised form 29 July 2006; accepted 1 August 2006
Available online 15 September 2006

Abstract

A fully automated flow-through microcolumn fractionation system with on-line post-extraction derivatization is proposed for monitoring of orthophosphate in solid samples of environmental relevance. The system integrates dynamic sequential extraction using 1.0 mol l^{-1} NH_4Cl, 0.1 mol l^{-1} NaOH and 0.5 mol l^{-1} HCl as extractants according to the Hieltjes–Lijklema (HL) scheme for fractionation of phosphorus associated with different geological phases, and on-line processing of the extracts via the Molybdenum Blue (MB) reaction by exploiting multisyringe flow injection as the interface between the solid containing microcolumn and the flow-through detector. The proposed flow assembly, capitalizing on the features of the multicommutation concept, implies several advantages as compared to fractionation analysis in the batch mode in terms of saving of extractants and MB reagents, shortening of the operational times from days to hours, highly temporal resolution of the leaching process and the capability for immediate decision for stopping or proceeding with the ongoing extraction. Very importantly, accurate determination of the various orthophosphate pools is ensured by minimization of the hydrolysis of extracted organic phosphorus and condensed inorganic phosphates within the time frame of the assay. The potential of the novel system for accommodation of the harmonized protocol from the Standards, Measurement and Testing (SMT) Program of the Commission of the European Communities for inorganic phosphorus fractionation was also addressed. Under the optimized conditions, the lowest detectable concentration at the 3σ level was $\leq$0.02 mg P l^{-1} for both the HL and SMT schemes regardless of the extracting media. The repeatability of the MB assay was better than 2.5% and the dynamic linear range extended up to 7.0 mg P l^{-1} in NH_4Cl and NaOH media and 15 mg P l^{-1} whenever HCl is utilized as extractant for both the HL and SMT protocols.

Keywords: Multisyringe flow injection; Microcolumn sequential extraction; Orthophosphate; Soil; Sediment

1. Introduction

Assessment of the bioavailability of macronutrients and trace elements in environmentally significant solid substrates is a key issue for ecology and environmental management. It is now widely accepted that the accessibility of the various elements for biota uptake depends strongly on their specific chemical forms and binding sites. A commonly used technique for identification of the phase associations of elements in solid phases is based on the application of sequential extractions [1–5]. These methods involve the rational use of a series of moderately selective reagents for releasing of targeted species from particular mineralogical fractions into the liquid phase under simulated natural and/or anthropogenic modifications of the environmental conditions. Sequential extraction procedures have been traditionally performed in a batchwise fashion. Yet, in the last decade, it has been realized that the conventional, manual procedures cannot mimic environmental scenarios accurately because naturally occurring processes are always dynamic, rather than static as they are identified by the traditional equilibrium-based approaches.

Recent trends have been focused on the development of alternative methods aimed at mimicking environmental events more correctly than their classical extraction counterparts [6]. Several

* Corresponding author. Tel.: +34 971 259576; fax: +34 971 173426.
E-mail address: manuel.miro@uib.es (M. Miró).

0039-9140/$ – see front matter © 2006 Elsevier B.V. All rights reserved.
doi:10.1016/j.talanta.2006.08.007

attempts have been made on the characterization and evaluation of dynamic (non-steady-state) partitioning methods, mostly exploiting continuous-flow or flow injection systems, where fresh portions of leaching agents are continuously provided to small containers or columns containing the solid material [7–18]. Dynamic approaches should be regarded as appealing avenues for fractionation assays not only because they alleviate the shortcomings of batch procedures including analyte re-adsorption and limited information on the size of actual available pools, but at the same time result also in improved precision and sample throughput. Furthermore, the overall leaching process may be monitored as a function of the exposure time, giving rise to a more realistic insight into the extractability of elements from different geological reservoirs. As a consequence of the development of flow-based extraction approaches, on-line leachate measurements are readily applicable, as deduced from current trends in the field [9,12–14,16,18,19]. However, most of the works capitalize on hyphenated analytical methods based on coupling of the miniaturizated column extraction manifold to continuously operating atomic spectrometers, such as flame atomic absorption spectrometry, inductively coupled plasma-mass spectrometry or inductively coupled plasma-atomic emission spectrometry, whereby the on-line generated extracts are directly injected into the detection system without any further treatment [9,13,14,16,18,19].

As a result of the precise fluidic control via syringe pumps, the second generation of flow injection (FI), namely, sequential injection (SI) analysis [20] has opened for new avenues in miniaturisation of sample processing including fractionation of solid samples [21]. While most FI-procedures employ continuous, uni-directional pumping of solutions, SI is based on exploiting programmable, bi-directional discontinuous flow as coordinated and controlled by a computer. Despite the well-recognized advantages of SI-microcolumn extraction as compared to its FI counterpart in terms of ruggedness, reagent consumption, precise handling of extracts and selection of the fractionation mode [6,22,23], automated post-column derivatization, which may be indispensable for macronutrient monitoring, is inherently hindered in SI due to the requirements of aspiration of the overall solutions into a holding coil [24].

To circumvent the above drawbacks, a hybrid flowing stream approach, the so-called multisyringe flow injection (MSFI) analysis [25–27], is here proposed as the interface between the microcolumn system and detector for on-line microfluidic manipulation of leachates and reagents. To the best of our knowledge, MSFI, which compiles the advantageous features of FI and SI systems, has not been exploited for dynamic fractionation assays so far.

The hyphenated MSFI-microcolumn set-up has been assembled for automated flow-through partitioning and accurate determination of the content of bioavailable forms of orthophosphate in soils and sediments utilizing the Molybdenum Blue method for extract processing. Although environmental solids contain both organic and inorganic forms of phosphorus [28,29], the latter are most relevant as a consequence of the well-known contribution to euthrophication [30]. In the terrestrial environment, phosphorus is an essential nutrient to support the plant growth; yet, direct uptake of organic forms is regarded to be unlikely. For the very same reason, it is essential that the analytical approach used ensures that distinction between readily available inorganic phosphorus and organic bound phosphate reliably can be accomplished.

In this communication, the potential of the MSFI set-up for accommodation of two sequential extraction schemes involving different operationally defined extracting conditions is assessed. In this context, the Hieltjes–Lijklema (HL) procedure [31] and the harmonized protocol from the Standards, Measurement and Testing (SMT) program of the European Commission [32] were selected and conducted in a dynamic fashion. Careful optimization of the chemical variables for the derivatization reactions is regarded to be crucial for appropriate performance of the analyzer due to the extreme pH conditions of the extracts obtained on-line in the various partitioning steps, not only to attain the desired selectivity, especially in regard to the presence of silicon, but also ensure the distinction between orthophosphate and organic-bound phosphorus.

2. Experimental

2.1. Instrumentation

The flow manifold devised for dynamic microcolumn fractionation and on-line spectrophotometric determination of orthophosphate is shown in Fig. 1. It comprises a 5000-step syringe pump (SP) (Crison Instruments, Alella, Barcelona, Spain) for handling of the leaching reagents and performance of fractionation analysis; a 10-port multiposition selection valve (SV, Valco Instruments, Houston, TX) for selection of the appropriate extractant, and a multisyringe piston pump (MSP, MicroBu 2030, Crison Instruments) for on-line post-column derivatization of the extracts. The automatic SP is furnished with a 5 ml syringe (Hamilton, Switzerland) and a three-way solenoid valve at its head (SP1), which allows connection with the manifold or the carrier (water) reservoir. The central port of the SV is connected to SP via a holding coil (HC; used to house the selected extractant), which consists of a 1.42 m long PTFE tubing (1.5 mm i.d.), with an inner volume of 2.5 ml.

The MSP is equipped with four syringes (S1-S4) of 5, 2.5, 2.5 and 2.5 ml, respectively, whose pistons are connected in block to the same stepper motor. The solenoid commutation valves (V1–V4) (N-Research, Caldwell, NJ) placed at the head of the syringes permit the connection of the liquid drivers with the manifold (On) or with reagent reservoir (Off) regardless of the motion of the piston pump. This module also incorporates two additional discrete three-way solenoid valves (V5 and V6) for effecting soil extraction and on-line extract analysis under optimum experimental conditions.

All the connections including the extract loop and knotted reactors (KR) are made from PTFE tubing of 0.87 mm i.d. The length of the extractant loop, KR1 and KR2 are 42, 65 and 51 cm, respectively, corresponding to ca. 250, 385 and 300 μl, respectively.

A diode-array spectrophotometer (Hewlett-Packard HP8452A) equipped with a flow-through cell (18 μl inner

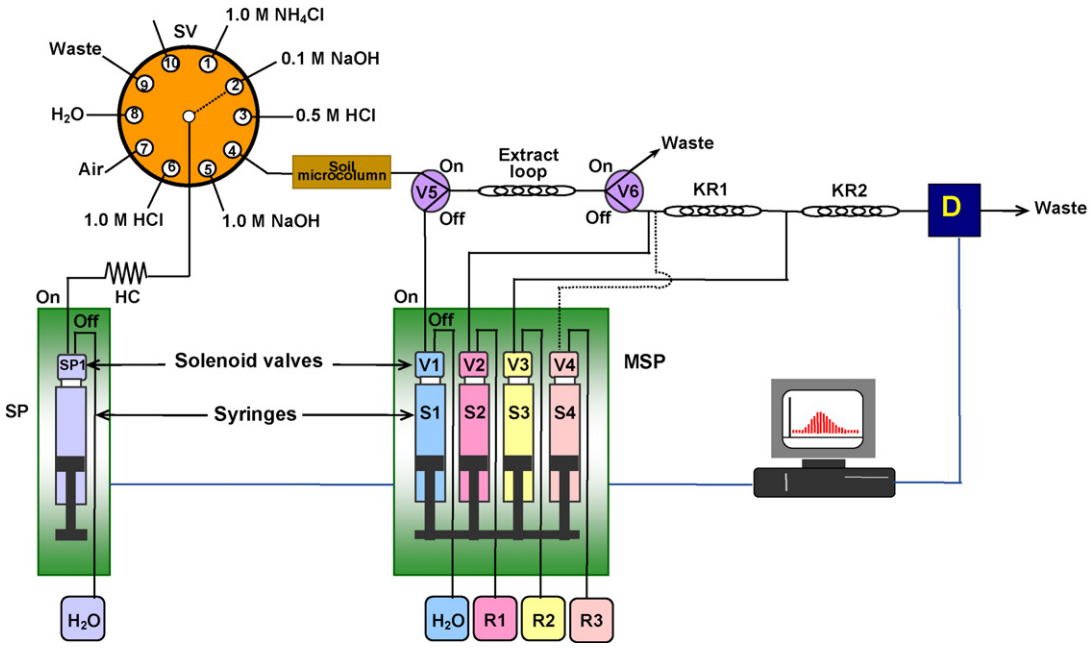

Fig. 1. Schematic diagram of the hybrid flow-through microcolumn extraction/MSFI system for automated fractionation and on-line determination of orthophosphate. R1: 6 g l^{-1} ammonium molydate + 0.125% (w/v) oxalic acid in 0.3 M H_2SO_4 (for HL scheme) or 6 g l^{-1} ammonium molydate + 0.25% (w/v) oxalic acid in 1.0 M H_2SO_4 (for NaOH-P in SMT); R2: 0.15 g l^{-1} $SnCl_2$ + 0.94 g l^{-1} $N_2H_4{\cdot}H_2SO_4$ in 0.25 M H_2SO_4; R3: 6 g l^{-1} ammonium molybdate in water (for HCl-P in SMT). SP: syringe pump; MSP: multisyringe pump; SV: selection valve, V: solenoid valve, KR: knotted reactor, D: detector.

volume, 1 cm optical path) is used as a detector. The analytical and reference wavelengths for monitoring of the Molybdenum Blue (MB) complex and minimization of Schlieren effects, respectively, are set at 690 and 530 nm. The transient spectrophotometric signals are acquired via an HP–IB interface at a frequency of 1.00 Hz. Instrumental control and data acquisition are performed using the software package AutoAnalysis 5.0 (Sciware, Spain).

2.2. Flow-through microcolumn assembly

The design of the extraction microcolumn has been described in detail in a previous work [22]. Made of PEEK, it comprises a central dual-conical shaped sample container for facilitating fluidized-bed like mixing conditions. The entire unit is assembled with the aid of filter supports and caps at both ends. The membrane filters (Fluoropore™, Millipore, 13 mm diameter with 0.45 and 1.0 μm pore sizes for sediment and soil samples, respectively) used at both ends of the extraction microcolumn allowed solutions and leachates to flow freely through but retained the particulate matter. Solid amounts up to 300 mg can be automatically processed without clogging effects as reported elsewhere [19].

2.3. Reagents, solutions and samples

All chemicals were of analytical-reagent grade and used as received. Solutions were prepared with double distilled water. A stock standard solution of orthophosphate (100 mg P l^{-1}) was prepared from KH_2PO_4 (Merck). Working solutions were prepared by stepwise dilution of the stock phosphorus solution. A stock standard solution of silicon (10 g Si l^{-1}) was prepared from $Na_2SiO_3{\cdot}5H_2O$, and diluted standards were used for the investigation of the effect of silicate on the analytical readouts.

The chemical extractants used in both the HL and SMT sequential extraction schemes are summarized in Table 1 along with the geological phosphorus fractions released.

The reagent utilized in the HL scheme (R1) for post-column formation of molybdophosphoric acid was composed of 6 g l^{-1} ammonium molybdate (Panreac) in 0.3 M H_2SO_4 (Merck) containing 0.125% (w/v) oxalic acid (Probus). For the determination of HCl and NaOH extractable phosphorus in the SMT scheme, a solution of 6 g l^{-1} ammonium molybdate was prepared in water (R3) and in 1.0 M H_2SO_4 containing 0.25% (w/v) oxalic acid (R1), respectively. A solution containing 0.15 g l^{-1} $SnCl_2$ (Scharlau) and 0.94 g l^{-1} hydrazine sulphate (Sigma) in 0.25 M H_2SO_4 (R2) was employed for on-line reduction of the molyb-

Table 1
Leaching reagents and corresponding phosphorus fractions in two extraction procedures

Procedure	Step I	Step II	Step III
Hieltjes–Lijklema	1.0 M NH_4Cl, pH 7 (Labile P)	0.1 M NaOH (Fe and Al-bound P)	0.5 M HCl (Ca-bound P)
SMT	1.0 M NaOH (Fe and Al-bound P)	1.0 M HCl (Ca-bound P)	

dophosphoric acid to the blue-coloured MB complex regardless of the fractionation scheme and extraction medium.

Two certified reference materials, namely SRM 2704 and SRM 2711, from the National Institute of Standards and Technology (NIST) were used for traceability studies. The SRM 2704 is a sediment collected from the Buffalo River in the area of the Ohio Street Bridge, NY, with a particle size distribution of 38–150 μm while the SRM 2711 is a pasture soil collected in the till layer of a wheat field (Montana, MT) with particle size <74 μm. The conical microcolumn was packed, in both cases, with 50 mg solid samples, the estimated free column volume being 250 μl.

2.4. Dissolution of solid residues and samples

Residues leftover after the sequential extraction schemes, and extracts collected downstream following post-column derivatization, were digested for quantitation of fixed and total released phosphorus, respectively. The microwave digestion procedure used can be regarded as a modified version of the EPA Method 3051 [33], named microwave-assisted acid digestion for sediments, sludges, soils, and oils. Hence, digestions were performed in a closed-vessel microwave system (Milestone, model MLS-1200 Mega, Italy) using 1.0 ml of concentrated HNO_3 (65%, Scharlau) and 3.0 ml of concentrated HCl (30%, Scharlau). The microwave digestion program consists of five steps each lasting 5 min. The power program applied is detailed as follows: 250 W/400 W/650 W/250 W/0 W. After cooling, if needed, the digests were filtered through 0.45 μm cellulose acetate filters (Minisartfilters, Sartorius, Göttinger). The clear digests were made up to 50 ml and the content of orthophosphate was determined by spectrophotometry using a batchwise standard addition method.

The pseudo-total (aqua regia) phosphorus content in the NIST 2711 was determined using the microwave digestion conditions detailed above.

2.5. General procedure for flow-through sequential extraction

The programmable flow-through fractionation assays were conducted with the aid of SP and SV. In the HL scheme, firstly, the HC was flushed with carrier (water), whereupon a 100 μl air plug from port 7 of SV and 2.0 ml of 1.0 M NH_4Cl from port 1 were consecutively aspirated into HC. Afterward, V5 and V6 were turned 'On' and SP was set to dispense 250 μl of 1.0 M NH_4Cl (which matches the free column volume) from HC through the microcolumn at a flow rate of 3.0 ml min^{-1}, allowing dynamic extraction to take place. The resulting leachate was stored into the extract loop and subsequently swept into the MSFI network for post-column derivatization and on-line determination of orthophosphate using a multicommutation protocol. The program was initially designed for eight cycle runs (equivalent to 2.0 ml of extractant volume) but the operational sequence proceeds until quantitative stripping of labile phosphorus forms.

Prior to continuing with the ensuing HL extraction step, a washing protocol is implemented by aspiration of 100 μl of air and 2.0 ml of H_2O from port 7 and 8, respectively, into HC, and using the same procedure described above for flow-through extraction. Thereafter, the next extractant (viz., 0.1 M NaOH or 0.5 M HCl) is aspirated repeatedly from the respective valve port and delivered to the soil containing microcolumn until completion of the phosphorus extraction.

For the SMT protocol, the dynamic fractionation was performed using an identical operational sequence with 1.0 M NaOH and 1.0 M HCl as leaching reagents.

2.6. Multicommutation protocol for on-line post-column derivatization

Two different multicommutation flow modalities for on-line injection of MB reagents, the so-called merging zones and sandwich-based approaches, were assayed. In both cases, switching of solenoid valves was effected during a single forward displacement of the piston bar of the MSFI pump. Both operational procedures are thoroughly described in the following:

2.6.1. Merging zones mode

As the name implies, the multicommutation protocol was programmed to merge the extract with the two reagent zones for development of the MB reaction as detailed in Table 2. After collection of the leachate in the extract loop, V1 and V2 were switched to 'On' while V5 and V6 were synchronously switched to 'Off'. As a result, the orthophosphate zone merged with a well-defined plug of ammonium molybdate to yield the heteropolyacid species in KR1. Subsequently, V3 was activated to 'On', whereby the reaction zone reaching the next confluence point overlapped with the reducing $SnCl_2$ segment to form the blue-coloured MB complex in KR2. The interdispersed zones were finally delivered downstream to the flow-through diode-array spectrophotometer by the carrier contained in S1, and the blue complex was monitored at 690 nm. Whenever the analysis

Table 2
Multicommuted merging zone protocol for on-line post-column derivatization

Multicommutation step	Solenoid valve position					Reagent (μl)		Carrier (μl)	Total flow rate (ml min^{-1})
	V1	V2	V3	V4	V5	R1	R2		
Merging of the extract and R1	On	On	Off	Off	Off	80	–	160	6.75
Delivery of the reaction zone to KR2	On	Off	Off	Off	Off	–	–	160	4.50
Merging of the reaction zone with R2	On	Off	On	Off	Off	–	120	240	6.75
Delivery of the MB zone to detector	On	Off	Off	Off	Off	–	–	2600	4.50

Table 3
Multicommuted sandwich-type protocol for on-line post-column derivatization

Multicommutation step	Solenoid valve position					Reagent (μl)		Carrier (μl) (S1)	Total flow rate (ml min^{-1})
	V1	V2	V3	V4	V5	R1	R2		
Fronting zone of R1	Off	On	Off	Off	Off	25	–	–	2.25
Simultaneous delivery of extract and R1	On	On	Off	Off	Off	80	–	160	6.75
Delivery of the rear end of extract into MSFI network	On	Off	Off	Off	Off	–	–	90	4.50
Tailing zone of R1	Off	On	Off	Off	Off	40	–	–	2.25
Injection of R2	On	Off	On	Off	Off	–	160	320	6.75
Delivery of the MB zone to detector	On	Off	Off	Off	Off	–	–	2440	4.50

was completed, all valves were returned to their original position for starting the following fractionation assay.

2.6.2. Sandwich-based mode

The multicommutation protocol involves the injection of two zones of molybdate which are stacked at each end of the leachate plug. The automated MSFI-multicommuted protocol using a sandwiched-based injection is summarized in Table 3. The method started when V2 was activated to 'On' and S2 was set to dispense 25 μl of molybdate into KR1. Thereafter, the combined extract/reagent zone was dispensed downstream. A second plug of molybdate (namely, 40 μl) was injected at the rear end of the leachate for sandwiching of the phosphorus containing segment. The reduction of molybdophosphoric acid to the Molybdenum Blue complex was performed in a merging zone fashion. To this end, 160 μl of $SnCl_2$ were injected at the front end of the interdispersed zone, and the transient signal of the MB complex was recorded by the detector.

3. Results and discussion

3.1. Configuration of the flow network for post-column phosphorus derivatization

3.1.1. Implementation of the HL sequential extraction scheme

In this three-step partitioning scheme, 1.0 M NH_4Cl, 0.1 M NaOH and 0.5 M HCl are used as leaching reagents for consecutive extraction of phosphorus pools associated with different geological phases. The flow system was devised aimed at monitoring the orthophosphate, released on-line, via the MB method. Preliminary experiments were carried out for optimization of the MSFI configuration attending the variable chemical composition of the extracts, the volume of which was maintained at 250 μl. Two different reagent injection modalities, namely, the merging zones and the sandwich-type approaches, were assayed as described under Experimental. The merging zones was finally selected over the sandwich mode because the axial interdispersion between segments is not favored in a knotted coil [34,35], thus rendering double peak profiles.

The effect of MB reagent volumes (viz., ammonium molybdate and tin(II) chloride) on the analytical readouts was investigated taking into consideration the different sizes of the various syringes. The analytical sensitivity improved by 75% when increasing the size of the molybdate plugs from 40 to 80 μl, and remained constant up to 130 μl. This might be attributed to the compensation of the better radial mixing of the reagent and extract plugs with the higher dilution of the extract for volumes above 80 μl. Reagent volumes above 130 μl are unnecessary for the present design because they lead to undue dilution. Similar trends were obtained for the optimization of tin(II)chloride volume. To prevent excessive consumption of reagents, the multicommutation protocol was programmed to merely inject 80 μl ammonium molybdate and 120 μl tin(II) chloride per assay.

The influence of the flow rate on the on-line MB derivatization reaction was evaluated over the range from 3.0 to 5.0 ml min^{-1} (for S1) for the three extractant media of the HL scheme. The higher the flow rate the lower was the yield for MB formation, which is not surprising considering the relative slow reaction rate of the derivatization reaction. In fact, the peak height dropped by 20% when increasing the flow rate from 3.0 to 4.5 ml min^{-1}. Yet, the higher the flow rate the lower is the yield of the competitive reaction for generation of the interfering molybdosilicate species and the better is the analytical throughput. Taking into account the variable sensitivity of the MB method in the various leachate solutions (see below) and the stripping of silicate from solid substrates in alkaline medium, the flow rate was fixed to 4.5 ml min^{-1} for processing of the extracts obtained in the first two steps of the HL method. Regarding the apatite-phosphate fraction, it should be born in mind that the kinetics of formation of molybdophosphoric acid are not favoured in the acidic leachate medium. Therefore, a flow rate of 3.0 ml min^{-1}, that can be programmed automatically, was utilized for monitoring of the orthophosphate released in the last step of the HL scheme.

3.1.2. Implementation of the SMT sequential extraction scheme

Within the framework of the Standards, Measurement and Testing Programme of the European Commission, a batch extraction protocol for fractionation of phosphorus in environmental solids was harmonized in order to improve the reproducibility among laboratories [32]. The so-called SMT protocol was originally designed to obtain five phosphorus fractions, namely, total phosphorus (TP), inorganic phosphorus (IP), organic phosphorus (OP), apatite phosphorus (Ca-bound P) and non-apatite phosphorus (Al and Fe-bound P). It should be taken into account that some of the SMT partitioning steps are performed in a single rather than sequential manner and that the calcination of the solid residue as demanded for the TP and OP assays cannot be effected in an on-line fashion. Consequently,

the potential implementation of the SMT fractionation assays related to the measurement of the inorganic (apatite + non-apatite) phosphorus fractions was ascertained. These two fractions are regarded as the most relevant ones for assessing the readily available phosphorus for plant uptake.

The SMT protocol is characterized for endorsing more aggressive leachants as compared with the HL scheme. The immediate consequence is that the optimal MSFI operational conditions for the HL fractionation as detailed above cannot be extrapolated directly to the SMT partitioning. The use of 1.0 M rather than 0.1 M NaOH for leaching of phosphorus associated to hydrous oxides of Al and Fe (non-apatite phosphorus) facilitates the concomitant release of large amounts of silicate. Actually, a 20% increase in the analytical signals was detected whenever the molybdate reagent for HL containing 0.125% (w/v) oxalic acid in 0.3 M H_2SO_4 was utilized for analyzing a 1.0 mg P l^{-1} standard containing 200 mg Si l^{-1} in 1.0 M NaOH. It is known that the interference of silicate on the orthophosphate MB determination can be minimized by increasing both the acidity of the reaction medium and the concentration of the masking organic acid [36–39]. The effect of the concentration of sulphuric acid was thus evaluated from 0.3 to 1.5 M while that of oxalic acid from 0.125 to 0.25% (w/v). Yet, since the acidity has opposite effects on the selectivity and sensitivity of the molybdophosphate formation [36–38], the molybdate reagent was finally prepared in a 1.0 M H_2SO_4 medium containing 0.25% (w/v) oxalic acid. Under these experimental conditions, silicate was tolerated up to 400 mg Si l^{-1} at the 10% interference level.

As to the SMT apatite fraction, the method's sensitivity using the HL reagent decreased dramatically as a result of the slow development of the reaction for molybdophosphoric acid formation under strong acidic conditions. Therefore, the heteropolyacid forming reagent was prepared in distilled water and the reaction flow rate was affixed at 3.0 ml min^{-1}. No appreciable increase of blank signals was detected, thus indicating that the acidity of the extractant suffices for preventing the self-reduction of molybdate. No oxalic acid was here added because of the negligible stripping of silicate from solids at low pH [40].

Although different reagents are needed for monitoring of the inorganic phosphorus in the HL and SMT extracts, a single MSFI assembly was arranged with no need for neither manual manipulations of reagents and leachates nor the changing of the composition of the carrier solutions for the various assays as demanded in previous flow systems for analyzing phosphorus containing soil solutions [40,41]. These facts emphasize the flexibility of MSFI for automated performance of derivatization reactions regardless of the variable chemical composition of the extracts in both fractionation schemes.

Fig. 2 illustrates the extraction patterns as obtained by on-line MSFI analysis of minute volumes of leachate (namely, 250 μl) for SRM 2704 and SRM 2711 following microcolumn extraction using both the HL and the SMT schemes. The extractograms give rise to valuable knowledge on: (i) the extraction kinetics, (ii) the content of phosphorus in available pools, (iii) the efficiency of the leachants and (iv) the actual extractant volumes for quantitative release of orthophosphate. The SMT extractograms show sharp leaching profiles while those of HL depict a gradual stripping of the nutrient species as a result of the milder leachants used. This is especially noticeable in the HCl extraction step in SRM 2704 where the amount of calcium bound phosphate leached in the first 2.0 ml in SMT is twofold higher to that of HL for the same extractant volume.

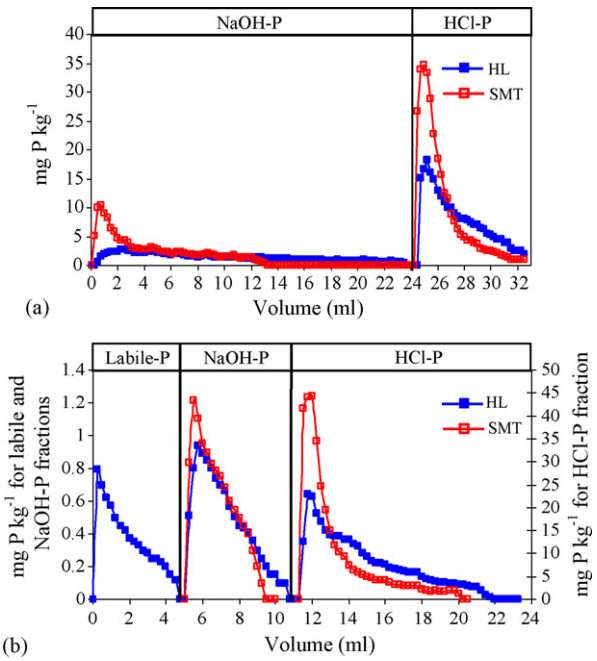

Fig. 2. Comparison of the on-line MSFI extraction profiles of orthophosphate in (a) SRM 2704 and (b) SRM 2711 as obtained by the application of HL and SMT protocols in a dynamic fashion. The labile phosphorus in 1.0 M NH_4Cl was <LOD for SRM 2704. The concentration of orthophosphate is given as mg P kg^{-1} sample.

The analytical results for SRM 2704 and SRM 2711 also evidence that different types of samples, in this case, agricultural soil and river sediment, behave differently under the same extraction conditions (see extraction patterns for the Al and Fe-bound phosphate in Fig. 2). This is attributed to the particular phosphorus soil phase associations existing in each kind of solid, thus, revealing the difficulty for setting a universal extraction protocol for dynamic fractionation of macronutrients.

3.2. Analytical performance of the MSFI analyzer

Under the optimized chemical and physical variables, the dynamic linear range of the multicommutated MB method was established over the range 0.05–7.0 mg P l^{-1} for the NH_4Cl and NaOH extraction media in the HL scheme, and 0.35–15 mg P l^{-1} for the 0.5 M HCl medium. For the NaOH and HCl steps in SMT, the regression lines extended from 0.1 to 7.0 and from 0.5 to 15 mg P l^{-1}, respectively. The limit of detection (LOD) assessed from three times the standard deviation of either the blank or a 50 μg P l^{-1} standard solution were 0.01, 0.01 and 0.02 mg P l^{-1} for NH_4Cl, NaOH and HCl steps in HL, respectively. In SMT, LODs of 0.02 and 0.01 mg P l^{-1} for 1.0 M NaOH and 1.0 M HCl were, respectively, obtained. Repeatability was estimated from 10 consecutive injections of a 1.0 mg P l^{-1} standard solution in each extracting medium. Relative standard deviations (R.S.D.)

Table 4
Comparison of the extraction/determination parameters for the HL scheme in SRM 2711 for three different procedures applied to phosphorus fractionation and extract analysis

Parameters	MSFIA (this work)		SI-MCE/FIA [42]		Batch [31]	
	Amount (mg)	Volume (μl)	Amount (mg)	Volume (μl)	Amount (mg)	Volume (μl)
1. Reagent consumption per extract analysis						
Ammonium molybdate	0.5	80	7.2	600	6.0	150
Reducing agent[a]	0.02	120	0.2	600	5.3	300
Masking agent[b]	0.1	80	2.4	1000	0.1	300
2. Extractant volume (ml)						
NH_4Cl fraction	4.5		25		2×50	
NaOH fraction	6		30		50	
HCl fraction	11		30		50	
3. Analysis time per extract (min)	0.77		0.74		20	
4. Operational time for overall fractionation and extract analysis per sample (h)	2.8		2.7		45.3	

[a] Tin(II) chloride was used as a reducing reagent for MSFIA and SI-MCE/FIA, while ascorbic acid was employed for batchwise analysis.
[b] Oxalic acid was employed as a masking agent for MSFIA, and tartaric acid for the SI-MCE/FIA and batch approaches.

of 1.0, 0.9 and 2.4% were obtained for the NH_4Cl, NaOH and HCl solutions in HL, respectively, and 1.0 and 2.2% for the NaOH and HCl media in SMT, respectively.

In Table 4, the analytical performance of the on-line MSFI analyzer for HL fractionation and orthophosphate determination is critically compared with that of the batchwise method [31] and an SI-microcolumn extraction (SI-MCE) system with further off-line analysis of the extracts by flow injection analysis [42]. A distinguishing feature of the MSFI-multicommutation set-up with respect to the FI and batch systems is the minimum consumption of reagents. Thus, in the proposed system, the consumption of MB chemicals is reduced more than 15-fold as regards to former methods. This is a consequence of the time-based injection of well-defined volumes of solutions at the precise instant for development of the reactions as effected via activation of the solenoid valves. Whenever not needed, the MB reagents are delivered to their respective reservoirs in lieu of being propelled downstream as occurs in continuous, forward-flow assemblies. Therefore, discontinuous-flow based MSFI analyzers might be viewed as environmental-friendly chemical processors.

The slightly higher operational time in MSFIA versus SI-MCE/FIA for fractionation/determination of orthophosphate has its origin in the different number of extracts analysed, that is, 86 extracts in the proposed on-line system as compared with merely 27 using the former FI set-up. Yet, the potential of the flow-through hyphenated MSFI system for handling of minute fractions of extract, that is $\leq$250 μl versus $\geq$5000 μl for methods involving fraction collection, ensures a unrivaled temporal resolution that yields a detailed insight into the leaching kinetics of phosphorus from the different soil/sediment compartments, as illustrated in Fig. 3. Hence, the content of inorganic phosphorus in readily mobilisable reservoirs can be more accurately estimated. At the same time, the sample mass to extractant volume ratio for each sequential extraction step can be calculated with improved accuracy, thereby avoiding the usage of any surplus of reagent for quantitative leaching of phosphorus in the various geological phases. According to Fig. 3 and data presented in Table 4, the leachant volumes used in the MSFI on-line fractionation system are three to four times lower to those required whenever off-line measurements are applied.

3.3. Accuracy of the proposed flow-through microcolumn extraction-multisyringe flow injection system for orthophosphate fractionation

The SRM 2704 river sediment and SRM 2711 Montana soil were utilized to evaluate the reliability and accuracy of the developed flow-through microcolumn hyphenated method. The amount of extractable orthophosphate in both standard reference materials resulting from the application of dynamic partitioning is listed in Tables 5 and 6 along with the certified total phosphorus content and the pseudo-total (aqua regia) phosphorus concentrations. The amount of extractable phosphorus for both solid substrates determined on-line by summation of all fractions plus residue is much lower than the certified values, while

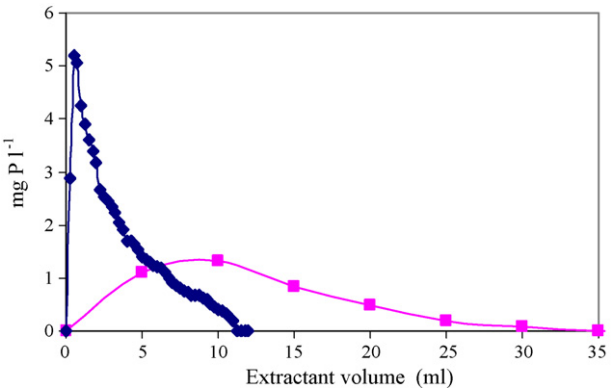

Fig. 3. Comparison of orthophosphate extractograms for the HCl step in the HL scheme for SRM 2711 as obtained by using off-line MB detection (5 ml per subfraction) and on-line MSFI spectrophotometric analysis (250 μl per subfraction).

Table 5
Comparison of extractable amounts of phosphorus in SRM 2711 (mg kg^{-1}) as obtained by using the Hieltjes–Lijklema and SMT sequential extraction schemes with on-line and off-line MB detection modes

Fractions	Hieltjes–Lijklema			SMT	
	On-line (MSFIA)	Off-line[a] (MWD)	Off-line[b] (SI-MCE) [42]	On-line (MSFIA)	Off-line[a] (MWD)
(1) Labile P	7 ± 1	36 ± 2	45 ± 5		
(2) Al and Fe-bound P	13.1 ± 0.4	84 ± 6	93 ± 10	11 ± 1	105 ± 2
(3) Ca-bound P	324 ± 45	370 ± 25	373 ± 18	365 ± 9	384 ± 9
(4) Residue	215 ± 14	215 ± 14	288 ± 43	202 ± 9	202 ± 9
Summation (1 + 2 + 3 + 4)	559 ± 47	705 ± 29	799 ± 48	578 ± 13	690 ± 13

Results are expressed as the mean of five fractionation assays ± S.D.; pseudo-total P: 700 ± 30 mg P kg^{-1}; certified value: 860 ± 70 mg P kg^{-1}; MWD: microwave digestion; SI-MCE: sequential injection-microcolumn extraction.
[a] The concentration of orthophosphate in the extracts is determined by batchwise MB standard addition.
[b] The concentration of orthophosphate in the extracts is determined by FIA-MB.

a good agreement, with maximum deviations of 8%, is obtained between the summation of fractions for SRM 2704 and SRM 2711 following acidic microwave digestion of the extracts collected downstream (after on-line detection) and the endorsed and pseudo-total concentrations, respectively.

According to the MB chemistry, only dissolved orthophosphate can react with MB reagents for generation of the reduced blue-coloured complex. Therefore, the on-line MSFI extraction system with spectrophotometric monitoring detects merely the extractable, reactive inorganic phosphorus. However, in the off-line assays, the extracts that may contain other phosphorus compounds, such as organic phosphorus and condensed inorganic phosphates (see below), can be degraded under microwave digestion into orthophosphate, thus providing information on the total phosphorus released. As a result, the total phosphorus content after appropriate processing of the MSFI extracts is not significantly different at the 0.05 significance level to the certified or pseudo-total phosphorus concentrations in both SRM materials, as shown in Tables 5 and 6.

3.4. Comparison of on-line and off-line modes for phosphorus determination in soil/sediment extracts

The phosphorus fractionation results using the on-line hyphenated MSFI assembly for SRM 2711 were contrasted with those previously obtained by sequential injection microcolumn extraction (SI-MCE) and fraction collection prior to off-line FI analysis [42]. As shown in Table 5, the extractable phosphorus monitored spectrophotometrically is severely affected by the mode of extract processing. It should be stressed that even though the HL and SMT schemes were originally designed for inorganic phosphorus fractionation, soil organic phosphorus can be concurrently released by the extracting reagents themselves. In fact, the most commonly accepted schemes for soil organic phosphorus fractionation [43,44] involve alkaline and acid extractions with 0.1–0.5 M NaOH and >0.1 M HCl, respectively, thus matching the chemical conditions for HL and SMT extractions. NaOH creates electrostatic repulsions by increasing the negative charge of both organic and mineral components [45] while HCl dissolves salts of some organic phosphate esters that are relatively insoluble in alkaline solution [43].

Furthermore, several organic phosphates are instable in alkaline and acid conditions, and therefore might be hydrolyzed under the fractionation conditions to free phosphate, thus leading to the overestimation of the content of readily accessible orthophosphate. The effects of alkaline and acid hydrolysis for a wide range of soil organic phosphorus compounds have been found to be markedly influenced by the nature of the phosphorus species [44,46,47]. The extraction of fast hydrolysable phosphorus forms (e.g., phosphatidyl choline) may hence explain the discrepancy in Table 5 between the on-line and off-line (SI-MCE) data for NaOH and HCl extracts in the HL scheme. Regarding the NH_4Cl extracts in HL, the contribution from organic phosphorus hydrolysis should here be negligible because organic substances cannot be leached under mild extraction media. Yet, common sources of readily hydrolysable phosphorusin soils, that might

Table 6
Comparison of extractable amounts of phosphorus in SRM 2704 (mg kg^{-1}) as obtained by using the Hieltjes–Lijklema and SMT sequential extraction schemes with on-line and off-line MB detection modes

Fractions	Hieltjes–Lijklema		SMT	
	On-line (MSFIA)	Off-line[a] (MWD)	On-line (MSFIA)	Off-line[a] (MWD)
(1) Labile P	<LOD	<LOD		
(2) Al and Fe-bound P	114 ± 14	103 ± 6	164 ± 18	177 ± 14
(3) Ca-bound P	310 ± 43	595 ± 17	288 ± 18	664 ± 21
(4) Residue	232 ± 26	232 ± 26	171 ± 5	171 ± 5
Summation (1 + 2 + 3 + 4)	656 ± 52	930 ± 32	623 ± 26	1012 ± 26

Results are expressed as the mean of five fractionation assays ± S.D.; certified value: 998 ± 28 mg P kg^{-1}; LOD: limit of detection.
[a] The concentration of orthophosphate in the extracts is determined by batchwise MB standard addition.

be released in the first extraction step of HL, are the condensed inorganic phosphates (e.g., pyrophosphate and polyphosphates) [44].

It should be noted that the hydrolysis of organic phosphorus and condensed inorganic phosphates in off-line based fractionation analysis might occur not only during the timeframe of the extraction but to a significant extent during the residence period prior to actual phosphorus determination. As opposed to batch partitioning and dynamic methods involving off-line or at-line analysis of phosphorus containing fractions, the novel multisyringe flow approach leads to a substantial shortening of the assay protocol, thus minimizing the potential decomposition of hydrolyzable phosphorus compounds. Each microvolume of extract leaving the microcolumn is readily treated on-line with MB reagents, while the released organic species in the batchwise method and SI-MCE system with off-line analysis remain in intimate contact with the extracting reagent for >15 and 3 h, respectively. Therefore, the flow-through MSFI fractionation analyzer with MB detection should be regarded as a unique tool for accurate monitoring of mobilisable orthophosphate in environmental solid substrates, even though organic phosphorus may be leached with the extracting reagents.

4. Conclusion

Multisyringe flow injection analysis has been presented as an appealing analytical tool for on-line processing of the extracts generated in flow-through dynamic fractionation assays. Prominent features of the assembled analytical set-up involving multicommutated post-column injection of reagents are the considerable saving of chemicals, the high temporal resolution of the leaching processes, the accurate evaluation of sample mass to leachant volume ratios, and the improved reliability, robustness and automation with respect to methods with off-line analysis of extracts.

The intrinsic versatility of the MSFI analyzer has been exploited for the accommodation in a single set-up of two well-accepted schemes for fractionation of inorganic phosphorus, i.e., the HL and SMT protocols, even though the chemical composition of the extracts resulting from both schemes is significantly different. As a consequence of the most aggressive extractants utilized in the SMT protocol, higher leachable contents and sharper extraction profiles were encountered as compared to the HL scheme. However, SMT does not give information on the labile inorganic phosphorus, which is regarded to be the readily available fraction for plant uptake. Furthermore, the extreme chemical conditions adopted in this scheme are unlikely to mimic the changes in the chemical properties of the solid occurring under environmental scenarios.

The flow-through microcolumn system hyphenated with spectrophotometric detection has been also proven unique for accurate monitoring of available orthophosphate in the extracts due to the minimization of the potential hydrolysis of extracted organic and condensed phosphorus into orthophosphate.

Further research is aimed at expanding the flexibility of the multisyringe flow injection analysis system for monitoring of ultratrace levels of pollutants, viz., heavy metals and metalloids, in solid substrates following dynamic fractionation and on-line solid-phase extraction for isolation and pre-concentration of the targeted species.

Acknowledgments

Janya Buanuam is grateful for financial support granted by the Royal Golden Jubilee Ph.D. Program of the Thailand Research Fund and to the Postgraduate Education and Research Program in Chemistry (PERCH) of the Higher Education Development Project of the Commission on Higher Education (Thailand). Manuel Miró is indebted to the Spanish Ministry of Education and Science for contract sponsorship through the *Ramón y Cajal* research program. The authors are grateful to the Spanish Ministry of Education and Science for financial support through projects CTQ2004-03256 and CTQ2004-01201. Special thanks are also due to Anders Sølby (DTU workshop) for construction of the extraction microcolumn.

References

[1] F.M.G. Tack, M.G. Verloo, Intern. J. Environ. Anal. Chem. 59 (1995) 225.
[2] G. Rauret, Talanta 46 (1998) 449.
[3] A.V. Filgueiras, I. Lavilla, C. Bendicho, J. Environ. Monit. 4 (2002) 823.
[4] C. Gleyzes, S. Tellier, M. Astruc, Trends Anal. Chem. 21 (2002) 451.
[5] J. Hlavay, T. Prohaska, M. Weisz, W.W. Wenzel, G.J. Stingeder, Pure Appl. Chem. 76 (2004) 415.
[6] M. Miró, E.H. Hansen, R. Chomchoei, W. Frenzel, Trends Anal. Chem. 24 (2005) 759.
[7] W. Tiyapongpattana, P. Pongsakul, J. Shiowatana, D. Nacapricha, Talanta 62 (2004) 765.
[8] J. Shiowatana, N. Tantidanai, S. Nookabkaew, D. Nacapricha, J. Environ. Qual. 30 (2001) 1195.
[9] D. Beauchemin, K. Kyser, D. Chipley, Anal. Chem. 74 (2002) 3924.
[10] P.S. Fedotov, A.G. Zavarzina, B.Ya. Spivakov, R. Wennrich, J. Mattusch, K. de P.C. Titze, V.V. Demin, J. Environ. Monit. 4 (2002) 318.
[11] H. Kurosaki, S.M. Loyland-Asbury, J.D. Navratil, S.B. Clark, Environ. Sci. Technol. 36 (2002) 4880.
[12] L.-M. Dong, X.-P. Yan, Talanta 65 (2005) 627.
[13] M. Jimoh, W. Frenzel, V. Müller, H. Stephanowitz, E. Hoffmann, Anal. Chem. 76 (2004) 1197.
[14] M. Jimoh, W. Frenzel, V. Müller, Anal. Bioanal. Chem. 381 (2005) 438.
[15] J. Shiowatana, N. Tantidanai, S. Nookabkaew, D. Nacapricha, Environ. Int. 26 (2001) 38.
[16] M. Schreiber, M. Otto, P.S. Fedotov, R. Wennrich, Chemosphere 61 (2005) 107.
[17] P.S. Fedotov, R. Wennrich, H.-J. Stärk, B.Ya. Spivakov, J. Environ. Monit. 7 (2005) 22.
[18] P.S. Fedotov, E.Yu. Savonina, R. Wennrich, B.Ya. Spivakov, Analyst 131 (2006) 509.
[19] R. Chomchoei, M. Miró, E.H. Hansen, J. Shiowatana, Anal. Chem. 77 (2005) 2720.
[20] C.E. Lenehan, N.W. Barnett, S.W. Lewis, Analyst 127 (2002) 997.
[21] M. Miró, E.H. Hansen, Anal. Bioanal. Chem. 382 (2005) 878.
[22] R. Chomchoei, E.H. Hansen, J. Shiowatana, Anal. Chim. Acta 526 (2004) 117.
[23] R. Chomchoei, M. Miró, E.H. Hansen, J. Shiowatana, Anal. Chim. Acta 536 (2005) 183.
[24] M. Miró, E.H. Hansen, Trends Anal. Chem. 25 (2006) 267.
[25] M.A. Segundo, L.M. Magalhaes, Anal. Sci. 22 (2006) 3.
[26] B. Horstkotte, O. Elsholz, V. Cerdà, J. Flow Injection Anal. 22 (2005) 99.
[27] M. Miró, V. Cerdà, J.M. Estela, Trends Anal. Chem. 21 (2002) 199.
[28] A. Barbanti, M.C. Bergamini, F. Frascari, S. Miserocchi, G. Rosso, J. Environ. Qual. 23 (1994) 1093.

[29] P. Pardo, J.F. López-Sánchez, G. Rauret, Anal. Bioanal. Chem. 376 (2003) 248.
[30] B.Ya. Spivakov, T.A. Maryutina, H. Muntau, Pure Appl. Chem. 71 (1999) 2161.
[31] A.H.M. Hieltjes, L. Lijklema, J. Environ. Qual. 3 (1980) 405.
[32] V. Ruban, J.F. López-Sánchez, P. Pardo, G. Rauret, H. Muntau, Ph. Quevauviller, J. Environ. Monit. 1 (1999) 51.
[33] US-EPA method 3051, Microwave Assisted Acid Digestion of Sediments, Sludges, Soils, and Oils, Code of Federal Regulations, 1991, Title 40, Part 136, Paragraph 33.
[34] B. Kalberg, G.E. Pacey, Flow Injection Analysis: A Practical Guide, Techniques and Instrumentation in Analytical Chemistry, vol. 10, Elsevier, 1989, p. 49.
[35] J. Ruzicka, E.H. Hansen, Flow Injection Analysis, 2nd ed., Wiley/Interscience, New York, 1988, pp. 105–106.
[36] T. Fujiwara, K. Kurahashi, T. Kumamaru, H. Sakai, Appl. Organometall. Chem. 10 (1996) 675.
[37] J.-Z. Zhang, C.J. Fisher, P.B. Ortner, Talanta 49 (1999) 293.
[38] S.-C. Pai, C.-C. Yang, J.P. Riley, Anal. Chim. Acta 229 (1990) 115.
[39] C.X. Galhardo, J.C. Masini, Anal. Chim. Acta 417 (2000) 191.
[40] W. Tiyapongpattana, Application of Continuous Flow Technique for Sequential Extraction and for Determination of Phosphorus in Soil and Sediment, Master thesis, Mahidol University, Bangkok, Thailand, 2002.
[41] N. Amornthammarong, P. Anujaravat, K. Sereenonchai, P. Chisuwan, P. Sastranurak, P. Wilairat, D. Nacapricha, Talanta 68 (2005) 480.
[42] J. Buanuam, M. Miró, E.H. Hansen, J. Shiowatana, Anal. Chim. Acta 570 (2006) 224.
[43] G. Anderson, in: A.D. McLaren, G.H. Peterson (Eds.), Soil Biochemistry, vol. 1, Marcel Dekker, New York, 1967, pp. 67–90.
[44] B.L. Turner, B.J. Cade-Menun, L.M. Condron, S. Newman, Talanta 66 (2005) 294.
[45] E.W. Russell, Soil Conditions and Plant Growth, 11th ed., Longman Scientific & Technical, Harlow, UK, 1988.
[46] M.I. Makarov, L. Haumaier, W. Zech, Soil Biol. Biochem. 34 (2002) 1467.
[47] B.L. Turner, N. Mahieu, L.M. Condron, Soil Sci. Soc. Am. J. 67 (2003) 497.

Anal Bioanal Chem (2006) 386: 363–369
DOI 10.1007/s00216-006-0633-9

ORIGINAL PAPER

Nattikarn Kaewkhomdee · Chatvalee Kalambaheti · Somrudee Predapitakkun · Atitaya Siripinyanond · Juwadee Shiowatana

Iron fractionation for corrosion products from natural gas pipelines by continuous-flow sequential extraction

Received: 29 April 2006 / Revised: 13 June 2006 / Accepted: 16 June 2006 / Published online: 28 July 2006

Abstract The forms and quantities of iron species in corrosion product samples from natural gas pipelines were examined, using a continuous-flow sequential extraction system. Sequential extraction consists of four steps that dissolve water soluble iron ($FeSO_4$), acid soluble iron ($FeCO_3$), reducible iron (Fe-(oxyhydr)oxides) and oxidisable iron (FeS_2) fractions, respectively. Selectivity of extracting reagents for particular iron species was evaluated by determination of co-extracted anions, using ion chromatography, and evolved CO_2, using indirect flame atomic absorption spectrometer (FAAS). Iron was found predominantly in the reducible fraction (61–99%), indicating that Fe-(oxyhydr)oxides are the major constituents of the corrosion products.

Keywords Corrosion product · Iron fractionation · Sequential extraction

Introduction

Steel pipelines are widely used in the petroleum and natural gas industries, and the deterioration due to corrosion is a well-known problem. The cost of corrosion and corrosion protection in the United States of America is estimated to be in excess of 276,000 million dollars per year [1]. In natural gas pipelines, iron corrosion is an extremely complex process, because a large number of parameters are involved. Firstly, gas contaminants are primary causes of corrosion. The most common gases are O_2, CO_2 and H_2S [2, 3]. O_2 is not normally present in natural gas but can pass through leaks. It can cause corrosion problems, even at very low concentrations. CO_2 and H_2S are weakly acidic gases and become corrosive when dissolved in water. The corrosion products from O_2, CO_2 and H_2S contaminants are Fe-(oxyhydr)oxides, $FeCO_3$ and Fe-sulphide, respectively. Fe-sulphide may be present as FeS or FeS_2, depending on the corroding condition [3]. Secondly, microbiologically influenced corrosion (MIC) can occur from sulphate-reducing bacteria (SRB) [4]. SRB consume sulphate ion (SO_4^{2-}) and produce CO_2 and H_2S, which, on the other hand, can also enter the corrosion processes from organic fermentation. Finally, water plays a very significant role in corrosion.

The corrosion mechanism can be indicated by the anion side of the corrosion products or the iron compounds. The analysis and identification of corrosion products can assist the engineer to solve a corrosion problem by giving information that may help in understanding (1) the nature and type of corrosive attack, (2) the metal or metal phase that has been attacked in an alloy, (3) the environmental conditions that contribute to the corrosion.

Corrosion products are generally investigated by surface characterisation techniques such as X-ray diffraction (XRD) [2, 5–11], X-ray photoelectron spectroscopy (XPS) [6, 11, 12], Mössbauer spectroscopy [6, 8], Raman spectroscopy [3, 10] and scanning electron microscopy (SEM) combined with energy dispersive spectrometry (EDS) [2, 7, 10]. These techniques have been used complementarily to allow complete characterisation of the corrosion products. One method alone often has limitations; for example, identification by XRD can be very difficult when the crystallinity is very low (this is often the case for corrosion products). Detection limits of XRD and SEM-EDS are poor, and results obtained from XRD are sometimes difficult to interpret. The disadvantages of XPS are the need of high vacuum, poor resolution and low sensitivity, while Raman spectroscopy has low selectivity.

The sequential extraction technique has been widely used to fractionate metals in a solid sample according to their leachability. A succession of chemical reagents was employed

N. Kaewkhomdee · A. Siripinyanond · J. Shiowatana (✉)
Department of Chemistry, Faculty of Science,
Mahidol University, Rama VI Road,
Bangkok, 10400, Thailand
e-mail: scysw@mahidol.ac.th
Tel.: +66-2201-5122
Fax: +66-2354-7151

C. Kalambaheti · S. Predapitakkun
Analytical and Petroleum Research Department,
PTT Research and Technology Institute,
PTT Public Company Limited,
Ayutthaya 13170, Thailand

to extract, sequentially, various targeted phases in the sample. The results are useful for obtaining information about origin, mode of occurrence, bioavailability, potential mobility and transport of elements in natural environments [13–16].

In our previous work [17, 18], a continuous-flow sequential extraction system was developed for simplicity, rapidity, less risk of contamination and improved accuracy of the traditional sequential extraction technique. The dynamic extraction system also provides kinetics data for detailed investigation [19].

The objective of this study was to apply the dynamic extraction system to determine the fractional distribution of iron in corrosion products. An important problem with sequential extraction techniques is the selection of suitable extractants (types, concentrations, pHs and temperatures) to obtain a good selectivity of sequential extraction of sulphate, carbonate, (oxyhydr)oxides and sulphide phases of corrosion products. Ideally, the extraction schemes are designed to dissolve specifically one mineralogical phase at a time. The lack of selectivity of extractants used in some extraction schemes for soils, which leads to errors in fractionation data, has been reported [15, 16, 20, 21].

For the selectivity of an extraction scheme for iron, Heron et al. [22] reported an extraction scheme to study the fractionation of iron in contaminated aquifer sediments. These results were used to quantify the iron species associated with the sediment samples. The scheme was applied to standard iron, and the selectivity was confirmed by SEM and XRD. Poulton and Canfield [23] developed an extraction scheme for fractionation of iron in modern and ancient sediments. The selectivity of the extraction scheme was tested on standard iron compounds and their mixtures. Each scheme used a variety of extractants, and the results were highly dependent on the extraction scheme used. Criteria for selection of an extraction scheme included (1) nature of sample such as pH and organic content and (2) ability for defining the desired phase of metals. In this work, the modified sequential extraction scheme of the Standard, Measurement and Testing Program (SM&T) (formerly BCR) [15] was used to selectively extract, water soluble iron ($FeSO_4$), acid soluble iron ($FeCO_3$), reducible iron (Fe-(oxyhydr)oxides) and oxidisable iron (Fe-sulphide) fractions using a dynamic continuous-flow extraction system coupled with appropriate detection techniques. The selectivity of extractants for iron fractionation in corrosion products was examined by simultaneous determinations of iron and co-extracted anions. Being leached at the same time as observed in the extractograms obtained indicates chemical association of the ions. The dynamic extraction system was finally applied to study the forms and quantities of iron species in corrosion products.

Experimental

Chemicals and apparatus

All chemicals were of analytical grade. Milli-Q water was used throughout. Standard iron solution (1,000 mg l^{-1}) was purchased from Merck (Darmstadt, Germany). The working standards were prepared when required. $FeSO_4 \cdot 7H_2O$, Fe_2O_3 and FeS_2, purchased from M&B (Dagenham, UK), Sigma (Missouri, USA) and Fisher (Loughborough, UK), respectively, were dried at 100 °C to constant weight and kept in a desiccator until required. Plastic containers and glassware were cleaned and soaked in 10% (v/v) HNO_3 for at least 24 h and rinsed three times with Milli-Q water.

A flame atomic absorption spectrometer (Perkin-Elmer Model 3100, Connecticut, USA) equipped with a deuterium background corrector was used for the determination of iron in the extracts. Absorbance measurements were made at 248.3 nm.

Corrosion product samples

Corrosion product samples were collected from natural gas pipelines. All samples were washed with methanol and petroleum benzene, dried and ground in an agate mortar to obtain homogeneity. The ground samples were stored in a desiccator until required.

Continuous-flow extraction system

Extraction chamber

The continuous-flow extraction system employed in this work has been previously described (Fig. 1a) [17, 18]. The extraction chamber was designed to allow containment and stirring of a weighed sample. Extractants could flow sequentially through the chamber and dissolve the targeted phases. The chamber and its cover were constructed from borosilicate glass to have a capacity of approximately 10 ml. The outlet of the chamber was furnished with a Whatman (Maidstone, UK) glass microfibre filter (GF/B, 47 mm diameter, 1 μm particle retention) to allow dissolved matter to flow through. Extractant was pumped through the chamber by a peristaltic pump [Micro tube pump, MP-3N, EYELA (Tokyo Rikakikai Co. Ltd)] at approximately 4 ml min^{-1} using Tygon tubing of 2.25 mm inner diameter. Heating of the extractant, when required, was carried out by passing the extractant through a glass heating coil approximately 120 cm in length, which was placed in a water bath before the extraction chamber.

Extraction procedure

A weighed sample (0.25 g) was transferred to a clean extraction chamber, together with a magnetic bar. A glass microfibre filter was then placed on the outlet, followed by a silicone rubber gasket, and the chamber cover was securely clamped in position. The chamber was connected to the extractant reservoir and the collector vial by Tygon tubing and placed on a magnetic stirrer. The magnetic stirrer and peristaltic pump were switched on to start the extraction. The extracting reagents were continuously

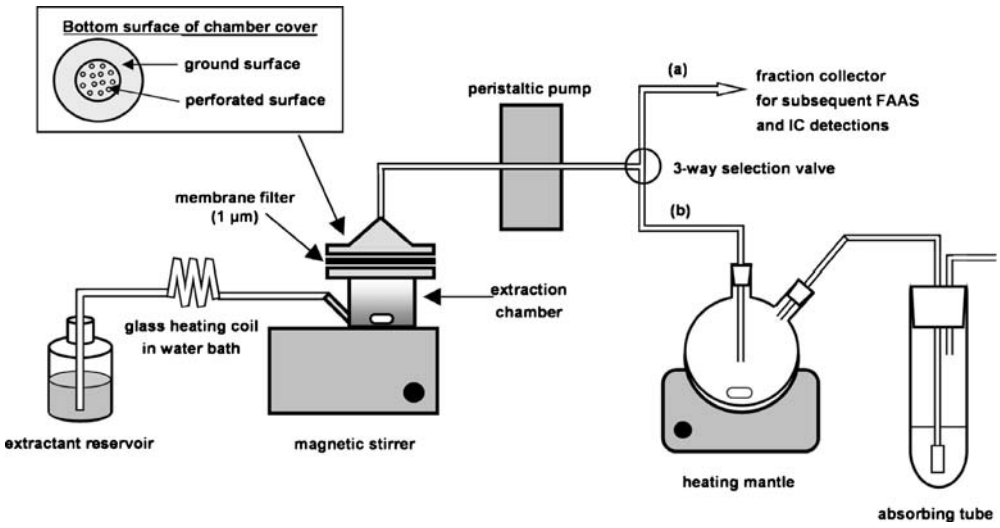

Fig. 1 Diagram of a continuous-flow sequential extraction system connected to (**a**) the fraction collector used in phases I, III and IV; (**b**) a unit used in phase II for collecting extract in the round-bottomed flask and CO_2 in the absorbing tube

moved through the chamber to effect a dynamic extraction process. The extract passed through the membrane filter, and collection of subfractions (60 ml volume intervals) was repeated until all four leaching steps had been completed.

Extraction scheme

The modified sequential extraction scheme of the Standard, Measurement and Testing Program (SM&T) (formerly BCR) [15] for iron was carried out on the following solutions:

Step I
: water, 70 °C (water soluble fraction)
Step II
: 0.11 mol l^{-1} CH_3COOH (acid soluble fraction)
Step III
: 0.1 mol l^{-1} $C_6H_8O_6$/ 0.2 mol l^{-1} $(NH_4)_2C_2O_4{\cdot}H_2O$ adjusted to pH 3.3 with HNO_3, 100 °C (reducible fraction)
Step IV
: 8: 3 v/v (30% H_2O_2: 0.02 mol l^{-1} HNO_3), 85 °C (oxidisable fraction)

Total dissolution of residue corrosion product samples and iron compounds

Residues from the extraction after steps I–IV or corrosion product samples (0.25 g) were digested with aqua regia (1:3 v/v mixture of concentrated HNO_3 and HCl) until the solutions were clear. After being cooled, the digested solutions were made up to volume in volumetric flasks. Iron compounds, i.e. $FeSO_4{\cdot}7H_2O$, Fe_2O_3 and FeS_2, were dissolved in pure hot water, concentrated HCl, and aqua regia, respectively. The dissolved solutions were diluted with pure water to the desired dilution factors.

Iron in extracts and digests were determined by flame atomic absorption spectrometer (FAAS) using external calibration.

Selectivity of extractants

For the selectivity study of extractants for the water soluble and oxidisable phases, the ion chromatographic equipment, consisting of a Waters Model 510 HPLC pump, an Alltech guard column and an Allsep Anion column (4.6 mm inner diameter), was used for sulphate separation. Detection was performed by a Waters Model 430 conductivity detector to monitor sulphate concentrations. Data were recorded with a Shimadzu Model C-R6A integrating recorder. An eluent of 4 mmol l^{-1} potassium hydrogen phthalate (KHP) was degassed ultrasonically before being used. For all samples, a 100 μl sample loop was used. The detection signal was recorded as peak height.

For the selectivity study of extractant for the acid soluble phase, the outlet tube of the extraction chamber was connected to a 250 ml two-necked round-bottomed flask, which was placed on a heating mantle. The other neck of the round-bottomed flask was connected to a Pyrex absorption tube, 25±200 mm, containing an absorbing solution (Fig. 1b). We evaluated the trapping efficiency of the absorbing solution by using successive absorbing tubes and found that only one absorbing tube was adequate to trap all the CO_2(g) evolved.

For this study the corrosion product sample was first treated with water to dissolve water soluble iron; the extracts were collected in fraction collectors. Then CH_3COOH at various concentrations (0.05 mol l^{-1}, 0.11 mol l^{-1}, 0.25 mol l^{-1}, 0.35 mol l^{-1} and 0.50 mol l^{-1}) was allowed to flow to leach the acid soluble iron. For this step the extract was collected in a two-necked round-bottomed flask, which was gently heated to purge the CO_2 quantitatively into an absorbing solution containing 2.5 mmol l^{-1} calcium hydroxide. The absorbing solution was centrifuged, and the amount of calcium in the supernatant was determined.

The amount of precipitated calcium carbonate ($CaCO_3$) was then calculated, and carbonate was determined. The concentrations of iron in the extracts and calcium were determined by FAAS.

In the reducible fraction the selectivity of extractant was not determined. Depending on the environmental conditions and oxidation pathways, different Fe-(oxyhydr)oxides can form [24], and, therefore, determination of the co-extracted anions is difficult. Therefore, the iron species of this phase is not specified in this paper. For the extractant used, ascorbic acid/oxalate solution was selected because of its reducing property and its high iron complexing capacity. This extractant has been widely used to dissolve metals in the reducible phase in many sequential extraction schemes [15].

Results and discussion

Typical extractogram of sequential extraction

With a continuous-flow extraction system, not only iron concentrations can be obtained, but also kinetics information of dissolution of various iron species from the sample can be observed in an extractogram (a graph of the metal concentration in a subfraction versus the corresponding subfraction number). A typical extractogram showing four iron species in corrosion product samples is given in Fig. 2. It also illustrates that the extractants are efficient in leaching the iron completely in each phase, because the iron concentration in the extract decreases to the baseline level before changing over to the next extractant. The extracted iron of each phase was determined by summation of the amounts in subfractions of the particular step. Overlaid extractograms of various species give additional information on their chemical association, as will be presented later in this manuscript.

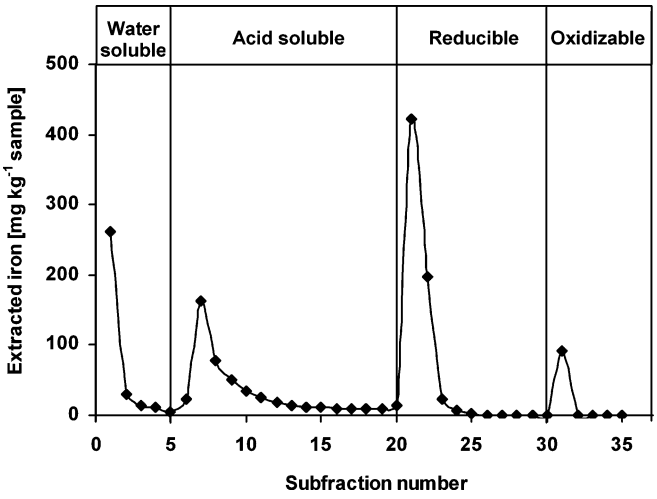

Fig. 2 Extractogram of iron for corrosion product sample as obtained by a continuous-flow sequential extraction system. Signals of water soluble, acid soluble and oxidisable phases were magnified ten times for clarity

Recovery of extraction of iron species

The efficiency of the four extractants employed in the modified SM&T extraction scheme for iron fractionation was primarily studied on pure iron compounds ($FeSO_4 \cdot 7H_2O$, Fe_2O_3 and FeS_2). The iron compounds and their mixture were subjected to total dissolution and sequential extraction followed by FAAS detection. Table 1 shows a very good selectivity of each extraction step, with less than 1% being extracted in other steps. Therefore, this extraction scheme showed satisfactory results for the possibility of studying iron species in real samples of corrosion products. Due to the complex nature of real samples, they may not behave similarly to the mixture of pure iron compounds. Therefore, the selectivity of the extractants for real samples was also investigated.

Selectivity of extractants

A number of sequential extraction schemes have been used for the elemental fractionation of soils and sediments. The accuracy of these schemes depends on many factors, especially the selectivity of the extractants used. In this work we performed a study of time-resolved extraction profiles of elements of concern to evaluate their co-elution, which, in turn, indicates chemical association. Ion chromatography was used to determine the sulphate concentration in the extracts of the water soluble and oxidisable steps. For the acid soluble extraction step, co-extracted carbonate was monitored. Carbonate ion generated in this step is not stable in the acidic medium. Therefore, the evolved CO_2 was trapped in a gas absorbing unit containing an absorbing solution with subsequent indirect FAAS measurement. Concentrations of iron, together with those of co-extracted anions, were plotted to confirm the association of iron with particular anions. Co-extraction and stoichiometric relationships of extracted iron and co-extracted anions were used to demonstrate the selectivity of extractant of each step.

Water soluble and oxidisable phases

In water soluble phase, iron sulphate ($FeSO_4$) was the main iron species in the samples. The selectivity of water for $FeSO_4$ was obvious from the solubility data of various forms of iron compounds likely to be present in the corrosion products, because $FeCO_3$, Fe-(oxyhydr)oxides and Fe-sulphide are not soluble in water. Nevertheless, this was confirmed by chromatographic determination of co-extracted sulphate in extracts. For the oxidisable extraction step, Fe-sulphides were oxidised by HNO_3/H_2O_2 to obtain ferric and sulphate ions (Eq. 1). Therefore, sulphate was also determined in this leaching step.

$$FeS_2(s)+7/2O_2+H_2O(aq) \rightarrow Fe^{3+}(aq)+2SO_4^{2-}(aq)+2H^+ \quad (1)$$

Table 1 Extraction recovery of iron from iron compounds in a four-step continuous-flow sequential extraction system (n=3) (*ND* not detectable)

Iron compound	Total iron [mg Fe]	Extracted iron [mg Fe]					Percentage of Fe recovered
		Water soluble phase	Acid soluble phase	Reducible phase	Oxidisable phase	Sum	
$FeSO_4 \cdot 7H_2O$	251±6	247±4	ND	ND	ND	247±4	98
Fe_2O_3	999±15	ND	ND	998±33	ND	998±33	100
FeS_2	258±8	ND	ND	2.0±0.1	245±8	247±8	96
$FeSO_4 \cdot 7H_2O^+$ Fe_2O_3+FeS_2	1,503±17	244±5	ND	991±20	245±7	1,480±28	98

At the selected experimental ion chromatographic conditions, carbonate, chloride, nitrate, oxalate, sulphate and thiosulphate can also be detected. Carbonate was eluted at void peak, while chloride, nitrate, oxalate, sulphate and thiosulphate can be detected at 5 min, 6 min, 7 min, 9 min and 12 min, respectively. The sulphate peak showed a well-defined resolved peak with no interfering anion peak. The calibration graph was rectilinear for 5-100 mg l^{-1} of sulphate, with a good linear regression (R^2=0.9998).

As can be seen in Fig. 3, no sulphate was detected in the extracts of acid soluble and reducible phases, and good correlation between the molar ratio of iron and sulphate in the water soluble (1:1) and oxidisable (1:2) steps confirmed the selectivity of water and 30% H_2O_2 in 0.02 mol l^{-1} HNO_3 for $FeSO_4$ and Fe-sulphide, respectively. In addition, the molar ratio of iron and sulphate in oxidisable phase from the extractograms was close to 2 indicating that FeS_2 was predominant in this phase. The extractograms demonstrated the usefulness of continuous-flow sequential extraction for chemical association studies. This type of study is not possible with a batch extraction, which gives only a single concentration of element for each step and does not provide a time-dependent extraction profile.

Acid soluble phase

CH_3COOH at various concentrations has been used to release metals associated with the carbonate fraction in soils [15, 16]. The efficiency of acid concentration in the extraction of this phase depends on several parameters, such as the nature and grain size of the sample and carbonate content. The effects on extractability of increasing the CH_3COOH concentration from 0.05 mol l^{-1} to 0.50 mol l^{-1} were investigated for corrosion products. Figure 4 shows that the amounts of extractable iron in the acid soluble phase depend on the concentration of CH_3COOH used. An increase in acid concentration causes a considerable increase in extractability. Low acid concentration was insufficient for the complete solubility of this carbonate phase, while higher concentration showed an improved efficiency of leaching but may cause partial dissolution of Fe-(oxyhydr)oxides, resulting in increased amounts of extractable iron. This could be a major source of overestimation of iron in the acid soluble step. Determination of co-extracted carbonate ion in the extracts by ion chromatography was not possible because the carbonate ion is not stable in the acidic medium. For this reason, the continuous-flow sequential extraction module was connected to a gas absorbing unit to monitor co-extracted carbonate ion for the study of selectivity of

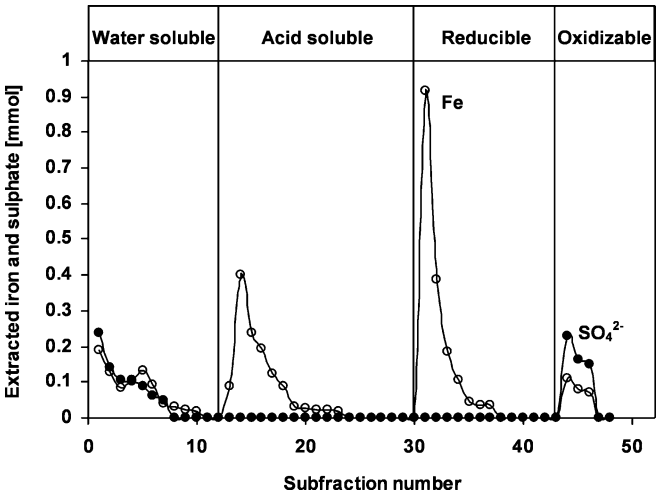

Fig. 3 Extractograms of iron (*open circles*) and sulphate (*closed circles*) for a corrosion product sample

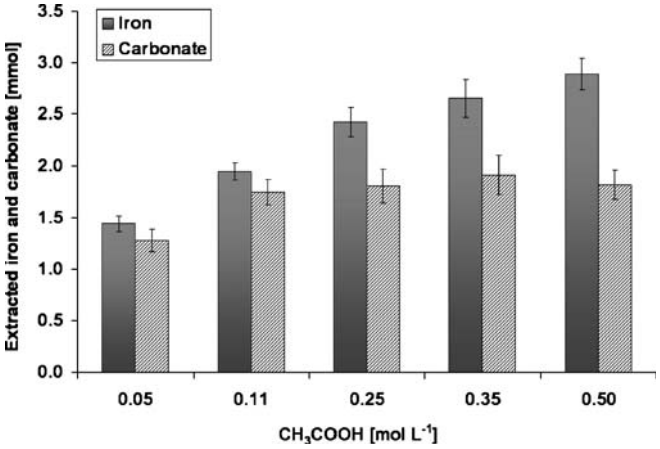

Fig. 4 Effect of the CH_3COOH concentrations on the extracted iron and carbonate (n=3)

Table 2 Iron species in corrosion product samples as determined by continuous-flow sequential extraction (n=3) (*ND* not detectable)

Sample ID	Extracted iron [mg Fe g^{-1} sample]				
	Water soluble phase	Acid soluble phase	Reducible phase	Oxidisable phase	Sum
001	ND	1.0±0.1	395.0±19.0	7.7±0.7	403.6±19.8
002	ND	58.4±3.9	334.6±8.7	3.8±0.9	396.7±12.4
003	3.9±0.2	22.1±1.9	185.2±18.2	1.7±0.5	213.0±20.5
004	0.1±0.0	0.7±0.1	318.8±21.4	ND	319.5±21.5
005	ND	42.4±5.0	367.3±23.1	1.5±0.0	411.3±28.1
006	ND	15.4±2.6	462.7±35.6	4.2±0.1	482.3±38.3
007	ND	2.8±0.2	371.9±8.2	8.9±0.5	383.5±8.7
008	ND	3.0±0.3	417.6±32.5	0.2±0.1	420.7±32.7
009	14.3±0.4	120.1±5.5	219.3±15.7	3.0±0.9	356.8±20.8
010	8.4±1.1	14.2±3.1	200.6±26.6	3.0±0.8	226.2±30.4
011	1.5±0.1	46.7±5.9	216.2±22.2	6.4±0.1	270.8±28.1

CH_3COOH in this extraction step. The concentrations of iron and co-extracted carbonate are used to evaluate the selectivity of the extractant. The results (Fig. 4) show that the amount of extracted iron increases at increasing concentrations of CH_3COOH. However, the co-extracted carbonate concentration becomes constant after 0.11 mol l^{-1} CH_3COOH, indicating that, at 0.11 mol l^{-1}, CH_3COOH is adequate to dissolve the carbonate phase. The increased amounts of iron at higher concentrations of CH_3COOH were due to partial dissolution of the Fe-(oxyhydr)oxides. For specific dissolution of $FeCO_3$, the molar concentrations of extracted iron and carbonate should be equal. The molar concentrations of iron and carbonate were found to be close to unity at 0.05 mol l^{-1} and 0.11 mol l^{-1} CH_3COOH, indicating selective leaching. Lower extractability at 0.05 mol l^{-1} CH_3COOH was due to incomplete dissolution. The higher extracted iron at CH_3COOH concentrations higher than 0.11 mol l^{-1} supported the aforementioned partial dissolution of Fe(oxyhydr)oxides and was further confirmed by the decreasing extracted iron in the reducible phase at increasing CH_3COOH concentrations. Therefore, the acid concentration of 0.11 mol l^{-1} was considered optimal for the acid soluble phase for corrosion product samples.

Application to corrosion product samples

The results presented above suggest that the extraction scheme developed can be used for evaluation of iron species in corrosion product samples. Results from its application to 11 samples (Table 2) showed the highest proportion of iron in the reducible fractions (61–99% of extractable iron). Fe-(oxyhydr)oxides appeared to be the major constituents of the corrosion products investigated, and, therefore, O_2 played an important role in the corrosion for these samples. Partial amounts of this phase may be transformed from $FeCO_3$. The study by Heuer and Stubbins [12] showed that $FeCO_3$ was unstable and quickly decomposed to Fe_2O_3 after contact with air. Very small proportions of iron were found in the water soluble and oxidisable fractions (0–4% of extractable iron). The sum of extracted and non-extracted iron (Table 3) from continuous-flow sequential extraction shows good agreement with the total concentration of iron obtained from acid

Table 3 Iron content in corrosion product samples as obtained from sequential extraction by continuous-flow system in comparison with acid digestion (n=3)

Sample ID	Extraction [%w/w]			Acid digestion [%w/w]
	Extracted[a]	Non-extracted (residue)	Sum	
001	40.4±2.0	1.6±0.7	41.9±1.3	42.9±0.4
002	39.7±1.2	0.0±0.0	39.7±1.2	39.1±1.6
003	21.3±2.0	1.2±0.2	22.5±1.9	24.1±0.2
004	32.0±2.1	16.7±3.9	48.6±1.8	49.6±0.4
005	41.1±2.8	12.1±0.4	53.3±2.4	55.5±1.6
006	48.2±3.8	0.3±0.4	48.5±3.4	50.0±3.8
007	38.4±0.9	4.7±1.0	43.1±0.6	44.5±2.0
008	42.1±3.3	4.8±1.2	46.9±2.3	47.1±0.3
009	35.7±2.1	6.4±0.4	42.0±2.1	44.2±0.2
010	22.6±3.0	13.4±1.4	36.0±2.1	36.2±0.8
011	27.1±2.8	5.4±1.2	32.5±2.3	33.1±0.3

[a]Summation of extracted iron from four extraction steps

digestion, with insignificant difference observed at the 95% confidence level. The non-extracted iron may be attributed to the iron associated with resistant complex species [25] that are insoluble in the extractants used. The residual or insoluble iron was difficult to dissolve and required aqua regia to facilitate solubilisation. The continuous-flow extraction method, with its collection of several subfractions, that we used in this work to obtain detailed extraction profiles could be tedious, and it required a large number of samples to be analysed. For practical use of this method, one fraction per step of sequential extraction is sufficient to obtain fractionation data. Additional advantages of the continuous-flow approach are the ease of operation and freedom from environmental and procedural contamination.

Conclusions

A continuous-flow sequential extraction was utilised to fractionate iron species in corrosion products from natural gas pipelines. Information on forms and quantities of iron in the samples can be obtained. The total concentration of iron was found to be in the range of 21–48% w/w. Iron is predominantly present in the reducible fraction. This indicates that corrosion products mostly result from O_2 (as gas contaminant) and water. Techniques such as ion chromatography and gas absorption with carbonate detection were applied to study the selectivity of extractants for the targeted iron phases. Ion chromatography was used to determine the amount of sulphate in the extracts of water soluble and oxidisable extraction steps to confirm the co-extraction of sulphate and sulphide. Simultaneous collection and determination of CO_2 generated from leaching of carbonate species revealed the association of iron and carbonate in the acid soluble fraction of corrosion products. The iron fractionation data can be used to understand the origins and mechanisms of corrosion and, consequently, to prevent or solve the corrosion problems in the petroleum and natural gas industries.

Acknowledgements The authors are grateful for the financial support of the Thailand Research Fund and the Postgraduate Education and Research Programme in Chemistry, Higher Education Development Project of the Commission on Higher Education. Funding from the Analytical and Petroleum Research Department, PTT Research and Technology Institute, PTT Public Company Limited, is also acknowledged.

References

1. Lee AK, Newman DK (2003) Appl Microbiol Biotechnol 62:134–139
2. Sembiring S (1999) Conference:‘ad infinitum’ a scope of science. Curtin University, Australia, pp 57–62
3. Bernard MC, Duval S, Joiret S, Keddam M, Ropital F, Takenouti H (2002) Prog Org Coat 45:399–404
4. Beech IB, Gaylarde CC (1999) Rev Microbiol 30:177–190
5. Peters NJ, Davidson CM, Britton A, Robertson SJ (1999) Fresenius J Anal Chem 363:562–565
6. Marco JF, Gracia M, Gancedo JR, Luengo MA, Joseph G (2000) Corros Sci 42:753–771
7. Roh Y, Lee SY, Elless MP (2000) Environ Geol 40:184–194
8. Rao TS, Sairam TN, Viswanathan B, Nair KVK (2000) Corros Sci 42:1417–1431
9. Peulon S, Antony H, Legrand L, Chausse A (2004) Electrochim Acta 49:2891–2899
10. Neff D, Dillmann P, Bellot-Gurlet L, Beranger G (2005) Corros Sci 47:515–535
11. Tang Z, Hong S, Xiao W, Taylor J (2006) Corros Sci 48:322–342
12. Heuer JK, Stubbins JF (1999) Corros Sci 41:1231–1243
13. Tessier A, Campbell PGC, Bisson M (1979) Anal Chem 51:844–851
14. Quevauviller Ph (1998) Trends Anal Chem 17:289–298
15. Gleyzes C, Tellier S, Astruc M (2002) Trends Anal Chem 21:451–467
16. Sahuquillo A, Rigol A, Rauret G (2003) Trends Anal Chem 22:152–159
17. Shiowatana J, Tantidanai N, Nookabkaew S, Nacapricha D (2001) Environ Int 26:381–387
18. Shiowatana J, Tantidanai N, Nookabkaew S, Nacapricha D (2001) J Environ Qual 30:1195–1205
19. Buanuam J, Shiowatana J, Pongsakul P (2005) J Environ Monit 7:778–784
20. Kheboian C, Bauer CF (1987) Anal Chem 59:1417–1423
21. Quan SX, Bin C (1993) Anal Chem 65:802–807
22. Heron G, Crouzet C, Bourg CM, Christensen TH (1994) Environ Sci Technol 28:1698–1705
23. Poulton SW, Canfield DE (2005) Chem Geol 214:209–221
24. Cornell RM, Schwertmann U (2003) in the iron oxides: structure, properties, reactions, occurrences and uses, 2nd edn. Wiley, Weinheim
25. Hall GEM, Vaive JE, Beer R, Hoashi M (1996) J Geochem Explor 56:59–78

Development of a simple extraction cell with bi-directional continuous flow coupled on-line to ICP-MS for assessment of elemental associations in solid samples†

Janya Buanuam,[a] Kasipa Tiptanasup,[a] Juwadee Shiowatana,*[a] Manuel Miró[b] and Elo Harald Hansen[c]

Received 4th September 2006, Accepted 18th October 2006
First published as an Advance Article on the web 26th October 2006
DOI: 10.1039/b612721e

A continuous-flow system comprising a novel, custom-built extraction module and hyphenated with inductively coupled plasma-mass spectrometric (ICP-MS) detection is proposed for assessing metal mobilities and geochemical associations in soil compartments as based on using the three step BCR (now the Measurements and Testing Programme of the European Commission) sequential extraction scheme. Employing a peristaltic pump as liquid driver, alternate directional flows of the extractants are used to overcome compression of the solid particles within the extraction unit to ensure a steady partitioning flow rate and thus to maintain constant operationally defined extraction conditions. The proposed flow set-up is proven to allow for trouble-free handling of soil samples up to 1 g and flow rates $\leq$10 mL min^{-1}. The miniaturized extraction system was coupled to ICP-MS through a flow injection interface in order to discretely introduce appropriate extract volumes to the detector at a given time and with a given dilution factor. The proposed hyphenated method demonstrates excellent performance for on-line monitoring of major and trace elements (Ca, Mn, Fe, Ni, Pb, Zn and Cd) released when applying the various extracting reagents as addressed in the BCR scheme, that is, 0.11 M CH_3COOH, 0.1 $NH_2OH \cdot HCl$ and 30% H_2O_2, even when a well recognized matrix-sensitive detector, such as ICP-MS, is used. As a result of the enhanced temporal resolution of the ongoing extraction, insights into the breaking down of phases and into the kinetics of the metal release are obtained. With the simultaneous multielement detection capability of ICP-MS, the dynamic fractionation system presents itself as an efficient front-end for evaluation of actual elemental association by interelement comparison of metals leached concurrently during the extraction time. Thus, the intimate elemental association between Cd and Zn in contaminated soils could be assessed.

1. Introduction

At present, it is widely accepted that risk assessment of trace elements contaminating environmental solid substrates is a topic of utmost relevance in environmental studies. This information can be used for evaluation of the impact on biota and serves as a reference of environmental policy decisions. In soil analysis, knowledge about the chemical forms of elements is required, because of its close link to the mobility and bioavailability of the species, which cannot be assessed by merely measuring the total concentration of the elements.

Batch sequential extraction procedures are conventionally employed for the fractionation of metals according to their leachability.[1–7] This technique makes use of suitable chemical reagents, which are applied, in a given order, to the sample to sequentially attack metals associated with different solid compartments. However, the batch procedures suffer from several shortcomings, such as being tedious, time consuming and being prone to risk of contamination and to metal adsorption/re-distribution phenomena, and, more importantly, they are able to provide neither information about the kinetics of leaching nor a detailed insight of the bindings of the metals within the solid phases.

Recent trends in the soil analysis field have been towards the development of methods aimed at tackling these drawbacks and additionally at mimicking environmental events more accurately than their classical extraction counterparts. The dynamic (non-equilibrium)-based extraction approach has proven to constitute an appealing alternative for trace element partitioning.[8] Thus, a number of research groups have proposed singular flow-through extraction systems[9–16] based on continuous or discontinuous delivery of fresh portions of the leaching reagents through small column-devices containing the solid material. A notable limitation of the flow-through extraction approach is the small inner dimension of the solid containers, the use of high amounts of sample can therefore cause unstable extraction flow rates due to blockage of the in-

[a] *Department of Chemistry, Faculty of Science, Mahidol University, Rama VI Road, Bangkok, 10400, Thailand. E-mail: scysw@mahidol.ac.th; Fax: +66-2354-7151; Tel: +66-2201-5122*
[b] *Department of Chemistry, Faculty of Sciences, University of the Balearic Islands, Carretera de Valldemossa km. 7.5, E-07122 Palma de Mallorca, Illes Balears, Spain*
[c] *Department of Chemistry, Technical University of Denmark, Kemitorvet, Building 207, DK-2800 Kgs. Lyngby, Denmark*
† The HTML version of this article has been enhanced with colour images.

line filters by solid particles. Even though fast extraction and screening of trace element release can be accomplished by using small amounts of sample (typically $\leq$ 25 mg),[10,13–15] this does require that highly homogeneous environmental solids should be used.

By using flow-through approaches, on-line extraction measurements have become possible.[10,13–15,17–19] Chomchoei *et al.*[19] described the feasibility of coupling flow-through microcolumn extraction to classical FAAS. However, the simultaneous monitoring of metals was inherently restricted due to the single element detection nature of the detector. Therefore, hyphenated techniques based on the combination of dynamic extraction systems with a powerful multielement detector, *i.e.* ICP-OES or ICP-MS, should prove especially attractive for metal fractionation in environmentally relevant solids. Not only saving of analysis time per fraction but more accurate information on interelement interaction in solid phases should make it appealing for on-line fractionation/detection protocols. The on-line analysis of the extracts by ICP-OES measurements has been recently demonstrated by Fedotov *et al.*[18] who used a rotating coiled column as sample compartment coupled with the detector. Unlike in Fedotov's work, Jimoh *et al.*[15] exploited a flow injection manifold as an interfacing unit between the soil microcartridge and the detector to allow for a flexible manipulation of the leaching agents and to provide a universal means of coupling to different analytical instruments. The main shortcoming of the microcartridge approach is the small sample size (5 mg) used for fractionation.

In this work, the potential of flow-through sequential extraction hyphenated on-line with ICP-MS for exploration of elemental distribution and associations within soil phases is demonstrated. A simple, continuous-flow set-up based on bi-directional flow extraction is proposed for preventing the clogging of the membrane surfaces incorporated within the extraction module by solid particles. The ability to handle larger sample amounts and higher extraction flow rates as compared with earlier works will be also ascertained.

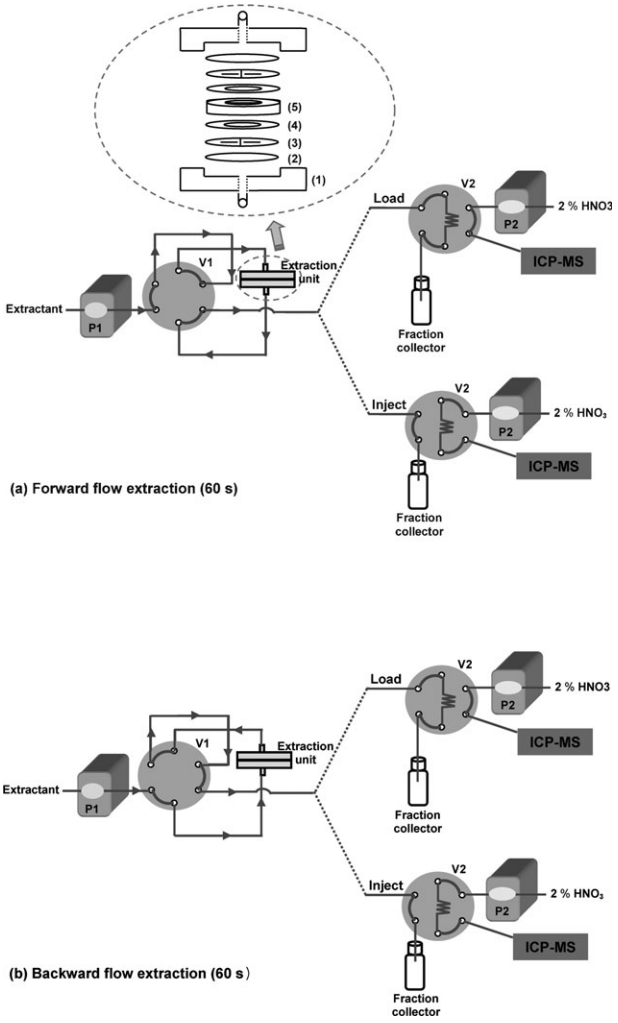

Fig. 1 Schematic diagram of the flow-through fractionation system coupled to ICP-MS for on-line elemental monitoring *via* the flow injection network; (a) forward and (b) backward extraction flow directions. P1 and P2, pumps; V1 and V2, 6 port rotary valves. (Top) Exploded view of the extraction unit comprising the following components: (1) extraction cap, (2) membrane filter, (3) filter support, (4) silicone gasket, (5) sample container. For operational details, see text.

2. Experimental

2.1 Preparation of standard solution and glassware

The chemical reagents used were of analytical grade. Ultrapure water from a Branstead water purification unit (Branstead International, IA, USA) was used throughout. Working standard solutions were prepared by appropriate dilution of the multi-element stock solution for ICP-MS (AccuStandard, Inc., CT, USA) with extracting reagents. All glassware and plastic containers were cleaned and soaked in 10% (v/v) HNO_3 for at least 24 h and rinsed with ultrapure water before use.

2.2 Extraction unit

The dedicated flow-through extraction unit employed in this work is shown in Fig. 1. It was machined out of polyoxymethylene that can tolerate the extractants used. The unit comprises two polyoxymethylene end-caps, glass microfibre membrane filters, PTFE membrane supports designed for maximizing extractant flow through the entire sample, silicone gaskets and a cylindrical sample container with an approximate inner volume of 2.8 mL. All parts were assembled according to the numbering order given in the figure. The amount of soil sample (up to 1.0 g) was placed in the sample container and sandwiched with glass microfibre filters (47 mm diameter, 1 μm pore size (Whatman, Maidstone, UK)) together with the PTFE membrane supports. The silicone gaskets were used to prevent leakage. The whole compartment was screwed tightly in position.

2.3 Soil material

The SRM 2711 from the National Institute of Standard and Technology was used for evaluation of accuracy and reliability of the proposed hyphenated technique and to allow for further

comparison of results. The soil material was collected from the tilled layer of a wheat field (MT, USA). It is a moderately contaminated pasture soil that was oven-dried, sieved and blended to achieve a high degree of homogeneity, the total concentration being certified for a number of elements.

A top soil sample (0–10 cm) from Tak Province, Thailand was used for evaluation of the ability of the designed extraction unit to handle different ranges of soil particle sizes as well as the maximum soil amount applicable without causing an unstable extraction flow rate. Being an alkaline sandy clay loam soil (pH 7.48) having 3.17% organic matter, the soil sample was ground and sieved for obtaining soil particle sizes of <150, 150–250 and >250 μm, respectively.

2.4 Extracting reagents

The BCR three-step sequential extraction scheme[4] was conducted in a dynamic fashion. The extracting reagents utilized and the corresponding targeted phases are detailed as follows: (i) 0.11 M CH_3COOH (metals bound to carbonate, the so-called acid soluble fraction); (ii) 0.1 M $NH_2OH \cdot HCl$ in 25% CH_3COOH adjusted to pH 2 with HNO_3 (metals bound to Fe or Mn oxides, the so-called reducible fraction); (iii) 30% H_2O_2 (metals bound to organic matter, the so-called oxidizable fraction)

2.5 Dissolution of soil residues

A closed-vessel microwave digestion system (Milestone model MLS-1200 Mega, Bergamo, Italy) was employed for pseudo-total digestion of residues. The residue leftover after the flow-through sequential extraction scheme was transferred to a digestion vessel of 20 mL capacity together with concentrated HNO_3 (5 mL) and 30% H_2O_2 (5 mL). The vessel was then tightly sealed and subjected to a microwave digestion protocol. The microwave digestion program consists of 5 steps, using power levels and durations of /250/400/500/600/0 W and /10/5/10/5/5 min, respectively. After cooling, the clear digests were transferred and made up to an appropriate volume with deionized water and the content of metals was determined by ICP-MS.

2.6 System configuration

The configuration of the bi-directional continuous-flow extraction system devised for dynamic metal fractionation and on-line monitoring of the extracts is depicted in Fig. 1. A peristaltic pump (P1) (Micro-tube pump, MP-3N, EYELA (Tokyo Rikakikai Co., Ltd.)) was employed for continuously propelling the leaching reagents through the extraction unit at varying flow rates. The alternate change of extractant flow direction was performed by the aid of the rotary valve (V1) (Upchurch Scientific, Inc., WA). The interfacing of the extraction unit with the detection device was effected *via* a discrete loop incorporated within a 6 port injection valve (V2) (Upchurch Scientific, Inc., WA), which upon actuation allowed the content of the loop to be introduced into the ICP-MS *via* a second peristaltic pump (P2). 2%HNO_3 was used as carrier and was continuously pumped to the nebulizer of the ICP-MS (Sciex Elan 6000, Perkin Elmer, CT) by P2 (Gilson, France) at a flow rate of 1.2 mL min^{-1}. All outlets of the rotary valves were connected through PEEK ferrules with rigid PTFE tubing (0.8 mm id). All connections consisted of Tygon tubing of 1.2 mm (id). The extract loop was also made of Tygon tubing (26.5 cm long, 1.2 mm id) with an internal volume of *ca.* 300 μL.

The ICP-MS operating conditions are as follow: RF power 1350 W; nebulizer, auxiliary and plasma gas flow rate are 0.99, 0.9 and 15 L min^{-1}, respectively; isotopes monitored being ^{44}Ca, ^{55}Mn, ^{54}Fe, ^{60}Ni, ^{66}Zn, ^{111}Cd and ^{208}Pb.

2.7 Operational procedure for bi-directional continuous-flow sequential extraction and on-line ICP-MS detection

An amount of 0.25 g of soil sample was selected for on-line fractionation studies. Initially, V1 and V2 were switched to the forward and load positions, respectively, and P1 was started to continuously pump 0.11 M CH_3COOH at the flow rate of 5.0 mL min^{-1} through the extraction unit for allowing the leaching of elements from the solid sample to take place. At this stage, the valve loop was filled with extract containing the released elements, the surplus flowing into the sample collector of 30 mL capacity. After 30 s of extraction, valve V2 was switched to the inject position and the extract zone entrapped within the sample loop was by means of P2 transferred to the ICP-MS as propelled by the carrier solution (2% HNO_3). When the extract had been flushed out from the extract loop, V2 was returned to its original position. After a total of 60 s of extraction in the forward direction, V1 was activated to the backward position (Fig. 1b.), causing the extracting reagent to flow in the opposite direction through the extraction unit for 60 s before being turned to the forward position once again. During the 60 s of backward flow, sampling by V2 was effected in the same manner as described for the forward flow direction. In general, the forward and backward extractions are repeated until the signals of the elements under investigation are close to baseline. Thereafter, the next extracting reagent (*viz.*, 0.1 M $NH_2OH \cdot HCl$ or 30% H_2O_2) is introduced and the operation repeated until all three extraction steps have been completed.

Apart from online ICP-MS detection, the extracts collected in each sample collector were analyzed by ICP-MS for metal quantification. The results were used for confirmation of the reliability of the proposed technique.

3. Results and discussion

3.1 Performance of the bi-directional continuous-flow extraction approach for sequential extraction

In on-line fractionation/detection schemes, a critical issue to take into account for successful coupling of the extraction module with the detection instrument is the requirement of a steady flow rate. Actually, an unstable extraction flow rate due to blocking of the in-line filters by solid particles would impede the metering of accurate volumes of leachates, thus hindering the real-time monitoring of the extracts. Non-constant extraction flow rates were, in fact, pronounced in our first design, namely, a continuous-flow stirred-flow cell unit, involving uni-directional flow of the extractants.[20,21] Although this problem recently most elegantly was solved by the development of a

new dynamic extraction approach[16] incorporating a bi-conical microcolumn within a sequential injection network, it requires more expensive, software-controlled instrumentation.

In order to provide a cost-effective flow-through partitioning system, the bi-directional continuous-flow extraction concept is therefore proposed. It is based on an alternate change of extractant's flow direction through the extraction chamber with two filtering membranes at both ends of the sample compartment. This approach prevents the compactness of solid particles on the membrane filter surface and at the same time favors an intimate sample–extractant contact. The bi-directional flow extraction system requires solely a peristaltic pump for continuous delivering of the extracting agents. Besides the cost effectiveness, simplicity and ease of operation are additional advantages. In order to assess the performance of the developed system, potential factors affecting the extraction flow rate were taken into consideration.

Fine solid particles as well as high delivery rates for the extractants are prone to cause the deterioration of the analytical performance of the ongoing extraction. Fine particles are easily retained within the membrane pores, while high pumping rates generate increased flow impedance. An unsteady extraction flow rate is especially noticeable whenever the extractant is continuously and unidirectionally pumped through the extraction vessel.[10,15,21] However, in the bi-directional continuous-flow system sample weights of 250 mg, soil particle sizes of even <150 μm, and extraction flow rates as high as 10 mL min^{-1} are admissible without any observable decrease of the extraction rate. As a result of the application of high extractant flow rates, the leaching behavior of readily mobilisable elements can be thoroughly investigated as opposed to previous reports where the extraction flow rate was ≤ 3 mL min^{-1}.[11,15–18]

A major issue in microcolumn fractionation approaches is the capability of handling environmentally representative sample amounts. Recent works reported the use of solid masses ≤ 25 mg,[10,13–15] which are only appropriate for highly homogeneous substrates. Beauchemin *et al.*[10] experienced significant flow back-pressure when scaling the sample size up from 25 to 250 mg in a microcolumn approach. By exploiting the devised extraction module with a top soil sample from Tak Province, Thailand (see Section 2.3), sample amounts as high as 1.0 g could be processed on-line without deterioration of the extraction flow rate when soil samples with particle sizes within the ranges of >250, 150–250 and <150 μm were analyzed at rates of ≤ 7.0 mL min^{-1}. Thus, soil particle size, extractant delivery rate and amount of sample had virtually no effect on the extraction flow rate.

3.2 Instrumental configuration of the hyphenated technique for on-line fractionation exploiting bi-directional flow

A bi-directional continuous-flow sequential extraction system hyphenated with ICP-MS *via* a flow injection network is here proposed for concurrently monitoring of the various trace and major metals released during the extraction protocols. This contrasts with recent publications from Beauchemin *et al.*[10] and Fedotov *et al.*[18] who directly coupled the extraction line with ICP-MS and ICP-OES, respectively. The interfacing of the extraction and detection streams *via* an FI manifold was selected in the present work because it offers several advantages, such as (i) independent control of the nebulization and the extraction flow rates, and (ii) the possibility of automatic on-line dilution of the extract matrix. Although ICP-MS has been considered as a powerful analytical tool for metal determinations as a result of its high sensitivity, wide linear range and multielemental capabilities, it is well known as a matrix-sensitive detector. The intrinsic low tolerance level of total dissolved solids[22,23] limits its potential use for metal determination in matrices containing high electrolyte concentrations. In fact, a dramatic decrease of the instrument's sensitivity was found within 1 h of operation when the CH_3COOH-extracts in the collected fractions were directly introduced into the nebulizer. The deposition of carbon and soil matrices on the sampler cone of the MS interface drastically affected the sensitivity and the stability of the signals. However, as a consequence of the dispersion/dilution of the minute extract volume within the carrier stream during transportation to the detector, the present set up expectedly yielded much fewer matrix interferences and generally did not give rise to problems for on-line detection of the various leachates. By using FI discrete sample introduction, the operational time can be extended significantly without observable reduction in sensitivity.

3.3 Data treatment and evaluation of the hyphenated bi-directional continuous flow sequential extraction set-up for the exploration of metal partitioning

Although membrane supports working as diffusers were inserted in the extraction unit to facilitate a close contact between soil particles and the leaching reagent, the extractability in the two flow directions was noticeably different, as can be observed in the raw signals illustrated in Fig. 2a. This happens regardless of the extraction unit orientation (horizontal or upright) or direction sequence (left to right or *vice versa*) of extraction. The occurrence was still observed when the internal volume of the extraction unit was reduced from 2.8 to 1.4 mL. This effect is very likely due to the different leachant fractions analyzed on-line, as a consequence of slight differences in the flowing paths of the leaching agents in both directions and the manual operation of the injection valves, while the influence of the flow direction on the fluidized bed-like extraction conditions might also play a role.

The raw extraction patterns were therefore processed in order to obtain a kinetic leaching profile. The final extractogram (Fig. 2b) was the result of averaging each pair of forward and backward peaks: each such average was plotted against the average exposure time. The quantification of the total extractable amount of elements was effected by integration of the processed extractogram.

The SRM 2711 was used to evaluate the accuracy and reliability of the hyphenated system. The extractable metal content obtained *via* on-line detection was compared with the off-line mode, involving the determination of metal concentrations in the fraction collectors and also with previously reported data of batchwise extraction.[24] As is apparent, both on-line and off-line modes in the proposed approach yielded

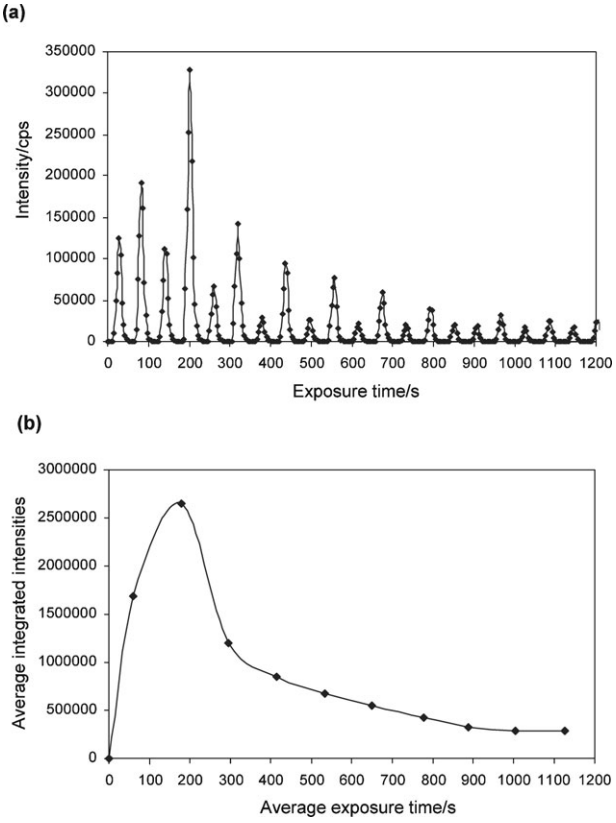

Fig. 2 Extraction profiles of Cd for the acid-soluble step, as obtained from the bi-directional continuous-flow extraction system coupled on-line to ICP-MS. (a) Raw signals showing alternate forward and backward peaks; and (b) processed profile obtained by averaging each pair of forward and backward peaks. Sample SRM 2711.

values which were insignificantly different at the significance level of 0.05 for every extraction step of all metals studied (see Table 1). Comparing batch and flow-through extraction, the percentage distribution of metals in the various fractions was significantly different. This is caused by the variable, operationally-defined, experimental conditions used in the two approaches. The redistribution/readsorption of leached metals onto the remaining solid substrate during a long extraction period, the different extraction times, and/or the incomplete metal leaching[25] in equilibrium-based extraction protocols may contribute to the different metal partitioning patterns. In contrast with batch extraction, the dynamic method minimizes the risk of readsorption due to the fact that the contact time between the solid and the liquid phases is minimized by the continuous delivery of fresh portions of leaching reagent through the soil container. However, the total concentrations of Cd, Ni, Pb and Zn obtained by summation of all fractions plus residue from the flow-through hyphenated technique as well as batch extractions are in good agreement with the certified concentrations in SRM 2711. However, those of Ca, Fe and Mn show lower recoveries probably due to the incomplete digestion in the pseudo-total analysis of the residual fraction.

3.4 Investigation of the metal soil phase associations

Apart from the detailed insight into metal distribution in the various phases, the extractogram of each element, as obtained by a graphical plot of the extracted concentration against the leaching time, can provide additional information. The appearance of leaching peaks in the extractograms enables an examination of the selectivity of extracting agents for each nominal soil phase and the binding between trace elements and soil parent phases. An illustration of this study is shown in Fig. 3. In the first step of extraction, CH_3COOH was used for dissolving $CaCO_3$ and releasing metals bound to that phase. For the second step, $NH_2OH \cdot HCl$ was used for attacking oxides/hydroxides of Fe and Mn. Therefore, simultaneous monitoring of the stripping of trace metals and major elements in solid phases, *i.e.* Ca, Fe and Mn, can be used for demonstrating how trace elements are bound to the particular soil phases.

As seen in the extractogram, peak positions and shapes between targeted metals (*viz.*, Cd and Pb) are all accompanied

Table 1 Comparison of extractable metal contents (mg kg^{-1}) for SRM 2711 as obtained by the bi-directional continuous-flow sequential extraction system with on-line and off-line ICP-MS detection modes and batchwise fractionation

		Step I	Step II	Step III	Residual	Sum	Certified value
Cd	This work (on-line)[a]	18.8 ± 0.5	13.7 ± 1.6	2.13 ± 0.25	2.82 ± 0.01	37.5 ± 1.7	41.70 ± 0.25
	This work (off-line)[a]	19.9 ± 0.5	14.5 ± 0.9	2.01 ± 0.1	2.82 ± 0.01	39.2 ± 1.0	
	Ho *et al.* (batch)[b]	28.6 ± 1.1	9.3 ± 0.6	2.4 ± 0.9	<1	40.2 ± 0.8	
Ni	This work (on-line)	2.7 ± 0.3	<D.L[c]	<D.L[c]	17.3 ± 2.0	20.0 ± 2.0	20.6 ± 1.1
	This work (off-line)	3.2 ± 0.1	<D.L	<D.L	17.3 ± 2.0	20.5 ± 2.0	
Pb	This work (on-line)	168 ± 11	517 ± 52	187 ± 15	149 ± 20	1021 ± 59	1162 ± 31
	This work (off-line)	187 ± 8	570 ± 24	212 ± 7	149 ± 20	1118 ± 33	
	Ho *et al.* (batch)	302 ± 27	349 ± 32	356 ± 85	97.9 ± 19.7	1100 ± 100	
Zn	This work (on-line)	94.9 ± 9.0	70.8 ± 1.7	129 ± 14	66.6 ± 2.3	361 ± 17	350.4 ± 4.8
	This work (off-line)	96.5 ± 6.9	73.8 ± 0.7	140 ± 7	66.6 ± 2.3	377 ± 10	
	Ho *et al.*(batch)	41.8 ± 1.2	62.2 ± 7.1	37.1 ± 13.3	206 ± 33	347 ± 34	
Ca	This work (on-line)	9630 ± 610	1910 ± 120	2100 ± 170	8500 ± 660	22 100 ± 900	28 800 ± 800
	This work (off-line)	9920 ± 430	2110 ± 50	2050 ± 60	8500 ± 660	22 600 ± 800	
Fe	This work (on-line)	301 ± 27	1771 ± 120	865 ± 76	18 270 ± 770	21 200 ± 800	28 900 ± 600
	This work (off-line)	310 ± 15	1900 ± 113	897 ± 54	18 270 ± 770	21 400 ± 800	
Mn	This work (on-line)	145 ± 4	211 ± 13	15.5 ± 1.3	159 ± 14	531 ± 20	638 ± 28
	This work (off-line)	157 ± 5	233 ± 5	15.4 ± 0.7	159 ± 14	564 ± 16	

[a] Results are expressed as the mean of 3 replicates ± standard deviation. [b] Former BCR scheme in batchwise extraction.[24] [c] The detection limits were 0.2 and 0.1 μg kg^{-1} for steps II and III of extraction, respectively.

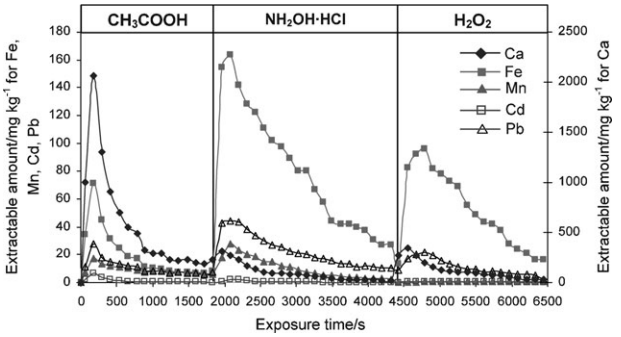

Fig. 3 Processed extractograms of trace and major elements in SRM 2711, as obtained from the three step BCR sequential extraction scheme performed in the proposed extraction system in hyphenation with on-line ICP-MS detection.

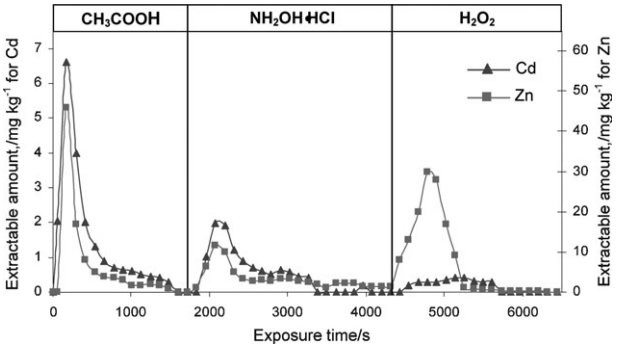

Fig. 4 Processed extraction profiles for Cd and Zn in SRM 2711.

by a Ca peak in step I and Fe and Mn peaks in step II. This can be taken as evidence that the release of Cd and Pb by CH_3COOH and $NH_2OH \cdot HCl$ is dependent on the dissolution of soil solid phase material. This proves that the fraction of both metals retained by exchangeable soil sites is not as relevant as the Ca-bound fraction. Therefore, the dynamic fractionation method should be regarded as appealing approach for discrimination of soil phase associations taking into account the lack of selectivity of the three BCR extracting reagents for a defined soil compartment.

A detailed extractogram also provides further knowledge on the homogeneity of binding and mobility of metals in the nominal phases. The surface bound metals would dissolve earlier than the remaining in the same soil fraction and generate a distorted peak profile.[26] It is clear that the present approach provides a better way for exploration of metal soil phase associations that can be of utmost importance to assess the impact of readily accessible trace elements in environmental substrates.

3.5 Applicability of the proposed approach for the study of the elemental associations

Traditionally, metal associations in soil have been ascertained by investigation of their correlation in soil phases. Due to the restrictions of the batchwise approach that provides solely a single value of extractable metals in each fraction, the statistical comparison of the content of metals in a particular phase of a number of samples is commonly performed.[27–29] When the contents of the elements correlate well, they are considered to be closely associated. This basis overlooks the fact that elements extracted in the same extraction step may not have dissolved simultaneously but at a different timing during that step. The present approach may thus offer a better evidence of elemental associations and may more accurately be exploited for correlation investigations.

Shiowatana *et al.*[21] and Hinsin *et al.*[30] demonstrated the potential of overlayed extractograms obtained from batch analysis of extract fractions resulting from continuous-flow partitioning systems for investigation of metal associations. Two elements are considered as closely associated if their peak profiles and shapes coincide with time during a given extraction step. Elemental associations can be more accurately detected by on-line ICP-MS interelement comparison as a consequence of the high temporal resolution of the leaching profile, as exemplified in this work by overlapping the on-line extractograms for Cd and Zn. The extraction profiles illustrated in Fig. 4 reveal a close association between Cd and Zn in the acid soluble and reducible fractions, but not in the oxidizable fraction. The strong overlapping of peak profiles for Cd and Zn indicates the simultaneous release of these two elements from the same solid compartment. Extractograms are not merely applicable to the evaluation of elemental distribution and soil phase associations, but they can be extended for the investigation of the homogeneity of solid materials,[30] readsorption behavior of trace elements[25,31] as well as the degree of anthropogenic soil contamination.[26,32]

4. Conclusion

The bi-directional continuous-flow hyphenated technique proposed herein has proven to be an appealing approach for conducting metal fractionation studies in environmental solid substrates. The non-steady flow rate during the fractionation protocol, as detected in former flow-through stirred cell systems, which hinders the coupling of the extraction units with atomic spectrometers, can be entirely circumvented by the alternate change of the flow direction of the extractant. Based on this concept, partitioning schemes can be carried out on-line with soil amounts of up to 1 g, thus assuring, as opposed to previous miniaturized microcolumn systems, sample representativeness and leaching flow rates of up to 10 mL min^{-1}. It can therefore be applied to various solid substrates for evaluation of metal accessibility under fast leaching conditions.

The hyphenated method offers not only information on trace element distribution but it constitutes itself as a powerful analytical tool for research in soil science in order to ascertain the modes of occurrence and accessibility of metals to biota as well as the detection of possible anthropogenic point sources. Thanks to the multielemental detection capacity of ICP-MS, interelemental comparison for exploration of metal associations in defined soil geological phases can be performed in a straightforward manner.

Although the alternate change of extractant flow direction through the extraction unit and the injection of discrete extract plugs into the ICP-MS were performed manually in this work,

it is also feasible to develop a computer-controlled hyphenated set-up for fully automated on-line soil processing.

Acknowledgements

The authors are grateful for financial support granted by the Royal Golden Jubilee PhD Program and the research grant from the Thailand Research Fund and to the Postgraduate Education and Research Program in Chemistry (PERCH) of the Higher Education Development Project of the Commission on Higher Education (Thailand). Manuel Miró is indebted to the Spanish Ministry of Education and Science for financial support through the "Ramon y Cajal" research program.

References

1 A. Tessier, P. G. C. Campbell and M. Bisson, *Anal. Chem.*, 1979, **51**, 844–851.
2 C. Kheboian and C. F. Bauer, *Anal. Chem.*, 1987, **59**, 1417–1423.
3 S. Xiao-Quan and C. Bin, *Anal. Chem.*, 1993, **65**, 802–807.
4 Ph. Quevauviller, *Trends Anal. Chem.*, 1998, **17**, 289–298.
5 C. Gleyzes, S. Tellier and M. Astruc, *Trends Anal. Chem.*, 2002, **21**, 451–467.
6 A. V. Filgueiras, I. Lavilla and C. Bendicho, *J. Environ. Monit.*, 2002, **4**, 823–857.
7 A. Sahuquillo, A. Rigol and G. Rauret, *Trends Anal. Chem.*, 2003, **22**, 152–159.
8 M. Miró, E. H. Hansen, R. Chomchoei and W. Frenzel, *Trends Anal. Chem.*, 2005, **24**, 759–771.
9 J. Shiowatana, N. Tantidanai, S. Nookabkaew and D. Nacapricha, *J. Environ. Qual.*, 2001, **30**, 1195–1205.
10 D. Beauchemin, K. Kyser and D. Chipley, *Anal. Chem.*, 2002, **74**, 3924–3928.
11 P. S. Fedotov, A. G. Zavarzina, B. Ya Spivakov, R. Wennrich, J. Mattusch, K. de P. C. Titze and V. V. Demin, *J. Environ. Monit.*, 2002, **4**, 318–324.
12 H. Kurosaki, S. M. Loyland-Asbury, J. D. Navratil and S. B. Clark, *Environ. Sci. Technol.*, 2002, **36**, 4880–4485.
13 L.-M. Dong and X.-P. Yan, *Talanta*, 2005, **65**, 627–631.
14 M. Jimoh, W. Frenzel, V. Müller, H. Stephanowitz and E. Hoffmann, *Anal. Chem.*, 2004, **76**, 1197–1203.
15 M. Jimoh, W. Frenzel and V. Müller, *Anal. Bioanal. Chem.*, 2005, **381**, 438–444.
16 R. Chomchoei, E. H. Hansen and J. Shiowatana, *Anal. Chim. Acta*, 2004, **526**, 117–184.
17 M. Schreiber, M. Otto, P. S. Fedotov and R. Wennrich, *Chemosphere*, 2005, **61**, 107–115.
18 P. S. Fedotov, E. Yu. Savonina, R. Wennrich and B. Ya. Spivakov, *Analyst*, 2006, **131**, 509–515.
19 R. Chomchoei, M. Miró, E. H. Hansen and J. Shiowatana, *Anal. Chem.*, 2005, **77**, 2720–2726.
20 J. Shiowatana, N. Tantidanai, S. Nookabkaew and D. Nacapricha, *Environ. Int.*, 2001, **26**, 381–387.
21 J. Shiowatana, R. G. McLaren, N. Chanmekha and A. Samphao, *J. Environ. Qual.*, 2001, **30**, 1940–1949.
22 A. Montaser, *Inductively Coupled Plasma Mass Spectrometry*, Wiley-VCH, New York, 1998, ch. 7.
23 J. M. Cano, J. L. Todolí, V. Hernandis and J. Mora, *J. Anal. At. Spectrom.*, 2002, **17**, 57–63.
24 M. D. Ho and G. J. Evans, *Anal. Commun.*, 1997, **34**, 363–364.
25 R. Chomchoei, J. Shiowatana and P. Pongsakul, *Anal. Chim. Acta*, 2002, **472**, 147–159.
26 J. Buanuam, J. Shiowatana and P. Pongsakul, *J. Environ. Monit.*, 2005, **7**, 778–784.
27 S. C. Jarvis, *J. Soil Sci.*, 1984, **35**, 431–438.
28 Z. Li, R. G. McLaren and A. K. Metherell, *New Zealand J. Agr. Res.*, 2001, **44**, 191–200.
29 Z. Li, R. G. McLaren and A. K. Metherell, *Aust. J. Soil Res.*, 2001, **39**, 951–967.
30 D. Hinsin, L. Pdungsap and J. Shiowatana, *Talanta*, 2002, **58**, 1365–1373.
31 R. Chomchoei, M. Miró, E. H. Hansen and J. Shiowatana, *Anal. Chim. Acta*, 2005, **536**, 183–190.
32 N. Tongtavee, J. Shiowatana and R. G. McLaren, *Int. J. Environ. Anal. Chem.*, 2005, **85**, 567–583.

Available online at www.sciencedirect.com
SCIENCE DIRECT®
Analytica Chimica Acta 570 (2006) 224–231
ANALYTICA CHIMICA ACTA
www.elsevier.com/locate/aca

On-line dynamic fractionation and automatic determination of inorganic phosphorus in environmental solid substrates exploiting sequential injection microcolumn extraction and flow injection analysis

Janya Buanuam [a], Manuel Miró [b,*], Elo Harald Hansen [c,**], Juwadee Shiowatana [a]

[a] *Department of Chemistry, Faculty of Science, Mahidol University, Rama VI Road, Bangkok 10400, Thailand*
[b] *Department of Chemistry, Faculty of Sciences, University of the Balearic Islands, Carretera de Valldemossa km. 7.5, E-07122 Palma de Mallorca, Illes Balears, Spain*
[c] *Department of Chemistry, Technical University of Denmark, Kemitorvet, Building 207, DK-2800 Kgs. Lyngby, Denmark*

Received 18 January 2006; received in revised form 14 March 2006; accepted 20 March 2006
Available online 28 April 2006

Abstract

Sequential injection microcolumn extraction (SI-MCE) based on the implementation of a soil-containing microcartridge as external reactor in a sequential injection network is, for the first time, proposed for dynamic fractionation of macronutrients in environmental solids, as exemplified by the partitioning of inorganic phosphorus in agricultural soils. The on-line fractionation method capitalises on the accurate metering and sequential exposure of the various extractants to the solid sample by application of programmable flow as precisely coordinated by a syringe pump.

Three different soil phase associations for phosphorus, that is, exchangeable, Al- and Fe-bound, and Ca-bound fractions, were elucidated by accommodation in the flow manifold of the three steps of the Hieltjes–Lijklema (HL) scheme involving the use of 1.0 M NH_4Cl, 0.1 M NaOH and 0.5 M HCl, respectively, as sequential leaching reagents. The precise timing and versatility of SI for tailoring various operational extraction modes were utilized for investigating the extractability and the extent of phosphorus re-distribution for variable partitioning times.

Automatic spectrophotometric determination of soluble reactive phosphorus in soil extracts was performed by a flow injection (FI) analyser based on the Molybdenum Blue (MB) chemistry. The 3σ detection limit was 0.02 mg P L^{-1} while the linear dynamic range extended up to 20 mg P L^{-1} regardless of the extracting media. Despite the variable chemical composition of the HL extracts, a single FI set-up was assembled with no need for either manifold re-configuration or modification of chemical composition of reagents.

The mobilization of trace elements, such as Cd, often present in grazed pastures as a result of the application of phosphate fertilizers, was also explored in the HL fractions by electrothermal atomic absorption spectrometry.

Keywords: Sequential injection; Dynamic fractionation; Inorganic phosphorus; Soil

1. Introduction

Phosphorus is an essential nutrient supporting the plant growth but it is also considered as a core factor for the eutrophication of rivers and lakes [1,2]. Accurate determination of inorganic phosphorus in natural waters and environmental solids is a current topic of major concern since this species is generally regarded as the limiting nutrient for biota growth. The quantitation of phosphorus in soils is aimed, for example, at the evaluation of the optimum soil phosphorus concentration required for plant growth; the determination of the phosphorus supplying capacity of soils according to the parental rocks; and most recently, the identification of scenarios where the prolonged application of superphosphate fertilizers might contribute to point source of trace element pollution.

In the geochemical, ecological and environmental fields, there has been an increasing interest for the chemical and physical characterization of the different forms of phosphorus in soils and sediments in order to determine the bioavailable fraction. A common route to estimate the stock of potentially accessible forms is to fractionate phosphorus according to the extractability by leaching reagents of increasing aggressiveness [3–8].

* Corresponding author. Tel.: +34 971 259576; fax: +34 971 173426.
** Corresponding author. Tel.: +45 4525 2346; fax: +45 4588 3136.
E-mail addresses: manuel.miro@uib.es (M. Miró), ehh@kemi.dtu.dk (E.H. Hansen).

0003-2670/$ – see front matter © 2006 Elsevier B.V. All rights reserved.
doi:10.1016/j.aca.2006.03.114

Sequential extraction techniques are traditionally conducted in a batch end-over-end fashion, which is rather laborious, tedious, time consuming and it is subjected to several potential errors including risks of contamination due to sample manipulation and underestimation of given fractions due to re-adsorption phenomena. Although naturally occurring processes inherently always are dynamic, batchwise extraction are nevertheless routinely performed with particular leaching agents for extended periods of time to ensure the establishment of steady-state conditions between the solid and liquid phases.

In order to alleviate these drawbacks, recent trends have been focused on the development of on-line extraction protocols. A number of research groups have directed their efforts into the characterization of dynamic fractionation systems, mostly involving continuous flow or flow injection approaches [8–15], where fresh portions of extracting reagents are continuously delivered to small containers or microcartridges containing the solid material. This approach offers enhanced information on the fractionation procedure as regards to the kinetics of the ongoing leaching process, chemical associations between elements and size of pools available under environmentally changing scenarios.

Tiyapongpattana et al. [8] reported a continuous flow method for sequential fractionation of inorganic phosphorus based on the principle of stirred flow cells. Soil samples are extracted in a closed extraction chamber furnished with a glass microfiber filter by the action of leaching reagents that are continuously propelled forward by means of a peristaltic pump. Besides its simplicity, the continuous flow system features a significant reduction in extraction time as compared with conventional batch protocols. However, the proposed configuration is not sufficiently rugged for on-line dynamic sequential extractions owing to the instability of the flow rate occasioned by the clogging of the in-line filter. In addition, the large dimensions of the sample container hinder appropriate resolution of the extraction profile.

The inherent shortcomings of stirred flow cell configurations are to be overcome by exploiting sequential injection microcolumn extraction (SI-MCE) [16], that should be regarded as a simple, robust and expeditious technique for ascertaining the fractional distribution and binding sites of specific elements in solid samples. The automated sequence comprises the consecutive aspiration of the individual extractants from different external ports of the valve, which, via flow reversal, sequentially are exposed to the solid sample as contained in the microcartridge attached externally to one of the port positions. To the best of our knowledge, SI-MCE has been merely utilized for exploration of the mobility and availability of trace metals in soils [16–18], but, so far, no work has been reported on the potential applicability to macronutrient fractionation.

Amongst the various operationally defined sequential extraction procedures for the determination of phosphorus forms in environmental solids, the Williams et al. [19] and Hieltjes–Lijklema (HL) [3] schemes have been commonly adopted as routine methods. Even though the former has been taken as a working basis for the harmonized protocol of the Standard, Measurement and Testing (SM&T) Program of the Commission of the European Communities [20], its adaptability to flow systems for on-line fractionation is rather cumbersome because of the single extraction nature of the several steps. Hence, the sequential HL method, which is established as the standard within the field of limnology for phosphorus fractionation [21] was herein selected for on-line SI-MCE. This scheme addresses three inorganic forms of phosphate, that is: (i) the fraction retained by exchange sites, (ii) the fraction associated with aluminium and iron oxyhydroxides and (iii) the calcium-bound fraction, generally referred to as apatite-phosphate.

In dynamic extraction approaches, in contrast to conventional fractionation protocols, a plethora of extract solutions are generated, thereby rendering rather time consuming procedures when performing the extract analyses in a batchwise mode [8,9,11,16,17]. This work was therefore also aimed at the development and characterization of an FI system based on Molybdenum Blue (MB) complex formation for automatic and rapid analysis of HL extracts. It should be noted that FI has been primarily utilized as an analytical tool for monitoring dissolved reactive phosphorus in freshwater systems [22–30], yet only a few papers have dealt with soil extract analysis [31–34].

2. Experimental

2.1. Apparatus

An FIAlab-3500 flow injection/sequential injection system (Alitea, USA) equipped with an internally incorporated 10-port multiposition selection valve (SV) and a syringe pump (SP, Cavro, Sunnyvale, USA) with a capacity of 5 mL was used. The SI-system was computer controlled by the associated FIAlab software. The extraction microcolumn was connected within the SI-system as an external module as shown in Fig. 1a and b. All outlets of the SV were connected through PEEK ferrules with rigid PTFE tubing (0.5 mm i.d.). The central port of the SV was connected to the SP via a holding coil (HC1), which consisted of a 5 m long PTFE tubing (0.8 mm i.d.), with an inner volume of ca. 2.5 mL. The holding coil for the extracts in Fig. 1b was also made of PTFE (HC2, 2.5 m long, 1.0 mm i.d.).

The FI manifold devised for determination of orthophosphate in the SI-MC soil extracts is depicted in Fig. 2. The flow system is composed of two low-pulsation multichannel peristaltic pumps with rate selector (Type IPS-4, Ismatec, Zurich, Swizerland) used for reagents/sample propulsion and sample loading, respectively. The flow rates of the various streams as well as the optimum dimensions of the reaction coils for heteropoly-acid complex formation and reduction by tin(II) chloride are shown in the figure. A minute volume of extract (viz., 25 μL) is injected into the flow network via a six-port rotary injection valve (Rheodyne, Type 5041). An UV–vis spectrophotometer (Jenway, Model 6300, UK) equipped with a 10 mm optical path flow-through cell was set at 690 nm and connected to a chart recorder (Radiometer, Model Rec 80 Servograph, Denmark) for monitoring of the molybdenum blue complex.

Determination of the concentration of cadmium in the HL fractions was performed by a Perkin-Elmer 2100 Electrothermal Atomic Absorption Spectrometer (ETAAS) equipped with

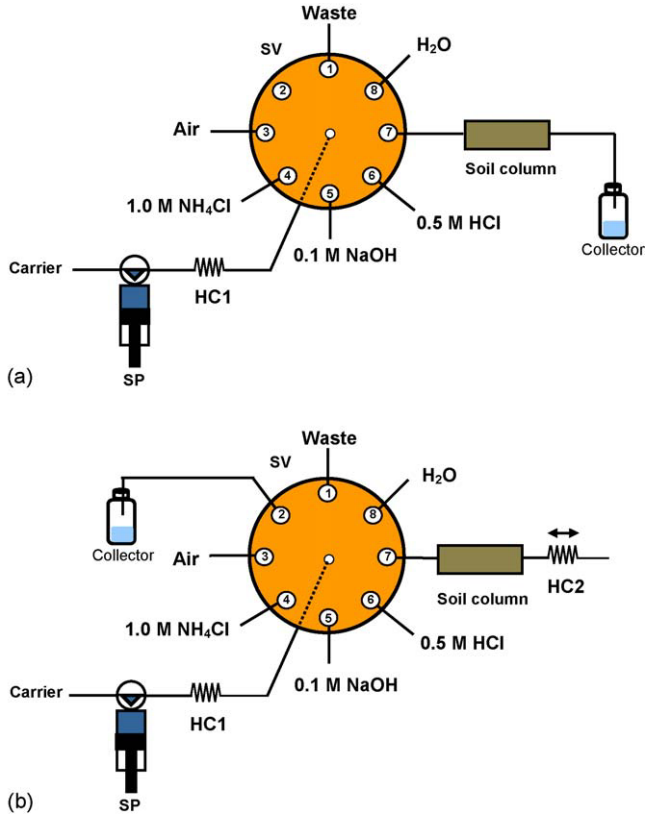

Fig. 1. Schematic diagrams of the sequential injection microcolumn set-ups for dynamic fractionation of inorganic phosphorus in soils as exploited for: (a) unidirectional and stopped flow and (b) bi-directional flow extraction. SP, syringe pump; SV, selection valve; HC1 and HC2, holding coils.

deuterium background correction, following manufacturer recommendations [35]. One microgram of $Pd(NO_3)_2$ was utilized as a matrix modifier.

2.2. Microcolumn assembly

The dedicated extraction microcolumn exploited in this work has been described in detail elsewhere [16,18]. Made of PEEK, it comprises a central dual-conical shaped sample container for facilitating fluidized-bed like mixing conditions. The entire unit is assembled with the aid of filter supports and caps at both ends. The membrane filters (Millipore, Fluoropore™ filter, 13 mm diameter, 0.45 μm pore size) used at both ends of the extraction microcolumn allowed solutions and leachates to flow freely through but retained particulate matter.

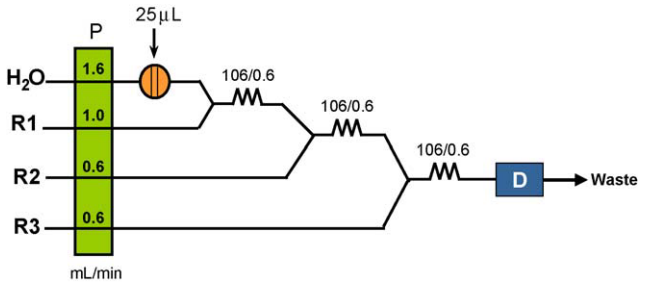

Fig. 2. Flow injection manifold for automatic monitoring of orthophosphate in soil extracts resulting from the Hieltjes–Lijklema scheme. R1, 2.4 g L^{-1} tartaric acid; R2, 12 g L^{-1} ammonium molybdate in 0.6 M H_2SO_4; R3, 0.3 g L^{-1} tin(II) chloride + 1.88 g L^{-1} hydrazinium sulphate in 0.5 M H_2SO_4.

2.3. Preparation of reagents

All glassware used was previously rinsed with 25% (v/v) concentrated nitric acid/water in a washing machine (Miehle, Model G 7735 MCU, Germany) and afterward rinsed with Milli-Q water. All chemicals were of analytical-reagent grade and Milli-Q water was used throughout. The various chemicals employed in this work are detailed as follows.

2.3.1. Standard solutions

A stock standard solution of orthophosphate (100 mg P L^{-1}) was prepared by dissolving 0.4392 g of KH_2PO_4 (Merck) in water and making up to a final volume of 1000 mL with Milli-Q water. The stock standard solution of cadmium (1000 mg L^{-1}) for AAS was purchased from Merck. Working standard solutions of P and Cd were obtained by stepwise dilution of the stock solutions.

2.3.2. Leaching reagents for sequential extraction

The chemicals utilized in the HL sequential extraction scheme are the following:

Step 1 1.0 M NH_4Cl adjusted at pH 7 with NH_4OH,
Step 2 0.1 M NaOH,
Step 3 0.5 M HCl,

which were aimed at stripping the labile, Fe- and Al-bound, and Ca-bound phosphorus fractions, respectively.

2.3.3. Reagents for flow injection analysis

According to the schematic diagram depicted in Fig. 2, R1 is composed of 2.4 g L^{-1} tartaric acid solution (Aldrich) in Milli-Q water, R2 involves 12 g L^{-1} ammonium molybdate (Riedel-de-Haën) in 0.6 M H_2SO_4 (Merck) and R3 comprises 0.3 g L^{-1} $SnCl_2$ (Merck) in 0.5 M H_2SO_4. The latter chemical also contains 1.88 g L^{-1} hydrazinium sulphate (J.T. Baker) for reagent preservation, whereby the combined solution is stable for, at least, 2 weeks.

2.4. Soil sample

A soil certified reference material from the National Institute of Standards and Technology, namely SRM 2711, was used for method validation. The soil material was collected from the tilled layer of a wheat field (MT, USA). It is a moderately contaminated pasture soil that was oven-dried, sieved and blended to achieve a high degree of homogeneity, the total concentration being certified for a number of elements, including phosphorus. The custom-built microcartridge was packed with 50 mg soil, thereby matching the sample weight endorsed in the batchwise HL scheme. Under these conditions, the free column volume (FCV) was estimated to be 250 μL.

2.5. Dissolution of soil residues

A closed-vessel microwave digestion system (Anton Paar Model Multiwave 3000, Austria) was used for digestion of residues after on-line fractionation. Residues from the extraction microcolumn were transferred to glass vessels as water slurries together with 2.0 mL of HNO_3 (65%, Merck) and 6.0 mL of HCl (30%, Merck). The vessels were then tightly sealed and subjected to a microwave digestion, according to manufacturer recommendations (1400 W, 30 min). After cooling, the digested solutions were made up to appropriate volume with Milli-Q water, and the content of orthophosphate was determined by spectrophotometry using a batchwise standard addition method.

2.6. Operational sequences for sequential injection microcolumn extraction

In this study, three applicable modes for the SI-MCE, that is, the uni-directional and stopped flow (see Fig. 1a) and the bi-directional flow (Fig. 1b), were investigated for inorganic phosphorus accessibility from soils. In all procedures, a maximum of 45 mL of each extractant was used. In order to avoid undue backpressure during extractant loading in those protocols involving flow reversal, merely 1 mL aliquots were manipulated at a time in the system using an air-sandwiched fashion. The complete sequential extraction procedure of the three approaches is described below.

2.6.1. Uni-directional flow

Before initialization of the extraction cycle, a 900 μL air plug is aspirated from port 3 of SV into HC1. Afterward, SP is set to aspirate 1.00 mL of 1.0 M NH_4Cl from port 4 into HC1 at a flow rate of 50 μL s^{-1}, whereupon the extractant and air plugs are pushed forward at the same rate through the microcolumn, allowing extraction to take place. For each five cycle runs, the extracts from the microcolumn are collected in a separate plastic vial, thus totally amounting to nine 5 mL subfractions for a complete set. Prior to continuing with the ensuing HL extraction step, a washing protocol is implemented by sequential aspiration of 900 μL of air and 1.00 mL of H_2O into HC1 which, via flow reversal, are delivered through the sample container into the fraction collector. This run is repeated five times. The amount of phosphorus leached in the cleansing step is summed to the content of the subfractions collected in the previous extraction. Thereafter, the next extractant (viz., 0.1 M NaOH or 0.5 M HCl) is automatically aspirated from the respective valve port and the collection of nine 5 mL subfractions repeated until all three leaching steps have been completed.

2.6.2. Stopped flow

The system operation was similar to that of the uni-directional flow procedure, except for the inclusion of an ancillary stopped flow stage. Here, a 900 μL air plug and 250 μL of extractant (that matches the free column volume) are consecutively pulled inwards into HC1 at 50 μL s^{-1}, the leaching reagent being dispensed afterwards via port 7 into the microcolumn where it remains halted for 30 s. Afterwards, the air segment in HC1 is dispensed forward to flush the leachant from the column into the fraction collector. The stopped flow mode is only programmed for the first step of the HL scheme, which estimates the loosely bound phosphorus fraction, in order to assess the possible re-adsorption of the target analyte on active soil sites. The extraction procedure was repeated with 20 cycle runs for each subfraction, thus amounting to a total of 9 subfractions for each set.

2.6.3. Bi-directional flow

SP is set to aspirate consecutively 900 μL of air and 1.00 mL of 1.0 M NH_4Cl into HC1 at a flow rate of 50 μL s^{-1}. The entire extractant plug is then delivered through the soil column at 50 μL s^{-1} and becomes positioned in HC2. Thereafter, the extract is aspirated backwards through the column and via the central port into HC1, and then finally dispensed to the collection vial attached to port 2. Again, the leaching process is repeated with five cycle runs for each subfraction, and totally nine subfractions for each set. Just as the stopped flow approach, this operational mode is merely applied to the first step of the HL scheme.

The amount of orthophosphate collected in the various subfractions was determined by flow injection spectrophotometry using the manifold depicted in Fig. 2. Accurate determination of trace concentrations of cadmium released during application of HL method was conducted by ETAAS via direct injection of 20 μL extracts.

3. Results and discussion

3.1. Configuration of the sequential injection microcolumn system for fractionation of inorganic phosphorus

Although originally conceived for automated liquid phase analysis, the scope of SI has been recently expanded to the on-line handling of solid materials [16–18], which is a consequence of its inherent flexibility for accommodating external modules into the flow network. Yet, there is still place for the improvement for the various SI operational extraction modes, that is, uni-directional, bi-directional and stopped flow-based fractionation. Even though SI is a discontinuously operating flow approach, a truly forward flow fractionation scheme has been designed in this work. This is carried out by sandwiching metered volumes of extractant between discrete air plugs, thus preventing a portion of the leaching reagent to reside in the sample line in intimate contact with the packed soil during loading of the next leachant zone into HC1. Therefore, the contact time is identical for the entire segment in each run of the iterative multiple-step protocol. In addition, the inexistence of a concentration gradient in HC1 is assured by hindering the dispersion of the aspirated reagent plug into the carrier solution.

As opposed to earlier works [16,17], there is no need for re-configuration of the SI-manifold for the bi-directional flow approach. This is circumvented by replacement of the pre-valve microcolumn arrangement for an in-valve column attached configuration (see Fig. 1b). Improvement of the stopped flow mode is made by calculating the free column volume of the soil-packed

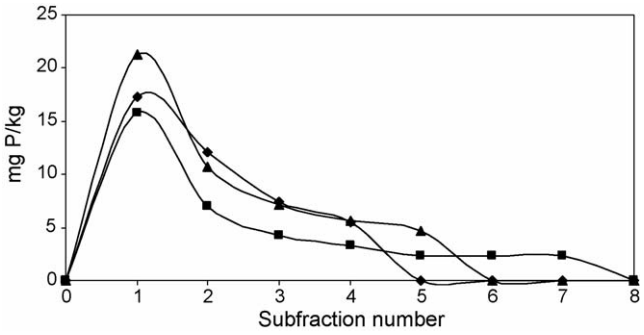

Fig. 3. Sequential injection extractograms of inorganic phosphorus in SRM 2711 as obtained from the application of three different operational modes for the step I of the Hieltjes–Lijklema scheme: uni-directional flow (♦); bi-directional flow (■); stopped flow (▲). Subfraction volume: 5 mL.

container and programming the liquid driver for accurate delivery of consecutive FCVs of extractant through the microcolumn prior to halting the flow in each single step of the analysis cycle.

In all cases, analysis of SI-MC extracts is conducted off-line because of the likelihood of effecting multiparametric sequential determinations of macronutrients and trace elements in each subfraction by spectrophotometry and atomic absorption spectrometry, respectively.

3.2. Sequential injection microcolumn for investigation of phosphorus re-adsorption

In sequential extraction techniques, aside from the non-selectivity of the extractant solutions, a crucial issue to be investigated is the extent of re-adsorption of leached elements onto the remaining solid phases during the time span of the extraction, which causes the underestimation of bioavailable fractions. Taking into account the versatility of movements of the syringe pump, the potential re-distribution of phosphorus during partitioning can be thoroughly studied by critical comparison of experimental data provided by the three aforementioned extraction modes for SI-MCE. It should be noted that the longer the intimate contact time between solid and leachant is, the higher becomes the probability that re-adsorption might occur. Therefore, the extraction time should be reduced to the extent possible [36], yet, a compromise should be reached regarding leaching kinetics for the targeted phases. Hence, the uni-directional flow, where the sample is continuously subjected to fresh extractant volumes ($t_{ext} = 5$ s) is expected to be free from re-adsorption as opposed to the bi-directional and stopped flow alternatives where the extracts remain longer ($t_{ext} = 10$ and 35 s, respectively) with the undissolved solid.

Fig. 3 shows the extractograms (graphical plots of extractable amounts versus subfraction number) recorded for the forward flow, bi-directional and stopped flow modes for the first step of the HL protocol. The investigation was restricted to the readily bioavailable phosphorus fraction because the re-distribution phenomenon is generally pronounced when employing mild extractants [37].

The fraction of exchangeable phosphorus determined by the uni-directional, bi-directional and stopped flow modes amounted to 0.0045 ± 0.0005, 0.0039 ± 0.0001 and 0.0043 ± 0.0007 mg P L^{-1}, respectively. The inexistence of significant differences at the significance level of 0.05 revealed that the re-adsorption was negligible for this particular solid material. This is attributed to the lack of selectivity of NH_4Cl, which is capable of removing partially carbonates from soil, thereby eliminating potential surfaces for phosphorus fixation [3,38]. The extraction patterns in Fig. 3 showed a dependence of the partitioning mode with the extraction rates, the highest rates being observed for the stopped flow approach.

3.3. Optimization of a flow injection system for monitoring of inorganic phosphorus in HL soil extracts

Two recent reports [31,39] have addressed the automatic determination of MB-reactive phosphorus in soil solutions resulting from batchwise fractionation via flow-based systems, namely FI and all injection analysis. However, Tiyapongpattana [39] claimed that it was a requirement to replace the carrier solution for each extractant medium to minimize the Schlieren effect, and Amornthammarong et al. [31] found that it was also required to adjust the concentration of sulphuric acid in the ammonium molybdate solution for the different leachant solutions. In this work, these flow manifolds were modified in order to design a simple set-up capable of admitting high electrolyte solutions as well as acidic and alkaline samples resulting from the HL scheme without changing neither the configuration of the system nor the chemical composition of the various streams. Schlieren effects were minimized by a 10-fold reduction of the sample volume used as compared to the earlier assembly [39] and a slight increase in residence time, thus promoting better axial mixing between the minute, well-defined volume of extract and the carrier solution (water) on their way towards the detector. On-line quantitation of soluble reactive phosphorus relies upon reaction of the target species with acidic molybdate to form molybdophosphoric acid which is subsequently reduced by tin(II) chloride to yield the blue-colored MB compound. Although the on-line formation of molybdosilicate is precluded by increasing the acidity of the reaction medium, the higher the acidity the lower the method's sensitivity due to the slow development of the reaction for molybdophosphate formation. Thus, the recommended concentration of sulphuric acid in the heteropolyacid forming reagent [39] was reduced from 1.0 to 0.6 M. The detection and determination limits for the optimized FI set-up at the 3 and 10σ levels were 0.02 and 0.09 mg P L^{-1}, respectively, regardless of the extraction medium, while the linear dynamic range extended up to 20 mg P L^{-1}. Actually, the tolerance of the flow injection method to metasilicate in 0.1 M NaOH, and in the presence of tartaric acid as a masking agent, is ca. 500 mg Si L^{-1}. Taking into account that silicate forms are hydrolysed, and thus mobilized, in alkaline solutions, and that the maximum available amount of silicon in SRM 2711 is merely 15 mg, the proposed method offers suitable selectivity for spectrophotometric monitoring of inorganic phosphorus in the selected material.

Table 1
Comparison of extractable amounts of inorganic phosphorus in SRM 2711 using the Hieltjes–Lijklema fractionation scheme as obtained with sequential injection microcolumn extraction and continuous flow stirred flow cell-based approaches

Flow-through method	Phosphorus content (%w/w)					
	1.0 M NH_4Cl	0.1 M NaOH	0.5 M HCl	Residue	Sum	Certified value
Continuous flow [8]	0.0189 ± 0.0006	0.0077 ± 0.0004	0.0413 ± 0.0006	0.0085 ± 0.0004	0.0764 ± 0.0011	0.086 ± 0.007
Sequential injection microcolumn[a] (this work)	0.0045 ± 0.0005	0.0093 ± 0.0010	0.0373 ± 0.0018	0.0275 ± 0.0048	0.0786 ± 0.0052	

[a] Results are expressed as the mean of five replicates ± standard deviation.

3.4. Accuracy of the proposed system and critical comparison of the analytical performance of SI-MCE with that of continuous flow systems

To evaluate the accuracy of the SI-MC system for phosphorus fractionation, a grazed soil with low organic phosphorus content, that is, the SRM 2711 Montana soil, was selected. Table 1 lists the amounts of orthophosphate extracted by on-line dynamic SI-MCE, which are compared with those recently reported for the same solid substrate using a continuous flow manifold with a stirred flow chamber [8]. The total phosphorus concentration obtained by summation of the entire set of fractions plus residue in SI-MCE showed a good agreement with the certified value and that obtained by fraction summation in the stirred flow cell method. Nevertheless, a significant difference in available phosphorus was distribution was found for the loosely bound fraction between the SI and the continuous flow method. This discrepancy is attributed to the different operationally defined extraction conditions for both procedures, such as, e.g., the partitioning time, and the non-selectivity of NH_4Cl for the targeted phase. In fact, the residence time of an extractant plug within the stirred chamber amounted to 120 s versus merely 5 s for the uni-directional SI-MC fashion. The shorter residence time in the proposed system would concurrently minimize the stripping of matrix ingredients which might potentially interfere in the determination step. Actually, while the standard addition method was mandatory for the determination of soluble reactive phosphorus in the NaOH and HCl extracts in the continuous flow system [8] owing to the poor performance of calibration protocols involving matrix matching with the pertinent extracting reagent, no multiplicative interferences were found in SI-MCE, whereby a straightforward external calibration approach with matrix matching was adopted.

The lack of selectivity of NH_4Cl for the exchangeable phosphorus fraction is occasioned by the capability of the reagent for attacking iron and aluminium hydroxy phosphate minerals, i.e., strengite and variscite, as a function of the contact time between solid and liquid phases [40]. This explains the overestimation of labile phosphorus and underestimation of aluminium- and iron-bound phosphorus in the continuous flow system as compared to SI-MCE (see Table 1).

The analytical performance of both batchwise and flow-through dynamic methods for fractionation of inorganic phosphorus according to the HL scheme is detailed in Table 2. The totally enclosed continuous flow system speeds up the extraction process as a result of the steady renewal of the leaching solutions and minimizes the risk of personal errors and contamination due to the avoidance of manual phase separations. Yet, the major problem posed by the application of continuous fractionation using stirred flow cells is the large dead volume of the sample container. Thus, a five-fold increase in soil amount versus batch fractionation is necessitated for attaining detectable signals due to the inherent dilution of released species. In addition, a larger consumption of reagents is concomitantly entailed for extraction until completion (≥300 mL versus 50–100 and 25–30 mL in batch and SI-MCE, respectively, for a single fraction). In fact, the stirred flow cell method was not deemed sensitive enough to be coupled to FI, for which reason the extracts were analysed by batch spectrophotometry. Furthermore, the fraction volumes collected in the continuous flow system, namely 60 mL, were 12-fold higher than those of SI-MC fractionation. The temporal resolution of the former method is therefore inappropriate for a detailed insight into leaching kinetics and phosphorus distribution in the soil phases, and only averaged leachable concentrations can be estimated. Finally, the instability of flow rates in the flow cell arrangement as a result of the pulsed flow of the peristaltic pump and blockage of the membrane filter with colloid particles, especially in the NaOH extraction step, was circumvented in SI-MCE by the novel design of the sample container and the ruggedness of the liquid driver.

Table 2
Analytical performance of batchwise and dynamic extraction methods based on Hieltjes–Lijklema scheme for fractionation of inorganic phosphorus in soils

Condition/parameter	Batch	Dynamic extraction	
		Continuous flow	SI-MCE
Sample (g)/extractant (mL)	1/1000	1/40[a]	1/5[b]
Extractant volume (mL)			
NH_4Cl fraction	2 × 50	540	25
NaOH fraction	50	300	30
HCl fraction	50	300	30
Extraction time per sample (h)	45[c]	3.8	2.1
Operational time for extract analysis (min)	20[d]	120[e]	20[f]

[a] Calculated as the ratio between sample weight and container volume.
[b] Calculated as the ratio between sample weight and free column volume.
[c] The length of the manual solid–liquid separations is not included.
[d] Only three extracts are analysed for the three-step fractionation procedure.
[e] The extracts containing NaOH and HCl extracted P are analysed by the standard addition method.
[f] The entire set of extracts is analysed by external calibration.

3.5. Applicability of Hieltjes and Lijklema scheme for cadmium fractionation in soil

Phosphorus is added to pasture soils by direct application of either reactive phosphate or acidulated rocks in the forms of single superphosphate, triple superphosphate or diammonium phosphate. These fertilizers contain varying concentrations of Cd depending on the particular phosphate mineral used as a raw material for their manufacture [41]. The Cd content of phosphate rocks varies widely, with the phosphate rocks of sedimentary origin having a very high concentration of Cd, and those of igneous origin having very low concentrations. The continuous use of fertilizers over a long time period might cause an undesired accumulation of Cd to levels above the maximum permissible concentrations set by regulatory authorities concerning human health. The impact of such fertilizers contaminated with trace elements, such as Cd, on the environment can be ascertained by sequential extraction. A multitude of partitioning schemes have been launched for evaluating the origin, mode of occurrence and mobility of trace elements in natural environments [37,42–45]. The potential applicability of the HL scheme to elucidate soil phase chemical associations not only for phosphorus but also for trace elements is, however, for the first time, investigated in this work. In fact, the HL procedure confines certain analogies with the well-established three-step fractionation scheme of the SM&T of the EU [45]. The first and third steps of HL, that involve the stripping of the exchangeable pools and phosphorus bound to calcium or adsorbed on calcium carbonate, are comparable with the first step of the SM&T protocol (i.e., acid soluble fraction) in terms of the nature of the soil phases solubilized. In fact, the summation of extractable Cd in SRM 2711 in steps I and III of the HL scheme performed in an MCE uni-directional flow fashion amounted to 37.9 ± 1.1 mg Cd kg^{-1}, which correlates well with the acid soluble Cd (viz., 36.2 ± 0.6 mg Cd kg^{-1}) as obtained from the step I of the SM&T protocol effected in a batchwise mode [46]. This good agreement between batch and flow-through partitioning methods is expected for labile, readily leachable elements, such as Cd. It should be also noted that the HL scheme offers, as opposed to SM&T, the possibility of discrimination of geologically relevant fractions (viz., exchangeable and acid soluble) which are of particular interest for readily mobilisable elements. The fractional distribution and extraction profiles of cadmium and phosphate using the HL protocol are schematically illustrated in Fig. 4. From the extractograms, it is feasible to discern the weakly adsorbed cadmium, probably as a free metal ion or chlorocomplex on ionic sites (step I in HL) from the cadmium carbonate (step III in HL) resulting from the isomorphic substitution of Ca by Cd in calcite minerals. The current impact of other potentially toxic elements in rock phosphates [47] such as As, Pb, Cr, Zn, Hg and F, which can be made available concurrently with phosphorus under environmentally changing conditions, might analogously be assessed via the HL partitioning method effected in a dynamic fashion.

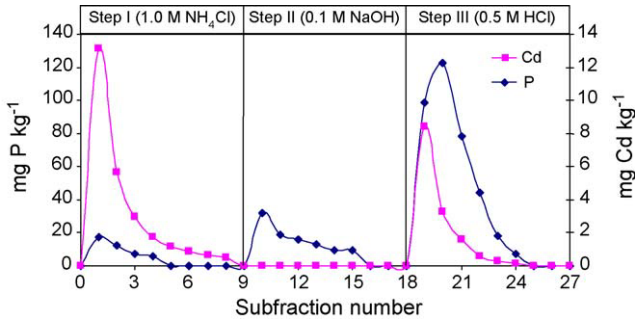

Fig. 4. Sequential injection extractograms of P and Cd in SRM 2711 as obtained from the application of Hieltjes–Lijklema scheme using the SI-MCE system in a uni-directional flow fashion. Subfraction volume: 5 mL.

4. Conclusion

The sequential injection microcolumn concept has been presented as a unique alternative to the batchwise and continuous flow counterparts for automatic fractionation of inorganic phosphorus in environmental solids. As opposed to previous flow-based approaches, the proposed SI-method features enhanced ruggedness and significant reduction of reagent consumption besides being characterized by rapidity, ease of operation and improved temporal resolution. The operational procedure and the configuration of the SI-MC system have been designed for on-line microfluidic handling of the HL leachant solutions and accurate control of partitioning time by exploiting programmable flow.

Bearing in mind the capability of SI to accommodate several operational fractionation modes in a dynamic fashion, i.e., uni-directional, bi-directional and stopped flow, the potential redistribution of phosphate for a particular extracting reagent can be assessed in a fully automated manner. In addition, a single flow injection system was assembled for facilitating the analyses of the HL extracts using the MB chemistry regardless of the composition of the extracting media.

The HL scheme, which offers enhanced phase resolution for readily mobilisable elements with respect to the harmonized SM&T protocol, was also utilized for the fractional distribution of cadmium in soils exposed to contamination via phosphate fertilizers. Experimental results revealed that both cadmium and phosphorus are predominantly bound to the calcium carbonate phase for the pasture soil (SRM 2711) analysed. Further research is being currently conducted in our group to exploit novel flow-based techniques, such as multicommutation flow analysis, multi-pumping flow analysis and multisyringe flow injection analysis, for on-line treatment of the multiple extracts obtained sequentially via dynamic SI-MC fractionation.

Acknowledgments

Janya Buanuam is grateful for financial support granted by the Royal Golden Jubilee Ph.D. Program of the Thailand Research Fund and to the Postgraduate Education and Research Program in Chemistry (PERCH) of the Higher Education Development Project of the Commission on Higher Education (Thailand).

Manuel Miró is indebted to the Spanish Ministry of Education and Science for financial support through the “Ramon y Cajal” research program. Special thanks are also due to Anders Sølby

(DTU workshop) for constructing the extraction microcolumn and Warawut Tiyapongpattana for valuable discussions.

References

[1] K. Pettersson, Hydrobiologia 373/374 (1998) 21.
[2] C. Forsberg, Water Sci. Technol. 37 (3) (1998) 193.
[3] A.H.M. Hieltjes, L. Lijklema, J. Environ. Qual. 9 (1980) 405.
[4] V. Istvánovics, Water Res. 28 (1994) 717.
[5] H.L. Goltherman, Hydrobiologia 335 (1996) 87.
[6] D.S. Ting, A. Appan, Water Sci. Technol. 34 (1996) 53.
[7] R.G. Perkins, G.J.C. Underwood, Water Res. 85 (2001) 1399.
[8] W. Tiyapongpattana, P. Pongsakul, J. Shiowatana, D. Nacapricha, Talanta 62 (2004) 765.
[9] J. Shiowatana, N. Tantidanai, S. Nookabkaew, D. Nacapricha, J. Environ. Qual. 30 (2001) 1195.
[10] D. Beauchemin, K. Kyser, D. Chipley, Anal. Chem. 74 (2002) 3924.
[11] P.S. Fedotov, A.G. Zavarzina, B. Ya Spivakov, R. Wennrich, J. Mattusch, K. de P.C. Titze, V.V. Demin, J. Environ. Monit. 4 (2002) 318.
[12] H. Kurosaki, S.M. Loyland-Asbury, J.D. Navratil, S.B. Clark, Environ. Sci. Technol. 36 (2002) 4880.
[13] L.-M. Dong, X.-P. Yan, Talanta 65 (2005) 627.
[14] M. Jimoh, W. Frenzel, V. Müller, H. Stephanowitz, E. Hoffmann, Anal. Chem. 76 (2004) 1197.
[15] M. Jimoh, W. Frenzel, V. Müller, Anal. Bioanal. Chem. 381 (2005) 438.
[16] R. Chomchoei, E.H. Hansen, J. Shiowatana, Anal. Chim. Acta 526 (2004) 117.
[17] R. Chomchoei, M. Miró, E.H. Hansen, J. Shiowatana, Anal. Chim. Acta 536 (2005) 183.
[18] R. Chomchoei, M. Miró, E.H. Hansen, J. Shiowatana, Anal. Chem. 77 (2005) 2720.
[19] J.D.H. Williams, J.-M. Jaquet, R.L. Thomas, J. Fish. Res. Board Can. 33 (1976) 413.
[20] V. Ruban, J.F. López-Sánchez, P. Pardo, G. Rauret, H. Muntau, P. Quevauviller, Fresenius J. Anal. Chem. 370 (2001) 224.
[21] H.L. Golterman, Hydrobiologia 450 (2001) 107.
[22] S. Auflitsch, D.M.W. Peat, I.D. McKelvie, P.J. Worsfold, Analyst 122 (1997) 1477.
[23] R.L. Benson, Y.B. Truong, I.D. McKelvie, B.T. Hart, Water Res. 30 (1996) 1959.
[24] S. Motomizu, Z.-H. Li, Talanta 66 (2005) 332.
[25] G. Hanrahan, M. Gledhill, P.J. Fletcher, P.J. Worsfold, Anal. Chim. Acta 440 (2001) 55.
[26] K. Grudpan, P. Ampan, Y. Udnan, S. Jayasvati, S. Lapanantnoppakhun, J. Jakmunee, G.D. Christian, J. Ruzicka, Talanta 58 (2002) 1319.
[27] I.P.A. Morais, M. Miró, M. Manera, J.M. Estela, V. Cerdà, M.R.S. Souto, A.O.S.S. Rangel, Anal. Chim. Acta 506 (2004) 17.
[28] F. Mas-Torres, J.M. Estela, M. Miró, A. Cladera, V. Cerdà, Anal. Chim. Acta 510 (2004) 61.
[29] T. Pérez-Ruiz, C. Martínez-Lozano, V. Tomás, J. Martín, Anal. Chim. Acta 442 (2001) 147.
[30] Y. Udnan, I.D. McKelvie, M.R. Grace, J. Jakmunee, K. Grudpan, Talanta 66 (2005) 461.
[31] N. Amornthammarong, P. Anujaravat, K. Sereenonchai, P. Chisuwan, P. Sastranurak, P. Wilairat, D. Nacapricha, Talanta 68 (2005) 480.
[32] C.X. Galhardo, J.C. Masini, Anal. Chim. Acta 417 (2000) 191.
[33] Z.-L. Chen, P. Grierson, M.A. Adams, Anal. Chim. Acta 363 (1998) 191.
[34] M.I.G.S. Almeida, M.A. Segundo, J.L.F.C. Lima, A.O.S.S. Rangel, Int. J. Environ. Anal. Chem. 85 (2005) 51.
[35] The THGA Graphite Furnace Manual: Techniques and Recommended Conditions, Bodenseewerk Perkin-Elmer GmbH, Überlingen, Germany, 1995.
[36] R. Chomchoei, J. Shiowatana, P. Pongsakul, Anal. Chim. Acta 472 (2002) 147.
[37] A.V. Filgueiras, I. Lavilla, C. Bendicho, J. Environ. Monit. 4 (2002) 823.
[38] A. Barbanti, M.C. Bergamini, F. Frascari, S. Miserocchi, G. Rosso, J. Environ. Qual. 23 (5) (1994) 1093.
[39] W. Tiyapongpattana, Application of continuous flow technique for sequential extraction and for determination of phosphorus in soil and sediment, Master Thesis, Mahidol University, Bangkok, Thailand, 2002.
[40] V. Ruban, J.F. López-Sánchez, P. Pardo, G. Rauret, H. Muntau, P. Quevauviller, J. Environ. Monit. 1 (1999) 51.
[41] P. Loganathan, M.J. Hedley, N.D. Grace, J. Lee, S.J. Cronin, N.S. Bolan, J.M. Zanders, Aust. J. Soil Res. 41 (2003) 501.
[42] C. Gleyzes, S. Tellier, M. Astruc, Trends Anal. Chem. 21 (2002) 451.
[43] G. Rauret, Talanta 46 (1998) 449.
[44] J. Hlavay, T. Prohaska, M. Weisz, W.W. Wenzel, G.J. Stingeder, Pure Appl. Chem. 76 (2004) 415.
[45] G. Rauret, J.F. López-Sánchez, A. Sahuquillo, R. Rubio, C.M. Davidson, A.M. Ure, P. Quevauviller, J. Environ. Monit. 1 (1999) 57.
[46] B.L. Larner, A.J. Seen, A.T. Townsend, Anal. Chim. Acta 556 (2006) 444.
[47] M.J. Mclaughlin, K.G. Tiller, R. Naidu, D.P. Stevens, Aust. J. Soil Res. 34 (1996) 1.

PAPER

Fractionation and elemental association of Zn, Cd and Pb in soils contaminated by Zn minings using a continuous-flow sequential extraction

Janya Buanuam,[a] Juwadee Shiowatana*[a] and Pichit Pongsakul[b]

[a] *Department of Chemistry, Faculty of Science, Mahidol University, Rama VI Road, Bangkok 10400, Thailand. E-mail: scysw@mahidol.ac.th; Fax: +66-2-3547-151; Tel: +66-2201-5122*
[b] *Department of Agricultural Science, Division of Soil Science, Ministry of Agriculture, Bangkhen, Bangkok 10900, Thailand*

Received 25th January 2005, Accepted 20th May 2005
First published as an Advance Article on the web 14th June 2005

Fractionation and elemental association of Zn, Cd, and Pb in soils near Zn mining areas were studied using a continuous-flow sequential extraction approach. The recently developed sequential extraction procedure not only gave fractional distribution data for evaluation of the mobility or potential environmental impact of the metals, but also the extraction profiles (extractograms) which were used for study of elemental association. In addition, the elemental atomic ratio plot extractogram can be used to demonstrate the degree of anthropogenic contamination. Seventy-nine soil samples were collected in the vicinity of a Zn mine and were fractionated into 4 phases *i.e.* exchangeable (F1), acid soluble (F2), reducible (F3) and oxidizable (F4) phases. Most samples were contaminated with Zn, Cd and Pb. The reducible phase is the most abundant fraction for Zn and Pb (> 50%) while Cd is concentrated in the first 3 extraction steps. The distribution patterns of Cd were obviously affected by soil pH. 55% of Cd appears predominantly in the F1 fraction for acidic soils while in neutral and alkaline soils, it was mostly (70%) found in the F2 + F3 fractions. The extractograms obtained from the continuous-flow extraction system revealed close association between Zn, Cd, Pb and Fe in the acid soluble phase, Cd–Pb and Zn–Fe in the reducible phase for contaminated soils. A correlation study of the 3 metals using a correlation coefficient was also performed to compare the results with the elemental association revealed by the extractograms. Atomic ratio plot extractograms of Zn/Fe, Cd/Fe and Pb/Fe in the reducible phase, where contaminated metals are predominant, can be used to evaluate the degree of anthropogenic contamination. From the elemental atomic ratio plot, it is obvious that the contaminants Cd and Pb are mostly adsorbed on the surface of Fe oxides. Zn, which is present in an approximately 1 : 1 ratio with Fe in contaminated soils, does not show a similar trend to that found for Cd and Pb.

Introduction

To understand the issue of metal contamination and its effect on ecosystems and living organisms, not only its occurrence but also its behavior in soil has been of particular interest. At present, it is recognized that the distribution, mobility and bioavailability of heavy metals depends not only on their total concentration but also on their forms in the solid phase to which they are bound. A sequential extraction technique is widely used to fractionate metals in solid samples due to their leachability.[1–4] This technique makes use of suitable chemical reagents which are applied in a given order to the sample to sequentially leach metals of different phases. The reagents used are dependent on the goals pursued and on the physical characteristics of the sample.

Sequential extraction procedures are mostly performed in a batch procedure. Recently, our group has developed a continuous-flow extraction system for sequential extraction[5] which has shown many advantages compared to a batch method. The flow system has the benefits of simplicity, rapidity, less risk of contamination, possibility for automation and provision of kinetic leaching information. In this report, the system was applied to soil samples taken from near a Zn mining area in Tak Province, Thailand. The first objective of the study is to examine fractionation of metals in soil samples resulting from Zn mining activities. Since the continuous-flow extraction can provide extractograms of kinetic leaching of elements, it is the second aim of this work to use the extractograms to study the chemical associations in soil fractions and to evaluate the degree of anthropogenic contamination. Finally, the mobility and potential bioavailability of Cd in the soil was studied by investigation of the correlation between Cd in rice grain and Cd in specific fractions.

The environmental problems resulting from Zn mining have been reported in many parts of the world such as Derbyshire in central England[6] and in southern Poland.[7,8] In those areas, a number of elements associated with Zn or Pb mineralization have been found to be highly elevated in soil contaminated by mining operations. Soils from the vicinity of a Zn/Pb mining and smelting complex in Poland were found to contain high total concentrations of Zn, Pb and Cd: 234–12 400; 42–3570; 2–73.2 mg kg^{-1}, respectively.[8]

Associations of heavy metals with Zn ore have been reported. Zn, Cd and Pb minerals often occur together because they have similar chemical behavior and they are often found to combine with sulfur as primary minerals.[9] Other heavy metals found as common impurities in Zn ores are Mn, Hg, Ge, Ag in sphalerite; Fe, Co, Cu, and Mn, in smithsonite and Mn and Fe in zincite.[10,11]

Chemical partitioning of heavy metals (Pb, Zn and Cd) in soils contaminated by past Zn/Pb mining and smelting activities was investigated by Li and Thornton.[12] They found that the main chemical phases of Pb are carbonates (24–55%) and Fe–Mn oxides (30%). Zn was found to be strongly associated with the Fe–Mn oxides (30%) and residual fractions (50%). For Cd, the exchangeable, carbonate and Fe–Mn oxide phases account for more than 70% of the total Cd content.

DOI: 10.1039/b500834d

In metal bioavailability studies of contaminated soil, it is generally accepted that metal bioavailability in soils depends on many factors. These factors are not completely understood and simple relationships are seldom found in natural soil systems between plant metal levels and total metal concentrations in soil.[13–15] In some investigations, correlations between specific metal fractions and plant metal contents were found. For example, in soils that had been amended with composted or liquid sewage sludge it was found that Zn in exchangeable and oxidizable fractions had a strong correlation with Zn in the leaves of barley (*Hordeum vulgar*).[16] A simple relationship existed between Co in the exchangeable fraction and the Co concentration in winter wheat (*Triticum aestivum* L.) and alfalfa (*Medicago sativa* L.) while the adsorption of Ni, Cu and Pb by plants could be predicted by a stepwise multiple regression procedure.[17] These studies show the possibility for using sequential extraction data to evaluate the correlation between metals in soil and plant uptake. Therefore, the relationship between plant uptake of metals and the metal concentration in some fractions was also investigated.

Experimental

Chemicals and apparatus

All chemicals used were of analytical grade. Multi-element stock solution for ICP-MS (AccuStandard, Inc. CT, USA) has been used for the preparation of standard solutions. Before use, all glassware and plastic containers were cleaned and soaked in 10% (v/v) HNO_3 for at least 24 h, followed by rinsing three times with ultra pure water.

Inductively coupled plasma mass spectrometry (ICP-MS, Perkin Elmer ELAN 6000) was used for the elemental determination of extracts.

Sample under investigation

Seventy-nine top soil samples (0–10 cm) near a Zn mining area in Tak Province, Thailand were sampled. All the samples were then sieved through a 2 mm sieve and milled in an agate mortar to fine particles, to obtain good homogeneity, which were used in the chemical analysis. Soil pH, soil texture and % organic matter (%OM), determined by the Walkley and Black method,[18] of the samples investigated are given in Table 1. The soil samples studied were slightly acidic, neutral or alkaline. Most samples (69 samples) had a %OM between 1.5–3.5%. Their textures were sandy loam, loam, sandy clay loam or clay loam.

Fractionation scheme

The modified Tessier sequential extraction scheme[4,19] was carried out using the following solutions:

Step 1 (F1): 0.01 M $Ca(NO_3)_2$ (exchangeable fraction)

Step 2 (F2): 0.11 M CH_3COOH (acid soluble fraction)

Step 3 (F3): 0.04 M $NH_2OH \cdot HCl$ adjusted to pH 2 with HNO_3, 85 °C (reducible fraction)

Table 1 Some chemical and physical properties of the soil used in the study

pH	*n*	Texture	*n*	%OM	*n*
4.5–5.0 (Very acid)	7	Sandy loam	21	<1.5	1
5.1–6.0 (Acid)	12	Loam	16	1.5–3.5	69
6.1–6.5 (Slightly acid)	13	Sandy clay loam	20	>3.5	9
6.6–7.3 (Neutral)	12	Clay loam	22		
7.4–7.8 (Slightly alkaline)	21				
7.9–8.4 (Alkaline)	14				

n = Number of samples.

Step 4 (F4): 8 : 3 v/v (30% H_2O_2 : 0.02 M HNO_3), 96 °C (oxidizable fraction)

Step 5 (F5): 1 : 1 v/v (conc. HNO_3 : 30% H_2O_2) (residual fraction)

Continuous-flow sequential extraction system

Extraction chamber. The continuous-flow extraction system as previously reported[5] was used. The extraction chamber was designed to allow containment and stirring of a weighed sample. Extractants could flow sequentially through the chamber and leach metals from the targeted phases. The chamber and its cover was constructed from borosilicate glass to have a capacity of approximately 10 ml. The outlet of the chamber was furnished with a Whatman (Maidstone, UK) glass microfibre filter (GF/B, 47-mm diameter, 1 μm particle retention) to allow dissolved matter to flow through. Extractant was pumped through the chamber using a peristaltic pump (Micro tube pump, MP-3N, EYELA (Tokyo Rikakikai Co. Ltd)) at varying flow rates using Tygon tubing of 2.25 mm inner diameter. Heating of the extractant in steps III and IV at 85 °C and 96 °C was carried out by passing the extractant through a glass heating coil approximately 120 cm in length which was placed in a waterbath before the extraction chamber. The temperature of the extractant, either 85 °C or 96 °C, in the chamber was achieved when the heating coil was immersed in a thermostatted water bath controlled at 88 °C and 99 °C respectively, due to slight heat loss.

Extraction procedure. A weighed sample (approx. 0.25 g) was transferred to a clean extraction chamber together with a magnetic bar. A glass microfibre filter was then placed on the outlet followed by a silicone rubber gasket, and the chamber cover was securely clamped in position. The chamber was connected to the extractant reservoir and the collector vial using Tygon tubing and placed on a magnetic stirrer. The magnetic stirrer and peristaltic pump were switched on to start the extraction. The extracting reagents were sequentially flowed through the chamber and the extraction took place. The extract passing the membrane filter was collected at 30 ml volume intervals to obtain 6 subfractions for each extractant. Extraction was carried out until all four extraction steps were completed.

Total dissolution of sample and dissolution of residue. A closed-vessel microwave digestion system (Milestone model MLS-1200 Mega, Bergamo, Italy) was used for pseudo-total digestion of soil samples and residues. Weighed soil samples (0.25 g) or residue from the extraction chamber were transferred to the vessels together with concentrated HNO_3 (5 ml) and 30% H_2O_2 (5 ml). The vessel was then tightly sealed and subjected to a microwave digestion. After cooling, the digested solutions were made up to volume in volumetric flasks.

Analysis of heavy metals in soil extracts and digests

Cr, Mn, Fe, Co, Ni, Cu, Zn, Cd and Pb in soil extracts and digests were determined by ICP-MS. The contents of Cr, Mn, Fe, Co, Ni, and Cu were found to be in the normal range while concentrations of Zn Cd and Pb were significantly elevated with respect to the background concentrations reported by Soil Science Division, Thailand. The high concentrations of Zn, Cd and Pb detected in the soil extracts indicate that these sites have been contaminated by these three metals. Therefore, this report will focus on Zn, Cd and Pb.

Quality control of analytical data. A soil certified reference material, National Institute of Standards and Technology (NIST) SRM 2711, was used for method validation. Further-

Table 2 Comparison of metals contents in SRM 2711 soil as determined by continuous-flow sequential extraction procedure and certified values

	Concentration/mg kg^{-1}, $n = 2$						
Element	F1	F2	F3	F4	F5	Total	Certified value
Cd	0.24 ± 0.09	30.1 ± 1.2	2.2 ± 0.9	0.5 ± 0.1	0.01 ± 0.00	33.1 ± 0.2	41.70 ± 0.25
Zn	0.0 ± 0.00	68.9 ± 6.2	165.3 ± 10.4	157.6 ± 54.3	1.64 ± 0.001	393.4 ± 50.1	350.4 ± 4.8
Pb	0.0 ± 0.00	631.1 ± 105.7	461.2 ± 110.0	25.9 ± 2.5	0.54 ± 0.15	1118.7 ± 6.7	1162 ± 31

more, one-third of the total number of samples examined were also subjected to residual analyses to obtain total concentrations by summation of all fractions. The results were compared with those obtained by total digestion of the corresponding samples.

Blank analysis was performed frequently and every time a change of reagents or materials was used. High blank values were sometimes found, particularly for zinc, from some batches of glass fiber filters. However, this was found to be no problem because the levels of zinc in almost all samples studied were very high, such that extracted amounts were much higher than the blank values.

Results and discussion

Evaluation of the continuous-flow sequential extraction system

Evaluation of the continuous-flow sequential extraction system was performed by comparison of the summation data of all fractions with the certified values for total metal concentrations of the NIST SRM 2711 (Table 2). The total concentrations of Cd, Zn and Pb by summation showed good agreement with the total concentration from the certified values with slightly lower Cd and Pb values. This was also observed in our previous work, probably because the concentrations of elements in extracts were often lower in the continuous-flow system due to a dilution effect and some subfractions of the extract may not be detectable. Zn was found to be slightly higher probably from the higher blank values as a result of leaching contamination.

Fig. 1 presents correlation plots between the total metal contents of 24 samples determined by a single digestion of non-fractionated soil and those obtained by summation of metal amounts of all fractions from continuous-flow sequential extraction. The results show very good correlations with R^2 being higher than 0.99 for the three elements studied. The values from summation of fractionation data were slightly lower than those of total digestion as depicted by slopes being 0.87, 0.83 and 0.86 for Cd, Zn and Pb, respectively. This was also found in our previous work and was likely to be due to the dilution effect which caused poorer detectability for sequential extraction procedures. These levels of recoveries can be considered acceptable for this type of determination which involves summation of several data from subfractions and a dilution effect.

Distribution of Cd, Zn and Pb in soil samples

Soil samples studied were measured for their total concentrations by pseudo-total digestion and divided into 4 groups according to their total Cd, Zn and Pb concentrations; background level, slightly contaminated (2–5 times of background level), moderately contaminated (6–50 times of background level), and highly contaminated (more than 50 times background level). Most soil samples are contaminated with Cd and Zn in moderate and high levels (62 samples for Cd and 52 samples for Zn). For Pb, 46 of 79 soil samples analyzed are at background level while 26 samples are slightly and 7 samples moderately contaminated.

The concentrations of Cd, Zn and Pb in soils adjacent to the zinc mining area are distinctly elevated. Cd, Zn and Pb concentrations were found to decrease with distance from the mining area (data not shown) indicating the likeliness of zinc mining as the point source of contamination.

Fractionation of Pb, Zn and Cd in soil samples of different pHs

It is well known that many soil properties such as soil organic matter, cation exchange capacity (CEC) and soil pH can affect the distribution of heavy metals. It is interesting to investigate the fractional distribution of Pb, Zn and Cd in various soil pHs. Soil pH in this study falls in a very acid zone to an alkaline zone. The numbers of soil samples in each soil property group are shown in Table 1. To study the effect of soil pH on metal retention, the relationship between total

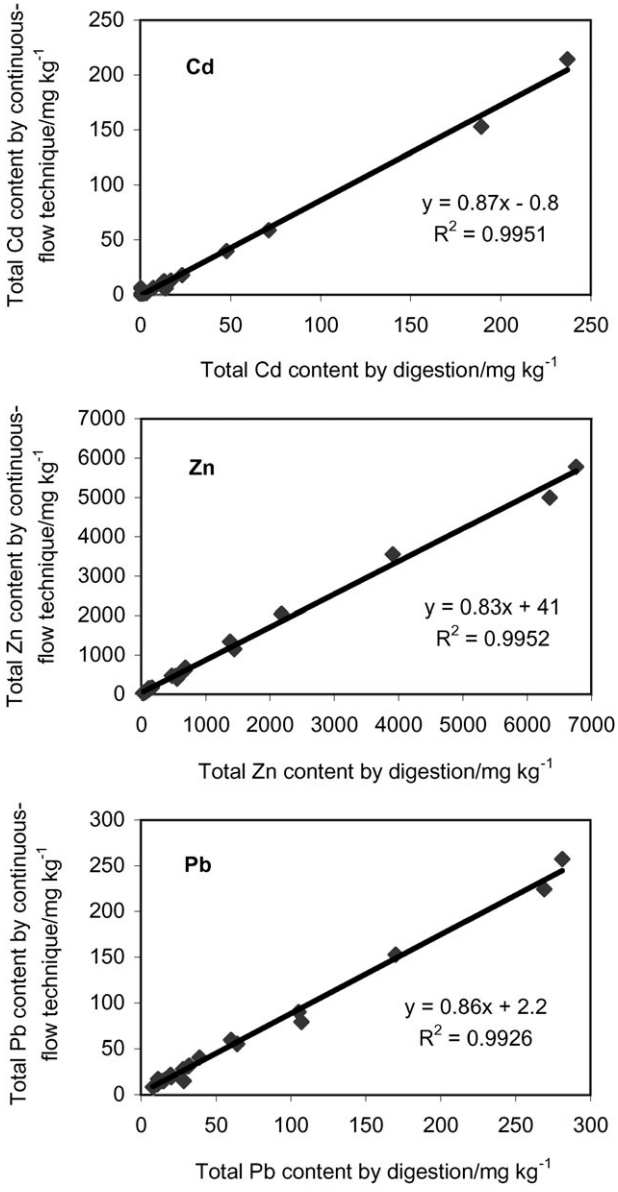

Fig. 1 Correlation plots of total metal contents determined by a single digestion of non-fractionated soil and by the continuous-flow sequential extraction procedure.

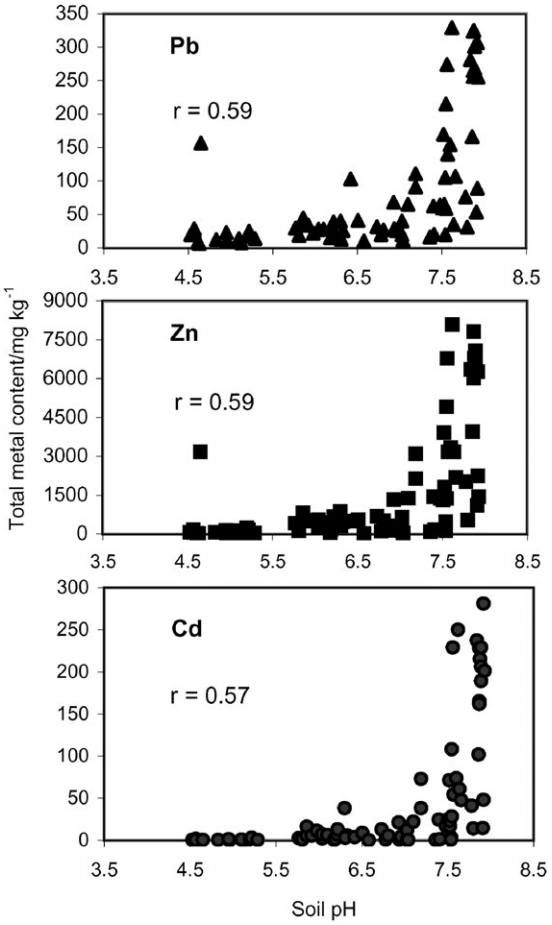

Fig. 2 Correlation plot between total metal contents and soil pH.

contents of Pb, Zn and Cd and soil pH was investigated. Fig. 2 shows clearly the pH dependence of metal retention in soil of the three elements. The three elements exhibit similar characteristics of pH dependence. Their total contents increase sharply with increasing pH from 7.0 to 7.9. Alkaline soils were proven to be a good scavenger of metals. This phenomenon is well-known and can be related to an increase of both specific and non-specific adsorption and to precipitation .[20]

The effect of soil pH on fraction distribution was also investigated. The average fraction distributions of Pb, Zn and Cd in 3 different soil pH zones, *i.e.* acidic (pH 4.5–6.5), neutral (pH 6.6–7.3) and alkaline (pH > 7.3) zones, are presented in Fig. 3. Samples with negligible amounts of extractable metals are not included in this investigation therefore the number of samples in acidic, neutral and alkaline zones are 32, 12 and 34 for Pb, 31, 12 and 34 for Zn, and 22, 8 and 32 for Cd, respectively.

For Pb, the most abundant fraction for the soils studied was found to be in the reducible phase (F3) regardless of soil pH. This fraction accounts for more than 70% of the extractable Pb content. The result agrees well with the observation of Li and Thornton[12] who found that a large amount of Pb in the soils at historical Pb mining and smelting areas was in the reducible fraction. The fraction distribution patterns of Pb are also very similar independent of the soil pH. The proportions of Pb were found to be in the order of: reducible (F3) > acid soluble (F2) > oxidizable (F4) > exchangeable (F1) fractions.

For Zn, about 50% of the extractable form was present in the F3 fraction for all three soil pH groups. Cadmium was predominantly (>55%) found in the first 2 fractions (F1 + F2) and mostly (>85%) in the first 3 fractions (F1 + F2 + F3). These results agree with many previous observations of Kuo *et al.*,[21] Hickey and Kittrick[22] and Xian[23] who reported that the organic/sulfide phase has only a minor role in binding Cd. The reducible phase was found to behave as an important scavenger of Pb and Zn and to a lesser degree for Cd.

In the case of Zn and Cd, soil pH shows a significant influence on the distribution patterns of these metals. Increasing soil pH caused a decrease in Cd and Zn contents in the exchangeable (F1) fraction but an increase in Cd and Zn contents in the acid soluble (F2) fraction. The effect of soil pH on the Cd distribution pattern has been explained[20,24] that as pH decreases, the solubility of the metal increases and metal is released in the forms of free or solvated ions. Therefore, lowering the pH of the soil can increase the concentration of metals in the soil solution.

Since exchangeable and acid soluble fractions (F1 + F2) are usually considered as mobile and having the most environmental impact, a comparison of their abundance in soil of different pHs was made. The Zn concentration in the mobile fraction (F1 + F2) in alkaline soils is higher than that in neutral soils and higher than that in acidic soils but that of Cd shows the opposite trend. The high Cd proportion in the mobile fraction (55–70%) clearly illustrates that Cd is more mobile and easily transported than Zn and Pb and it is therefore of particular concern, even without considering its higher toxicity.

The distribution of Zn and Cd in the oxidizable fraction (F4) is also affected by soil pH. Zn and Cd contents in this fraction seem to decrease with increasing soil pH. A clear explanation of changes in the percentage distribution of Zn and Cd in the F4 fraction is not possible in this study. Metal binding with organic matter *i.e.* humic acids was considered to be complex and dependent on many factors[25] such as pH and the presence of other metal ions.

Elemental associations in soil fractions using correlation study and extractograms

Generally, the association between metals in soils has been studied by investigation of their correlation in soil phases. This is performed by comparison of contents of two elements in a particular fraction of a number of samples. When the contents of two elements correlate well, they are considered to be closely associated. One of the problems when studying elemental association by this approach is the non-absolute evidence of elemental associations. Elements extracted in the same extrac-

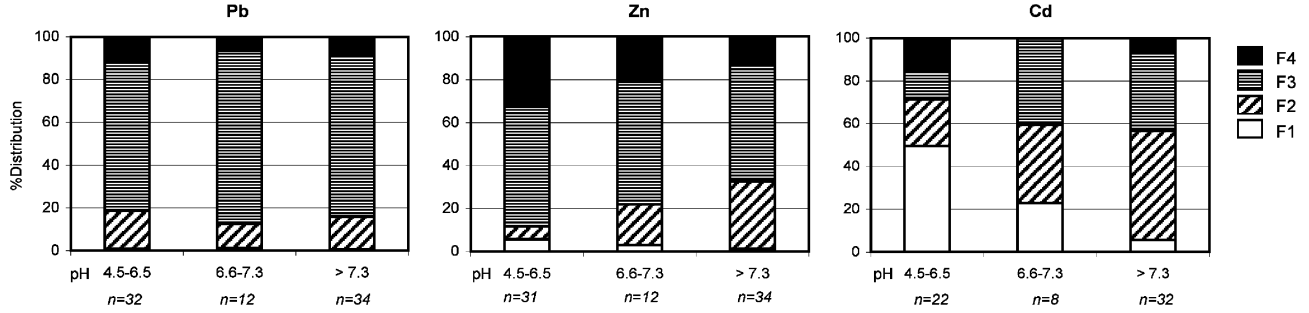

Fig. 3 Average % Pb, Zn and Cd distribution in soils of different soil pHs.

Table 3 Correlation coefficient between metal in soil fractions with other metal in corresponding soil fractions

	F1		F2		F3		F4	
	Cd	Zn	Cd	Zn	Cd	Zn	Cd	Zn
Group I (Cd $<$ 0.15–0.75 mg kg^{-1}), $n = 17$								
Zn	0.000		0.577		0.714[a]		−0.067	
Pb	0.000	−0.087	−0.133	−0.167	0.562	0.576	0.876[a]	0.310
Group II (Cd $>$ 0.75 mg kg^{-1}), $n = 62$								
Zn	0.372[a]		0.807[a]		0.848[a]		0.417[a]	
Pb	−0.019	0.109	0.752[a]	0.630[a]	0.851[a]	0.950[a]	0.396[a]	0.643[a]

[a] Correlation coefficient is significant at $p < 0.01$.

tion step may not have dissolved simultaneously but at a different time during that step. In other words, correlation of elements may not be a true elemental association. Such study of the relationship between metals in individual fractions by correlation study may be better referred to as 'elemental correlation'.

For investigation of elemental association, the overlayed extractograms obtained from a continuous-flow extraction can be used. Shiowatana *et al.*[26] and Hinsin *et al.*[27] used extractograms for evaluating the elemental associations in soils and iron hydroxide precipitates. The elemental associations for different elements can be studied by comparing detailed peak profiles and peak shapes of extractograms. Such detailed comparison is impossible using batch fractionation data alone, where the only possible comparison is between the elements extracted in a particular phase. The elemental correlation by considering the correlation coefficient and elemental association from extractograms are discussed using the data obtained in this study as follows:

The elemental correlations between Zn–Cd, Zn–Pb and Cd–Pb in individual fractions of soils are shown in Table 3. Because soils with high and low Cd contents may show different elemental correlations and in order to have a large enough number of samples in each group for correlation study, samples are divided into 2 groups based on the total content of Cd. In Table 3, the first group represents data from soils containing a total Cd content of $<$0.15–0.75 mg kg^{-1} (uncontaminated to slightly contaminated soil). The second group contains $>$0.75 mg kg^{-1} (moderately to highly contaminated soil).

The correlations between metals in the two groups of soil samples are different. For group I, correlation between Cd–Zn, Cd–Pb was found only in F3 ($r = 0.714$) and F4 ($r = 0.876$), respectively but significant correlations between Zn, Cd and Pb were found in group II for F2, F3 and F4 where contaminated metals were predominant.

Considering the elemental association in a particular fraction by using the extractograms, Fig. 4 shows the extractograms of Zn, Cd and Pb in highly, moderately contaminated and uncontaminated soil. The results show close associations between Zn, Cd and Pb and Fe in the acid soluble phase for the highly contaminated soil (Fig. 4a). In the reducible fraction, Cd and Pb appear to dissolve at the same time and earlier than Zn and Fe which appear together in the later part of the leaching. This indicates a strong association of Zn with Fe oxides which are important constituents of soil in the reducible fraction. The results of the relationship between metals in individual fractions from the two methods are obviously different because the two methods were based on different approaches as previously indicated.

Elemental atomic ratio plots for evaluation of the degree of anthropogenic contamination

The degree of contamination can be studied by the continuous-flow sequential extraction. This is obtained by a graphical plot of the elemental atomic ratio of metals of interest *versus* the subfraction number in a particular phase. The atomic ratio plots of Cd/Fe, Pb/Fe and Zn/Fe for highly contaminated, moderately contaminated and uncontaminated soils are shown in Fig. 5.

The extent of Cd, Pb and Zn adsorption on Fe oxides in the reducible fraction can be clearly observed in Fig. 5. For Cd in highly contaminated soil, high ratios of Cd/Fe were found in the early subfractions and decreased with subfraction number to approach a constant value. The atomic ratio of Cd/Fe in moderately contaminated soil differs from highly contaminated soil in that the atomic ratio is very low and almost constant for all subfraction numbers. Cd contents in uncontaminated soil

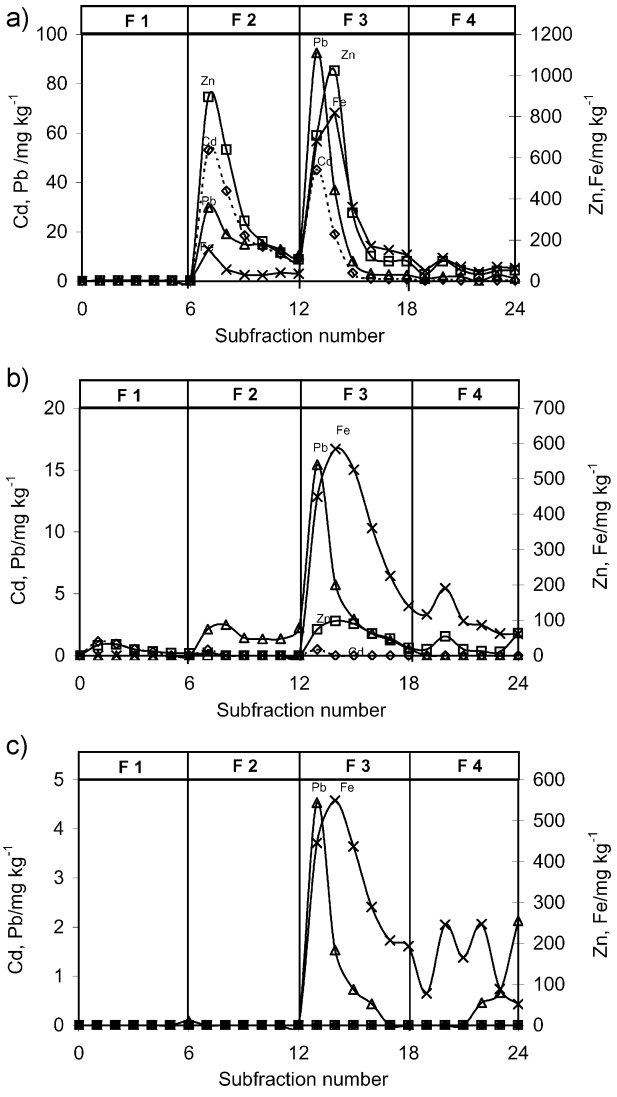

Fig. 4 Extractograms for Zn, Cd, Pb and Fe for highly (a), moderately (b) and uncontaminated (c) soils.

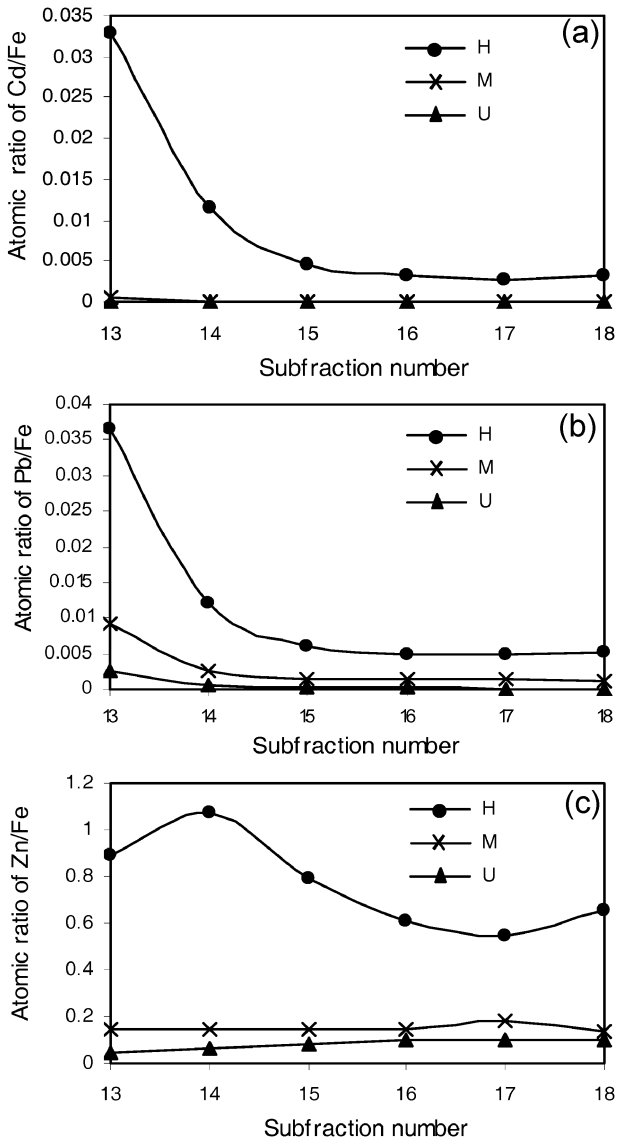

Fig. 5 Elemental atomic ratio of Cd/Fe (a), Pb/Fe (b) and Zn/Fe (c) plotted against subfraction number in the reducible phase, H = highly, M = moderately and U = uncontaminated soils.

are too low to be detectable; therefore, atomic ratio of Cd/Fe of the soil could not be determined. The results indicate that the contaminated Cd is mostly adsorbed on the surfaces of Fe oxides. The atomic ratio plots of Pb/Fe (Fig. 5b), show the same tendency as those of Cd. It appears that the atomic ratio plot can be used as a tool for identification of anthropogenic origin and degree of contamination. The atomic ratio of Zn/Fe in highly contaminated soil varied in the range 0.6–1.1 (Fig. 5c) while that of moderately contaminated and uncontaminated soil are lower than 0.2. The atomic ratio plot of Zn/Fe in highly contaminated soil does not show a similar trend as found for Cd and Pb.

Correlation between metal in rice grain and metal fractions

Heavy metal uptake by plants in contaminated soils has been extensively studied. The sequential extraction method has been used in an attempt to evaluate the relationship between the bioavailable fraction of metal in soil and the metal content in plant. Mench *et al.*[28] found that Cd and Ni uptake by maize was correlated with their contents in the exchangeable fraction. In this study, correlations between metal in rice grain, total metal contents, exchangeable (F1), acid soluble (F2) fractions and the summation of exchangeable and acid soluble (F1 + F2) fractions were studied. Pb in soil samples was mostly found near background levels or slightly contaminated therefore Pb is not included in this study. The correlation coefficients between metal in rice grain and their different fractions in soil collected from the corresponding field of rice grain samples are listed in Table 4.

Table 4 Correlation coefficient between metals in rice grain, total metal contents, exchangeable (F1), acid soluble (F2) and the summation of exchangeable and acid soluble (F1 + F2) fractions

	Metals in soil			
Metal in rice grain	Total	F1	F2	F1 + F2
Cd	0.341	0.680[a]	0.266	0.298
Zn	0.115	0.133	0.301	0.172
Fe	N.A.	0.567	0.079	0.034

N.A. = Not available. [a] Correlation coefficient is significant at $p < 0.01$.

A significant correlation was found between Cd in the F1 fraction and Cd in rice grain ($r = 0.680$). The result from fractionation shows the predominant Cd content in F1 for acidic soils. This implies that rice will uptake more Cd in acidic soil than neutral and alkaline soils. In other word, Cd uptake can be regulated by pH control of the soil. The present study agrees with previous reports which found that the uptake of Cd into crops grown on contaminated soils was correlated with Cd in the exchangeable fraction which was governed by soil pH.[7,29]

Total metal contents were poorly correlated with metal concentrations in rice grains ($r = 0.341$, 0.115 for Cd and Zn, respectively). These results agree with previous studies.[13,30–32] The different physical and chemical properties of soil have prevented the obtainment of direct relationships between the total metal contents in soil and plants.

The correlations between Fe and Zn in rice grain, total metal contents, concentrations of F1, F2 and F1 + F2 were also studied. The contents of Fe and Zn in the soil fractions do not correlate with the metal contents in rice grain. No significant correlation for these two elements was found.

Conclusions

A continuous-flow sequential extraction was utilized to study fractionation and elemental association of Zn, Cd and Pb in soil contaminated from zinc mining activities. Zn and Pb are predominantly present in the reducible fraction while Cd is concentrated in the first three fractions. Soil pH strongly affects the distribution of Cd but has no effect on Pb. The elemental associations were investigated from extractograms obtained. The results show close associations between Zn, Cd, Pb and Fe in the acid soluble phase for the contaminated soil. In the reducible fraction, Cd and Pb appear to dissolve at the same time and earlier than Zn and Fe, which appear together in the later part of the leaching. The extractograms provide detailed information that is not possible to obtain using a batch extraction technique. The data from elemental atomic ratio plot extractograms of Cd/Fe and Pb/Fe and Zn/Fe in the reducible phase confirm the information obtained from extractograms that contaminated Cd and Pb is adsorbed on the surface of Fe oxides. The higher the degree of contamination, the higher the Cd/Fe and Pb/Fe atomic ratio in the earlier subfractions of extraction. The two additional advantages of the continuous-flow extraction, *i.e.* using extractograms to study elemental association and use of elemental atomic ratio plots as a tool for identification of the anthropogenic origin and degree of contamination, have proved the continuous-flow extraction as an efficient system for detailed investigation of

soil contamination. However, the continuous-flow extraction does have some drawbacks concerning the larger numbers of analyses of subfractions required and the dilution effect from the flowing stream of extractant.

Acknowledgements

The authors would like to thank the Royal Golden Jubilee Scholarship for JB and research grant from the Thailand Research Fund and the Postgraduate Education and Research Program in Chemistry (PERCH), Higher Education Development Project of the Commission on Higher Education for partial support.

References

1 A. Tessier, P. G. C. Campbell and M. Bisson, *Anal. Chem*., 1979, **51**, 844.
2 C. Kheboian and C. F. Bauer, *Anal. Chem*., 1987, **59**, 1417.
3 S. Xiao-Quan and C. Bin, *Anal. Chem*., 1993, **65**, 802.
4 Ph. Quevauviller, *Trends Anal. Chem*., 1998, **17**, 289.
5 J. Shiowatana, N. Tantidanai, S. Nookabkaew and D. Nacapricha, *J. Environ. Qual*., 2001, **30**, 1195.
6 X. Li and I. Thornton, *Appl. Geochem*., 1993, **S2**, 51.
7 S. M. Ullrich, M. H. Ramsey and E. Helios-Rybicka, *Appl. Geochem*., 1999, **14**, 187.
8 J. F. Verner, M. H. Ramsey, E. Helios-Rybicka and B. Jêdrzejczyk, *Appl. Geochem*., 1996, **11**, 11.
9 B. J. Skinner, *Earth Resources*, Prentice-Hall Inc., Englewood Cliffs, NJ, 2nd edn., 1976, p. 88.
10 B. J. Alloway, *Heavy Metals in Soils*, Chapman & Hall, London, 2nd edn., 1995, p. 43.
11 *Econ. Geol. Bull. (Thailand Dep. Miner. Resour., Econ. Geol. Div.)*, 1982, **32**, pp. 16–17.
12 X. Li and I. Thornton, *Appl. Geochem*., 2001, **16**, 1693.
13 S. S. Iyengar, D. C. Martens and W. P. Miller, *Soil Sci. Soc. Am. J*., 1981, **45**, 735.
14 J. T. Sims, *Soil Sci. Soc. Am. J*., 1986, **50**, 367.
15 J. T. Sims and J. S. Kline, *J. Environ. Qual*., 1991, **20**, 387.
16 J. P. LeClaire, A. C. Chang, C. S. Levesque and G. Sposito, *Soil Sci. Soc. Am. J*., 1984, **48**, 509.
17 J. Qian, Zi-jian Wang, Xiao-quan Shan, Q. Tu, B. Wen and B. Chen, *Environ. Pollut*., 1995, **91**, 309.
18 A. Walkley and J. A. Black, *Soil Sci*., 1934, **37**, 29.
19 C. W. Gray, R. G. McLaren, A. H. C. Roberts and L. M. Condron, *Commun. Soil Sci. Plant Anal*., 2000, **31**, 1261.
20 M. B. McBride, *Environmental Chemistry of Soil*, Oxford University Press, New York, 1994, p. 320.
21 S. Kuo, P. E. Heilman and A. S. Baker, *Soil Sci*., 1983, **135**, 101.
22 M. G. Hickey and J. A. Kittrick, *J. Environ. Qual*., 1984, **13**, 327.
23 X. Xian, *Environ. Pollut*., 1989, **57**, 127.
24 R. N. Yong, A. M. O. Mohamed and B. P. Warkentin, *Principles of Contaminant Transport in Soil*, Elsevier, Amsterdam, 1992.
25 L. K. Koopal, W. H. van Riemsdijk and D. G. Kinniburgh, *Pure Appl. Chem*., 2001, **12**, 2005.
26 J. Shiowatana, R. G. McLaren, N. Chanmekha and A. Samphao, *J. Environ. Qual*., 2001, **30**, 1940.
27 D. Hinsin, L. Pdungsap and J. Shiowatana, *Talanta*, 2002, **58**, 1365.
28 M. J. Mench, E. Martin and P. Solda, *Water, Air, Soil Pollut*., 1994, **75**, 277.
29 T. Asami, M. Kubota and K. Orikasa, *Water, Air, Soil Pollut*., 1995, **83**, 187.
30 D. Voutsa, A. Grimanis and C. Samara, *Environ. Pollut*., 1996, **94**, 325.
31 S. Shallari, C. Schwartz, A. Hasko and J. L. Morel, *Sci. Total Environ*., 1998, **209**, 133.
32 K. Chojnacka, A. Chojnacki, H. Górecka and H. Górecki, *Sci. Total Environ*., 2005, **337**, 17.

Anal. Chem. **2005,** *77,* 2720−2726

Automated Sequential Injection-Microcolumn Approach with On-Line Flame Atomic Absorption Spectrometric Detection for Implementing Metal Fractionation Schemes of Homogeneous and Nonhomogeneous Solid Samples of Environmental Interest

Roongrat Chomchoei,[†] Manuel Miró,[‡] Elo Harald Hansen,*[,§] and Juwadee Shiowatana[†]

Department of Chemistry, Faculty of Science, Mahidol University, Rama VI Road, Bangkok 10400, Thailand, Department of Chemistry, Faculty of Sciences, University of the Balearic Islands, Carretera de Valldemossa Km. 7.5, E-07122 Palma de Mallorca, Illes Balears, Spain, and Department of Chemistry, Technical University of Denmark, Kemitorvet, Building 207, DK-2800 Kgs. Lyngby, Denmark

An automated sequential injection (SI) system incorporating a dual-conical microcolumn is proposed as a versatile approach for the accommodation of both single and sequential extraction schemes for metal fractionation of solid samples of environmental concern. Coupled to flame atomic absorption spectrometric detection and used for the determination of Cu as a model analyte, the potentials of this novel hyphenated approach are demonstrated by the ability of handling up to a 300 mg sample of a nonhomogeneous sewage amended soil (viz., CRM 483). The three steps of the endorsed Standards, Measurements, and Testing sequential extraction method have been also performed in a dynamic fashion and critically compared with the conventional batchwise protocols. The ecotoxicological relevance of the data provided by both methods with different operationally defined conditions is thoroughly discussed. As compared to traditional batch systems, the developed SI assembly offers minimal risks of sample contamination, the absence of metal redistribution/readsorption, and dramatic saving of operational times (from 16 h to 40−80 min per partitioning step). It readily facilitates the accurate manipulation of the extracting reagents into the flow network and the minute, well-defined injection of the desired leachate volume into the detector. Moreover, highly time-resolved information on the ongoing extraction is given, which is particularly relevant for monitoring fast leaching kinetics, such as those involving strong chelating agents. On-line and off-line (for Cu, Pb, and Zn) single extraction schemes are also proven to constitute attractive alternatives for fast screening of metal pollution in solid samples and for predicting the current, rather than the potential, element bioavailability by the assessment of the readily mobilizable metal forms.

Sequential injection (SI) analysis has already been established as a powerful, fully automated computer-controlled sample pretreatment tool for wet chemical analysis.[1−4] Basically, SI encompasses a multiposition selection valve with a central communication line that can be made to address each of its peripheral ports (refer to Figure 1), and which, by means of a syringe pump, is used for sequentially aspirating well-defined segments of the various constituents of the assay, situated at the individual ports, and placing them into a holding coil. Afterward, the segments are, via flow reversal, propelled toward the detector, the manifold allowing appropriate unit operations to be executed by incorporation of packed column reactors, reaction coils, dilution chambers, digestion or extraction units, or gas diffusion/dialysis modules.[5,6] The system, moreover, allows metering of minute volumes (down to a few tenths of microliters), and the use of a syringe pump readily and reproducibly permits automatic microfluidic handling and operation at variable flow rates at will.[7]

Despite the recognized advantages of SI with respect to the first generation of flow injection (FI),[8−9] manipulation of solid materials into the microchannels of the SI network remains a challenge for analytical chemists. Yet, this flow approach entails inherent potentials for on-line processing of solid samples, as recently demonstrated in our research group,[10] which should

* Corresponding author. Telephone: +45-4525-2346. Fax: +45-4588-3136. E-mail: ehh@kemi.dtu.dk.

[†] Mahidol University.

[‡] University of the Balearic Islands.

[§] Technical University of Denmark.

(1) Wang, J.-H.; Hansen, E. H.; Miró, M. *Anal. Chim. Acta* **2003**, *499*, 139−147.
(2) Lenehan, C. E.; Barnett, N. W.; Lewis, S. W. *Analyst* **2002**, *127*, 997−1020.
(3) Fang, Z.-L. *Anal. Chim. Acta* **1999**, *400*, 233−247.
(4) van Staden, J. F.; Stefan, R. I. *Talanta* **2004**, *64*, 1109−1113.
(5) Marshall, G.; Wolcott, D.; Olson, D. *Anal. Chim. Acta* **2003**, *499*, 29−40.
(6) Cerdà, V.; Cerdà, A.; Cladera, A.; Oms, M. T.; Mas, F.; Gómez, E.; Bauzá, F.; Miró, M.; Forteza, R.; Estela, J. M. *Trends Anal. Chem.* **2001**, *20*, 407−418.
(7) Wang, J.-H.; Hansen, E. H. *Anal. Lett.* **2004**, *37*, 345−359.
(8) Hansen, E. H. *Talanta* **2004**, *64*, 1076−1083.
(9) Hansen, E. H.; Wang, J.-H. *Anal. Chim. Acta* **2002**, *467*, 3−12.

10.1021/ac048233m CCC: $30.25
Published on Web 03/17/2005

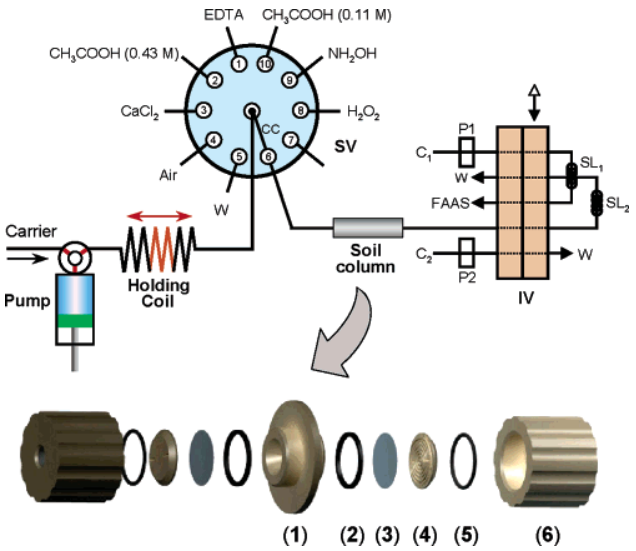

Figure 1. (Top) Schematic diagram of the hybrid FI/SI system with on-line FAAS detection for metal partitioning studies, comprising a syringe pump, a 10-port selection valve (SV) with a central communication channel (CC), a holding coil, a soil column, and a two-position injection valve (IV) accommodating sample loops SL_1 and SL_2. C_1 and C_2, carrier solutions; P1 and P2, peristaltic pump; W, waste. (Bottom) Exploded view of the extraction microcolumn, comprising the following components: (1) dual-conical sample container, (2) silicone gasket, (3) membrane filter, (4) filter support, (5) O-ring, and (6) end screw cap. The total volume of the sample container is ca. 400 μL. Bottom figure adapted with permission from ref 10. Copyright 2004 Elsevier Science Publishers.

attract the interest of practitioners in other scientific fields, such as soil science. In this discipline, fractionation analysis is currently regarded as a powerful tool for the identification and quantification of trace pollutants (e.g., anthropogenic metal species) bound to predefined geological phases in the soil sample. The batchwise procedures conventionally used are effected in a single or sequential extraction fashion under operationally defined conditions by attacking pollutant soil phase associations with solely one chemical reagent or by the sequential action of various extractants of increasing aggressiveness to leach the target species from particular soil compartments. Single extractions are mostly exploited to evaluate the exchangeable fraction of trace elements in soils, to estimate the fraction of total metal content available for root uptake,[11] and to predict pools of contaminants mobilizable via acidification or complexation processes.[12] Sequential extractions, though more laborious and time-consuming, provide enhanced information on the leachability of metal forms in different targeted phases. The ultimate aim of these fractionation schemes is to acquire knowledge on items of major environmental concern such as the origin, mode of occurrence, bioavailability, potential mobility, and the transport of the elements in natural scenarios.[13−17]

Although both single and sequential extraction protocols, such as the well-established three-step scheme from the Standards, Measurements and Testing (SM&T) Program of the European Commission[18,19] (formerly BCR), originally were devised to simulate natural conditions, researchers have more recently realized that naturally occurring processes are, in fact, always dynamic,[20,21] rather than static as they are identified by the traditional equilibrium-based methods. In addition, these batch ("end-over-end") extraction schemes suffer from several limitations regarding practicability (e.g., lack of automation, potential risks of contamination, labor-intensive and time-consuming protocols) and the significance of information provided, due to the inherent phase overlapping as a consequence of phase transformations, readsorption, and re-distribution of extracted elements.

In recent years, a number of groups have developed clever dynamic fractionation methods capitalizing on the advantageous features of FI schemes to circumvent the abovementioned drawbacks.[20−25] In all cases, the solid sample, as contained in small containers or microcartridges, is continuously subjected to the effect of fresh portions of a given leaching agent provided in a semiautomated fashion. These strategies have already opened new avenues for exploring the kinetics of the leaching processes as a function of exposure time and for obtaining a more realistic insight into metal lability from the different soil fractions. However, the manipulation of the extractant into the FI network to allow for increasing contact times with the solid substrate is rather cumbersome due to the intrinsic rigidity of the FI manifold and the progressive aging of the flexible tubes of the peristaltic pumps demanding a high frequency of maintenance. Although hyphenated microanalytical techniques for on-line detection of released species have been proposed recently, metal fractionation studies have merely been performed by increasing the concentration of the nitric acid supplied to the packed sample.[21,23] To the best of our knowledge, the application of a complete sequential extraction scheme in a fully automated mode along with on-line detection has not yet been reported.

In this paper, SI is exploited for the first time as a versatile and automated approach for the implementation of both single and sequential metal extraction/fractionation protocols in a single, compact module furnished with a dedicated dual-conical microcolumn, which can be hyphenated with atomic spectrometers (e.g., ICP-AES, ICP-MS, or AAS) for on-line leachate measurements. While it would be preferable to use a multielement detection device, a flame-AAS (FAAS) instrument was used in this investigation to exploit the principle applicability of the methodology.

(10) Chomchoei, R.; Hansen, E. H.; Shiowatana, J. *Anal. Chim. Acta* **2004**, *526*, 177−184.
(11) Pueyo, M.; López-Sánchez, J. F.; Rauret, G. *Anal. Chim. Acta* **2004**, *504*, 217−226.
(12) Sahuquillo, A.; Rigol, A.; Rauret, G. *Trends Anal. Chem.* **2003**, *22*, 152−159.
(13) Kennedy, V. H.; Sanchez, A. L.; Oughton, D. H.; Rowland, A. P. *Analyst* **1997**, *122*, 89R−100R.
(14) Gleyzes, C.; Tellier, S.; Astruc, M. *Trends Anal. Chem.* **2002**, *21*, 451−467.
(15) Das, A. K.; Chakraborty, R.; Cervera, M. L.; de la Guardia, M. *Talanta* **1995**, *42*, 1007−1030.
(16) Filgueiras, A. V.; Lavilla, I.; Bendicho, C. *J. Environ. Monit.* **2002**, *4*, 823−857.
(17) Hlavay, J.; Prohaska, T.; Weisz, M.; Wenzel, W. W.; Stingeder, G. J. *Pure Appl. Chem.* **2004**, *76*, 415−442.
(18) Ure, A. M.; Quevauviller, Ph.; Muntau, H.; Greepink, B. *Int. J. Environ. Anal. Chem.* **1993**, *51*, 135−151.
(19) Rauret, G.; López-Sánchez, J. F.; Sahuquillo, A.; Rubio, R.; Davidson, C. M.; Ure, A. M.; Quevauviller, Ph. *J. Environ. Monit.* **1999**, *1*, 57−61.
(20) Fedotov, P. S.; Zavarzina, A. G.; Spivakov, B. Ya.; Wennrich, R.; Mattusch, J.; Titze, K. de P. C.; Demin, V. V. *J. Environ. Monit.* **2002**, *4*, 318−324.
(21) Jimoh, M.; Frenzel, W.; Müller, V.; Stephanowitz, H.; Hoffmann, E. *Anal. Chem.* **2004**, *76*, 1197−1203.
(22) Shiowatana, J.; Tantidanai, N.; Nookabkaew, S.; Nacapricha, D. *J. Environ. Qual.* **2001**, *30*, 1195−1205.
(23) Beauchemin, D.; Kyser, K.; Chipley, D. *Anal. Chem.* **2002**, *74*, 3924−3928.
(24) Morales-Muñoz, S.; Luque-García, J. L.; Luque de Castro, M. D. *Anal. Chim. Acta* **2004**, *515*, 343−348.
(25) Dong, L.-M.; Yan, X.-P. *Talanta* **2004**, *65*, 627−631.

Detailed information about the kinetics of the ongoing extraction process and the current mobility of the various chemical forms of the target elements may thus be obtained. By taking advantage of the multiposition selection valve and the accurate microfluidic handling of the syringe pump, the different and well-accepted SM&T single and sequential extraction solutions can be precisely aspirated and dispensed through the soil microcolumn, whereupon the stripped target species are immediately injected into the detection device via a straightforward FI interface. Controllable on-line dilution to account for the variability of metal concentrations in the various extracts is readily accomplished by programming the portion of the FI sample loop to be filled by the leachate.

To ascertain the potentials of the hyphenated technique, a nonhomogeneous metal-contaminated complex sample was employed, namely, the sewage amended CRM 483 soil, with certified metal extractable contents for single extraction procedures (acetic acid and ethylenediaminetetraacetic acid (EDTA)), using Cu as the model of an anthropogenic metal ion of major concern, for instance in mining areas.[26] The dynamic information obtained with the microanalytical automated flow system is also critically compared with that previously reported for batch fractionations.

EXPERIMENTAL SECTION

Instrumentation. A FIAlab-3500 flow injection/sequential injection system (FIAlab, USA) equipped with an internally incorporated ten-port selection valve (SV), and a syringe pump (SP, Cavro, Sunnyvale, CA) with a capacity of 5 mL was used. The SI system was computer-controlled by the associated FIAlab software. The extraction microcolumn was incorporated within the SI system, and the outlet of the sample container was connected to a ten-port two-position injection valve (IV), acting as interface to a flame atomic absorption spectrometer (FAAS, AAnalyst 100, Perkin-Elmer), as depicted schematically in Figure 1. All ports of the SV and IV were connected through PEEK ferrules with rigid PTFE tubing (0.5 mm i.d./1.60 mm o.d.). The central port of the SV was connected to the holding coil (HC), which consisted of PTFE tubing (1.32 mm i.d./1.93 mm o.d.), the length being 110 cm, corresponding to a volume of 1.5 mL. The lengths of the PTFE tubing from port 6 of SV to the microcolumn and from the outlet of the microcolumn to IV were each 20 cm, corresponding to a volume of 40 μL. The IV was furnished with two sample loops (SL_1 and SL_2) each of 175 μL capacity. The connecting line between the IV and the FAAS nebulizer, which contributes to leachate dilution, was 19 cm long. The carrier solutions (C_1, and C_2; Milli-Q water) were pumped by means of a multichannel peristaltic pump (Ismatec, SA 8031) furnished with Tygon tubing. The peristaltic pump (in Figure 1 for graphical reasons depicted as two separate pumps, P1 and P2) was set at a slightly higher flow rate (viz., 6.2 mL min^{-1}) than the uptake rate of the FAAS (viz., 6.0 mL min^{-1}) to deliver the extract into the nebulizer by a positive pressure.

For on-line FAAS detection of Cu the wavelength and slit width were 324.5 nm and 0.7 nm (except for the extracts obtained in the EDTA single extraction method, where 216.5 nm and 0.2 nm were used). The same conditions were used in the off-line measurements of Cu, while the analytical wavelengths and slit widths for Pb and Zn were fixed at 283.3 nm and 0.7 nm, and 213.9 nm and 0.7 nm, respectively. Electrothermal atomic absorption spectrometry (ETAAS, Perkin-Elmer 2100) was exploited as a detection system to determine Pb in the acetic acid subfractions. The temperature program was executed according to the manufacturer's recommendations,[27] yet a 0.17 M $NH_4H_2PO_4$ solution was used as a modifier to increase the pyrolysis temperature to 850 °C.

Microcolumn Assembly. The purpose-made extraction microcolumn exploited in this work (Figure 1, bottom) was made of PEEK and comprised a central dual-conical shaped sample container with an inner volume of approximately 400 μL.[10] The entire unit is assembled with the aid of filter supports and caps at both ends. The membrane filters (Millipore, Fluoropore membrane filter, 13 mm diameter, 1.0 μm particle retention) used at both ends of the sample holder retains efficiently the solid particles while allowing solutions and leachates to flow freely with no backpressure effects.

Soil Sample. A certified reference material from the Standards, Measurements and Testing Program, namely, CRM 483 soil, was used to evaluate both the EDTA and the acetic acid single extractions, and the endorsed SM&T three-step sequential extraction method.[19] The solid material (sewage sludge amended soil) containing high levels of organic matter (viz., 12%) was collected from Great Billings Sewage Farm (Northampton, U.K.), as reported elsewhere.[28]

It should be stressed that the pretreatment steps for the preparation of this reference material involved sieving through a 2 mm round-hole sieve and mixing thoroughly by rolling for several days. The resulting material is, thus, characterized by a poor homogeneity, so that when the conical microcolumn was packed with the 300 mg soil, used in all experiments herein, it was guaranteed to constitute a representative fraction of the CRM 483 material.[29] It should be stressed that the selected soil cannot be handled reliably with previously reported FI/continuous microcartridge extraction techniques utilizing minute quantities of solid sample (5−25 mg).[21,23,25]

Reagents and Solutions. All chemicals were, at least, of analytical-reagent grade, and Milli-Q water was used throughout. Working standard solutions of metal ions were prepared by appropriate dilution of 1000 mg L^{-1} stock standard solutions (Merck) with 0.1 M nitric acid. The various chemicals employed in this work are detailed as follows: glacial acetic acid (Merck), EDTA free acid (Sigma), hydroxylammonium chloride (Merck), hydrogen peroxide (30%; Merck), calcium chloride dihydrate (Merck), Suprapur ammonia (25%; Merck), Suprapur nitric acid (Merck), Suprapur perchloric acid (Merck), and hydrofluoric acid (Merck).

Prior to use, all glassware was rinsed with 25% (v/v) concentrated nitric acid/water in a washing machine (Miehle, Model G 7735 MCU, Germany) and afterward rinsed with Milli-Q water.

Single Extraction and Modified SM&T Sequential Extraction Schemes. The reagents used in the single and sequential

(26) Grzebisz, W.; Kocialkowski, W. Z.; Chudzinski, B. *J. Geochem. Explor.* **1997**, *58*, 301−307.

(27) *Handbook of Analytical Techniques for Furnace Atomic Absorption Spectrometry: Recommended Conditions*, Manual B3205; Bodenseewerk Perkin-Elmer GmbH: Überlingen, Germany, 1987.

(28) Quevauviller, Ph.; Rauret, G.; López-Sánchez, J. F.; Rubio, R.; Ure, A.; Muntau, H. *Fresenius' J. Anal. Chem.* **1997**, *357*, 611−618.

(29) Chomchoei, R.; Miró, M.; Hansen, E. H.; Shiowatana, J. *Anal. Chim. Acta*, in press.

extraction schemes according to the SM&T recommendations are presented in the following sections:

Single Extraction Scheme. A 0.05 mol L^{-1} amount of EDTA was prepared as the ammonium salt solution by adding in a fume cupboard 14.61 g of EDTA free acid to 80 mL water and by partially dissolving it by stirring in 13 mL of 25% ammonia solution. The addition of ammonia was continued until all the EDTA was dissolved. The obtained solution was filtered through filter paper into a 1.00 L polyethylene volumetric flask and diluted with water to 0.9 L. The pH was adjusted to 7.00 ± 0.05 by addition of a few drops of ammonia or hydrochloric acid as appropriate. Finally, the solution was diluted with water to 1.00 L, well-mixed, and stored in a stoppered polyethylene container.

A 0.43 M solution of acetic acid was prepared by adding in a fume cupboard 25 mL of glacial acetic acid to about 500 mL of water in a 1.00 L polyethylene volumetric flask. The solution was diluted with water to 1.00 L volume, well-mixed, and stored in a stoppered polyethylene container.

A 0.05 M aqueous solution of calcium chloride was prepared by weighing 7.35 mg of the dried salt and then diluting it to 1.00 L volume with water.

Three-Step Modified Sequential Extraction Scheme. Step I (acid soluble fraction): A 0.11 M acetic acid solution was obtained by appropriate dilution of the 0.43 M acetic acid stock solution prepared previously.

Step II (reducible fraction): A 0.5 M hydroxylamine solution was prepared daily by dissolving 3.48 g of hydroxylamine hydrochloride in the minimum volume of water (ca. 10 mL) to which was added 1.6 mL of 2 M HNO_3. The solution was finally diluted to 100 mL with water.

Step III (oxidizable fraction): A 30% hydrogen peroxide solution was used as supplied by the manufacturer.

Dissolution of Residues. The residues from the extraction microcolumn were transferred to a PTFE vessel and, following addition of 6.0 mL of concentrated nitric acid and 5.0 mL of concentrated hydrofluoric acid, then heated gently to near dryness in a sand bath, with the temperature not exceeding 200 °C. Upon complete dissolution, the samples were cooled and 5 mL of perchloric acid was added, whereafter they were heated again to near dryness and diluted with 0.1 M HNO_3 to 50 mL prior to atomic absorption spectrometric measurements.

General Procedure for On-Line Single and Sequential Extraction. Initially, the holding coil was filled with the carrier solution (Milli-Q water) and all tubing from the peripheral SV ports were filled with the respective leaching solutions, while an air segment was delivered to the SL_2 interface via the assembled soil containing microcartridge. Since the total volume of the conduits between the holding coil (HC) and the FAAS (including microcolumn and sample loop) was 655 μL, SP was set to aspirate an equivalent volume of the desired extractant into HC and, then, the entire extractant plug was dispensed (10 μL s^{-1}) from HC directly to the microcolumn, allowing soil phase dissolution to take place, along with leachate collection into loop SL_2. After a delay time of 3 s, during which the pump was stopped, IV was switched (downward direction of the arrow in Figure 1) to make SL_2 part of the conduit between P2 and the FAAS and the extract was injected into the detector by means of carrier C_2. The 3 s delay time was incorporated first to engage the FAAS measurement and second to avoid creation of a pressure change during the valve shift.

Then SP was set to aspirate consecutively 100 μL of air from port 4 and 1050 μL of extractant into HC (at the rate of 100 μL s^{-1}). The role of the air segment is to prevent dispersion of the leaching reagent into the carrier solution. Solely 175 μL of the extractant plug (i.e., equal to the volume of the loops SL) was dispensed (10 μL s^{-1}), at each time, through the microcolumn into the SI−FAAS interface, in this case loop SL_1. The IV was again turned and the leachate, supplied to the nebulizer by carrier C_1, was analyzed on-line. The described procedure, alternately filling loops SL_1 and SL_2, was continued with a given reagent until no detectable amount of metal was leached (i.e., the signal was below LOD), or the increase was lower than 5% of the total metal leached. For elements continuously leaching from slowly accessible pools, as occurring in the acetic acid single extraction, a sample weight to extractant volume ratio similar to that of the batch method was selected.

The quantification of target analytes was done by peak integration (6 s) and summing up the peak areas of the particular metal fraction. All determinations were made using external calibration with standards prepared in diluted nitric acid. Although a common practice in batchwise fractionation is the use of calibration protocols based on matrix matching with the pertinent extracting reagent,[11,30] in our case, under the operationally selected conditions for CRM 483 partitioning, no multiplicative matrix interferences were encountered, as revealed by the application of the method of standard additions. This is a consequence of the discrete injection of minute, well-controlled volumes of extract into a continuously flowing carrier stream prior to FAAS detection, thus ensuring a high wash-to-sample exposure time, which diminishes risks of burner blockage.

RESULTS AND DISCUSSION

SI Analyzer for Single and Sequential Extraction Schemes. Dynamic extraction procedures for monitoring metal ion release from solid samples can be categorized into continuous[20−23] and discontinuous leaching processes[10] by exploiting the first (FI) and second (SI) generations of flow injection analysis, respectively. SI is more advantageous than FI in terms of accurate handling of microvolumes at predefined uniform flow rates through the solid substrate, because the flows are precisely controlled via the syringe pump with no need for frequent system recalibration. Furthermore, back-pressure or clogging effects in SI assemblies housing solid samples can, if called for, efficiently be alleviated by accommodating bidirectional flow approaches.

In our case, however, the SI setup with unidirectional flow fashion was entirely free from increase in flow resistance, even after long-term use. This is a result of the optimum hydrodynamic features of the dedicated biconical shaped microcolumn design (refer to Figure 1), which, in fact, accepts considerable amounts of solid material (up to 300 mg), so that solid materials lacking homogeneity can, also, be pretreated fully automatically without problems.

With regard to on-line detection, the discontinuous operational nature of SI must be taken into account for appropriate hyphen-

(30) Rauret, G.; López-Sánchez, J. F.; Sahuquillo, A.; Barahona, E.; Lachica, M.; Ure, A. M.; Davidson, C. M.; Gomez, A.; Lück, D.; Bacon, J.; Yli-Halla, M.; Muntau, H.; Quevauviller, Ph. *J. Environ. Monit.* **2002**, *2*, 228−233.

ation with the detection instrument. Electrothermal atomic absorption spectrometry (ETAAS) is inherently the most attractive detector for trace metal monitoring following SI extraction. Yet, the accommodation volume of the graphite tube (<50 μL) is unnecessarily small even for monitoring fast leaching kinetics, and the extraction schemes can therefore be excessively prolonged as a consequence of the resulting low measurement frequency of ETAAS.

Although ICP-AES and ICP-MS nowadays have been consolidated as routine tools for metal determinations because of their high sensitivity and multielemental capabilities, their intrinsic low tolerance to total dissolved salts[31,32] limits their potential uses. For ICP-MS, spectral interferences arising from isobaric overlapping, and the presence of polyatomic ions, further makes its application troublesome.[33]

From an operational point of view and despite its single-element capability, FAAS should be regarded as an attractive alternative for on-line analysis of metal contaminated soil samples using the well-accepted SM&T extractants. Not the least because the moderate dilution required to bring the analyte concentrations into the linear dynamic range can be readily performed in the microconduits of the flow setup. Furthermore, this detection principle has proven to be compatible with direct FI injection of the leaching agents with negligible matrix interferences.

To make compatible techniques of different nature, an external FI device was required, thereby yielding a SI−FI hybrid approach. It should be stressed that while the free uptake rate of FAAS usually ranges from 4 to 10 mL min^{-1}, the packed microcolumn accepts maximum delivery flow rates of ca. 1.0 mL min^{-1}. As can be seen in Figure 1, a leachate injector furnished with two sample loops was used to ensure optimum performance of the SI and FAAS systems, and allowing consecutive measurements to be effected, that is, the leaching process itself became the limiting step of the overall procedure.

As opposed to unidirectional continuous extraction protocols in FI systems, the hybrid SI−FI extraction technique allows all of the extract to be subjected to analysis, and hence an almost continuous extraction profile can be recorded (whenever required, in-line dilution can be realized via the software-controlled injection of a well-defined microvolume of leachate into the carrier of the SI−FAAS interface). Thus, by using volumes equal to only 175 μL of extract per injection, detailed knowledge on the leaching kinetics is gained, which otherwise could not be obtained, as off-line FAAS detection in the continuous-mode requires more than 1000 μL solution for reliable measurements.

In the following, discussions of the two extraction schemes with on- or off-line detection are offered in more detail.

Single Extraction Schemes with Off-Line Detection. Weak acid and strong complexing solutions are commonly used to assess trace-element availability in soil sciences. Complexing agents extract both carbonate and organically bound fractions, whereas weak acids mimic the effect of an acid input, such as acid rainfall or an anthropogenic spill, onto solid substrates of environmental origin.[12,13] Therefore, one of the aims of the present work was critically to compare the analytical results from the proposed dynamic method as achieved with the CRM 483 soil with those obtained under equilibrium conditions. The SI extraction system with off-line detection was assembled for fractionation explorations of three trace elements of different recognized lability (viz., Pb, Cu, and Zn). While Zn is considered as a typical mobile element, Cu is regarded as a metal of intermediate mobility and Pb as a fixed element.[12] The automated extraction was performed in the unidirectional flow mode as reported before,[10] yet at a perfusate flow rate of 10 μL min^{-1} with collection of 1 and 2 mL per subfraction for EDTA and CH_3COOH, respectively.

Table 1. Extractable Contents of Trace Metals (mg kg^{-1}) in CRM 483 As Obtained by the Single Extraction Procedure Using the SI Extraction System with Off-Line Detection[a]

	acetic acid (n = 3)		EDTA (n = 3)	
element	obtained	certified value	obtained	certified value
Pb	1.4 ± 0.1	2.10 ± 0.25	206 ± 9	229 ± 8.0
Cu	19 ± 2	33.5 ± 1.6	227 ± 11	215 ± 11
Zn	637 ± 38	620 ± 24	617 ± 5	612 ± 19

[a] Soil sample, 300 mg; extraction flow rate, 10 μL s^{-1}; subfraction volume/total extractant used, 1 mL/50 mL and 2 mL/12 mL for EDTA and CH_3COOH, respectively.

Table 1 is a compilation of the extractable amounts of Pb, Cu, and Zn from the CRM 483 soil as obtained by resorting to the SI single extraction schemes with off-line detection. For the CH_3COOH extraction of Pb and Cu, the total volume of the extractant was fixed at 12 mL to maintain a soil mass/volume ratio identical to that in the batchwise method. For these two nonreadily accessible metal ions, a nearly constant, continuous leaching profile was detected, due to the nonselectivity of the reagent,[34] which is also capable of releasing different metal pools prone to acidification processes. On the other hand, Zn was rapidly leached from the sewage amended soil. The CH_3COOH extraction pattern was monitored until the increase of metal leached in five consecutive subfractions was less than 5% of the accumulated amount. As shown in Table 1, the extractable content of Zn via SI−CH_3COOH extraction is statistically comparable to the certified value, thereby indicating that both, conceptually different methods yield similar results whenever applied to weakly retained forms. This also holds true for reagents with a strong capacity for metal mobilization and stabilization, such as EDTA, thus minimizing readsorption and re-distribution drawbacks. In fact, several researchers have employed chelating agents aimed at limiting precipitation and sorption of solubilized forms during batch procedures.[35] In this context it should be born in mind that EDTA is not merely capable of mobilizing carbonate and organic metal forms by competing complexing reactions but also metals entrapped in hydrous oxides of iron because of the high stability constant of the Fe−EDTA chelates (viz, log K = 25). This explains the good agreement between the SI and the batch results for the EDTA extractable fractions of the entire set of target elements.

In contrast, the leachable content under dynamic mode for less labile forms, such as acid soluble Pb and Cu, is appreciably lower

(31) Wang, J.-H.; Hansen, E. H. *J. Anal. At. Spectrom.* **2002**, *17*, 1278−1283.
(32) Cano, J. M.; Todolí, J. L.; Hernandis, V.; Mora, J. *J. Anal. At. Spectrom.* **2002**, *17*, 57−63.
(33) Montaser, A. *Inductively Coupled Plasma Mass Spectrometry*, WILEY−VCH: New York, 1998; Chapter 7.
(34) Whalley, C.; Grant, A. *Anal. Chim. Acta* **1994**, *291*, 287−295.
(35) Raksasataya, M.; Langdon, A. G.; Kim, N. D. *Anal. Chim. Acta* **1997**, *347*, 313−323.

Table 2. Extractable Contents of Trace Metals (mg kg^{-1}) for CRM 483 As Obtained by the Single Extraction Procedure and the Modified SM&T Three-Step Sequential Extraction Procedure Using the SI Extraction System with On-Line FAAS Detection

		single extraction ($n = 3$)		sequential extraction ($n = 3$)				
element	method	acetic acid	EDTA	step I	step II	step III	residue	total (I + II + III + residue)
Cu	proposed system (automated)	26 ± 1	221 ± 5	12 ± 1	198 ± 8	39 ± 3	112 ± 6	361 ± 11
	reported value (batchwise)	33.5 ± 1.6[a]	215 ± 11[a]	16.8 ± 1.5[b]	141 ± 20[b]	132 ± 29[b]	43.3 ± 3.8[b]	335 ± 35[b]
								362 ± 12[c]

[a] Certified value. [b] Taken from ref 30: soil sample, 300 mg; extraction flow rate, 10 μL s^{-1} (except step III, 5 μL s^{-1}); subfraction volume, 175 μL; total extractant used, 12 and 18 mL for CH_3COOH and EDTA (single extraction) and 12, 24, and 12 mL for steps I, II, and III (sequential extraction), respectively. [c] Total aqua regia digestion value.[30]

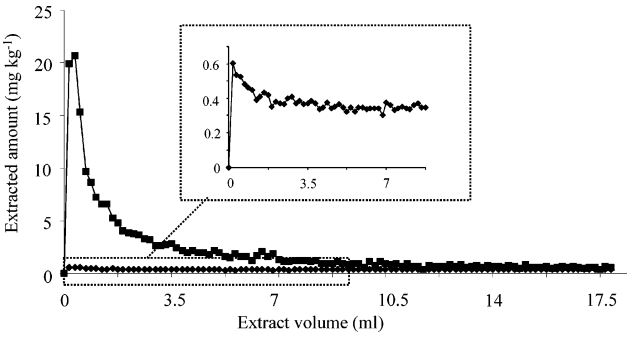

Figure 2. Extractograms for Cu in CRM 483, as obtained from single extraction on-line FAAS detection: (■) EDTA extraction; (◆) CH_3COOH extraction; subfraction volume, 175 μL; extraction flow rate, 10 μL s^{-1}. In the insert is shown a close-up of the extractogram within the first 8 min using CH_3COOH.

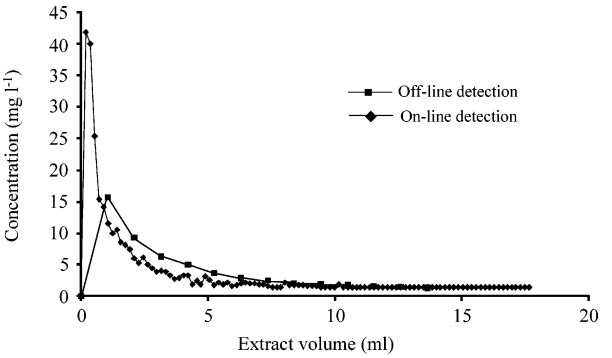

Figure 3. Extractograms for Cu with EDTA extraction, comparing the concentration of Cu in each subfraction when using off-line (1.0 mL per collected subfraction) and on-line FAAS detection (175 μL per subfraction).

than that obtained under a steady-state regime. This is a consequence of the inherently longer intimate contact time between soil and solution in the batchwise method. Actually, the results provided by both procedures are expected to differ considerably whenever the leaching agent attacks soil phases containing large available pools of slowly accessible elements. Yet, when increasing the acidic extractant volume in the SI method up to 50 mL, the leached amount for Pb and Cu was 3- and 2-fold higher, respectively, than the certified values due to the continuous shift of the metal distribution equilibria. Therefore, it is possible to conclude that the automated fractionation studies are better suited than their traditional counterparts for predicting actual risks associated with soil contamination.

Automated Single and Sequential Extraction Schemes with On-Line Detection. Microcolumn-based single and sequential extraction schemes were equally well accommodated in the fully automated SI setup for element partitioning studies. Besides preventing contamination risks, the totally enclosed environment reduces auxiliary sample manipulations dramatically, as neither separation nor dilution steps are needed. Very importantly, the microanalytical hyphenated technique ensures highly time-resolved information on the ongoing extraction process. Hence, fast leaching processes, such as those involving EDTA, can be appropriately monitored as depicted in Figure 2. For the particular reference material under investigation, more than 45% of the Cu(II) potentially prone to complexation is released in the first 2 mL of EDTA solution. Figure 3 clearly illustrates the different kinetic information rendered by the on-line analysis of minute volumes of leachate and, for comparison, measurements after manual dilution of 1 mL subfractions. The averaged concentrations of the semiautomated procedure are, thus, inadequate for short-term assessment of the ecological impact of pollutants liberated under the action of soluble ligands.

For the first time, the use of the three reagents in the well-established (sometimes termed standard[36]) SM&T extraction scheme[19] has been effected in a dynamic flow-through mode. According to previous researchers,[20] the third step of the procedure was realized at room rather than at elevated temperature, yet the flow rate was half (viz. 5 μL s^{-1}) of that for the other extractants in order to increase the contact time between the oxidizing agent and the sample. It should be emphasized that the methodology applied in the standard scheme for organic matter degradation solely is useful to estimate the total metal content associated with oxidizable soil phases. The oxidation at room temperature is a more realistic measure of the current, rather than potential, availability of metal ions by changes in oxidizing conditions or microbial activity in real-life samples, as metals associated with refractory organic compounds included in the mineral soil compartments are assumed to remain in the sample matrix for longer periods.[13]

As shown in Table 2, the fully automated single CH_3COOH extraction method renders, similarly to the off-line detection scheme, lower Cu recoveries than the batch protocol. Yet, the on-line available fraction (i.e., 26 mg kg^{-1} Cu) differs from that achieved under nonequilibrium regime but with fraction collection

(36) Filgueiras, A. V.; Lavilla, I.; Bendicho, C. *Anal. Bioanal. Chem.* **2002**, *374*, 103−108.

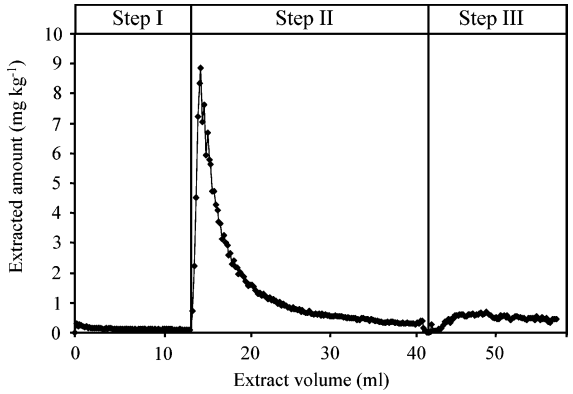

Figure 4. Extractogram for Cu in CRM 483 using the three-step sequential extraction scheme in the proposed SI system with on-line FAAS detection. Subfraction volume, 175 μL.

(i.e., 19 mg kg^{-1} Cu). These discrepancies are the result of the differences of the two operational procedures, since the delay time per subfraction required in the on-line method between extraction and measurement causes longer extractant−sample contact times (viz., 42 s/(mL of reagent)). The leaching patterns are obviously unaffected by the detection mode, as deduced from Figure 2 and the comments in the above section.

To compare critically both the dynamic and the batch extraction techniques, it should be noted that the contact time between the soil and the solution in the latter one is 16 h, so that metal re-distribution processes most likely take place. Gómez-Ariza et al.[37] reported that the percentages of readsorption of metals were strongly dependent upon the Fe−Mn oxide and organic matter content. In this context, Chomchoei et al.[38] demonstrated that the higher the organic matter content, the higher the readsorption of leached divalent metals, such as Cu, was encountered. Therefore, when the manual sequential extraction method is applied to soils containing high levels of organic matter, the first two steps are expected to be influenced by re-distribution processes. The higher recovery of Cu associated with easily reducible phases (mostly, manganese oxyhydroxides) for the sewage amended CRM 483 soil using the hybrid SI/FI system (see Table 2) as compared with the standard procedure is, hence, to be explained by the contribution of this phenomenon from step II to step III. The metal content liberated from oxidizable phases, cannot, however, be strictly compared because of the variable operational conditions of both methods.

In Figure 4 is illustrated the three-step Cu extractogram for the CRM 483 using the proposed flow system with on-line FAAS detection. The extraction profile renders an additional insight into the chemical associations of the elements within the soil compartments and into the leaching kinetics through continuous monitoring of the overall partitioning protocol.

As detailed in Table 2, the accuracy of the proposed approach is assessed by comparing statistically the summation of the extracted concentrations in each operationally defined phase plus the residue fraction with the reported total concentrations using aqua regia digestion. No significant differences existed between the total metal contents provided by the two methodologies. Thus, the extractable amount of Cu obtained by summation of steps I, II, and III (i.e., 249 mg kg^{-1}) is fairly similar to that mobilized using the EDTA single extraction method (i.e., 221 mg kg^{-1}). Therefore, the EDTA scheme can be regarded as a valuable tool for fast screening of metal pollution and measurement of readily bioavailable forms.

The most easily accessible pool of Cu from the CRM 483 was also monitored by resorting to the McLaren−Crawford scheme, originally developed for copper fractionation in soils.[39] The first two steps of this procedure, involving 0.05 M $CaCl_2$ for mobilization of water-soluble and exchangeable fractions and 0.43 M CH_3COOH for the acid soluble phases (or metals weakly bound to specific sites), were compared with the SM&T acetic acid single extraction scheme. The metal concentrations found in the exchangeable and acid soluble fractions were 1.8 ± 0.2 and 25 ± 2 mg kg^{-1}, respectively. The summation of these two fractions is statistically comparable to that of the SM&T method (viz., 26 ± 1 mg kg^{-1}), thereby demonstrating that single extractions are time and cost-effective alternatives to the sequential procedures for empirical assessment of the ecotoxicological significance of a given element in environmentally relevant solid samples, as also pointed out by several researchers.[13,36]

ACKNOWLEDGMENT

R.C. is grateful for financial support granted by The Royal Golden Jubilee Ph.D. Program of the Thailand Research Fund and to The Postgraduate Education and Research Development Program in Chemistry (PERCH) of the Commission on Higher Education (Thailand). M.M. is indebted to the Spanish Ministry of Education and Science for financial support through the "Ramon y Cajal" research program. Special thanks are also due to the mechanical workshop of the Department of Chemistry at Technical University of Denmark (headed by John Madsen), and especially to Anders Sølby, for constructing the extraction microcolumn.

(37) Gómez-Ariza, J. L.; Giráldez, I.; Sánchez-Rodas, D.; Morales, E. *Anal. Chim. Acta* **1999**, *399*, 295−307.
(38) Chomchoei, R.; Shiowatana, J.; Pongsakul, P. *Anal. Chim. Acta* **2002**, *472*, 147−159.
(39) McLaren, R. G.; Crawford, D. V. *J. Soil Sci.* **1973**, *24*, 172−181.

Received for review November 30, 2004. Accepted February 5, 2005.

AC048233M

Available online at www.sciencedirect.com
SCIENCE DIRECT®
Analytica Chimica Acta 536 (2005) 183–190
ANALYTICA CHIMICA ACTA
www.elsevier.com/locate/aca

Sequential injection system incorporating a micro-extraction column for automatic fractionation of metal ions in solid samples Comparison of the extraction profiles when employing uni-, bi-, and multi-bi-directional flow plus stopped-flow sequential extraction modes

Roongrat Chomchoei[a], Manuel Miró[b], Elo Harald Hansen[c,*], Juwadee Shiowatana[a]

[a] *Department of Chemistry, Faculty of Science, Mahidol University, Rama VI Road, Bangkok 10400, Thailand*
[b] *Department of Chemistry, Faculty of Sciences, University of the Balearic Islands, Carretera de Valldemossa Km. 7.5, E-07122 Palma de Mallorca, Illes Balears, Spain*
[c] *Department of Chemistry, Technical University of Denmark, Kemitorvet, Building 207, DK-2800 Kgs. Lyngby, Denmark*

Received 14 October 2004; received in revised form 22 December 2004; accepted 22 December 2004
Available online 21 January 2005

Abstract

Recently a novel approach to perform sequential extractions (SE) of elements in solid samples was developed by this group, based upon the use of a sequential injection (SI) system incorporating a specially designed extraction microcolumn. Entailing a number of distinct advantages as compared to conventional batch methods, this fully automated approach furthermore offers the potentials of a variety of operational extraction protocols. Employing the three-step sequential extraction BCR scheme to a certified homogeneous soil reference material (NIST, SRM 2710), this communication investigates four operating modes, namely uni-, bi- and multi-bi-directional flow and stopped-flow, allowing comparison of the metal fractionation profiles. Apart from demonstrating the versatility of the novel approach, the data obtained on the metal distribution in the various soil phases might offer valuable information as to the kinetics of the leaching processes and chemical associations in different soil geological phases. Special attention is also paid to the potentials of the microcolumn flowing technique for automatic processing of solid materials with variable homogeneity, as demonstrated with the sewage amended CRM483 soil which exhibits inhomogeneity in the particle size distribution.

Keywords: Sequential extraction; Sequential injection; Soil; Leaching kinetics; Microcolumn; Metal fractionation

1. Introduction

Sequential extraction is one of the most important tools to assess the impact of trace elements in solid samples (namely, soils, sediments, solid wastes, sludges, airborne particulates, biological tissues and foodstuffs) [1]. The results offer detailed information about the origin, mode of occurrence, bioavailability, potential mobility, and the transport of the elements in the natural environment [1–5]. When sequential extraction is practiced in the batch mode, there is, however, a high risk of sample contamination. Moreover, the classical manual procedures are tedious, time consuming, labor intensive and subject to several potential errors.

Exploiting the benefits of the manipulatory advantages of sequential injection (SI) [6–9], this group recently developed a novel, robust approach to perform sequential extraction of element in solid soil samples by using an SI-system incorporating a specially designed extraction microcolumn [10]. In this context, it was especially useful that SI-systems are based on using programmable, bi-directional discontinuous

* Corresponding author. Tel.: +45 4525 2346; fax: +45 4588 3136.
E-mail address: ehh@kemi.dtu.dk (E.H. Hansen).

0003-2670/$ – see front matter © 2004 Elsevier B.V. All rights reserved.
doi:10.1016/j.aca.2004.12.068

flow as precisely co-ordinated and controlled by a computer. Therefore, the flow network is easy and simple to reprogram from one application to another, notable advantages being that it allows the exact metering of even small volumetric volumes and that it readily and reproducibly permits flow reversals. Furthermore, sample/reagent consumption, operating times, as well as risks of contamination and analyte loss due to manipulation are considerably reduced in comparison with conventional batchwise systems. In this context, it should be stressed that the latter operationally-defined procedures are performed under pseudo-equilibrium conditions, so that kinetic information on the mobility of a given element is lost.

Based on the operation of the syringe pump, four operational modes are potentially feasible, comprising uni-directional flow, bi-directional flow, multi-bi-directional flow and stopped-flow, which are critically compared in this work aimed at metal fractionation explorations in solid samples. Sequential injection analysis is, thus, used as a powerful automated technique for accurate handling of micro-volumes of extracting solutions through the soil microcolumn in whatever desired sequence, and also as a promising tool in looking into the kinetics of the leaching processes as a function of exposure time, and into the chemical associations of the different components of the solid materials in the various leaching protocols.

In order to ascertain the results, the flow system was tested on two different certified reference materials with variable particle size distribution, namely, the homogeneous SRM 2170 pasture soil using the three-step BCR extraction scheme, and the heterogeneous sewage amended CRM 483 soil with single extraction protocols. It should be mentioned that the latter soil cannot be handled with reported flow injection/continuous microcartridge extraction techniques utilising minute amounts of solid sample [11–13], since the packed material cannot necessarily be considered as representative of the bulk medium. Though the emphasis herein is more on the potentials of the SI-microextraction technique as a novel operational concept able to integrate extraction schemes for metal fractionation in samples of different complexity, an interpretation of the behavior of the individually extracted metal species in the various operational modes is also provided for the SRM 2710 soil.

2. Experimental

2.1. Instrumentation

A FIAlab-3500 flow injection/sequential injection system (Alitea, USA) equipped with an internally incorporated 10-port selection valve (SV), and a syringe pump (SP, Cavro, Sunnyvale, USA) with a capacity of 10 ml was used. The SI-system was computer controlled by the associated FIAlab software. The extraction microcolumn was connected within the SI-system as shown in Fig. 1. All outlets of the SV were

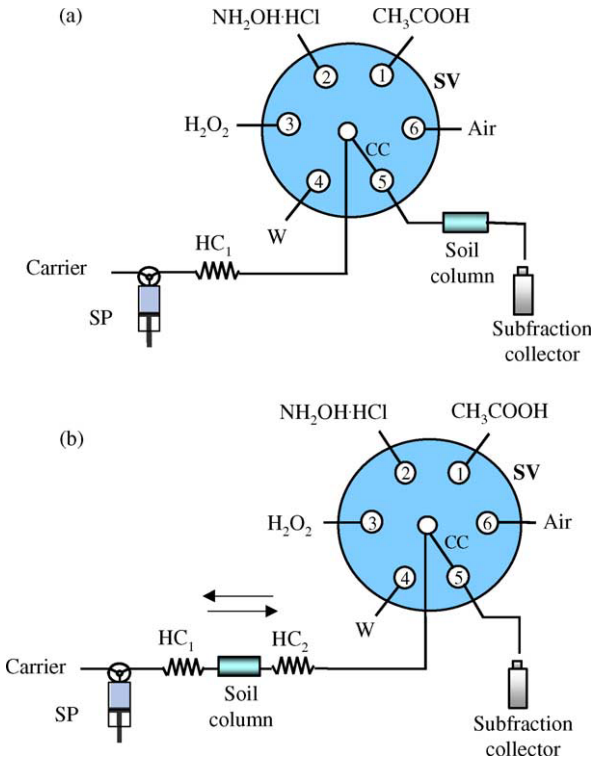

Fig. 1. Schematic diagram of the SI/SE systems used: (a) uni-directional flow and stopped-flow systems; (b) bi-directional flow and multi-bi-directional flow system. SV, selection valve; CC, central communication channel; SP, syringe pump; HC_1 and HC_2, holding coils number 1 and 2; W, waste; carrier, Milli-Q water (from Ref. [10] by permission of Elsevier Science Publishers).

connected through PEEK ferrules with rigid PTFE tubing (0.5 mm i.d./1.60 mm o.d.) (Bohlender, Germany). The central port of the SV was connected to the holding coil (HC), which consisted of PTFE tubing (1.32 mm i.d./1.93 mm o.d.) (Cole-Parmer Instrument Company, USA), the length being 110 cm, corresponding to a volume of 1.5 ml.

Determination of the concentrations of the individual metal species was performed by using a Perkin-Elmer Analyst 100 flame atomic absorption spectrometer (FAAS) equipped with deuterium background correction.

When required, heating of extractants was made by means a thermostated hotplate allowing the solutions to obtain the required temperature before aspiration into the system.

2.2. Apparatus and procedure

The extraction microcolumn employed in this work has been described in detail previously [10]. Made of PEEK, and comprising a central bi-conical shaped sample container, with a volume of ca. 359 μl, and equipped with filters and filter supports and caps at both ends, the entire unit is ca. 43 mm long when fully assembled. The membrane filters (Millipore, Fluoropore™ membrane filter, 13 mm diameter, 1.0 μm particle retention) used at both ends of the extraction microcolumn allowed dissolved matter to flow freely through.

Table 1
Experimental details of the three-step BCR sequential extraction scheme performed in the flow-through automated fashion

Step	Extracting reagent	Fraction
I	0.11 mol l^{-1} acetic acid, room temperature	Acid soluble
II	0.1 mol l^{-1} hydroxylamine hydrochloride, pH 2.0, 65 ± 5 °C	Reducible
III	8.8 mol l^{-1} hydrogen peroxide, pH 2.0, 85 ± 5 °C	Oxidisable

In this study, the three-step sequential extraction scheme of the Community Bureau of Reference (BCR) [14] was carried out as shown in Table 1.

2.3. Soil sample

A soil certified reference material from the National Institute of Standards and Technology (NIST), SRM 2710, was used. The soil material was collected from a pasture land (Montana, USA) affected by the deposition of creek sediments. It is a highly contaminated soil, the certified total concentration values of a number of elements being given. According to the certification report, this material was carefully prepared to achieve a high degree of homogeneity, its primary mission in this work being to provide a convenient way for evaluation of the accuracy of the proposed schemes. The extracts obtained automatically from the highly contaminated soil in the different extraction steps of the various operational SI-modes were processed by FAAS.

In this investigation, the dedicated microcolumn was packed with merely 25 mg of SRM 2710 soil. However, acceptable results when working with such low amounts of homogeneous solid materials have been verified previously [10] and also reported in the literature [11–13,15].

As a model solid sample to assess the potentials of the automated SI-extraction system, another certified reference material was also used, i.e., CRM 483 from BCR, which is a heterogeneous sewage sludge amended soil containing high levels of organic matter.

2.4. Preparation of reagents

All reagents were of analytical grade. Milli-Q water was used throughout. Working standard solutions were prepared by diluting 1000 mg l^{-1} stock standard solutions (Merck).

Other chemicals employed in the experiments were Suprapur nitric acid (65%, Merck), Suprapur perchloric acid (70%, Merck), hydrofluoric acid (40%, Merck), hydrogen peroxide (30%, Merck), glacial acetic acid (100%, Merck), and hydroxylammonium chloride (Merck).

Prior to use all glassware was rinsed by 25% (v/v) concentrated nitric acid in a washing machine (Miehle, Model G 7735 MCU, Germany) and afterwards cleaned with Milli-Q water.

2.5. Dissolution of residues and determination of total concentrations of metals

Residues from the extraction column were transferred to a PTFE vessel and then 3.0 ml of nitric acid (65%) and 3.0 ml of hydrofluoric acid (40%) were added and heated gently to near dryness in a sand bath, with temperature not exceeding 140 °C, as reported elsewhere [16]. The samples were cooled and 1 ml of perchloric acid was added, thereafter they were heated again to near dryness and finally diluted with 2% nitric acid. All the sample solutions were then further properly diluted to make the analyte concentrations within the linear dynamic range of the FAAS instrument.

2.6. Operating procedures

In this study, four applicable modes of the sequential injection/sequential extraction (SI/SE) procedure were investigated, that is, the uni-directional flow and the stopped-flow as shown in Fig. 1(a), and the bi-directional flow and triple bi-directional flow as depicted in Fig. 1(b). In all procedures, a total of 50 ml of each extractant was used. However, in order to ensure appropriate temperature control of the solutions, and to avoid back-pressure effects during extractant loading in those protocols involving flow reversal, only 1 ml aliquots were manipulated at a time in the system. The complete sequential extraction procedure of the four approaches thus runs through the following sequences.

Uni-directional flow. SP was set to aspirate consecutively 300 μl of air from port 6 and 1.00 ml of 0.11 M CH_3COOH from port 1 into HC_1 (at a rate of 100 μl s^{-1}). The role of the air segment is to prevent dispersion of the leaching reagent into the carrier solution. The entire extractant plug was then dispensed (50 μl s^{-1}) from HC_1 directly to port 5 and then passed through the microcolumn, allowing extraction to take place. For each five cycle runs, the extracts from the microcolumn were collected in a separate plastic vial, thus totally amounting to ten 5 ml subfractions for a complete set. Thereafter, the next extractant was automatically aspirated from the respective valve port and the collection of ten 5 ml subfractions repeated until all three leaching steps had been completed.

Stopped-flow. The system operation was similar to that of the uni-directional flow procedure, except that the procedure included the extra stopped-flow step. After aspiration of the air and of the extractant segment into HC_1, 800 μl of the leaching agent was dispensed (50 μl s^{-1}) from HC_1 directly to port 5 to wash out the former extract and stop the next fraction volume into the microcolumn, the stop period being affixed to 2 min. Afterwards, the remaining extractant in HC_1 was dispensed to pass through the column, thereby transporting totally 1.00 ml to the subfraction collector. The stopped-flow step was performed only in step I (acid soluble fraction) to assess the possible re-adsorption of the various elements on the soil particle surface, as well as the influence on the metal extractability by application of the ensuing

reducing and oxidising leaching agents. The extraction procedure was repeated with five cycle runs for each subfraction and totally ten 5 ml subfractions for each set. Extractions with the following two extractants were made as described in the uni-directional flow procedure above.

Bi-directional flow. SP was set to aspirate 1.00 ml of 0.11 M CH_3COOH (50 $\mu l\,s^{-1}$) from port 1 to pass through the microcolumn to HC_1. To ensure that all of the extractant actually had been passed through the column, the central communication channel (CC) in the SV was immediately, after the loading of the extractant, switched to port 6 and SP made to aspirate 1.00 ml of air (50 $\mu l\,s^{-1}$) which hence became positioned in HC_2. The extract was then dispensed backward (50 $\mu l\,s^{-1}$) through the column, HC_2, port 5 and finally collected in the subfraction collector. Again, the leaching process was repeated with five cycle runs for each subfraction, amounting to a total of 10 subfractions for each set. Identical protocols were executed for the consecutive steps of the sequential extraction scheme.

Triple bi-directional flow. The operation of the system was similar to that of the bi-directional flow procedure, except that the extractant in each cycle run was passed through the extraction microcolumn backward and forward totally six times (3× bi-directional). The triple bi-directional step was performed merely in the first step of the SE protocol, so that the extraction yields of the acid soluble fraction are to be compared for the various SI-extraction modes handled, that is, the following extractants were used as described in the bi-directional flow procedure.

The extracts were subjected to FAAS measurement after the overall automated extraction steps were completed. All determinations were made using external calibration without matrix matching, as this previously has been found unnecessary for this particular reference material [10]. The total metal concentrations were obtained for each extraction mode by summation of the metal content in the soil phase associations sensitive to acidification and redox processes, and the residual fraction, allowing statistical comparison with the certified values.

3. Results and discussion

3.1. Extraction by the SI/SE system

By exploiting the SI/SE microcolumn set-up illustrated in Fig. 1, and taking advantage of the versatility of the movements of the syringe pump, four modes of extraction are practicable, that is, uni-directional flow, bi-directional flow, multi-bi-directional flow, and stopped-flow, being also readily applicable to single extraction schemes.

In the uni-directional flow the extractant plugs are delivered only once through the microcolumn. This approach is simple, rapid and easy to perform. Moreover, in contrast to the other extraction protocols, and to batch-mode extractions, the uni-directional multiple-step scheme minimizes the problem of readsorption and redistribution of released species during extraction, because the extractant is being continuously renewed, and the contact time between the leachant solution and soil sample is, to a great extent, reduced. Thus, this dynamically operating mode can be regarded as an elegant solution to reduce the readsorption effects, which may dramatically affect trace metal extractability in the earlier steps of sequential extraction protocols, as reported by different researchers [17–19].

Yet, in order to obtain additional kinetic insight and valuable information on the various metal pools available, longer contact time between the extractant and the soil sample might be profitable, which can readily be achieved by exploiting the stopped-flow and the forward–backward flow approaches. The bi-directional flow mode must also be considered as a suitable alternative whenever back-pressure effects are encountered in the uni-directional approach due to the progressive tighter packing of the solid material. In the present application, however, the uni-directional operation turned out to be entirely trouble-free, and neither flow resistance nor tendency of clogging was observed even after long-term use at the moderately high flow rates applied (namely 3.0 ml min^{-1}), which is attributed to both the minute amounts of solid material employed and the optimum hydrodynamics of the custom-built microcolumn.

3.2. Comparison of the extractable amount of metals by different modes of extraction

One of the aims of the present work was to critically compare the analytical performance of the various SI-extraction procedures performed in an automated fashion in terms of extractability and acceleration of the operationally-defined SE schemes, thus reducing the number of subfractions. As a consequence of the longer contact times between the extractant plugs and the packed soil sample in the triple bi-directional flow and stopped-flow with respect to the uni- and bi-directional approaches, higher extraction efficiencies might be expected. On the other hand, it should be also kept in mind that problems due to metal readsorption/redistribution processes might emerge. If that is the case, the extractable amount of target metals by using the two former modes should decrease in step I and increase in either step II or III. Therefore, in this study, triple bi-directional flow and stopped-flow were executed solely in step I.

It is important to emphasise the existence of a correlation between the contact time and the extent of the redistribution/readsorption phenomenon, as the larger the extraction time the larger influence of this phenomenon is expected. However, it is possible to discern between both effects by comparison of the metal leachable contents obtained for the stopped-flow and forward–backward approaches for a given extraction time. In fact, the stopped-flow mode provides relevant information on the readsorption process as a consequence of the stagnant nature of the leaching solution, whereas the effect of the contact time may be

Table 2
Extractable amounts of Pb, Cu, Zn, and Mn for the various operationally-defined automated extraction modes using the SI/SE microcolumn set-up

Element	Mode	Amount extracted (mg g^{-1}) ± S.D. (n = 3)				Total (mg g^{-1})	Certified values (mg g^{-1})
		Step I	Step II	Step III	Residue		
Pb	Uni-directional	1.0 ± 0.1	2.11 ± 0.03	<0.36[a]	2.3 ± 0.1	5.5 ± 0.1	5.53 ± 0.08
	Bi-directional	0.97 ± 0.02	2.6 ± 0.1	0.5 ± 0.1	1.45 ± 0.09	5.5 ± 0.2	
	Stopped-flow	1.04 ± 0.01	2.48 ± 0.01	< 0.36[a]	2.10 ± 0.05	5.62 ± 0.05	
	Triple bi-directional	0.9 ± 0.1	2.39 ± 0.06	0.6 ± 0.1	1.5 ± 0.1	5.5 ± 0.2	
Cu	Uni-directional	1.38 ± 0.09	0.53 ± 0.02	0.15 ± 0.01	0.75 ± 0.07	2.8 ± 0.1	2.9 ± 0.1
	Bi-directional	1.46 ± 0.06	0.65 ± 0.05	0.14 ± 0.06	0.71 ± 0.06	3.0 ± 0.1	
	Stopped-flow	1.56 ± 0.09	0.73 ± 0.02	0.22 ± 0.04	0.40 ± 0.09	2.9 ± 0.1	
	Triple bi-directional	1.6 ± 0.1	0.70 ± 0.09	0.17 ± 0.08	0.4 ± 0.1	2.9 ± 0.2	
Zn	Uni-directional	1.62 ± 0.02	1.4 ± 0.1	1.1 ± 0.1	2.7 ± 0.2	6.9 ± 0.2	6.95 ± 0.09
	Bi-directional	1.65 ± 0.04	1.48 ± 0.03	1.27 ± 0.06	2.5 ± 0.3	6.9 ± 0.3	
	Stopped-flow	1.7 ± 0.1	1.52 ± 0.03	1.04 ± 0.03	2.7 ± 0.1	6.9 ± 0.1	
	Triple bi-directional	1.75 ± 0.09	1.53 ± 0.05	1.04 ± 0.01	2.6 ± 0.2	6.9 ± 0.2	
Mn	Uni-directional	1.9 ± 0.2	0.44 ± 0.02	0.63 ± 0.03	6.9 ± 0.7	9.9 ± 0.7	10.1 ± 0.4
	Bi-directional	0.95 ± 0.03	1.62 ± 0.04	0.46 ± 0.05	6.8 ± 0.8	9.9 ± 0.8	
	Stopped-flow	1.78 ± 0.05	1.5 ± 0.1	0.6 ± 0.1	6.2 ± 0.1	10.0 ± 0.2	
	Triple bi-directional	1.92 ± 0.07	1.6 ± 0.3	0.55 ± 0.02	5.9 ± 0.1	10.0 ± 0.3	

Sample, SRM 2710 soil; S/C ratio, 1:14; extraction flow rate, 50 μl s^{-1}.
[a] Below the FAAS detection limit.

ascertained via the bi-/multi-bi-directional modes since the diffusion layer of the extractant solution in contact with the soil matrix—containing the highest concentration of released metal species—is renewed for each extraction step.

Table 2 shows the extractable amounts of Pb, Cu, Zn and Mn for the SRM 2710 soil as obtained with the SI/SE system exploiting various automated extraction protocols. Despite the uni-, bi-, triple bi-directional and stopped-flow intrinsically give rise to different extraction times (namely, 7, 14, 48 and 120 s, respectively, for a loading flow rate of 50 μl s^{-1}), the extractability of trace metals from each soil phase association is by and large similar. However, the contribution of re-distribution processes can be detected for Pb and Cu due to the appreciable increase in the extractability for the reducing agent using the backward–forward (ca. 18 and 28%, respectively) and stopped-flow (ca. 17 and 38%, respectively) modes in comparison with the uni-directional flow. In fact, the phenomenon of re-distribution for the batchwise SE schemes has been found particularly relevant for Cu and Pb, the manganese oxide and humic acids being mostly responsible for this effect [2].

Moreover, as opposed to Pb, the SI-extraction yields for Cu using the chemical extractant with the lowest leachant strength, i.e., 0.11 M acetic acid, improved to some extent (≤15%) by increasing the leaching time, which can be explained according to the different mobility of both metal ions: While Cu is regarded as an element of intermediate mobility, with pools of the readily leachable carbonate bound phase, Pb is considered as a typical fixed element [5]. In addition, whereas the Pb fraction susceptible of oxidation processes is not significantly different for the bi- and triple bi-directional flow, both the uni-directional and stopped-flow modes yielded lower extraction yields. This behavior might be explained by the difference of the extracting operations, because the uni-directional flow and the stopped-flow are basically based on the same operating approach, just as are the bi- and the triple bi-directional flow procedures.

The behavior of manganese was somewhat different from that of the remaining metals explored. It should, however, be taken into account that Mn, as opposed to Pb, Cu and Zn, is a major element in soil matrices. Although hydrous oxides of manganese are commonly described as easily reducible soil phases [2], manganese should be regarded in SRM 2710 as a non-labile element, being strongly associated to the residual fraction. According to Table 2, the extractable amounts associated to carbonates for the bi-directional flow, and the reducible fraction for the uni-directional flow are lower than those attained by the other modes of extraction. This is probably caused by the insufficient contact time between soil and extractant.

3.3. Kinetic leaching and chemical associations in the soil sample

Apart from the information on metal distribution in the various phases, extractograms of each element [20] as obtained by a graphical plot of extracted concentration and subfraction number can provide an additional useful insight into the kinetics of the leaching processes and the chemical associations of the elements within the solid phases.

According to the extractograms of Pb, Cu, Zn, and Mn resulting from the application of the different SI/SE operational modes to the SRM 2710 soil (see Fig. 2 for further details), the most labile elements, i.e. Zn and Cu, are specially sensitive to acidification processes, so that more than 25% of the total metal content is bound to carbonates.

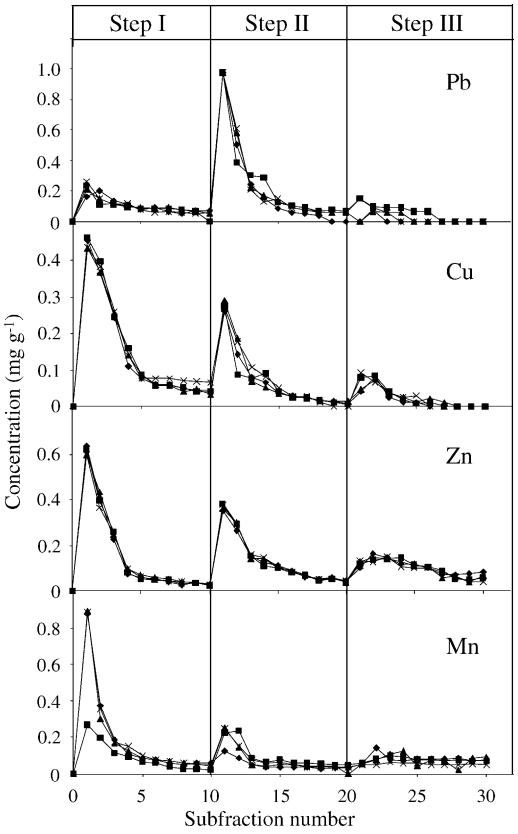

Fig. 2. SI/SE extractograms of metals in the SRM 2710 reference soil resulting from the application of different operational modes: uni-directional flow (♦); bi-directional flow (■); stopped-flow(▲); and triple bi-directional flow (×). Sample, 25 mg; subfraction, 5 ml; extraction flow rate, 50 μl s^{-1}.

Moreover, the target phases are rapidly leachable, since more than 80% of the maximum metal available is obtained in the first four subfractions. On the other hand, lead is highly affected by reduction processes since the maximum extractability (ca. 45%) was obtained in step II of the SE scheme. This result agrees with previous researchers [21,22] who found that fixed elements, such as lead, are bound to easily or moderately reducible fractions (namely, manganese oxyhydroxides and amorphous iron oxides).

When comparing the leaching patterns of the various metals in SRM 2710 for the uni-directional mode (Fig. 3), it is noticeable that the kinetics of metal release from the solid material follow the same trends for all trace metals: each target analyte is mostly leached in the first subfraction (>30% for Cu, and >40% for Zn and Pb), and the concentration in solution rapidly decreases in the following subfractions. Similar pictures are encountered when exploiting the remaining dynamic extraction sequences, and virtually the same leaching profiles are obtained.

Another outstanding asset of the SI/SE system is the feasibility of comparing both the peak positions and the profile shapes between elements to identify pollutant–soil phase interactions. In order to gain more detailed information of the leaching kinetics and elemental association, the

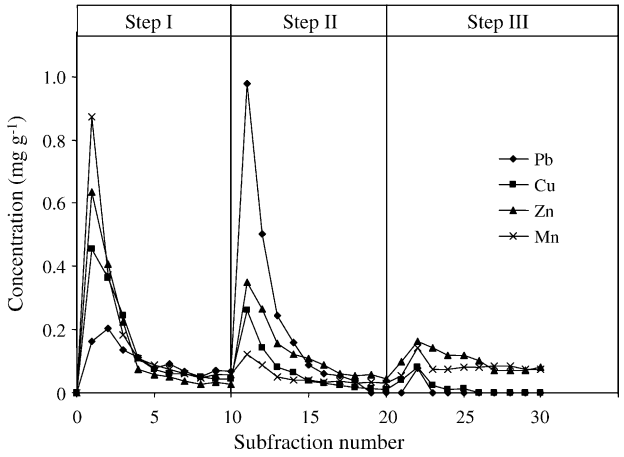

Fig. 3. Extractograms of metals in the SRM 2710 reference soil resulting from the application of the BCR three-step sequential extraction protocol using the SI-microanalytical system in a uni-directional fashion. Sample, 25 mg; extraction flow rate, 50 μl s^{-1}; subfraction volume, 5 ml.

detailed, continuous extractograms are to be explored. This can either be effected by collection of smaller volumes of extract per subfraction, or, as this group presently is engaged in, by interfacing the SI-microcolumn set-up directly with an appropriate flow-through detector, thereby allowing on-line determination of the individual metals.

3.4. Particle size and soil homogeneity

The proposed SI/SE concept with automatic handling of solutions can be regarded as a versatile tool and supplementary technique to the flow injection/continuous flow microcolumn schemes [11–13,23] that have recently attracted special interest for on-line fractionation of metal ions in solid materials and assessment of leaching kinetics to receive valuable information on metal mobility and availability to biota.

Although the use of minute amounts of solid samples, even lower than 10 mg [11], have been reported recently, it should be born in mind that the reliability of the leaching assays is to be strongly influenced by the particle size distribution, which, in turn, depends on the sample preparation protocols effected prior to initialisation of the extraction tests. As suggested by Beauchemin et al. [12], the treatment of solid materials with poor homogeneity by automated microextraction techniques could be troublesome due to the limited capacity of the sample container and the increase of flow resistance. Yet, the feasibility of handling heterogeneous soil samples into flow manifolds is a current subject of exploration in our research group. To this end, the sewage sludge amended CRM 483 soil with certified release concentrations of anthropogenic metals following standardised single extraction procedures [24] is being used as a model of heterogeneous material with particle size up to 2 mm, as compared with <74 μm in the SRM 2710 pasture soil. The experiments have been scaled up to

evaluate the maximum sample amount to be accommodated in the dedicated microcolumn. Sample size is proven to be readily enlarged up to 300 mg with minimum back-pressure increase, because of the favourable hydrodynamics of the dual-conical shaped column. The perfusing extractant flow rate should, however, be tailored to the dimensions of the column for appropriate long-term performance of the micro-analytical system. Thus, the coefficients of variation for lead in consecutive uni-directional single extractions for CRM 483 have been reduced from 35 to 5% by increasing the sample mass from 25 to 300 mg, rendering R.S.D. values comparable, and even better, to those of the homogeneous SRM 2710 soil (see Table 2 for further information).

As a result, the proposed configuration has opened new avenues for automatic extraction schemes of environmentally relevant parameters in soils with different morphology and variable homogeneity. Current research is also being focused on the implementation of single and sequential extraction protocols in a single, compact and miniaturised SI-manifold aiming at developing a robust tool with inherent capabilities for fast screening of soil pollution and at-site monitoring of soil phase associations.

3.5. Validation of the proposed system

The accuracy of the proposed approach was evaluated by analyzing the SRM 2710 certified reference material, and comparing statistically the summation of extracted concentrations in each operationally-defined phase and residue fraction with the certified total concentrations detailed in Table 2. The *t*-test for mean comparison was applied as a significance test [25]. Since the experimental *t*-values for Pb, Zn, Cu and Mn were lower than the critical value of $|t|$ (viz., 2.23, $P = 0.95$) no significant differences were encountered between the certified values and the sum of concentrations at the 5% significance level. As a consequence, the SI/SE method is free from both additive and multiplicative matrix interferences, making the application of the method of the standard additions unnecessary.

The correlation between the uni-directional flow (UNI) and the bi-directional (BI), triple bi-directional (TR) and stopped (ST) flow modes was assessed via statistical treatment of the regression curves obtained from the overall results listed in Table 2 for trace elements. The correlation lines were as follows: $\mathrm{UNI} = (1.16 \pm 0.22)\,\mathrm{BI} - (0.09 \pm 0.28)$; $\mathrm{UNI} = (1.10 \pm 0.20)\,\mathrm{TR} - (0.04 \pm 0.27)$ and $\mathrm{UNI} = (1.09 \pm 0.21)\,\mathrm{ST} + (0.003 \pm 0.27)$.

As deduced from the above equations, the calculated slopes and intercepts do not differ significantly from 1 and 0, respectively, thus confirming the inexistence of systematic differences between the various operational modes for the SRM 2710 reference material. It can be concluded from these results, that this homogeneous, highly contaminated soil contains large pools of easily mobilisable metal fractions, so that the uni-directional flow provides extraction yields which are statistically comparable with that of the other automated protocols. However, the application of operational modes involving longer extraction times should be desirable to enhance the extraction efficiency in soils, sediments or sludges with large fractions of slowly accessible metals, as currently being investigated in our laboratory exploiting both single and sequential extraction approaches in an automated flow fashion.

Acknowledgements

Roongrat Chomchoei is grateful for financial support granted by The Royal Golden Jubilee Ph.D. Program of the Thailand Research Fund and to The Postgraduate Education and Research Development Program in Chemistry (PERCH) of the Commission on Higher Education (Thailand). Manuel Miró is indebted to the Spanish Ministry of Education and Science for financial support. Special thanks are also due to the mechanical workshop of the Department of Chemistry at Technical University of Denmark (headed by John Madsen), and especially to Anders Sølby, for constructing the extraction microcolumn.

References

[1] A.K. Das, R. Chakraborty, M.L. Cervera, M. De la Guardia, Talanta 42 (1995) 1007.
[2] A.V. Filgueiras, I. Lavilla, C. Bendicho, J. Environ. Monit. 4 (2002) 823.
[3] V.H. Kennedy, A.L. Sanchez, D.H. Oughton, A.P. Rowland, Analyst 122 (1997) 89R.
[4] C. Gleyzes, S. Tellier, M. Astruc, Trends Anal. Chem. 21 (2002) 451.
[5] A. Sahuquillo, A. Rigol, G. Rauret, Trends Anal. Chem. 22 (2003) 152.
[6] Z.-L. Fang, Anal. Chim. Acta 400 (1999) 233.
[7] E.H. Hansen, J.-H. Wang, Anal. Chim. Acta 467 (2002) 3.
[8] C.E. Lenehan, N.W. Barnett, S.W. Lewis, Analyst 127 (2002) 997.
[9] V. Cerdà, A. Cerdà, A. Cladera, M.T. Oms, F. Mas, E. Gómez, F. Bauzá, M. Miró, R. Forteza, J.M. Estela, Trends Anal. Chem. 20 (2001) 407.
[10] R. Chomchoei, E.H. Hansen, J. Shiowatana, Anal. Chim. Acta 526 (2004) 177.
[11] M. Jimoh, W. Frenzel, V. Müller, H. Stephanowitz, E. Hoffmann, Anal. Chem. 76 (2004) 1197.
[12] D. Beauchemin, K. Kyser, D. Chipley, Anal. Chem. 74 (2002) 3924.
[13] L.-M. Dong, X.-P. Yan, Talanta 65 (2005) 627.
[14] A.M. Ure, Ph. Quevauviller, H. Muntau, B. Griepink, Int. J. Environ. Anal. Chem. 51 (1993) 135.
[15] A.V. Filgueiras, I. Lavilla, C. Bendicho, Anal. Bioanal. Chem. 374 (2002) 103.
[16] X.-B. Long, R. Chomchoei, P. Gała, E.H. Hansen, Anal. Chim. Acta 523 (2004) 279.
[17] A.V. Hirner, Int. J. Environ. Anal. Chem. 46 (1992) 77.
[18] M. Raksasataya, A.G. Langdon, N.D. Kim, Anal. Chim. Acta 347 (1997) 313.
[19] R. Chomchoei, J. Shiowatana, P. Pongsakul, Anal. Chim. Acta 472 (2002) 147.
[20] J. Shiowatana, N. Tantidanai, S. Nookabkaew, D. Nacapricha, J. Environ. Qual. 30 (2001) 1195.

[21] A. Sahuquillo, A. Rigol, G. Rauret, J. Environ. Monit. 4 (2002) 1003.
[22] B. Pérez-Cid, M. de Jesús-González, E. Fernández-Gómez, Analyst 127 (2002) 681.
[23] S. Morales-Muñoz, J.L. Luque-García, M.D. Luque de Castro, Anal. Chim. Acta 515 (2004) 343.
[24] Ph. Quevauviller, G. Rauret, J.F. López-Sánchez, R. Rubio, A. Ure, H. Muntau, Fresenius J. Anal. Chem. 357 (1997) 611.
[25] J.C. Miller, J.N. Miller, Statistics for Analytical Chemistry, 3rd ed., Ellis Horwood, Chichester, 1993, p. 55.

Available online at www.sciencedirect.com

SCIENCE DIRECT®

Science of the Total Environment 348 (2005) 244–256

Science of the Total Environment
An International Journal for Scientific Research into the Environment and its Relationship with Humankind

www.elsevier.com/locate/scitotenv

Assessment of lead availability in contaminated soil using isotope dilution techniques

N. Tongtavee[a,*], J. Shiowatana[a], Ronald G. McLaren[b], Colin W. Gray[b]

[a]*Department of Chemistry, Faculty of Science, Mahidol University, Rama VI Road, Bangkok 10400, Thailand*
[b]*Soil and Physical Sciences Group, Agriculture and Life Sciences Division, PO Box 84, Lincoln University, Canterbury, New Zealand*

Received 8 June 2004; accepted 10 December 2004
Available online 8 March 2005

Abstract

Isotope dilution methods using a stable isotope tracer (^{207}Pb) were developed for the determination of Pb availability in contaminated soils. The methods included determination of E values (isotopically exchangeable pool), L values (plant labile pool) and isotopic exchange kinetics (IEK). Isotopically exchangeable Pb was monitored at different exchange times based on measurement of the ^{207}Pb/^{208}Pb ratio in soil solution following addition of the tracer. The rate of decrease in the ^{207}Pb/^{208}Pb ratio in solution could be described by using the same IEK equation as used previously with radioisotope tracers. The amounts of isotopically exchangeable Pb in Pb-contaminated soils estimated from long-term IEK parameters were in good agreement with directly determined E values up to 15 days. However, values of some of the fitted IEK parameters cast doubts on the validity of using the IEK approach with ^{207}Pb, most probably as a result of irreversible fixation of some of the spike by reactive surfaces in the soils. Estimation of isotopically exchangeable Pb using short-term kinetics data was unsuccessful, substantially underestimating E values. Results for the control (uncontaminated) soil were highly variable, most probably as a result of fixation of tracer by the soil and poor analytical precision due to low solution Pb concentrations. A compartmental analysis of the variation in E values with time indicates a good potential for estimating bioavailable Pb in contaminated soils. The amounts of available Pb obtained from summation of the $E_{1\ \mathrm{min}}$ and $E_{1\ \mathrm{min–24\ h}}$ pools ($E_{(\mathrm{available})}$), accounting for an average of 57.62% of total soil Pb, were significantly correlated with both the L values and with Pb extracted from soil with EDTA.

Keywords: Isotopic exchange kinetics; Lead; Bioavailability

1. Introduction

The present amount of lead (Pb) in the environment is a result of release by natural processes and a long history of anthropogenic use of Pb. The increasing uses of Pb have resulted in recurring

* Corresponding author. Tel.: +662 664 1000; fax: +662 259 2097.
E-mail address: namfon@swu.ac.th (N. Tongtavee).

0048-9697/$ - see front matter © 2005 Elsevier B.V. All rights reserved.
doi:10.1016/j.scitotenv.2004.12.066

environmental contamination in developing and industrialised areas of the world. Contamination of soil with Pb from the main recognised sources is well documented, i.e. mining and smelting, automotive emissions, Pb-based paints and industrial activity (e.g. Haack et al., 2003; Wong and Li, 2004; Ettler et al., 2004; Monastra et al., 2004). Accumulation of lead in surface soils can impact on environmental health and can affect food quality and human health. It is widely recognized that the mobility and bioavailability of metals in the environment depend not just on their total concentrations. Hence, determination of metal availability is important for the assessment of metal toxicity in contaminated soils. In response to this concept, there has been a great deal of research conducted to find suitable methods for the determination of available Pb in contaminated soils (e.g. McLaughlin et al., 2000; Bacon et al., 2004; Bäckström et al., 2004).

In relation to the mobility and plant uptake of elements, isotope dilution techniques have been used for investigating elemental dynamics in the soil–plant system (Tiller et al., 1972; Fardeau, 1993; Singh and Pandeya, 1998; Gérard et al., 2000). These techniques are based on the assumption that isotopic tracers added to the soil solution will exchange with the potentially available and mobile forms of elements present in the soil solid phase (often referred to as the labile pool). In principle, the isotopic exchange procedure can be performed using both radioactive and stable isotope as tracers. In previous studies, isotopic exchange with radioactive isotopes has been used mainly for the determination of labile forms of metals such as Cd, Zn and Ni in soils (e.g. Echevarria et al., 1998; Hamon et al., 1998; Smolders et al., 1999). There are two main types of labile pool measurements by isotopic exchange, i.e. the determination of E and L values. The E value is a direct measurement of the isotopically exchangeable metal pool obtained by equilibrating soil suspension with a radioisotope spike, followed by measurement of the specific activity of the soil solution after equilibration. For the determination of L values, plants are grown in soils spiked and pre-equilibrated with the radioisotope. Measurement of the specific activity of the isotope in the plants is then used to compute the labile pool in the soil. Some studies have suggested that E and L values produce different estimates of the labile pool. (Tiller et al., 1972; Smolders et al., 1999; Gray et al., 2001). In contrast, Echevarria et al. (1998) found that E and L values for Ni were similar. Errors may arise with L values because the specific activity of the exchangeable metal as sampled by plants can be affected by many complex chemical and biological processes in the soil.

For additional information, a method has been developed to study isotopic exchange as a function of time. This approach is usually referred to by the term isotope exchange kinetics (IEK) (Fardeau et al., 1985). The IEK method has been successfully applied to describe the kinetic transfer of radioactive phosphate ions ($^{32}PO_4$) from the soil solution to the solid phase (Fardeau, 1996; Frossard and Sinaj, 1997). It has been shown that the IEK technique is very useful in describing P availability in terms of the concepts of intensity, quantity and capacity factors. More recently, the IEK technique has been applied successfully to study Zn exchangeability in soils (Sinaj et al., 1999), and Echevarria et al. (1998) used IEK to assess Ni phytoavailability in Ni polluted soils. Gérard et al. (2000) and Gray et al. (2004) have used the IEK technique to investigate Cd availability in cadmium-contaminated soils.

All the above studies of IEK have used radioisotopes tracers. However, procedures employing radioisotopes generally require special facilities for the safe handling and final disposal of radioactive materials. In addition, for Pb there is no radioisotope tracer that can be used for isotopic exchange studies. In contrast to use of radioisotopes, there have been only a handful of studies that have used stable isotopes to measure labile metals in soils. Given some of the advantages that stable isotopes offer over radioisotopes as outlined by Vanhaecke et al. (1997), and the increasing availability and sophistication of mass spectrometry (MS) instruments, there is now increased interest in using analytical techniques that rely on stable tracers to measure labile fractions of heavy metals. For example, in recent years, analytical techniques using inductively coupled plasma-mass spectrometry (ICP-MS) coupled with using stable isotopes have been developed and applied to study the bioavailability (labile fraction) of metals in soils by Gäbler et al. (1999), Ahnstrom and Parker (2001), Ayoub et al. (2003) and by Gray et al. (2003). The labile fraction is defined as that portion of an element

in a soil that rapidly exchanges with an added spike which contains a known quantity of the element of interest, artificially enriched with one of the isotopes of the element. In the case of Pb, the determination of ^{207}Pb and ^{208}Pb can be easily carried out using quadrupole-based ICP-MS instruments (ICP-QMS) (Becker, 2002).

The labile pool of a metal in soil, whether determined by radioactive or stable isotopes, can be considered as a relatively unambiguous assessment of the chemical and biological reactivity of that metal in soil compared with fractions isolated by chemical extractants (e.g. Nakhone and Young, 1993). However, it should be recognised that isotopic exchange determinations are based on the assumption that the added spike (radioisotope or stable isotope) remains 100% available for exchange. Examination of the equations for the calculation of *E* values shows that fixation ('irreversible' sorption) of some of the spike by reactive soil phases results in an overestimate of the size of the labile pool. In the case of relatively mobile elements such as Cd and Zn, the assumption that 100% of the spike remains available for exchange appears reasonable, although, in some cases, some fixation of the spike may occur even with these elements. For example, Tiller et al. (1972) reported evidence of fixation of spiked radioactive Zn by soils. They found quite erratic overestimates of isotopically exchangeable Zn for alkaline soils, sometimes even exceeding the total amount of soil Zn. In the case of Pb, fixation of the spike could potentially be a considerable problem since Pb is known to be very strongly bound by soil surfaces. Indeed, examination of the results of Gäbler et al. (1999) suggests that fixation may be a real issue. Their values for isotopically exchangeable Pb, determined in water or 1M NH_4NO_3, were actually higher than the concentration of EDTA-extractable Pb determined for their study soil. This would seem a somewhat unlikely situation. In addition, several recent isotope studies examining isotopic signatures of different soil Pb pools show that there is considerable Pb isotopic heterogeneity between pools, and at best, exchange between fractions and homogenisation of isotopic ratios must be extremely slow (e.g. Emmanuel and Erel, 2002; Wong and Li, 2004; Bacon et al., 2004).

In the present study we have examined the use of an enriched stable Pb isotope to determine the pool of isotopically exchangeable Pb in soils (*E* value). We have also investigated whether it is possible, using the IEK approach, to predict isotopically exchangeable Pb for long-term exchange times, i.e. up to 15 days, from short-term data (1–100 min). Our study also includes the measurement of isotopically exchangeable Pb based on plant uptake (*L* value). With all methods, we examine the data for evidence that fixation of the spike may limit or invalidate their usefulness. Finally we compare the different measurements of labile Pb with a single soil extraction with ethylenediaminetetraacetate disodium salt (EDTA).

2. Materials and methods

2.1. Description of study site and soil samples

Surface soil samples (0–10 cm) were sampled from the area surrounding a small lead smelter located near the town of Rangsit, approximately 110 km north of Bangkok, Thailand. The smelter, has been operating for the last 10 years and is used essentially to re-cycle lead (Pb) from old batteries. Sampling was carried out at distances of between 0 and 2.5 km from the smelter by taking several sub samples at each location with a trowel from an area of approximately 0.5 m^2 and bulking. A preliminary sampling of the site was carried out and the total concentrations of Pb in these samples were determined. The results showed that total Pb concentrations varied in the range of 20–250 mg/kg Pb. Five samples were chosen for use in this study to represent a range from background to high concentrations of Pb. The background soil was sampled at a distance of 2 km from the smelter. The chemical and physical properties of these five soils are shown in Table 1. Soil samples were dried at 30 °C in an oven for 5 days. All the samples were then ground and sieved through a 2 mm stainless steel sieve. All soils were stored in a desiccator prior to laboratory analysis. Soil pH was measured in a water suspension using a soil/solution ratio of 1:2.5 after the suspensions were shaken for 24 h on a reciprocating shaker at 20 °C (Blakemore et al., 1987). Total carbon content was determined by LECO CNS 2000 Analyser. Soil texture was measured by the Malvern

Table 1
Properties of the experimental soils

Soil	Total Pb (mg/kg)	pH	Sand (%)	Silt (%)	Clay (%)	Org. C (%)	Total Fe (%)	Total Al (%)
C1	21.2	5.54	21.3	56.9	21.8	2.23	5.1	1.8
S1	69.9	6.51	20.5	63.6	15.9	2.89	7.6	1.2
S2	99.2	6.17	24.6	61.9	13.5	1.47	4.7	0.8
S3	143.0	5.91	17.1	65.1	17.8	1.81	3.3	1.1
S4	246.6	5.73	20.5	61.4	18.1	2.65	3.4	1.1

Laser Sizer method (Singer et al., 1988). Total Pb, Fe and Al were determined by acid digestion as described by Kovács et al. (2000), followed by atomic absorption spectrophotometry or ICP-QMS using a Perkin Elmer SCIEX model ELAN 6000.

2.2. Reagents

All chemicals used were of Analytical Reagent grade and obtained from BDH Chemicals (Poole, Dorset, UK). High purity water was used throughout with a metered resistivity ≥18 MΩ. Elemental Pb enriched with ^{207}Pb (≥94.6% ^{207}Pb) was purchased from Novachem Pty. Ltd. (Australia). The enriched Pb was initially dissolved in HNO_3 and then diluted with water to give a stock solution of approximately 1800 mg/L.

2.3. Theory

2.3.1. Isotopically exchangeable Pb

When a spike solution enriched with ^{207}Pb is added to a soil, it is assumed to equilibrate with all forms of soil Pb that constitute the overall labile pool. At equilibrium, the Pb isotope ratios of the solution and solid isotopically exchangeable phases should be the same (in our case we measured the ^{207}Pb/^{208}Pb ratio). The amount of isotopically exchangeable metal, at equilibrium time t (E_t) in the soil can be calculated using Eq. (1) (Gäbler et al., 1999).

$$E_{(t)} = \frac{V_{spike} \cdot C_{spike-solution} \cdot M \cdot (h_{spike}^{light} - r \cdot h_{spike}^{heavy})}{m_{sample} \cdot N_A \cdot (r \cdot h_{sample}^{heavy} - h_{sample}^{light})} \cdot 10^6 \quad (1)$$

Where V_{spike} is the volume of the added spike solution (mL), $C_{spike\ solution}$ is the concentration of the element in the spike solution (atom/mL), M is the molar mass (g/mol) of the element, N_A is Avogadro's constant, m_{sample} is the mass of the sample (g), h is the isotopic abundance of the lighter (^{207}Pb) or heavier (^{208}Pb) isotope in the spike solution or the natural isotopic abundance in the sample, r is the measured ^{207}Pb/^{208}Pb isotope ratio in solution after isotopic exchange. The natural isotopic abundance of Pb occurring in each contaminated soil sample, h_{sample} was determined for each sample by ICP-QMS. Eq. (1) can also be used to calculate L values from plant uptake studies. In this case, r is the ^{207}Pb/^{208}Pb ratio measured in plants grown in spiked soil.

2.3.2. Isotopic exchange kinetics

The principle of IEK employing a radioactive tracer has been described in a number of recent papers (Echevarria et al., 1998; Sinaj et al., 1999; Gray et al., 2004). When radioactive ions are added carrier free to a soil solution system at a steady state, the quantity of radioactivity in solution (r_t) decreased as a function of time, t (min) for the duration of the isotopic exchange according to the following Eq. (2) (Fardeau et al., 1985).

$$r_{(t)}/R = [r_{(1)}/R]\left\{t + [r_{(1)}/R]^{1/n}\right\}^{-n} + r_{(\infty)}/R \quad (2)$$

Where R is the total introduced radioactivity (MBq) and $r_{(1)}$ and $r_{(\infty)}$ are the radioactivity (MBq) remaining in the solution after 1 min and an infinite exchange time, respectively. The value n is a parameter describing the rate of disappearance of the radioactive tracer from the solution for times longer than 1 min of exchange.

The present IEK study was carried out using a stable isotope as a tracer. In this case, the rate of decrease in ^{207}Pb/^{208}Pb ratio in solution, as a result of ^{207}Pb exchange with Pb on the solid phase, was

assumed to follow the same behaviour as previously observed with radioactive tracers (Eq. (2)). Therefore, with reference to Eq. (2), $r_{(t)}$ is defined as the $^{207}Pb/^{208}Pb$ ratio in solution at time (t) and R is the $^{207}Pb/^{208}Pb$ ratio of the spike solution. The $r_{(1)}$ and $r_{(\infty)}$ values are the $^{207}Pb/^{208}Pb$ ratios in the solution after 1 min and an infinite exchange time, n is a parameter describing the rate of decrease in $^{207}Pb/^{208}Pb$ ratio in solution for times longer than 1 min of exchange.

2.4. Procedure for determination of E values and IEK

Generally, for isotope exchange determinations, tracers (radioactive or stable) are added to soil suspensions already at chemical equilibrium. However, the length of time taken for soils to achieve chemical equilibrium for metals in water, or weak salt solutions can be quite variable, ranging from a few hours to several days (e.g. Tiller et al., 1972; Sinaj et al., 1999; Gray et al., 2004). We selected a 3-day equilibrium period before adding tracer to the soil suspension. An important factor of concern when using stable isotope tracers is the amount of spiking tracer added. Ideally, the amount of tracer added should ensure a significant and detectable change in the isotope ratio in the soil solution ($^{207}Pb/^{208}Pb$) from that in unspiked samples, even after isotopic equilibration has taken place. Gäbler et al. (1999) successfully determined amounts of isotopically exchangeable Pb in soils using a spike of 10^{16} atom/g soil. Since the total soil concentrations of Pb in our study were in the same range as those reported by Gäbler et al. (1999), we also added the stable isotope tracer at a rate of 10^{16} atom/g soil.

Samples of soil (3.00 g) were equilibrated with 30 mL deionized water on an end-to-end shaker for 3 days. At this time (t=0 min), 60 μL of an enriched ^{207}Pb solution (^{207}Pb; 94.6% and ^{208}Pb; 2.9%) was spiked into the equilibrated soil suspension (2.148×10^{16} atom/g soil). The soils were then re-suspended and shaken further. At intervals of 1, 10, 40 and 100 min, 1, 2, 3, 7, 11 and 15 days, duplicate samples were removed from the shaker, centrifuged (10 000 rpm for 10 min) and filtered through a 0.45 μm cellulose acetate membrane. Concentrations of ^{207}Pb and ^{208}Pb were determined in the filtrates by ICP-QMS.

2.5. Procedure for determination of L values

Five soils were spiked with a ^{207}Pb-enriched solution for use in a plant growth study. A 40 mL volume of ^{207}Pb-enriched solution was added to 400 g of sieved dried soil to give a final mean soil atom of approximately 1.597×10^{16} atom/g soil. The soils and ^{207}Pb spiking tracer were then mixed manually together with an additional 56 mL of a mixed nutrient solution of KNO_3 (6.5 mM), NH_4NO_3 (7.5 mM), $MgSO_4$ (2 mM) and KH_2PO_4 (0.6 mM). After mixing, the soil was divided into four and placed into acid washed plastic pots, lined with perforated plastic bags. Each spiked soil (approximately 125 g moist soil at 80% of the water holding capacity) was covered and left to incubate for 1 week.

Seeds of wheat (*Triticum aestivum* L. cv. Monad) were then placed just below the soil surface, at a sowing density of 9 seeds per pot, and thinned to 6 plants following seedling development to remove late germinating and unhealthy seedlings. Four replicates of each soil were arranged in a randomized block design and the plants were grown in a controlled environment growth chamber (15/20 °C, 8 h dark/16 h light). The moisture content was maintained at 80% of the water holding capacity by watering to weight with de-ionized water daily. Every 2 weeks, a further addition of the mixed nutrient solution was made. Plant shoots were harvested after 6 weeks, at which time there was sufficient plant material for analysis. Plants were rinsed in deionized water and then dried at 80 °C for 48 h, and the dry weights recorded. Then the dried plants were finely ground and digested in 10 mL HNO_3 over 7 h. Following HNO_3 digestion, the lead isotope ratio of $^{207}Pb/^{208}Pb$ in the digested solution was determined by ICP-QMS.

2.6. Single extraction with 0.04 M EDTA

EDTA-extractable Pb was determined by extraction of 10 g of soil with 25 mL of 0.04 M EDTA at 20 °C for 2 h on an end-over-end shaker. After extraction the soil suspension was centrifuged at 10 000 rpm for 10 min and then filtered through Whatman 42 filter paper before Pb measurements by ICP-QMS. The filtered solutions were diluted 50 times with deionized water and spiked with ^{115}In as an internal standard prior to ICP-QMS measurements. The extractable

amounts of ^{207}Pb and ^{208}Pb isotopes provided the 'natural' isotopic abundance of ^{207}Pb and ^{208}Pb for each soil sample prior to addition of the ^{207}Pb enriched spike. In fact, there was no significant difference in this value between the five soils.

2.7. Data analysis

For all five soil samples, long-term isotopic kinetics was carried out. The IEK procedure was carried out for 1, 10, 40 and 100 min, and then for a further 1, 2, 3, 7, 11 and 15 days of isotopic exchange. The ^{207}Pb/^{208}Pb ratio in the soil solution was then determined by ICP-MS at each interval. At each sampling interval for these five soils, $r_{(t)}$ values were used to calculate directly the isotopically exchangeable Pb, $E_{(t)}$ using Eq. (1) (up to 15 days). We refer to these data as measured E-values (E_{meas}).

To calculate long-term kinetic parameters, data for $r_{(t)}/R$ at any time, t (min) was fitted to Eq. (2) using on iterative nonlinear regression algorithm (REGRESSION WIZARD, SigmaPlot, Version 6.0) to obtain $r_{(1)}/R$, n and $r_{(\infty)}/R$ kinetic parameters. The fitting procedure constricted the value for $r_{(\infty)}/R$ to values equal to or above the value obtained assuming complete dilution of the spike by the total Pb in the soil sample (see short-term calculation below). This was done because, in reality, no values for $r_{(\infty)}/R$ can be smaller than the estimates made assuming that all the soil Pb is ultimately isotopically exchangeable. Using the fitted parameters, $E_{(t)}$ values were then calculated from Eqs. (2) and (1). We refer to these calculated values as long-term predicted E-values ($E_{\text{long-pred}}$).

For relatively short periods of exchange (we used 100 min), Eq. (1) simplifies to (Fardeau et al., 1991):

$$r_{(t)}/R = r_{(1)}/R[t]^{-n} \tag{3}$$

So the values of $r_{(1)}/R$ and n can be estimated from a linear regression plot between log $r_{(t)}/R$ and log t. The value of $r_{(\infty)}/R$ can be estimated by assuming complete dilution of the spike by the total Pb in the soil sample.

$$r_{(\infty)}/R = \frac{(94.6 \times 7.4 + \text{Pb}_t \times 22.2)}{(2.9 \times 7.4 + \text{Pb}_t \times 52.3)} \times 1/32.62 \tag{4}$$

Where Pb_t=total soil lead concentration (mg/kg), The values of 94.6 and 2.9 are the percentage abundances of ^{207}Pb and ^{208}Pb in the added spike. The values of 22.2 and 52.3 are the measured natural abundance of ^{207}Pb and ^{208}Pb in the soils. The value of 32.62 is the ^{207}Pb/^{208}Pb ratio (R) in the spiking solution. The estimated values of $r_{(1)}/R$, $r_{(\infty)}/R$ and n were then used to calculate $E_{(t)}$ values for periods up to 15 days (Eqs. (1) and (2)). We refer to these values as short-term predicted E-values ($E_{\text{short-pred}}$).

The results obtained from the IEK technique can be interpreted using compartment analysis (Fardeau et al., 1991). A compartment is defined as a homogenous unit pool in which all the ions have the same kinetic properties and exchange at the same rate of exchange with the same ions present in other compartments of the system (Sheppard, 1962; Atkins, 1973). We have chosen to analyze soil isotopically exchangeable Pb with a three-pool model consisting of $E_{1\ \text{min}}$, $E_{1\ \text{min–24 h}}$ and $E_{>24\ \text{h}}$.

2.8. Quality control

For the isotope ratio measurements of ^{207}Pb and ^{208}Pb, the ICP-QMS measurement parameters were daily optimized before use according to the manufacturers recommendation using a mixed standard solution containing Ba, Ce, Mg, Pb and Rh, and also

Table 2
ICP-MS operating parameters

Plasma conditions	
RF power	1050–1100 W
Nebulizer flow rate	1.0 mL/min
Auxiliary gas flow rate	0.9 mL/min
Plasma gas flow rate	15 L/min
Mass spectrometer setting	
Analog stage voltage	−2500 V
Pulse stage voltage	1400 V
AC rod offset	−5 V
Sampler cone	Nickel
Skimmer cone	Nickel
Measurement parameters	
Mode	Peak hopping
Resolution	Normal
Dwell time (isotope)	50 ms (Pb-207 and Pb-208)
Number of sweeps per reading	40
Number of replicate	3
Sample introduction	
Sample uptake flow rate	1.0–1.2 mL/min

including mass tuning to obtain separate well-defined peaks between ^{207}Pb and ^{208}Pb (Reference: Perkin-Elmer mass spectrometry manual instruction). The general operating conditions of the ICP-MS are shown in Table 2. The resolution of mass separation with the quadruple mass detector used in this work is 1 amu, with general well-defined peak widths of 0.7 amu each. The concentrations of ^{207}Pb and ^{208}Pb were determined together with an internal standard ^{115}In (Indium). The limit of detection for Pb was 0.05 μg/L. For a 'natural' Pb standard of 10 μg/L, the measured ^{207}Pb/^{208}Pb was 0.423+0.005 (n=10).

2.9. Statistical analysis

All statistical analyses were performed using the statistics program in MS-Excel'97. Long-term, n, $r_{(1)}/R$ and $r_{(\infty)}/R$ parameters were obtained using the nonlinear regression algorithm (REGRESSION WIZARD, Sigma Plot, Version 6.0).

3. Results and discussion

3.1. Change in E-value with time

The quantity of isotopically exchangeable Pb (E_{meas}) was calculated for each sampling period during the 15 day study. For all of the contaminated soils, the calculated E values increased rapidly during the first 24 h (1440 min) of exchange, followed by much slower rates of exchange (Fig. 1). The E values appeared to plateau at between 3 and 7 days (4000–10 000 min), indicating that isotopic equilibrium had

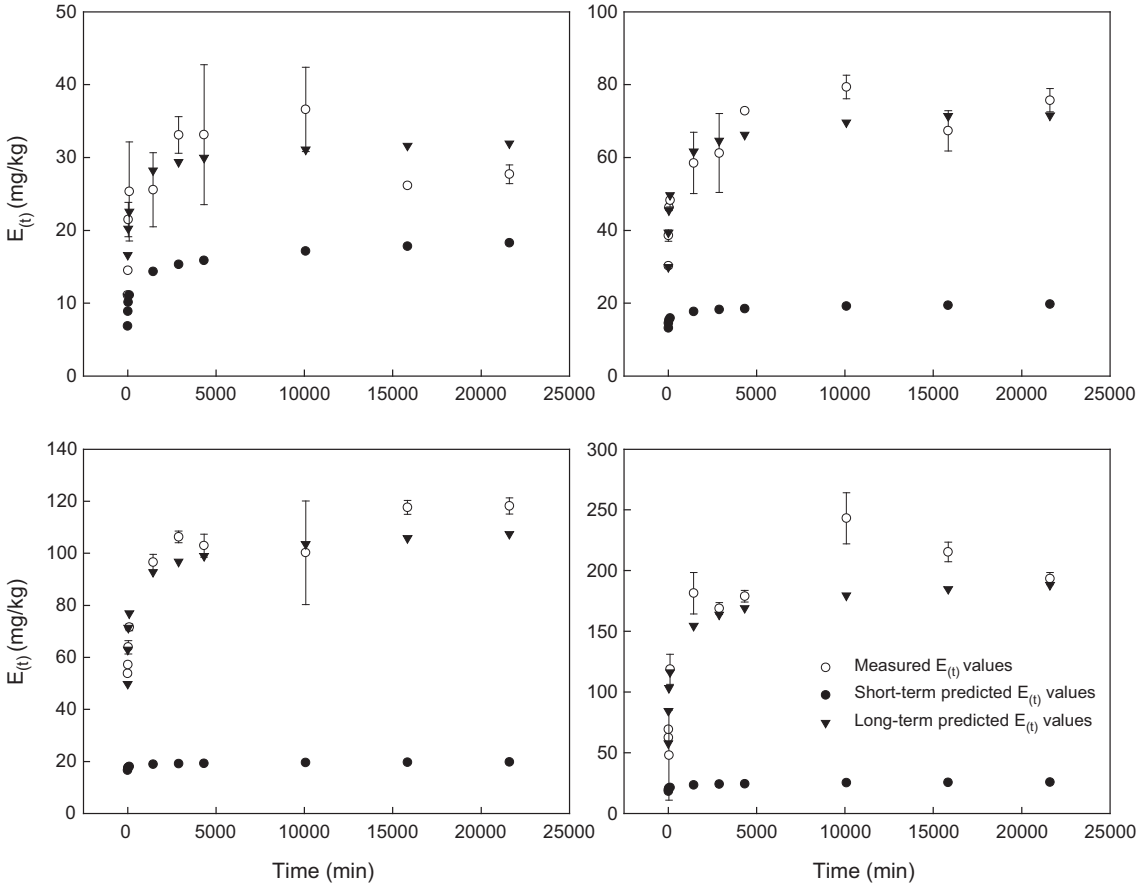

Fig. 1. Comparison between measured, long-term predicted, and short-term predicted $E_{(t)}$ values for contaminated soils S1 to S4. Error bars for measured $E_{(t)}$ values are ±S.E. of duplicate determinations.

largely been achieved by this stage. For soils S2, S3 and S4 in particular, the $E_{(meas)}$ values lay on relatively smooth curves with increasing time (Fig. 1). In contrast, for the control (C1) soil (Fig. 2), and for contaminated soil S1, the data points between 3 and 7 days showed considerable fluctuation. The reasons for this may be related to a combination of some of the analytical and fixation problems discussed elsewhere in this paper.

Our results appear similar to previous reports for Zn and Cd (Sinaj et al., 1999; Gray et al., 2004). Sinaj et al. (1999) investigated labile Zn in both polluted and non-polluted soils, their results showing an increase in the quantity of isotopically exchangeable Zn during 15 days with a fast exchange in the early stages. Gray et al. (2004) found that the isotopic exchange process for Cd is relatively fast during the first 24 h of exchange. These results are similar to those found in the current work, which clearly indicated that the isotopic exchange of Pb is initially a relative fast process (1 min–1 day), followed by a period of much slower exchange.

In an attempt to examine the use of the IEK approach for a stable isotope, Eq. (2) was used to model the decrease in the $^{207}Pb/^{208}Pb$ ratio in solution with time after addition of the spike. For the contaminated soils (S1, S2, S3 and S4), Eq. (2) provided a reasonable fit to the experimental data as shown in Fig. 1 (R^2>0.91) and the long-term kinetics parameters; $r_{(1)}/R$, n and $r_{(\infty)}/R$ could be estimated from the equation fitting procedure (Table 3). Statistical tests demonstrated reasonable good agreement between values of $E_{(meas)}$ and the corresponding E values ($E_{long\text{-}pred}$) calculated from the IEK parameters. The results indicated that the behavior of isotopically exchangeable Pb was similarly to that of Zn, Cd and phosphate ions that have previously been successfully fitted to Eq. (2). In contrast, for the control soil (C1),

Table 3
Comparison of kinetic parameters using IEK data between short-term and long-term exchange

Soil	$r_{(1)}/R$	n	$r_{(\infty)}R$	R^2
Short-term				
Control C1	0.153	0.228	0.032	0.931
Soil S1	0.053	0.115	0.019	0.970
Soil S2	0.026	0.047	0.017	0.987
Soil S3	0.021	0.020	0.016	0.907
Soil S4	0.020	0.039	0.015	0.896
Long-term				
Control C1	0.125	0.448	0.040	0.919
Soil S1	0.025	0.289	0.024	0.931
Soil S2	0.0094	0.179	0.017	0.979
Soil S3	0.0054	0.163	0.016	0.914
Soil S4	0.0054	0.226	0.015	0.926

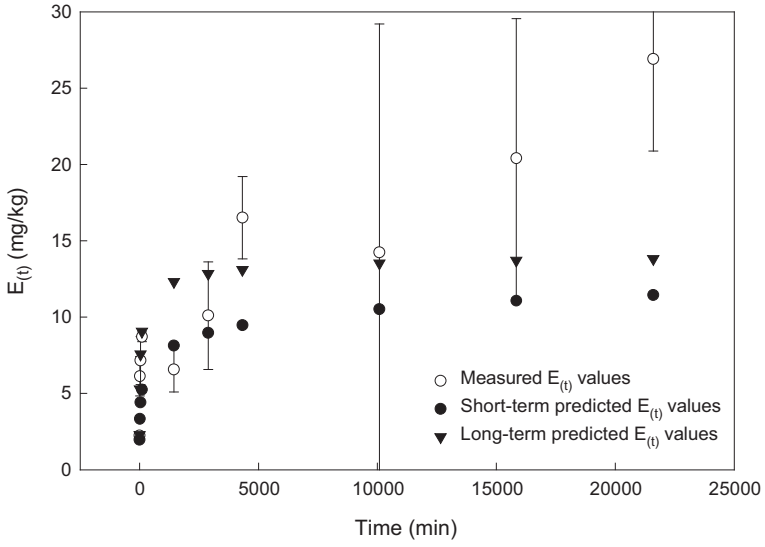

Fig. 2. Comparison between measured, long-term predicted, and short-term predicted $E_{(t)}$ values for the control soil (C1). Error bars for measured $E_{(t)}$ values are ±S.E. of duplicate determinations.

although the R^2 obtained from long-term kinetics fitting is relatively high (0.919) (Table 2), agreement between the $E_{(\text{long-pred})}$ and $E_{(\text{meas})}$ values is generally poor. It seems most likely that the poor fitting of the control soil data is related to the analytical errors for this soil, caused by the very low concentrations of Pb involved.

Attempts to use short-term data (up to 100 min) to predict E values ($E_{\text{short-pred}}$), for periods up to 15 days were not successful (Fig. 1). It was found that the $E_{\text{short-pred}}$ values were underestimated compared to the $E_{(\text{meas})}$ values for all soil samples. Our short-term kinetics approach shows that it is not possible, in the soil samples studied, using short-term parameters (1–100 min of isotopic exchange) to predict the amounts of isotopically exchangeable Pb for longer-term period (up to 15 days). To a certain extent, these large errors may be due to a lack of precision in the values used for time (t). For short equilibrations the length of time taken to separate solution from soil by centrifugation and filtration could have introduced substantial errors into the first two data points (1 and 10 min). However, Gray et al. (2004) also found that data from short-term kinetics data were only successful in predicting long-term exchangeable Cd for two out of six soils, even when they filtered soil suspensions immediately after sampling. For other soils, short-term IEK could predict exchangeable Cd only up to 24 h of exchange. After 24 h, $E_{\text{short-pred}}$ values were overestimated. In contrast, Sinaj et al. (1999) demonstrated that the results derived from a short-term IEK experiment (1–100 min) allowed for a precise prediction of exchangeable Zn up to 15 days in some soil samples. However, this was not possible for soils with high pH and low total Zn contents. From all of these studies, it would seem that short-term IEK procedures have some limitations for predicting long-term E values.

3.2. Validity of the IEK approach

Although as described above, Eq. (2) appeared to provide good fits to the experimental data (high R^2 values, Table 3), a closer examination of some of the parameters derived from the fitting process raises doubts about its validity for use in this study. In the case of three of the soils (S2, S3 and S4), the fitted values for $r_{(\infty)}/R$ are the minimum values possible, implying that ultimately all Pb in the soils is isotopically exchangeable. This seems extremely unlikely. More importantly the fitted $r_{(1)}/R$ values are lower than the $r_{(\infty)}/R$ values, which is of course an impossibility. This implies that Eq. (2) is inappropriate for modelling the isotopic exchange process, or that in this study the decrease in $^{207}Pb/^{208}Pb$ ratio in solution is not due solely to isotopic exchange. Fixation of some of the ^{207}Pb spike in non-isotopically exchangeable forms could account for this problem, and additional evidence of fixation occurring in this study is described below. In view of this issue, the use of Eq. (2) in this study should be regarded simply as a mathematical curve-fitting procedure enabling the 'smoothing' of the experimental data. On this basis it is probably unwise to pay much attention to the fitted values for the various parameters (Table 3) or make comparisons with values obtained for other metals such as Zn, Cd and Ni obtained in previous studies (e.g. Echevarria et al., 1998; Sinaj et al., 1999; Gérard et al., 2000; Diesing et al., 2002).

3.3. Compartment analysis of isotopically exchangeable lead

Previous studies have demonstrated that availability of metals is not a simple matter of labile and non-labile pools (Sinaj et al., 1999; Gray et al., 2004). In this present study, a three-compartment model was used to describe isotopically exchangeable Pb in our soil samples. The three compartments are $E_{1\ \text{min}}$, $E_{1\ \text{min–24 h}}$ and $E_{>24\ \text{h}}$ pool, respectively. The results of compartment analysis estimated from the long-term kinetics data are summarized in Table 4. They indicate that the $E_{1\ \text{min}}$ pool contained between 10.75% and 34.82% of the total soil Pb. This pool

Table 4
Isotopically exchangeable Pb in designated pools predicted from long-term IEK data

Soil	Pool 1: $E_{(1\ \text{min})}$ (mg/kg)	Pool 2: $E_{(1\ \text{min–24 h})}$ (mg/kg)	Pool 3: $E_{(>24\ \text{h})}$ (mg/kg)
Control C1	2.28 (10.75)	10.04 (47.36)	8.80 (41.89)
Soil S1	10.92 (15.92)	17.29 (24.74)	41.69 (59.64
Soil S2	29.98 (30.22)	31.63 (31.89)	37.59 (37.89)
Soil S3	49.79 (34.82)	43.02 (30.08)	50.19 (35.10)
Soil S4	57.66 (23.38)	96.78 (39.25)	92.16 (37.37)

Figures in parenthesis show % of total Pb in each pool.

represents Pb that is isotopically exchangeable during the first minute of exchange and corresponds to the instantaneously isotopically exchangeable Pb ions. The Pb present in this pool is composed of Pb^{2+} in the soil solution and adsorbed or chelated Pb that is very rapidly exchangeable. This pool must be considered as the pool of Pb ions directly available for plants. The size of the $E_{1\ min–24\ h}$ pool ranges between 24.74% and 47.36% of the total soil Pb. According to our data, the amounts of isotopically exchangeable Pb increased rapidly during the first day of exchange (Figs. 1 and 2), so that it is highly likely that Pb in the $E_{1\ min–24\ h}$ pools is also relatively plant available. Finally, the pool containing Pb that is either slowly exchangeable (i.e. between 24 h and 15 days), or not exchangeable with the spike, for instance Pb occluded in minerals or strongly adsorbed onto soil particles, is in the $E_{>24\ h}$ pool. Lead in this pool ranges between 35.10% and 59.64% of total soil Pb. For the five soil samples, the proportions of Pb present in the $E_{1\ min}$, $E_{1\ min–24\ h}$ and $E_{>24\ h}$ pools were on average 22.96%, 34.66% and 42.38%, respectively.

3.4. L values from plant uptake study

As mentioned in the introduction, there is no previous report examining the use of the L value for determination of available lead in soils. In our work, L values have been determined by spiking of soils with a stable isotope tracer (^{207}Pb) and measuring the $^{207}Pb/^{208}Pb$ ratio in plants grown in the soils. The L values determined are shown in Table 5. The L value for the control soil (C1) shows a totally unrealistic value vastly exceeding the total content of soil Pb. This overestimation may result from the fixation at strongly binding sites in the soil. Fixation is considered to be a much more likely problem to occur in the control soil. In the current study, the fixation problem may be related to the high Fe content of our soils (Table 1). In the contaminated soils, fixation also probably occurred but may have had much less overall influence on the isotopic exchangeable process than in the control soil. In the contaminated soils, the most strongly fixing sites on the soil oxide surfaces are more likely to be already occupied by anthropogenic Pb prior to spiking. In our procedure for determination of the L value, Pb fixation could have occurred during the period of incubation with ^{207}Pb for 7 days, before seeding.

Table 5
Comparison of amounts of available Pb determined using different methods

Soil	$E_{(available)}$[a] (mg/kg)	L value (mg/kg±S.D.)	EDTA-extractable Pb (mg/kg)
Control C1	12.32	184.1±57.7	3.78
Soil S1	28.21	55.2±15.5	18.50
Soil S2	61.61	73.1±11.9	53.21
Soil S3	92.81	93.9±26.2	76.83
Soil S4	154.44	133.8±25.3	130.87

[a] $E_{(available)}=E_{(1\ min)}+E_{(1\ min–24\ h)}$.

3.5. Comparison of available Pb determined by different methods

Estimates of labile pools of Pb are generally regarded as providing an indication of plant available Pb in the soil. The mean E values estimated from the long-term IEK fitting procedure were compared with the amounts of labile Pb determined using two other techniques, i.e. L values and single extraction with EDTA. Table 5 shows the comparison of the estimates of available Pb determined using the different methods. The $E_{(available)}$ values consist of Pb present in the $E_{1\ min}$ plus $E_{1\ min–24\ h}$ pools. For the three most highly contaminated soils (S2, S3 and S4) there is relatively good agreement between the $E_{(available)}$ pool estimated from long-term IEK data and the corresponding L values. However, because of fixation of Pb as discussed in the previous section, there is no agreement between the two types of estimate for the control soil. The L value for the least contaminated soil (S1) is also much higher than the corresponding $E_{(available)}$ value, suggesting that Pb fixation may also have been an issue with this soil.

The amounts of available Pb estimated from a single EDTA extraction are generally lower than those estimated by $E_{(available)}$ or L values, again suggesting that fixation of the Pb spike may have resulted in an overestimate of labile/available Pb. However, in the case of the three most highly contaminated soils, the differences are not large. Many laboratory studies have shown that EDTA is effective in removing Pb, Zn, Cu and Cd from contaminated soils (Elliotte and Brown, 1989; Brown and Elliott, 1992). EDTA is a very commonly used

soil extractant because of its strong chelating ability for different heavy metals. In spite of the potential fixation issue, labile Pb as predicted from both E and L values (L value for control (C1) soil excluded) is highly correlated with EDTA extractable soil Pb (Fig. 3). On this basis, EDTA would appear to be an effective extractant for estimating the amounts of labile Pb in contaminated soils.

Some previous studies have reported the correlation between the IEK-derived estimates of plant availability and plant uptake of elements. Frossard et al. (1992) have reported that P exchangeable between 1 min and 24 h correlated with root uptake of P from soils. Echevarria et al. (1998) have successfully used the IEK approach to assess Ni phytoavailability in Ni polluted soils. Gray et al. (2004) reported that the IEK compartment analysis showed clear differences in the distribution of Cd between exchange pools between soils where Cd was derived from phosphate fertilizer and those where Cd was derived from biosolids, especially Cd located in the $E_{1\ \mathrm{min}-24\ \mathrm{h}}$ pool. The results suggested that biosolids-derived Cd was more bioavailable than that derived from phosphate fertilizer. It can therefore be concluded that the proposed IEK approach is a useful method for characterizing the availability of these metals. However, because of the potential fixation of the Pb spike by soils, the characterization of Pb availability using the IEK approach appears to have some limitations.

4. Conclusions

Initially, our results indicated that the IEK equation used for radio-isotopic exchange processes also appeared to be an effective model for kinetics studies using a stable isotope. The fitted curves illustrate that isotopic exchange of Pb was a relatively fast process in the early stages (<24 h), followed by a much slower rate of exchange. The results found in our study were similar to those found in previous studies for Zn and Cd. However, a close examination of some of the IEK parameters derived from the fitting process raises doubts about its validity for use with the stable Pb isotope. Some limitations of the isotopic exchange approach have been observed where irreversible fixation of added Pb has appeared to occur. This fixation significantly affects the basic assumptions underlying this approach. Fixation of Pb coupled with errors associated with low concentrations of Pb in soil solution lead to unrealistically high E and L values, in particular for the control soil. It was also not possible to use short-term kinetics parameters (derived from 1–100 min) to predict the isotopically exchangeable Pb in the long-term (up to 15 days). Clearly, fixation of the added tracer by soil requires further investigation. It may well have been exacerbated in the current study by using soils with such high Fe oxide contents.

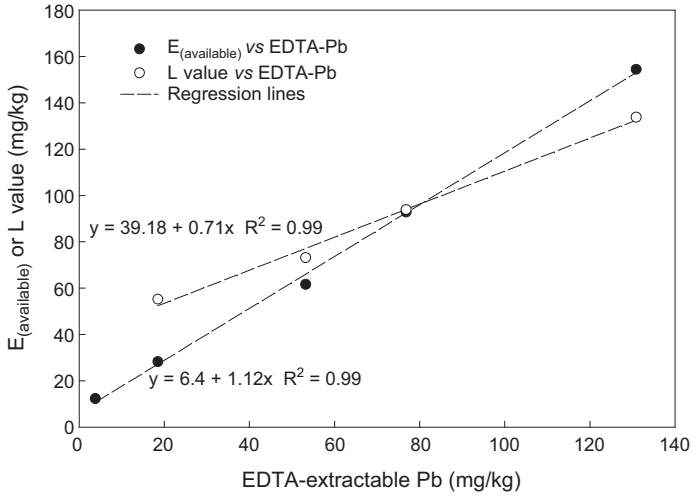

Fig. 3. Relationships between $E_{(\mathrm{available})}$ and L values and EDTA-extractable Pb concentrations.

In spite of problems with using the IEK approach, other than as a simple mathematical curve-fitting exercise, the amounts of available Pb (E values), determined during 24 h of exchange were significantly correlated with the plant uptake method (L values), and with EDTA-extractable Pb for all contaminated soils.

Acknowledgements

The authors would like to gratefully thank the Royal Golden Jubilee Grant and the Thailand Research Fund for funding this project, and the Postgraduate Education and Research Program in Chemistry (PERCH) for partial support.

References

Ahnstrom ZAS, Parker DR. Cadmium reactivity in metal-contaminated soils using a coupled stable isotope dilution-sequential extraction procedure. Environ Sci Technol 2001;35: 121–6.

Atkins GL. Modèles à compartiments multiples pour les systèmes biologiques. Paris: Gauthier-Villars; 1973.

Ayoub AS, McGaw BA, Shand CA, Midwood AJ. Phytoavailability of Cd and Zn in soil estimated by stable isotope exchange and chemical extraction. Plant Soil 2003;252:291–300.

Bäckström M, Karlsson S, Allard B. Metal leachability and anthropogenic signal in roadside soils estimated from sequential extraction and stable lead isotopes. Environ Monit Assess 2004;90:135–60.

Bacon JR, Hewitt IJ, Cooper P. Origin of lead associated with different reactive phases in Scottish upland soils: an assessment made using sequential extraction and isotope analysis. J Environ Monit 2004;6:766–73.

Becker JS. State-of-the-art and progress in precise and accurate isotope ratio measurements by ICP-MS and LA-ICP-MS, Plenary Lecture. J Anal At Spectrom 2002;17:1172–85.

Blakemore LC, Searle PL, Daly BK, Methods for chemical anaslysis of soils. Department of Scientific and Industrial Research, New Zealand Soil Bureau Scientific Report No. 80. 1987.

Brown GA, Elliott HA. Influence of electrolytes on EDTA extraction of Pb from polluted soil. Water Air Soil Pollut 1992;62:157–65.

Diesing W, Frossard E, Sinaj S. A comparison of short and long term isotopic exchange kinetics parameters used to predict zinc exchangeability in six heavy metal polluted soils. Proc of rhizosphere, preferential flow and bioavailability; A holistic view of soil-to-plant transfer, 21–23 September 2002, p. 27–30 Ascona, Switzerland.

Echevarria G, Morel JL, Fardeau JC, Leclerc-Cessac E. Assessment of phytoavailability of nickel in soil. J Environ Qual 1998;27: 1064–70.

Emmanuel S, Erel Y. Implications from concentrations and isotopic data for Pb partitioning processes in soils. Geochim Cosmochim Acta 2002;66:2517–27.

Elliotte HA, Brown GA. Comparative evaluation of NTA and EDTA for extractive decontamination of Pb-polluted soils. Water Air Soil Pollut 1989;45:361–9.

Ettler V, Mihaljevic M, Komarek M. ICP-MS measurements of lead isotopic ratios in soils heavily contaminated by lead smelting: tracing the sources of pollution. Anal Bioanal Chem 2004;378:311–7.

Fardeau JC. Le phosphore assimilable des sols Sa représentation par un medèle fonctionel à plusieurs compartiment. Agronomie 1993;13:317–31.

Fardeau JC. Dynamics of phosphate in soils. An isotopic outlook. Fert Res 1996;45:91–100.

Fardeau JC, Morel C, Jappé J. Cinétique d'échange des ions phosphate dans les systémes sol:solution Vérification expérimentale de l'équation théorique. CR Séances Acad Sci Paris t 300 III 1985;8:371–6.

Fardeau JC, Poss R, Saragoni H. Potassium release and fixation in Ferralsols (Oxisols) from Southern Togo. J Soil Sci 1991; 42:649–60.

Frossard E, Sinaj S. The isotope exchange kinetic technique: a method to describe the availability of inorganic nutrients applications to K, P, S and Zn. Isot Environ Health Stud 1997;33:61–77.

Frossard E, Fardeau JC, Ognalaga M, Morel JL. Influences of agricultural practices, soil properties and parent material on the phosphate buffering capacity of cultivated soils developed on temperate climates. Eur J Agron 1992;1:45–50.

Gäbler HE, Bahr A, Mieke B. Determination of the interchangeable heavy-metal fraction in soils by isotope dilution mass spectrometry. Fresenius' J Anal Chem 1999;356:409–14.

Gérard E, Echevarria G, Sterckeman T, Morel JL. Cadmium availability to three plant species varying in cadmium accumulation pattern. J Environ Qual 2000;29:1117–23.

Gray CW, McLaren RG, Roberts AHC. Cadmium phytoavailability in a New Zealand pastoral soil. Chemical bioavailability in the terrestrial environment workshop, 18–20 November 2001, Adelaide, Australia, p. 85–6.

Gray CW, McLaren RG, Shiowatana J. The determination of labile cadmium in some biosolids-amended soils by isotope dilution plasma mass spectrometry. Aust J Soil Res 2003; 41:589–97.

Gray CW, McLaren RG, Günther D, Sinaj S. An assessment of cadmium availability in cadmium-contaminated soils using isotope exchange kinetics. Soil Sci Soc Am J 2004;68:1210–7.

Haack UK, Heinrichs H, Gutsche FH, Plessow K. The isotopic composition of anthropogenic Pb in soil profiles of northern Germany: evidence for pollutant Pb from a continent-wide mixing system. Water Air Soil Pollut 2003;150:113–34.

Hamon RE, McLaughlin MJ, Naidu R, Correll R. Long-term changes in cadmium bioavailability in soil. Environ Sci Technol 1998;32:3699–703.

Kovács B, Prokisch J, Györi Z, Kovács AB, Palencsér AJ. Studies on soil sample preparation for inductively coupled plasma atomic emission spectrometry analysis. Commun Soil Sci Plant Anal 2000;31:1949–63.

McLaughlin MJ, Zarcinas BA, Stevens DP, Cook N. Soil testing for heavy metals. Commun Soil Sci Plant Anal 2000;31:1949–63.

Monastra V, Derry LA, Chadwick OA. Multiple sources of lead in soils from a Hawaiian chronosequence. Chem Geol 2004; 209:215–31.

Sheppard CW. Basic principles of the tracer method Introduction to mathematical tracer kinetics. New York: John Wiley and Sons; 1962. 282 pp.

Sinaj S, Machler F, Frossard E. Assessment of isotopically exchangeable Zn in polluted and nonpolluted soils. Soil Sci Soc Am J 1999;63:1618–25.

Singer JK, Anderson JB, Ledbetter MT, McCave IN, Jones KPN, Wright R. An assessment of analytical techniques for the size analysis of fine grained sediments. J Sediment Petrol 1988; 58:534–43.

Singh AK, Pandeya SB. Modelling uptake of cadmium by plants in sludge-treated soils. Bioresour Technol 1998;66:51–8.

Smolders E, Brans K, Földi A, Merckx R. Cadmium fixation in soils measured by isotopic dilution. Soil Sci Soc Am J 1999;63: 78–85.

Tiller KG, Honeysett JL, De Vries MPC. Soil zinc and its uptake by plants: I. Isotopic exchange equilibria and the application of tracer techniques. Aust J Soil Res 1972;10:151–64.

Vanhaecke F, Moens L, Dams R, Papadakis I, Taylor P. Application of high-resolution ICP-mass spectrometry for isotope ratio measurements. Anal Chem 1997;69:268–73.

Wong CSC, Li WXD. Pb contamination and isotopic composition of urban soils in Hong Kong. Sci Total Environ 2004;319: 185–95.

กรดอินทรีย์ในอาหารไทยเพิ่มการนำไปใช้ได้ของแคลเซียม

ORGANIC ACIDS IN THAI FOODS CAN ENHANCE CALCIUM BIOAVAILABILITY

ยุวดี เชี่ยววัฒนา *Juwadee Shiowatana Sottimai*
อทิตยา ศิริภิญญานนท์ *Atitaya Siripinyanond*
สุทธินันท์ แต่บรรพกุล *Sutthinun Taebunpakul*
อัปสร โสตธิมัย *Upsorn*

ABSTRACT

Vegetable is an important source of dietary calcium. Unfortunately, they contain substances, i.e., dietary fiber, phytate, and oxalate which can inhibit the bioavailability of calcium. Two vegetables were selected for study: kale and spinach which are representative of vegetables with high and low calcium bioavailability, respectively. The effect of adding these vegetables in different dishes on calcium bioavailability were investigated using an *in vitro* dialysis method. Four dishes: fish Tom Yam, fish Kaeng Som, fish soup, and fish soup with lime juice were prepared to study the effect of ingredients on calcium *in vitro* dialyzability of vegetables.

A novel continuous-flow dialysis method with flame atomic emission spectrometric detection (flame AES) was applied to estimate the dialyzability of minerals in dishes prepared. The method involves a simulated gastric digestion with pepsin, followed by dialysis occurring during a continuous flow of dialyzing solution ($NaHCO_3$). Using the proposed system, the enhancement of calcium dialyzability for kale was observed for fish Tom Yam (28%), and fish soup with lime juice (15%). For fish soup and fish Kaeng Som, no significant enhancement in calcium dialyzability for kale was found in these dishes. For spinach, the depression of calcium dialyzability was found in all dishes. The enhancement of bioavailability found could be attributed to the organic acids, especially citric acid in the dishes containing lime juice.

Key words : *In vitro* method, bioavailability, calcium, Thai dishes.

ภาควิชาเคมี คณะวิทยาศาสตร์ มหาวิทยาลัยมหิดล ราชเทวี เขตพญาไท กรุงเทพมหานคร 10400

Department of Chemistry, Faculty of Science, Mahidol University, Rajthevi, Phayathai, Bangkok 10400

บทคัดย่อ

ผักเป็นแหล่งของแคลเซียมที่สำคัญในอาหาร แต่ผักบางชนิดประกอบด้วยสารซึ่งสามารถยับยั้งการนำไปใช้ของแคลเซียม เช่น เส้นใยอาหาร ไฟเตต และออกซาเลต งานวิจัยนี้ได้ทำการศึกษาการนำไปใช้ได้ของแคลเซียมในตัวอย่างผักสองชนิด คือ ผักคะน้า และผักปวยเล้ง ซึ่งเป็นตัวแทนของผักที่มีแคลเซียมที่ร่างกายดูดซึมได้สูงและต่ำตามลำดับ และศึกษาผลของการนำผักเหล่านี้มาปรุงเป็นอาหาร 4 ชนิด ได้แก่ ต้มยำปลา แกงส้มปลา แกงจืดปลา แกงจืดปลาใส่น้ำมะนาว เพื่อศึกษาผลของส่วนประกอบในอาหารที่มีต่อการนำไปใช้ได้ของแคลเซียมโดยใช้วิธีในหลอดแก้วในการประเมินความสามารถในการนำไปใช้ได้ของแคลเซียม

วิธีในหลอดแก้วแบบไหลต่อเนื่องแนวใหม่ โดยการตรวจวัดด้วยเทคนิคอะตอมมิคอิมิสชันแบบเปลวไฟ ได้นำไปศึกษาปริมาณแร่ธาตุที่ไดอะไลส์ได้โดยเลียนแบบการย่อยในกระเพาะอาหารด้วยเอนไซม์เปปซินตามด้วยกระบวนการไดอะไลซิสภายในหลอดไดอะไลซิส โดยการผ่านสารละลายโซเดียมไบคาร์บอเนตอย่างต่อเนื่อง จากการใช้ระบบที่เสนอ พบการเพิ่มขึ้นของปริมาณที่ไดอะไลส์ได้ของแคลเซียมในคะน้า เมื่อนำคะน้าไปปรุงในอาหารที่ใส่น้ำมะนาว ได้แก่ ต้มยำปลา (28%) และแกงจืดปลาใส่น้ำมะนาว (15%) ในขณะที่แกงจืดปลาและแกงส้มปลา ไม่พบว่ามีการเพิ่มขึ้นของปริมาณที่ไดอะไลส์ได้ของแคลเซียม สำหรับอาหารข้างต้นที่เติมผักปวยเล้ง พบการลดลงของปริมาณที่ไดอะไลส์ได้ของแคลเซียมในอาหารที่ศึกษา การเพิ่มขึ้นของปริมาณที่ไดอะไลส์ได้ คาดว่าเป็นผลมาจากกรดอินทรีย์ โดยเฉพาะอย่างยิ่งกรดซิตริกในอาหารที่มีการเติมน้ำมะนาว ส่วนการลดลงน่าจะเป็นผลจากสารยับยั้งต่าง ๆ เช่น ออกซาเลต และไฟเตต เป็นต้น

บทนำ

โรคกระดูกพรุนจัดเป็นปัญหาสำคัญในทางสาธารณสุข เกิดจากการได้รับแคลเซียมไม่เพียงพอ ซึ่งมักพบในผู้ป่วยสูงวัย เนื่องด้วยเป็นวัยที่มีอัตราการสลายของธาตุแคลเซียมสูง เพื่อลดอุบัติการณ์ของภาวะกระดูกพรุน การรณรงค์ให้บริโภคอาหารที่มีแคลเซียมอย่างเพียงพอตั้งแต่วัยเยาว์ เพื่อเสริมสร้างกระดูกและลดอัตราการสูญเสียแคลเซียมเมื่อสูงวัยเป็นสิ่งสำคัญ อย่างไรก็ดีนอกจากปริมาณแคลเซียมที่บริโภคแล้ว ความสามารถในการนำแคลเซียมไปใช้ได้ในอาหารชนิดนั้นก็เป็นสิ่งที่ควรจะนำมาพิจารณา

อาหารที่พบแคลเซียมในปริมาณสูง ตัวอย่างเช่น นม และผักชนิดต่าง ๆ โดยเฉพาะอย่างยิ่งผักใบเขียวจัดเป็นแหล่งที่สำคัญที่สุดแหล่งหนึ่งของแคลเซียม ค่าความสามารถของร่างกายในการนำแคลเซียมไปใช้ได้ในผักเหล่านี้อยู่ในช่วงระหว่าง 5-50% (Sottimai *et al*., 2003) โดยผักบางชนิดแม้จะมีปริมาณของแคลเซียมสูง แต่ร่างกายนำไปใช้ได้ต่ำมาก ทั้งนี้เพราะผักเหล่านี้มีสารบางชนิดเช่น ไฟเตต ออกซาเลต และไฟเบอร์ ซึ่งสามารถรวมตัวกับแคลเซียมเกิดเป็นสารประกอบที่ร่างกายไม่สามารถดูดซึมได้ (Lombardi-Boccia *et al*., 1998; Weaver *et al*., 1999; Kamchan *et al*., 2004) เนื่องจากแคลเซียมเป็นแร่ธาตุที่สำคัญ จึงได้มีผู้ทำการศึกษาหาแนวทางการเพิ่มปริมาณการนำไปใช้ได้ของแร่ธาตุ ตัวอย่างเช่น การใช้อาหารเสริมในรูปยาเม็ด การเสริมธาตุที่ต้องการในอาหารที่บริโภคโดยตรง หรือแม้กระทั่งการใช้ปุ๋ย เพื่อส่งเสริมให้พืชสะสมธาตุอาหารที่ต้องการได้มากขึ้น หรือลดสารยับยั้งบางชนิดลง รวมถึงการใช้กระบวนการพันธุวิศวกรรมปรับปรุงพันธุ์พืช (Frossard *et al*., 2000)

ในหลายปีที่ผ่านมาได้มีการศึกษาเกี่ยวกับส่วนประกอบในอาหารที่อาจส่งผลต่อการนำแคลเซียมไปใช้ โดยสามารถแบ่งออกได้เป็น 2 ประเภท คือ ปัจจัยที่ส่งเสริมการนำแคลเซียมไปใช้ เช่น น้ำตาลแลคโตส วิตามินดี วิตามินเค กรดอินทรีย์บางชนิด และปัจจัยที่ลดการนำแคลเซียมไปใช้ เช่น ไฟเบอร์ ไฟเตต ออกซาเลต โปรตีนบางชนิด ไขมัน และเกลือ (Gueguen *et al*., 2000; Kennefick *et al*., 2000) จากการศึกษาเบื้องต้นของคณะวิจัยก็พบ

ผลของกรดอินทรีย์ชนิดต่าง ๆ ที่สามารถเพิ่มการนำแคลเซียมไปใช้ได้ โดยพบว่ากรดซิตริก กรดทาร์ทาริก กรดมาลิก และกรดแอสคอร์บิกเพิ่มการนำไปใช้ได้ของแคลเซียมในตัวอย่างผักที่มีค่าการนำไปใช้ได้ต่ำ (Sottimai *et al*., 2003) อย่างไรก็ตามโดยทั่วไปเราไม่ได้บริโภคผักโดด ๆ แต่จะปรุงเข้ากับส่วนประกอบอื่น ๆ งานวิจัยนี้จึงมีวัตถุประสงค์ในการศึกษาถึงอิทธิพลของกรดอินทรีย์ที่มีในเครื่องปรุงของอาหารไทยที่มีต่อการดูดซึมได้ของแคลเซียมในผัก โดยเลือกอาหารไทยที่มีรสเปรี้ยวจากการมีกรดอินทรีย์ในส่วนประกอบ เช่น ต้มยำมีกรดซิตริกจากน้ำมะนาว แกงส้มมีกรดทาร์ทาริกจากน้ำมะขามเปียก การศึกษาได้นำเอาวิธีในหลอดแก้วแบบไหลต่อเนื่องแนวใหม่ที่พัฒนาขึ้นครั้งแรกจากคณะวิจัยไปใช้ในการศึกษาการนำแคลเซียมไปใช้ในตัวอย่างผักต่าง ๆ และในอาหารไทย โดยผักที่เลือกศึกษามี 2 ชนิดคือ ผักคะน้า และปวยเล้งซึ่งเป็นผักที่มีแคลเซียมที่ร่างกายดูดซึมได้สูงและต่ำตามลำดับ โดยนำมาทำการปรุงเป็นอาหารไทย 4 ชนิด ได้แก่ ต้มยำปลา แกงส้มปลา แกงจืดปลา และแกงจืดปลาใส่น้ำมะนาว เพื่อทำการศึกษาผลของเครื่องปรุงในอาหารเหล่านี้ที่มีต่อการนำไปใช้ได้ของแคลเซียม

อุปกรณ์และวิธีการ

1. การเตรียมตัวอย่างผักและอาหาร

ผักสด (ผักคะน้าและปวยเล้ง) ซื้อจากตลาดสด และห้างสรรพสินค้าในเขตกรุงเทพมหานคร โดยนำมาล้างด้วยน้ำปราศจากไอออน ทำการอบให้แห้งที่อุณหภูมิ 65°C จนกระทั่งน้ำหนักคงที่ ทำการปั่นให้ละเอียด และเก็บไว้ในโถอบแห้ง สำหรับไว้ใช้ตลอดการศึกษา

อาหาร (ต้มยำปลา แกงส้มปลา แกงจืดปลา และแกงจืดปลาใส่น้ำมะนาว) เตรียมได้จากวิธีการปรุงในตำราอาหารไทย (มูลนิธิการแพทย์แผนไทยพัฒนา, 2544; วัลยา ภู่ภิญโญ, 2544) โดยนำผักคะน้าหรือปวยเล้ง (A) ประมาณ 80 กรัม ปรุงด้วยเครื่องปรุงอื่น ๆ (B) เป็นอาหาร 4 ชนิด ดัง Table 1.

Table 1. Ingredients for samples of fish Tom Yam, fish Kaeng Som, fish soup, and fish soup with lime juice.

Ingredients	Fish Tom Yam (B)	Fish Kaeng Som (B)	Fish soup (B)	Fish soup with lime juice (B)
Boiled fish (g)	120.60	119.84	120.59	120.59
Tom Yam Chilli paste (g)	31.46	-	-	-
Kaeng Som Chilli paste (g)	-	40.30	-	-
Lime juice (g)	15.00	-	-	20.00
Tamarind juice (g)	-	15.50	-	-
Fish sauce (g)	5.50	10.00	5.48	5.48
Sugar (g)	-	4.00	-	-
Deionized water (mL)	250	300	250	250

อาหารที่เตรียมได้ จะนำมาปั่นด้วยเครื่องปั่นอาหาร และทำการอบให้แห้งที่อุณหภูมิ 65°C จนกระทั่งน้ำหนักคงที่ ทำการปั่นให้ละเอียดอีกครั้ง และเก็บไว้ในโถอบแห้งจนกระทั่งวิเคราะห์ โดยสามารถทำการทดลองกับตัวอย่างซ้ำเมื่อต้องการ

2. การวิเคราะห์หาปริมาณแคลเซียมทั้งหมดในตัวอย่าง

ตัวอย่างอาหารแห้งที่ได้ประมาณ 0.5 กรัม ชั่งโดยละเอียด นำมาย่อยด้วยสารละลายเข้มข้นของ HNO_3: H_2O_2 3:2 (v/v) ปริมาตร 10 mL โดยวิธีการย่อยด้วยไมโครเวฟ สารละลายใสที่ได้นำมาทำการเจือจางด้วยน้ำปราศจากไอออนให้มีปริมาตรเป็น 50.0 mL แล้วทำการตรวจวิเคราะห์ปริมาณโดยใช้ Flame AES

3. การวิเคราะห์หาปริมาณที่ไดอะไลส์ได้ของแคลเซียม

ปริมาณการนำแคลเซียมไปใช้ได้ในตัวอย่างผักและอาหาร ศึกษาได้จากวิธีในหลอดแก้วแบบไหลต่อเนื่องแนวใหม่ (Sottimai *et al*., 2003) ซึ่งประกอบด้วยขั้นตอนหลัก ๆ 3 ขั้นตอนได้แก่ การจำลองสภาพการย่อยในกระเพาะอาหาร การหาความเข้มข้นที่เหมาะสมของสารละลาย $NaHCO_3$ และการจำลองสภาพการย่อยในลำไส้เล็ก

3.1 การจำลองสภาพการย่อยในกระเพาะอาหาร ทำได้โดยวิธีของ Miller

3.2 การหาความเข้มข้นที่เหมาะสมของสารละลาย $NaHCO_3$ ทำได้โดยหาค่าสภาพกรดของตัวอย่าง (titratable acidity) ที่ได้จากการไทเทรตสารผสมของ pepsin digestate (2.5 g) กับ pancreatin bile extract mixture (625 µL) ด้วย 0.1 M NaOH ค่าที่ได้นี้สามารถนำไปใช้ในการคำนวณหาความเข้มข้นที่เหมาะสมของ $NaHCO_3$ เพื่อใช้ปรับ pH ของอาหารที่ผ่านการย่อยในกระเพาะอาหารซึ่งมีค่าประมาณ 2.0 ให้เป็น 5.0 ซึ่งเป็น pH ในลำไส้เล็กภายในเวลา 30 นาที โดยพบว่า ความเข้มข้นที่เหมาะสมของ $NaHCO_3$ มีความสัมพันธ์เป็นเส้นตรงกับค่า titratable acidity ซึ่งหาได้จากสมการดังต่อไปนี้ สำหรับกรณีอาหารที่ศึกษาในงานวิจัยนี้

$$\text{Optimum } NaHCO_3 \text{ concentration} = (\text{Titratable acidity in Molarity})/36$$

3.3 การจำลองสภาพการย่อยในลำไส้เล็ก ทำได้โดยการบรรจุ pepsin digestate 2.5 กรัม ลงในถุงไดอะไลซิส (MWCO 12-14 kDa) นำไปติดตั้งตาม Figure 1. จากนั้นทำการผ่านสารละลาย $NaHCO_3$ ความเข้มข้นที่เหมาะสม ด้วยอัตราการไหล 1 mL/min แล้วทำการเก็บสารที่ไดอะไลส์ได้ในขวดเก็บสาร โดยภายหลัง 30 นาทีนับจากเริ่มต้นเก็บ ทำการฉีด pancreatin bile extract mixture 625 µL เข้าไปในถุงไดอะไลซิสผ่านวาล์วฉีดสาร และทำการผ่านสารละลาย $NaHCO_3$ อย่างต่อเนื่องอีก 2 ชั่วโมง ทำการเก็บสารที่ไดอะไลส์เป็นระยะ ๆ (10 mL/ fraction) จากนั้นจะทำการตรวจวัดด้วยเทคนิค flame AES ต่อไป

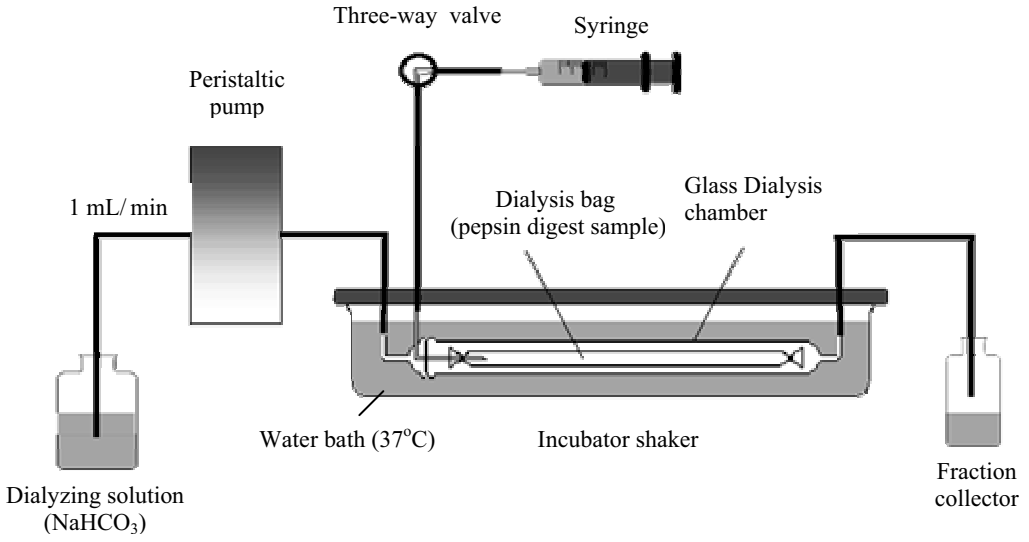

Figure 1. Diagram of a novel continuous-flow dialysis system.

4. การประเมินค่าความสามารถในการไดอะไลส์ได้ของแคลเซียม

ค่าความสามารถในการไดอะไลส์ได้ของแคลเซียม อาจใช้ในการชี้บอกถึงความสามารถในการนำแคลเซียมไปใช้ได้ของอาหารชนิดนั้น ซึ่งหาได้จากสมการ

$$\text{Dialyzability (\%)} = \frac{D \times 100}{W \times A}$$

โดยที่ D = ปริมาณของแคลเซียมที่ไดอะไลส์ได้ทั้งหมดในเวลา 150 นาที เมื่อหักลบออกจากค่าที่ได้จากการทำแบลงก์ (µg)

W= น้ำหนักตัวอย่างอาหารแห้ง (g)

A = ความเข้มข้นของแคลเซียมในตัวอย่างอาหารแห้ง (µg/g)

5. การประเมินค่าการเพิ่มขึ้นหรือลดลงของแคลเซียมที่ไดอะไลส์ได้ เมื่อนำผักไปประกอบเป็นอาหาร

$$\text{Dialyzability Enhancement (or Depression) (\%)} = \frac{[D_{AB} - (D_A+D_B)]}{(D_A+D_B)} \times 100$$

เมื่อ D_{AB} = ปริมาณการไดอะไลส์ได้ของแร่ธาตุ เมื่อนำผัก (A) และเครื่องปรุงอื่น ๆ (B) มาปรุงเข้าด้วยกันและทำให้สุก

D_A, D_B = ปริมาณการไดอะไลส์ได้ของแร่ธาตุในผัก (A) หรือเครื่องปรุงอื่น ๆ (B) เมื่อทำให้สุกโดดๆ

ถ้าค่าการเพิ่มขึ้นหรือลดลงของแคลเซียมที่ไดอะไลส์ได้ดังกล่าวมีค่าสูงกว่าหรือต่ำกว่ามากกว่า 10% จึงจะถือว่าเครื่องปรุงอื่น ๆ ในอาหารนั้นส่งผลให้มีการไดอะไลส์ได้เพิ่มขึ้นและลดลงของผัก

ผลและวิจารณ์

1. ผลการศึกษาปริมาณการนำแคลเซียมไปใช้ได้ในตัวอย่างผัก

ผักคะน้า

ผักปวยเล้ง

ผักที่เลือกทำการศึกษามี 2 ชนิด ได้แก่ ผักคะน้าและปวยเล้ง ซึ่งเป็นตัวแทนของผักที่มีความสามารถในการนำแคลเซียมไปใช้ได้สูงและต่ำตามลำดับ จากการศึกษาโดยใช้วิธีในหลอดแก้วแบบไหลต่อเนื่อง ผลที่ได้ใน

กราฟแสดงการเปลี่ยนแปลงของการไดอะไลส์ของแคลเซียมตามเวลาของการไดอะไลส์ และค่าการเปลี่ยนแปลงของ pH ในระหว่างการไดอะไลซิส (Figure 2.)

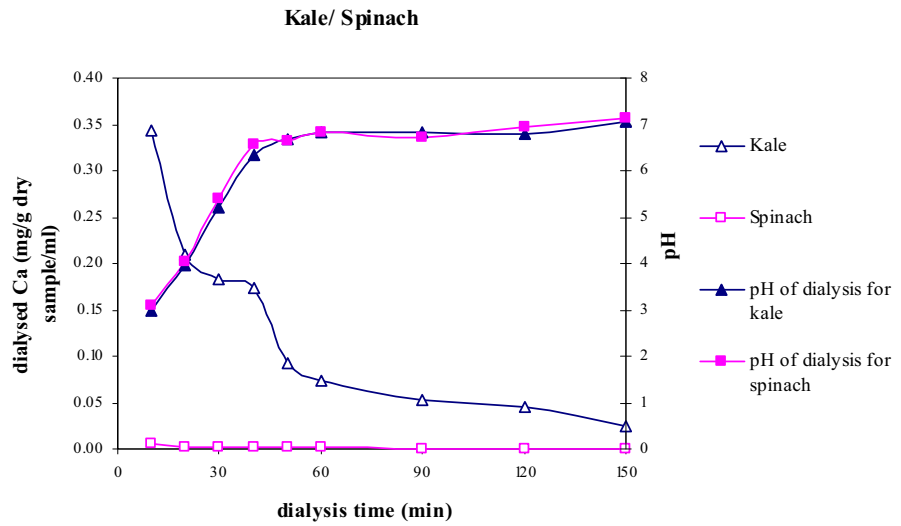

Figure 2. The profile of dialyzed calcium and pH change during dialysis for kale and spinach by continuous-flow dialysis method.

จากผลแสดงให้เห็นว่าวิธีที่เสนอขึ้นนี้ให้ค่าการเปลี่ยนแปลงของ pH ในระหว่างการไดอะไลซิสสอดคล้องกับสภาพ pH ในระบบทางเดินอาหารของมนุษย์ โดยมีการเปลี่ยนแปลง pH ในกระเพาะอาหารจาก 2.0 เป็น 5.0 ซึ่งเป็น pH ในลำไส้เล็กภายในเวลา 30 นาที สำหรับผลการเปรียบเทียบค่าความสามารถในการนำแคลเซียมไปใช้ของผักคะน้าและปวยเล้ง แสดงไว้ใน Table 2.

Table 2. The comparison of calcium bioavailability for kale and spinach by the continuous-flow dialysis and *in vivo* method.

Method	% Ca bioavailability	
	Kale	Spinach
<u>*In vitro* method</u>		
Continuous-flow dialysis (this study)	42.2 ± 0.2	2.89 ± 0.17
Continuous-flow dialysis (Sottimai *et al*., 2003)	52.9 ± 1.1	4.6 ± 0.5
<u>*In vivo* method</u>		
Dual isotope tracer (Weaver *et al*., 1994)	58.8	5.1
Dual isotope tracer (Weaver *et al*., 1999)	49.3	5.1
Dual isotope tracer (Heaney *et al*., 1990)	40.9	4.55

จากตารางจะเห็นว่าค่าที่ได้จากการศึกษาด้วยวิธีนี้ให้ค่าที่ใกล้เคียงกับการศึกษาด้วยวิธีในร่างกาย ความแตกต่างของค่าเหล่านี้ที่อาจมีบ้าง อาจเกิดจากหลายปัจจัยด้วยกัน เช่น อายุของผัก สิ่งแวดล้อม และสภาพดินที่ปลูกผักนั้น เหตุที่ผักปวยเล้งมีค่าการนำแคลเซียมไปใช้ต่ำมาก เป็นเพราะการมีปริมาณของออกซาเลตสูง ซึ่ง

สามารถรวมตัวกับแคลเซียมแล้วเกิดเป็นเกลือแคลเซียมออกซาเลตที่ร่างกายไม่สามารถนำแคลเซียมไปใช้ได้ (Reykdal *et al*., 1991; Savage *et al*., 2000) ในทางตรงข้ามคะน้าเป็นผักที่มีออกซาเลตต่ำ เช่นเดียวกับบรอคโคลี่ และ กะหล่ำปลี ทำให้ผักเหล่านี้มีค่าการนำแคลเซียมไปใช้สูง (Heaney *et al*., 1990; Heaney *et al*., 1993)

2. ผลการศึกษาความสามารถในการนำแคลเซียมไปใช้ได้ จากการนำผักคะน้าปรุงเป็นอาหารไทยต่างชนิดกัน

จากการศึกษาเบื้องต้น ถึงอิทธิพลของกรดอินทรีย์ต่าง ๆ เช่น กรดซิตริก กรดทาร์ทาริก กรดมาลิก และกรดแอสคอร์บิกในการเพิ่มการนำแคลเซียมไปใช้ได้ในผักโขม พบว่าให้ผลดัง Table 3. ซึ่งแสดงผลการเพิ่มขึ้นของแคลเซียมที่ไดอะไลส์ได้ เมื่อมีกรดอินทรีย์ชนิดต่าง ๆ ในความเข้มข้นที่ต่างกัน

Table 3. The percent increase of calcium dialyzability in the presence of organic acid for amaranth as determined by continuous-flow dialysis method.

Organic acid	% increase of dialyzability in the presence of organic acid		
	1%	2.5%	5%
Ascorbic acid	0	15.1	29.1
Citric acid	32.8	54.5	65.7
Malic acid	0	33.2	46.1
Tartaric acid	26.6	41.6	55.8

การศึกษานี้จึงสนใจที่จะศึกษาดูว่ากรดอินทรีย์ที่มีอยู่ในอาหารไทยมีผลช่วยเพิ่มความสามารถในการดูดซึมของแคลเซียมได้หรือไม่ โดยเลือกผักคะน้าทำการปรุงเป็นอาหารไทยทั้งชนิดที่มีและไม่มีส่วนผสมของกรดอินทรีย์ โดยทำการศึกษาในอาหาร 2 ชนิดคือ ต้มยำปลาใส่ผักคะน้า (มีกรดซิตริกจากมะนาว) และแกงส้มปลาใส่ผักคะน้า (มีกรดทาร์ทาริกจากมะขาม) นอกจากนี้ยังได้ศึกษากรณีของแกงจืดปลาใส่คะน้าและแกงจืดปลาใส่คะน้าและน้ำมะนาวด้วยเพื่อยืนยันผลของน้ำมะนาวที่มีต่อการนำไปใช้ได้ของแคลเซียม จากการศึกษาพบว่าให้ผลเป็นดัง Table 4. Figure 3-4. เป็นกราฟแสดงการเปลี่ยนแปลงของการไดอะไลส์ของแคลเซียมตามเวลาของการไดอะไลส์ และค่าการเปลี่ยนแปลงของ pH ในระหว่างการไดอะไลซิส

Table 4. Calcium dialyzability of kale alone(A) and in different dishes(AB) and enhancement (depression) effect from ingredients.

Menu	% organic acid	Total calcium (mg/serving)	Dialyzed Calcium (mg/serving), n=3	% enhancement (or depression)
1. <u>Fish Tom Yam with kale</u>				
- Boiled kale alone(A)	(0.1)	55.1 ± 4	25.4 ± 0.6 (46.0%)	
- Fish Tom Yam alone(B)	0.61[a]	39.5 ± 3.6	19.0 ± 2.1 (48.1%)	+28%
- Fish Tom Yam with kale(AB)	0.50[a]+(0.1)	109 ± 1	56.7 ± 1.9 (52.0%)	
2. <u>Fish Kaeng Som with kale</u>				
- Boiled kale alone(A)	(0.1)	55.1 ± 4	25.4 ± 0.6 (46.0%)	
- Fish Kaeng Som alone(B)	0.10[b]	71.7 ± 4.9	35.6 ± 1.1 (49.7%)	+7%
- Fish Kaeng Som with kale(AB)	0.08[b]+(0.1)	132 ± 13	65.1 ± 2.5 (49.4%)	Insignificant effect
3. <u>Fish soup with kale</u>				
- Boiled kale alone(A)	(0.1)	82.8 ± 0.7	41.3 ± 0.9 (49.9%)	
- Fish soup alone(B)	0.00	8.78 ± 0.53	3.71 ± 0.20 (42.4%)	+6%

- Fish soup with kale(AB)	0.00+(0.1)	90.8 ± 3.6	47.5 ± 3.1 (52.3%)	Insignificant effect
4. <u>Fish soup with lime juice with kale</u> - Boiled kale alone(A) - Fish soup with lime juice alone(B) - Fish soup with lime juice with kale(AB)	 (0.1) 0.40[a] 0.33[a]+(0.1)	 79.3 ± 0.7 10.7 ± 1.2 86.6 ± 1.6	 39.6 ± 0.8 (49.9%) 4.98 ± 0.25 (46.6%) 51.2 ± 0.8 (59.1%)	 +15%

* Values in brackets are percent dialyzability.

[a] Citric acid containing in the dish.
[b] Tartaric acid containing in the dish.

จากการศึกษานี้พบว่ากรดอินทรีย์ในส่วนประกอบของอาหารเพิ่มความสามารถในการนำแคลเซียมไปใช้ได้ ซึ่งชี้ให้เห็นว่ากรดซิตริกจากน้ำมะนาวเพิ่มการนำไปใช้ของแคลเซียมที่ดีกว่ากรดทาร์ทาริกจากน้ำมะขามเปียก แต่อย่างไรก็ตามค่าการเพิ่มขึ้นนี้ก็ยังขึ้นอยู่กับปริมาณของกรดอินทรีย์ที่อยู่ในอาหารด้วย โดยเปอร์เซ็นต์การเพิ่มขึ้นของแคลเซียมที่ไดอะไลส์ได้ เพิ่มตามความเข้มข้นของกรดอินทรีย์ที่มีในอาหารซึ่งเป็นแนวโน้มเดียวกับการศึกษาในเบื้องต้นดัง Table 3 โดยกรดอินทรีย์นั้นทำให้แคลเซียมอยู่ในรูปที่สามารถไดอะไลส์ได้มากขึ้น (Benway *et al*., 1993; Lyon *et al*., 1984) ในการยืนยันผลการเพิ่มขึ้นของการไดอะไลส์เนื่องจากน้ำมะนาว ได้ทำการศึกษาเปรียบเทียบอาหาร 2 ชนิด คือ แกงจืดปลาใส่ผักคะน้า และแกงจืดปลาใส่ผักคะน้าใส่น้ำมะนาว พบว่าน้ำมะนาวซึ่งมีกรดซิตริก สามารถเพิ่มการไดอะไลส์ของแคลเซียมได้จริง ซึ่งไม่เพียงแต่กรดซิตริกจะช่วยเพิ่มการไดอะไลส์ได้ของแคลเซียมในผักคะน้าเท่านั้น แต่ยังช่วยเพิ่มการไดอะไลส์ได้ในเนื้อปลาด้วย (42% เพิ่มเป็น 47% เมื่อพิจารณาค่า B ของแกงจืดปลาและแกงจืดปลาใส่น้ำมะนาวใน Table 4.)

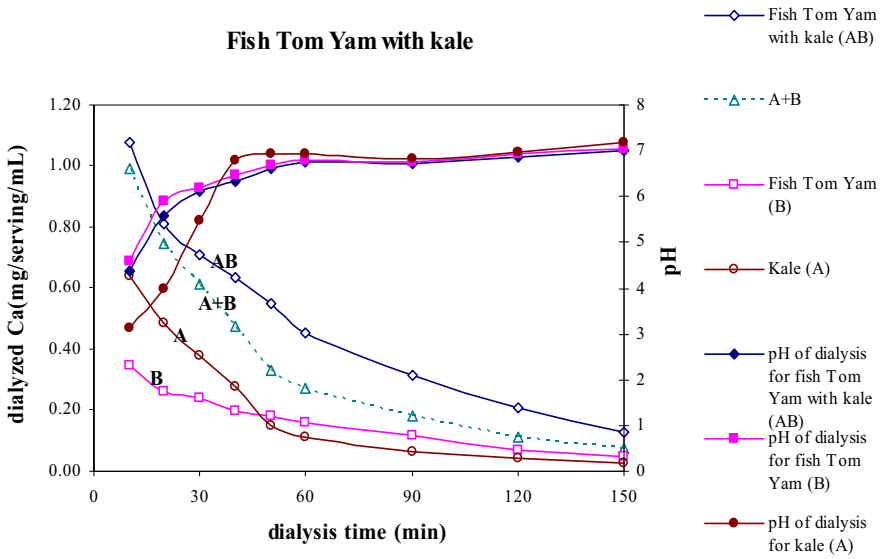

Figure 3. The profile of dialyzed calcium and pH change of fish Tom Yam with kale by continuous-flow dialysis method.

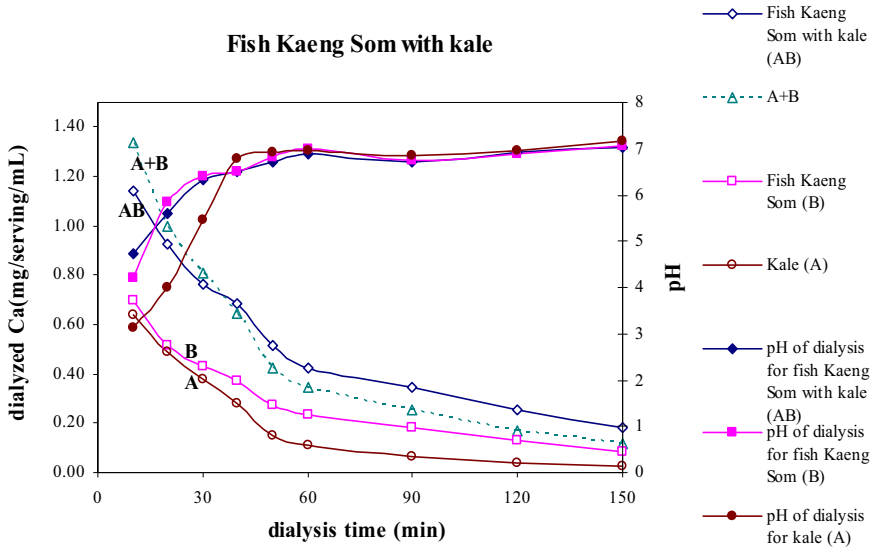

Figure 4. The profile of dialyzed calcium and pH change of fish Kaeng Som with kale by continuous-flow dialysis method.

จาก Figure 3-4 จะเห็นได้ว่า อาหารบางชนิดให้การเปลี่ยนแปลงของ pH ในระหว่างการไดอะไลซิสในชั่วโมงแรกช้ากว่า ทั้งนี้อาจเป็นเพราะ การมีองค์ประกอบบางอย่างในอาหารที่อาจไปขัดขวางการปล่อยออกของกรดสู่ภายนอกเมมเบรน ทำให้มีการเปลี่ยนแปลงของ pH ที่ช้ากว่า

3. ผลการศึกษาความสามารถในการนำแคลเซียมไปใช้ได้ จากการนำผักปวยเล้งปรุงเป็นอาหารไทยต่างชนิดกัน

ในทำนองเดียวกับการศึกษากับผักคะน้า การศึกษานี้ใช้ผักปวยเล้งทำการปรุงเป็นอาหาร 2 ชนิดคือ ต้มยำปลาใส่ผักปวยเล้ง แกงส้มปลาใส่ผักปวยเล้ง โดยผลการศึกษาเป็นไปดัง Table 5.

Table 5. Calcium dialyzability of spinach alone(A) and in different dishes(AB) and enhancement (depression) effect from ingredients.

Menu	% organic acid	Total calcium (mg/serving)	Dialyzed Calcium* (mg/serving), n=3	% enhancement (or depression)
1. <u>Fish Tom Yam with spinach</u>				
- Boiled spinach alone(A)	0.00[a]	34.1 ± 1.6	0.98 ± 0.06 (2.89%)	
- Fish Tom Yam alone(B)	0.61[a]	58.5 ± 4.2	27.1 ± 0.1 (46.3%)	-78%
- Fish Tom Yam with spinach(AB)	0.52[a]	100 ± 4	6.14 ± 0.12 (6.14%)	
2. <u>Fish Kaeng Som with spinach</u>				
- Boiled spinach alone(A)	0.00[b]	29.5 ± 1.4	0.85 ± 0.05 (2.89%)	
- Fish Kaeng Som alone(B)	0.10[b]	96.1 ± 5.0	39.2 ± 2.0 (40.8%)	-72%
- Fish Kaeng Som with spinach(AB)	0.08[b]	128 ± 2	11.1 ± 0.4 (8.70%)	

* Values in brackets are percent dialyzability.

[a] Citric acid containing in the dish.

[b] Tartaric acid containing in the dish.

จากตารางแสดงให้เห็นว่าปริมาณการนำแคลเซียมไปใช้นั้นลดลงอย่างมากในอาหารที่ศึกษา ผลเหล่านี้เกิดจากการมีสารยับยั้งโดยเฉพาะอย่างยิ่งออกซาเลตในรูปที่ละลายน้ำได้ในผักปวยเล้งที่พบในปริมาณสูง อาจถึง

737 ± 20 mg/100g (Brogren *et al*., 2003) ซึ่งนอกจากออกซาเลตในผักสามารถรวมตัวกับแคลเซียมในตัวมันเองแล้ว ยังรวมถึงแคลเซียมในส่วนประกอบของอาหารอื่น ๆ ส่งผลให้การนำไปใช้ของแคลเซียมที่อยู่ในส่วนประกอบอาหารลดลงด้วย ผลเหล่านี้สอดคล้องกับการศึกษาในมนุษย์ ซึ่งพบว่า การดูดซึมแคลเซียมในนมเมื่อบริโภคร่วมกับอาหารเช้านั้นมีค่า 27.6% แต่เมื่อบริโภคผักปวยเล้งร่วมกับอาหารเช้าพบว่าเหลือเพียง 5.1% เท่านั้น (Heaney *et al*., 1988) และจากการศึกษาในหนูทดลอง โดยเมื่อให้การดูดซึมของแคลเซียมในนมเป็น 100% พบว่าการดูดซึมสัมพัทธ์ของผักปวยเล้งมีค่า 47% และเมื่อบริโภคผักปวยเล้งร่วมกับนมจะมีค่าเพียง 52% (Poneros-Schneier *et al*., 1989)

การศึกษานี้แสดงให้เห็นว่ากรดอินทรีย์ในอาหารไม่สามารถต้านอิทธิพลของสารยับยั้งทำให้การไดอะไลส์ของแคลเซียมลดน้อยลงอย่างมาก (78% และ 72% ในต้มยำและแกงส้ม) อาจเป็นเพราะปริมาณของกรดอินทรีย์ไม่มากพอที่จะเอาชนะผลของออกซาเลตซึ่งมีอยู่ในปริมาณที่มากได้

สรุป

วิธีในหลอดแก้วแบบไหลต่อเนื่อง สามารถใช้ศึกษาแนวโน้มการนำแร่ธาตุไปใช้ได้ โดยเป็นเครื่องมือที่มีประโยชน์ในการประมาณค่าการนำไปใช้ได้ของแร่ธาตุในอาหาร หลักการวิธี *in vitro* นี้ สามารถใช้ศึกษาเบื้องต้นถึงปัจจัยที่มีผลต่อการนำแคลเซียมไปใช้ ก่อนทำการศึกษาจริงในมนุษย์เพื่อยืนยัน เพราะวิธี *in vitro* เป็นวิธีที่ง่ายทำให้รวดเร็วและค่าใช้จ่ายน้อย

จากการศึกษานี้ชี้ให้เห็นว่า ส่วนประกอบในอาหารสามารถส่งผลต่อการนำแคลเซียมไปใช้ โดยกรดอินทรีย์ในอาหารไทย เช่นกรดซิตริกจากน้ำมะนาวสามารถเพิ่มการนำแคลเซียมไปใช้ได้ในผักคะน้า ในการเสริมธาตุแคลเซียม แหล่งของแคลเซียมเป็นสิ่งสำคัญที่ควรพิจารณา โดยจะต้องพิจารณาทั้งปริมาณแคลเซียมที่มีในอาหารนั้นและสารที่เป็นปัจจัยเสริมหรือเป็นปัจจัยยับยั้งการดูดซึมด้วย จากการศึกษานี้พบว่าผักคะน้าเป็นแหล่งของแคลเซียมที่ดี ถ้าบริโภคร่วมกับส่วนประกอบที่มีกรดอินทรีย์สูงและไม่มีสารยับยั้ง

อย่างไรก็ตามเนื่องจากหลักการนี้ไม่สามารถที่จะเลียนแบบให้เหมือนกับกระบวนการเมทาบอลิสมต่าง ๆ ในร่างกายมนุษย์โดยสมบูรณ์ จึงควรนำไปใช้อย่างพิเคราะห์

กิตติกรรมประกาศ

ขอขอบพระคุณโครงการพัฒนาบัณฑิตศึกษาและการวิจัยทางเคมี (PERCH) ทุนวิจัยจากสำนักงานกองทุนสนับสนุนการวิจัยที่ได้สนับสนุนค่าใช้จ่ายต่าง ๆ ตลอดการศึกษาครั้งนี้ และภาควิชาเคมี คณะวิทยาศาสตร์ มหาวิทยาลัยมหิดล ที่เอื้ออำนวยความสะดวกในด้านเครื่องมือในการวิเคราะห์

เอกสารอ้างอิง

มูลนิธิการแพทย์แผนไทยพัฒนา โครงการพัฒนาตำรา กองทุนสนับสนุนกิจกรรม 2544. อาหารเพื่อสุขภาพ. โรงพิมพ์องค์การรับส่งสินค้าและพัสดุภัณฑ์ กรุงเทพมหานคร. 154 หน้า.

วัลยา ภู่ภิญโญ 2544. ต้นไม้ ผักหญ้า อาหารและสมุนไพร. ดุจลดา กรุงเทพมหานคร. 234 หน้า.

Benway DA, Weaver CM.1993. Assessing chemical form of calcium in wheat, spinach, and kale. *J Food Sci*. 58 : 605-608.

Brogren M, Savage GP. 2003. Bioavailability of soluble oxalate from spinach eaten with and without milk products. *Asia Pacific J Clin Nutr*. 12 : 219-224.

Frossard E, Bucher M, Machler F, Hurrell R. 2000. Review potential for increasing the content and bioavailability of Fe, Zn and Ca in plants for human nutrition. *J Sci Food Agric*. 80 : 861-879.

Gueguen L, Pointillart A. 2000. The bioavailability of dietary calcium. *J Am Coll Nutr*. 19 : 119S-136S.

Heaney RP, Weaver CM. 1989. Oxalate: effect on calcium absorbability. *Am J Clin Nutr*. 50 : 830-832.

Heaney RP, Recker RR, Weaver CM. 1990. Absorbability of calcium sources: The limited role of solubility. *Calcif Tissue Int*. 46 : 300-304.

Heaney RP, Weaver CM. 1990. Calcium absorption from kale. *Am J Clin Nutr*. 51 : 656-657.

Heaney RP, Weaver CM, Hinders SM, Martin B, Packard PT. 1993. Absorbability of calcium from *brassica* vegetables: broccoli, bok choy, and kale. *J Food Sci*. 58 : 1378-1380.

Kamchan A, Puwastien P, Sirichakwal PP, Kongkachuichai R. 2004. *In vitro* calcium bioavailability of vegetables, legumes and seeds. *J Food Comp Anal*. 17 : 311-320.

Kennefick S, Cashman KD. 2000. Investigation of an *in vitro* model for predicting the effect of food components on calcium availability from meals. *Int J Food Sci Nutr*. 51 : 45-54.

Lombardi-Boccia G, Lucarini M, Lullo GD, Puppo ED, Ferrari A, Carnovale E. 1998. Dialysable, soluble and fermentable calcium from beans (*Phaseolus vulgaris* L.) as model for *in vitro* assessment of the potential calcium availability. *Food Chemistry*. 61 : 167-171.

Lyon DB. 1984. Studies on the solubility of Ca, Mg, Zn, and Cu in cereal products. *Am J Clin Nutr*. 39 : 190-195.

Miller DD, Schricker BR, Rasmussen RR, Campen DV. 1981. An *in vitro* method for estimation of iron availability from meals. *Am J Clin Nutr*. 34 : 2248-2256.

Poneros-Schneier AG, Erdman JW. 1989. Bioavailability of calcium from sesame seeds, almond powder, whole wheat bread, spinach and nonfat dry milk in rats. *J Food Sci*. 54 : 150-153.

Reykdal O, Lee K. 1991. Soluble, dialyzable and ionic calcium in raw and processed skim milk, whole milk and spinach. *J Food Sci*. 56 : 864-866.

Sottimai U. 2003. Development of a continuous-flow *in vitro* method for estimation of calcium bioavailability and application for various vegetables. M.Sc. Thesis in Applied Analytical and Inorganic Chemistry, Faculty of Graduate studies, Mahidol University. 91 p.

Weaver CM, Martin BR, Ebner JS, Krueger CA. 1987. Oxalic acid decrease calcium absorption in rats. *J Nutr*. 117 : 1903-1906.

Weaver CM, Plawecki KL. 1994. Dietary calcium: adequacy of a vegetarian diet. *Am J Clin Nutr*. 59(suppl) : 1238S-1241S.

Weaver CM, Proulx WR, Heaney R. 1999. Choices for achieving adequate dietary calcium with a vegetarian diet. *Am J Clin Nutr*. 70(suppl) : 543S-548S.

Wolters MGE, Diepenmaat HB, Hermus RJJ, Voragen AGJ. 1993. Relation between in vitro availability of minerals and food composition: a mathematical model. *J Food Sci*. 58 : 1349-1355.